Environmental Records from Corals and Coralline Sponges

By
Stewart John Fallon

A Thesis submitted for the degree
of Doctor of Philosophy
of The Australian national University

October 2000

The work described in this thesis was carried out while I was a full-time student at the Research School of Earth Sciences, at the Australian National University between April 1997 and October 2000. Except where mentioned in the text, the research described here is my own. No part of this thesis has been submitted to any other university or similar institution.

Stewart John Fallon
October 2000

ACKNOWLEDGMENTS

Truly no PhD project could be accomplished without the help of many people. Firstly, I would like to thank my supervisor **Malcolm McCulloch** for helping me get to RSES, your enthusiasm and support enabled me to finish within the overseas guidelines. Well, the fieldtrips in-between lab work and writing didn't hurt either. I've enjoyed my time here from your office discussions to 5 m underwater drilling corals. The rest of my committee consisted of **Vicki Harriott**, **Chantal Alibert** and **Brad Opdyke**. Thanks Vicki for helping me with discussions, editing and memorable field trips from mud/coral drilling in Moreton Bay to the reefs of Lord Howe Island to the solitary diving on Middleton Reef. I'll skip the bit about bobbing around on the RV Franklin. Chantal, thanks for many discussions about corals, trace elements and your help with techniques. Thanks Brad for valuable comments at the midpoint of my project.

I received quite a lot of help from **Les Kinsley**. Les, your expertise in mass spectrometers, lasers and everything else I bugged you about "Hi Les, got a minute?" has been greatly appreciated, thanks. **Graham Mortimer** has been very helpful with chemistry, discussions and TIMS & THUG measurements and any other questions I could ask him. Thanks to the rest of the Environmental Geochemistry and Geochronology group for their help; thanks to **Candace Martin** for discussions and sharing an office with a cluttered person, **Lois Taylor** for the fantastic cakes. Thanks also to **Mike Gagan** and **Heather Scott-Lynch** for discussions, stable isotope measurements and the exciting fieldwork in Indonesia. **Joe Cali** also helped with stable isotope questions. In the administration department thanks go to **Wayne Hampton**, **Tracy Coombes** and **Marina Lukatela** for their behind the scenes help taking care of everything, enabling more time to be spent on my project. The workshop group, **Bob Waterford**, **Chris Morgan**, **Roger Willison** thanks for help constructing, inventing and fixing coral drilling gear when I needed it, usually at the last minute. And thanks to the rest of the RSES staff, no matter how busy people were they always had time to answer questions, do favors and provide help.

Outside the school, I would like to thank the group at AIMS; **Janice Lough** for her help with projects, discussions, coral material, data and for making me feel so welcome my first days in Australia at the AUSCORE meeting, **Dave Barnes** for discussions, questions

(both answering and asking), **Monty Devereux** for coral access, arranging density scans and help during my visit, **Ray Taylor** for discussions about coral and sponge growth and signal smoothing. I'd also like to thank **John Hooper** (Queensland Museum) for access to sponge samples. **Gert Wörheide** for all his help with coralline sponges, thanks for showing me how to "sniff" out the *Astrosclera*, and his generosity in providing samples. Thanks to **Donovan Whitford** for his help with collecting sponges in Indonesia. **Steve Eggins** provided answers and lots of help with the laser ablation system.

I have gained a lot of knowledge from my fellow students; my thanks to my officemate **John Marshall** and our lunchtime discussions that solved all the trace element coral questions, **Erica Hendy** for discussions, and possibly doing more analyses than I, **Dan Sinclair** for getting me started on LA-ICP-MS and many discussions about coral trace elements and laser ablation standards etc… I would also like to thank my former officemates (and fellow Americans) **Chuck Magee** and **Eleanor Dixon** for fun discussions and homesickness prevention. I would also like to thank morning and afternoon tea, because good discussions and ideas do flow by way of *Earl Grey*.

Extracurricular activities like mountain biking and Ultimate provided the necessary distractions for the completion of a successful project. The many hours of riding in vans to tourneys in Sydney etc. with **Leon**, **Ian**, **Nikki**, **Davey**, **Anna** and **Michael** and the rest of the gang, **Gman**, **Helen**, **Sue** and **Jon**…(I can't name you all) gave me fond memories that I'll remember forever, the after training at ABN will also be missed.

I especially want to thank my family. My mother and father who have provided many years of support, emotionally, financially and have given me so many opportunities, thank you both so much!! My sister you have helped me more than you know, our talks and your persistence to become a MD inspired me greatly. However, I got my letters first ☺. And to my new family, Christina, finding you has made life incredible, with your help and support I made it to the end. Thank you for your love and encouragement.

Abstract

This research centers on the extraction of environmental information stored in the calcium carbonate skeletons of corals (*Porites*) and coralline sponges (*Astrosclera willeyana*). Elemental variations are measured in these samples using laser ablation inductively coupled plasma mass spectrometry. During this project, techniques were refined and developed to quantitatively measure major (B, Mg, Sr, Ba, U) and minor (Mn, Zn, Pb, REE's) elemental abundances in corals and coralline sponges.

This method was used to extract seasonal records from a high latitude coral living at its limits of cold-water tolerance in Japan. Seasonal cycles of major elements (B, Mg, Sr, U) were calibrated against *in situ* instrumental temperature monitors. Calibrations were in good agreement with other published reports. This coral also recorded wind-induced upwelling (both annual and El Niño related) by increases in the Ba/Ca ratio. The trace element annual patterns and slow growth rate also indicated that this coral had very slow/no extension during the cold winter months when water temperature was below 18 ºC.

Cores from *Porites* sp. coral colonies were also collected from inshore, mid-shelf and outer reef localities (central Great Barrier Reef) to test the robustness of the major elemental SST and runoff proxies (B/Ca, Mg/Ca, Sr/Ca, Ba/Ca, U/Ca). The inshore reefs selected for this study are heavily influenced by river runoff whereas the mid-reef and outer-reef locations are not. It is shown that Ba/Ca provides an excellent proxy for river runoff. Time series analyses of Sr/Ca, U/Ca, B/Ca and Mg/Ca are compared to *in situ* sea surface temperature (SST) and/or IGOSS NMC weekly satellite SST to provide calibrations for these elements. Previous workers have noted differences in the calibration of Sr/Ca vs. SST; this LA-ICP-MS dataset shows a slight variation between different corals. This suggests small-scale intra-coral variability. Both the U/Ca and Mg/Ca have calibrations within error for mid-shelf and outer reef corals but the calibrations differ for the inshore corals. Sr/Ca and B/Ca appear to be the most robust of the elemental temperature proxies in terms of recording water temperature. Measurements of coral manganese suggest a seasonal cycle closely linked to solar radiation

and wind. Increased solar radiation may increase the dissolved seawater Mn that result in corals having elevated concentrations of Mn during the summer.

The use of corals as recorders of marine pollution was examined on the island of Misima in Papua New Guinea where open-cut gold mining commenced in 1989. This mining caused increased sedimentation affecting the nearby fringing coral reef to varying degrees, causing coral mortality (complete suffocation) in some areas. This sediment is made up of completely weathered quartz feldspar, greenstone and schist. These rocks have distinct chemical constituents (rare earth elements [REE], zinc and lead etc.), which are entering the near-shore environment in considerably higher than normal concentrations. Eight coral colonies (2 from high sedimentation, 2 transitional, 2 minor and 2 unaffected control sites) were analyzed for Mn, Y, La, Ce, Zn and Pb. All sites show low steady "background" levels prior to the commencement of mining. After mine construction began in 1988, all sites aside from the control show dramatic increases of Mn, Y, La, and Ce associated with the increased sedimentation. Zn and Pb increase after 1989 when ore processing began. The concentration of these elements in these corals decreases as the distance from the mine increases. Rare earth elements (REE) measured in two corals suggest a pattern different from "normal" seawater. When the coral REE pattern is compared to seawater an enrichment of the light and middle REE's appear. The heavy REE's are depleted relative to the seawater pattern. This suggests the nearshore seawater REE's are influenced by island weathering.

Coralline sponges have been proposed as a new source of tropical paleoclimatic information. Profiles of $\delta^{13}C$ in coralline sponges have documented (better and more accurately than corals) the atmospheric increase of ^{12}C associated with increased fossil fuel consumption. Due to their very slow growth rates ~0.2 mm yr^{-1} sponges are better suited to recording and providing long-term environmental information rather than annual information. These sponges appear to smooth the record stored in their skeleton by adding secondary aragonite near the base of the living tissue layer. This smoothing limits their use as annual environmental recorders but still enables their use for decadal or longer environmental fluctuations. Smoothed records of Sr/Ca from five sponges around the Southwest Pacific

suggest that these sponges are able to capture 5 yr. and longer seawater temperature anomalies over the past 50-200 years. The temperature sensitivity of Sr/Ca in sponges is 7 to 12 times larger than corals with ~0.7-0.9 mmol/mol ΔSr/Ca per ºC for sponges compared to ~0.07 mmol/mol ΔSr/Ca per ºC for corals.

Table of Contents

List of Figures

List of Tables

Chapter 1: Introduction

General circulation models (GCM's) illustrate the interaction between atmospheric and ocean circulation and their effects on climate throughout time. The tropical oceans play an important role in the distribution of heat and atmospheric moisture content by way of seawater temperature. Understanding the structure of tropical sea surface temperature variability is critical to accurately predicting future climate change. In order to increase our confidence in these models, rigorous testing with paleo-records is needed from time periods outside of human influence. The production of high fidelity records from multiple locations is critical to evaluate the patterns and mechanisms of natural climate variability. Only with a good understanding of natural climate variability can we assess the impact of human influence (increased greenhouse gasses, changed land practices and pollution). Corals are one such proxy that can provide the spatial and time coverage required to produce these records.

Environmental indicators preserved in the chemistry of coral skeletons provide important information about the past climate in the tropics (Knutson *et al*., 1972; Dodge and Vaisnys, 1975; Highsmith, 1979). Time series of environmental conditions can be constructed because corals deposit their aragonitic ($CaCO_3$) skeleton in alternating high-density and low-density band couplets that are revealed by X-radiography (Knutson *et al*., 1972). It has been shown that these density bands can be correlated to approximately one year of colony growth. Changing skeletal chemistry in coral growth bands reveals a time series of changing environmental conditions.

Corals incorporate elements in near proportion to the element/calcium ratio of the surrounding seawater. The partitioning of some of these elements into coral aragonite is influenced by temperature. Elemental ratios, Sr/Ca, U/Ca, Mg/Ca and B/Ca have all been shown to be useful for monitoring the seawater temperature surrounding a growing coral (e.g. Beck *et al*., 1992; Mitsuguchi *et al*., 1996; Alibert and McCulloch, 1997; Sinclair *et al*., 1998). Similarly, rainfall, runoff and upwelling events have been identified through the use of $\delta^{18}O$, Ba/Ca and Cd/Ca (e.g. Lea *et al*., 1989; Linn *et al*., 1990; Shen *et al*., 1992a; Gagan *et al*., 1998). Corals can also document anthropogenic changes related to pollution and land use (e.g. Cu, Zn, Pb, Mn, Cd, Rare Earth

Elements, Howard and Brown, 1986; Brown, 1987; Shen and Boyle, 1987; Hanna and Muir, 1990; Scott, 1990; Sholkovitz and Shen, 1995; Bastidas and Garcia, 1999).

In order to understand variations of past SST, climate and anthropogenic change, rigorous testing and confirmation of multiple proxy methods is needed. A relatively new analytical method laser ablation ICP-MS has been used to investigate the "major" elemental proxies in corals (B/Ca, Mg/Ca, Sr/Ca, Ba/Ca, U/Ca) and to test their variability in corals from different environments. A high latitude reef *Porites* coral (Shirigai Bay, Japan) was chosen because its location provided a 'unique' opportunity to study the response of trace element systematics and coral growth in an environment where the SST ranged from 15-29ºC. *Porites* corals were also collected from inshore, mid-shelf and the outer reef of the Great Barrier Reef to test the effects of runoff and nearshore processes on these "major" elemental proxies. A set of *Porites* corals collected for a study on the impact of sediment on coral growth, extension and calcification by J. Lough and D. Barnes (Australian Institute of Marine Science) was used to examine whether metals associated with sediments would preserve a record of impact. These corals were collected from nearby a gold mine on the island of Misima in Papua New Guinea.

Finally, a new proxy indicator, *Astrosclera willeyana* has been examined to test whether trace elemental variations (Sr/Ca etc.) can be used to reconstruct environmental parameters. These sponges are slow growing (0.1 – 0.5 mm yr^{-1}) and therefore are suited to the high resolution LA-ICP-MS method. They are very long lived (up to 1000 yrs) and consequently have the potential to provide longer-term records of climate with less sample expense. They also inhabit a wider depth range then corals (10-185 m) and may be able to provide information about the water column as well as the sea surface.

Chapter Summaries

Chapter 2

This chapter reports on the analytical methods used for this project. Topics include coral core collection, cutting, cleaning and instrumentation used to measure the trace elements in the corals and coralline sponges.

Chapter 3

This chapter reports my enhancements to the LA-ICP-MS method as applied to corals that was first developed at ANU by D. Sinclair (Sinclair, 1999). The construction and calibration of a coral pressed powder standard enabled accurate fully quantitative measurements of B, Mg, Sr, Ba, U in corals. The accuracy and reproducibility using the coral pressed powder standard is also discussed. The technique to measure "minor" elements (Mn, Zn, Pb, Y, REE's) in corals using the commercial silicate standard NIST 614 is also discussed.

Chapter 4

This chapter presents a review on the factors affecting "major" and "minor" element incorporation into coral skeletons based on the existing literature. Factors such as seawater concentration, incorporation of elements into carbonates, factors affecting partitioning (temperature, salinity, biologic factors) are discussed.

Chapter 5

This chapter discusses the records of B/Ca, Mg/Ca, Sr/Ca, Ba/Ca and U/Ca extracted from a *Porites* coral living in one of the most northern reefs of Japan. The effect of cold winter water is discussed in relation to coral extension and trace element kinematics.

Chapter 6

This chapter presents the data collected from six corals collected and analyzed from a transect that covers the inshore; mid-shelf and outer reef section of the Great Barrier Reef. Influences of nearshore processes (runoff, particle resuspension and particle reactions) on corals is discussed. The water temperature proxies B/Ca, Mg/Ca, Sr/Ca and U/Ca are examined relative to each other and to other published calibrations. Ba/Ca is evaluated as a river runoff proxy and manganese is examined as a measure of nearshore particle interaction.

Chapter 7

This chapter presents the data collected from eight corals subjected to varying degrees of increased sedimentation due to open-cut gold mining on Misima Island, PNG. Variations in the concentration of the metals Mn, Zn, Pb and REE's are discussed relative to the sediment impact gradient and different source rock types.

Chapter 8

This chapter discusses the coralline sponge *Astrosclera willeyana* and the records obtained by Sr/Ca, $\delta^{18}O$ and $\delta^{13}C$. Temperature dependence on sponge Sr/Ca is discussed relative to corals as well as the effect of biomineralization on the recovered records.

Chapter 2: Analytical Methods

2.1 Coral Collection

Coral cores were collected underwater using SCUBA and a hand held pneumatic air drill in contrast to the larger systems of for example, Isdale and Daniel (1989). A surface compressor or most often a SCUBA tank located on a dingy or underwater powered the air drill. The core barrel is capable of removing a 55 mm diameter, 550 mm long coral core. Special tungsten carbide cutting tips designed and constructed by the RSES workshop are attached to the end of the barrel. Through the use of extension rods the collection of longer cores, up to 1.5 m is possible. Once a suitable *Porites* coral is found, the driller uses a guide board to start the hole and commence drilling (Figure 2.1).

Figure 2.1 D. Whitford drilling *Porites* coral Alor, Indonesia.

The driller must clear the cuttings every 5 - 10 mm to prevent seizure of the core barrel (Figure 2.2). When the desired core length is achieved a ring is slipped around the core and pushed to the bottom of the hole. A chain attached to the ring feeds around a sprocket and an aluminum core extractor snaps the core at the bottom of the hole

(Figure 2.3). The core is then removed and returned to the surface by the support diver (Figure 2.4)

Figure 2.2 D. Whitford using core barrel to flush cuttings to prevent core barrel seizure.

Figure 2.3 D. Whitford using ring and core extractor to remove coral core.

Figure 2.4 J. Marshall showing coral core from *Porites* at Old Reef, GBR. Photo by Viv Moran.

An extension rod can then be used to remove longer sections of coral; this system is very effective for 1 m long cores but can be extended to ~ 2 m (Figure 2.5). Cores are soaked in freshwater. Some had tissue removed with a water hose, and were then dried before being packed for transport to Canberra. This system has been developed over several years in close collaboration with the RSES workshop (C. Morgan).

2.1.1 Cutting Corals

Coral cores were glued to brackets (Araldite™) for mounting onto a specially modified end mill. A 23 mm diameter (2 mm thick) diamond-impregnated saw blade was mounted on the end mill specifically to cut coral. The cores move ~ 0.5 mm sec^{-1} past the blade with fresh water used as a lubricant. Three to four 7.0 mm thick slices were obtained from each core. The slices were soaked in 18 Ω water and air-dried.

Figure 2.5 Extension rod for obtaining longer coral cores.

The slices were taken to National Capital Diagnostic Imaging for X-ray analysis. The images are taken on Kodak emulsion film on a Lamenex screen. Contact prints were made for ease of handling. Density profiles and preliminary chronologies were obtained from the contact prints. A 20 - 25 mm wide strip including a major growth axis was then cut from the slice. The strip was sub-sectioned into 45 mm lengths for laser analysis. The 45 mm lengths were not cut all the way through. Approximately 1 mm is left at the base of the section to preserve the continuous record. The pieces are separated by hand with very little loss of material between pieces.

2.1.2 Cleaning

Prior to the analysis, the 45 mm sections were placed in an ultrasonic bath of 18 Ω water for 30 minutes. Some of the samples were also cleaned in 15 – 30 % H_20_2 for 30 minutes to remove organics. The samples were then treated with an ultrasonic probe in 18 Ω water. Both surfaces were cleaned 2-3 times, changing water after 2 passes with the probe. Six passes were used to clean one side. The corals were then placed on lint-free tissue and dried overnight at 40 ºC. Plastic gloves are used to handle the corals subsequently to prevent contamination.

Laser Cleaning

A laser slit 200 x 800 μm (normal analysis slit 50 x 500 μm) was used in a two stage cleaning process. The laser is pulsed at 50 Hz with a laser energy of 100 mj. The coral moves beneath the laser at ~ 150 μm sec^{-1}. A second ablation at 5 Hz, 100 mj and a speed of 30 μm sec^{-1} removes any loose debris. This two stage cleaning procedure removes ~ 5 – 10 μm of coral from the sample surface exposing clean fresh material. The sample and standards can been seen in (Figure 2.6).

Figure 2.6 Close up of sample holder, NIST 614 glass standard (top left), coral pressed powder standard (bottom left), 45 mm coral piece (right).

2.2 Hardware

2.2.1 Inductively Coupled Plasma Mass Spectrometer

The main instrument used throughout this project was a PlasmaQuad PQII. The standard operating conditions for both laser and solution are given in Table 2.1.

Table 2.1 ICP-MS Configuration, Laser and Solution.

	Laser	**Solution**
ICP-MS	PlasmaQuad PQ II	
Forward Power	1350 W	1350 W
Reflected Power	< 1 W	< 1 W
Gas Flow Rate:		
Cool Gas	13 - 14 l min^{-1}	13 - 14 l min^{-1}
Auxiliary	0.5 – 1 l min^{-1}	0.5 – 1 l min^{-1}
Nebulizer Ar	0.99 l min^{-1}	0.99 l min^{-1}
Nebulizer He (into cell)	0.3 l min^{-1}	
Cone Composition	Aluminum or Nickel	Nickel
Detector Mode	Pulse Counting	Dual
Acquisition Mode	Time Resolved	Normal
Isotope Dwell Time	25 – 60 ms	Adjustable
Points per Peak	3	3
Time Slice	~ 1 s	-
Nebulizer	-	Meinhardt
Counting Time	-	60 s
Uptake Time	-	90 s
Wash-out Time	-	120 s (for each of Triton sol'n, HNO_3, and 18Ω water)

2.2.2 Laser

The laser used was an ArF excimer laser constructed by Lambda Physik (Table 2.2). It operates at a wavelength of 193 nm with an energy density of 5 – 10 J cm^{-2}. A significant advantage of this laser is the large output beam (3 cm x 1 cm) and its uniform energy density (Table 2.2). The large output beam enables almost any shape of mask to be used (spots, rectangles etc). The laser has a long focal length (15 cm) and the mask image is demagnified 20x at the sample. Under normal operating conditions (70 μm spot, 5 Hz and 100 mJ) approximately 0.1 μm of sample is removed per pulse on an NBS glass standard (for more information see Eggins *et al*., 1998; Sinclair, 1999).

For coral work, the laser beam is masked to produce a rectangle 50 μm tall by 500 μm wide (Figure 2.7). The size of this slit minimizes depth-related fractionation by limiting the amount of material removed from the bottom of holes (corals are very porous) (Eggins *et al*., 1998; Sinclair *et al*., 1998). The slit size is a compromise between sample resolution and the amount of material sampled. Too much material causes plasma instabilities, cone degradation and can overwhelm the detector (Sinclair, 1999). For coral work we used an energy of 50 mJ with a 50% partially reflecting mirror to

produce an effective sample energy of 25 mJ. This provided a good range of counts across the mass range of interest for coral analysis. Figure 2.7 shows parallel laser tracks on a coralline sponge. Tracks are not readily visible on corals.

Table 2.2 Operating Parameters for ArF Excimer Laser.

	Setting
Laser	Lambda Physik LPX 120i
Gas Mix	ArF
Wavelength	193 nm
Output Beam	3 cm x 1 cm
Focal Length	15 cm
Focusing	20x reduction
Spot Dimensions	X = 500 μm Y = 50 μm
Energy Density	5 – 10 J cm^{-2}
Sample Energy	50 mJ with 50% partially reflecting mirror
Pulse Rate	5 – 10 Hz
Drill Rate	0.1 μm s^{-1} (NIST glass)
Sample Scan Speed	~ 30 μm s^{-1}

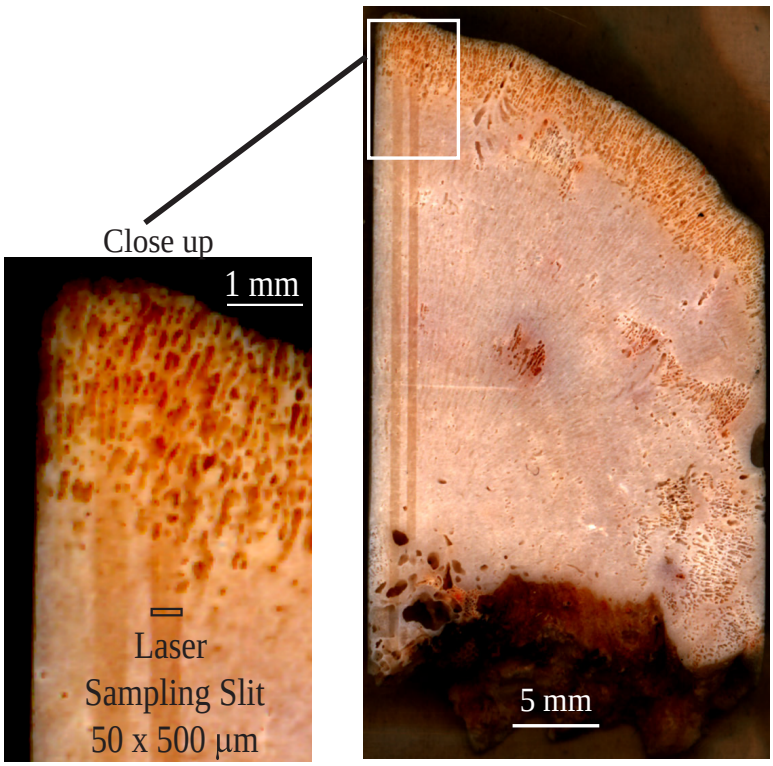

Figure 2.7 Laser sampling on a coralline sponge showing two parallel tracks (right picture) and close up of boxed section (left side) of the laser sampling slit. Laser tracks are not observable on corals due to surface porosity.

2.2.3 Sampling Cell

Samples were mounted in the sample holder (Figure 2.6). The sample holder is moved beneath the laser beam by a DC motor calibrated in millimeters (Figure 2.8). The speed of the motor is adjustable and continuous scanning occurs in one direction. Coral samples are moved underneath the laser at ~ 30 μm s^{-1}. The samples are ablated in a sealed Perspex chamber under a helium atmosphere (Figure 2.8) (Eggins *et al*., 1998; Sinclair, 1999). The ablated material is entrained in argon and helium gas for entrance into the ICP-MS. The cell is designed to ensure ablation occurs in helium and not argon, which improves sample removal efficiency and decreases the ablation blanket deposited on the sample (Eggins *et al*., 1998).

Before the sample reaches the ICP-MS it is passed through a smoothing manifold to reduce signal fluctuations caused by a pulsing laser. The manifold splits the sample/gas mixture stream into 8 parts having slightly different residence times and then recombines them into one coherent stream for analysis over the 1-s time slice.

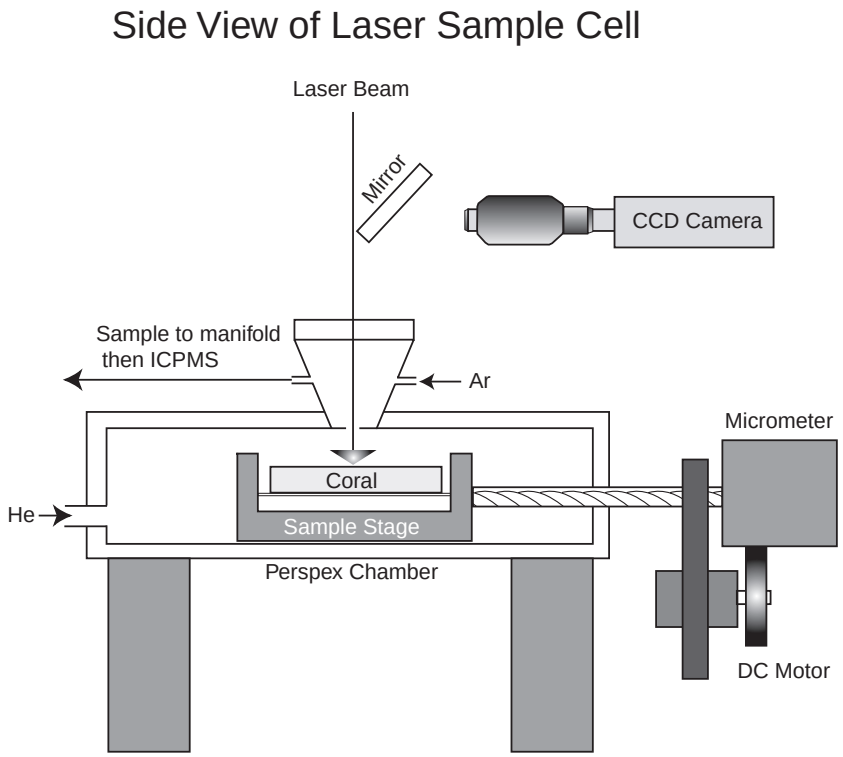

Figure 2.8 Side view of laser sample cell at RSES. Coral is ablated in sealed Perspex chamber under a helium atmosphere. Sample stream is entrained in argon and enters smoothing manifold before entrance to ICP-MS. Sample is viewed by CCD video camera. A DC motor moves samples underneath the laser enabling continuous sampling.

2.3 LA-ICP-MS Analytical Method

2.3.1 Summary of Method

Table 2.3 is a summary of the LA-ICP-MS method used to analyze corals and coralline sponges (methods based on Sinclair *et al*., 1998). The first two steps are cleaning steps. During the first step the laser is pulsed at 50Hz and the sample moves at ~150 μm s^{-1}. The laser is then pulsed at 5 Hz and 30 μm s^{-1} to clean loose debris and precondition ICP-MS to analyze carbonate material. This step helps increase short-term stability of the LA-ICP-MS system. The laser slit is then changed to either 50 x 500 μm for the "major" suite of elements or 100 x 500 μm for the "minor" elements.

The laser is pulsed at 5 Hz, 50 mJ using a 50 % partially reflecting mirror. The time resolved analysis program is started and 60-90 seconds of blank/background is collected while the laser is off. The coral pressed powder standard is then analyzed for 60-90 s, equating to approximately 2-3 mm in length. The sample is then analyzed from top to bottom and the top 5 mm is reanalyzed as a drift check. The sample moves beneath the laser at a speed of 30 μm s^{-1}. Another 60-90 s of standard is analyzed followed by 60-90s of blank/background with the laser off. This method is adjusted slightly when "minor" elements are analyzed. During "minor" element analyses an additional standard (NIST 614) is analyzed before the first coral pressed powder standard and after the second coral pressed powder standard (Table 2.3). The laser is pulsed at 10 Hz and 100 mJ to provide higher count rates for the low concentration elements. Parallel tracks are usually analyzed and averaged to obtain a more representative analysis (Figure 2.7).

2.3.2 *Isotopes Monitored*

The "major" element isotopes monitored for coral analysis are ^{10}B, ^{25}Mg, ^{43}Ca, ^{84}Sr, ^{138}Ba and ^{238}U. Crosschecks were also undertaken using additional isotopes ^{11}B, ^{26}Mg, ^{46}Ca and ^{137}Ba, which produce near identical results. "Minor" element isotopes monitored were ^{10}B, ^{31}P, ^{46}Ca, ^{55}Mn, ^{66}Zn, ^{84}Sr, ^{89}Y, ^{114}Cd, ^{137}Ba, ^{139}La, ^{140}Ce, ^{208}Pb and ^{238}U although not all elements were measurable in every coral.

Table 2.3 Summary of LA-ICP-MS Analytical Method

Procedure list for LA-ICP-MS of corals
1. Pre-ablate coral with high laser repetition rate to reveal clean surface (50 Hz)
2. Pre-condition ICP-MS during second pre-ablation at 5 Hz
3. Collect 60 – 90 s of background counts (laser off)
4. Collect 60 – 90 s of data from secondary standard (NIST 614) if necessary
5. Collect 60 – 90 s of data from pressed coral powder standard
6. Analyze the length of coral
7. Re-analyze the top 5 mm of coral as an instrumental drift check
8. Collect another 60 – 90 s of data from pressed coral powder standard
9. Collect another 60 – 90 s of data from secondary standard (NISTS 614) if necessary
10. Collect another 60 – 90 s of background (laser off)

2.3.3 Dwell Time (Instrument integration per isotope)

The dwell times for each isotope in the "major" element suite is 50ms while measuring 3 points per isotope peak. The ICP-MS quadrapole has a settling time of 10 ms between isotope peak jumps. This dwell time provides a time slice of ~ 1 s for the time resolved analysis. A 1 s time slice is a good compromise between counting statistics and reducing the amount of time between calcium concentration estimates. Minimizing the time between calcium concentration estimates is important because the laser is constantly analyzing new sections of coral and the variability of the coral surface porosity causes variations in count rate. These variations must be accounted for to ensure proper normalization of element/calcium ratios. When analyzing the "minor" element suite a 1 s time slice is still used. The dwell times for elements with high-count rates are reduced and the dwell times for the lower concentration elements are increased to improve counting statistics during the "minor" element analysis.

2.3.4 Data Processing

The data from the ICP-MS is downloaded as comma delimited text format with sample header information and the counts per second for each isotope versus time slice. A Visual Basic program was written within Excel to speed data reduction and processing. Normally ~ 3000 data points are acquired for each isotope during a typical coral analysis. The processing steps include: selecting the beginning and ending sections for the first background, first standard, beginning and ending of coral and coral repeat and

beginning and ending of second standard and background. For the "minor" element processing, a second spreadsheet was designed to handle the additional standard (NIST 614). The user must select the beginning and ending sections for each group (background 1, standard 1, etc), the program uses these sections to perform the processing steps; background subtraction, normalization to calcium, standardization and signal smoothing. These steps are described in more detail below. A typical count rate vs. time showing backgrounds, standards and coral sections is seen in Figure 2.9.

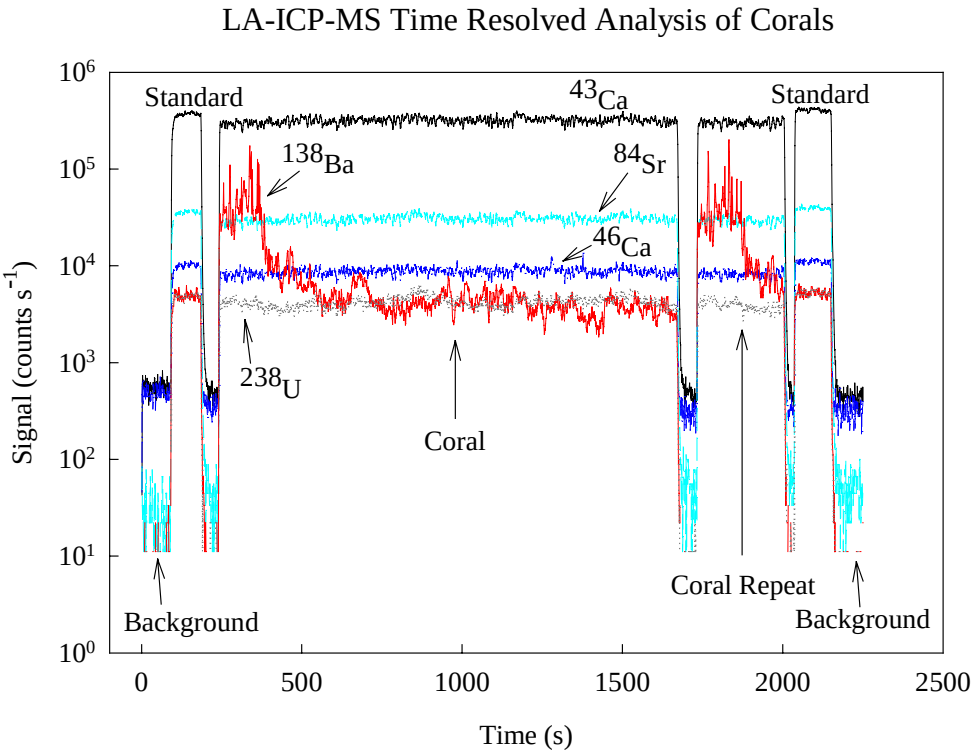

Figure 2.9 Time resolved data (counts s^{-1}) showing components of typical coral analysis. Samples are bracketed by standards and backgrounds.

Background/Blank Subtraction

The background/blank values are measured with the laser turned off and represent the signal due to gas contamination and machine noise. For many elements, the background values are extremely low compared to the sample signal. In this case the background subtraction is insignificant. However when analyzing "minor" elements this is not always the case. The 60-90 s of background acquired from the beginning and ending background are averaged to one value. If the background values differ from beginning to end they are assumed to have drifted linearly with time. A linear equation is interpolated from the beginning and ending background values to the appropriate time

slice. This equation is then subtracted from all the data. This removes the background/blank from the signal as well as accounting for any drift in the background. The spreadsheet performs this task automatically.

Normalization to Calcium

In order to account for changes in the amount of material ablated, the elements are standardized to an isotope of calcium. The isotope ^{43}Ca (0.135 % of Ca) is used as the index isotope to account for variable sample count rates due to coral surface porosity. ^{46}Ca (0.004 % of Ca) is used for the "minor" elements because the counts for ^{43}Ca are off scale when measuring the "minor" elements (this will be discussed in the standards section 3.5). All elemental counts are divided by the calcium counts and hereby referred to as calcium normalized.

Standardization

The next step is to relate the calcium-normalized signal to the calcium-normalized signal of the standards. The instrument sensitivity can change over time and can change by different amounts for each element of the mass range. This sensitivity drift can also be approximated by a linear function. The standard values from the beginning and end of the analysis are interpolated using a linear equation to correct each point (same as background subtraction). The calcium-normalized signal is divided by this equation using the time slice as the dependent variable. This correction accounts for ICP-MS sensitivity-related drift assuming that it is linear. Figure 2.10 shows a calcium-normalized scan without standardization (note linear drift) and with the linear drift removed from the standardized scan. The standardized values are then multiplied by the element/Ca concentration (mol/mol) in the coral pressed powder standard. The use of standards for absolute concentrations and calibrations will be discussed in Chapter 3.

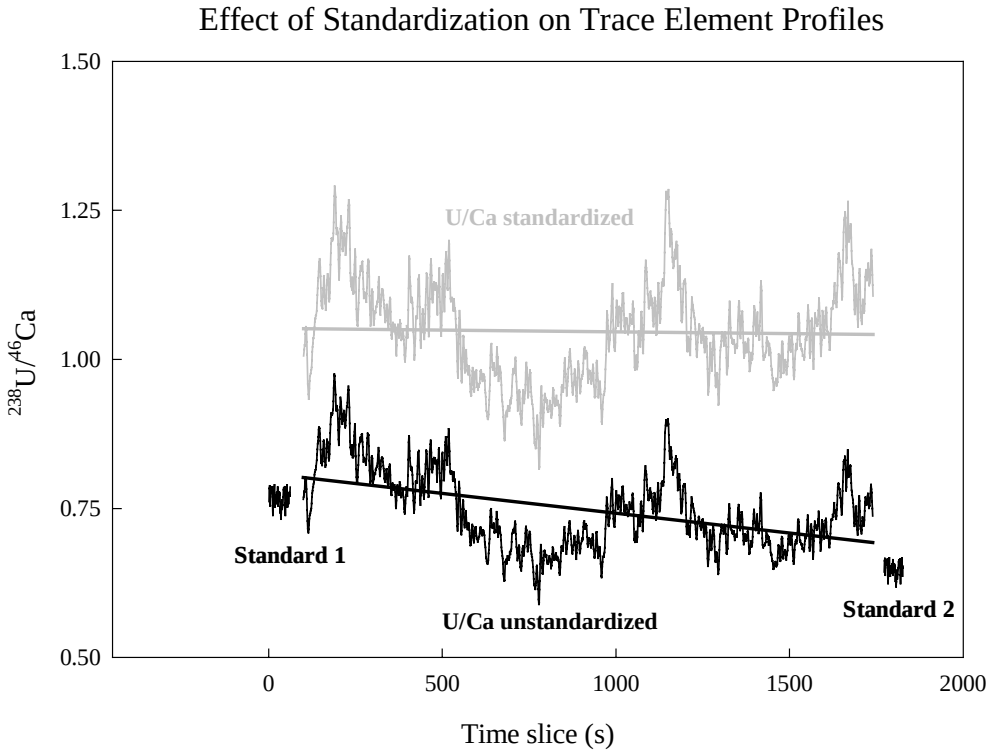

Figure 2.10 Effect of standardization on trace element profiles. $^{238}U/^{46}Ca$ vs. time slice. Bottom curve (black) shows unstandardized linear drift with a standard bracketing the beginning and end of the analysis. Top curve (gray) shows same profile after standardization, with the linear drift removed.

Data Averaging

The laser-sampling window is 50 μm in the y direction; the coral is scanned at 30 μm s^{-1} in the y direction. Under these conditions one spot on the coral is pulsed by the laser 9-10 times over a 2 s period. The 1 s integrated samples are essentially a running average over the coral. Sinclair (1999) discussed several methods for trace element smoothing in corals, running median filters, running average filters and Fourier filters etc. All of the filtering methods examined result in similar trace element profiles. For this project, the data is discretely averaged at ~0.25 mm. This still provides "high" resolution information with data on the shorter scales (< weekly) averaged out. This is feasible because corals have been found to be heterogeneous at small scales and the environmental information at this scale is probably not informative (Allison and Tudhope, 1992; Allison, 1996b; Hart and Cohen, 1996; Sinclair, 1999). The effect of the averaging can be seen in Figure 2.11.

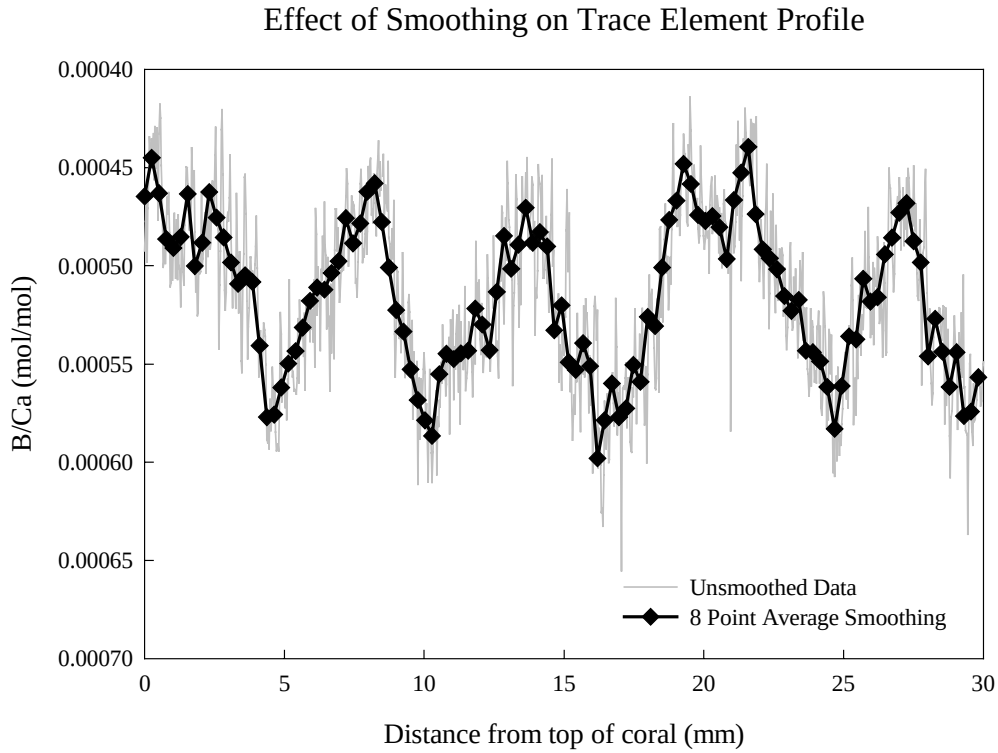

Figure 2.11 B/Ca (mol/mol) vs. distance from top of coral. Gray line is unsmoothed data, black line with diamond symbols is "smoothed" data. The "high" frequency (<weekly) data (noise) is removed leaving a "cleaner" signal.

Chapter 3: Enhancements to the LA-ICP-MS Method

3.1 Major Element Standards

For LA-ICP-MS, an ideal standard should be chemically and physically matched to the unknown (Perkins *et al*., 1991; Pearce *et al*., 1992; Jarvis and Williams, 1993; Morrison *et al*., 1995; Sylvester and Ghaderi, 1997). However, finding appropriate matrix matched standards for the analysis of carbonates by LA-ICP-MS is difficult. Two in-house standards were used in this project. The first was a $CaSiO_3$ glass synthesized and described by Sinclair *et al*. (1998). However, there were problems with this glass standard with respect to accuracy and long-term reproducibility. Sinclair *et al*. (1998) concluded that matrix-related fractionation occurred when coral (calcium) silicate is used as a standard. Therefore, the non-matrix matched coral silicate standard does not provide the accuracy or long-term reproducibility necessary for fully quantitative analysis of corals and has now been replaced. The current standard is a pressed powder disc similar to ones developed by Perkins *et al*. (1991).

3.1.1 Crushed Coral Pressed Powder Standard

The coral powder was processed and cleaned by Dan Sinclair as described in Sinclair (1999). In summary, a section of coral material was removed from a *Porites* coral collected at Davies Reef, Great Barrier Reef, and crushed into fragments ~ 2.5 cm^3 in size. A cleaning protocol modified from Shen and Boyle (1988) was applied, involving Milli-Q (18 Ω) water, H_2O_2 and hydrazine with heating steps (Sinclair, 1999). The coarse fragments were finally leached in a 5% solution of citric acid and rinsed in Milli-Q water before a final crushing in an agate mortar.

Using this cleaned coral powder I prepared a pressed coral standard using the following procedure. Two grams of well-mixed powder was transferred to clean Teflon containers and mixed with 5 drops of 5% poly-vinyl alcohol binder (PVA). This was then transferred to a clean pellet press and pressed at 20 tons into a 7 mm diameter disc, similar to Perkins *et al* (1991) and Pearce *et al* (1992) (Figure 3.1). Thin Teflon sheets

placed on both sides of the pellet press were used to minimize contamination during the pressing procedure. However, subsequent analyses indicate some contamination, possibly during the pressing, for heavy metals (Pb). The standards were then placed into 2.54 mm diameter Teflon cups to fit into the sample holder (Figure 2.6).

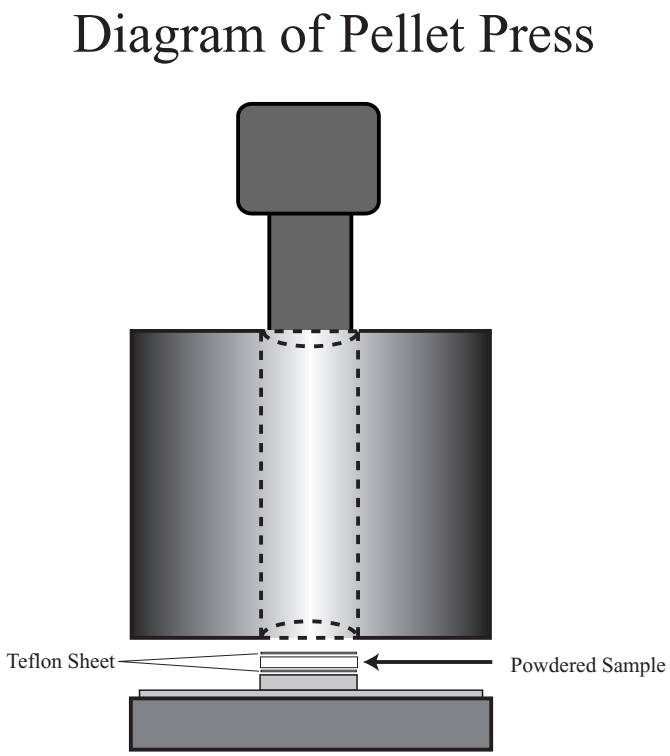

Figure 3.1 Side view of steel pellet press. Powdered samples are pressed at 20 tons to form 7 mm discs.

Powdered coral and marine carbonate samples

Additional pressed powder samples were constructed from a *Porites* coral (Huon, Papua New Guinea coral), an aragonite sponge (*Astrosclera willeyana*) and a calcite sponge (*Acanthochaetetes* sp.). These bulk samples were crushed into ~2 cm^3 fragments and subjected to 15% H_2O_2. They were rinsed in Milli-Q (18 Ω) water and dried completely. They were then placed into a clean automated agate mortar and crushed. The powder was then placed into clean containers and sub-samples were pressed in the same manner as the coral standard (see above description).

Teflon binder

Standards have also been constructed using 1 and 12 μm Teflon beads mixed with the coral powder as a binder. This method provides a "dry" binder and when using a shaker it mixes quite well with the coral powder. These standards ablate very similarly to the PVA binder standards even though Teflon ablation is poor. During the construction of the 2 g coral pressed powder standard, 0.2 g of Teflon is mixed with 1.8 g of coral powder. These Teflon standards are not currently being used but after further testing they will probably replace the PVA binder standards.

3.1.2 Solution based ICP-MS

Isotope dilution solution ICP-MS was used to calibrate the coral carbonate standards. For isotope dilution ICP-MS, the ratios $^{10}B/^{11}B$, $^{24}Mg/^{25}Mg$, $^{84}Sr/^{86}Sr$, $^{137}Ba/^{138}Ba$, $^{235}U/^{238}U$ and $^{45}Sc/^{43}Ca$ were measured on the carbonate material samples. About 1mg of material was dissolved and spiked with a 2% HNO_3 mixed spike containing ^{10}B, ^{137}Ba, ^{235}U and ^{45}Sc (Concentrated Mix Spike #1) and diluted with 2% HNO_3 to a weight of 10g and mixed (Table 3.1). A 1g aliquot was then removed and spiked with ^{84}Sr and ^{25}Mg (Dilute Mix Spike #2) and diluted with 2% HNO_3 to a final weight of 10g (Table 3.1). A sample run consisted of 6 replicates each of 60-s duration. The dwell time was 24ms and data was collected using 3 points per peak in peak jumping mode. Mass discrimination was corrected by repeated measurements of a calibrated in-house coral standard. The precision on the isotopic ratios was typically 0.3-0.8%.

Table 3.1 Concentration of Spikes

Concentrated Mix Spike #1	**Concentration (nmol/g)**	**Dilute Mix Spike #2**	**Concentration (nmol/g)**
^{10}B	0.4129	^{84}Sr	1.1676
^{45}Sc	0.0215	^{25}Mg	4.974
^{137}Ba	10.0092		
^{235}U	10.0484		

The measurement sequence consisted of a procedural blank, standard coral, spiked standard coral, sample 1, sample 2, sample 3, procedural blank, standard coral, spiked

coral. Milli-Q, a dilute detergent (Triton) and 2% HNO_3 were run between each measurement to "clean" the system. All samples were blank corrected before the measured isotope ratios were converted to elemental concentrations. The concentration of calcium was determined by using ^{45}Sc as an internal standard, the latter is very useful in this application as its mass lies in the middle of the calcium range and its ionization energy is very similar (Lea and Martin, 1996; LeCornec and Correge, 1997). The concentration of ^{45}Sc in corals is insignificant and the spike did not cross contaminate the samples. The samples were spiked to achieve a 1:1 ratio in the $^{45}Sc/^{43}Ca$ ratio and near optimal spike ratios for the other elements. The concentrations in the samples were calculated using the isotope dilution equation (Equation 1). The spike isotope ratios and the natural ratios are shown in Table 3.2.

Equation 1
$$\frac{\left(^{86}Sr_{Sa}\right)}{\left(^{86}Sr_{Spk}\right)} = \frac{\left(\frac{84}{86}Mix - \frac{84}{86}Spk\right)}{\left(\frac{84}{86}Sa - \frac{84}{86}Mix\right)}$$

where:

$^{86}Sr_{Sa,\ Spk}$ = moles of Sr in sample and spike

$$\frac{84}{86}Mix, Spk, Sa = \frac{84}{86}\text{Sr ratio in mix, spike and sample}$$

Table 3.2 Isotopic ratios for Spike and Normal

	Spike	**Normal**
10/11	18.798	0.24844
25/24	6.05998	0.1266
84/86	15.15968	0.00674
137/138	9.261	0.15662
235/238	99.0	0.00725

3.1.3 Calibration of Standard

The concentrations of the Davies pressed powder standard; Huon, *Astrosclera* and *Acanthochaetetes* powders were determined by ID-ICP-MS. There values are shown in Table 3.3. Boron contamination of the glass spray chamber was difficult to remove. Therefore B/Ca was only measured on the original Davies powder.

Table 3.3 Elemental concentrations from the 4 pressed powder samples/standards measured by ID-ICP-MS and LA-ICP-MS.

Method/standard	B/Ca (mmol/mol)	Mg/Ca (mmol/mol)	Sr/Ca (mmol/mol)	Ba/Ca (μmol/mol)	U/Ca (μmol/mol)
Davies Reef, GBR Coral*					
ID-ICP-MS	0.571 ± 0.006	4.43 ± 0.05	8.863 ± 0.017	3.81 ± 0.04	1.08 ± 0.01
Huon Peninsula, PNG Coral					
ID-ICP-MS[1]	-	4.99 ± 0.11	8.90 ± 0.06	2.89 ±0.03	1.09 ± 0.01
LA-ICP-MS[2]	0.528 ± 0.004	5.18 ± 0.25	8.96 ± 0.12	2.83 ± 0.15	1.06 ± 0.05
Aragonite Sponge, GBR					
ID-ICP-MS[1]	-	1.35 ± 0.09	10.68 ± 0.07	3.71 ± 0.04	2.75 ± 0.02
LA-ICP-MS[3]	0.224 ± 0.007	1.23 ± 0.11	10.63 ± 0.13	3.80 ± 0.14	2.72 ± 0.10
Calcite Sponge, GBR (Hi Mg Calcite)					
ID-ICP-MS[1]	-	-	0.154 ± 0.001	2.25 ± 0.04	0.227 ± 0.01
LA-ICP-MS[4]	0.130 ± 0.004	-	0.158 ± 0.003	2.28 ± 0.09	0.232 ± 0.01

* Average of 10 measurements by ID-ICP-MS.
[1] Average of 5 measurements by ID-ICP-MS, B/Ca not measured.
[2] Average of 12 individual measurements made over a 1-month period using coral pressed powder standard.
[3] Average of 50 individual measurements made over a 3-month period using the coral pressed powder standard. (All data in Figure 3.8 and Appendix 1)
[4] Average of 5 individual measurements made over a 1-month period using the coral pressed powder standard.

3.2 Accuracy

3.2.1 TIMS and LA-ICP-MS

Two methods were utilized to test the accuracy of measuring corals by LA-ICP-MS. The first method only tests the Sr/Ca accuracy. Coral samples that have already been analyzed by TIMS for Sr/Ca were resampled for laser analysis. The samples collected for TIMS analysis were removed by a computerized mill with a 2 mm diameter drill bit. Samples are normally collected in 0.25 or 0.5 mm increments (Gagan *et al*., 1994;

McCulloch *et al*., 1994; Alibert and McCulloch, 1997). When trying to compare the two methods, a number of factors must be considered, e.g. sample volume and sample resolution (sample distance differences).

Sample volume

There is a significant difference in the amount of material analyzed by the laser versus 'conventional' bulk sampling in TIMS and $\delta^{18}O$. TIMS samples are approximately 0.25 x 2 x 2.5 mm rectangles which is approximately 1.25 mm^3 or around 1500 μg of coral per sample, depending on the porosity of the sample. The laser-sampling rectangle is 50 x 500 μm x ~ 0.1 μm per pulse depth, corresponding to ~2500 μm^3 per pulse. In one second this is equivalent to ~ 20 ng of sample (assuming ~ 50% coral porosity). Since the laser data is averaged to an approximate resolution of 0.25 mm (8 one second time slices) the total material sampled per data point is ~ 160 ng (again assuming ~ 50% coral porosity). This is approximately 7500 times less material for LA-ICP-MS than milled for TIMS. The actual TIMS measurement consists of a ~ 100 μg sub-sample (McCulloch *et al*., 1994; Alibert and McCulloch, 1997).

Sample resolution

Another consideration is the sampling resolution; for comparisons the laser data needs to be averaged to the same resolution as the TIMS data. The averaged laser data however has only an approximately similar x-distance so direct comparisons cannot be made. This is adequate for overall comparisons but if one wants to directly compare sections of corals, both datasets need to have the same distance axis. This is achieved by re-sampling the laser data at the same sample intervals as the TIMS data. This action can be performed by many time-series analysis packages. In this project, the software package Analyseries (Paillard *et al*., 1996) was utilized, which uses linear interpolation to resample the laser data. When both datasets have a common distance axis, direct comparisons and correlations between the two methods can be achieved. This was done before comparisons between TIMS and laser were attempted.

Coral Scans

Four different coral samples were analyzed both by TIMS and LA-ICP-MS; Davies 2 and Wheeler Reef (Alibert and McCulloch, 1997), Myrmidon (J. Marshall, pers. comm.) and a coral from Japan (see Chapter 5). The comparison between the two different analytical techniques is shown in Figures 3.2 - 3.5. There is quite good agreement between the two methods. Annual averages and intra-annual variations in the TIMS data are reproduced by the LA-ICP-MS measurements. However the higher amplitude variations in the LA-ICP-MS data reinforces the belief that corals are heterogeneous at small scales (Allison and Tudhope, 1992; Hart and Cohen, 1996; Sinclair, 1999). Also shown on the graphs is the % difference between the laser values and the TIMS values. The % difference is defined in Equation 2.

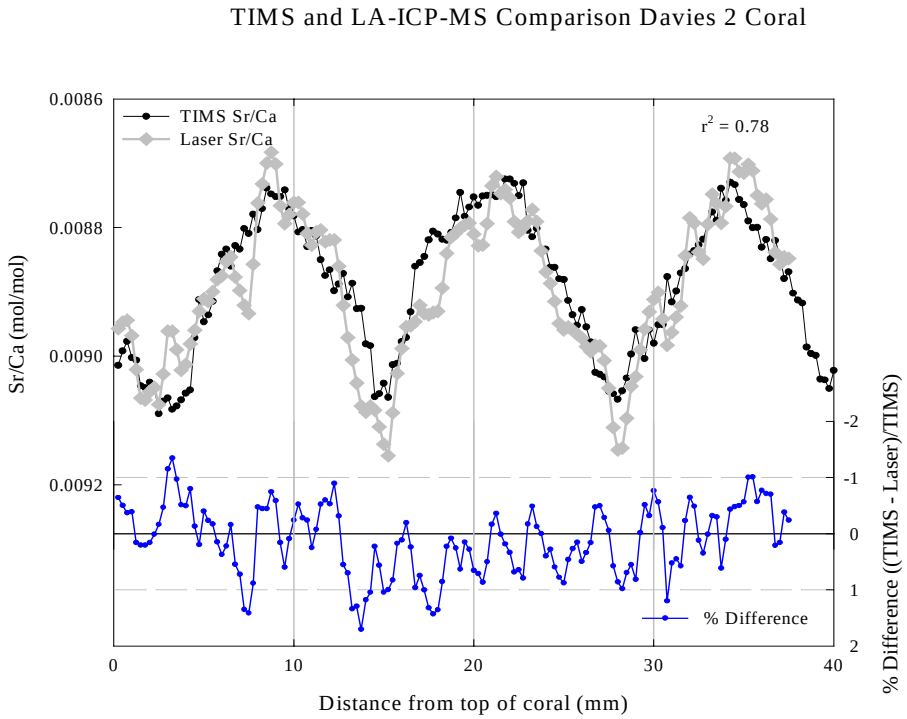

Figure 3.2 TIMS Sr/Ca and LA-ICP-MS Sr/Ca vs. distance from top of the Davies 2 coral (TIMS data from Alibert and McCulloch, 1997). The bottom panel shows the % Difference between the two methods (see Equation 2).

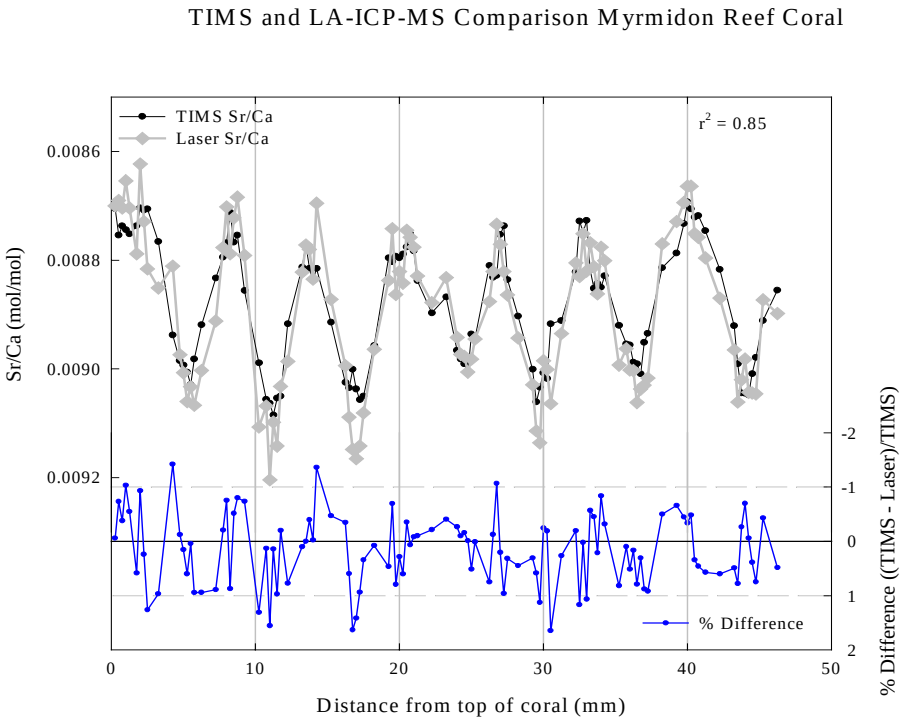

Figure 3.3 TIMS Sr/Ca and LA-ICP-MS Sr/Ca vs. distance from top of the Myrmidon Reef coral (TIMS data from J. Marshall). The bottom panel shows the % Difference between the two methods (see Equation 2).

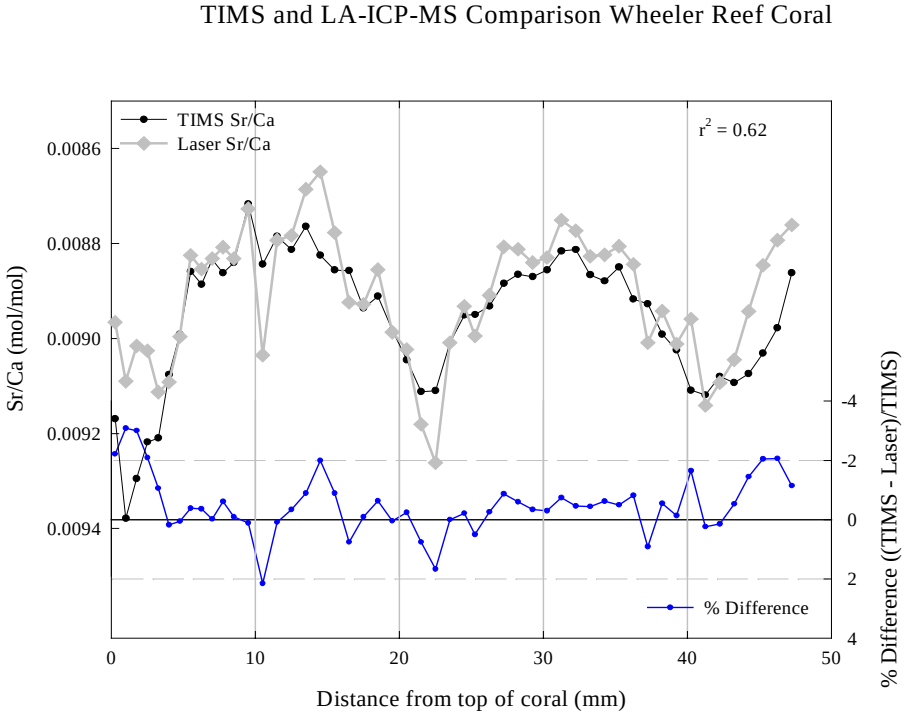

Figure 3.4 TIMS Sr/Ca and LA-ICP-MS Sr/Ca vs. distance from top of the Wheeler Reef coral (TIMS data from Alibert and McCulloch, 1997). The bottom panel shows the % Difference between the two methods (see Equation 2).

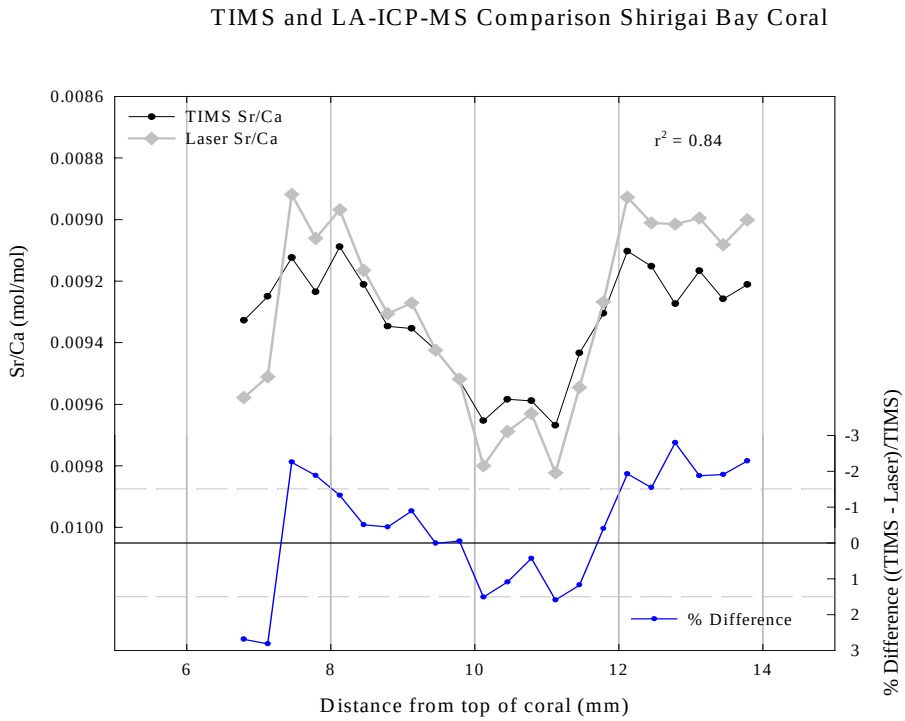

Figure 3.5 TIMS Sr/Ca and LA-ICP-MS Sr/Ca vs. distance from top of the Shirigai Bay coral (see Chapter 7). The bottom panel shows the % Difference between the two methods (see Equation 2).

Equation 2 $$\%\,\text{Difference} = \frac{\text{Laser Value - TIMS Value}}{\text{TIMS Value}} * 100$$

Most of the % difference values are within the quoted analytical uncertainty of 1.6 % (see section 3.3) but there are a few points in the Wheeler Reef coral and Japanese coral that are outside the analytical error (Figures 3.5, 3.6). In the case of the Japanese coral, the amplitude of the TIMS values are smaller than the laser in both winter (higher Sr/Ca) and summer (lower Sr/Ca) (Figure 3.5). I believe this is due to time averaging. The growth direction was not perpendicular to the coral slice and was dipping at a significant angle. Thus during milling, the sample analyzed does not equate to the same time period as the laser sample. Because the mill collects 2 mm thick samples the samples are probably averaging over 1-2 months, resulting in a smoothed signal relative to the LA-ICP-MS data (most coral cores are not affected to this extent). The piece analyzed from the Wheeler coral came from an adjacent core slice. This different slice

and different growth axis could account for the differences observed between the two methods (Figure 3.4).

Another way to examine the two methods is by scatter plots and linear regressions (Figure 3.6). The correlation between the two methods is good but the slopes of the regression differ from a perfect correlation of 1 (Figure 3.6). The Wheeler Reef coral and the Japanese coral slopes are the furthest from a 1:1 relation and this difference may be caused by the factors discussed previously.

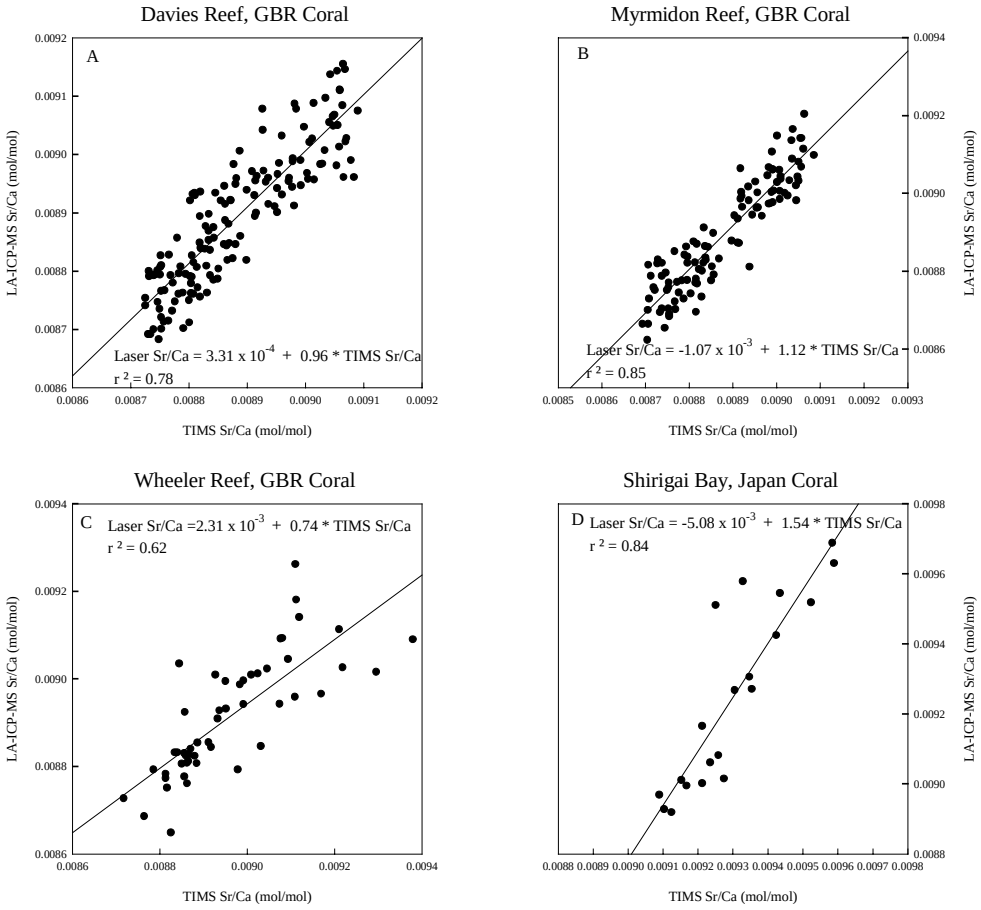

Figure 3.6 A) Linear regression between TIMS Sr/Ca and LA-ICP-MS Sr/Ca Davies 2 coral. B) Linear regression between TIMS Sr/Ca and LA-ICP-MS Sr/Ca Myrmidon Reef coral. C) Linear regression between TIMS Sr/Ca and LA-ICP-MS Sr/Ca Wheeler Reef coral. D) Linear regression between TIMS Sr/Ca and LA-ICP-MS Sr/Ca Shirigai Bay coral.

3.2.2 ID-ICP-MS and LA-ICP-MS

The second method used to determine accuracy was the analysis of three other pressed powder samples. As previously discussed, a coral from Huon, PNG, an aragonite

coralline sponge (*Astrosclera*) and a calcite coralline sponge (*Acanthochaetetes*) were finely crushed and pressed into pellets. The concentration of Mg/Ca, Sr/Ca, Ba/Ca and U/Ca of the bulk powders were measured by ID-ICP-MS and the values are reported in Table 3.3. The pressed powder samples have been analyzed by laser (2-3 mm sections). The Huon sample was measured 12 times over a 1-month period, the *Astrosclera* sample 50 times over a 3-month period and the *Acanthochaetetes* sample 5 times in one day. The mean values for both the laser and solution estimates are within error (Table 3.3). Figure 3.7 shows the values, along with the regression lines and equations. The values have regression slopes very close to 1 indicating good agreement between the two methods. Using a pressed powder standard constructed from a calibrated coral provides accurate fully quantitative LA-ICP-MS for $CaCO_3$ (corals and sponges) with differing concentrations. This is a significant improvement over the original calcium silicate standard used by Sinclair (1999).

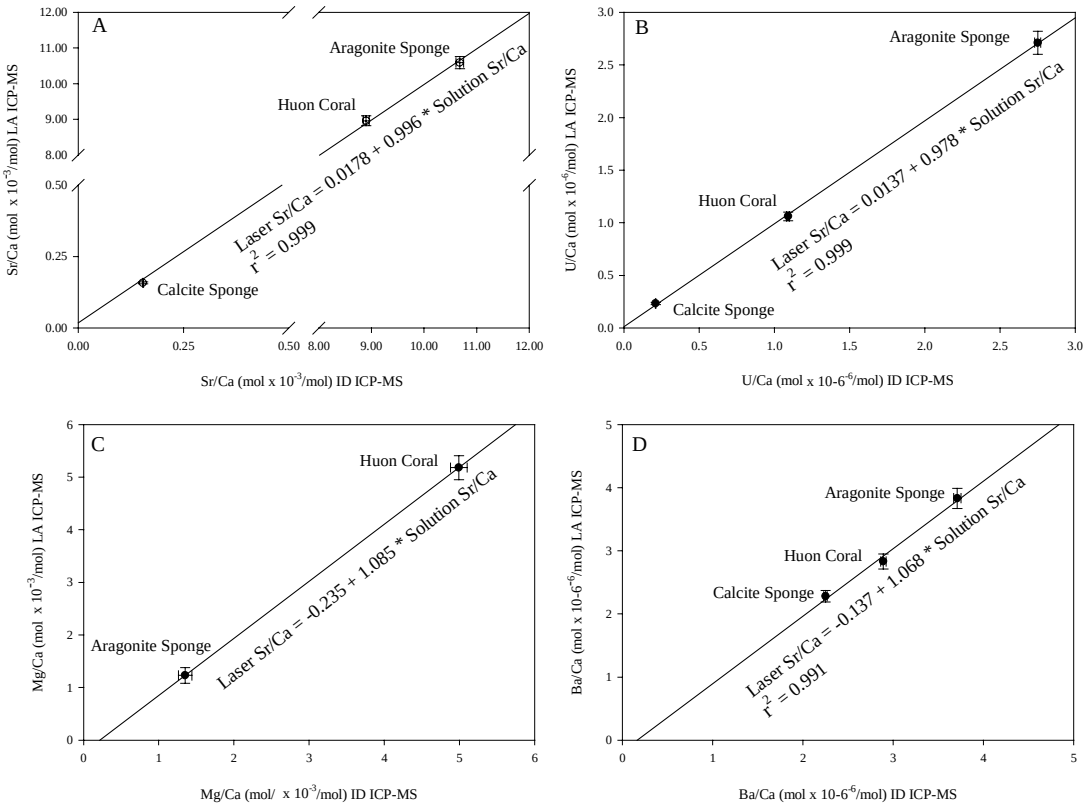

Figure 3.7 Comparisons between the ID-ICP-MS and LA-ICP-MS for the three pressed powder samples. A) Sr/Ca B) U/Ca C) Mg/Ca (Mg not measure in Mg calcite sponge) D. Ba/Ca. Also shown are linear regression and correlations.

3.3 Analytical Uncertainty

The main component that contributes to the analytical uncertainty of this method is the heterogeneity of the standard. Minor components are a combination of counting statistics and calibration of the standard. Estimates for the errors associated with counting statistics, standard calibration and standard heterogeneity are given in Table 3.4. These errors can be added in quadrature to provide an estimate of the overall uncertainty. The overall uncertainty is defined as:

Equation 3 $$\sigma_{uncert.} = \sqrt{\sigma^2_{cs} + \sigma^2_{calib} + \sigma^2_{std}}$$

where σ_{uncert} = Overall uncertainity

σ^2_{cs} = Counting Statistics % St. Dev.

σ^2_{calib} = % St. Dev. of 10 ID - ICP - MS measurements on the standard

σ^2_{std} = % St. Dev. of 60 - 90s scan on standard

The counting statistics errors are estimated by count rate and dwell time. The count per second data have been multiplied by 120 ms, a 40 ms dwell time with 3 points per peak to obtain the total counts. The standard deviation of the counting statistics has been given as the √n, where n is the counts. The percentage standard deviation for each element and calcium were combined to produce the counting uncertainty in Table 3.4. When measuring the minor elements this component will increase because of the lower count rates (see next section on minor isotopes).

The second minor component is the reproducibility and precision of the solution ICP-MS and TIMS measurements in the calibration of the standards. This component was estimated as the percentage standard deviation of 10 solution ICP-MS analyses of the powder; Sr/Ca was measured by TIMS (Table 3.4). This gives a constant bias but should still be considered in the overall errors. The main component is the heterogeneity of the standard. This is calculated as the percentage standard deviation of a 60 – 90s scan. The overall analytical uncertainty of this LA-ICP-MS technique is 3.8% B/Ca, 4.2 % Mg/Ca, 1.6% Sr/Ca, 4.3 % Ba/Ca and 3.9 % U/Ca (Table 3.4). This is between 1-4 % higher than solution based ICP-MS analyses for these ratios in corals

(LeCornec and Correge, 1997; Schrag, 1999). Table 3.4 also lists the equivalent temperature uncertainties using the "element"/Ca – SST calibrations from Chapter 6.

Table 3.4 Estimates of Analytical Uncertainties and Reproducibility for LA-ICP-MS of corals.

Error	B/Ca	Mg/Ca	Sr/Ca	Ba/Ca	U/Ca
Counting Uncertainty	1.8%	0.5%	0.6%	1.2%	1.6%
Calibration of standard	1.1%	1.7%	0.02%*	1.0%	0.9%
Heterogeneity of standard[1]	3.2%	3.8%	1.5%	4.0%	3.4%
Overall Uncertainty	**3.8%**	**4.2%**	**1.6%**	**4.3%**	**3.9%**
Temperature Equivalent[2]	0.9°C	1.1°C	2.2°C	-	0.8°C
Daily reproducibility[3]	1.7%	2.1%	0.5%	2.5%	1.5%
Pressed Sample Monthly reproducibility[4]	2.8%	3.4%	0.8%	3.2%	2.9%
Coral Monthly reproducibility[5]	2.5%	4.9%	1.1%	3.3%	3.3%

*Calibrated using TIMS.
[1] 1σ standard deviation on a 60 sec. scan.
[2] Calculated from the temperature equations in this paper.
[3] Based on 1σ standard deviation of repeated daily measurements of the *Astrosclera* coralline sponge pressed sample (See Appendix 1 for data).
[4] Based on 1σ standard deviation of 50 replicates (over 3 months) of the *Astrosclera* coralline sponge pressed sample (See Appendix 1 for data).
[5] Based on 1σ standard deviation of 4 replicates over a 86mm length section of Shirigai Bay coral during a 5 month period (Figure 3.9)

3.4 Reproducibility

3.4.1 Pressed Powder Reproducibility

The *Astrosclera* pressed powder sample was analyzed 50 times to test short and long-term reproducibility. The samples were analyzed in the same manner as the corals; each *Astrosclera* sample was bracketed by background and standard measurements. Each analysis was 60-90 s in duration and the data is presented in Figure 3.8.

The analyses have been grouped into days, analytical conditions (laser spot size, repetition rate, laser energy etc.) were held approximately constant. Different sections of the 7 mm diameter disc were analyzed on the different days. To determine the daily reproducibility, the analyses from each day were averaged into one point and the mean

and percentage standard deviation was calculated for all eight days. This daily uncertainty is 1.7 % for B/Ca, 2.1 % for Mg/Ca, 0.5 % for Sr/Ca, 2.5 % for Ba/Ca and 1.5 % for U/Ca (Table 3.4). The longer term reproducibility, defined as the percentage standard deviation for the entire dataset is 2.8 % for B/Ca, 3.4% for Mg/Ca, 0.8% for Sr/Ca, 3.2 % for Ba/Ca and 2.9 % for U/Ca (Table 3.4).

3.4.2 Coral Reproducibility

An estimate of coral reproducibility has been obtained by 4 replicate analyses of a 96 mm section of the coral from Shirigai Bay, Japan (Chapter 5). The sampling (analytical) parameters were the same for each replicate. One component that could not be repeated was the aligning of the laser sampling tracks, as previous tracks are invisible on corals. However these repeat tracks were probably within 2 mm of each other. A subsection of the data from these four replicates is shown in Figure 3.9. The long-term reproducibility is calculated by averaging the data of each elemental ratio into a single point. The percentage standard deviation of the four replicates (long-term reproducibility) is 2.5 % for B/Ca, 4.9 % for Mg/Ca, 1.1 % for Sr/Ca, 3.3 % for Ba/Ca and 3.3 % for U/Ca (Table 3.4). These values are similar to the long-term values for the pressed powder samples (Table 3.4).

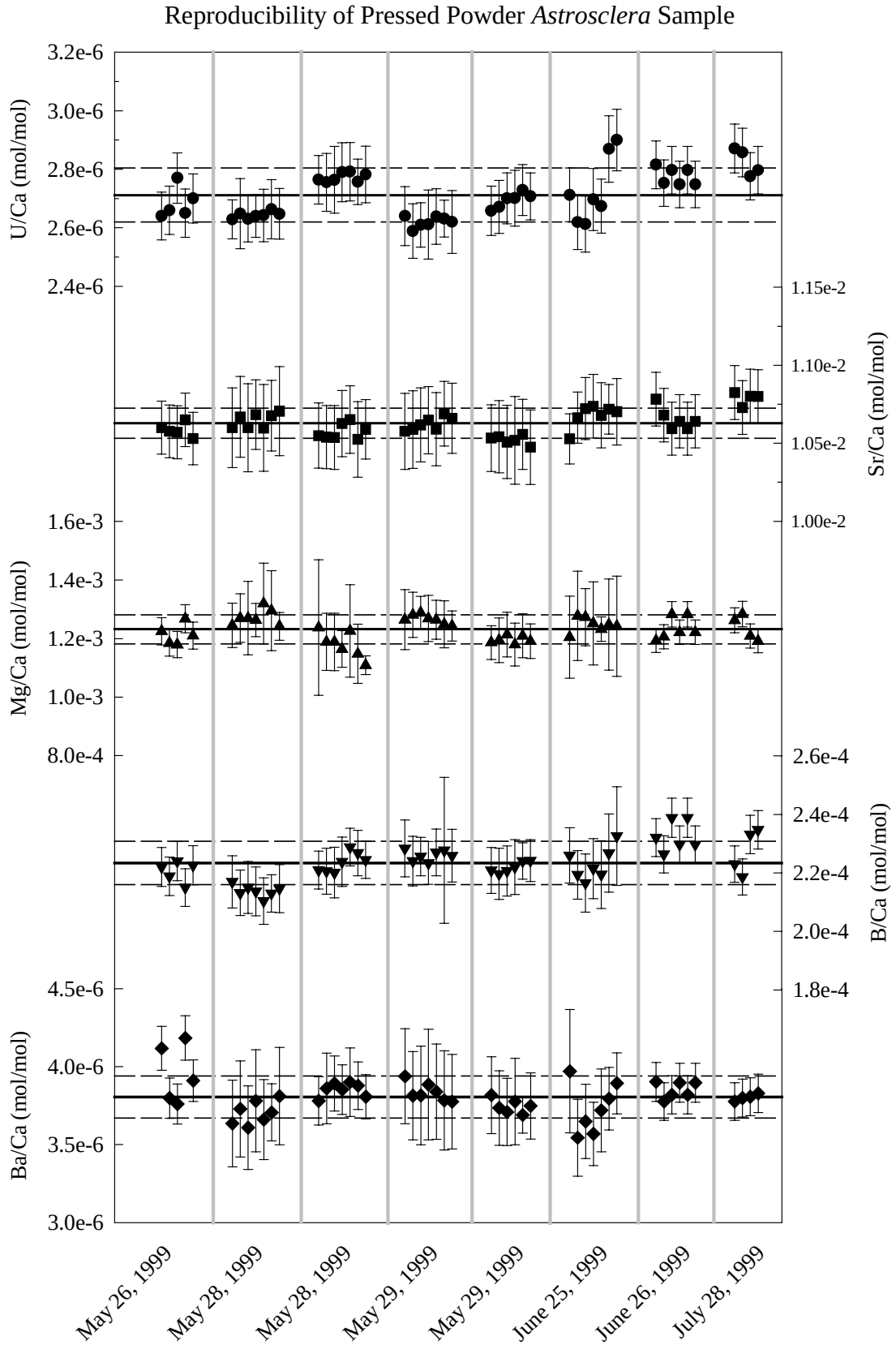

Figure 3.8 Multiple daily measurements of the *Astrosclera* pressed powder sample. Error bars are 1σ standard deviation of the 60-90 s analyses. Solid line is long-term mean and dashed lines show 99% confidence interval (Table 3.3). Data values in Appendix 1.

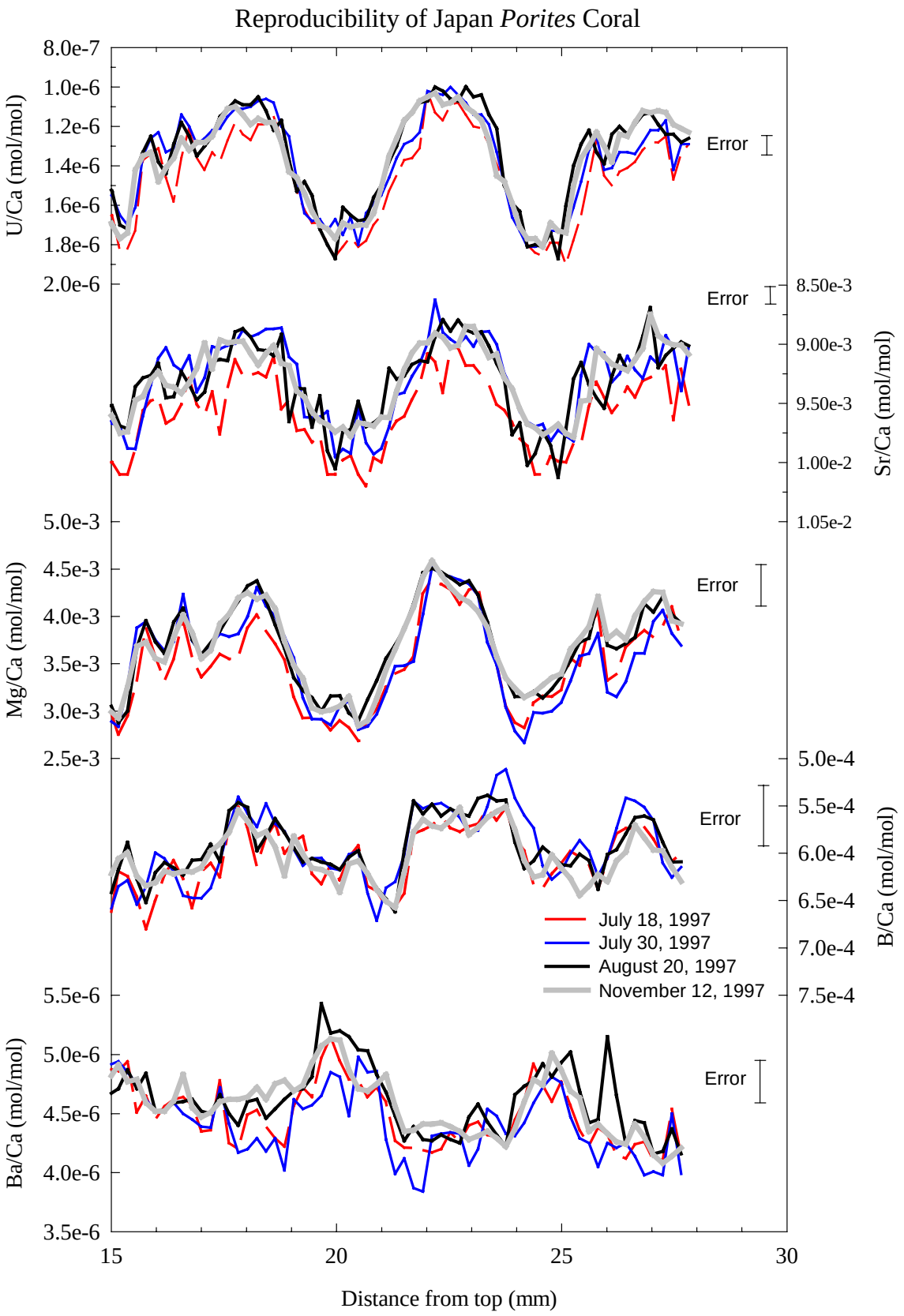

Figure 3.9 Long term reproducibility for the 5 elemental ratios (U/Ca, Sr/Ca, Mg/Ca, B/Ca and Ba/Ca) of the LA-ICP-MS method by measuring the Shirigai Bay coral 4 times over a 5-month period.

3.5 Minor Element Standards

Low-level sub-ppm trace element carbonate standards are not readily available. The United States National Institute of Standards (NIST) produces commercially available standards that are used for low-level trace element analysis. A suite of synthetic silicate glasses are available with major element concentrations of 72% SiO_2, 12 % CaO, 14 % Na_2O and 2% Al_2O_3 and minor element concentrations of 500, 50 and 1 $\mu g\ g^{-1}$ for 61 elements. They are known as NIST 610, 612 and 614 respectively. These glasses were made carefully and manufactures claim < 5 % heterogeneity. Many current studies are using the NIST suite of glasses to accurately measure elemental abundances from a variety of different matrices (Chen *et al*., 1997; Gunther *et al*., 1997; Horn *et al*., 1997; Nesbitt *et al*., 1997; Perkins *et al*., 1997; Sylvester and Ghaderi, 1997; Butler and Nesbitt, 1999).

These glasses have some advantages over the pressed powder standards discussed previously. They are very homogenous and since they are available commercially they have been well calibrated. They are also easy to clean and polish and laser tracks are visible so re-analyzing the same track is easy. However there are also some serious disadvantages in using them as standards for coral analyses (especially for the "major" elements). These silicate standards are a poor chemical matrix match for carbonates. Sinclair (1999) reported poor reproducibility when measuring "major" elements using the NIST 612 standard. Another potential problem is the compositional concentrations in these glasses are very different than in corals. The NIST 612 has low concentrations of Mg, Sr and Ca while corals have high concentrations of those elements.

3.5.1 Coral "Minor" Elements using NIST 614

In order to measure "minor" elements in corals we examined the NIST 614 as a possible standard. The LA-ICP-MS method was adjusted slightly to include a measurement of the NIST 614 prior to the coral pressed powder standard in the beginning of the analysis and after the coral pressed powder standard at the end of the analysis (See Table 2.3 and Section 2.4.1). The NIST 614 contains 61 elements with an approximate concentration of 1 $\mu g\ g^{-1}$ and has 11.85% CaO (Horn *et al*., 1997). Accepted and certified values for the elements of interest are given in Table 3.5 (Horn *et al*., 1997), six measurements of

element concentrations for the NIST 614 using the NIST 612 as a standard are also shown in Table 3.5. A published value for Zinc was not available so we currently used 2.26 μg g^{-1}, the cross calibration value from the NIST 614 (Table 3.5). We used the other reported and certified values in our calibration calculations (Table 3.5). The isotopes that we measure regularly with this method are ^{55}Mn, ^{66}Zn, ^{89}Y, ^{139}La, ^{140}Ce and ^{208}Pb.

Table 3.5 Cross calibration of NIST SRM 614 by NIST SRM 612.

Concentration ($\mu g\ g^{-1}$)	Mn	Zn	Sr	Mo	Cd	Ba	La	Ce	Nd	Sm	Eu	Gd	Yb	Pb	Th	U
Preferred value 614	1.37		45.8	0.81		3.15	0.71	0.78	0.74	0.78	0.76	0.735	0.785	2.32	0.748	0.823
Preferred value 612	36.9	37.92	78.4	39.6	28.32	37.74	35.77	38.35	35.24	36.72	34.44	36.95	39.95	38.57	37.79	37.38
Mean LA-ICP-MS	1.35	2.26	45.3	0.83	0.52	3.07	0.70	0.77	0.72	0.76	0.78	0.75	0.75	2.24	0.75	0.83
% 1 s S.D.	1.44	6.29	0.58	1.02	3.41	0.95	0.75	1.10	2.24	1.42	1.83	2.15	1.39	5.22	0.93	1.32
29-Jul-99	1.327	2.000	45.207	0.831	0.527	3.101	0.704	0.781	0.692	0.765	0.803	0.728	0.761	2.043	0.751	0.832
29-Jul-99	1.343	2.348	45.127	0.828	0.500	3.092	0.695	0.769	0.740	0.747	0.764	0.748	0.758	2.166	0.735	0.835
29-Jul-99	1.352	2.249	44.921	0.817	0.529	3.022	0.698	0.761	0.717	0.749	0.767	0.748	0.735	2.324	0.741	0.815
29-Jul-99	1.382	2.226	45.493	0.817	0.501	3.064	0.706	0.780	0.730	0.774	0.778	0.760	0.750	2.268	0.750	0.841
29-Jul-99	1.341	2.321	45.651	0.838	0.542	3.081	0.704	0.776	0.719	0.763	0.788	0.766	0.764	2.298	0.752	0.837
29-Jul-99	1.365	2.404	45.337	0.823	0.506	3.051	0.708	0.764	0.721	0.768	0.778	0.773	0.749	2.354	0.751	0.817

Red values from Horn et al. (1997)
Blue values certifeid by US NBS

Detection Limits

Due to the low concentration of the "minor" elements in corals, the LA-ICP-MS detection limits play an important role. The detection limit for an element is defined as the concentration equivalent to three times the standard deviation of the background counts. Detection limits can be adjusted by changing laser spot size, energy and ablation rate. We report detection limits based on measurements of the NIST 614 using the large coral laser mask (100 x 500 μm). The detection limits can vary from day to day and analysis to analysis. Table 3.6 shows the calculated detection limits for 12 analyses measured over 3 days of analytical time. The isotope monitored is shown in parentheses. The detection limits varied by 10 - 20 % over the three days most likely due to ICP-MS stability. The counts per second "minor" element data for a scan on the Misima Island TO5BO3A coral is shown in Figure 3.10. This graph also shows the detection limit values (based on counts and not concentration) to compare with the coral signal counts.

Accuracy and Reproducibility

The accuracy of this technique (using the non-matrix matched NIST 614 standard) was difficult to assess because of a lack of independent $CaCO_3$ standards. The NIST 614 standard was considered for use because the concentration of the elements (~μg g^{-1}) is the closest match to the concentrations we wanted to measure in the corals (ng g^{-1} to μg g^{-1}) in the Misima corals (See Chapter 7). During the routine analysis of a set of corals from Misima Island, both the NIST 614 and Davies pressed powder standards were analyzed. A total of 24 comparisons over 3 days were made. Only Ba and U are found in corals at the low μg g^{-1} level similar to the levels in the NIST 614. The U concentration in the Davies pressed powder standard is 2.49 ± 0.07 μg g^{-1} and Ba is 5.01 ± 0.05 μg g^{-1}, these concentrations were determined by ID-ICP-MS and discussed in Section 3.1.3.

Table 3.6. Detection limits for "minor" elements.

Concentration (mg g^{-1})	(11) B	(46) Ca	(55) Mn	(66) Zn	(89) Y	(137) Ba	(139) La	(140) Ce	(208) Pb	(238) U
Feb. 3, 2000	0.022	0.012	0.020	0.033	0.0017	0.0055	0.0007	0.0006	0.003	0.0004
Feb. 3, 2000	0.035	0.025	0.025	0.047	0.0022	0.0047	0.0010	0.0008	0.003	0.0003
Feb. 3, 2000	0.042	0.031	0.023	0.042	0.0021	0.0041	0.0006	0.0006	0.006	0.0003
Feb. 4, 2000	0.025	0.011	0.017	0.026	0.0012	0.0040	0.0006	0.0004	0.003	0.0002
Feb. 4, 2000	0.027	0.015	0.016	0.024	0.0011	0.0038	0.0006	0.0005	0.002	0.0003
Feb. 4, 2000	0.029	0.018	0.019	0.023	0.0014	0.0039	0.0006	0.0005	0.002	0.0003
Feb. 4, 2000	0.040	0.028	0.026	0.037	0.0016	0.0044	0.0007	0.0006	0.002	0.0002
Feb. 9, 2000	0.043	0.027	0.023	0.044	0.0021	0.0057	0.0008	0.0007	0.003	0.0003
Feb. 9, 2000	0.033	0.020	0.016	0.028	0.0019	0.0085	0.0007	0.0006	0.003	0.0002
Feb. 9, 2000	0.064	0.021	0.024	0.020	0.0024	0.0140	0.0009	0.0007	0.003	0.0003
Feb. 9, 2000	0.063	0.020	0.022	0.041	0.0020	0.0098	0.0010	0.0006	0.003	0.0002
Feb. 9, 2000	0.051	0.021	0.019	0.048	0.0019	0.0086	0.0007	0.0007	0.005	0.0002
Average (mg g^{-1})	0.039	0.021	0.021	0.034	0.002	0.006	0.001	0.001	0.003	0.0003

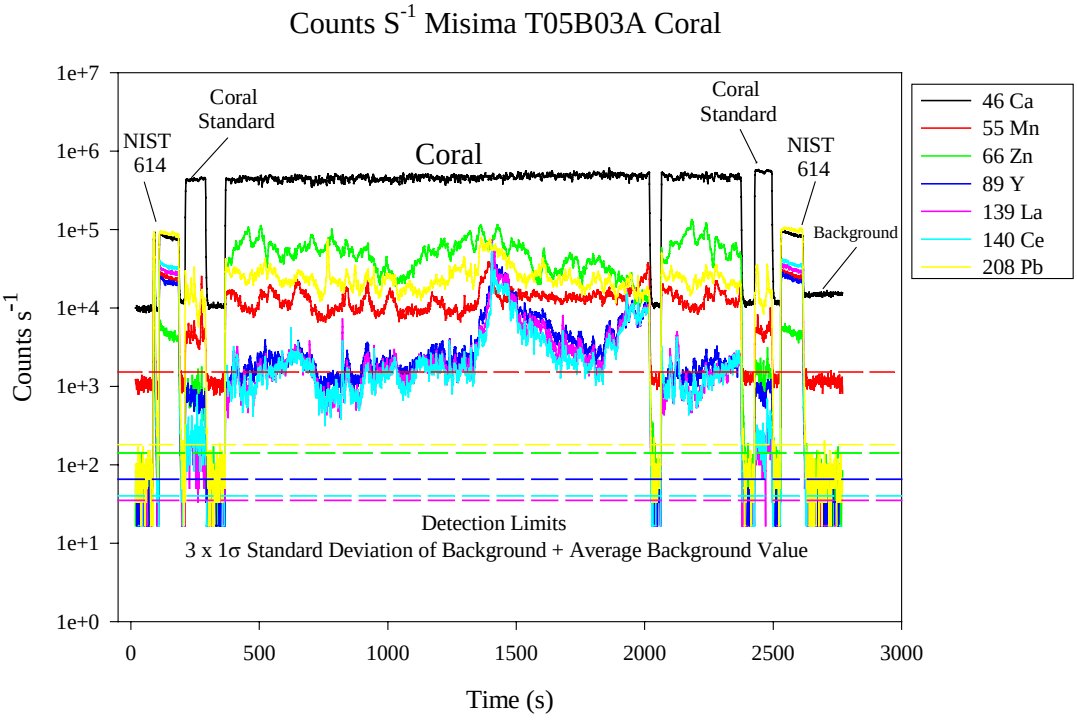

Figure 3.10 Misima Island TO5BO3A Coral, Raw counts s^{-1} vs. time slice, showing background, NIST 614 and coral pressed powder standard, coral, repeat of first section of coral and detection limit values based on count rate.

The concentration of U in the Davies pressed powder using the NIST 614 as the calibration standard is 2.57 ± 0.16 μg g^{-1} and is within error of the solution measurement although the values have a large spread (**Error! Not a valid bookmark self-reference.**). The estimate of Ba by the NIST 614 standard is 5.49 ± 0.22 μg g^{-1} and is approximately 10 % higher than the solution value. This is outside of analytical error and may be indicative of the accuracy when using non-matrix matched standards, or the value of 3.15 μg g^{-1} that was used for the Ba concentration in the NIST 614 may be too high. Our own cross calibration between NIST 612 and NIST 614 indicate the Ba concentration in the NIST 614 should be closer to 3.07 μg g^{-1} which would bring our LA-ICP-MS estimate closer to the solution value, but it would still be slightly outside of analytical error.

Without the use of other calibrated carbonate standards, we were unable to assess the accuracy of Mn, Zn, Y, La, Ce or Pb measurements. It was decided that a coral with the highest concentrations of the elements (MIST05B03A) would be analyzed as a secondary standard. This would make it possible to normalize the data if the NIST 614 standard caused significant calibration offsets during different analytical sessions.

Table 3.5 ID-ICP-MS and LA-ICP-MS measurements of Davies pressed powder standard. LA-ICP-MS is calibrated using NIST 614 standard.

	Ba (μg g^{-1})	**U (μg g^{-1})**
ID-ICP-MS[1]	**5.01 ± 0.05**	**2.49 ± 0.07**
LA-ICP-MS[2]	**5.49 ± 0.22**	**2.57 ± 0.16**
Feb. 3, 2000	5.81	2.72
″	5.43	2.50
″	5.72	2.65
″	5.21	2.25
″	5.46	2.59
″	5.30	2.31
Feb. 4, 2000	5.78	2.76
″	5.57	2.55
″	5.43	2.80
″	5.38	2.45
″	5.57	2.82
″	5.49	2.45
″	5.72	2.72
″	5.64	2.67
″	5.68	2.67
″	5.21	2.28
Feb. 9, 2000	5.81	2.72
″	5.54	2.43
″	5.01	2.59
″	5.18	2.35
″	5.55	2.62
″	5.55	2.42
″	5.50	2.71
″	5.26	2.55

[1] 10 repeat measurements
[2] Average and Standard Deviation of the 24 measurements shown.

The Misima suite of corals (8 in total, 2 pieces for each coral) was analyzed on 3 days, Feb. 3-4, 9, 2000. The coral MIST05B03A had also been previously analyzed in August 1999. Figure 3.11 A-F shows the comparison between the four replicates for the elements Zn, Mn, Pb, Y, La and Ce. All four analyses agree well so no additional normalization was performed on the other corals analyzed on those days (see Chapter 7, Misima). Under close inspection, both the low background and peak levels are consistent. Figure 3.11 D-F also show a close-up of the scans between 10-20 mm. Even at these low concentrations ~ 0.03 – 0.05 μg g^{-1} (only 10 times detection limit) the four analyses of Y, La and Ce replicate quite well. The Zn data is ~ 100x greater than detection level where Mn, Pb, Y, La and Ce are only ~ 10x greater than detection level. The reproducibility of Mn from the 4 replicates is 3.5%, Zn is 4.5%, Y is 3.5%, La is 5.5%, Ce is 3.6% and Pb is 4.1%. This is based on a 1σ standard deviation of the four replicates. This data suggest that the NIST 614 standard provided reproducible results

even if we are unable to independently determine the corals "absolute" accuracy. At this point the NIST 614 standardization technique provides semi-quantitative concentrations for Mn, Zn, Y, La, Ce and Pb in corals as the matrix effect cannot be fully assessed for each element. By analogy with Ba it is possible that the non-matrix matched NIST 614 introduces systematic errors of ~ ± 10%. In the case of the Misima Island corals (Chapter 7) the relative change between sites is robust (the most important factor) due to the analysis of the "secondary coral" standard.

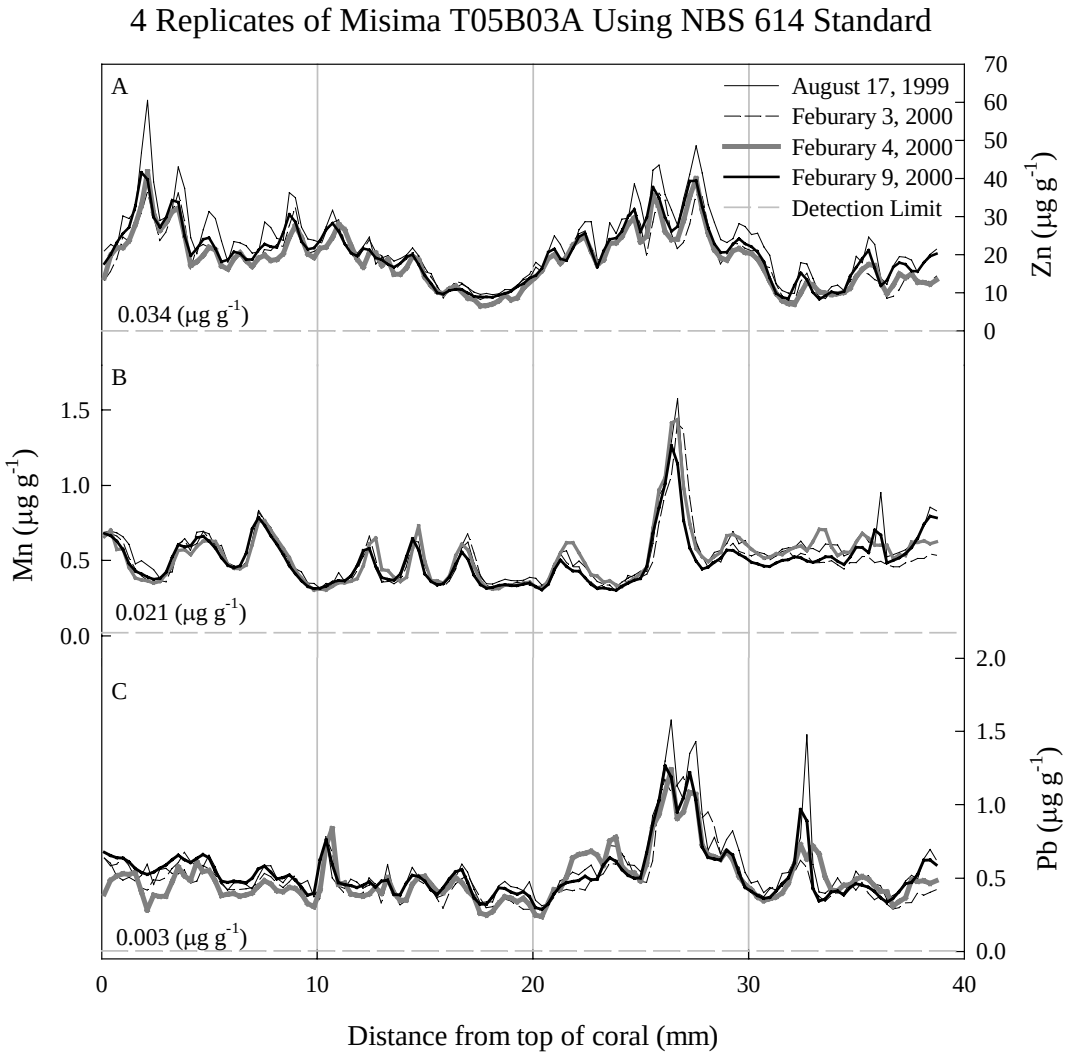

Figure 3.11 Four replicates of the MIST05B03A coral using the NIST 614 as the standard. A) Zn µg g^{-1} vs. Distance from the top of the coral. B) Mn µg g^{-1} vs. Distance from the top of the coral. C) Pb µg g^{-1} vs. Distance from the top of the coral. Also shown on graph is the detection limits for these elements (gray dashed lines and values).

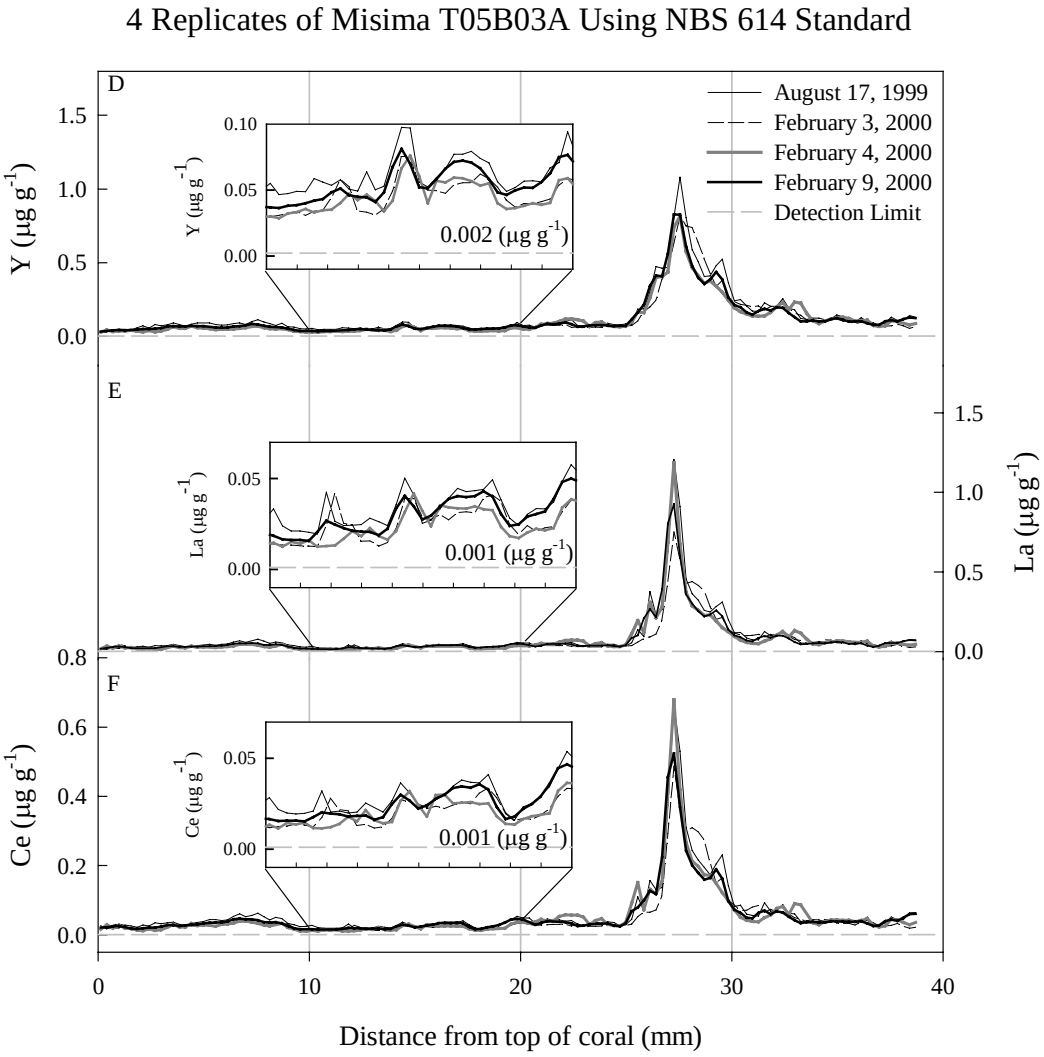

Figure 3.11 Continued D) Y µg g^{-1} vs. Distance from the top of the coral. Inset is close-up of section 10-20 mm showing the reproducibility of the non-peak values. E) La µg g^{-1} vs. Distance from the top of the coral. Inset is close-up of section 10-20 mm showing the reproducibility of the non-peak values. F) Ce µg g^{-1} vs. Distance from the top of the coral. Inset is close-up of section 10-20 mm showing the reproducibility of the non-peak values. The detection limits are shown in the gray dashed line.

3.5.2 Alternate Cleaning

An alternate cleaning strategy was employed on the sample MIST05B03A to test whether the minor elements were affected by contamination. Cleaning methods for minor elements in corals have been developed by Shen and Boyle (1988) using dilute acid leaching coupled with oxidative and reductive steps to remove organic material and Fe and Mn oxyhydroxides. However their techniques were developed for crushed coral fragments and not solid coral slabs. The modified cleaning protocol is as follows:

1) The samples cleaned in 18 Ω water while subject to ultrasonic agitation for 10 minutes (repeated 3x).
2) The samples are cleaned in 30% H_2O_2 while subject to ultrasonic agitation for 10 minutes, then rinsed with 18 Ω water (repeated 3x).
3) The samples are cleaned in 0.06 N HNO_3 for 2 minutes while subject to ultrasonic agitation. Then the samples are rinsed with 18 Ω water and subject to ultrasonic agitation (repeated 3x)
4) The samples are cleaned in 0.2N NH_4OH while heated at 50 ºC. The samples are subject to 5 min. of ultrasonic agitation then heated for 2 min (repeated 4 x).
5) The samples are rinsed 5 times with 18 Ω water and dried at 40 ºC.
6) The analyses were preformed on the new Agilent 7500s ICP-MS.

Approximately 4% of material was lost during this cleaning. The same six elements used in the reproducibility test of the NIST 614 were analyzed. Figure 3.12 shows the elements before and after cleaning steps. There is no systematic variation observed by these cleaning methods or the time of the analyses (July vs. Feb. 2000). The variations shown between the cleaning steps was similar to the variation observed by using the non-matrix matched NIST 614. This cleaning test is not absolutely definitive as the cleaning protocol can only clean the outer surfaces of the coral slab. It appears that our laser cleaning protocols, (ultrasonic and pre-ablations) do as good as a job of cleaning the outer surfaces as the chemical treatments when samples are analyzed by LA-ICP-MS.

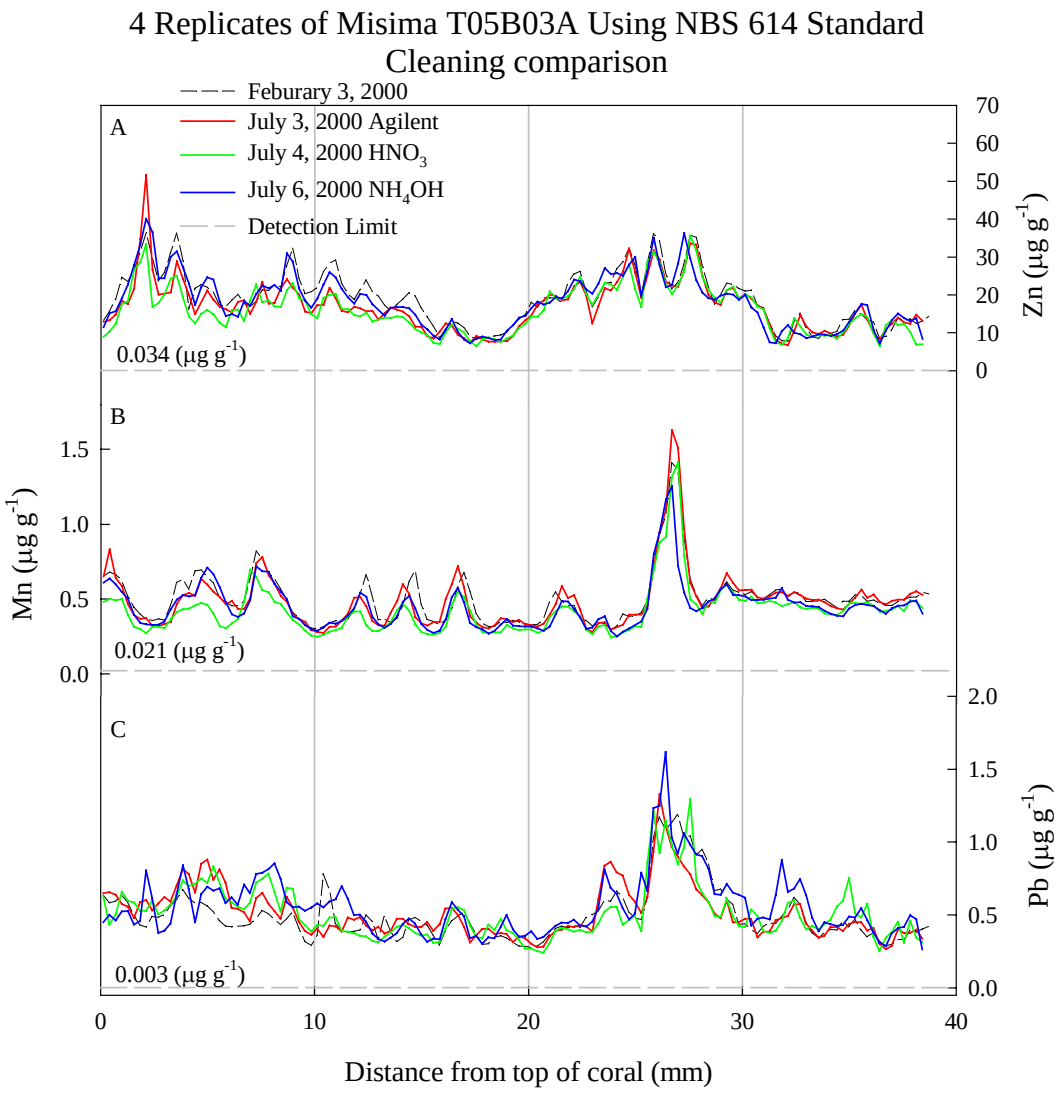

Figure 3.12 Four replicates of the MIST05B03A coral after the alternate cleaning strategy using the NIST 614 as the standard. A) Zn µg g^{-1} vs. Distance from the top of the coral. B) Mn µg g^{-1} vs. Distance from the top of the coral. C) Pb µg g^{-1} vs. Distance from the top of the coral. Also shown on graph is the detection limits for these elements (gray dashed lines and values).

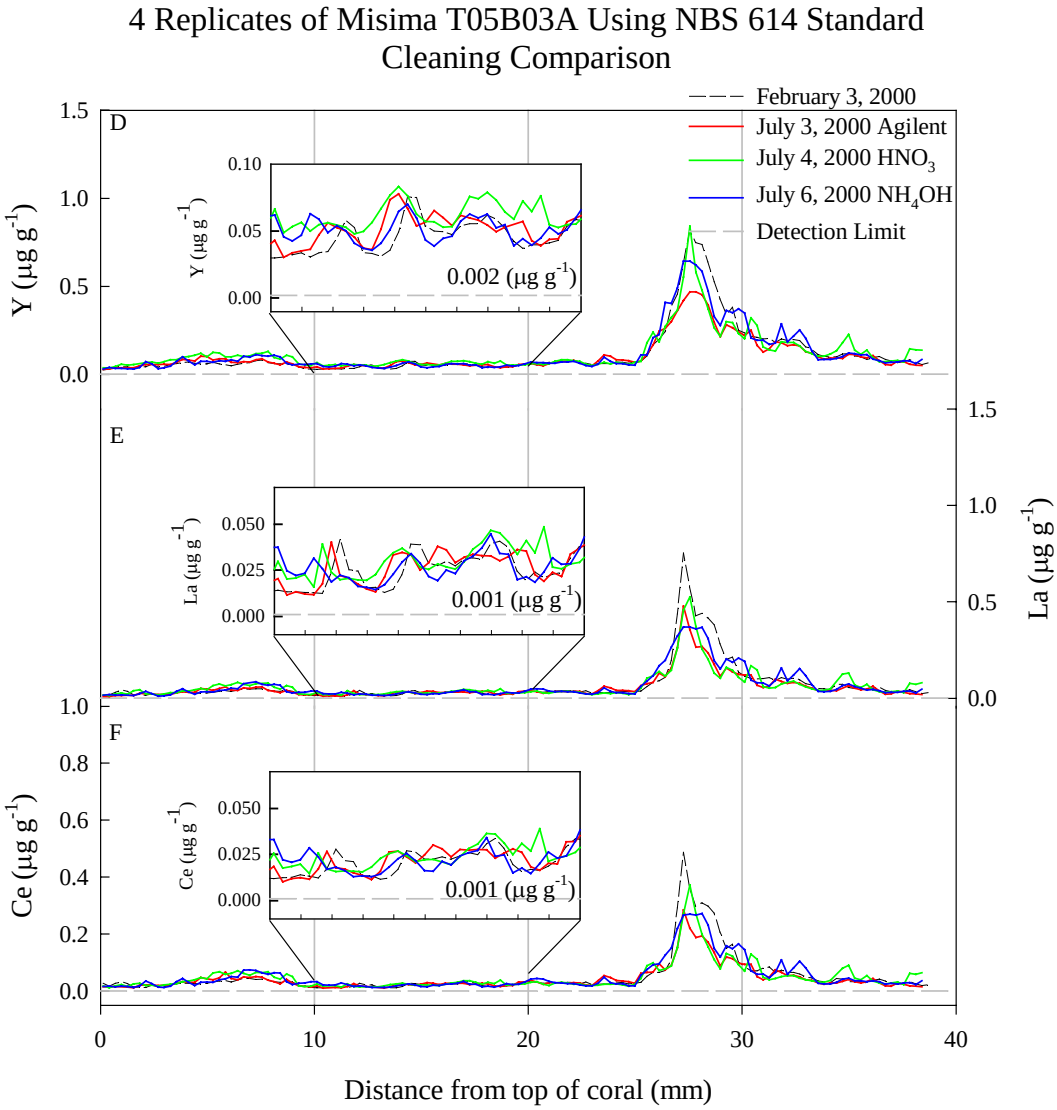

Figure 3.12 Continued D) Y µg g^{-1} vs. Distance from the top of the coral. Inset is close-up of section 10-20 mm showing the reproducibility of the non-peak values. E) La µg g^{-1} vs. Distance from the top of the coral. Inset is close-up of section 10-20 mm showing the reproducibility of the non-peak values. F) Ce µg g^{-1} vs. Distance from the top of the coral. Inset is close-up of section 10-20 mm showing the reproducibility of the non-peak values. The detection limits are shown in the gray dashed line.

Chapter 4: Literature Review: Coral Trace Elements/Proxies

4.1 Introduction

The chemical constituents of coral skeletons have been the subject of many studies. These studies have compared the chemical signatures with environmental parameters; seawater temperature, upwelling, runoff and pollutants. However during these studies a comprehensive and clear understanding of the mechanisms of incorporation of these elements into the coral skeleton has not been achieved. This chapter summarizes the available literature concerning the incorporation and partitioning mechanisms of boron, magnesium, strontium, uranium and barium in coral skeletons and how they relate to environmental factors. This chapter also summarizes the information available on the minor elements; Cd, Mn, Pb, rare earth elements and other pollutants/heavy metals and discusses their environmental chemistry.

4.2 Boron

4.2.1 Boron in Seawater

In seawater, boron has a concentration range of 3.5 – 5 ppm (Schwarcz *et al*., 1969; Spivak and Edmond, 1987; Gaillardet and Allegre, 1995). Boron exists primarily as either boric acid ($B(OH)_3$) or borate ion ($B(OH)_4^-$) (Hershey *et al*., 1986). In seawater, pH ~ 8, the majority of boron (~80%) exists as $B(OH)_3$ and as the pH increases, $B(OH)_4^-$ becomes the dominant species (Figure 4.1) (Hershey *et al*., 1986; Hemming and Hanson, 1992). A slight temperature dependence also exists on the two species, as the temperature increases the ratio of $B(OH)_4^-$ to $B(OH)_3$ decreases (Hershey *et al*., 1986; Hemming and Hanson, 1992). Boron also has a long residence time in oceans of 16-20 million years making studies of isotopic and boron concentration robust over long time scales (Taylor and Mclennan, 1985; Spivack *et al*., 1993).

4.2.2 Incorporation of Boron into Carbonates

The incorporation of boron into coralline aragonite has not been extensively studied although possible mechanisms of incorporation have been examined for inorganic calcite/aragonite and other marine carbonates (ex. mollusks, Ichikuni and Kikuchi, 1972; Taylor and Mclennan, 1985; Spivack *et al*., 1993; Hemming *et al*., 1995). Three possible mechanisms of incorporation were discussed by Ichikuni and Kikuchi (1972), they are:

- Co-precipitation of calcium borate with calcium carbonate
- Substitution of boron for carbon
- Adsorption of boron species $B(OH)_3$ or $B(OH)_4^-$ onto calcium carbonate.

The adsorption of boron species is most probable due to the low amounts of calcium borate and because BO_3^{3-} (B substitute for C) only occurs in highly alkaline conditions (Ichikuni and Kikuchi, 1972).

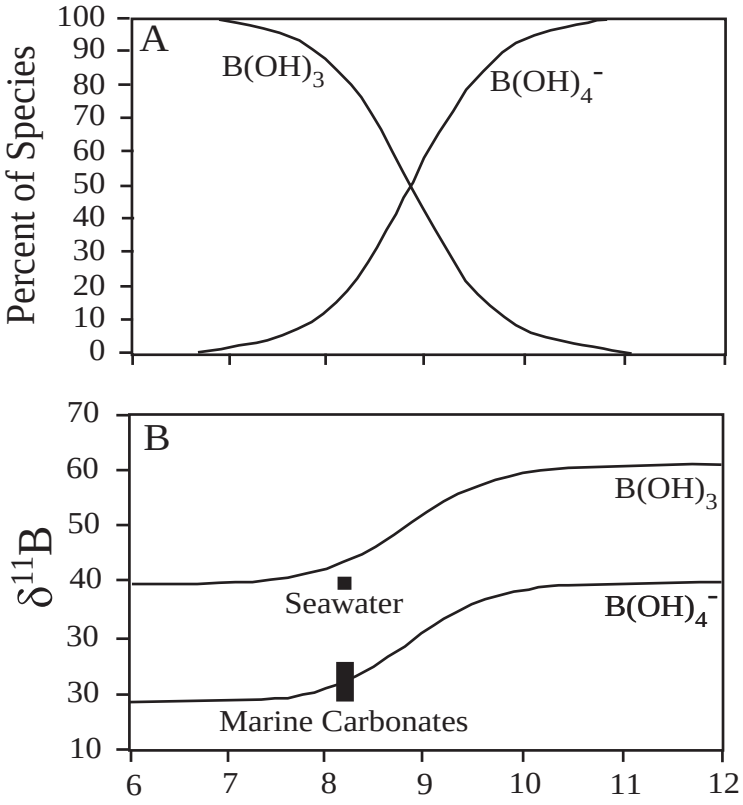

Figure 4.1 A) Distribution of boron species in seawater as a function of pH. B) Isotopic ratio of boron species as a function of pH, shown is seawater and marine carbonate values. Figure adapted from (Kakihana *et al*., 1977; Hemming and Hanson, 1992).

Evidence for the Incorporation of $B(OH)_4^-$ into Marine Carbonates

Adsorption of boron is affected by temperature, salinity and species, ($B(OH)_3$, $B(OH)_4^-$) (Ichikuni and Kikuchi, 1972). It was first thought that boron incorporation did not favor either species (Ichikuni and Kikuchi, 1972). However, the effect of species on adsorption is significant because $B(OH)_4^-$ has a negative electrostatic force that would be attracted to the positively charged sites in $CaCO_3$, the uncharged $B(OH)_3$ would not be attracted in the same way (Ichikuni and Kikuchi, 1972; Lahann, 1978; Given and Wilkinson, 1985). These results are based on $\delta^{11}B$ measurements from various marine and inorganic carbonates. The isotopic composition of boron species are fractionated, $B(OH)_4^-$ is enriched in ^{10}B (Vengosh *et al*., 1991; Hemming and Hanson, 1992; Hemming *et al*., 1995; Sanal *et al*., 2000).

A fractionation of approximately 22‰ exists between the two species, and at a pH of ~8 the $\delta^{11}B$ of $B(OH)_3$ is 42‰ and $B(OH)_4^-$ is 20‰ (Vengosh *et al*., 1991; Hemming and Hanson, 1992). The seawater $\delta^{11}B$ is 39.5‰ which at a pH of ~8 is a balance between the heavy $B(OH)_3$ and the light $B(OH)_4^-$ (the distribution of $B(OH)_3$ and $B(OH)_4^-$ are pH dependent, see Figure 4.1) (Spivack *et al*., 1987; Vengosh *et al*., 1991; Hemming and Hanson, 1992).

Marine carbonates precipitated from seawater have similar $\delta^{11}B$ values and an average value of 22‰ (Vengosh *et al*., 1991; Hemming and Hanson, 1992; Gaillardet and Allegre, 1995; Hemming *et al*., 1995; Hemming *et al*., 1998). At the pH of seawater (7.5-8.4), the $\delta^{11}B$ of $B(OH)_4^-$ is 19-24‰ (Figure 4.1) (Kakihana *et al*., 1977; Hemming and Hanson, 1992). This is offset from seawater but is very similar to the marine carbonate average of ~22‰ (e.g. Hemming and Hanson, 1992). At this same pH, the $\delta^{11}B$ of $B(OH)_3$ is 40-45‰ (Kakihana *et al*., 1977; Hemming and Hanson, 1992), very close to seawater (its dominant species) but significantly offset from marine carbonates (Figure 4.1). This observation and the fact that $B(OH)_4^-$ is charged leads to the conclusion that $B(OH)_4^-$ is the dominant species in the incorporation of boron into marine carbonates (Vengosh *et al*., 1991; Hemming and Hanson, 1992; Gaillardet and Allegre, 1995). The most probable location for boron substitution is the CO_3^{2-} site (Hemming and Hanson, 1992; Gaillardet and Allegre, 1995), this is shown in Equation 4.1:

Equation 4.1 $CaCO_{3solid} + B(OH)_{4\ aqueous}^{-} \rightarrow Ca(HBO_3)_{solid} + HCO_{3\ aqueous}^{-} + H_2O$

This is possible because HBO_3^{2-} and CO_2^{3-} have similar ionic size and charge (Hemming and Hanson, 1992).

Calcite vs. Aragonite

Studies have determined that in fluids of similar boron concentration aragonite incorporates 1-5 times more boron than calcite, with the concentration of boron in HI-Mg calcite being intermediate (Furst *et al*., 1976; Kitano *et al*., 1978; Hemming and Hanson, 1992; Sen *et al*., 1994). Sen *et al*. (1994) used ^{11}B MAS NMR techniques to conclude that boron resides in the structural sites of aragonite and calcite, with aragonite favoring the tetrahedral boron coordination and calcite the trigonal coordination ($B(OH)_4^-$ is tetrahedral, $B(OH)_3$ is trigonal). However, experimental synthetic calcite and aragonite show boron isotopic composition identical to the $B(OH)_4^-$ of the parent fluid (Hemming *et al*., 1995). Since we have previously argued that $CaCO_3$ prefers $B(OH)_4^-$ this suggests that the surface adsorbed $B(OH)_4^-$ species keeps its tetrahedral coordination but must change its coordination to trigonal for calcite (Sen *et al*., 1994). If this coordination change is not favored then this could account for the different amounts of boron (from the same parent fluid) being incorporated into calcite, compared to aragonite.

4.2.3 Factors Affecting Partitioning into Carbonates

The boron concentration and isotopic composition in carbonates can be affected by several distinct and separate factors. Hemming and Hanson (1992) separated these into 7 factors:

- pH – according to Equation 4.2

Equation 4.2 $B(OH)_3 + H_2O \leftrightarrow B(OH)_4^- + H^+$

- Biologic controls (calcification in microenvironments)
- The ratio of borate to carbonate in seawater
- Temperature – increased $B(OH)_3$ with higher temperatures

- Salinity
- Calcite vs. aragonite mineralogy
- Kinetic factors.

Marine aragonites have a wide range of boron concentrations, 2-80 ppm (Vengosh *et al*., 1991; Hemming and Hanson, 1992; Sen *et al*., 1994). As was previously noted, the main species in seawater is $B(OH)_3$ at a pH of 8.2 (Kitano *et al*., 1978) but the relationship has a very steep slope in the region of 7-10 pH units (Figure 4.1) (Hemming and Hanson, 1992). Since $B(OH)_4^-$ is the species incorporated into aragonite an increase in pH will result in an increase in the $B(OH)_4^-$ species and therefore more boron is available to be incorporated into the coral aragonite skeleton.

Since seawater is well buffered and rapid large changes in pH will probably not occur, the sites of calcification in marine carbonates play an important role in the incorporation of boron. In some carbonates, calcification takes place in an internal microenvironment, like mollusks, which have lower pH or $B(OH)_4^-/HCO_3$ ratio. This could account for the lower boron concentration in these bivalves (Furst *et al*., 1976). Kűhl *et al*. (1995) have also documented pH changes in the microenvironments of corals. They showed that pH increased as photosynthesis increased, making $B(OH)_4^-$ more available to the carbonate. However, this pH change can also affect the CO_3^{2-} concentration, which is the anion site the boron competes with. This relationship between increasing pH, HBO_3^{2-} and CO_3^{2-} is not straightforward and needs to be examined more closely to determine its influence on boron incorporation into coralline aragonite.

Temperature

Temperature also plays a role in the partitioning of boron into carbonates, as the temperature increases the $B(OH)_3/B(OH)_4^-$ ratio increases (Hemming and Hanson, 1992). The influence of temperature on boron in corals was first noted by Hart and Cohen (1996) by ion-microprobe measurements. They demonstrated a seasonal cycle for B/Ca that was correlated to Sr/Ca. More recently Sinclair *et al*. (1998) and Fallon *et al*. (1999b) have shown B/Ca to be a faithful recorder of seawater temperatures with B/Ca changing by about 3-5% per ºC. The B/Ca relationship to temperature can be seen in Figure 4.2.

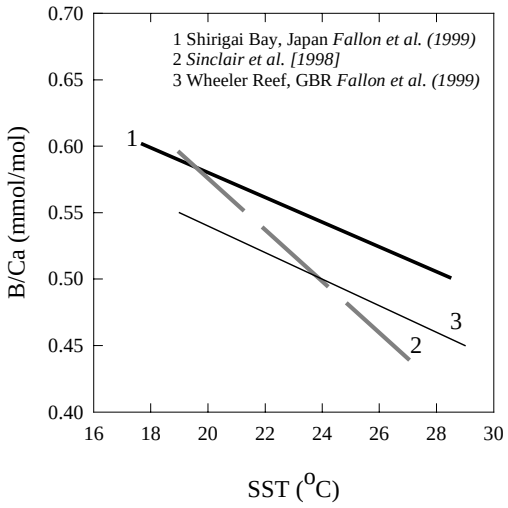

Figure 4.2 B/Ca vs. SST from Sinclair *et al*. (1998) and Fallon *et al*. (1999b)

Salinity

In mollusc shells a correlation between seawater salinity and boron concentration was observed (Furst *et al*., 1976). As the salinity increased so did the boron concentration. In studies of inorganic calcite and aragonite, Kitano *et al*. (1978) noted a positive correlation between salinity and B concentration in calcite but a negative correlation of B in aragonite. The effects of salinity on the boron concentration in corals have not been documented but they should be small as the changes in salinity surrounding corals are usually small.

4.3 Magnesium

4.3.1 Magnesium in Seawater

The magnesium concentration in seawater is ~1300 ppm and exists primarily as Mg^{2+} (89.9%), -SO_4 (8.9%), -HCO_3 (0.6%) and -CO_3 (0.3%) (Hanor, 1969; Schifano, 1982). A small correlation between the Mg content and the salinity of the water also exists (Schifano, 1982). The residence time of magnesium in seawater is long (13 million years, Broecker and Peng, 1982) indicating long term stability for paleoreconstructions.

4.3.2 Incorporation of Magnesium into Carbonates

The incorporation of magnesium into carbonates has been widely studied because of its effect on generating different carbonate forms (calcite, aragonite, HI-Mg calcite) from parent solutions of differing Mg concentration. The majority of this work deals with Mg incorporation into calcite and the effects of diagenesis (e.g. Chave, 1954; Katz, 1973; Folk, 1974; Walls *et al*., 1977). At seawater Mg concentrations the majority of carbonates are in the form of aragonite (Katz, 1973; Folk, 1974; Berner, 1975; Lahann, 1978; Oomori *et al*., 1987). The mechanisms controlling incorporation of Mg^{2+} into coral skeletons has not been well established (Katz, 1973; Oomori *et al*., 1987) and the possible locations for Mg^{2+} in corals are: loosely bound in the aragonite crystal lattice, bound to metal sites of organic compounds or adsorbed to crystal surfaces (Amiel *et al*., 1973a; Walls *et al*., 1977).

A study by Kinsman (1970) suggested magnesium was incorporated into the crystal lattice of inorganically precipitate aragonite but this was never substantiated. Indirect evidence based on cleaning and leaching indicated that organic and adsorbed Mg^{2+} was a small proportion compared to lattice Mg^{2+} because little was lost during these procedures (Delaney *et al*., 1996; Mitsuguchi *et al*., 1996). This agrees with Amiel *et al*. (1973a) who determined 70-80% of Mg existed in mineral phases.

If Mg is in a mineral phase where does it substitute? The difference in size (ionic radius) between the Ca^{2+} and Mg^{2+} cations is large, 1.06 Å vs. 0.78 Å respectively. A variation of more than 15% between cations usually precludes substitution (Amiel *et al*., 1973a). Aragonite has an orthorhombic structure whereas in the presence of Mg^{2+} the $CaCO_3$ – $MgCO_3$ solid solution is distorted into a rhombohedral structure, not fitting neatly in aragonite (Mitsuguchi *et al*., 1996). This structural difference may account for the low Mg concentration and distribution coefficient in aragonite compared to HI-Mg-calcite, D_{Mg} aragonite = 0.00016 (Oomori *et al*., 1987). The distribution coefficient (D_{Metal}) is defined as:

Equation 4.3 $$D_{metal} = \frac{M/Ca_{coral}}{M/Ca_{seawater}}$$ where M = B, Mg, Sr, Ba, U etc..

Adsorbed and/or Organic sites

In an effort to locate Mg in corals Amiel *et al*. (1973a) suspended corals in distilled water and then measured the Mg content of the water over a range of time intervals. Their results indicate incongruent dissolution; there was a higher concentration of Mg in the water than in the skeleton. This finding led to the conclusion that Mg was also adsorbed to the crystal surface or that it occurred in minerals more soluble than aragonite (Amiel *et al*., 1973a). In Holocene and older corals affected by diagenesis (most probably exposed to fresh water) Mg concentrations decreased (Cross and Cross, 1983), consistent with the previous findings of Amiel *et al*. (1973a). Allison (1996b) determined corals were heterogeneous with respect to Mg incorporation at small scales (ion microprobe). It was determined that centers of calcification had higher Mg concentration; consistent with Mg being an adsorbed cation (Allison, 1996b).

The organic component of corals has a substantial capacity for metal binding and coral tissue has higher concentrations of many metals (Mitterer, 1978; Howard and Brown, 1987; McConchie and Harriott, 1992). However, Amiel *et al*. (1973a) found corals only contain small amounts of organic matter ~0.1%. The concentration of Mg found in the organic matter by Amiel *et al*. (1973a) was ~300 ppm and only accounted for a small fraction of the total coral magnesium.

4.3.3 Factors Affecting Partitioning into Carbonates

Mineralogy

The mineralogy is the most important parameter affecting magnesium partitioning, with calcite having 1-20 mol % Mg, and aragonite <1 mol % Mg (Chave, 1954). In seawater, the presence of magnesium has been shown to inhibit calcite formation in favor of aragonite or HI-Mg-calcite (>10 mol % Mg) (Katz, 1973; Folk, 1974; Berner, 1975). During experimental precipitations of carbonates aragonite was formed when the Mg/Ca ratio exceeded 2:1 (Katz, 1973; Folk, 1974). This has important implications for marine carbonates as the Mg/Ca ratio in seawater is close to 4:1.

Temperature

In early studies on calcite, temperature appeared to play a significant role in the incorporation of magnesium (Chave, 1954; Katz, 1973; Kolesar, 1978; Lorens and Bender, 1980; Oomori *et al*., 1987). In inorganic and foraminiferal calcite positive relationships exist between water temperature and magnesium concentration (Chave, 1954; Katz, 1973; Oomori *et al*., 1987). In early studies on coral the temperature relationship was not very clear, although small positive correlations with sea surface temperature were noted (Chave, 1954; Weber, 1974; Oomori *et al*., 1982; Oomori *et al*., 1987). The lack of a temperature relationship in the early work (Chave, 1954; Weber, 1974) was probably due to a combination of large sampling volume, different coral genera and different locations (Mitsuguchi *et al*., 1996).

Subsequently Goreau (1977) noted a seasonal cycle for Mg/Ca and other researchers have documented seasonal variations in Mg/Ca (Hart and Cohen, 1996; Mitsuguchi *et al*., 1996; Sinclair *et al*., 1998; Fallon *et al*., 1999b). The positive Mg/Ca-SST relationships found by these authors are shown Figure 4.3. At this point no definitive explanations for the positive relationship between Mg/Ca and temperature for corals have been proposed, although it is noted that Mg is the only major cation in coral to have a substantially smaller ionic radius than Ca.

Several possible mechanisms for this positive relationship were discussed by Kinsman and Holland (1969) and Swart (Swart, 1981). One possibility is Mg^{2+} distorts the crystal lattice and the crystal lattice tolerance to distortion increases with increasing temperature thereby increasing the Mg/Ca ratio with increasing temperature (Kinsman and Holland, 1969). Swart also proposed the positive relationship between Mg/Ca and temperature to be related to temperature. When a solution is heated the molecules around the ion expand causing increased complex formation. The activity coefficient of Ca^{2+} and Mg^{2+} decreases with increasing temperature but the activity coefficient of Ca^{2+} is lower than Mg^{2+} resulting in an increase of the Mg^{2+}/Ca^{2+} ratio with increasing temperature (Swart, 1981).

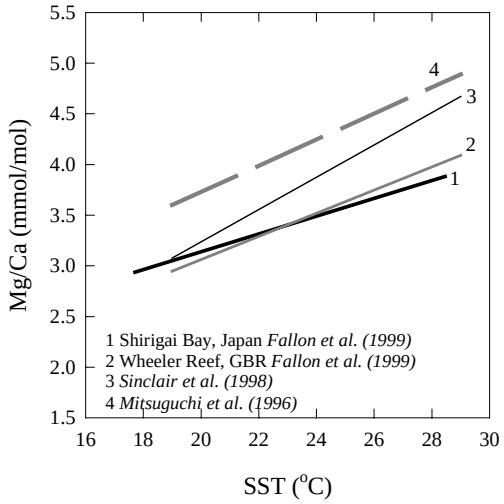

Figure 4.3 Mg/Ca vs. SST, showing positive relationship.

Biologic Factors

There is a large variation in the Mg content of corals; ranges of 700-2400 ppm have been reported (Chave, 1954; Weber, 1974; Swart, 1981; Oomori *et al*., 1982; Cross and Cross, 1983; Mitsuguchi *et al*., 1996). This variation cannot be accounted for by changes in water chemistry or temperature (Cross and Cross, 1983; Allison and Tudhope, 1992). This leads to the conclusion that the Mg/Ca ratio in corals is also affected by physiology (Weber, 1974; Cross and Cross, 1983; Hart and Cohen, 1996).

One type of physiological parameter that has been discussed as influential is growth rate, however its effect is not consistent. Faster growth rates have been shown to produce both higher Mg/Ca ratios (Dodd, 1967; Weber, 1973b), and lower Mg/Ca ratios (Kolesar, 1978) as well as having no effect at all (Lorens and Bender, 1980). In corals, Weber (1974) did not find any evidence of a link between growth rate and magnesium concentration, but Oomori *et al*. (1982) did note that slower growing corals had higher magnesium concentration. However, this observation could have been related to a phylogenic effect, as the corals compared were from different genera. Swart (1981) noted a positive correlation between growth rate and magnesium content in one coral but this could not be confirmed and may be a species or habitat effect.

4.4 Strontium

4.4.1 Strontium in Seawater

The concentration of strontium in seawater is ~8000 μg/L (Brass and Turekian, 1974; Chester, 1990). The main species of strontium in seawater is Sr^{2+} (Hanor, 1969). Strontium exhibits a conservative behavior with a slight surface depletion (1-3%) in some nutrient rich waters (Chester, 1990; de Villiers *et al*., 1994). This slight depletion is similar to elements with a "nutrient-type" behavior. In oligotrophic waters strontium is depleted relative to deeper waters (de Villiers *et al*., 1994). This depletion/enrichment from shallow to deep is most likely due to the formation of celestite ($SrSO_4$) skeletons by radiolaria at the surface and their dissolution at depth (Brass and Turekian, 1974). Strontium also has a long residence time of 4-5 million years which lends to it use in paleo-studies (Holland, 1978; Beck *et al*., 1992).

4.4.2 Incorporation of Strontium into Carbonates

Lattice Substitution

Strontium forms an orthorhombic isomorph of aragonite called strontianite ($SrCO_3$) (Speer, 1983). In solid solution with aragonite, Sr^{2+} mainly substitutes for Ca^{2+} in the crystal lattice (Kinsman and Holland, 1969; Speer, 1983; Greegor *et al*., 1997). The chemistry of Sr^{2+} is very similar to Ca^{2+} and therefore its behavior should be similar (Kinsman and Holland, 1969) even though its ionic radius (Sr 1.31 Å) is larger than Ca^{2+} (1.06 Å). Most studies suggest that Sr^{2+} directly substitutes for Ca^{2+} in corals but others suggest that it occurs in another phase (e.g. strontianite) (Cross and Cross, 1983; Rasmussen, 1988; Greegor *et al*., 1997). Harriss and Almy (1964) suggested that the substitution of calcium by strontium has a stabilizing effect on biogenic aragonite. Dissolution experiments by Amiel *et al*. (1973a) indicated Sr^{2+} lattice substitution for Ca^{2+} with no strontium in exchangeable sites. In substitution experiments Sr^{2+} releases in the presence of Ca^{2+} which is also an indication of lattice substitution (Amiel *et al*., 1973a). Organic phases were also found to contain strontium at a concentration of ~ 500 ppm, which is equivalent to only ~ 7% of the total strontium (Amiel *et al*., 1973a). Greegor *et al*. (1997) found evidence for strontianite ($SrCO_3$) with some solid solution

of $SrCO_3$-$_{CaCO3}$. They proposed that 60% of the strontium substitutes for calcium and the rest is in a $SrCO_3$ phase.

4.4.3 Factors Affecting Strontium Partitioning in Carbonates

Temperature

An inverse relationship between strontium incorporation and temperature was observed during inorganic precipitation of aragonite (Kinsman, 1969). The distribution coefficient (D_{Sr}) goes from1.17 at 16ºC to 0.88 at 90ºC (Figure 4.4) (Kinsman, 1969). They also noted a positive relationship between D_{Sr} and the strontium concentration in the parent fluid.

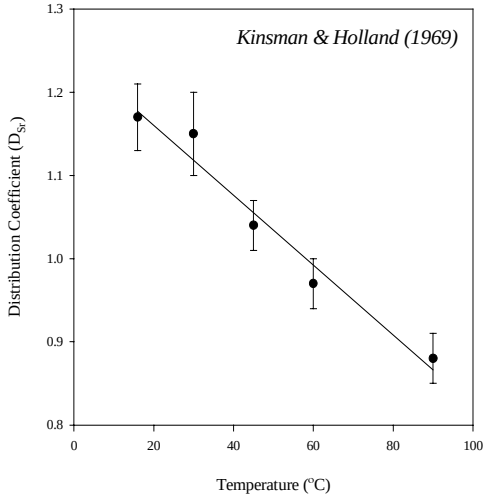

Figure 4.4 The distribution coefficient for strontium in inorganic aragonite vs. temperature. A negative linear correlation is observed.

Early studies on corals suggest that Sr/Ca and temperature were not associated (e.g. Thompson and Livingston, 1970; Goreau, 1977). Weber (1973a) attributed this to sampling locations, misidentification of corals and depth. Most likely it was the low precision analytical methods available at the time. Weber (1973a) found that D_{Sr} and temperature were negatively related (like inorganic) but it was offset from the inorganic value, corals D_{Sr} = 0.96 – 1.09. This variation may be attributed to their "bulk" sampling methods. The first significant linear relationship between Sr/Ca and temperature became apparent when smaller samples were analyzed. Both Houck *et al*. (1977) and Smith *et al*. (1979) reported good correlations between water temperature

and Sr/Ca in corals. However it wasn't until Beck *et al*. (1992) produced high-precision Sr/Ca using ID-TIMS that the use of Sr/Ca as a temperature proxy became more widespread. This has lead to other estimates of D_{Sr} in corals; McCulloch *et al*. (1994) determined it to be ~ 1.1 at 20 ºC. The difference between inorganic and biogenic D_{Sr} is ~ 4-6 % and may be related to some type of biological effect (Swart, 1981).

Swart (1981) proposed that the inverse relationship between temperature and Sr/Ca in corals could be related to ion complexation. As temperature increases the water molecules around the ion expand and the proportion of the element in its ionic form decreases. In seawater the activity coefficients for Sr^{2+} and Ca^{2+} both decrease with increasing temperature but the activity coefficient for Sr^{2+} is lower resulting in a decrease of Sr/Ca with increasing temperature. This is opposite of the Mg/Ca relationship discussed earlier (Swart, 1981).

Since 1992, various labs have been measuring Sr/Ca and trying to obtain calibrations with SST (e.g. de Villiers *et al*., 1994; McCulloch *et al*., 1994; Shen *et al*., 1996; Alibert and McCulloch, 1997). The conclusion from these studies was that the Sr/Ca-SST relationship was not straightforward and differed between locations and coral genera. At specific locations high correlations between Sr/Ca and SST were observed but individual calibrations did not agree very well (Figure 4.5). In one case, three corals collected from nearby (< ~100m distance) locations in Hawaii had distinctly different calibrations (de Villiers *et al*., 1994), but some of this variation could be due to sampling different growth axes. Many of the published calibrations have similar slopes (similar temperature dependence) but are not all within error. Their differences have been attributed to other factors; seawater, growth rate and species.

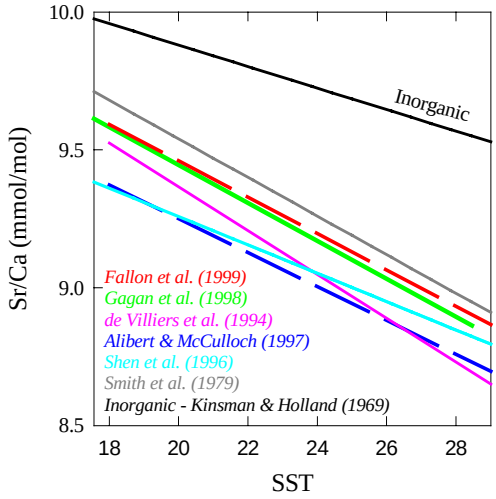

Figure 4.5 Sr/Ca vs. SST for various coral genera and locations. Variations in the calibrations can be seen, also shown is the inorganic temperature relationship.

Seawater

Shen *et al*. (1996) suggested that to compare calibrations between localities a correction based on the seawater Sr/Ca was needed. When they corrected the calibrations of de Villiers *et al*. (1994) and Beck *et al*. (1992) and compared it to their calibrations they found that at 24ºC all the calibrations give similar Sr/Ca values. However, the slopes of the three equations are different which causes different Sr/Ca values at low and high temperatures between the three equations (Shen *et al*., 1996). This indicates seawater Sr/Ca is not the only variable.

Salinity

The influx of river runoff was theorized to affect local seawater Sr/Ca through dilution as the Sr/Ca of river water is usually low. All available data indicate that the influence of freshwater on coral Sr/Ca is negligible (Schneider and Smith, 1982; McCulloch *et al*., 1994; Alibert and McCulloch, 1997).

Growth Rate / Extension / Calcification

If Sr/Ca partitioning in corals is under kinetic control, calcification (coral density x extension) should affect Sr/Ca incorporation (Weber, 1973a; Alibert and McCulloch, 1997). Studies on inorganic aragonite found no relationship between strontium incorporation and precipitation (Kinsman and Holland, 1969; Mucci *et al*., 1989). de

Villiers *et al*. (1994) argue that the D_{Sr} for corals is lower than inorganic aragonite because corals precipitate aragonite ~ 6 times faster than inorganic aragonite. They analyzed two sections of the same coral, one extending 4-7 mm yr^{-1} and the other 11-12 mm yr^{-1}. They found that the Sr/Ca was lower in the faster growing section. However they did not measure density so it is impossible to tell whether extension or calcification caused the lower Sr/Ca. McCulloch *et al*. (1994) found that during El Niño years the cold winter waters were causing decreased extension and calcification and resulting in more strontium incorporation and the D_{Sr} (1.1 at 20ºC) approaching the inorganic value of 1.15. Shen *et al*. (1996) and Alibert and McCulloch (1997) determined that extension had little effect on coral Sr/Ca as long as a main growth axis was sampled. If samples are obtained from a growth margin the Sr/Ca was shifted to higher values (Alibert and McCulloch, 1997). They attribute these higher Sr/Ca values to sub-optimal growth conditions resulting in smaller corallites, lower skeletal density and lower calcification. Their study reinforces the need for good, consistent sampling of a main growth axis for reproducible results.

Species

The effect of species on strontium content in corals has been observed (Thompson and Livingston, 1970; Weber, 1973a; Houck *et al*., 1977). Weber (1973a) found ranges of 7000-8000 ppm between different coral species growing in nearby locations at Heron Island, Australia. Houck *et al*. (1977) reported different Sr/Ca for corals of different species growing in the same aquaria. These studies lead to another factor (physiological) that affects strontium incorporation in corals. This physiological effect could also account for the differences between D_{Sr} inorganic and D_{Sr} corals.

4.5 Uranium

4.5.1 Uranium in Seawater

The oceanic average concentration of uranium is 3.3 μg/L (~3.3 ppb) (Ku *et al*., 1977; Djogic *et al*., 1986). Ku *et al*. (1977) noted variability in worldwide U concentration, with ranges of 2.9 - 3.6 μg/L; these differences were attributed to waters with salinities of 30.3 and 36.1 ‰, respectively. U has a residence time in seawater of ~ 300,000

years, making $^{234}U/^{238}U$ ratio a useful tracer in the analysis of old corals (Ku *et al*., 1977).

Similar to boron, uranium has several aqueous species, these are: UO_2^{2+}, $UO_2CO_3^0$, $UO_2(CO_3)_2^{2-}$, $UO_2(CO_3)_2^{4-}$ (Langmuir, 1978; Djogic *et al*., 1986). The most prevalent species at pH ~ 8 is $UO_2(CO_3)_2^{4-}$, with $UO_2(CO_3)_2^{2-}$, $UO_2CO_3^0$ and UO_2^{2+} becoming more prevalent with decreasing pH (Langmuir, 1978; Djogic *et al*., 1986).

4.5.2 Incorporation of Uranium into Carbonates

The incorporation of uranium in carbonates favors aragonite over calcite (Kitano and Oomori, 1971; Meece and Benninger, 1993). One possible reason is that the aragonite structure is more open than calcite and can accommodate ions with larger ionic radii (Kitano and Oomori, 1971; Meece and Benninger, 1993). This reasoning has lead toward lattice substitution of uranium in aragonite (Meece and Benninger, 1993).

The possible substitution equations for uranium into coralline aragonite are:

Equation 4.4 $UO_2^{2+}{}_{sw} + UO_2(CO_3)_2^{2-}{}_{sw} \leftrightarrow UO_2CO_{3aragonite} + CO_3^{2-}{}_{sw}$

This mode of substitution is favored by Min *et al*. (1995). Their reasoning is based on UO_2^{2+} having the same valence as Ca^{2+}, the slightly larger size and different shape of UO_2^{2+} substitutes preferentially in aragonite (Meece and Benninger, 1993) and the form UO_2CO_3 is a naturally occurring orthorhombic carbonate (rutherfordine), like aragonite (Christ. *et al*., 1955).

Equation 4.5 $CaCO_{3arag.} + UO_2(CO_3)_2^{2-}{}_{sw} \leftrightarrow CaUO_2(CO_3)_{2arag.} + CO_3^{2-}{}_{sw}$

This mode is favored by Swart and Hubbard (1982) and Shen and Dunbar (1995). However with this route one difficulty is that the uranyl carbonate group is much larger ionic radii than the carbonate group (Shen and Dunbar, 1995).

Equation 4.6 $CaCO_{3arag.} + UO_2CO_3^0{}_{sw} \leftrightarrow UO_2CO_{3arag.} + CaCO_{3arag.}$

One difficulty with these three equations is that at seawater pH $UO_2(CO_3)_2^{4-}$ is the dominant species (Langmuir, 1978; Djogic *et al*., 1986). This suggests that the coral must have some control over uranium speciation (Shen and Dunbar, 1995). Another possibility for uranium incorporation is interstitial insertion of uranium between planes and/or vacant lattice positions (Veizler, 1983).

In controlled experiments, Swart and Hubbard (1982) found that uranium concentrations in corals were directly related to the uranium content of the water and that the concentration of calcium (in the water) did not affect the coral uranium concentration. This suggests that different mechanisms are responsible for uranium and calcium incorporation into skeletal aragonite (Swart and Hubbard, 1982). The mode (Equation 4.5) favored by Swart and Hubbard (1982) and Shen and Dunbar (1995) suggests uranium incorporation through intercellular inorganic carbonate pathways (Weber and Woodhead, 1972; Swart and Hubbard, 1982). The distribution coefficient (D_U) between coral U/Ca and seawater is ~ 1 (Kitano and Oomori, 1971; Flor and Moore, 1977; Swart and Hubbard, 1982; Shen and Dunbar, 1995).

Adsorbed and/or Organic sites

Amiel *et al*. (1973b) suggested uranium could be adsorbed onto the surface of skeletal aragonite in an exchangeable form and/or be associated with organic components. The adsorbed component on skeletal aragonite was shown to be ~40-60 ppb and could be readably leached and/or exchanged (Amiel *et al*., 1973b). This component is low in concentration because of the low surface area in coralline aragonite and is about 2% of the total uranium (Amiel *et al*., 1973b).

The uranium concentration of organic phases associated with corals can be very high, 20-30 times higher than the skeleton (Amiel *et al*., 1973b; Flor and Moore, 1977). However outside of the tissue zone, corals were found to be very low in organics, ~0.1%, and will not make a significant contribution to the overall uranium concentration (Amiel *et al*., 1973b). These factors lead to the conclusion that most of the uranium in corals is lattice bound (Amiel *et al*., 1973b; Swart and Hubbard, 1982; Shen and Dunbar, 1995).

4.5.3 Factors Affecting Partitioning into Carbonates

pH and Carbonate Species

The uranium speciation in seawater is governed by these three equations:

Equation 4.7 $UO_2^{2+}{}_{sw} + CO_3^{2-}{}_{sw}^{-} \leftrightarrow UO_2CO_3^{0}{}_{sw}$

Equation 4.8 $UO_2CO_3^{0}{}_{sw} + CO_3^{2-}{}_{sw}^{-} \leftrightarrow UO_2(CO_3)_2^{2-}{}_{sw}$

Equation 4.9 $UO_2(CO_3)_2^{2-}{}_{sw} + CO_3^{2-}{}_{sw}^{-} \leftrightarrow UO_2(CO_3)_2^{4-}{}_{sw}$

The CO_3^{2-} activity in seawater varies as a function of pH, temperature and total CO_2 (Min *et al*., 1995). Their model suggests that coralline U/Ca is sensitive to pH and total CO_2 changes and that the microenvironments involved in coral calcification have a buffer/control over the aqueous carbonate species. This agrees with the conclusions of Swart and Hubbard (1982) and Shen and Dunbar (1995) that corals must have control over uranium speciation. If pH and/or total CO_2 decrease then U/Ca in the coral will increase (Min *et al*., 1995).

Temperature

In early studies on corals no seasonality was found in the U/Ca ratio, this was probably due to analytical limitations (Veeh and Turekian, 1968; Schroeder *et al*., 1970; Amiel *et al*., 1973b). More recently Shen and Dunbar (1995) showed seasonal variations of U/Ca that correlated with $\delta^{18}O$ in Galapagos corals. In the same journal issue, Min *et al*. (1995) went one step further and showed strong correlations between U/Ca and Sr/Ca and SST from New Caledonia and Tahiti corals. The inverse relationship between U/Ca and temperature has been documented in many locations since (Fallon, 1996; Fallon *et al*., 1999b; Sinclair *et al*., 1998). The published U/Ca-SST relationships are shown in (Figure 4.6). The absolute values of the equations are different but they all have similar slopes, indicating common temperature dependence. The U/Ca thermometer appears to have a sensitivity of about 3-5 % per ºC (Min *et al*., 1995; Shen and Dunbar, 1995; Fallon, 1996; Sinclair *et al*., 1998; Fallon *et al*., 1999b).

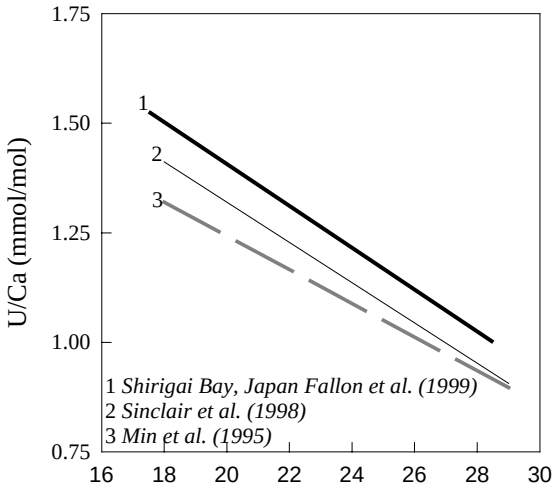

Figure 4.6 U/Ca and SST showing inverse relationship.

Seawater

The concentration of uranium in seawater may be influenced (diluted or enhanced) by high rainfall or runoff (Shen and Dunbar, 1995). In areas of high freshwater influence stratification can occur in the upper surface waters of the West Pacific (Lukas and Lindstrom, 1991). This low salinity could potentially cause a 10% dilution of uranium (Shen and Dunbar, 1995). The majority of rivers are low in uranium (Magini *et al*., 1979; Palmer and Edmond, 1993), but some have higher uranium content due to carbonate weathering (Shen and Dunbar, 1995). However the most significant source of excess uranium in river waters is phosphate fertilizers (Spalding and Sackett, 1972; Magini *et al*., 1979; Bloch, 1980; Palmer and Edmond, 1993). These fertilizers can contain 50-200 μg/L uranium depending on the percentage of phosphate; this could cause significant local estuarine/seawater uranium enrichments (Spalding and Sackett, 1972; Magini *et al*., 1979; Bloch, 1980; Palmer and Edmond, 1993).

Growth Rate

A growth rate effect was suggested by Cross and Cross (1983) for U because of the different uranium concentrations in slower and faster growing corals, but this may be a species artifact. Schroeder *et al*. (1970) reported small-scale heterogeneities along the internal corallites, which they associated with differing calcification rates. However, Swart and Hubbard (1982) and Shen and Dunbar (1995) and Fallon *et al*. (1999b) found no systematic effects on uranium incorporation related to changing extension or calcification. Shen and Dunbar (1995) analyzed slower and faster growing portions of the same coral to arrive at this conclusion.

Species

The effect of species on uranium content in corals has not been fully tested. Gvirtzman *et al*. (1973) found that uranium concentrations in various corals were relatively uniform. Shen and Dunbar (1995) examined corals of different species and found different uranium concentrations but this difference was attributed to water temperature. Min *et al*. (1995) found a noticeable difference between *Acropora* and *Porites* U/Ca that was not attributable to temperature suggesting that coral U/Ca can be controlled in part by species.

4.6 Barium

4.6.1 Barium in Seawater

The distribution of barium in seawater is different to the previous elements discussed, i.e. boron, magnesium, strontium and uranium. Barium has a "nutrient-type" distribution in seawater as opposed to the more "conservative" distribution of B, Mg, Sr and U (Chester, 1990). The profile of dissolved barium indicates enrichment in deep water and depletion in the surface water (Figure 4.7). The surface waters are ~ 4.5 ppb and increase to 15-30 ppb in deep water (Riley and Chester, 1971; Bacon and Edmond, 1972; Bernat *et al*., 1972).

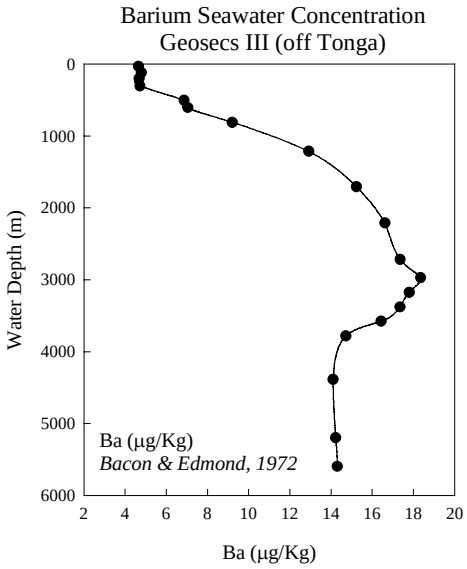

Figure 4.7 Profile of barium seawater concentration from GEOSECS III station off Tonga. Shows "nutrient-type" behavior of barium in seawater.

The higher concentration of barium in deep water is due to the production of barite ($BaSO_4$) by marine organisms (Dehairs *et al*., 1980; Monnin *et al*., 1999). Barium has an average residence time in seawater of ~84,000 years (Riley and Chester, 1971).

4.6.2 Incorporation of Barium into Carbonates

Barium forms an isomorph of aragonite called witherite ($BaCO_3$) (Speer, 1983). This is also an orthorhombic carbonate and matches the orthorhombic structure of aragonite (Speer, 1983). Barium should substitute into the lattice of aragonite corals because of this solid-solution between witherite and aragonite (Speer, 1983) and this incorporation should be proportional to the seawater concentration (Lea *et al*., 1989). It is thought that the incorporation of Ba^{2+} should be similar to that of Sr^{2+} as they are both alkaline earth elements with ionic radii larger than calcium (1.47 Å for Ba, 1.31 Å for Sr), strontium also forms an orthorhombic isomorph, strontianite ($SrCO_3$) (Speer, 1983; Lea *et al*., 1989). In ion-microprobe studies of corals by Allison and Tudhope (1992) they found high barium concentrations in the centers of calcification and microborings. This finding indicates that Ba^{2+} replaces Ca^{2+} and also that it exists in a contaminant phase.

Organic and/or Adsorbed sites

The small contaminants in corals can have high barium concentrations and can play a significant role in the overall coral barium concentration (Allison and Tudhope, 1992; Tudhope *et al*., 1996). Some of these contaminants could be associated with organic matter trapped in the interstices and pores of the corals (Allison and Tudhope, 1992; Tudhope *et al*., 1997). The coral tissue also has been shown to have higher concentrations of barium than the surrounding tissue (Flor and Moore, 1977; Buddemeier *et al*., 1981; Tudhope *et al*., 1996). Using SEM, Tudhope *et al*. (1996) found the presence of barite crystals in the tissue zone of a cleaned coral. However no barite has been found away from the tissue zone in the skeletal area (Hart and Cohen, 1996; Tudhope *et al*., 1996; Hart *et al*., 1997). In an effort to examine a possible relationship between barium and organics, Hart *et al*. (1997) extracted organic carbon from coral skeletons but did not find any associations with high barium concentrations. This supports their conclusion that the barium concentration in corals was not directly controlled by organic material.

Using experimental data from Gafford (1969), Pingitore *et al*. (1989) suggest adsorption as the main mechanism for barium incorporation in corals. This is based on the increasing distribution coefficient of barium in aragonite with increasing rates of precipitation (Gafford (1969) quoted by Pingitore *et al*., 1989). The adsorption mechanism was proposed because as precipitation increases more ions would be incorporated as the surface grows, this mechanism agrees with the Gafford (1996) conclusions cited by (Pingitore *et al*., 1989).

Overall, it appears that some barium is lattice bound, some adsorbed and some occurs in a yet identified contaminant phase (Pingitore *et al*., 1989; Hart and Cohen, 1996; Tudhope *et al*., 1996; Hart *et al*., 1997).

4.6.3 Factors Affecting Partitioning into Carbonates

Variations in Seawater Barium Concentration

The concentration of an element in seawater plays a critical role in its final concentration in coral aragonite. The previously discussed elements (B, Mg, Sr, U) have very little concentration variation in surface seawater. Sea surface barium

concentrations can be influenced by upwelling of deeper water (Figure 4.7) (Lea *et al*., 1989; Shen *et al*., 1992a; Fallon *et al*., 1999b) and by river runoff (Shen and Sanford, 1990; Tudhope *et al*., 1997; Fallon *et al*., 1999a).

Upwelling of cold, nutrient rich (high barium concentration) waters can increase the barium concentration of waters surrounding the corals while they are growing. Studies by Lea *et al*. (1989) and Shen *et al*. (1992a) show that coralline Ba/Ca follows the water temperature at Galapagos as it is influenced by changes in thermocline depth and upwelling. Shen *et al*. (1992a) suggested some of the major upwelling changes were associated El Niño and its effect on the depth of the thermocline. In a more recent paper, an association between coralline Ba/Ca and wind-induced upwelling was observed (see Chapter 5, Fallon *et al*., 1999b).

Another significant source of barium to the oceans is river runoff. The desorption of barium from particulate matter increases the seawater barium concentration (Riley and Chester, 1971). This desorption occurs when barium particulate laden freshwater is mixed with seawater; barium is released by ion-exchanging processes involving sodium, magnesium, potassium and calcium (Riley and Chester, 1971; Hanor and Chan, 1977; Edmond *et al*., 1985). This process can increase seawater barium concentration near coastal regions by 50% or more (Hanor and Chan, 1977; Carroll *et al*., 1993). Corals collected from Barbados show strong correlations between Amazon discharge and Ba/Ca (Shen and Sanford, 1990). Recent studies by Sinclair (1999) and Fallon *et al*. (1999a) have shown clear relationships between Ba/Ca in near shore GBR corals and Burdekin River runoff.

Temperature

Temperature is known to play an important role in the portioning of B, Mg, Sr and U (earlier in this chapter) but its influence on Ba partitioning is not well documented. Lea *et al*. (1989) suggested that Ba might have a temperature dependence similar to Sr since they are both alkali earth elements with larger ionic radii that calcium. Based on Sr/Ca-SST this would suggest ~ 0.7% change in Ba/Ca per ºC (e.g. Smith *et al*., 1979; Beck *et al*., 1992; Alibert and McCulloch, 1997). This temperature effect would enhance the Ba/Ca record due to upwelling, as the cold deep water has higher barium and the relationship between Sr/Ca and SST is inversely proportional (see previous section on

Strontium). This potential temperature influence on barium only accounts for ~ 4% of a 20-25% range in Ba/Ca observed in upwelling regions of Galapagos (Lea *et al*., 1989; Shen *et al*., 1992a). However, this temperature effect has never been documented from any locations, even ones far removed from upwelling and/or river runoff influences.

Biologic Factors

Pingitore *et al*. (1989) suggest that the incorporation of barium is related to the rate of precipitation. Citing experiments by Gafford (1969), Pingitore *et al*. (1989) said the distribution coefficient for barium in aragonite precipitated from seawater increased with increasing rates of precipitation. Pingitore *et al*. (1989) also compared barium concentration from *Acropora* (fast growing) and *Montastrea* (slow growing) and showed that the slowest growing part of *Acropora* had barium concentrations very similar to *Montastrea*.

4.7 Minor Elements

4.7.1 Cadmium

Cadmium has a nutrient like oceanic behavior (similar to barium) and is enriched in upwelled waters and low in oligotrophic waters (Boyle *et al*., 1976). The pattern of cadmium in seawater closely resembles that of phosphate (Boyle *et al*., 1976). Cadmium has a very similar ionic radius to calcium and has a known carbonate mineral phase in solid solution with calcite, $CdCO_3$ (Otavite) (Speer, 1983). A lattice bound component of cadmium was documented by Shen and Boyle (1988) and a distribution coefficient of (D_{Cd}) ~ 1 was determined. Cd/Ca in corals has mostly been used as a paleofertility tracer in association with upwelling off the Galapagos (Shen and Sanford, 1990). Other variations in the Cd/Ca ratio in corals have been attributed to aeolian flux; (industrial cadmium in Bermuda corals Shen *et al*., 1987), rainfall (island runoff and resuspension of particulate cadmium, Tarawa Shen and Sanford, 1990), or inconclusive patterns not associated with any environmental signals (Linn *et al*., 1990; Delaney *et al*., 1993). The Cd/Ca in corals is ~ 5-15 nmol/mol (Shen *et al*., 1987; Linn *et al*., 1990; Delaney *et al*., 1993).

4.7.2 Manganese

The Mn/Ca ratio has been measured in corals from several locations. These corals tend to show seasonal variations (Linn *et al*., 1990; Shen *et al*., 1991; Delaney *et al*., 1993) and in some cases a cyclicity related to El Niño (changing wind patterns Shen *et al*., 1991). The concentration of manganese in seawater is affected by proximity to coastlines. In coastal areas manganese is enriched by riverine manganese (both dissolved and particulate), shelf sediments and aeolian inputs (Bender *et al*., 1977; Shen *et al*., 1991). Away from the coasts aeolian supply is the main contributor to the high surface seawater Mn concentration (Klinkhammer and Bender, 1980). The concentration then decreases with depth except for a mid-depth maxima coincident with the oxygen minimum zone (Klinkhammer and Bender, 1980). Because of these factors manganese has a high spatial variability in seawater (Shen *et al*., 1991). In corals the Mn/Ca is ~ 15-300 nmol/mol and is mostly lattice bound (Linn *et al*., 1990; Shen *et al*., 1991; Delaney *et al*., 1993). However it appears that manganese is discriminated against in the coral lattice, the D_{Mn} is ~ 0.2 – 0.6 (Shen *et al*., 1991). Regardless, Mn/Ca has been used to track surface ocean currents (Linn *et al*., 1990; Shen *et al*., 1991; Delaney *et al*., 1993), local volcanism from seafloor hydrothermal plumes (Shen *et al*., 1991), and manganese released from nearshore and lagoonal sediments by wave action (Shen *et al*., 1991).

4.7.3 Lead

Lead forms an orthorhombic carbonate similar to strontianite ($SrCO_3$) and witherite ($BaCO_3$); called cerussite ($PbCO_3$) (Speer, 1983). The lead concentration in corals ranges from 10-100 ppb (20 – 150 nmol/mol) (Dodge and Gilbert, 1984; Shen and Boyle, 1987; Shen and Boyle, 1988). The increases of Pb/Ca measured in corals is mostly attributed to anthropogenic input, fossil fuel burnings etc. (Shen and Boyle, 1987) but some has also been attributed to local inputs (sewage) (Dodge and Gilbert, 1984). Lead appears to substitute directly into the coral lattice and is enriched in the coral skeleton relative to seawater, the D_{Pb} ~ 2.3 (Shen and Boyle, 1987; Shen and Boyle, 1988). The lead record in Bermuda corals closely follows the record of US Alkyl lead production and consumption (Shen and Boyle, 1987). Two samples from St. Croix US Virgin Islands record increases of Pb from 1950 – 1980 (anthropogenic) and

one site from nearby a harbor and sewage outfall records excess lead associated with this pollution (Dodge and Gilbert, 1984). These studies indicate that corals can record local and global oceanic lead inputs (Dodge and Gilbert, 1984; Shen and Boyle, 1987; Shen and Boyle, 1988).

4.7.4 Rare Earth Elements

The measurement of rare earth elements (hereby referred to as REE) in corals can be potentially very useful for identifying sources of dissolved trace elements and documenting weathering histories of drainage basins (Sholkovitz and Shen, 1995). This can be accomplished because rock weathering alters riverine REE patterns and they can be significantly different to seawater patterns (Sholkovitz and Shen, 1995; Naqvi *et al*., 1996). Corals incorporate REE's in proportion to their seawater concentration and have $D_{REE} \sim 1$ with concentrations in the ppb range (Sholkovitz and Shen, 1995; Naqvi *et al*., 1996). In seawater REE exist primarily as REE-carbonate species, light REE's are more easily adsorbed to surfaces than the heavy REE's (Sholkovitz and Shen, 1995). REE's form a coherent group of elements and their chemical properties vary systematically across the REE series. Different source materials will have different REE patterns. Naqvi *et al*. (1996) used REE patterns to distinguish between monsoon and non-monsoon time periods in corals, the patterns reflected different amounts of terrigenous influence.

4.7.5 Pollution and Heavy Metals

Corals have been used to monitor environmental pollution for a number of years. Many different elements have been used to document this pollution (e.g. Hg, Cu, Zn, Pb, Mn, Fe, V, Cd, REE's etc. Veeh and Turekian, 1968; Brown and Holley, 1982; Dodge and Gilbert, 1984; Dodge *et al*., 1984; Denton and Burdon-Jones, 1986; Howard and Brown, 1986; Brown, 1987; Howard and Brown, 1987; Shen and Boyle, 1987; Harland and Brown, 1989; Hanna and Muir, 1990; Scott, 1990; Brown *et al*., 1991; Shen *et al*., 1991; Allison and Tudhope, 1992; Guzman and Jimenez, 1992; McConchie and Harriott, 1992; Sholkovitz and Shen, 1995; Allison, 1996a; Guzman and Jarvis, 1996; Bastidas and Garcia, 1999). Pollution can be characterized as either point, non-point or unpredictable point source; examples of point source pollution are ports, dockyards,

sewage, mining, and dredging; non-point sources are agriculture and soil erosion; unpredictable point sources are, oil spills etc. (Guzman and Jimenez, 1992). These pollutant metals can arrive in coral skeletons either as dissolved or particulate metals. Figure 4.8 indicates some possible metal pathways into coral skeletons (Brown, 1987). Dissolved metals can enter the coral directly in the lattices (e.g. Pb, Cd Shen and Boyle, 1988) or by way of zooxanthallae and/or plankton (Figure 4.8) (Brown, 1987). Particulate matter in seawater consists of clay minerals, colloids, organic material and plankton which all have high metal binding capacity (St.John, 1974). These particulates may be "accidentally" incorporated during calcification (St.John, 1974) or fill open skeletal spaces appearing as detritus. Detrital material has been observed in many corals through the use of scanning electron microscocopy (Barnard *et al*., 1974; Naqvi *et al*., 1996). Another incorporation mechanism proposed by Brown *et al*. (1991), based on iron measurements, suggests that during stress coral tissue retracts leaving their mucus exposed. This exposed mucus has a high affinity to bind metals and when conditions improve the tissue grows back over the exposed skeletal spines and the metals are calcified over (Brown *et al*., 1991). The metal entrapment of these particles or precipitated material would be resistant to conventional cleaning methods because it is trapped in the skeleton.

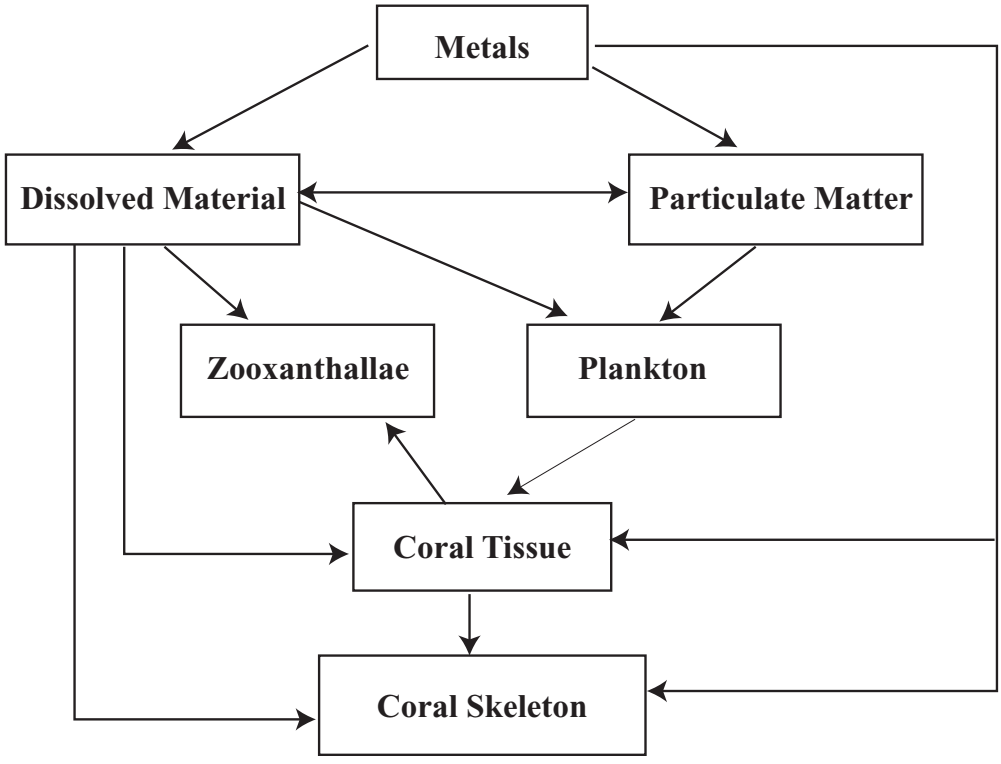

Figure 4.8 The possible pathways for metal accumulation in corals, from (Brown, 1987).

The variability of these different incorporation mechanisms may account for the large range of reported metal concentrations (Table 4.1). Some researchers propose extensive and rigorous cleaning mechanisms to isolate lattice metals (e.g. Shen and Boyle, 1988; Sholkovitz and Shen, 1995). Others suggest that the combination of lattice and sediment bound particles are a more useful indicator of the coastal environment (e.g. Guzman and Jimenez, 1992). Either way, the conclusion is that corals have the necessary requirements to be used as biomonitors of pollution (e.g. Brown and Holley, 1982; Hanna and Muir, 1990; Guzman and Jimenez, 1992).

Table 4.1. Minor element concentrations in corals.

Element (ppm)	Fe	Mn	Zn	Pb	V	Cd	Y	Cu	Reference
	1.3 - 300		0.8 - 42	0.03 - 4.7	.03 - 1.6			3.3 - 89	Bastidas and Garcia (1999)
	45 - 94		1.4 - 3.7					0.8 - 1.6	Brown and Holley (1982)
	70 - 113	7	9.0 - 10	32	40	7.6		2.0 - 4	Guzman and Jimenez (1992)
	11.0 - 38	5.6 - 6.8	3.4 - 9.3	44 - 51	5.9 - 7.6	0.04 - 0.06		0.78 - 0.84	Hanna and Muir (1990)
		1.4 - 4.7		0.18 - 0.58		0.06 - 0.14			McConchie and Harriott (1992)
				0.2 - 0.8	0.1 - 0.8	ppb - 2	0.05 - 0.15	8	Scott (1990)
			2.4	0.27					St. John (1974)
			1.8 - 12				1.5 - 3		Howard and Brown (1986, 1987)
		0.008 - 0.02	0.02 - 0.07	0.01 - 0.1	0.05	0.0008 - 0.008			Shen and Boyle (1988)

Chapter 5: Corals at their latitudinal limits: Shirigai Bay, Japan

5.1 Introduction

Coral reefs are under increasing threat not only from direct human impacts but also from changing climatic patterns. Corals growing in environments close to their survivability are likely to be those most sensitive to climate change. Hence, developing a better understanding of factors controlling coral reef growth and long-term sustainability is of general importance. A *Porites lobata* coral core was collected from one of the most northern coral reefs of Japan (Shirigai Bay, 32°46′ N, 132°42′ E) (VanWoesik, 1995). This location provides a 'unique' opportunity to study the response of trace element systematics and coral growth over a wide range of environmental conditions, where the SST ranges from 15-29°C. Corals from locations with winter temperature extremes may also provide an important insight into reef growth during glacial conditions. The following chapter is an abbreviated excerpt from the published manuscript of Fallon *et al*. (1999b). A reprint of the publication is in Appendix 2.

5.2 Location

A core was extracted from a 2m diameter *Porites lobata* coral in Shirigai Bay, Shikoku Island, Japan (32°46′ N, 132°42′ E) in 1993 (Figure 5.1). Shirigai Bay supports a 2.5-hectare reef coral community and is one of the most northern coral communities in the world. The warm Kuroshio Current, which originates in equatorial waters extends north to Shirigai Bay and beyond. The bay has a wide diversity of corals, ~ 63 scleractinian coral species (Veron, 1992), covering approximately 70% of the rocky substrate. No carbonate accumulation is evident. Outside the bay, tides flood to the west and ebb to the east. A deep channel (15 m) splits the bay entrance, which occasionally brings cold,

nutrient rich, jets of deep water into the bay. This form of "local" upwelling is most likely related to shifting wind patterns, when the summer southwesterly is replaced by a northwesterly pattern. The SST in the bay ranges from ~15°C in February to ~29°C in August (Komame station data, See Figure 5.1).

Figure 5.1 Sampling location in Japan. The *Porites* coral core was collected from Shirigai Bay (32°46´N, 132°42´E), the instrumental SST record used was from Komame (an aquaculture station ~2-3 km south of Shirigai Bay).

5.3 Methods

The coral was analyzed using the methods described in Chapter 2. The coral sample was cut parallel to the axis of growth in 7 mm slabs and X-rayed to reveal the density variations. A sampling transect along the slice was chosen to follow the main axis of growth (Alibert and McCulloch, 1997).

5.4 **Results and Discussion**

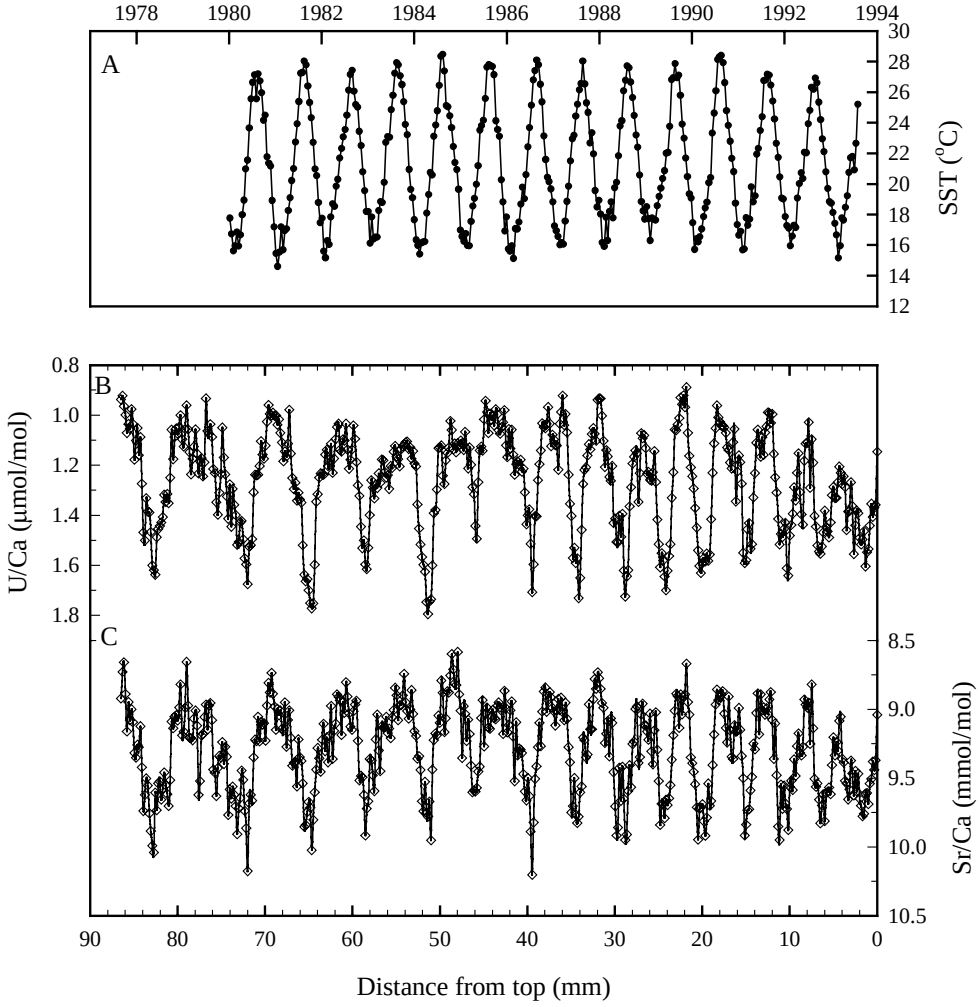

Figure 5.2 A) Fortnightly SSTs from Komame station. B) U/Ca vs. distance from the top of the Shirigai Bay *Porites* coral. C) Sr/Ca vs. distance from the top of the Shirigai Bay *Porites* coral. Diamonds represent individual measurements.

A 9 cm length of the Shirigai Bay coral core was analyzed for B, Mg, Sr, Ba and U. The Sr/Ca and U/Ca data is shown in Figure 5.2. The average annual extension of this coral is 5.3 ± 1.2 mm yr^{-1} and the scan therefore covers approximately 16 years of coral growth. Each data point shown (Figure 5.2) is a running average of 5 seconds of analytical time resulting in an effective resolution of 0.15mm which is similar to the coral calix depth. This sampling interval provides approximately fortnightly resolution.

5.4.1 Correlations Between Elements

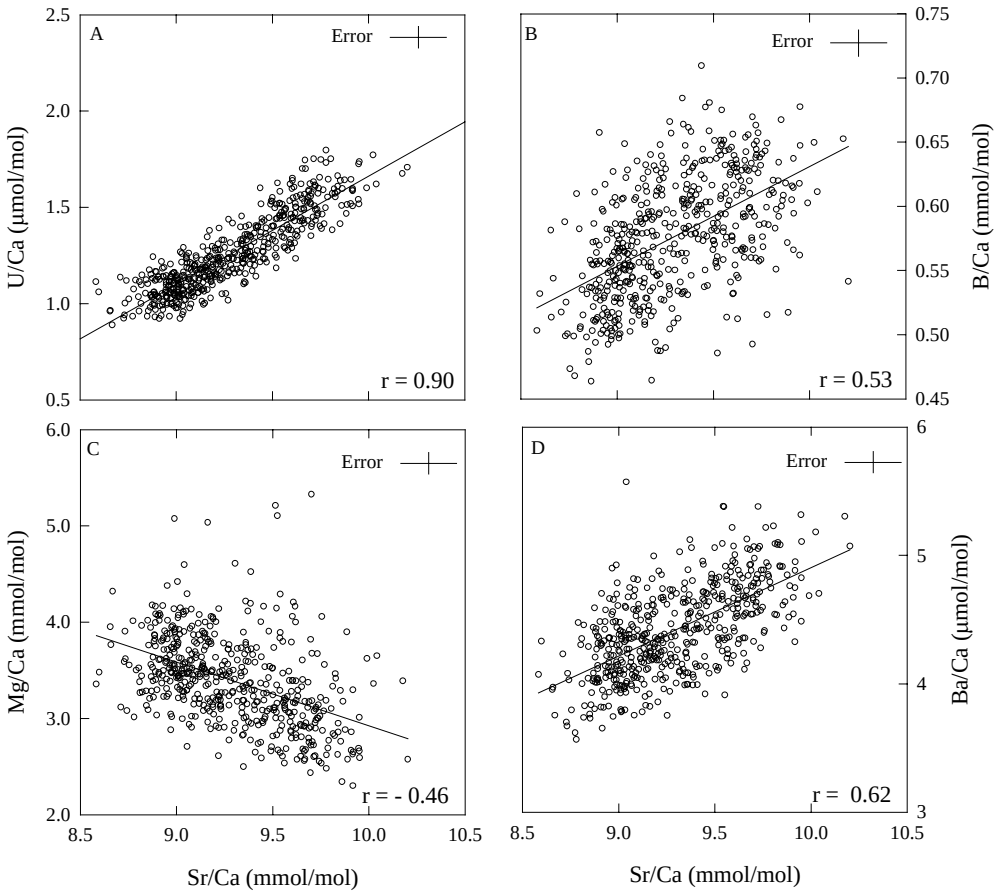

Figure 5.3 A) Linear regression of U/Ca vs. Sr/Ca. B) Linear regression of B/Ca vs. Sr/Ca. C) Linear regression of Mg/Ca vs. Sr/Ca. D) Linear regression of Ba/Ca vs. Sr/Ca.

Regression of Sr/Ca vs. U/Ca, B/Ca and Mg/Ca are given in Figure 5.3. A strong correlation ($r = 0.9$, $p < 0.0001$) exists between Sr/Ca and U/Ca, which agree with previous results (Min *et al*., 1995). However, the correlations between Sr/Ca and Mg/Ca and Sr/Ca and B/Ca ($r = -0.46$ and 0.53 respectively) are not as high as previously reported by Mitsuguchi *et al*. (1996) and Sinclair *et al*. (1998) indicating that B and Mg may be influenced by other factors aside from temperature.

5.4.2 Length to time translation

Translating from distance to time usually involves correlating the “element”/Ca to SST maximum and minimum and assuming linear growth between these “marker” points.

This approach is not adequate for this coral because of the extreme summer to winter growth bias. Evidence for a marked decrease, or cessation, of winter growth can be seen in Figure 5.2, where the winters are under represented as sharp spikes compared to the broad peaks for summer. A quantitative representation of this effect is shown in the histogram of the number of data points sampled at ~0.15 mm growth increments (Figure 5.4). The measured SST has approximately a sinusoidal pattern with winter having a slightly higher abundance of points than summer (Figure 5.4A), whereas for the coral ~ 3 times more points (U/Ca and Sr/Ca) were sampled in summer versus winter (Figure 5.4 B, C). The "arched" shape of the trace element profiles is very similar to model simulations of coral growth with variable intra-annual extension rates by Barnes *et al*. (1995). These workers showed that trace element profiles took on an "arched" shape when summer extension increased relative to winter extension. Our data reproduces the sharp/narrow winter peaks observed by the model simulated trace element profiles when winter extension is stopped (Barnes *et al*., 1995). Using the simulations as a guide, we tested the correlation between U/Ca and SST by assuming variations in winter extension.

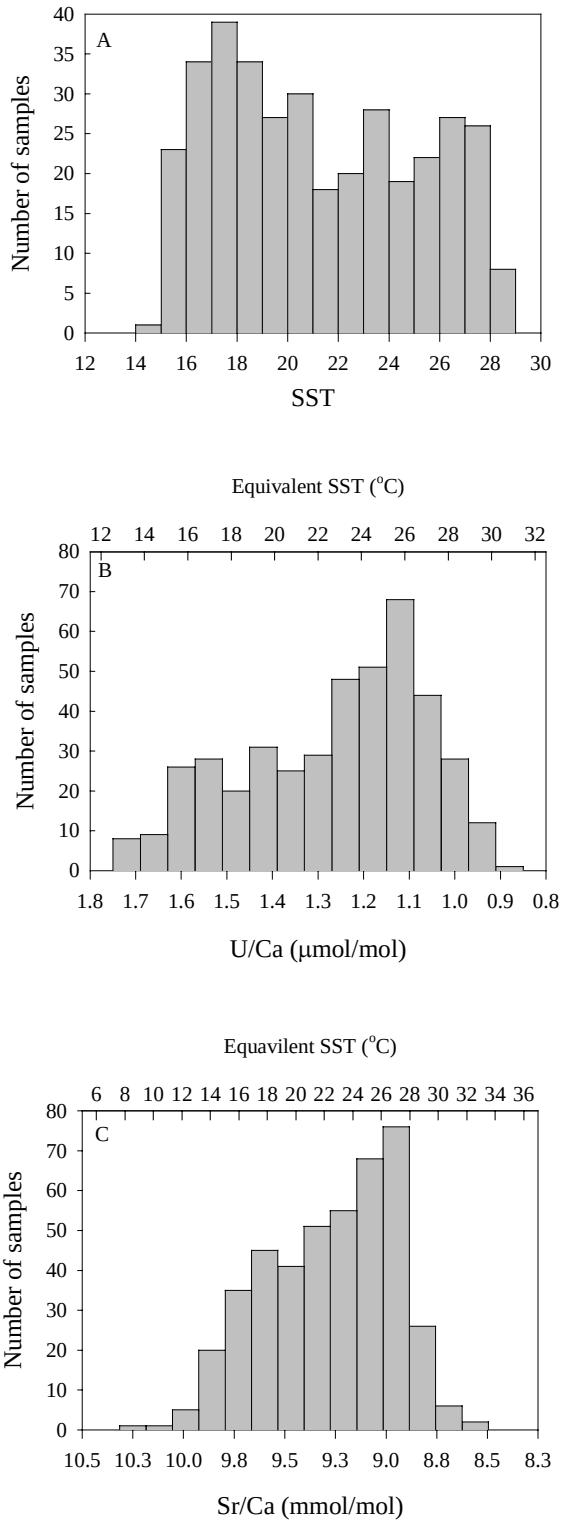

Figure 5.4 A) Histogram of Komame sea surface temperatures (SSTs), number of observations vs. SSTs. Notice a slightly higher abundance of data points sampled between 16° and 19°C. B) Histogram of U/Ca values. Notice a higher abundance of data points sampled between 1.25-1.1 μmol/mol, which is approximately equivalent to 23-26°C (top X-axis). C) Histogram of Sr/Ca values. Notice a higher abundance of data points sampled between 9.2-8.9 mmol/mol, or at 24-28 °C.

Based on the assumption that little to no growth was occurring during the winters, a time gap was inserted during each winter minimum. Using the minimum measured SST's as a guide, the effects of assuming non-uniform growth for different periods was examined (1week to 4 months). The optimum fit for the U/Ca (and Sr/Ca) ratios was obtained for an ~2-month cessation of growth between early January and late March when SST < 18 °C. Linear growth was then assumed to occur within the remaining interval, that is from spring to late fall. It is noted that an absence of winter growth for 2 months is a simplifying assumption that cannot be resolved from very slow (< 1 mm yr^{-1}) winter growth rates.

A comparison of the best fits for U/Ca (and Sr/Ca) and measured SST versus time is shown for the two cases, i.e. uniform annual growth (Figure 5.5 A) versus an absence of winter growth (Figure 5.5 B, C). For uniform annual growth, the relationship of U/Ca to SST has a correlation coefficient of r = -0.71, compared to an r = -0.84 for the 2 month cessation of winter growth. Inputting an absence of growth considerably improves the U/Ca/SST interpretation, however there are still outliers. This has been noted previously by McCulloch *et al*. (1994) for coral growth during winter in the inshore region of the GBR where cool (< 20°C) temperatures are sometimes recorded.

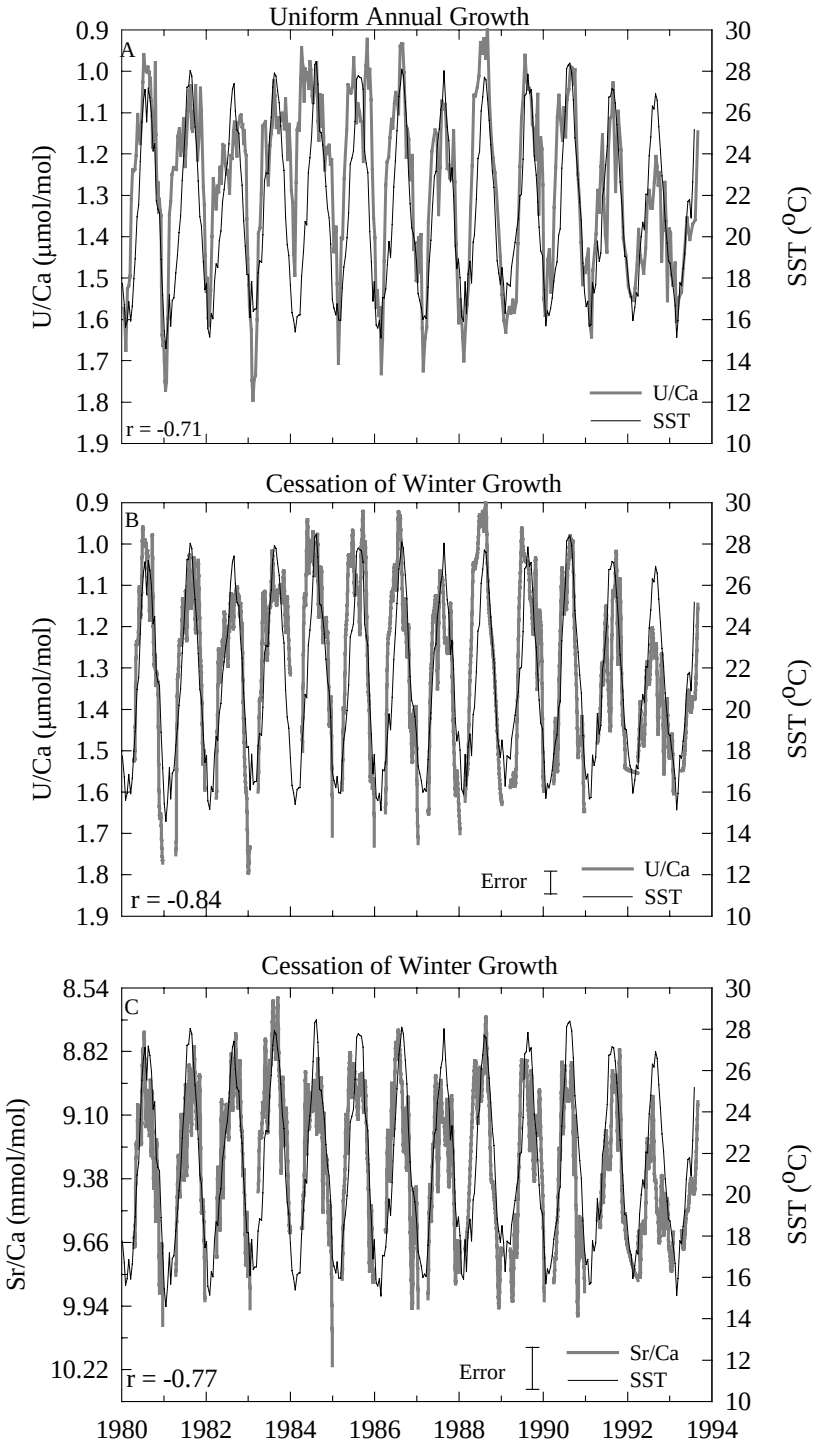

Figure 5.5 A) U/Ca and Komame SSTs vs. time assuming uniform growth between winter minimum and summer maximum SSTs. Note the U/Ca curve is much broader from early spring to late autumn. Correlation coefficient for this least squares regression is r = -0.71. B) U/Ca and SST vs. time using 2-month cessation of growth model. By assuming little/no growth during the winter (SST < 18°C) we assigned marker points then assumed linear growth between these points. The result is a better visual and statistical fit (r = -0.84). C) Sr/Ca and SST vs. time using the 2-month cessation of growth model, this also provides a better fit between the data and SSTs.

5.4.3 SST and Elemental Calibrations

Using this chronology the elemental ratios are compared with the fortnightly SST record. Linear regressions between U/Ca, Sr/Ca, B/Ca and Mg/Ca vs. SST were computed and are shown in Figure 5.6. The least squares regression equations for these elements are:

$U/Ca * 10^6 = 2.26 (\pm 0.05) - 0.044 (\pm 0.022) * SST (°C)$ r = -0.84
$Sr/Ca * 10^3 = 10.76 (\pm 0.08) - 0.063 (\pm 0.003) * SST (°C)$ r = -0.77
$B/Ca * 10^3 = 0.767 (\pm 0.015) - 0.009 (\pm 0.001) * SST (°C)$ r = -0.74
$Mg/Ca * 10^3 = 1.38 (\pm 0.161) + 0.088 (\pm 0.007) * SST (°C)$ r = 0.66

Under the assumption of cessation of growth, the regression equations are not applicable to temperatures below 18°C.

The calibrations presented here are similar to previously reported calibrations with some discrepancies (Figure 5.6) (de Villiers *et al*., 1994; Min *et al*., 1995; Mitsuguchi *et al*., 1996; Alibert and McCulloch, 1997; Gagan *et al*., 1998; Sinclair *et al*., 1998). The calibration of Sr/Ca to water temperature has been the most widely studied of the temperature proxies and several calibrations exist for the genera *Porites*. Calibrations from Alibert & McCulloch (1997), de Villiers *et al*. (1994) and Gagan *et al*. (1998) are plotted for comparison with our dataset (Figure 5.6 A). There is a wide range of published calibrations, and considering the larger error associated with our laser ablation technique our calibration falls closely within the reported range (Figure 5.6A). However, no good explanation has been provided for the offsets reported between high-precision TIMS Sr/Ca calibrations. But, more importantly the slope and temperature dependence provided by our calibration is very close to the previously reported calibrations (Beck *et al*., 1992; de Villiers *et al*., 1994; Shen *et al*., 1996; Alibert and McCulloch, 1997; Gagan *et al*., 1998).

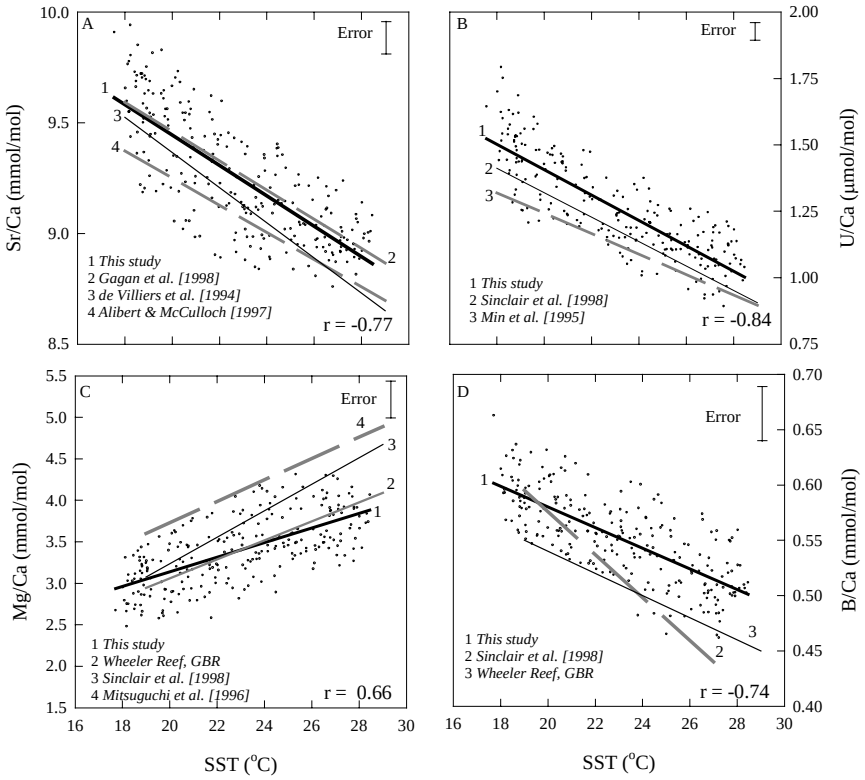

Figure 5.6 A) Linear regression of Sr/Ca vs. Komane SSTs. Also shown are calibration lines from de Villiers *et al*. (1994), Alibert & McCulloch (1997) and Gagan *et al*. (1998). b) Linear regression of U/Ca vs. SST. Also shown are calibration lines from Sinclair *et al*. (1998) and Min *et al*. (1995). c) Linear regression of Mg/Ca vs. SSTs. Also shown are calibrations from Mitsuguchi et at. (1996), Sinclair *et al*. (1998) and a coral from Wheeler Reef (see Chapter 6). d) Linear regression of B/Ca vs. SST. Also shown are calibration lines from Sinclair *et al*. (1998) and a coral from Wheeler Reef (see Chapter 6).

Two previously reported calibrations for U/Ca and temperature from Min *et al*. (1995) and Sinclair *et al*. (1998) are plotted for comparison with our dataset (Figure 5.6 B). Our calibration is offset from Min *et al*. (1995) and Sinclair *et al*.(1998), and gives temperatures between 2-4 °C higher, although the slope and temperature dependence are both very similar (Figure 5.6 B). It appears that discrepancies similar to those for Sr/Ca may exist for the U/Ca temperature calibrations.

5.4.4 Mg/Ca

The annual cycles of Mg/Ca are clearly visible (Figure 5.7 A) but are weakly correlated with SST (r = 0.66) (Figure 5.6 C). This is generally consistent with previous measurements of the Mg/Ca ratio in corals (Oomori *et al*., 1982; Hart and Cohen, 1996;

Mitsuguchi *et al*., 1996; Sinclair *et al*., 1998). Calibration lines for Mg/Ca, based on data from Mitsuguchi *et al*. (1996), Sinclair *et al*.(1998) and Wheeler Reef, GBR (see Chapter 6) are shown in Figure 5.6C. The calibration from Wheeler Reef, GBR is very similar to the Shirigai Bay coral however a large offset (outside analytical error) exists for the data of Mitsuguchi *et al*. (1996) (Figure 5.6C). The calibration provided by Sinclair *et al*. (1998) falls between the two with a much steeper slope (Figure 5.6C). We do not attribute these calibration offsets to inaccuracy of the laser method, more likely they are due to different environmental conditions of the coral or to differing biologic factors affecting the incorporation of magnesium.

However, large variations across short distances (weeks to months) approaching 50-60% of the annual signal were observed in some sections of the record (Figure 5.7 A). This short time scale variability cannot be associated with any SST variations but must be attributed to another mechanism. Micro-scale heterogeneity has also been observed in corals analyzed by Allison and Tudhope (1992), Allison (1996b) and Sinclair *et al.* (1998). The high-resolution nature of laser and other micro beam techniques may enhance the observation of this heterogeneity. In a study by Mitsuguchi *et al*. (1996), a more coarse sampling approach was undertaken (each sample equivalent to ~ 3 weeks of growth) and this fine scale heterogeneity was not observed. It appears that bulk sampling may smooth some of the heterogeneity.

Amiel *et al*. (1973a) suggested that Mg^{2+} could occur either in adsorbed sites or in organic phases as well as in the crystal lattice, with the lattice component easily displaced by Ca^{2+} during leaching. Amiel *et al*. (1973a) also suggested that different amounts of organic phases, adjacent to each other, could possibly explain this fine scale heterogeneity. The variability in the metal binding capacity of the coral tissue organic matrix, and its heterogeneity throughout the depth of the coral, may also play an important role (Mitterer, 1978; Allison and Tudhope, 1992; Allison, 1996b). Clearly more work is needed to understand the fine scale variations of Mg in corals.

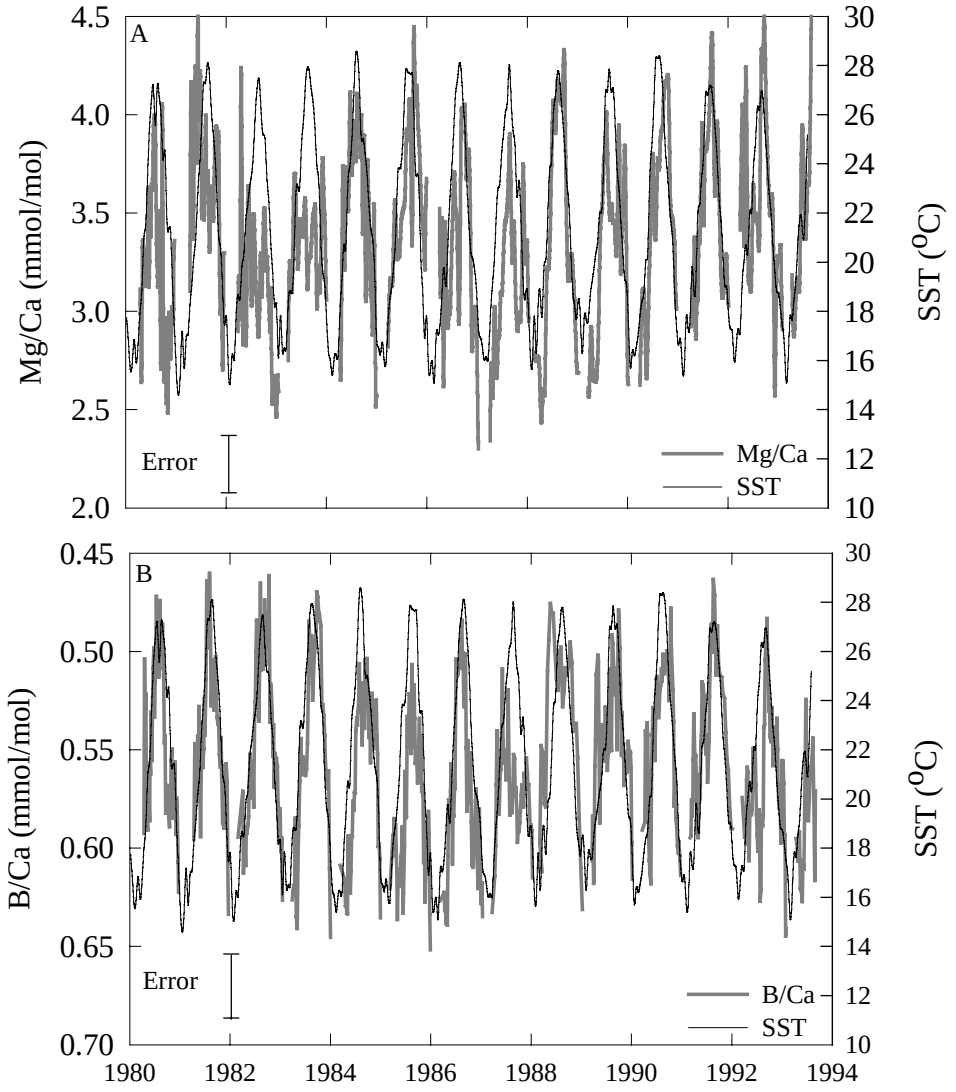

Figure 5.7 A) Mg/Ca and Komame SSTs vs. time using 2-month cessation of growth model. B) B/Ca and Komame SSTs vs. time using 2-month cessation of growth model.

5.4.5 B/Ca

The B/Ca ratio in corals has been suggested to be a paleothermometer by Hart and Cohen (1996) and Sinclair *et al*. (1998). The only previously published calibration for B/Ca is from Sinclair *et al*. (Sinclair *et al*., 1998) and there is a large discrepancy when this is compared to this data (Figure 5.6 D). The calibration for the coral from Wheeler Reef, GBR (see chapter 6) is also shown for comparison. The slopes of the Shirigai Bay coral and the Wheeler Reef coral are very similar but the temperature offset is on the order of 4-6°C (Figure 5.6 D).

The speciation of boron in seawater can be affected by many factors, including: pH, temperature, borate to carbonate ratio in seawater, and biological and kinetic factors (Vengosh *et al*., 1991; Hemming and Hanson, 1992; Gaillardet and Allegre, 1995). Sinclair *et al*. (1998) noted a high correlation between B/Ca and SST (r = -0.91) for a mid-reef site in the GBR. In this study we observe a moderate correlation between B/Ca and SST (r = -0.74, $p < 0.0001$) (Figures 5.6D, 5.7D). As mentioned previously for Mg/Ca, we also observed large elemental excursions across short distances approaching 60-70% of the annual signal (Figure 5.7B). Large shifts, not attributable to SST, may limit the use of B/Ca as a paleothermometer but when used in conjunction with U/Ca or Sr/Ca these fine-scale variations may be able to provide additional information on other environmental influences. Clearly more work is needed in order to establish the veracity of B as a temperature proxy.

5.4.6 Winter Growth Changes

Decreased extension and hence calcification during cold winter temperatures has been noted previously (Buddemeier and Kinzie, 1975; Houck *et al*., 1977; Crossland, 1981; Wellington and Glynn, 1983). Reduced growth rates of *Pavona* sp. corals on the western side of the Galapagos Islands, as opposed to other locations on the islands, have been attributed to reduced SST in winter that are triggered by upwelling events (SST 17-18 °C) (Wellington and Glynn, 1983). In studies on *Porites lobata*, Houck *et al*. (1977) noted a growth rate decrease of up to 2x the summer rate when SST approached 22°C. The evidence shown in other studies suggest a decrease in winter growth, but not a full cessation of growth as shown in the present study.

Jacques *et al*. (1977) suggested calcification rates approached zero as temperature reached 16°C. Our coral grew in temperatures below 16°C for ~3 to 4 weeks every year and below 18°C for 2-3 months (Figure 5.2A). In conjunction with the trace element profiles showing sharp winter peaks and few samples, we conclude that *Porites* corals essentially cease extension in winter in high latitude habitats with a temperature cut-off of ~ 18°C.

5.4.7 SST Variations, Upwelling and Ba/Ca

The summer SST's during 1982, 1991 and 1992 are cooler than the "average" summer, (Figure 5.5 A) consistent with the U/Ca ratios that also indicate cooler than normal summer water temperatures (Figure 5.5 B). These cooler summer temperatures coincide with years characterized as El Niño periods. One factor that may play a role in determining which years have cooler summer SST's is local upwelling. In Shirigai Bay, along the coast of Shikoku, local upwelling occurs when the summer SW airflow is replaced by a winter NW wind pattern. Data from buoys in the bay suggest a deep-water channel (15m) on the eastern side of the bay provides an access for cold, nutrient rich, water to enter into the shallow coral zones. The effects of upwelling on SST at this site will be discussed later.

Barium can substitute for calcium into the aragonitic crystal lattice of reef corals. The concentration of Ba in seawater increases from low values in warm surface water to high values in deep, cold, and nutrient rich water. Therefore cycles in the Ba/Ca ratio in corals, away from coastal river runoff, are most likely controlled by the strength of local upwelling (Lea *et al*., 1989; Tudhope *et al*., 1996). However, it has been suggested that the barium distribution coefficient has a slight temperature dependence but this hasn't been verified (Lea *et al*., 1989; Shen *et al*., 1992a). However, if it exists it will be small compared to the upwelling signature recorded by this coral.

The observed range of Ba/Ca in this coral is approximately 3.9-5.1 μmol/mol. Using a distribution coefficient of 1.27 (Lea *et al*., 1989), the coralline Ba/Ca can be converted to an estimate of seawater barium content. The seawater barium concentration ranges from a low of 31 nmol/Kg in the summer to a high of 41 nmol/Kg in the winter. These values are consistent with inferred seawater barium concentrations from corals in an upwelling zone of the Galapagos, whose values ranged from 32-40 nmol/Kg (Lea *et al*., 1989; Shen *et al*., 1992a).

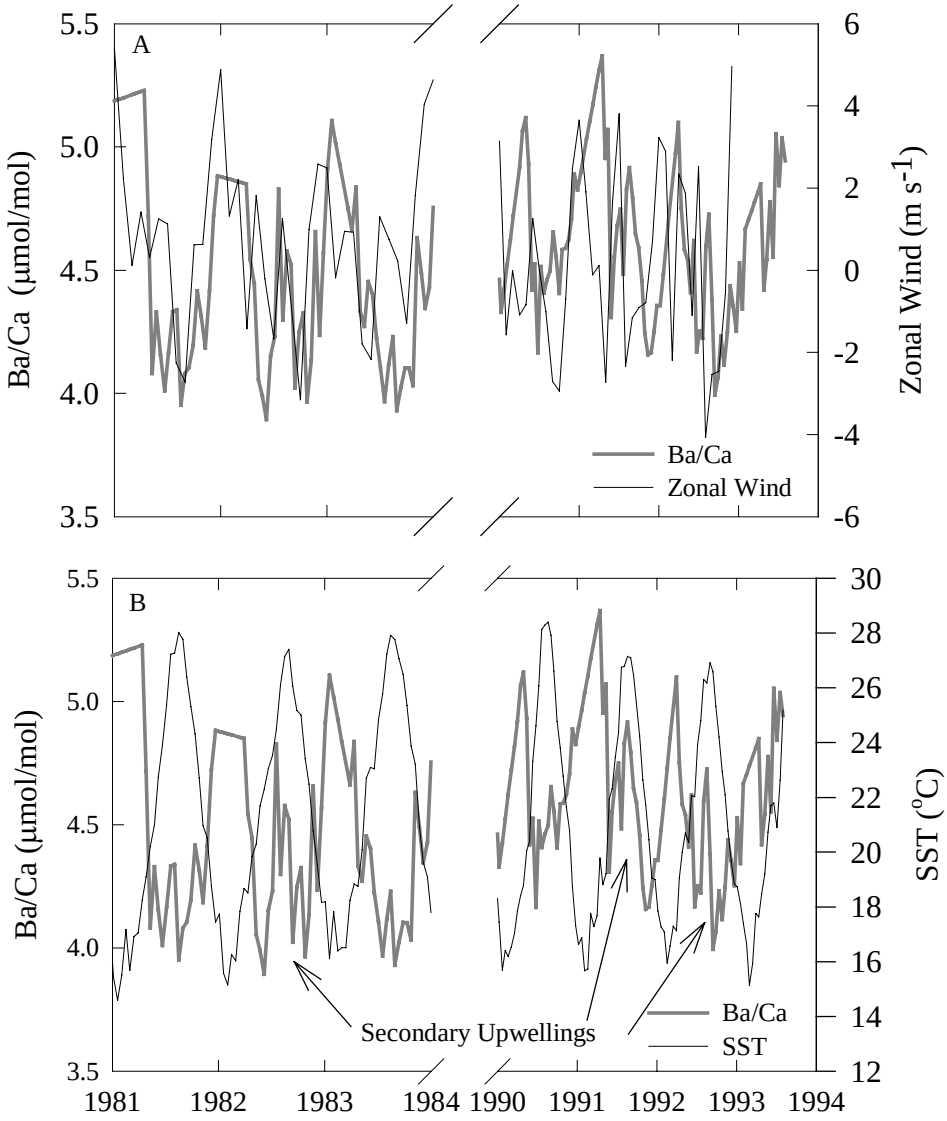

Figure 5.8 A) Ba/Ca and Zonal wind velocity vs. time. Zonal wind dataset from COADS (2°x2°) grid centered on 33ºN, 133ºE. Note positive zonal wind peaks lead Ba/Ca peaks by ~ 2 months. During the El Niño years (1982, 1987, 1991, 1992) multiple peaks in both the zonal wind and Ba/Ca occur. Cross correlation indicates a 2 month lag by the Ba/Ca to the zonal winds r = 0.51. B) Close-up of Ba/Ca and SST vs. time from 1981-84 and 1990-94 showing secondary upwelling in the summers of 1982, 1991 and 1992.

The Ba/Ca cycles in the *Porites* coral peak just after a positive peak in the zonal wind speed (Figure 5.8 A). The wind direction appears to be forcing upwelling thereby bringing colder, Ba enriched water to the surface. Wind data from COADS (Slutz *et al.*, 1985) indicate that the shift to the NW wind pattern usually precedes the winter SST minimum by ~1-2 months (Figure 5.8A). The main inferred Ba/Ca upwelling peaks coincide with the U/Ca and Sr/Ca maximum and the SST minimum (Figure 5.8B). Cross correlation indicates the Ba/Ca lags the zonal wind by 2 months (r = 0.51 when

lagged by 2 months, no lag r = 0.25). Thus winter upwelling contributes to the extremely cold winter SST's measured in this area.

During the years 1982, 1987, 1991 and 1992 (the cooler summers) there are secondary peaks in both the zonal winds and Ba/Ca (Figure 5.8 A). It appears that there are changes in the "normal" atmospheric wind patterns during these periods that are associated with El Niño Southern Oscillation. The change in wind patterns observed in this coral is recorded as a second-stage increase in Ba/Ca during the summer (Figure 5.8). This suggests several upwelling events during these years. This second upwelling event is at least partly responsible for the cooler than average summer SST's during 1982, 1987, 1991 and 1992 (Figures 5.5B, 5.8B). The double upwelling signature identified in this study appears to be a useful proxy for the reconstruction of paleo-El Niño in this region.

5.5 Conclusions

The "arched" shape of our trace element profiles is indicative of increased extension in summer relative to winter. This is corroborated by model simulations of trace element profiles with little to no winter extension (Barnes *et al*., 1995). Our data suggest a marked decrease and/or cessation of extension and hence calcification during winter. A decrease or cessation of growth during cold winters has important implications for coral calcification and overall carbonate/reef accumulation.

U/Ca, Mg/Ca and B/Ca appear to exhibit similar calibration offsets as the Sr/Ca thermometer. It is expected however that as the database for these elements increase, factors influencing the temperature relationships and their (B, Mg, Sr, U) respective elemental budgets will be enhanced

The Shirigai Bay coral has an approximately linear response of U/Ca and Sr/Ca to temperatures above 18°C. Below this temperature there appears to be an increase in elemental incorporation during times of extreme cold and/or little to no growth. This study reinforces the notion that factors aside from temperature (i.e. adsorbed sites or variability in metal binding capacity of the organic matrix) could be affecting the Mg/Ca ratio. It also appears that other factors are influencing the B/Ca ratio aside from

temperature. The usefulness of Ba/Ca as an upwelling indicator is confirmed as well as showing how upwelling can influence SST. A secondary upwelling event occurs during El Niño summers causing cooler summer SST's, and may provide a proxy for detecting paleo-events in similar locations.

Chapter 6: Cross Shelf Coral Transect, GBR

6.1 Introduction

Through the chemical constituents trapped in their skeletons, corals can provide records of water temperature, salinity, runoff and upwelling intensity. Before they can be used to document these environmental parameters with confidence rigorous testing of these chemical proxies (Sr/Ca, U/Ca, Mg/Ca, B/Ca, Ba/Ca) must occur. An examination of the corals ability to faithfully record water temperature while influenced by fresh water (both rainfall and river flood plumes) is important. After testing, confidence in the fidelity of coralline paleoclimate records estimates of natural climate variability can be assessed. Our current climate system can then be compared and anthropogenic influences (e.g. Greenhouse gases and land use) can be assessed.

In this chapter I am testing the effects of proximity to the coastline on the water temperature (Sr/Ca, U/Ca, Mg/Ca, B/Ca), runoff/upwelling (Ba/Ca), and particle suspensions (Mn) proxies. Corals were analyzed and collected from an inshore, mid-shelf and outer shelf transect across the central Great Barrier Reef (GBR). The consistency between the temperature calibrations for these elements in *Porites* corals from different environments is also examined. In this transect the inshore reefs are heavily influenced by runoff from the Burdekin River (Figure 6.1). The mid and outer reefs are relatively unaffected by nearshore processes with the possible exception of sediment resuspension and are considered “open-ocean”.

6.2 Methods and Locations

The “major” elements (B, Mg, Sr, Ba, U) and “minor” elements (Mn) were analyzed using LA-ICP-MS. The coral collection, processing and analytical methods are described in detail in Chapter 2 & 3. The corals were collected from reefs across the central GBR corresponding to inshore reefs (Havannah Island, Orpheus Island, Pandora Reef), mid-shelf (Davies Reef, Wheeler Reef) and outer-shelf (Myrmidon Reef) (Figure 6.1).

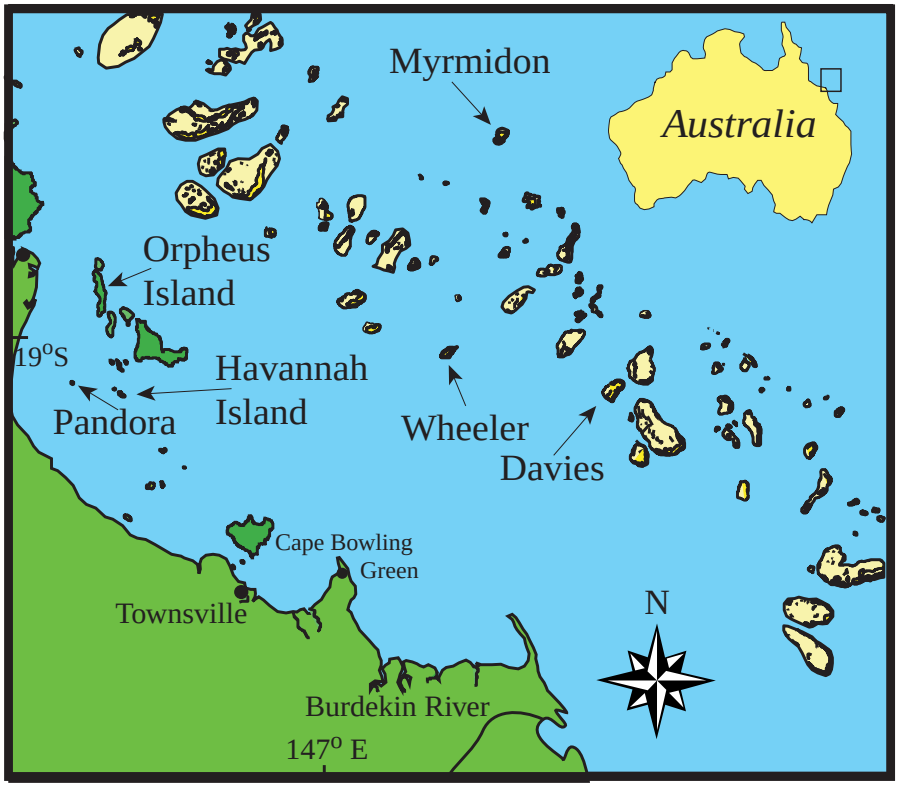

Figure 6.1 Map of sample locations for the GBR transect. Havannah Island, Orpheus Island and Pandora Reef make up the inner shelf corals. Mid-shelf corals were collected from Wheeler and Davies Reefs. Outer shelf corals were collected from Myrmidon Reef.

6.2.1 Inshore Reefs

Pandora Reef

Pandora reef is a small platform reef located approximately 17 km from the shore (Figure 6.1). There are few islands surrounding the reef indicating oceanographic conditions should well mixed. A *Porites* coral was drilled in October 1998 (by S. Fallon and coworkers) at a water depth of 2m. Two cores were collected from one colony; one core was partially bleached on top, the other core appeared to be unbleached. They were labeled Pan 1-98a; Pan 1-98b, both will be discussed in this section. Fluorescent lines are visible in both of the coral cores. These lines have been attributed to Burdekin River runoff (Isdale, 1984; Boto and Isdale, 1985; Isdale *et al*., 1998). A section of Pan 1-98a, 138 mm in length encompassing the time period 1990-1998 was analyzed by LA-ICP-MS. A 46 mm section of Pan 1-98b (1996-1998) was also analyzed.

Orpheus Island

Orpheus Island is located ~ 25 km from the coast and is ~ 28 km North from Pandora Reef (Figure 6.1). The coral was drilled by the Australian Institute of Marine Sciences (AIMS). The coral was collected in 2.5 m water depth ~ 100m off the northern tip of the island. The environment surrounding the coral was well mixed as it was on the edge of a point. Orpheus Island is considered to be on the interface between inshore and the inner part of the mid-shelf. The piece analyzed was 48 mm in length and encompasses the time period 1989-1992. Fluorescent lines are also visible indicating river runoff, most likely from the Burdekin River (see Sinclair, 1999).

Havannah Island

Havannah Island is approximately 25 km from the coast and is almost directly east of Pandora Reef (Figure 6.1). The coral core was collected in October 1998 by S. Fallon and coworkers at a depth of 2.5 m. A 120 mm section was analyzed by LA-ICP-MS and this covers the time frame 1993-1998. Fluorescent lines are also visible in this coral indicating the influence of the Burdekin River. The area around this coral is relatively shallow water and the coral record may not necessarily correspond to well mixed marine conditions.

6.2.2 Mid-Shelf Reefs

Davies Reef

Davies Reef is located on the mid-shelf of the central GBR (Figure 6.1). It is ~ 100 km east of Townsville. A full description of oceanographic conditions and coral collection is found in Alibert and McCulloch (1997). In brief, this mid-shelf location is a well-flushed lagoon and is not affected by nearshore processes (Alibert and McCulloch, 1997). Two corals form Davies Reef were examined for this study (Davies 2, Davies 8). The Davies 2 coral core was collected from 3.1 m water depth. The Davies 8 coral was collected at 6.5 m water depth. The cores were collected in October 1993. A 95 mm piece of Davies 2 was analyzed encompassing the time frame 1986-1993. A 46 mm piece of Davies 8 was analyzed and encompasses 1990-1993. This location is not affected by Burdekin River runoff.

Wheeler Reef

Wheeler Reef is also approximately 100 km from the coast and is 14 km west of Davies Reef (Figure 6.1). This site is also considered to be well mixed (Alibert and McCulloch, 1997). The coral core was drilled by AIMS in 1985. A 48 mm piece from 1982-1985 was analyzed by LA-ICP-MS.

6.2.3 Outer Shelf Reef

Myrmidon Reef

Myrmidon Reef is located on the outer shelf of the central GBR (Figure 6.1). It is approximately 150 km from the coastline, north of Townsville (Figure 6.1). This location is not affected by nearshore processes but may be subject to upwelling events (Marshall, in prep). D. Burrows collected the Myrmidon 2 coral in 1996. A detailed description of the location and cores can be found in Marshall (in prep). A 46 mm section was analyzed that covers the period 1988 – 1996.

6.3 Results

6.3.1 Sea Surface Temperatures (SST's)

The inshore *in situ* SST data come from data loggers installed at Orpheus Island by Great Barrier Reef Marine Park Authority (GBRMPA). The SST ranges from 20.8 ºC to 30.5 ºC with a mean value of 25.8 ºC during the time period 1993-1999 (Figure 6.2). This range is probably indicative of the inshore water temperatures at Pandora Reef and Havannah Island. The SST at Davies Reef ranges from 22.3 – 29.5 ºC with a mean value of 25.8 ºC (Figure 6.2). The outer reef station at Myrmidon Reef has SST ranging from 24.9 – 29.5 ºC; the mean SST is 27.4 ºC (Figure 6.2). Both of the latter datasets are from the AIMS weather stations (data courtesy of J. Lough). Also used is the IGOSS-NMC satellite-derived SST (see http://ingrid.ldeo.columbia.edu/). Weekly SST's are available for 1º latitude by longitude boxes across the globe. The data presented in Figure 6.2 is the box centered on 147.5º E, 18.5ºS. The satellite-derived SST indicates a range of 22.1 – 29.9 ºC with a mean of 26.2 ºC (Figure 6.2). In contrast to the satellite SST *in situ* data loggers suggest that winter temperatures were cooler for

reefs closer to the coast. The summer SST's are consistent between the sites. Only during a few summer months are the inshore SST's slightly higher (Figure 6.2).

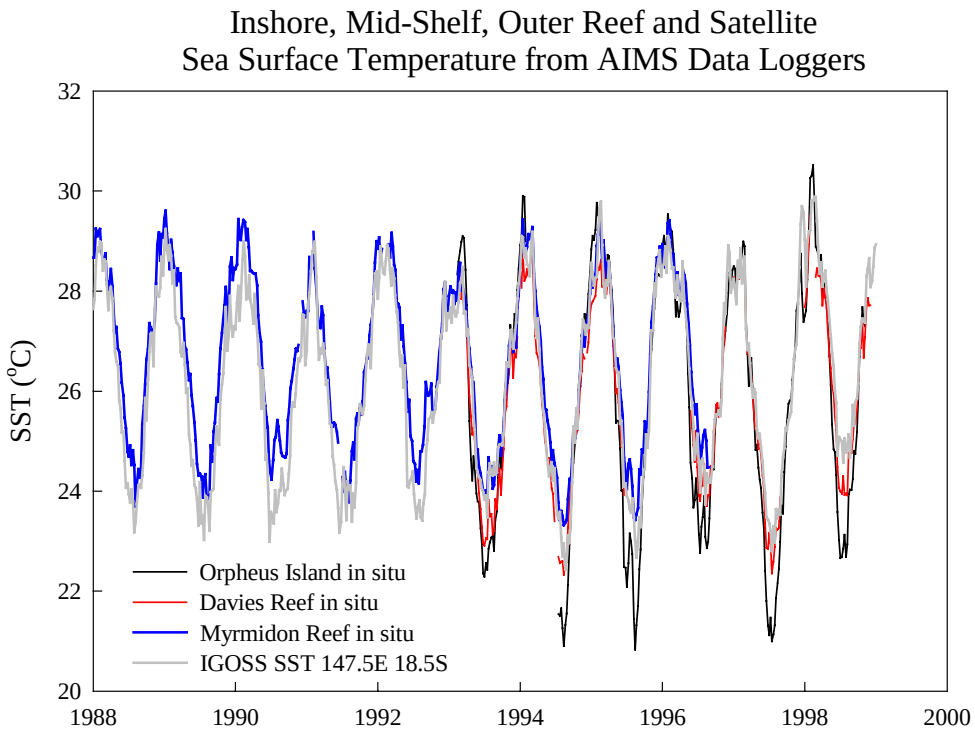

Figure 6.2 Sea surface temperature from Orpheus Island *in situ* data loggers (black), Davies Reef (red), Myrmidon Reef (blue) and IGOSS satellite (gray). In general winter SST's are cooler closer to the coast. All data is weekly resolution.

A limitation of data from *in situ* data loggers is that records are often of limited length or there can be missing data. To obtain more complete SST datasets with which to compare to the coral records, correlations were examined between the *in situ* SST and the satellite-derived SST (Figure 6.3). Very strong correlations exist between all the datasets (Figure 6.3). The satellite-derived SST records the rapid (weeks to months) variability that is observed by the *in situ* data loggers except that the satellite-derived SST is usually lower in amplitude (Figure 6.2). Davies Reef has the highest correlation to the IGOSS dataset, which is expected as it is near the center of the satellite grid box and should closely represent the "average" SST derived by the satellite. Composite SST's were constructed for the inshore, mid-shelf and outer reefs using the linear relationships of shown in Figure 6.3. The composite SST's are used to calibrate the trace element signals described in the next section.

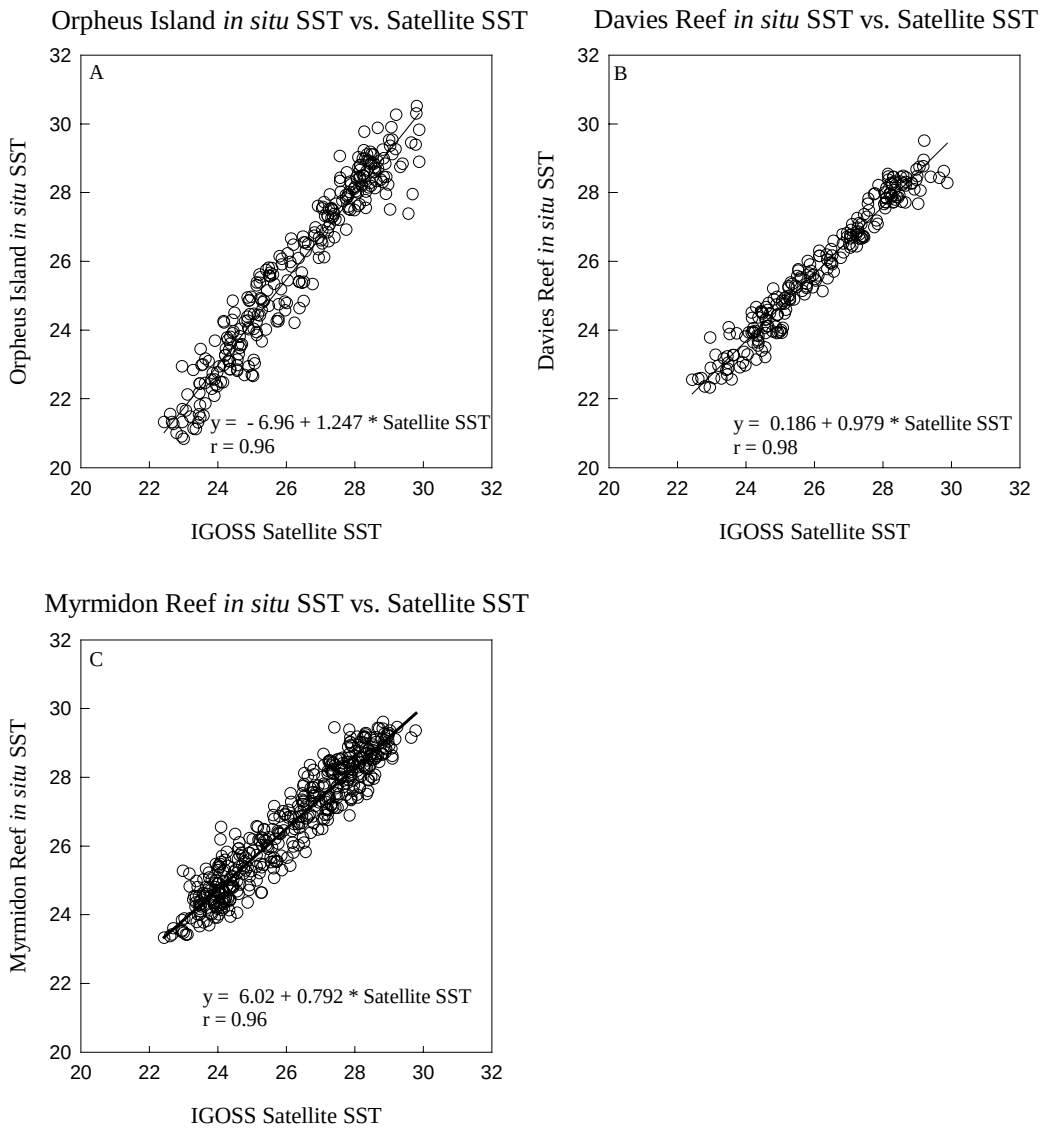

Figure 6.3 a) In situ SST from Orpheus Island vs. Satellite SST 147.5E 18.5 S (IGOSS). b) In Situ SST from Davies Reef data logger vs. Satellite SST 147.5E 18.5 S (IGOSS). c) In situ SST from Myrmidon Reef data logger vs. Satellite SST 147.5E 18.5 S (IGOSS). Linear correlations are shown for each comparison. Data obtained from AIMS.

6.3.2 Length to Time Translation of Coral Elemental Ratios

Seasonal cycles of Sr/Ca were used to construct time series for all corals except the Havannah Island coral where Mg/Ca was used due to the absence of a clear Sr/Ca seasonal cycle. Maximum Sr/Ca values (minimum SST) were matched to minimum SST values and minimum Sr/Ca was matched to maximum SST values using the Analyseries program (Paillard *et al.*, 1996). Linear growth was assumed to occur between summer and winter marker points. This assumption provides a reasonably good approximation for this transect. All data was then resampled to the same weekly

resolution to facilitate comparisons between weekly SST datasets and other elemental ratios using the Analyseries program (Paillard *et al.*, 1996).

6.3.3 Inshore Reefs

Pandora Reef

The Pandora reef coral record encompasses the time period Dec. 1990 – Oct. 1998. All elements aside from Ba/Ca show clear seasonal cycles (Figure 6.4). Sr/Ca, U/Ca,

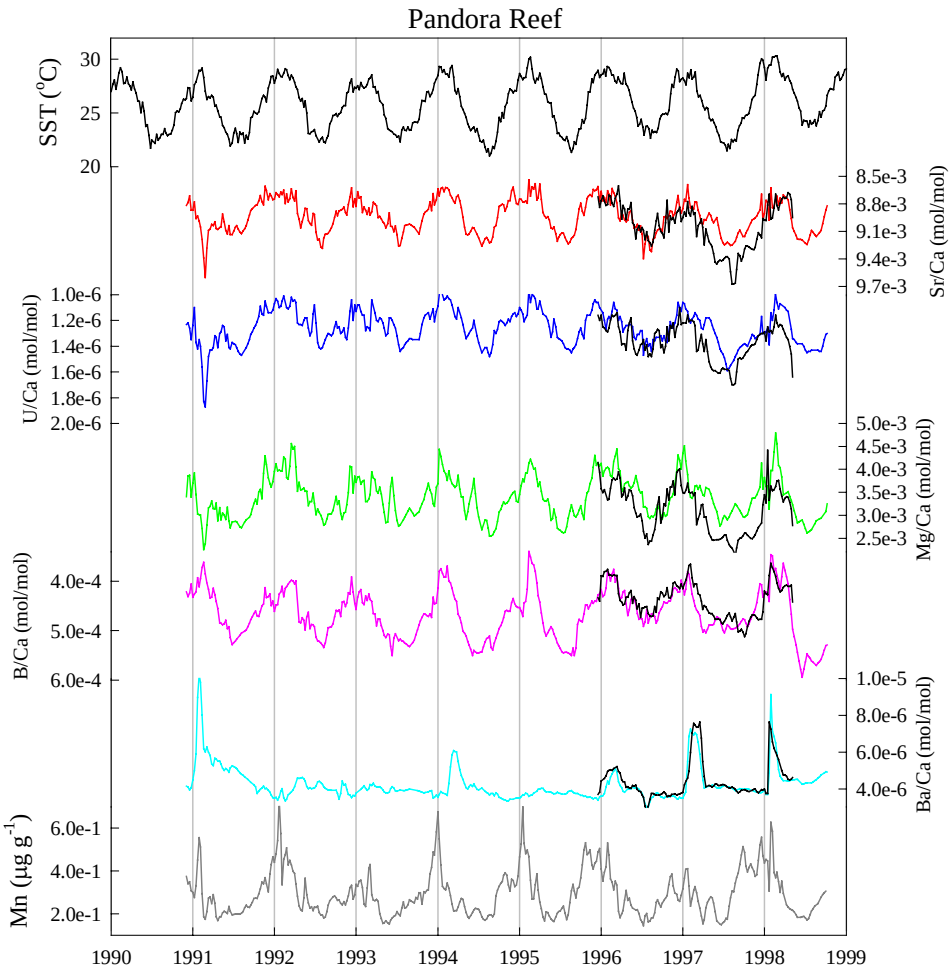

Figure 6.4 Trace element profiles from Pandora Reef corals vs. time. IGOSS SST adjusted to reflect inshore variations from equation in Figure 6.3a shown for comparison. Colored lines indicate coral Pan 1-98a, black overlay is coral Pan 1-98b. Y-axes for Sr/Ca, U/Ca, B/Ca and Mg/Ca are scaled to reflect temperature.

Mg/Ca and B/Ca vary in conjunction with observed changes in water temperature (Figure 6.4). Pan 1-98b was not alive on top when collected in October 1998.

Comparison between trace element signals between the two cores indicate that pan 1-98b probably stopped recording environmental information ~ March/April 1998. This was 2-4 months after the January bleaching event. The Ba/Ca record recovered from both cores show increases at the same time. These increases have been attributed to nearshore barium release during Burdekin River floods (Sinclair, 1999). The manganese signal shows a clear annual signal too, increasing in spring, max in early summer followed by slow decrease toward winter (Figure 6.4). Pan 1-98b was not analyzed for Mn.

Orpheus Island

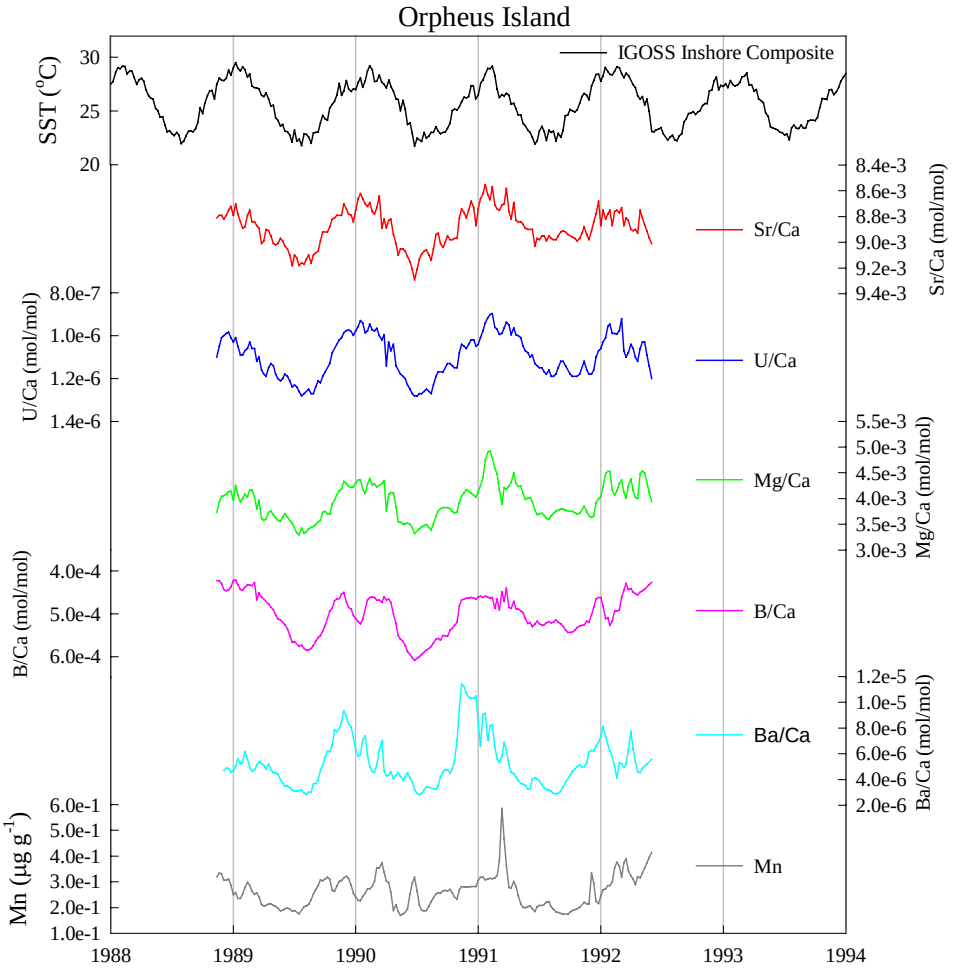

Figure 6.5 Trace element profiles from Orpheus Island corals vs. time. IGOSS SST adjusted to reflect inshore variations from equation in Figure 6.3a shown for comparison. Y-axes for Sr/Ca, U/Ca, B/Ca and Mg/Ca are scaled to reflect temperature.

The Orpheus Island coral record covers the time period Dec. 1989 – May 1992. Sr/Ca, U/Ca, Mg/Ca and B/Ca also show annual variations consistent with SST (Figure 6.5). Ba/Ca shows increases consistent with Burdekin river runoff of 1990 and 1991 as well as an "anomalous" component (Figure 6.5). Mn has an annual signal similar to the Pandora coral (Figure 6.5). Part of this coral (B/Ca and Ba/Ca) was analyzed and discussed by D. Sinclair in his thesis (Sinclair, 1999). For this project I have reanalyzed this sample (all elements) using the coral pressed powder standard discussed in Chapter 3. Sinclair (1999) did not use this standard during his analyses.

Havannah Island

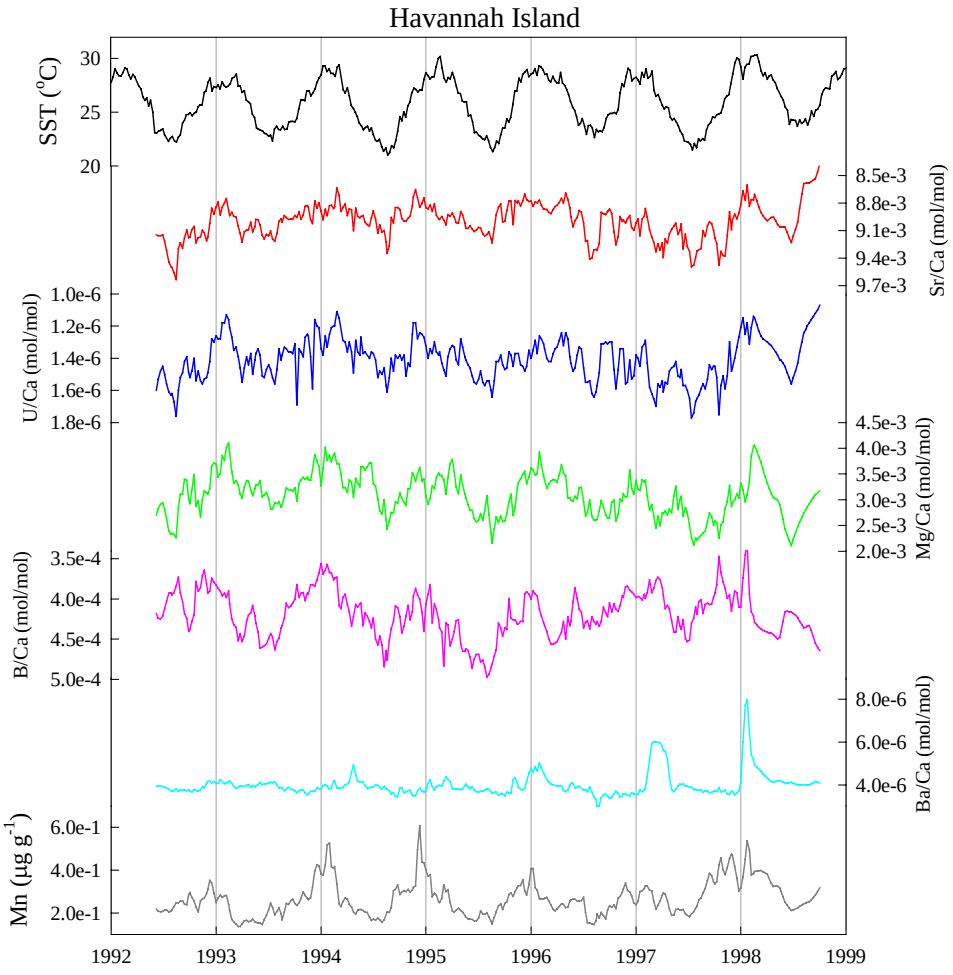

Figure 6.6 Trace element profiles from Havannah Island corals vs. time. IGOSS SST adjusted to reflect inshore variations from equation in Figure 6.3a shown for comparison. Y-axes for Sr/Ca, U/Ca, B/Ca and Mg/Ca are scaled to reflect temperature.

The Havannah Island coral record spans the time period Apr. 1992 – Oct 1998. This coral displays a relatively poor seasonal signal with respect to Sr/Ca, U/Ca and B/Ca

(Figure 6.6). The Ba/Ca displays the "inshore" signal of peak values that are consistent with the Pandora coral and Burdekin river runoff (discussed later) (Figure 6.6). Manganese displays a seasonal signal and the pattern is very similar to the Pandora coral Mn signal (Figures 6.4, 6.6).

6.3.4 Mid-Shelf Reefs

Davies Reef

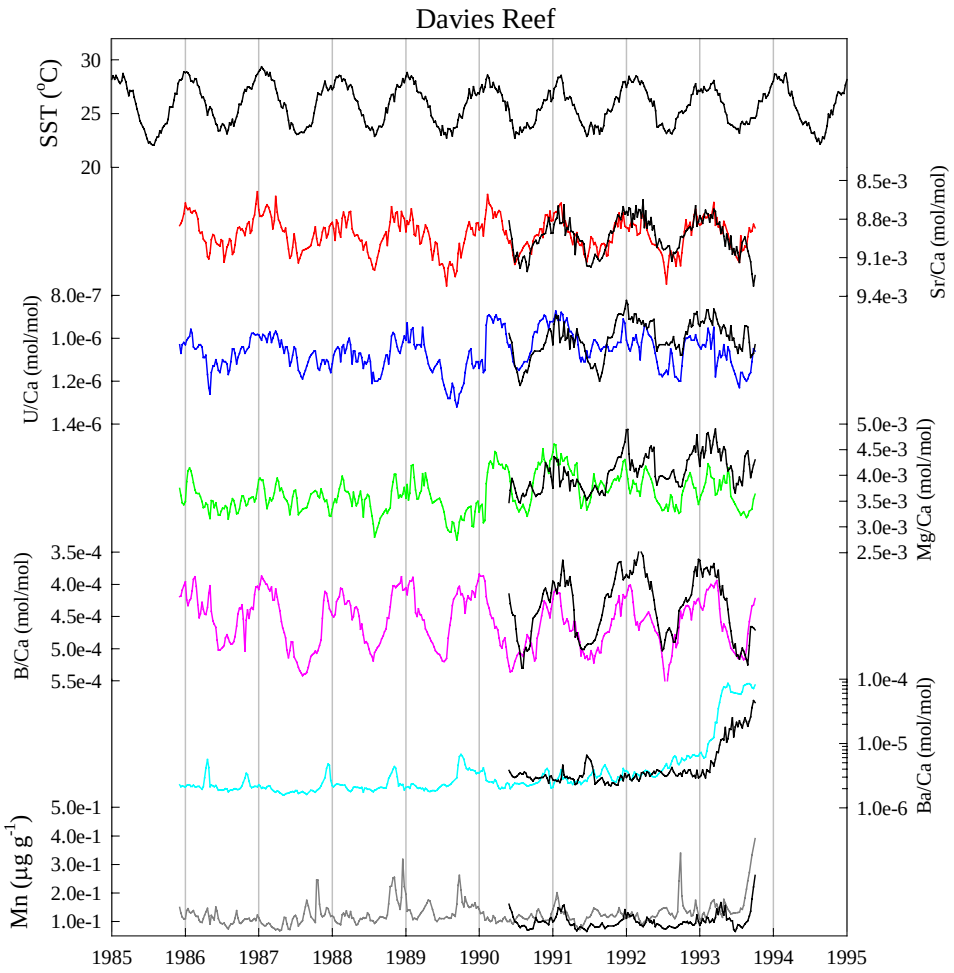

Figure 6.7 Trace element profiles from Davies Reef corals vs. time. IGOSS SST adjusted to reflect mid-shelf variations from equation in Figure 6.3b shown for comparison. Colored lines indicate coral Davies 2, black overlay is coral Davies 8. Y-axes for Sr/Ca, U/Ca, B/Ca and Mg/Ca are scaled to reflect temperature. Ba/Ca y-axis is shown as a log scale to preserve small fluctuations and high outer edge concentrations.

The Davies 2 coral spans the time period Dec. 1985 – Oct. 1993, Davies 8 only covers Apr. 1990 – Oct 1993. The trace elements from the top section (0 – 45 mm from top of coral) were measured and discussed by D. Sinclair (Sinclair *et al.*, 1998; Sinclair, 1999).

I again reanalyzed this piece using the coral pressed powder standard. TIMS Sr/Ca were analyzed and presented by Alibert and McCulloch (1997). The relationship between TIMS and LA-ICP-MS was presented in Chapter 3. Sr/Ca and B/Ca from both corals show clear seasonal cycles while Mg/Ca and U/Ca cycles are not as consistent (Figure 6.7). The two corals show reasonably consistent trace element records (Figure 6.7). Ba/Ca shows lower "background" levels (~ 2 e-6 mol/mol) than the inshore corals (~3.5 e-6 mol/mol) (Figure 6.7). However at the outer tissue layer the Ba/Ca concentration increases dramatically (~ 15x) (Figure 6.7). Davies 2 also shows short sharp peaks that appear to be "anomalous". Mn shows no seasonality unlike the inshore corals.

Wheeler Reef

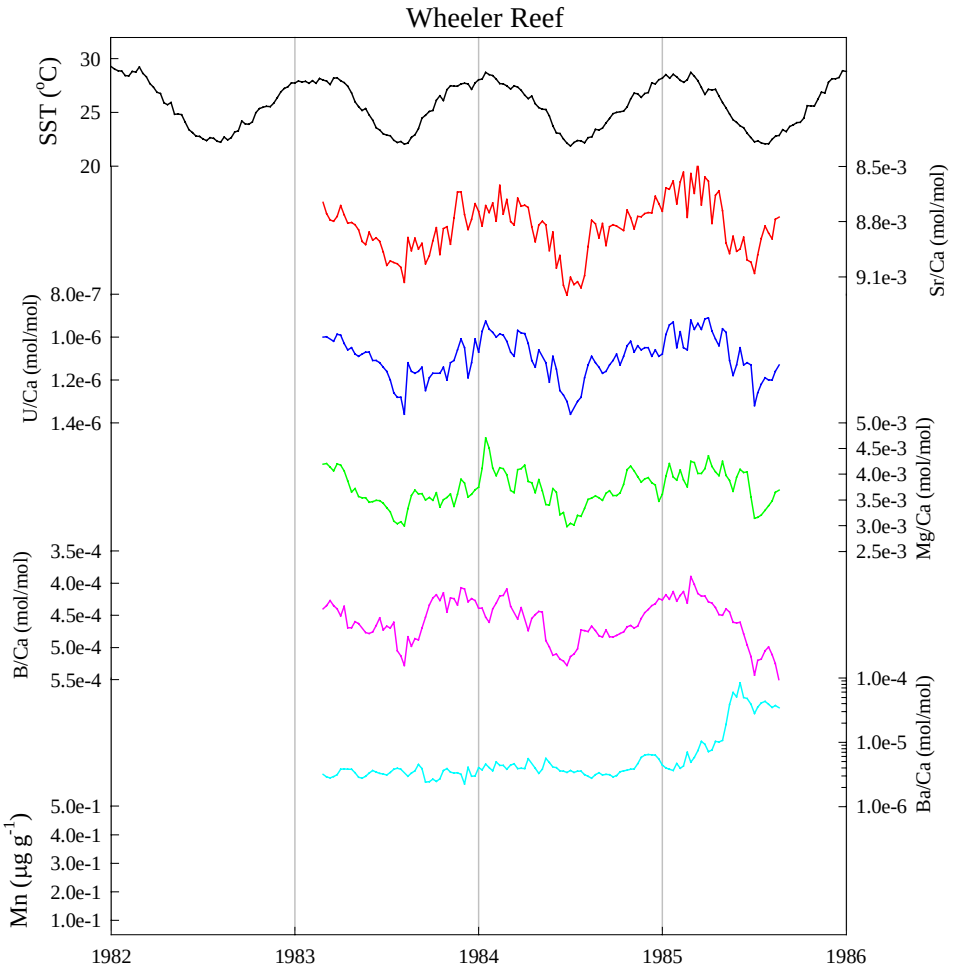

Figure 6.8 Trace element profiles from Wheeler Reef corals vs. time. IGOSS SST adjusted to reflect mid-shelf variations from equation in Figure 6.3b shown for comparison. Ba/Ca y-axis is shown as a log scale to preserve small fluctuations and high outer edge concentrations.

The Wheeler Reef coral only covers the time period Feb. 1983 – Jun. 1985. Sr/Ca, U/Ca, Mg/Ca and B/Ca show seasonal cycles consistent with SST but also have intra-annual fluctuations that can be ~ ½ the annual signal (Figure 6.8). Ba/Ca also displays a lower "background" concentration than the inshore corals (~ 2 e-6 mol/mol). This coral also displays the significant Ba/Ca increases associated with the outer edge (tissue layer) similar to the Davies Reef corals (Figures 6.7, 6.8). Mn was not analyzed.

6.3.5 Outer Reef

Myrmidon Reef

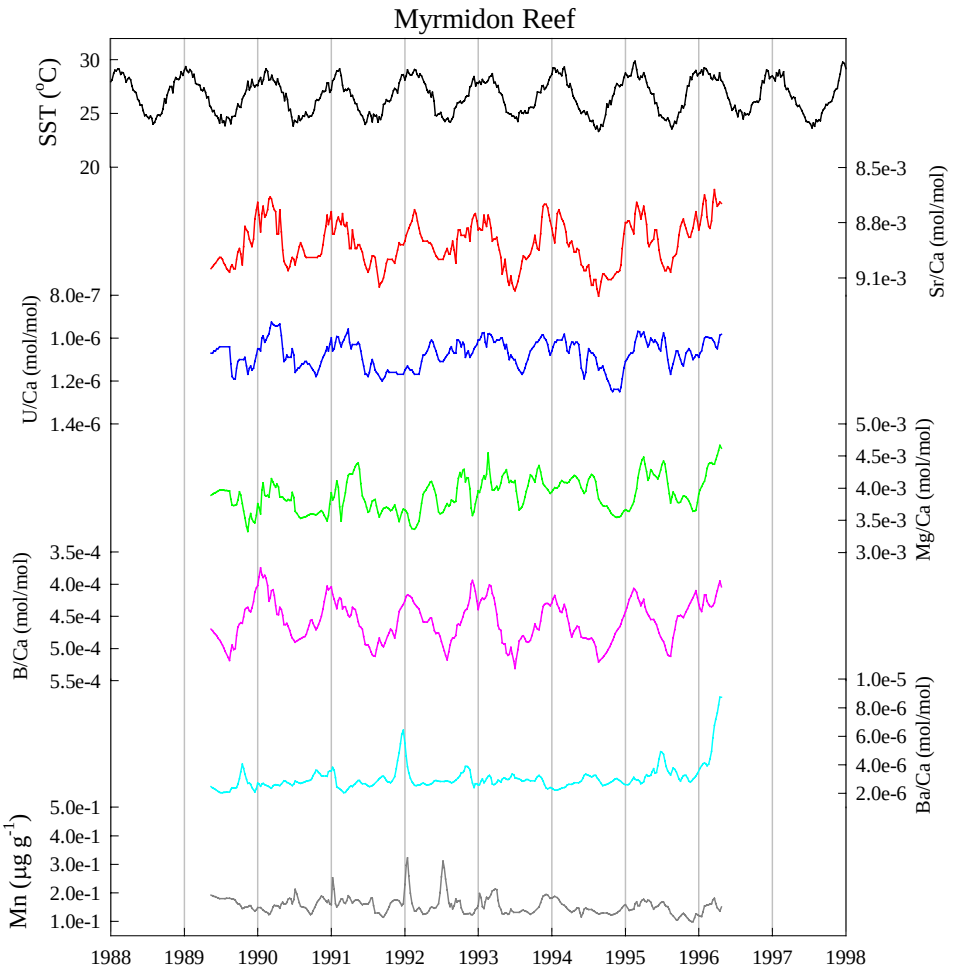

Figure 6.9 Trace element profiles from Myrmidon Reef corals vs. time. IGOSS SST adjusted to reflect outer reef variations from equation in Figure 6.3c shown for comparison.

The Myrmidon Reef coral spans the time frame Mar. 1989 – Mar. 1996. Sr/Ca and B/Ca both have very clear seasonal cycles (Figure 6.9). Mg/Ca and U/Ca do not show

clear seasonal cycles but show consistency between each other (Figure 6.9). Ba/Ca displays the low "background" levels similar to the mid-shelf corals but also has a few peaks (1992, 1995) (Figure 6.9). Ba/Ca also increases as the outer living surface (tissue layer) is approached (Figure 6.9). Mn does not display seasonal cycles similar to the mid-shelf corals but does show some variability (Figure 6.9).

6.3.6 Correlation Between Elements

Figure 6.10 shows the scatter plot comparisons between Sr/Ca, B/Ca, Mg/Ca and U/Ca. The linear regression line for each elemental correlation is shown in Figure 6.11. Correlation coefficients are listed in Table 6.1. Good correlations ($r > 0.73$) exist between Sr/Ca and U/Ca at all locations aside from Myrmidon ($r = 0.57$). This is consistent with the notion that U/Ca is influenced by temperature although probably not exclusively (Min *et al*., 1995; Fallon *et al*., 1999b; Sinclair, 1999).

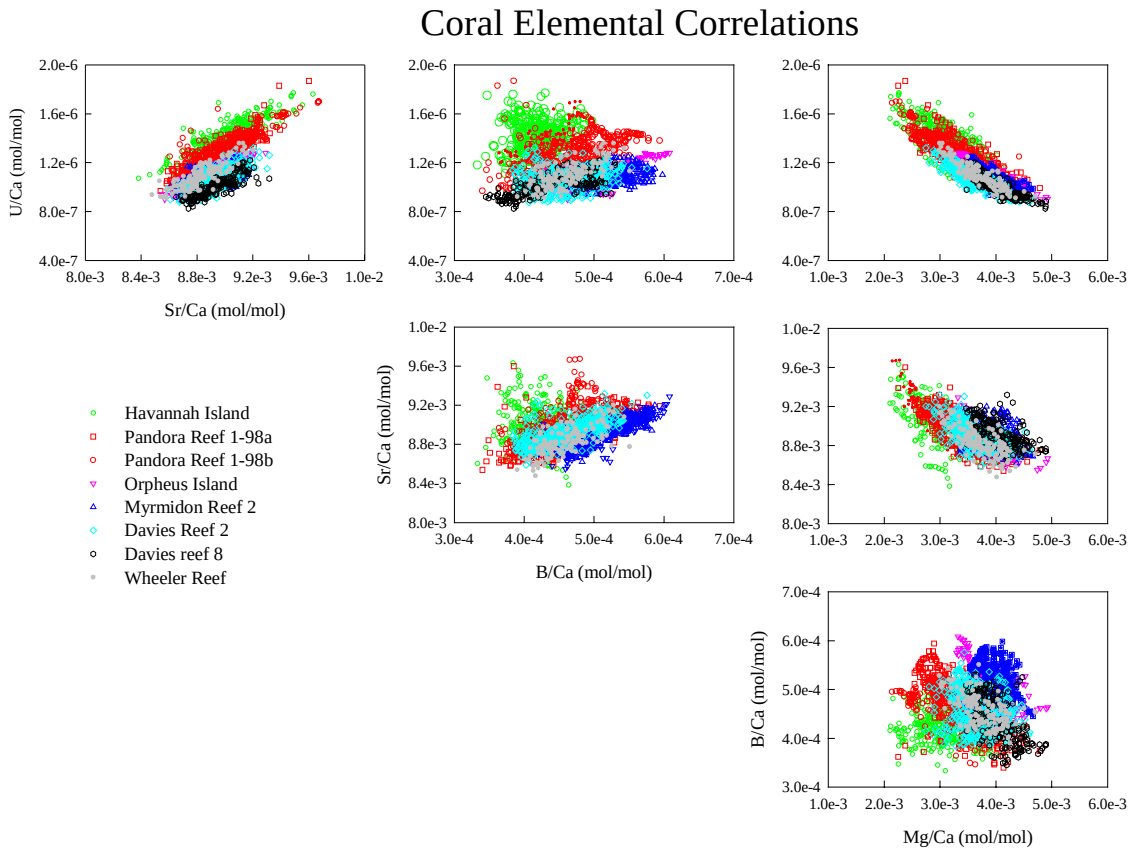

Figure 6.10 Elemental correlations between all sites. Color codes for each coral stay the same for the Figures 6.10 – 6.15.

In most cases good correlations exist between the other elements most likely reflecting the influence of temperature incorporation of these elements (Table 6.1). However the seasonal cycle of some elements, Mg/Ca and U/Ca from Davies 2 and Myrmidon (Figures 6.7, 6.9) breaks down resulting in lower correlations between them and B/Ca and Sr/Ca (Table 6.1). The Havannah coral has poor seasonal cycles resulting in very low/no correlations between B/Ca, Sr/Ca, U/Ca and Mg/Ca (Table 6.1). One important observation is that U/Ca and Mg/Ca always seem to be well correlated on both the annual and intra-annual scale regardless of how well each element tracks temperature (Table 6.1, Figure 6.11). The correlation between these two elements at all scales has been noted in other studies (Fallon *et al.*, 1999b; Sinclair, 1999; Marshall, in prep). Along with this observation it appears that the relationship between these two elements is more robust between sites than the other elements (Figure 6.10). This is seen as the tight cluster of points for the U/Ca vs. Mg/Ca graph in Figure 6.10 relative to the other elemental correlations. The coupling may be indicative of related incorporation mechanisms for these two elements.

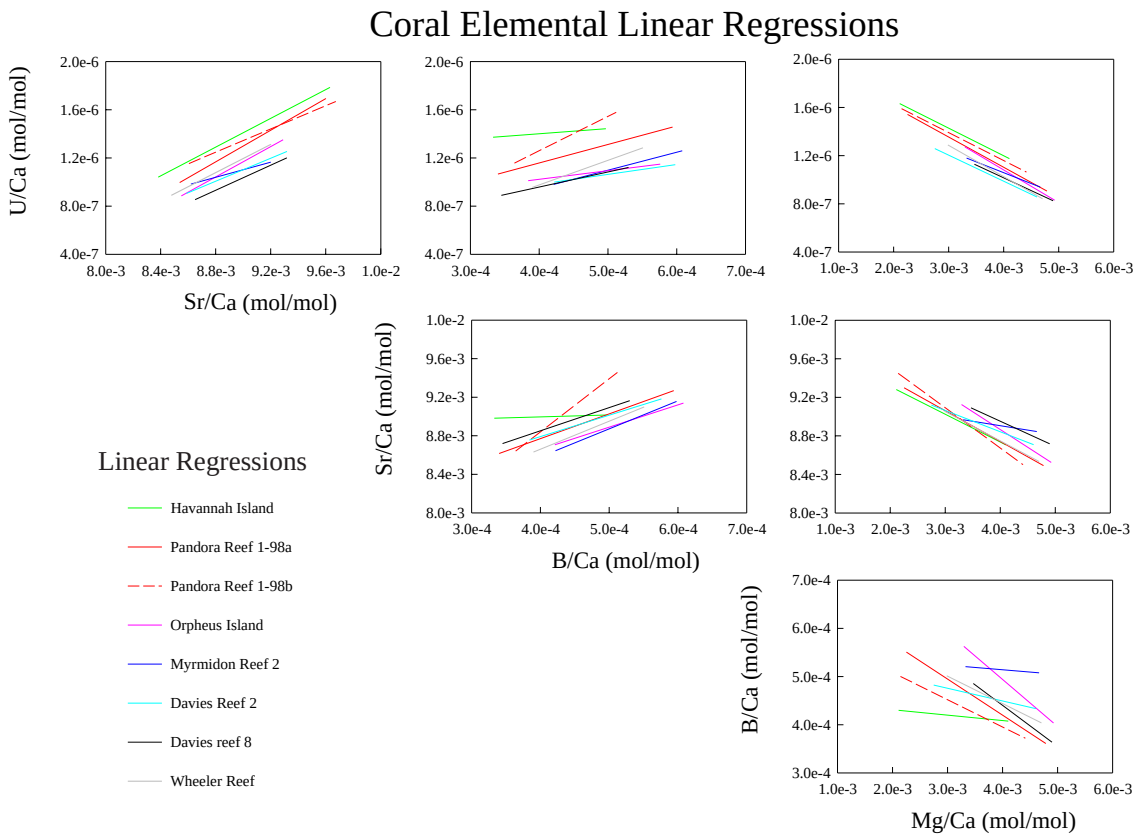

Figure 6.11 Coral elemental linear regressions for all elements. Lines shown without data for easier comparisons.

Table 6.1 Correlation coefficients between elements from Figures 6.10, 6.11.

Havannah Island	B/Ca	Mg/Ca	Sr/Ca	Myrmidon Reef	B/Ca	Mg/Ca	Sr/Ca
Mg/Ca	-0.14			Mg/Ca	-0.06		
Sr/Ca	-	-0.62		Sr/Ca	0.86	-0.17	
U/Ca	0.09	-0.72	0.88	U/Ca	0.45	-0.71	0.57
Pandora Reef 1-98a	**B/Ca**	**Mg/Ca**	**Sr/Ca**	**Davies Reef 2**	**B/Ca**	**Mg/Ca**	**Sr/Ca**
Mg/Ca	-0.69			Mg/Ca	-0.22		
Sr/Ca	0.69	-0.79		Sr/Ca	0.69	-0.58	
U/Ca	0.56	-0.84	0.88	U/Ca	0.33	-0.87	0.73
Pandora Reef 1-98b	**B/Ca**	**Mg/Ca**	**Sr/Ca**	**Davies Reef 8**	**B/Ca**	**Mg/Ca**	**Sr/Ca**
Mg/Ca	-0.75			Mg/Ca	-0.59		
Sr/Ca	0.79	-0.88		Sr/Ca	0.85	-0.64	
U/Ca	0.72	-0.85	0.85	U/Ca	0.71	-0.85	0.84
Orpheus Island	**B/Ca**	**Mg/Ca**	**Sr/Ca**	**Wheeler Reef**	**B/Ca**	**Mg/Ca**	**Sr/Ca**
Mg/Ca	-0.70			Mg/Ca	-0.58		
Sr/Ca	0.75	-0.86		Sr/Ca	0.68	-0.72	
U/Ca	0.71	-0.93	0.92	U/Ca	0.69	-0.89	0.84

6.4 Discussion

6.4.1 SST Calibrations

Sr/Ca

All sites (inshore, mid-shelf, outer) were compared to their respective IGOSS adjusted SST's (from section 6.3.1) using the equations from Figure 6.3. Figure 6.12A-C shows Sr/Ca vs. SST from all the sites. Figure 6.12D shows the linear regression lines for each location to compare them more easily. Also shown are 5 other published Sr/Ca-SST calibrations (dashed lines). The equations for these lines, correlation coefficients and % change per ºC at 25 ºC are given in Table 6.2. The calibration lines for all of the sites form a relatively tight cluster (Figure 6.12B). All sites have good correlations with temperature (r = 0.77 – 0.91) aside from Havannah, which only has a correlation coefficient of 0.5 (Table 6.2). The slopes of the calibration lines are different but the % change per ºC is similar between the sites with a value of ~ 0.7 % change per ºC at 25 ºC (Table 6.2). There is no systematic change in the calibrations between nearshore, mid-shelf and outer reef (Figure 6.12). This suggests that Sr/Ca is not influenced by nearshore processes (runoff etc.) at the level resolvable with LA-ICP-MS analyses.

The calibration of Sr/Ca versus SST has been the most studied elemental proxy aside from $\delta^{18}O$ (e.g. Beck *et al*., 1992; McCulloch *et al*., 1994; Shen *et al*., 1996; Alibert and McCulloch, 1997). A wide range exists between published Sr/Ca-SST calibrations. For equivalent Sr/Ca values, temperature differences can be 2–3.5 ºC higher/lower depending on the calibration used (Figure 6.12D). However the slopes and more importantly the % change per ºC between the published calibrations are very similar with values of ~0.7 % per ºC at 25 ºC (Table 6.2). One unresolved observation is that the regression line from Gagan *et al*. (1998) (Figure 6.12D) is from another coral at Orpheus Island. This offset between the two Orpheus corals is troubling. Seawater temperatures reconstructed using their equation result in values ~3 – 4 ºC higher than any of the calibrations from this GBR dataset. At this point no suitable reasons for this offset have been found.

There have been various discussions concerning the variability of the Sr/Ca-SST calibrations. Differences such as coral collection, sampling, SST measurements, inter-laboratory spikes and analysis may be some causes for these differences (Gagan *et al*., 2000). Or as some may suggest the differences may be real. Another subject of contention is that seawater Sr/Ca may vary between sites, but this could only account for < 1 ºC difference between sites and not the 2 – 3.5 ºC observed from sites across the Pacific (de Villiers *et al*., 1994; Shen *et al*., 1996; Gagan *et al*., 2000). Here Sr/Ca is confirmed as being a good tool for extracting paleo-SST's from corals, both living and fossil. An important caveat in this study is the errors associated with the LA-ICP-MS (~ 2 ºC, Table 3.2), are too large for precise temperature reconstructions but are nevertheless adequate to provide a basis to compare the other "temperature" proxies obtained with this technique.

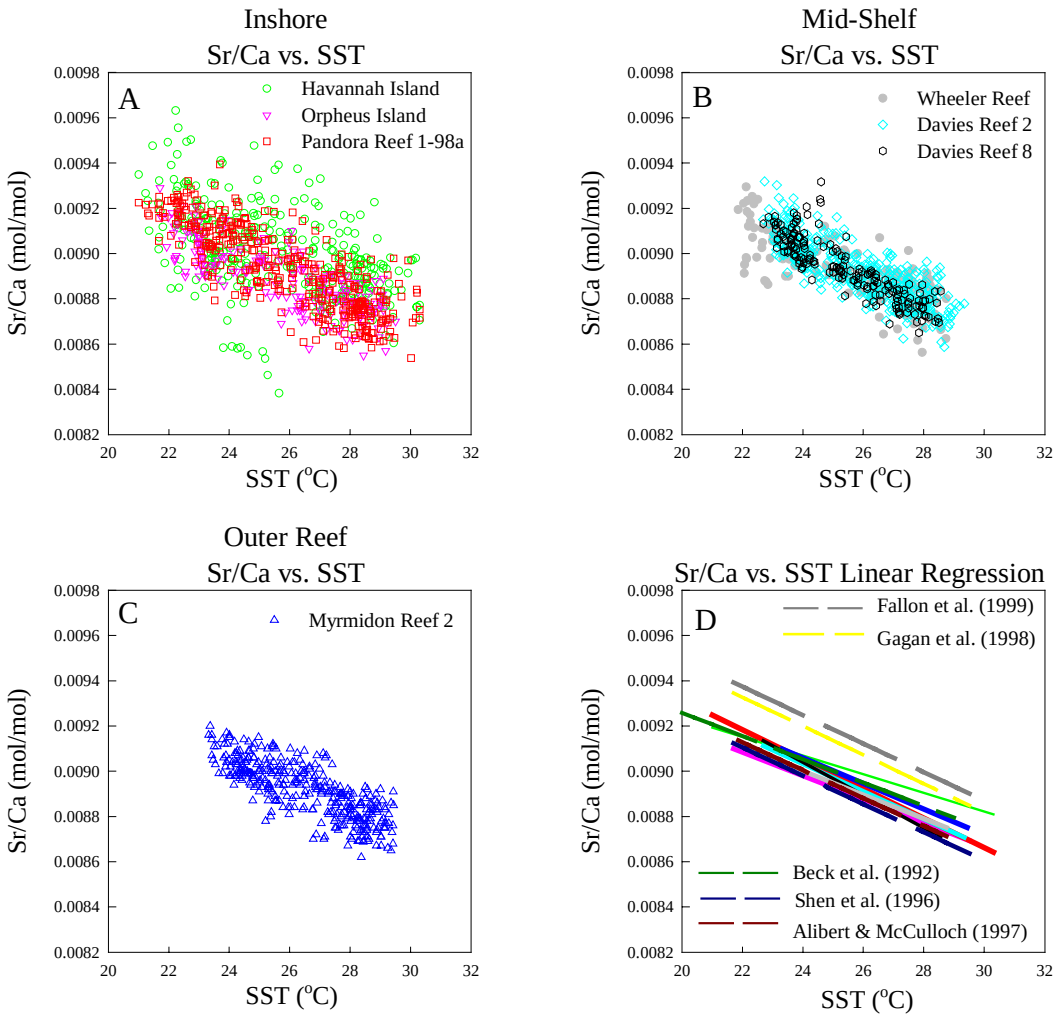

Figure 6.12 a) Sr/Ca vs. SST for Inshore Reefs (Havannah, Pandora, Orpheus). b) Sr/Ca vs. SST for Mid-shelf Reefs (Davies, Wheeler). c) Sr/Ca vs. SST for Outer Shelf Reefs (Myrmidon). d) Linear regression equation lines from Table 6.2 for all sites. Also shown are several published Sr/Ca-SST calibrations.

Table 6.2 Element – Temperature relationship for *Porites* corals from the Great Barrier Reef

	Coral Species	a[1]	b[1]	r	% change per ºC at 25 ºC
Sr/Ca (mol/mol)					
Havannah Island	*Porites* sp.	0.01011	4.12e-5	-0.5	0.455%
Pandora Reef 1-98a	*Porites* sp.	0.01062	6.52e-5	-0.83	0.728%
Orpheus Island	*Porites* sp.	0.01023	5.20e-5	-0.79	0.584%
Davies Reef 2	*Porites* sp.	0.01039	6.02e-5	-0.84	0.680%
Davies Reef 8	*Porites* sp.	0.01073	7.07e-5	-0.91	0.792%
Myrmidon Reef 2	*Porites* sp.	0.01042	5.65e-5	-0.79	0.629%
Wheeler Reef	*Porites* sp.	0.01035	5.95e-5	-0.82	0.674%
Alibert & McCulloch (1997)	*Porites* sp.	0.01048	6.15e-5		0.690%
Beck *et al*. (1992)	*Porites lobata*	0.010479	6.245e-5		0.703%
Fallon *et al*. (1999)	*Porites lobata*	0.01076	6.3e-5	-0.77	0.688%
Gagan *et al*. (1998)	*Porites lutea*	0.01073	6.39e-5		0.702%
Shen *et al*. (1996)	*Porites* sp.	0.010286	5.14e-5		0.573%
B/Ca (mol/mol)					
Havannah Island	*Porites* sp.	5.328e-4	4.436e-6	-0.37	1.06%
Pandora Reef 1-98a	*Porites* sp.	9.093e-4	1.707e-5	-0.80	3.60%
Orpheus Island	*Porites* sp.	8.19e-4	1.457e-5	-0.76	3.26%
Davies Reef 2	*Porites* sp.	9.247e-4	1.805e-5	-0.79	3.89%
Davies Reef 8	*Porites* sp.	1.098e-3	2.609e-5	-0.89	6.03%
Myrmidon Reef 2	*Porites* sp.	8.952e-4	1.65e-5	-0.87	3.48%
Wheeler Reef	*Porites* sp.	7.88e-4	1.288e-5	-0.83	2.80%
Fallon *et al*. (1999)	*Porites lobata*	7.66e-4	9.33e-6	-0.74	1.77%
U/Ca (mol/mol)					
Havannah Island	*Porites* sp.	2.165e-6	2.94e-8	-0.53	2.08%
Pandora Reef 1-98a	*Porites* sp.	2.36e-6	4.31e-8	-0.79	3.42%
Orpheus Island	*Porites* sp.	2.001e-6	3.51e-8	-0.78	3.17%
Davies Reef 2	*Porites* sp.	1.806e-6	2.86e-8	-0.60	2.66%
Davies Reef 8	*Porites* sp.	2.02e-6	3.98e-8	-0.78	3.96%
Myrmidon Reef 2	*Porites* sp.	1.46e-6	1.469e-8	-0.37	1.35%
Wheeler Reef	*Porites* sp.	2.03e-6	3.64e-8	-.079	3.30%
Fallon *et al*. (1999)	*Porites lobata*	2.215e-6	4.539e-8	-0.84	4.29%
Min *et al*. (1995)	*Porites* sp.	2.386e-6	5.30e-8		5.12%
Quinn (in press)	*Porites lutea*	1.959e-6	3.2e-8		2.80%
Mg/Ca (mol/mol)					
Havannah Island	*Porites* sp.	1.04e-4	-1.160e-4	0.66	-3.79%
Pandora Reef 1-98a	*Porites* sp.	-6.03e-4	-1.155e-4	0.80	-4.93%
Orpheus Island	*Porites* sp.	1.044e-3	-1.123e-4	0.73	-2.87%
Davies Reef 2	*Porites* sp.	1.338e-3	-8.934e-5	0.47	-2.47%
Davies Reef 8	*Porites* sp.	7.037e-4	-1.321e-4	0.65	-3.24%
Myrmidon Reef 2	*Porites* sp.	3.73e-3	-6.61e-6	0.04	-0.17%
Wheeler Reef	*Porites* sp.	7.59e-4	-1.161e-4	0.73	-3.12%
Fallon *et al*. (1999)	*Porites lobata*	1.38e-3	-8.79e-5	0.66	-2.43%
Mitsuguchi *et al*. (1996)	*Porites* sp.	1.15e-3	-1.29e-4		-2.91%
Quinn (in press)	*Porites lutea.*	1.90e-3	-1.28e-4		-2.48%

[1] Calibration equation is X/Ca = a – b * SST.

U/Ca

U/Ca has also been shown to co vary with Sr/Ca and therefore temperature (Min *et al*., 1995; Fallon *et al*., 1999b). All corals, aside from Havannah and Myrmidon, have good correlations with temperature (r = 0.74 – 0.89; Table 6.2). The scatter plots and linear regression equations for the corals are shown in Figure 6.13. There is more variation in the U/Ca-SST calibrations between the sites than for Sr/Ca-SST (Figures 6.12, 6.13). Two of the inshore corals (Havannah and Pandora) have higher U/Ca concentrations than the mid-shelf and outer reef corals. However the Orpheus coral (inshore) has a U/Ca concentration very similar to the mid-shelf and outer reef corals (Figure 6.13).

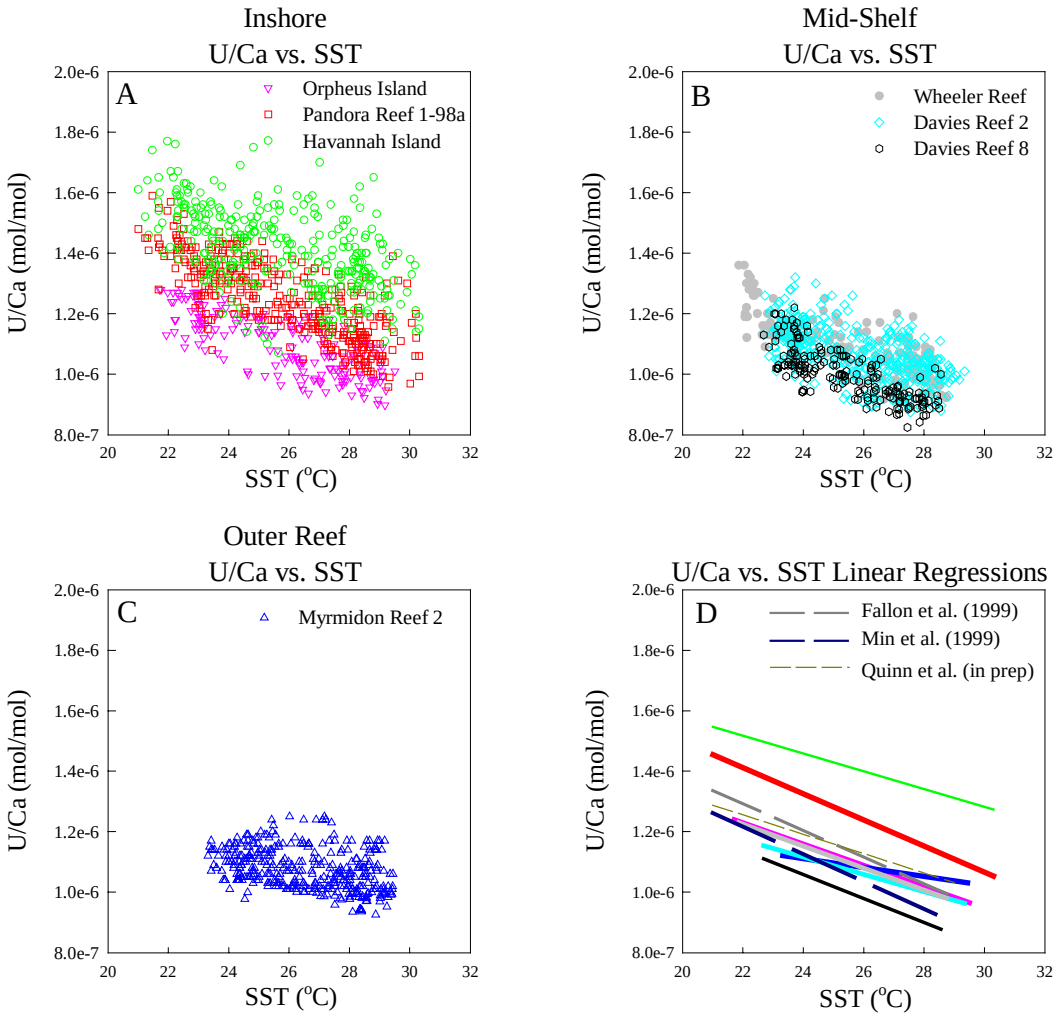

Figure 6.13 a) U/Ca vs. SST for Inshore Reefs (Havannah, Pandora, Orpheus). b) U/Ca vs. SST for Mid-shelf Reefs (Davies, Wheeler). c) U/Ca vs. SST for Outer Shelf Reefs (Myrmidon). d) Linear regression equation lines from Table 6.2 for all sites. Also shown are several published U/Ca-SST calibrations.

U/Ca has now been reported for corals from several locations and it appears that the U/Ca-SST calibrations may vary more than the Sr/Ca-SST calibrations. At a single

U/Ca value (e.g. 1.1 e-6 mol/mol) the GBR calibrations can give SST's that differ by 6 ºC, excluding the Havannah coral (Figure 6.13D). Previously published calibrations lie within the variability of the GBR corals (Figure 6.13D). The GBR corals have similar temperature dependencies (% change per ºC), ~ 3.5% (Table 6.2). This temperature dependency is lower that that suggested by Shen and Dunbar (1995) and Min *et al*. (1995) of ~ 5 % per ºC. The variability observed in the U/Ca-SST proxy may indicate the potential influences on coral U/Ca aside from temperature (pH, total CO_2, runoff) (Min *et al*., 1995; Shen and Dunbar, 1995). For U/Ca the LA-ICP-MS technique can provide temperature accurate to within ~ 1 ºC (Table 3.2), if corrections are made for the higher U/Ca of inshore corals.

B/Ca

B/Ca was first suggested to vary in response to SST by Hart and Cohen (1996) and Sinclair *et al*. (1998). However there are many factors that can influence seawater boron speciation and incorporation into $CaCO_3$ (see Section 4.2). Regardless of these potential influences B/Ca seems to be robust at documenting SST (Sinclair *et al*., 1998; Fallon *et al*., 1999b). Figure 6.14 shows the scatter plots and linear regression lines of B/Ca vs. SST for all the GBR corals. All of the sites have good to strong correlations to SST (r = 0.74 – 0.89) except for Havannah (Table 6.2). The regression lines cluster neatly together except for Havannah and Davies 8 (Figure 6.14). Davies 8 has a steeper slope that corresponds to almost a 2x increase in the temperature sensitivity compared to the other GBR corals, 6% per ºC vs. 3.5 % per ºC (Table 6.2). This temperature dependence (~ 3.5%) is similar to that of U/Ca (Table 6.2). Based on the errors for the B/Ca measurement our temperature reconstructions are accurate to ~ 1 ºC (Table 3.2).

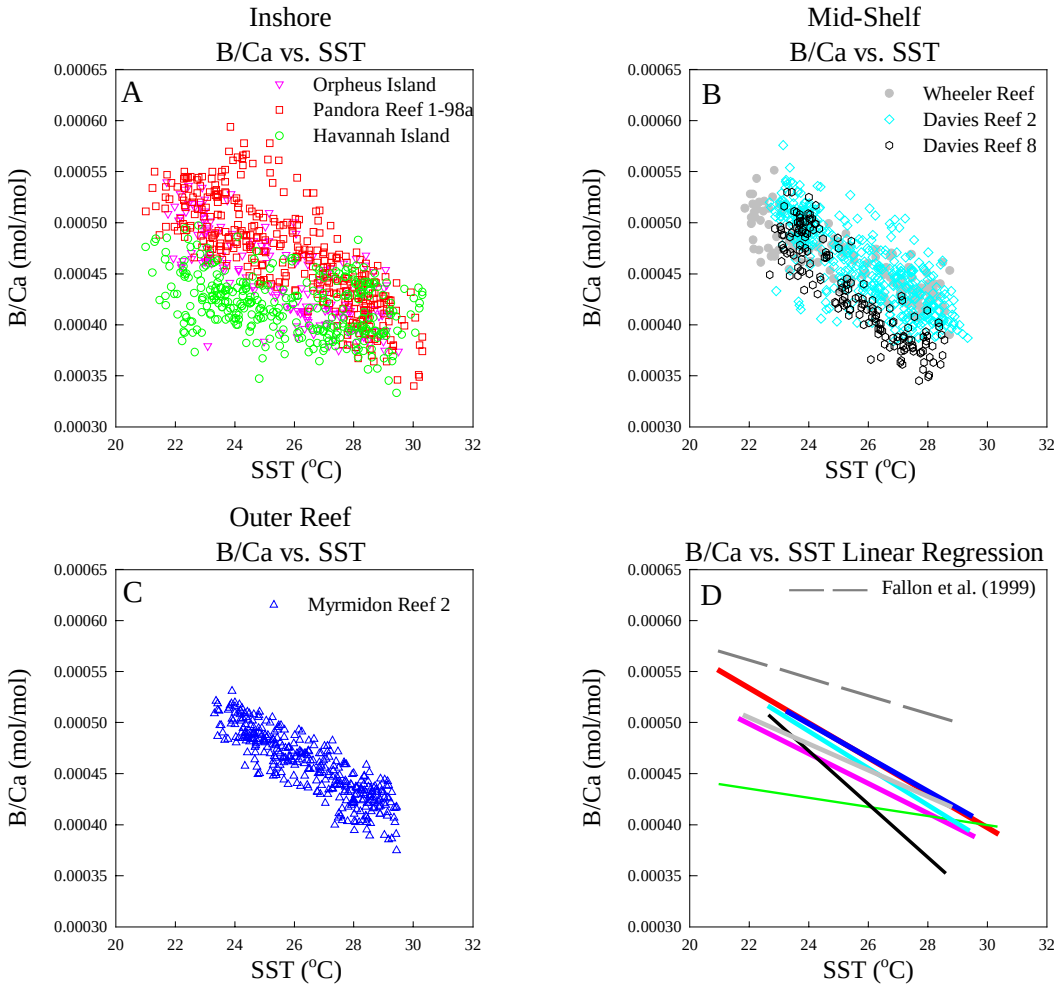

Figure 6.14 a) B/Ca vs. SST for Inshore Reefs (Havannah, Pandora, Orpheus). b) B/Ca vs. SST for Mid-shelf Reefs (Davies, Wheeler). c) B/Ca vs. SST for Outer Shelf Reefs (Myrmidon). d) Linear regression equation lines from Table 6.2 for all sites. Also shown are several published B/Ca-SST calibrations.

B/Ca displays the "cleanest" seasonal cycles of all the elements measured. However it is also influenced by other factors aside from temperature. Some of the corals display intra-annual fluctuations of half to equal the annual amplitude (Figures 6.4 – 6.7). The linear regression slopes and the % change per ºC are steeper and larger, respectively, than a *Porites* coral from Japan (Table 6.2). This difference could be indicative of *Porites* corals, similar to offsets for Sr/Ca and U/Ca – SST calibrations.

Mg/Ca

Mg/Ca has a clear annual signal in the Pandora, Orpheus and Wheeler corals. However this annual signal breaks down in the Myrmidon, Davies and Havannah corals. Figure 6.15A-C shows the scatter plots of Mg/Ca vs. SST for all the corals. The linear regression equation lines from Table 6.2 are shown in Figure 6.15D. The disruption of

the annual signal is reflected by the lower correlation coefficients that range from 0.65 to 0.80 (Table 6.2). Mg/Ca has the largest spread of calibrations. This is indicative of significant variation in Mg/Ca concentration between the corals which is not temperature related (Figure 6.15). The slopes of the linear regressions are similar and within 10% of values reported by Mitsuguchi *et al*. (1996). The % change per ºC (~ 3%) is also similar between the GBR corals and the previously published calibrations (Table 6.2).

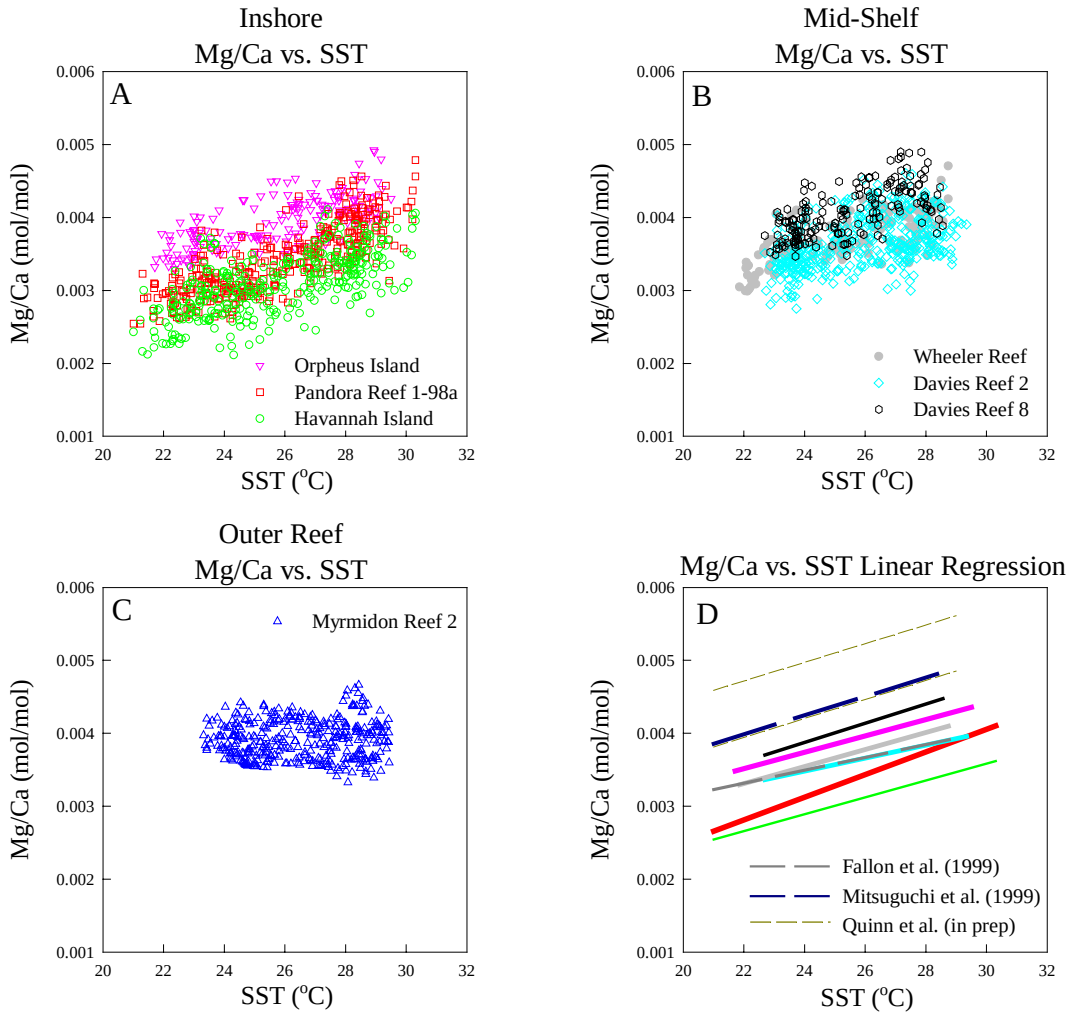

Figure 6.15 a) Mg/Ca vs. SST for Inshore Reefs (Havannah, Pandora, Orpheus). b) Mg/Ca vs. SST for Mid-shelf Reefs (Davies, Wheeler). c) Mg/Ca vs. SST for Outer Shelf Reefs (Myrmidon). d) Linear regression equation lines from Table 6.2 for all sites. Also shown are several published Mg/Ca-SST calibrations.

It is apparent that the Mg/Ca – SST proxy is influenced by factors aside from temperature (Fallon *et al*., 1999b; Schrag, 1999; Sinclair, 1999). Again in this set of corals (as seen in Chapter 5, Japan coral) intra-annual variations equivalent to the annual cycle are often present (ex. Figure 6.4). Short-term variability on this scale

cannot be attributed to SST variations and must be caused by other factors. Variations similar to this have been noted using other micro-beam techniques (Allison and Tudhope, 1992; Allison, 1996b; Fallon *et al*., 1999b; Sinclair, 1999). As discussed previously (Chapter 5) the high-resolution nature of micro-beam techniques may enhance the heterogeneity of the recovered Mg/Ca signal. Coarser sampling (~ monthly) does not show these high-frequency variations (Mitsuguchi *et al*., 1996). Factors such as the incorporation mechanism of Mg into the coral skeletal lattice (see Chapter 4.3) could be responsible for this heterogeneity. Organic phases and/or metal binding capacity of coral tissue could affect the recovered Mg/Ca record (Amiel *et al*., 1973a; Mitterer, 1978; Allison and Tudhope, 1992; Allison, 1996b). Problems such as these have been noted by other researchers and may limit the use of Mg/Ca as a SST proxy (Schrag, 1999).

6.4.2 Inshore Corals

Ba/Ca

The Ba/Ca ratio in corals can be influenced by upwelling (Lea *et al*., 1989; Shen *et al*., 1992a; Tudhope *et al*., 1996; Fallon *et al*., 1999b) or in coastal corals, river runoff (Shen and Sanford, 1990; Tudhope *et al*., 1997; Sinclair, 1999). The study sites are not affected by upwelling with the exception of possibly Myrmidon. It has been suggested that minor upwelling influences Myrmidon Reef, but this probably would not affect corals living on the lagoon side of the reef. The inshore corals of the GBR have been shown to record river runoff in the form of increases in Ba/Ca (Sinclair, 1999). The influence of river runoff on GBR corals is also recorded as luminescent or fluorescent lines/bands in the corals (Isdale, 1984; Boto and Isdale, 1985; Isdale *et al*., 1998). The three inshore corals studied in this project all display these luminescent/fluorescent lines synchronous to runoff from the Burdekin River. However not all floods are recorded, most likely because runoff did not reach the sites.

The three inshore coral Ba/Ca records and the Burdekin River runoff record are plotted in Figure 6.16. The Havannah and Pandora 1-98a coral overlap and record the floods of 1994, 1996, 1997 and 1998. The Pandora coral also records part of the 1991 flood. The Ba/Ca record from the Orpheus coral shows the 1989, 1990 and 1991 floods as well as an “anomalous” component from Oct. to Dec. of each year (will be discussed later). The relation between river discharge and coral Ba/Ca is not necessarily linear; with

factors such as wind and ocean current conditions affecting the path of the flood plumes. Sinclair (1999) reported that two equal sized floods had very different Ba/Ca concentrations (1970, hi Ba/Ca; 1971 low Ba/Ca) measured in another coral from Pandora Reef. This difference may be explained by recent Burdekin flood plume modeling that suggests the 1970 flood plume impacted the Pandora reef more than the 1971 flood (McAllister *et al*. 1999). The Havannah coral generally has lower peak Ba/Ca than the Pandora coral (1997, 1998; Figure 6.16) even though there is only ~ 10 km separating the two sites. This is most likely due to dissipation of the plume as it moves offshore.

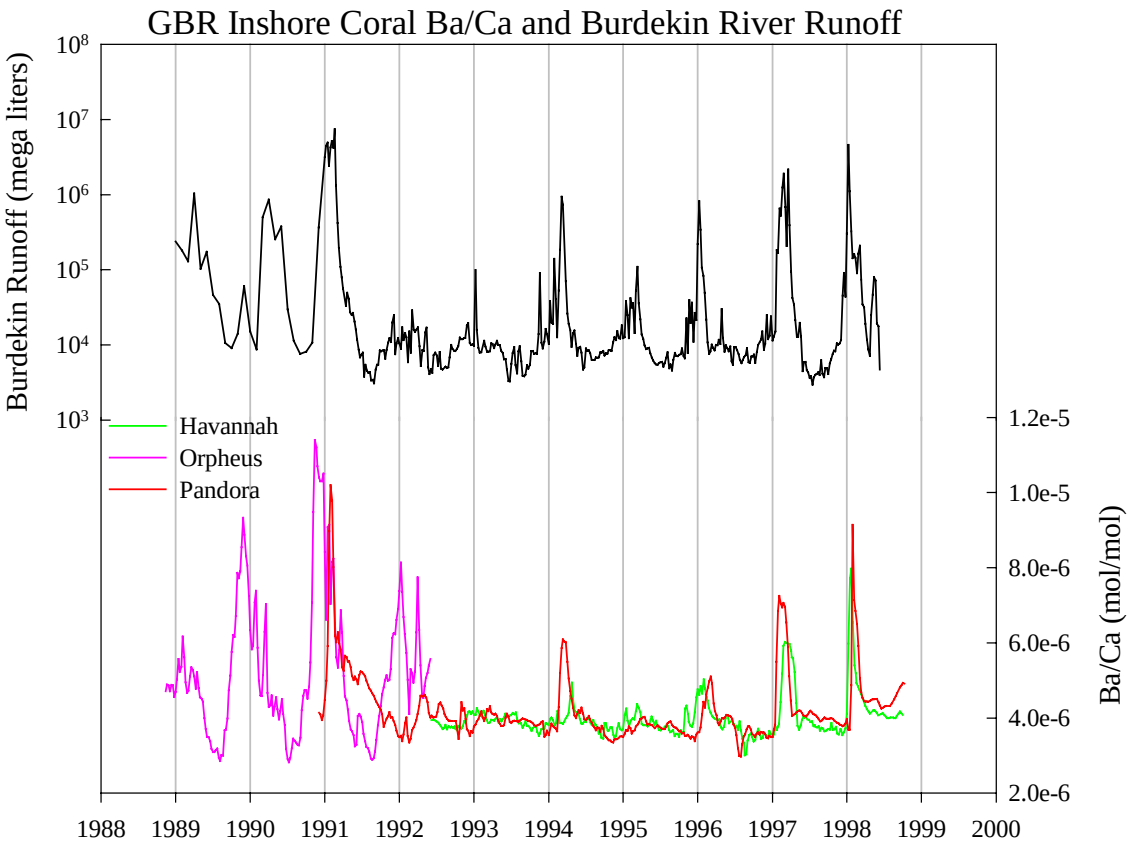

Figure 6.16 Burdekin River Runoff in mega liters (log scale) (courtesy of Queensland Department Natural Resources, Mick O'Connor). 1989-1991 samples are monthly averages, after 1991 data is weekly averages. Bottom graph is Ba/Ca vs. time from Havannah (green), Pandora (red) and Orpheus (pink) corals.

Barium Between Sites

Inshore corals have a slightly higher concentration of "background" Ba/Ca, ~4e-6 (mol/mol) relative to the value of ~2e-6 (mol/mol) for the mid-shelf and outer reef corals (Figures 6.16, 6.17). One would assume that this difference could be explained by the riverine barium input except that flood plumes are present for weeks/months and not all year. The Burdekin River flood plume directions and duration have been modeled by McAllister *et al*. (1999). They suggest that low salinities surround the areas (Pandora, Havannah) for short time periods (weeks-months). Seawater barium measurements suggest that during non-flood times the inshore, mid-shelf and outer reef have similar concentrations and do not follow the trend observed by the corals (C. Alibert pers. comm.). Another interesting feature of the Davies 2, Davies 8 and Wheeler coral is the extremely high values in the tissue layer (~15x the background level; Figures 6.7, 6.8). Other researchers have observed this behavior in corals and determined that the high values could not be removed during rigorous cleaning (Tudhope *et al*., 1996). During the 1998 collecting trip, coral cores had their tissue hosed off immediately with fresh water to help eliminate mold. Eight cores from the three reefs do not show this elevated tissue barium (Havannah, Pandora and Frankland Islands - M. McCulloch pers. comm.). The other corals Davies, Wheeler and Myrmidon were not subjected to this treatment. During the next field collection this tissue removal method will be further examined. If the elevated "tissue" barium values can be removed then valuable Ba/Ca records from near the tissue zone can be observed (as seen in the Pandora and Havannah corals, Figure 6.16, 1998).

Anomalous Barium

The Davies 2, Orpheus and possibly the Myrmidon coral display an "anomalous" barium behavior similar to that described by Sinclair (1999). Sinclair (1999) used this term to describe the sharp short barium spikes observed in a coral from the Whitsunday Islands (GBR) and the early peak (Nov-Dec.) in the Orpheus coral. These "anomalous" spikes occur regularly (Oct.-Dec.) in the Davies 2 and Orpheus coral (Figure 6.17). This time frame is close to the Whitsunday coral, which has spikes occurring around Sep.-Oct. (Sinclair, 1999). As Sinclair (1999) discussed the 1991 Ba/Ca increase in the Orpheus coral occurs before the fluorescent band, therefore making it "anomalous" (Figure 6.16). I tested whether the barium signal was consistent laterally within a coral by analyzing 24, 12 mm long (0.5 mm wide) parallel tracks on the Orpheus coral. The

"box" covers a fluorescent band and a surface map of coral Ba/Ca was produced (Figure 6.18). The Ba/Ca profile shows that the spikes and runoff signal persist laterally (at least 12 mm) and are parallel to the growth bands (Figure 6.18). The Ba/Ca signal precedes the flood indicator (fluorescent band), this is the "anomalous" barium discussed by Sinclair (1999) (Figure 6.18). The lateral consistency shown by Ba/Ca in this coral suggests that barium is incorporated reliably even if anomalously.

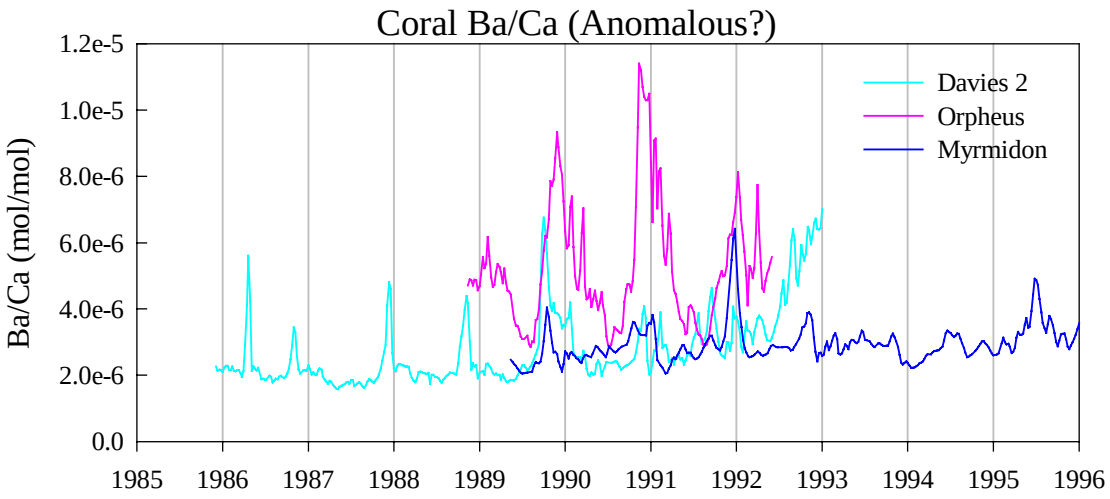

Figure 6.17 Ba/Ca vs. time from Davies 2 (cyan), Orpheus (pink) and Myrmidon (blue) corals. Mid-shelf and outer reef coral Ba/Ca has "background" levels ~2e-6 (mol/mol). Davies 2, Orpheus and perhaps Myrmidon have "anomalous" barium spikes that are not associated with runoff/upwelling.

Anomalous barium has also been observed in other corals during mid-summer (Hart and Cohen, 1996; Tudhope *et al.*, 1996; Hart *et al.*, 1997). Both of these publications discussed sharp spikes of barium that are not directly linked to runoff or upwelling. An extensive discussion based on the possible environmental factors causing the anomalous barium values in the GBR corals (e.g. wind, tides, water temperature, light, nutrients, spawning, anthropogenic and plankton blooms) was discussed by Sinclair (1999). His final summary suggests that none of these environmental factors are fully consistent with the observed barium spikes but spawning and/or plankton blooms cued by environmental factors were his best hypothesis. However if spawning was the culprit this behavior should be observed in more corals. The "anomalous" barium spikes observed in the Davies 2 coral cannot be related to runoff or upwelling and are probably related to the spikes in the Orpheus and Whitsunday corals discussed by Sinclair (1999).

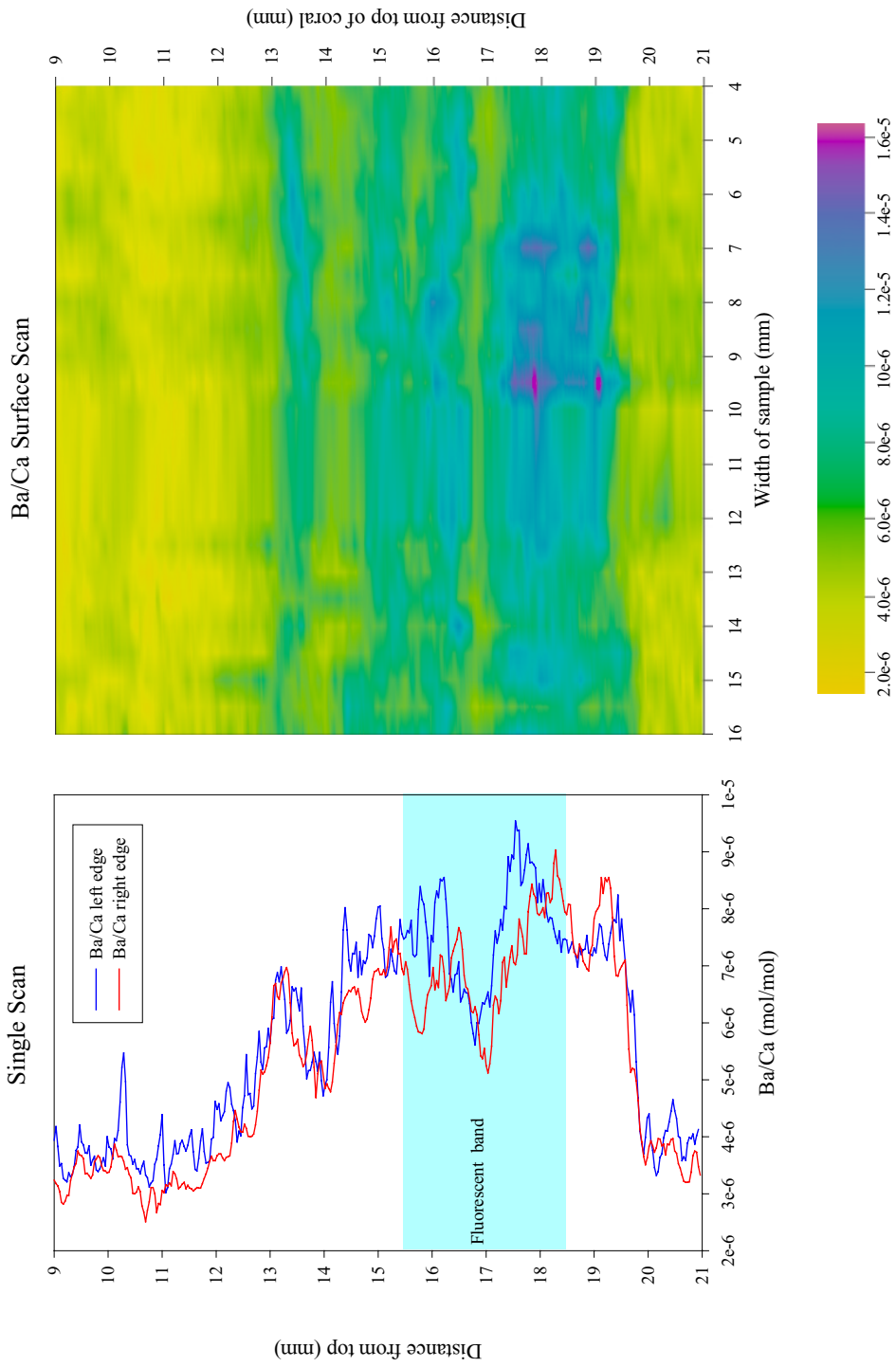

Figure 6.18 Ba/Ca surface map from Orpheus coral. Left graph shows the single scans from the left edge (blue) and right edge (red). The blue box shows the position of the fluorescent band. The right graph is a 2-D surface map covering a 12 x 12 mm box of Ba/Ca concentration. The scale bar shows the concentration range. The scan is made up of 24, 0.5 mm wide laser tracks. The data is high resolution with each sample equivalent to 0.1 mm.

Manganese (Mn)

Manganese has been measured in corals from near coastal locations (Gulf of Panama, Shen and Sanford, 1990), the Galapagos Islands (Linn *et al*., 1990; Shen *et al*., 1991; Delaney *et al*., 1993) and open ocean (Tarawa Atoll, Shen *et al*., 1992b). In these studies Mn displays clear strong annual signals, less clear annual signals (Shen and Sanford, 1990; Delaney *et al*., 1993) and pulse type events (Shen *et al*., 1992b). The Mn seawater concentration is normally dominated by proximity to coastlines. Dissolved and particulate Mn from rivers, reduction of Mn in shelf sediments and aeolian inputs dominate the coastal seawater Mn concentrations (Bender *et al*., 1977; Shen *et al*., 1991). Away from coastal locations aeolian input is the main contributor to surface Mn concentrations (Klinkhammer and Bender, 1980).

The GBR inshore corals (Pandora, Havannah, Orpheus) all show clear annual cycles of Mn (Figures 6.4 – 6.6). This annual cycle is offset from seawater temperature with Mn peaks preceding the summer SST maximum (Figure 6.18A). This timing offset most likely precludes temperature as a factor controlling the Mn variations. Other possible parameters that have the correct timing and can affect seawater Mn concentration are solar radiation and wind. The solar radiation recorded at Cape Bowling Green (Figure 6.1) and the meridional wind component is highly correlated (Figure 6.18B) reflecting the affects of land heating during spring and summer.

In other corals with clear annual cycles the Mn maximum occurs during warm and sunny conditions (Shen *et al*., 1991; Delaney *et al*., 1993). The inshore GBR corals have Mn maxima when the southeasterly winds slacken and reverse which is coincident with the solar radiation annual maximum (Figure 6.18B). The data from the three inshore corals displayed such consistent Mn cycles that the data was combined to produce an inshore Mn composite, shown in Figure 6.. The variations in the meridional wind velocity explain 59% of the Mn variations whereas the solar radiation explains 51% of the Mn variations (Figure 6.) making it difficult to separate each parameters influence on seawater and therefore coralline Mn.

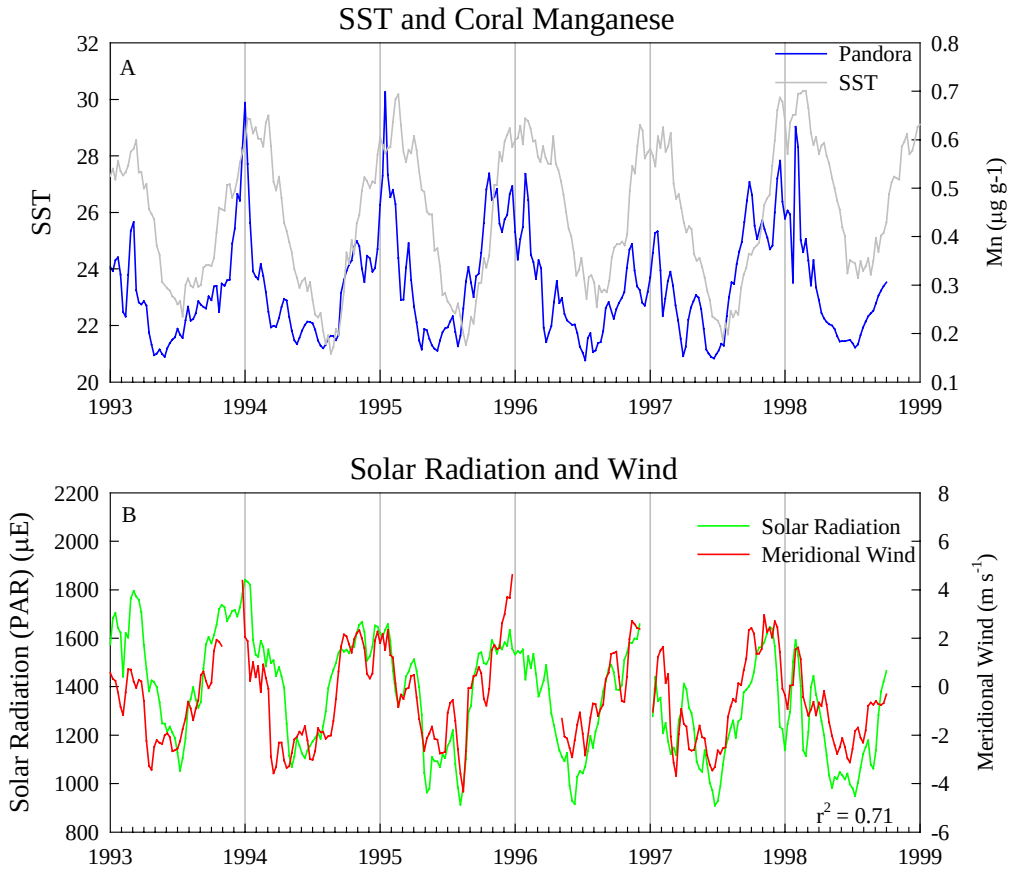

Figure 6.18 a) Pandora Mn (blue) and Inshore SST (gray) vs. time. b) Solar radiation (green) and Meridional Wind velocity (red) vs. time from the AIMS Weather Station located at Cape Bowling Green, Qld. Data plotted is a two week average of daily data. There are several gaps visible in both datasets. The solar radiation data has a decreasing trend reflecting increased summer cloud cover; when this trend is removed the wind and solar radiation are well correlated ($r^2 = 0.71$). Data was provided by J. Lough.

Mn records in corals from previous publications pointed to annual upwelling of low concentration Mn waters diluting the surface seawater at Galapagos during half the year as the cause for the annual signal (Shen *et al*., 1991; Delaney *et al*., 1993). The high surface Mn was most likely sustained by aeolian inputs and/or shelf/riverine manganese (Shen *et al*., 1991). Other sites have shown Mn spikes that were speculated to be caused by volcanism (Shen *et al*., 1991). At Tarawa lagoon westerly wind bursts were speculated to generate wind waves that stirred up particulate and diagenetically remobilized manganese from lagoon sediments (Shen *et al*., 1992b). Factors that only influence the inshore reef are needed to explain the annual Mn cycling as the mid-shelf and outer reef corals do not show this seasonality (Figures 6.7 – 6.9).

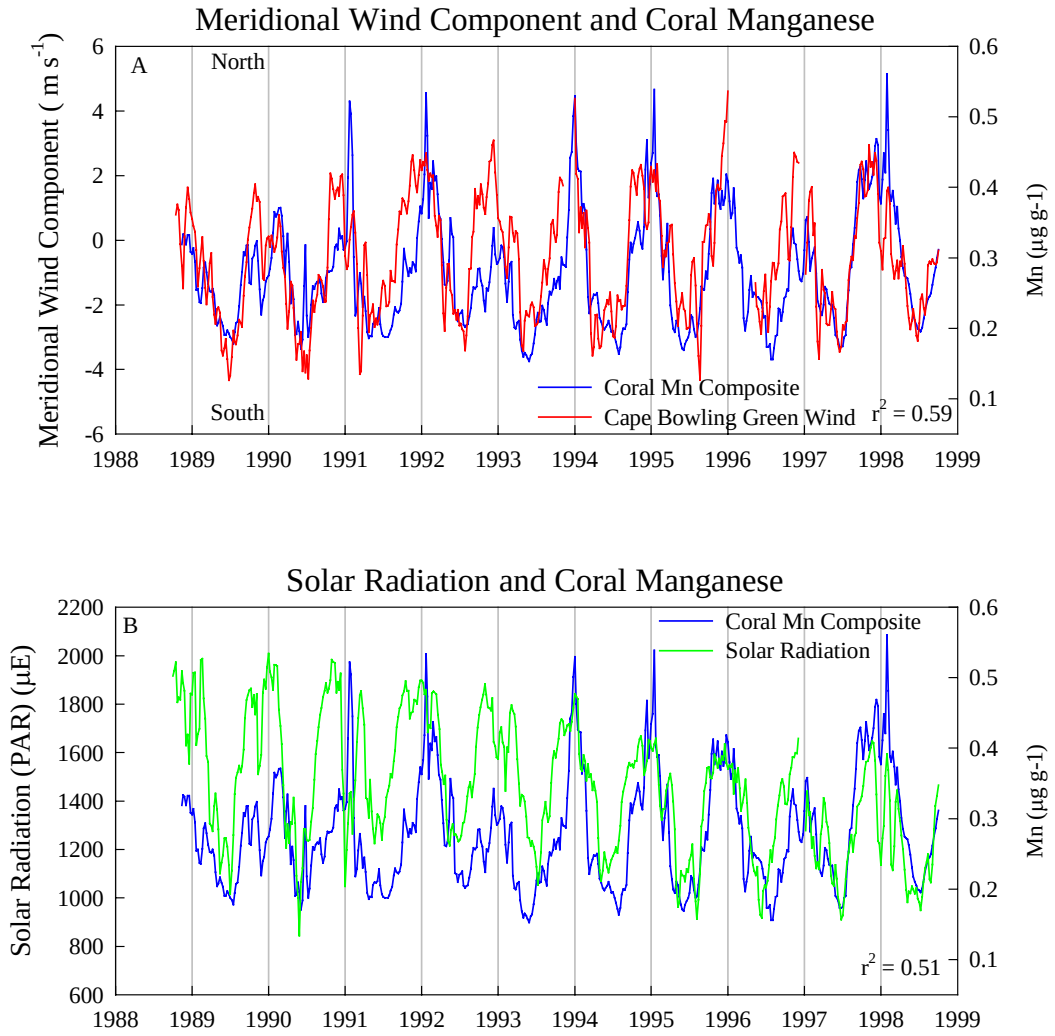

Figure 6.20 a) Cape Bowling Green meridional wind component (red) and inshore coral Mn composite (blue) vs. time. The three inshore corals were combined to produce the inshore coral Mn composite. The Cape Bowling Green meridional wind explains 59% of the Mn variations. b) Cape Bowling Green solar radiation (green) and the inshore coral Mn composite blue vs. time. When solar data is de-trended it explains 51% of the Mn variations making it difficult to separate the two factors influence on inshore coral Mn.

On the GBR, aeolian input of Mn is probably not the main cause of Mn cycles. If it were, all the measured corals in this study would show the annual cycles. As mentioned previously, the inshore reefs are influenced by riverine inputs, which most likely carry particulate and dissolved Mn. Spikes in the Pandora coral occur in Jan. 1991 and Jan. 1998 at the same time as the Ba/Ca runoff spikes, indicating a possible river connection (Figures 6.16, 6.20). These runoff events are pulse events and cannot explain the annual Mn cyclisity. These flood plumes and therefore particulates do not reach the mid-shelf and outer reef, which may account for the lower coral Mn concentration and lack of seasonality.

Some possible explanations to account for this annual seasonality revolve around sunlight and wind. One possibility is that the stronger winter winds keep particles stirred up enough to scavenge Mn from the reducing sediments. Then during the low spring/summer winds the particles drop out of the water column allowing Mn to diffuse into the seawater from anoxic sediments. Another explanation is that sunlight is influencing the surface seawater Mn concentration. Photoreduction of manganese oxides has been shown to increase in the presence of full sunlight (Sunda and Huntsman, 1988). The formation of particulate manganese is decreased during increased sunlight through the photoinhibition of manganese oxidizing microorganisms (Sunda and Huntsman, 1988). During the winter, the winds probably stir up particles, then as the solar radiation increases, photoreduction of particulate Mn oxides occurs releasing soluble Mn. This soluble Mn is not scavenged to particulates because of photoinhibition. Therefore the higher dissolved seawater Mn would be available for incorporation into the coral. Corals most likely incorporate Mn as a dissolved component and not as a particulate (Shen *et al*., 1991). The influence of wind and solar radiation on particles may also work in the opposite direction. During some summers (1990,1991,1992,1993,1995, maybe 1997 and 1998) a shift in the meridional wind occurs from positive (north) to slightly negative and a decrease in the solar radiation result in a decrease of coral Mn (Figure 6.). At this point neither the solar radiation nor wind can be linked as the major influence on coral Mn. One other unresolved issue is that Mn peaks during Jan. of most years are not directly accounted for by either the winds or solar radiation.

6.5 Conclusions

The use of B/Ca, Mg/Ca, Sr/Ca and U/Ca has been investigated as proxies for SST in corals from inshore, mid-shelf and outer reef locations in the GBR. From this dataset Sr/Ca and B/Ca appear to be the most faithful in recording seawater temperature. Sr/Ca also appears to be the least influenced in regards to coastline proximity and runoff. B/Ca may be influenced slightly. U/Ca and Mg/Ca both had sites where correlations to SST were both good and poor suggesting they may also be influenced by factors aside from temperature. The average concentration of U/Ca and Mg/Ca may also be influenced by the corals proximity to the coast. The Pandora and Havannah coral have on average higher U/Ca and lower Mg/Ca than either the mid-shelf and outer reef corals. The coastline proximity (runoff) does not dilute the U/Ca as some may suggest (Shen and Dunbar, 1995; Wei *et al*., 2000). The use of multiple SST proxies is very

valuable to coral studies and during the construction and reconstruction of long records the ability to examine different elements can increase the value of the information received.

Nearshore processes, specifically river runoff, influence inshore corals on the GBR. The inshore corals in this study show increases of Ba/Ca coincident with Burdekin River flood plumes. This study helps reinforce the use of Ba/Ca as an indicator of river runoff. However, corals with "anomalous" spikes of barium were also found. Spikes in the Davies 2, Myrmidon and Orpheus corals occurring in Oct. – Dec. may confound the barium record. These "anomalous" spikes have also been observed in other corals (Hart and Cohen, 1996; Tudhope *et al*., 1996; Hart *et al*., 1997; Sinclair, 1999). One positive note is that not all corals show this "anomalous" behavior but the ones that do share a commonality that the spikes are sharp and of short duration. They should be noticeable when compared to Ba/Ca upwelling or river runoff.

Inshore corals also show good annual cycles of manganese. The timing of the Mn increases coincides with annual increases of solar radiation and weakening of the winter south easterlies. Increased solar radiation may act to reduce particulate formation through photoinhibition and increased photoreduction of manganese oxides. The wind may act to increase particle suspension during the winter. The abundance of particles can then be reduced during the warmer months causing local surficial manganese increases that are recorded by the corals.

This study shows the benefit of LA-ICP-MS, whereby the simultaneous measurement of multiple elements is possible. These elements have been shown to provide records of water temperature, runoff and possibly wind direction. This study has only concentrated on short time scales from corals across the GBR and obviously the potential now exists for paleo-reconstructions over longer time scales (10^2 years).

Chapter 7: Trace Elements in Misima Island Corals Record Increased Sedimentation

7.1 Introduction

A major environmental issue especially in tropical regions is marine sedimentation, primarily caused by soil erosion from deforestation and agriculture. Localized increases in sedimentation have also been caused by urbanization and mining. A gold and silver mine on Misima Island, Papua New Guinea (PNG) has caused a significant increase in the local sediment load through the construction and operation of an open-cut mine and ore-processing plant (Figure 7.1). Construction of the open cut mine at Misima Island began in April 1988. A platform (150 m wide) was constructed at the end of the haul road on top of the fringing reef (Figure 7.1) to accommodate the disposal of soft waste (soil and highly friable rock). Approximately 50 x 10^6 tons of waste was dumped over the edge of the reef into deep water from Apr. 1988 to Nov. 1993 (Misima Mines Limited (MML), unpublished data). However, runoff from the disturbed (mined) sites, via the two creeks on either side of the plant site, is also a very significant source of sedimentation onto the reef (Figures 7.1, 7.2) (Done and Turak, 1994).

Barnes and Lough (1999) examined whether the growth characteristics (average annual density, annual extension and annual calcification) from 93 *Porites* colonies collected from various locations around the southeastern portion of Misima Island changed in response to an increase in the sediment load (Figure 7.1). They reported that the density, extension and calcification were lower in the period after mining when compared to the pre-mining levels. As this result was not associated with distance from the mine site, it was concluded that some other environmental parameter not associated with the mine (e.g. temperature) was the cause of this change. However, they did note that tissue layer thickness (a potential monitor of coral stress) significantly decreased with increasing proximity to the mine (Barnes and Lough, 1992; Barnes and Lough, 1999). The increase in sediment had little effect on growth related mechanisms aside from decreasing tissue layer thickness (Barnes and Lough, 1999).

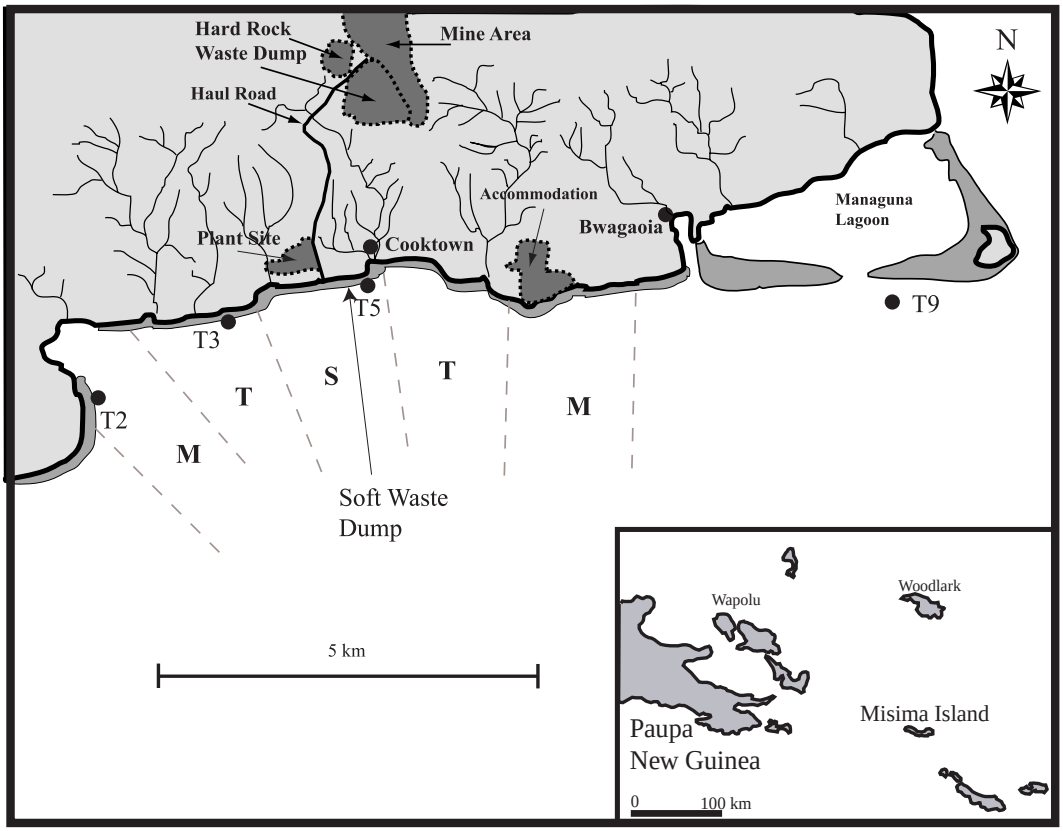

Figure 7.1 Location map of Misima Island and the Misima Mines Ltd open cut operation, Papua New Guinea. The plant site, pit, waste dumps and main creek systems are indicated as well as reef impact zones (S-severe, T-Transitional and M-Minor) and sample sites (T2, T3, T5 and T9).

Figure 7.2 Aerial photo of Misima Island Mine showing sediment runoff from Cooktown Creek. Photo courtesy of MML.

As has been discussed previously, methods have been developed that enable corals to be used as biomonitors of environmental pollution by measuring trace metals, such as Hg, Cu, Zn, Pb, Mn, Fe, V, Cd, rare earth elements (REE's) etc. (e.g. Howard and Brown, 1986; Brown, 1987; Shen and Boyle, 1987; Hanna and Muir, 1990; Scott, 1990; Sholkovitz and Shen, 1995; Guzman and Jarvis, 1996; Bastidas and Garcia, 1999). Incorporation of trace metals into corals can be the result of dissolved metal incorporation into the crystal lattice (substitution for Ca), particulate (detritus) matter trapped within skeletal cavities, organic matter from coral tissue or by coral feeding (Barnard *et al*., 1974; St.John, 1974; Howard and Brown, 1984; Brown, 1987; Hanna and Muir, 1990). Regardless of the incorporation mechanism, corals have been shown to be good tracers of pollutants in the marine environment (Dodge and Gilbert, 1984; Howard and Brown, 1987; Shen and Boyle, 1987; Hanna and Muir, 1990; Scott, 1990; Guzman and Jimenez, 1992; Guzman and Jarvis, 1996; Bastidas and Garcia, 1999).

In this chapter, results are reported for analyses of eight *Porites* corals two corals from each of four transects (T2, T3, T5, T9). Sites T2, T3 and T5 (minor, transitional and severe, respectively) were affected by varying amounts of sediment and site T9 was a control (Figure 7.1). We measured Mn, Y, La and Ce (construction and clay overburden elements) and Zn, Pb (ore zone, "fresh" rock elements) using laser ablation inductively coupled plasma mass spectrometry (LA-ICP-MS) to determine whether the increased sedimentation could be monitored by these elements. The entire REE suite of elements was also analyzed to determine if the seawater patterns around Misima Island were similar to other REE patterns from mainland PNG.

7.2 Location and Mineralization

The Misima gold and silver mine is located at the southeastern side of Misima Island, which is ~ 200 km east of the mainland of PNG (10.6°S, 152.8°E) (Figure 7.1). Misima Island is a mountainous island consisting of vertical limestone cliffs bordered by a narrow (<100m wide) fringing reef that drops steeply to depths exceeding 1000m (Barnes and Lough, 1999). The mineral deposits are located in steep hilly terrain approximately 4 km from the coast (Figure 7.1). The silver gold mineralization occurs in veins within breccia. The following gangue minerals (in order of abundance) are associated with the ore mineralization; illite-sericite, quartz, calcite, manganese oxides,

pyrite (FeS_2), sphalerite (ZnS), galena (PbS) and chalcopyrite ($CuFeS_2$). The ore body is overlain by highly weathered and oxidized material. Four main rock types were identified in this weathered material, quartz feldspar porphyry, feldspar porphyry, greenstone and schist (NSR, 1987). These dominant rock types typified the waste disposed via the soft waste dump as well as the material entrapped in mine site runoff.

A detailed description of the location, transect sites, coral and sediment traps can be found in Barnes and Lough (1999) and Done (1994). In summary, Natural Systems Research (NSR) Environmental Consultants established 10 transects on both sides of the mine. The reef immediately adjacent to the mine was divided into one of three impact zones; severe, transitional and minor (see Figure 7.1). Two transects were established in each of the severe (T4 & T5) and minor (T2 & T8) impact zones, with three located in the transitional zones (T3, T6 & T7). A further three transects (T1, T9&T10) were established outside of the impact zone as control sites. Corals were collected from a depth of 6-8m and sediment traps were placed adjacent to the coral collections at depths of 9-10m, 1m above substrate (J. White, pers. comm.). Daily sedimentation rate (mg cm^{-2} d^{-1}) was calculated for the time period 1988 to 1994 and monthly rainfall records were collected at Umuna Mine Site (MML unpublished data, Barnes and Lough, 1999).

7.3 Methods

Trace elements were measured using the LA-ICP-MS method. The laser setup and standardization was discussed in Chapter 3.5. In addition the REE suite of elements was analyzed on a recently acquired Agilent 7500s ICP-MS using the previously described laser system. The isotopes monitored were; ^{139}La, ^{140}Ce, ^{141}Pr, ^{146}Nd, ^{147}Sm, ^{153}Eu, ^{157}Gd, ^{159}Tb, ^{163}Dy, ^{165}Ho, ^{166}Er, ^{169}Tm, ^{172}Yb and ^{175}Lu again using ^{46}Ca as the index isotope. The laser repetition rate was increased to 20Hz to provide more material to the ICP-MS. This ICP-MS has improved sensitivity when compared to the older PQ2 and has enabled us to analyze the low REE concentrations.

7.4 Results

Figure 7.3 shows the daily sedimentation rate (mg cm^{-2} day^{-1}) for each of the four study sites (T2, T3, T5 and T9) plus the rainfall for each collection period. Sedimentation rates measured in the three months prior to the mine construction averaged 1.06 ± 0.9 mg cm^{-2} day^{-1} for the four sites. Once mining operations started the sedimentation rate at the severe site (T5) quickly increased ~100 fold and stayed quite high until mid-1992 (Figure 7.3A). Sedimentation rate at the transitional site (T3) increased ~20-80 times then tapered off until mid-1992 (Figure 7.3B). The minor site showed slight increases of 10-20 times in sedimentation rate during this same time period (Figure 7.3C). The control sites recorded low sedimentation rates < 2 mg cm^{-2} day^{-1}during the entire collection period indicating that these sites were unaffected by increases in sedimentation/mine associated activities (Figure 7.3D). Pre-mining and construction levels of sedimentation were approached by all transects after 1993 when dumping ceased and more importantly drought conditions occurred (Figure 7.3E) (NSR, 1987; Barnes and Lough, 1999). Monitoring after cessation of soft waste dumping confirms that rainfall and thus runoff is the primary source of sediment (J. White, pers. comm.). Higher sedimentation rates at the severe, transitional and minor zones were associated with high rainfall events in mid-1989 and late-1991 (Figure 7.3E).

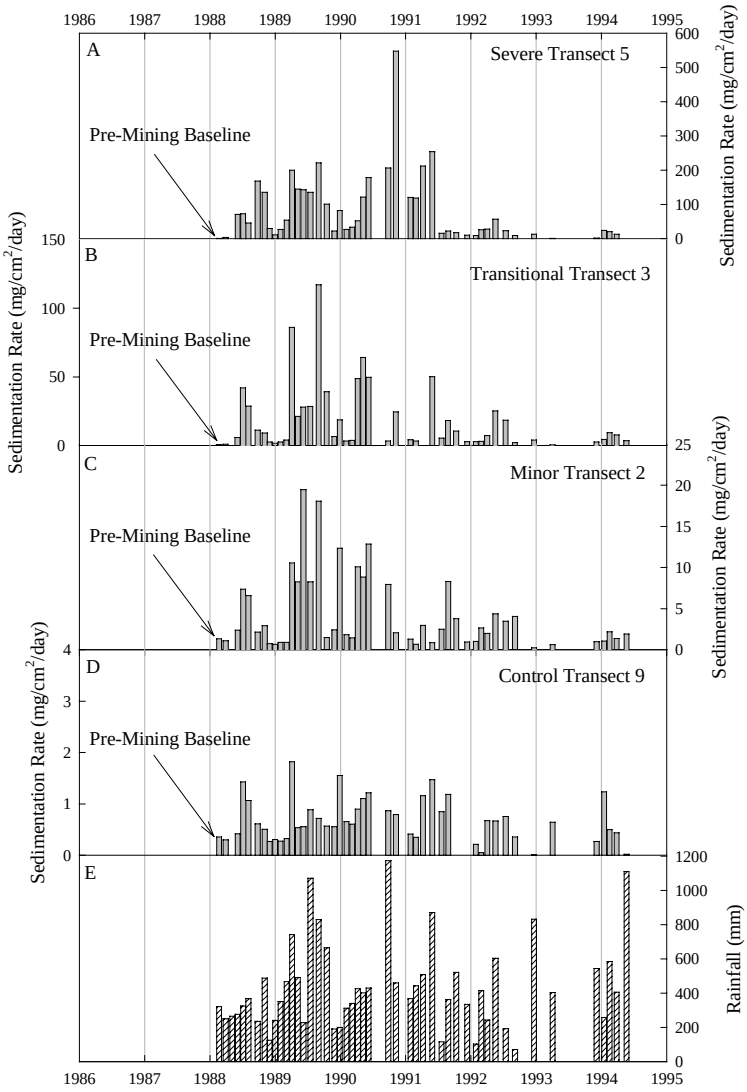

Figure 7.3 A-D) Sedimentation rate (mg cm^{-2} d^{-1}) from sediment traps at the four transects. E) Rainfall (mm) Umuna Pt. (MML data).

7.4.1 Reproducibility of Coral Records

Two corals were analyzed from each site and both corals show very similar, highly reproducible trace element patterns for each transect. The trace element patterns of Y and Zn from the two severe site corals (T05B03, T05B08) can been seen in Figure 7.4A,B. Examination of the X-ray confirms a visual gap in the coral slice T05B08 around 1992 indicating that a growth stoppage occurred at that time. When this is accounted for, the Y peaks and the Zn increases are synchronous (Figure 7.4A,B). Two other elements (La and Pb) were compared between the two corals from the transitional site (T03B03, T03B07) in Figure 7.4 C,D. Both corals show synchronous peaks in La and increases of Pb.

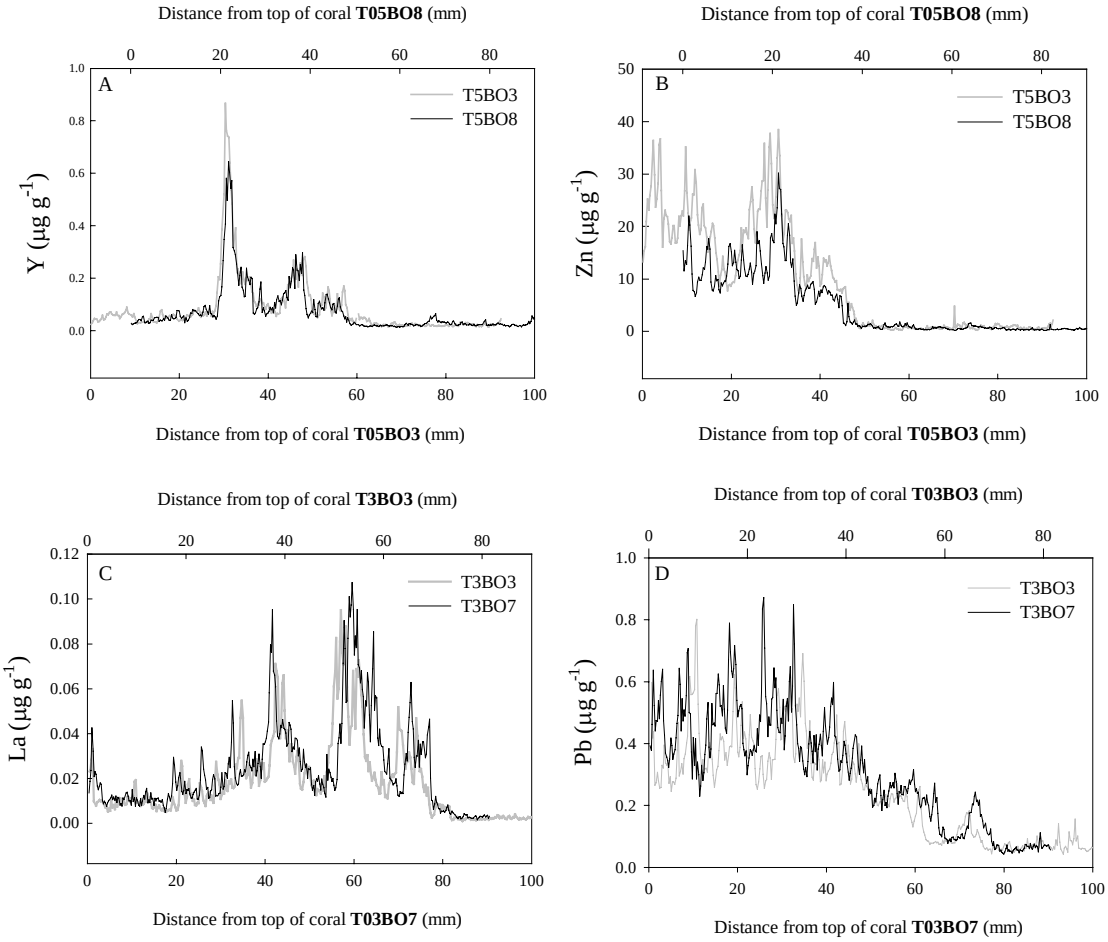

Figure 7.4 A) Y (µg g^{-1}) vs. Distance from the top of the coral (mm) for both severe site corals. B) Zn (µg g^{-1}) vs. Distance from the top of the coral (mm) for both severe site corals. C) La (µg g^{-1}) vs. Distance from the top of the coral (mm) for both transitional site corals. D) Pb (µg g^{-1}) vs. Distance from the top of the coral (mm) for both transitional site corals. The graphs have different x-axis scales to account for variations in growth rate between the two corals

7.4.2 Distance to Time Translation

Time series were constructed using seasonal cycles of U/Ca and B/Ca (proxies for SST, Fallon *et al*., 1999b) by matching winter SST minima to U/Ca and B/Ca maxima. Data from each coral was re-sampled to weekly resolution (52 samples yr^{-1}) using the time series program Analyseries (Paillard *et al*., 1996) and the two corals from each site were averaged to produce one record for each transect. This enhances the common features between the coral records. Since a minimal amount of time marker points were chosen this chronology may suffer during times of non-linear extension/growth but should be accurate to within ± 1 month.

7.4.3 Yttrium, Lanthanum and Cerium

The three rare earth elements, La, Ce and Y from the 4 transects all track each other and were associated with an increase in runoff of weathered topsoil (Figure 7.5). Pre-mining levels (< 1988) for these elements were similar between the 4 transects, 0.02, 0.004, and 0.003 μg g^{-1} for Y, La, and Ce respectively (Table 7.1). Severe, transitional and minor transects all increased after the mine construction began in 1988 (Figure 7.5A-C). During heavy runoff events the concentrations of these elements in the corals increased consistently with the amount of sediment collected by the sediment traps (Figures 7.3, 7.5). After 1992 (when sedimentation rate dropped sharply, Figure 7.3) the concentration of Y, La, and Ce from the minor and control site corals returned to pre mining levels (Table 7.1). The concentrations of Y, La, and Ce in the severe and transitional site corals were still ~ 2x higher than the pre-mining after 1992 (Table 7.1). The control site corals showed low, relatively steady concentrations of the elements throughout all the rainfall periods indicating runoff or soft waste dumping was not affecting them.

Table 7.1 Concentrations in the corals from all sites before (< 1988) and after (>1992) sediment increase.

	Mn (μg g^{-1})		Zn (μpg g^{-1})		Pb (μg g^{-1})		Y (μg g^{-1})	
	<1988	>1992	<1988	>1992	<1988	>1992	<1988	>1992
Severe	0.190	0.490	0.680	19.9	0.241	0.468	0.024	0.048
Trans.	0.160	0.305	0.160	12.7	0.071	0.428	0.016	0.030
Minor	0.090	0.189	0.286	2.25	0.051	0.127	0.017	0.021
Control	0.094	0.104	0.350	0.393	0.051	0.053	0.022	0.018

	La (μg g^{-1})		Ce (μg g^{-1})	
	<1988	>1992	<1988	>1992
Severe	0.006	0.026	0.006	0.022
Trans.	0.003	0.011	0.002	0.009
Minor	0.002	0.005	0.002	0.004
Control	0.004	0.004	0.003	0.002

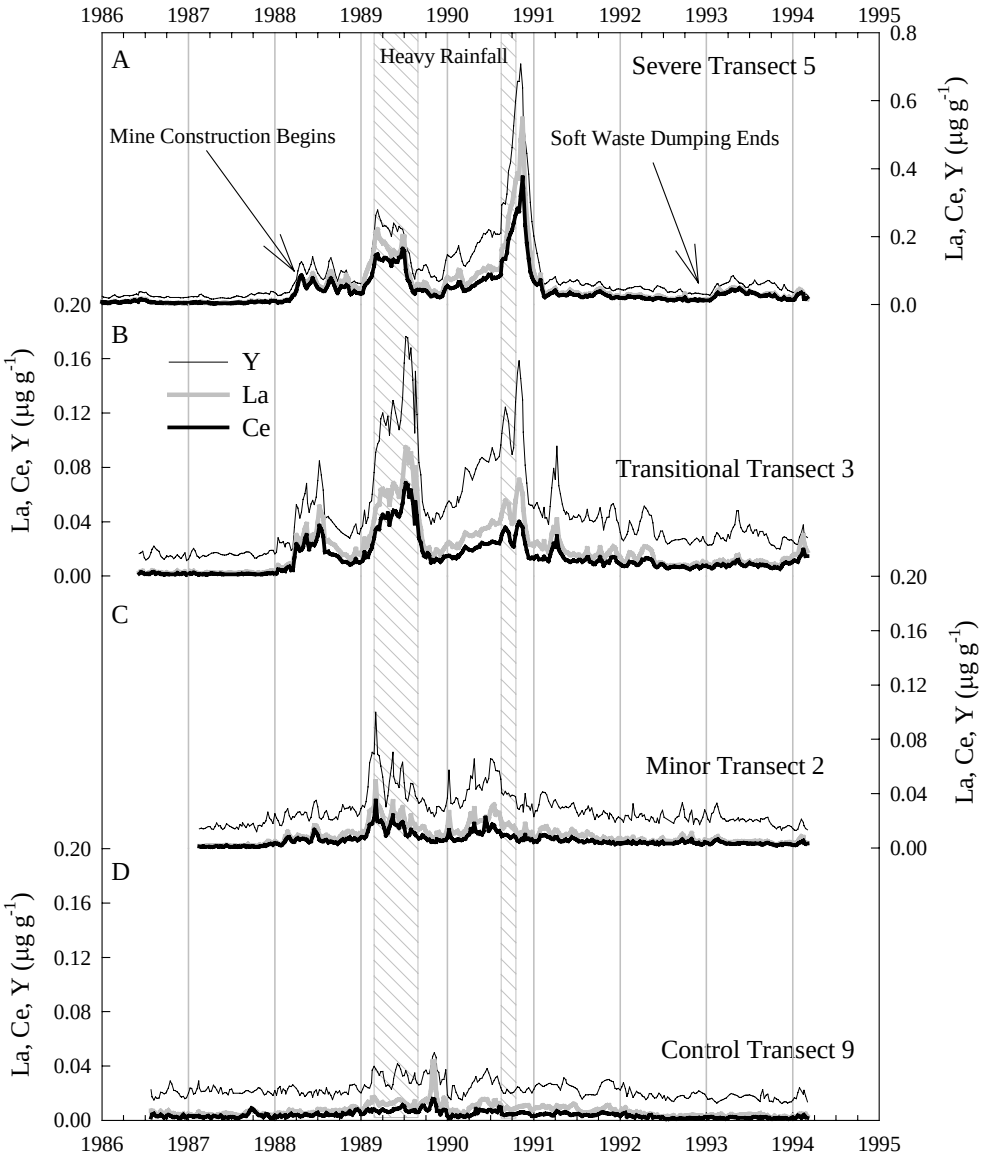

Figure 7.5 La, Ce, Y (μg g^{-1}) vs. time from all four transects. These elements record the onset of mine construction in 1988 and show peak values during heavy rainfall events. Note y-axis scaled differently for each transect.

7.4.4 Manganese

The concentration of Mn also increased after 1988 in both the severe, transitional and to some extent the minor site corals (Figure 7.6A-C). The three peaks in the severe site corals also coincide with increases in sediment and Y, La and Ce peaks, although the peak values were slightly offset (Figures 7.5, 7.6). The average Mn concentration for the pre-mining time period ranged from 0.09-190 μg g^{-1} with the control and minor corals at 0.09, the transitional at 0.160 and the severe at 0.190 μg g^{-1} (Figure 7.6, Table

7.1). After 1992, the three affected sites had an average concentration ~ 2x higher than the pre-mining level (similar to Y, La, Ce), 0.490 severe, 0.305 transitional and 0.190 μg g^{-1} minor (Figure 7.6A-C, Table 7.1). The control site had steady low "background" levels throughout the period analyzed (Figure 7.6D, Table 7.1).

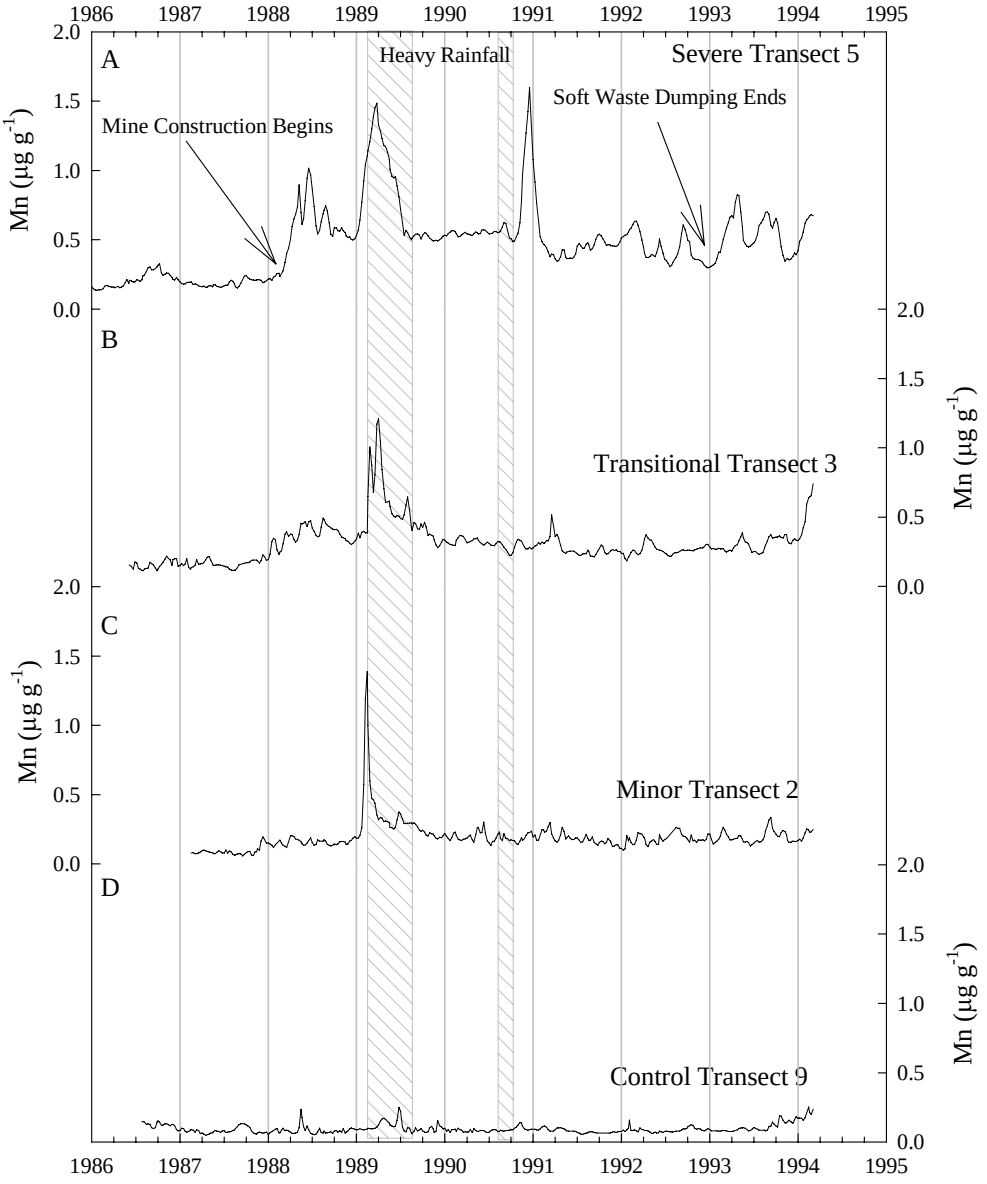

Figure 7.6 Mn (μg g^{-1}) vs. Time from all four transects. This element also shows increases coincident with the mine construction and peaks associated with heavy rainfall.

7.4.5 Zinc and Lead

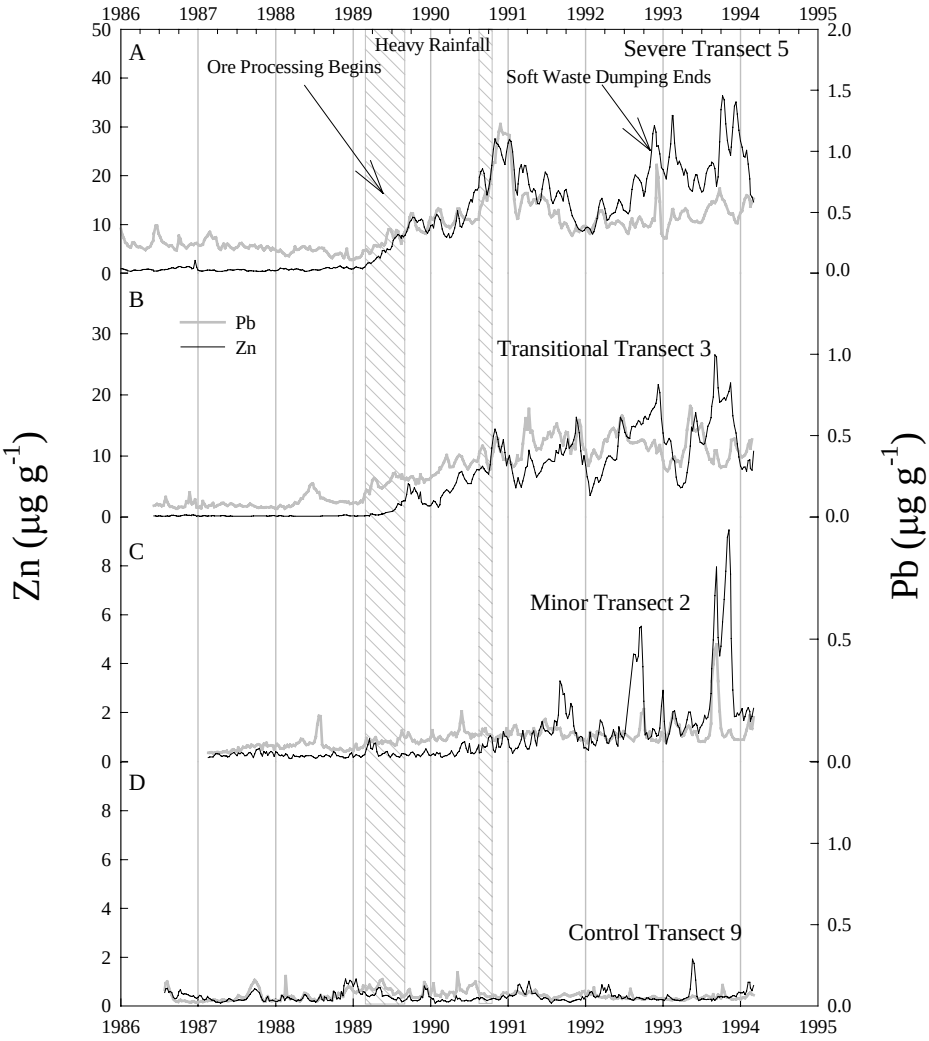

Figure 7.7 Zn and Pb (μg g^{-1}) vs. time from the four transect sites. Zn and Pb do not increase until ore processing begins and "fresh" rock is exposed. y-axis scales different for different transects.

The concentration of Zn and Pb in the corals from the severe and transitional sites began to increase after 1989 when ore processing began and "fresh" rock was exposed from the pit (Figure 7.7A,B). The minor transect corals showed a slight increase in Zn after 1991, but the Pb was relatively steady at background levels. The control site did not show any variations of Zn or Pb coincident with mining or runoff (Figure 7.7D). The average pre-mining Zn concentration was 0.68, 0.16, 0.286 and 0.350 from the severe, transitional, minor, and control site corals respectively (Table 7.1). After 1992, the average Zn concentration was dramatically higher for the three affected sites, remaining substantially above the pre-mining concentrations, 19.9 (severe), 12.7 (transitional), 2.25 (minor), and 0.393 μg g^{-1} for the control site corals (Table 7.1).

7.4.6 Rare Earth Element Pattern Data

Sections of four corals (2 from severe sites and 2 from transitional sites) were selected to analyze the entire REE suite. These corals had the highest La and Ce values providing us with the best opportunity to obtain meaningful concentration data from the very low concentration REE's. The scan for the severe site coral (T05B03, Figure 7.8) encompasses the sediment increase (1988, ~ 60 mm from top of coral) to after the largest peak (Nov.-Dec. 1990, ~ 25 mm from top of coral) (Figures 7.5, 7.8). Figure 7.8 also displays the coherent nature of REE's as each one reproduces the detail in all the peaks. All of the peak data (the sections covered by the shaded area, Figure 7.8) was considerably above instrumental detection limits (Table 7.2). The pre-mining values for the lower concentration REE's (Eu, Tb, Ho, Tm, Lu) were only slightly above the detection limits (Table 7.2).

Data were grouped and averaged from each peak value (shaded area on Figure 7.8) to enhance counting statistics. Table 7.2 lists the average concentration for each REE from two peak sections of the severe and transitional site corals. A "(1)" indicates the average value for the peak section June 1990 – Jan. 1991 and a "(2)" is the average of the Feb. 1989-Aug. 1989 section (Figure 7.8, Table 7.2A). These are the only two sections of each coral presented in the REE pattern data.

To interpret REE data, samples are usually normalized to upper continental crust or chrondrites. In this instance we normalized to the mean value of North American, European and Russian shales used by Sholkovitz *et al*. (1999).

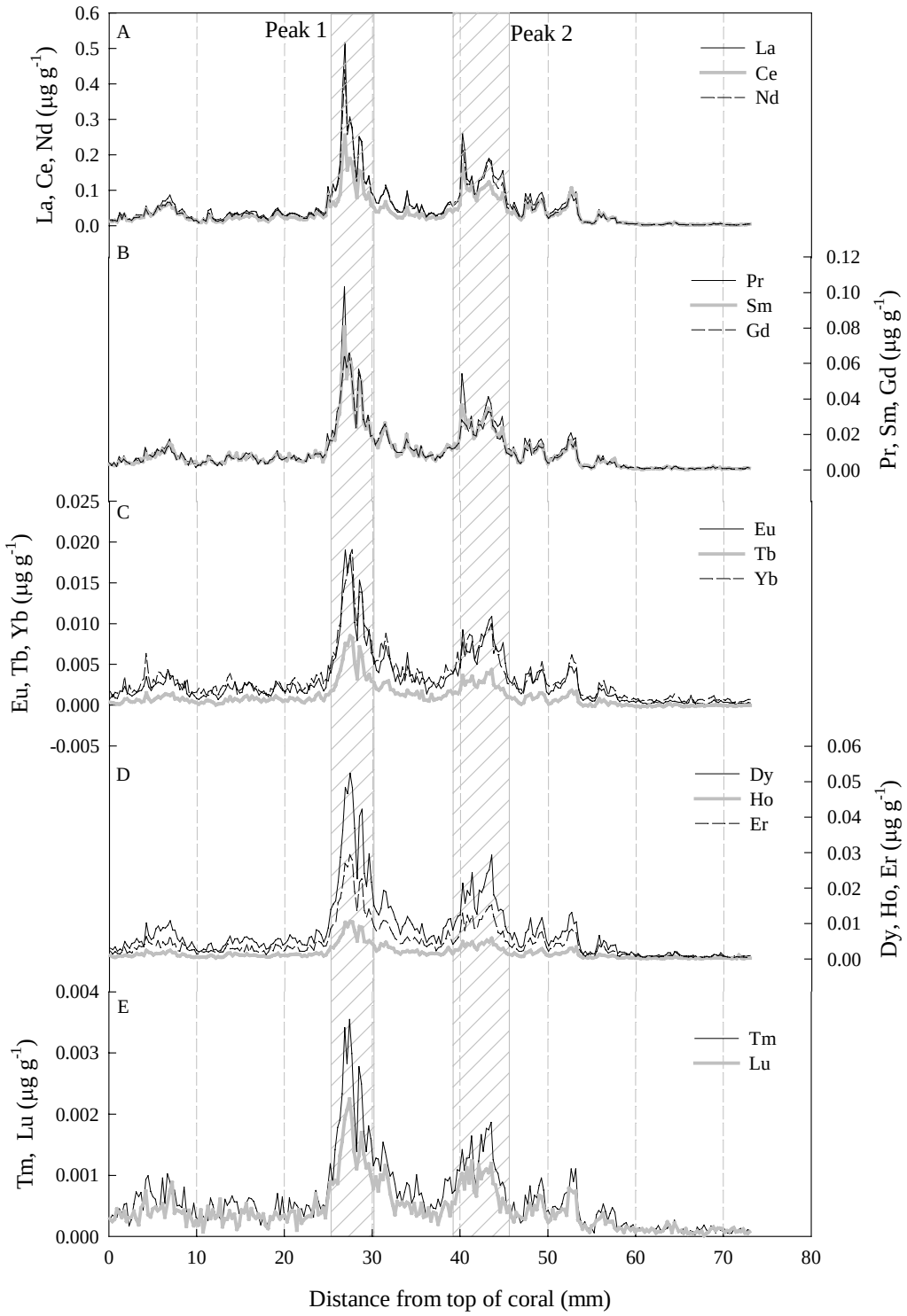

Figure 7.8 REE vs. Distance from top of coral (mm) from the severe site coral T5B03. Shaded area corresponds to “Peak 1” and “Peak 2” sections. The data was integrated over this area to construct REE normalized graphs.

Table 7.2 REE data from Severe and Transitional Corals and Sepik and Fly River estuary waters and sediments. Also shown is Coral Sea water and Shale concentrations.

(A) Coral Samples ($\mu g\ g^{-1}$)

	Severe Site Corals		Transitional Site Corals						
	T5B3 (1)	T5B3 (2)	T5B8 (1)	T5B8 (2)	T3B3 (1)	T3B3 (2)	T3B7 (1)	T3B7 (2)	DL*
La	0.1590	0.1256	0.2706	0.1999	0.0639	0.0329	0.0748	0.0412	0.00008
Ce	0.0946	0.0861	0.1772	0.1290	0.0400	0.0226	0.0455	0.0272	0.00007
Pr	0.0333	0.0259	0.0566	0.0394	0.0129	0.0064	0.0154	0.0078	0.00006
Nd	0.1503	0.1144	0.2592	0.1775	0.0561	0.0261	0.0680	0.0332	0.00032
Sm	0.0303	0.0224	0.0534	0.0355	0.0120	0.0053	0.0139	0.0066	0.00046
Eu	0.0089	0.0065	0.0154	0.0107	0.0035	0.0017	0.0043	0.0021	0.00011
Gd	0.0311	0.0208	0.0551	0.0353	0.0114	0.0057	0.0146	0.0068	0.00037
Tb	0.0039	0.0025	0.0073	0.0044	0.0016	0.0008	0.0019	0.0009	0.00029
dy	0.0254	0.0163	0.0458	0.0283	0.0103	0.0048	0.0124	0.0055	0.00029
Ho	0.0055	0.0035	0.0100	0.0060	0.0023	0.0011	0.0029	0.0013	0.00007
Er	0.0146	0.0094	0.0270	0.0164	0.0066	0.0032	0.0076	0.0034	0.00014
Tm	0.0018	0.0012	0.0033	0.0020	0.0010	0.0005	0.0011	0.0005	0.00003
Yb	0.0094	0.0065	0.0179	0.0113	0.0059	0.0031	0.0058	0.0027	0.00012
Lu	0.0012	0.0008	0.0022	0.0014	0.0008	0.0005	0.0009	0.0005	0.00004

(B) Water Samples (pmol/kg) Sediments (ppm)

	PNG River Waters[a]		Coral Sea Water			
	Fly	Sepik	SA-7 Composite[b]	Fly River[a]	Sepik River[a]	Shale[a]
La	108	164	4.12		21.4	41
Ce	252	390	5.0	71	47	83
Pr			0.77			10
Nd	178	250	3.53	32	25	38
Sm	50.3	63.0	0.66	7.4	4.7	7.5
Eu	13.9	18.3	0.2	1.4	1.07	1.6
Gd	55.5	66.7	1.08	6.9	4.22	6.4
Tb		9.59	0.2			1.2
dy	39.6	50.4	1.57	5.0	4.19	5.5
Ho			0.44			1.3
Er	18.6	23.6	1.43	3.0	2.40	3.8
Tm			0.19			
Yb	13.36	18.4	1.05	2.8	2.45	3.5
Lu	1.7	2.91	0.17	0.36	0.386	0.6

*DL = Detection Limit = Concentrat ion based on 3 x standard deviation of background counts

[a]Sholkovitz et al. (1999)

[b]Zhang and Nozaki (1996) Composite 0 - 248 m, n = 8

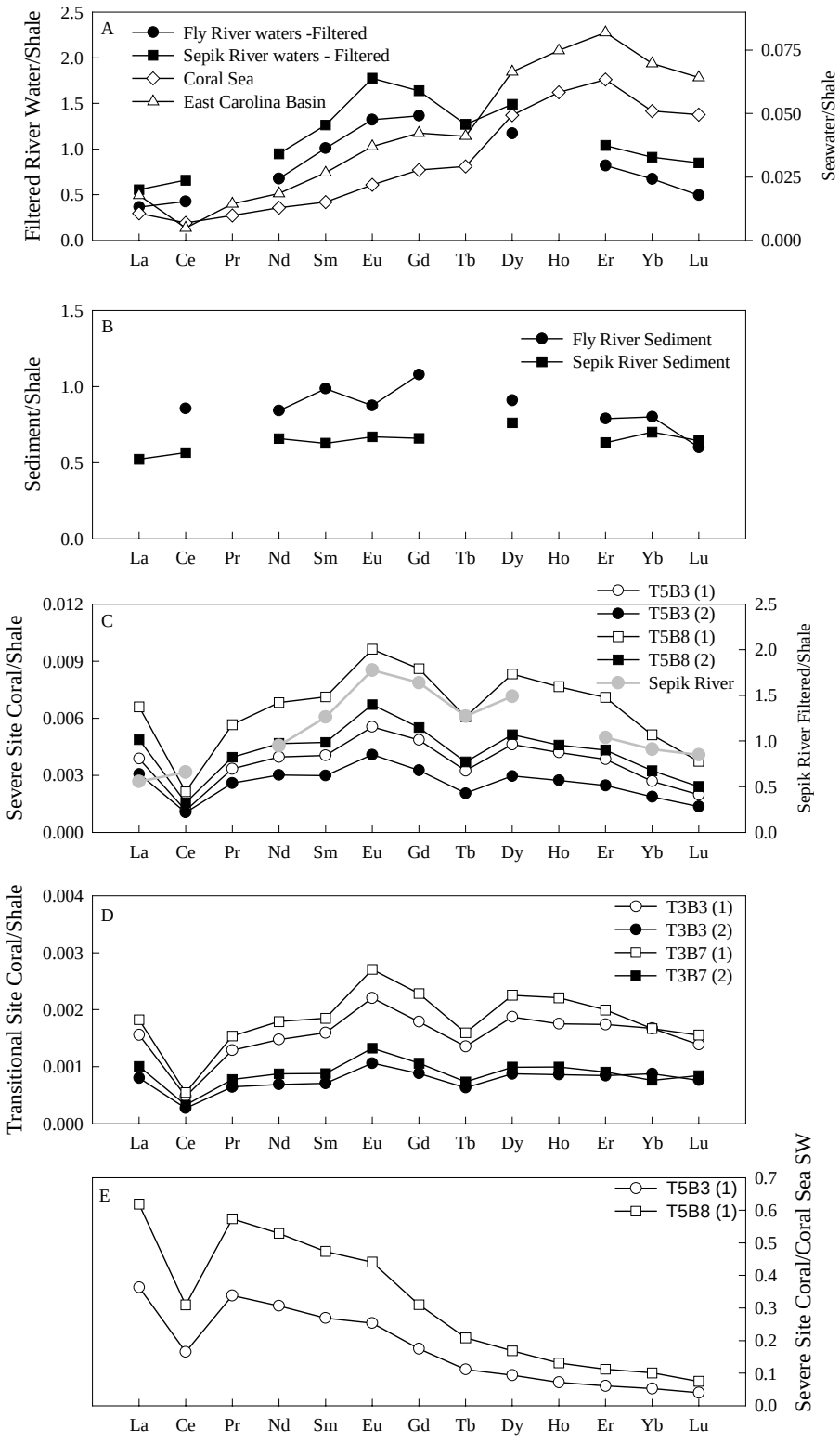

Figure 7.9 a) Shale normalized filtered Fly and Sepik river REE concentrations and Coral Sea Water (Zhang and Nozaki, 1996; Sholkovitz *et al*., 1999). b) Shale normalized sediment REE's from Fly and Sepik rivers (Sholkovitz *et al*., 1999). c) Shale normalized REE data from severe site corals and Sepik river REE values (Sholkovitz *et al*., 1999) on right axis. d) Shale normalized REE data from transitional site corals. e) Coral Sea seawater normalized data from severe site corals.

Figure 7.9 shows the shale normalized REE patterns of PNG river water (Fly and Sepik estuary), Coral Sea water, Fly and Sepik sediments and the coral data, all data is listed in Table 7.2. The values of the Coral Sea water come from a composite of 8 measurements of water samples from 0-248 m depth used by Sholkovitz *et al*. (1999), data from Zhang and Nozaki (1996) (Table 7.2B). The shale values used for normalization are also shown in Table 7.2B and come from Sholkovitz *et al*. (1999). Both estuary river waters were enriched in the middle REE's (MREE's) and depleted in the heavy REE's (HREE's) relative to Coral Sea water (Figure 7.9A) (Zhang and Nozaki, 1996; Sholkovitz *et al*., 1999). The REE pattern of sediments from both the Fly and Sepik rivers were different to the filtered river water. Neither pattern showed MREE enrichment (Figure 7.9B) (Sholkovitz *et al*., 1999). Figure 7.9C,D shows the shale-normalized data from the four corals; the Sepik river data is also plotted in Figure 7.9C for comparison. The REE pattern data from the two peaks in each of the four corals were in excellent agreement (Figure 7.9C,D). The coral data REE pattern was remarkably similar to the filtered estuarine river water pattern. When the coral data is normalized to Coral Sea seawater the differences between the two patterns emerge (Figure 7.9E). The light to MREE is enriched relative to the Coral Sea seawater while the HREE's are depleted (Figure 7.9E). The coral data also have a different pattern compared with the Fly and Sepik sediment data (Figure 7.9B,C).

7.5 Discussion

7.5.1 Sediments

The soft waste dump was not the major source of sediment collected by the transect sediment traps. There was very little correspondence between the soft waste dumped and the sediment at the severe site transect (T5) (Figure 7.10) (Done and Turak, 1994). The majority of dumping occurred from 1991-1993, which corresponded with a very low sedimentation rate. This low sediment trap accumulation occurred because the soft waste formed a density current which caused the waste to flow rapidly down the steep submarine slope to ~ 1500 m depth and not along the shore (Figure 7.10). This re-affirms the conclusions that creek runoff was the major source of sediment input into the near shore environment at Misima (Done and Turak, 1994).

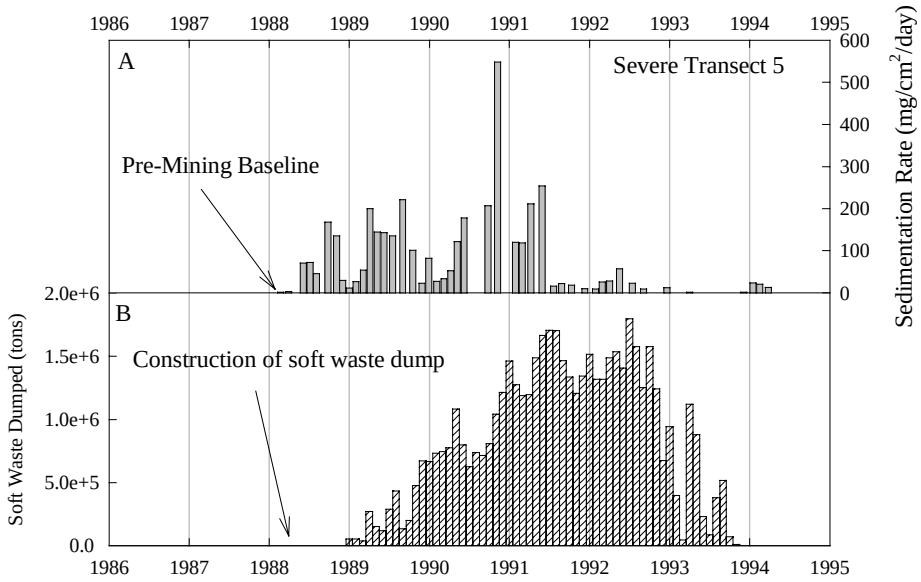

Figure 7.10 a) Sedimentation rate (mg cm^{-2} d^{-1}) from the severe site transect. b) Weight of soft waste dumped (tons) per month. Note the lack of correlation between the two datasets.

7.5.2 Manganese

In coastal areas, seawater Mn is mainly controlled by dissolved and particulate Mn derived from river or shelf sediments. At Misima, the reef shelf (~ 10m depth) along the coast adjacent to the mine site is about 50m wide (max) with a steep submarine slope (1:1.6). Resuspension does occur but little longshore movement of sediments occurs as they are moved offshore. Steep cliff like slopes in places also prevent longshore movement, as sediments tend to flow down rather than along the shore. This suggests that riverine input was the main source of the nearshore Mn. Mn has been hypothesized to substitute for Ca in the $CaCO_3$ lattice but may also be adsorbed or occluded within aragonite as an oxide or in some organic phase (Shen *et al*., 1991). Mn also appears to be discriminated against in the coral lattice with a distribution coefficient of 0.1 – 0.5 (Shen *et al*., 1991). This makes extrapolation back to seawater Mn or source sediment Mn difficult.

Mn followed a similar pattern to Y, La and Ce in the Misima corals. This probably indicates a relationship between the source materials of these elements. The likely source material for Y, La and Ce is weathered material (feldspar and greenstone) present in high quantities in the porphyry (J. White pers. comm.). Mn is also suggested to be enriched in this weathered zone as evidenced by sections of the porphyry that have

a strong "pink" or "browny-black" tint (J. White pers. comm.). This Mn is present as manganese "wad" which consists of various Mn oxides and Ferro-Mn oxides (MML pers. comm., Lewis and Wilson, 1990). The Mn concentration of the weathered material ranged from 200 ppm for "normal" soil to 4290 ppm for the "pink/brown" material (J. White, MML data). Various concentrations of MnO (0 – 0.3 wt. %) have also been reported for the greenstones, schists and porphyry of the pit area (MML data). These enriched Mn concentrations reach the rivers and creeks and increase both the dissolved and particulate Mn.

In estuarine environments, Mn has been shown to display non-conservative mixing behavior (Knox *et al*., 1981). At low salinities (2-5‰) dissolved Mn is removed especially in the presence of particulates. As salinities increase (6-20‰), Mn is added back to solution, and then removed again as salinities approach 35 ‰ (Knox *et al*., 1981). There are no estuarine environments near the mine site but a small mixing zone close to the creek site would approximate this type of environment. The severe site is expected to have the highest Mn concentrations from creek runoff. The concentration decreases at the transitional and minor transect sites through non-conservative mixing and seawater dilution.

The concentration of Mn in "cleaned" (Shen and Boyle, 1988) corals ranges from 8 – 400 ppb (Linn *et al*., 1990; Shen and Sanford, 1990; Shen *et al*., 1991; Delaney *et al*., 1993), which is similar to the baseline values measured in the Misima suite of corals (Pre-mining ~ 90-190 ppb, Table 7.1). The average value of Mn in corals collected from Galapagos is ~40-50 ppb but these corals are a different genus and are well away from riverine inputs of Mn (Linn *et al*., 1990; Shen *et al*., 1991; Delaney *et al*., 1993). Another *Pavona* coral collected from the Gulf of Panama has a Mn concentration range of 200-400 ppb with a peak value of ~ 600 ppb (Shen and Sanford, 1990). This site has a riverine influence and peak values were most likely due to Mn flux released through this runoff (Shen and Sanford, 1990). In earlier studies of "non-cleaned" corals concentrations of up to 15 ppm were measured (Harriss and Almy, 1964; Livingston and Thompson, 1971). The severe site corals had Mn peaks approaching 1.6 ppm (Figure 7.6).

7.5.3 Lead and Zinc

Lead and zinc measured in corals mostly have an anthropogenic or pollutant source. Lead appears to substitute directly for calcium in the coral lattice and is enriched relative to the surrounding seawater (Distribution coefficient = 2.3, Shen and Boyle, 1987; Shen and Boyle, 1988). Less is known about zinc, but it probably substitutes for calcium in the coral lattice although it appears that zinc is also enriched in the coral skeleton relative to seawater (Distribution coefficient = 11, Shen and Boyle, 1988). Wide ranges of concentrations have been reported for Pb and Zn in corals from "polluted" and "pristine" environments. Lead levels range from 0.03 $\mu g\ g^{-1}$ (Bastidas and Garcia, 1999) to 51 $\mu g\ g^{-1}$ (Hanna and Muir, 1990) in *Porites* sp. corals (Table 7.3). Corals from the severe site at Misima Island had peak values of 1.22 $\mu g\ g^{-1}$ and averages ~ 0.5 $\mu g\ g^{-1}$. These values are within the range reported for other *Porites* sp. (Table 7.3). The zinc values for Misima Island approached the highest zinc values measured ~ 40 $\mu g\ g^{-1}$ (Bastidas and Garcia, 1999). These high zinc values also come from corals influenced by a heavy sediment load.

Table 7.3 Zinc and Lead concentrations reported for *Porites* sp. corals.

Location	Zn ($\mu g\ g^{-1}$) Range	Pb ($\mu g\ g^{-1}$) Range	Comments-Reference
Severe	0.68-36.5	0.24-1.22	This study
Transitional	0.16-26.5	0.07-0.68	″
Minor	0.29-9.5	0.05-0.47	″
Control	0.35-1.9	0.05-0.21	″
Venezuela	3-42	0.03-1.4	high sediment (Bastidas and Garcia, 1999)
Venezuela	0.8-37	0.03-4.7	low sediment (Bastidas and Garcia, 1999)
Thailand	1.4-3.7		(Brown, 1987)
Red Sea	3	44	unpolluted (Hanna and Muir, 1990)
Red Sea	9	51	dredging, polluted (Hanna and Muir, 1990)
Great Barrier Reef	4.7	0.58	Heron Island marina (McConchie and Harriott, 1992)
Great Barrier Reef	1.4	0.18	Witsari reef (McConchie and Harriott, 1992)
Hong Kong		0.2-0.8	(Scott, 1990)
GBR	2.4	0.27	(St.John, 1974)

Both zinc and lead (at the severe site) were significantly higher after mining began and show some similarity with each other (Figure 7.7). Zinc and lead were present in the ore body as sphalerite (ZnS) and galena (PbS). They are part of the silver-lead-zinc mineralization (Feldspar porphyry). Soils collected from the mine site in 1999 showed Zn concentrations ranging from 200-800 ppm and lead concentration ranging from 70-580 ppm (MML unpublished data). These elements (Pb, Zn) can be released from the

sulfide minerals by oxidation. Measurements of sulfate in the Cooktown Creek (Figure 7.1) were ~ 10-30 ppm in 1998 (pre-mining, MML unpublished data). By 1994 sulfate levels were ~ 200 ppm, with subsequent monitoring indicating the concentration has stabilized at ~ 450 ppm (MML unpublished data). This increase in sulfate concentration was most likely due to oxidation of sulfidic minerals, including sphalerite and galena. Zinc and lead are then free to dissolve or form particulates as they mix with fresh and seawater.

Another possible source of zinc increases was the soft waste material. Preliminary results (MML unpublished data) for zinc suggested high solubility in both the weathered greenstones and feldspar components of the soft waste. Fine particulates of both rocks were shown to release zinc in the presence of seawater (NSR, 1987). If this were the source the zinc increases would coincide with the onset of soft waste dumping and not 1989-90 which was when "fresh rock" and ore-zone material was exposed (MML unpublished data). This indicates the soft waste dump had little influence on the nearshore seawater metal concentrations.

7.5.4 REE's

REE-carbonate complexes are the dominant species in seawater with light REE's (LREE's) preferentially adsorbed to surfaces while HREE's remain in solution (Sholkovitz and Shen, 1995). These elements have been measured in a few coral samples and have been shown to incorporate in proportion to the seawater REE concentration (Sholkovitz and Shen, 1995). A slight enrichment for both La and Ce occurs in corals relative to seawater (D_{La} = 1.6, D_{Ce} = 2.9, Sholkovitz and Shen, 1995). The low pre-mining values for La and Ce were within the range reported by Sholkovitz and Shen (1995) for lattice bound REE's (Table 7.4). The range of measured values from all the Misima corals was similar to the range of other REE measurements in corals (Table 7.4) (Schofield and Haskin, 1964; Scherer and Seitz, 1980; Naqvi *et al*., 1996).

Table 7.4 Lanthanum and Cerium concentration in corals from this study and other published reports.

Location	La ($\mu g\ g^{-1}$) Range	Ce ($\mu g\ g^{-1}$) Range	Comments-Reference
Severe	0.006-0.54	0.006-0.037	This study
Transitional	0.003-0.09	0.002-0.07	″
Minor	0.002-0.05	0.002-0.03	″
Control	0.004-0.04	0.003-0.02	″
Kalpeni Atoll	0.4-1.8	0.1-0.33	(Naqvi *et al*., 1996)
Bermuda/Tarawa	0.0009-0.0036	0.0024-0.0085	(Sholkovitz and Shen, 1995)
Florida Bay	0.08	0.27	(Schofield and Haskin, 1964)
Bahamas	0.27	0.17	(Scherer and Seitz, 1980)

The increased land disturbance around the Misima mine provided an easier mechanism for weathered material to enter the nearshore environment. The REE's can enter the nearby creeks in dissolved form or as particulates. At low salinities, dissolved REE's can be removed from river water on colloids and other particulates (Sholkovitz, 1993). However as the salinity increases (6-34.5‰) Sholkovitz (1993) reported that dissolved REE's increased in Amazon estuaries. Sholkovitz (1995) reported that REE's could be desorbed from particulates and colloids when mixed with seawater. In more recent experiments, Sholkovitz *et al*. (1999) noted that large removal of dissolved REE's occurred in low salinity regions of the Fly and Sepik river estuaries of mainland PNG. This was due to the coagulation of iron-humic colloids. These authors also noted that release of REE's from particulates/colloids (based on Nd data) occurred in the Fly estuary as the salinity increased. However the Sepik estuary showed relatively steady Nd concentration throughout with increasing salinity (Sholkovitz *et al*., 1999).

The source of the high amount of dissolved and particulate REE's (Y, La, Ce) entering the nearshore environment of Misima Island is most likely the weathered topsoil. La and Ce measured in the weathered rocks ranged from ~ 5-30 ppm and ~10-40 ppm, respectively (MML unpublished data). The rocks measured were feldspar porphyry, schists and greenstone (MML unpublished data). The Y, La and Ce patterns appeared to follow the sedimentation rate patterns observed for the three affected transects. This provides reasonable evidence that the sediment is causing increased REE concentration in the nearshore environment. The similarity between the sedimentation rate and the Y, La and Ce signals was not perfect and this most likely reflects the complex nearshore estuarine mixing processes.

7.5.5 REE Patterns

The filtered river water data from the Fly and Sepik estuaries on mainland PNG show dissolved REE patterns that are MREE enriched (Figure 7.9A) (Sholkovitz *et al*., 1999). Sholkovitz *et al*. (1999) suggest this pattern reflects the weathering of rocks on PNG. They have also shown that particulates from the Fly and Sepik rivers preferentially release MREE's during mixing with seawater. This is significant because the suspended particles and sediments do not display the MREE enrichments (Figure 7.9A,B) (Sholkovitz *et al*., 1999). Sholkovitz *et al*. (1999) termed this MREE enrichment an "island weathering signature" and found evidence that it affects the East Carolina Basin seawater which has slight but measurable MREE enrichment when compared to Coral Sea surface water.

It is inferred here that Misima Island has a similar weathering history to mainland PNG and that its sediments, particulates and dissolved water REE patterns would be similar. Under this assumption the nearshore seawater REE patterns are probably similar to the dissolved river (Fly and Sepik estuary) patterns. Corals have been shown to incorporate REE's in proportion to their seawater concentration (Sholkovitz and Shen, 1995). All of their corals when normalized to shale have filtered seawater patterns that suggest their corals are incorporating dissolved seawater REE's. The REE patterns from corals off India have been shown to change seasonally in response to increased continental weathering during monsoon season (Naqvi *et al*., 1996). These authors noted that LREE's were enriched during monsoon seasons relative to HREE enrichments during non-monsoon seasons. The REE concentrations for Misima Island reported here lie between values measured by Sholkovitz and Shen (1995) and Navqi *et al*. (1996). The higher REE concentrations recorded by Misima Island corals and Indian corals (Naqvi *et al*., 1996) most likely reflect higher sediment input. Sholkovitz and Shen (1995) measured corals living away from heavy sediment inputs, Bermuda and Tarawa.

From these observations we can infer that the REE's recorded in the Misima Island corals came from the dissolved seawater component. If particulates or sediments were the main mode of incorporation the Misima coral REE patterns would resemble the Fly and Sepik sediment patterns of Sholkovitz and Shen (1995) (Figure 7.9A,C,D). This data lends support that PNG sediments are influencing the seawater REE pattern

observed by the "island weathering signature" for the PNG waters proposed by Sholkovitz *et al* (1999).

7.5.6 Metal Incorporation

Corals collected from the severe site (T5) at Misima Island contained higher concentrations of Mn, Y, La, Ce, Zn and Pb than the transition, minor or control sites (Figures 7.5 – 7.7). This can be attributed to the different sediment loads affecting each transect. Incorporation of these metals into corals can either be the result of dissolved metal incorporation, included particulate material absorbed by coral tissue or by coral feeding (Barnard *et al*., 1974; St.John, 1974; Brown, 1987; Hanna and Muir, 1990). During heavy rainfall events some corals near the Cooktown creek were partially covered by sediment (J. White pers. comm.). It is possible that these elements could be trapped as particulates in cavities, or incorporated into the skeleton through damaged polyps or cuts as suggested by Barnard *et al*. (1974), but the robustness of *Porites* sp. corals indicate that they can slough off some of this sediment. However, on occasion, high levels of clays smothered non-massive corals, in some cases horizontal planes on the corals died but vertical planes survived. In this study only live corals were chosen for this study.

Detritus particles may be incorporated into corals by direct deposition on skeleton through polyp damage or surface lesions (Macintyre and Smith, 1974; Dodge *et al*., 1984). Detritus particles may then be covered by new skeleton as the coral grows over the damaged portions. If this were the incorporation mechanism, consistent polyp damage (or surface scarring) throughout 2-3 years and over distances of several km would be necessary to generate the coherent and reproducible signals recorded by the two corals from each of the 3 (severe, transitional and minor) sites. This seems highly unlikely and detritus particles are probably not the dominant mode of incorporation. Detritus incorporation would most likely appear as a random trace element signal with erratic variations within and between sites (Goreau, 1977) and not as the consistent record we observed (Figures 7.5 – 7.7). However, it is still possible that some clay material may make its way into the skeleton. If these small particles become trapped in the coral skeleton even extensive oxidative-reductive cleaning procedures (Shen and Boyle, 1988) would probably not remove them. To test the clay particle theory,

measurements of aluminum (Al) and thorium (Th) were performed on the coral T05B03. The laser sampling slit was reduced to ~ 20 μm wide (to allow small concentration spikes to be observed). There were no indications of Al or Th increases corresponding to the sediment peaks or in any part of that coral.

Two corals at each transect were recording the same trace element signatures in proportion to the increased sedimentation. All elements showed a linear relationship between the amount of sediment collected and the average metal concentration from 1988 to 1993. This indicates these corals were recording their seawater environment consistently and in proportion to the amount of material entering the nearshore environment. This result alludes to common metal incorporation between these 8 *Porites* corals. If the incorporation mechanisms were influenced by multiple (possibly conflicting) parameters then this linear relationship should break down. The data also suggest that at these concentrations the coral are not excluding any of these metals (in terms of poisoning factors).

A non-random method of incorporation is necessary to produce such consistent records of trace metals in coral skeletons. The most likely mechanism is a combination of seawater soluble metals and incorporation via coral polyp feeding (Howard and Brown, 1984). Rivers can have very different soluble and particulate metal concentrations so both constituents may be very important to the final coral skeletal concentrations. Incorporation by coral feeding can be accomplished in two ways. Firstly, tentacular capture of zooplankton where the zooplankton are exposed and accumulate metals (Cd, Mn, Pb, Zn etc, Martin, 1970). A second mechanism is mucus nets that trap zooplankton and fine particulate material, which is periodically ingested by the corals. St. John (1974) indicates that metal concentrations in corals are enhanced due to feeding on bacterial plankton and inorganic matter. Either mechanism will cause corals exposed to elevated soluble and particulate metals to have increased skeletal concentrations.

7.6 Conclusions and Implications

This chapter shows that low concentration elements (ppm and lower) incorporated into corals can be measured by LA-ICP-MS and that the values are reproducible. By analyzing two corals from each location we have also shown that corals from the same

locations can record the seawater environment consistently. These corals at Misima Island appear to be faithfully recording their environment relative to the impact received. This dataset benefited by having well documented impact gradients (sediment traps) to compare with the metal records extracted from the corals. By examining different metals in the corals we were able to distinguish between two different rock source sediments entering the nearshore environment. The weathered topsoil has a distinctive signature of Mn and REE's and appears first in the corals and therefore the nearshore environment (1988). The Zn and Pb do not increase in the corals until "fresh" rock (ore zone material) was exposed for processing (1989).

This study suggests that the most probable mode of metal incorporation in these corals is by seawater soluble metals or coral polyp feeding. The consistent metal patterns within and between sites would indicate that we are not measuring detritus particles trapped in skeletal cavities or lesions overgrown by new skeleton but are measuring a more consistent type of metal incorporation. Direct incorporation of detritus is also excluded by the lack of correlated variation in Th and Al. The REE pattern data also suggests that we are measuring dissolved REE's and not particulates as the coral REE patterns are similar to dissolved river REE's and not river sediment/particulates from PNG (Sholkovitz *et al*., 1999).

This unique dataset shows that through trace metals *Porites* corals can record varying levels of disturbances, ranging from heavy to minor sediment impacts. Having documented impact information in the form of coral metal concentrations gives us a baseline against which to analyze older and longer coral cores to view the effects of changing land practices. In the Great Barrier Reef long coral records are available from nearshore, river runoff affected sites (e.g. Lough *et al*., 1999). We now plan to analyze dated sections from the past to test whether river runoff (sediments etc…) has different signatures to the post-European settlement (farming, fertilizing and industrialization) runoff signatures measured in recent corals. This may provide a clue as to how land clearing/farming and industrialization has affected the Great Barrier Reef over the last century. This technique could also be used to examine land use practices from other coral locations. Corals could document runoff/sediment variability of the Amazon, and other South American rivers. Significant sedimentation changes are also occurring throughout Southeast Asia. Reefs from the Philippines to Indonesia (just to name a few) are continually under threat by soil erosion from deforestation and/or agriculture.

Using time series of coral trace elements we could document these changes and present background data to help with land management in these areas.

Chapter 8: Environmental Records from Coralline Sponges

8.1 Introduction

Coralline sponges are slow growing (0.15 to 0.5 mm yr-1), long lived and their calcareous skeletons can provide proxy records of salinity, water temperature and atmospheric CO_2 over the 100 to 1000 year time range. Their compressed record (slow growth) make them ideal for the high-resolution trace element analytical technique of LA-ICP-MS. Coralline sponges are also found in a much larger depth range than corals. Specimens have been observed in depths ranging from 10-185 m, therefore providing unique information on the history of the upper water column. Their skeleton is extremely dense providing more resistance to diagenesis than corals. They can be used to augment and in some cases replace records obtained from coral skeletons, and have the advantage that they are in chemical equilibrium with the surrounding seawater for carbon and oxygen. Here I evaluate the potential of using variations of trace elements in coralline sponges as potential proxies for reconstructing environmental parameters (e.g. SST).

Measurements of $^{18}O/^{16}O$ and $^{13}C/^{12}C$ (ratio of carbon-13 to carbon-12) have been reported on coralline sponges (*Astrosclera* sp. and *Ceratoporella* sp.) and are providing information about long-term water temperature and atmospheric CO_2 (Druffel and Benavides, 1986; Böhm *et al*., 1996; Wörheide, 1998). The concentration of CO_2 in the atmosphere has been increasing steadily since the late 1800's (Figure 8.1) causing the carbon isotopic ratio ($\delta^{13}C$) in the atmosphere to decrease (Nozaki *et al*., 1978; Druffel and Benavides, 1986; Freidli *et al*., 1986). The continuous decrease of $\delta^{13}C$ is attributable to the burning of fossil fuels that are isotopically light in carbon (^{13}C depleted) (Nozaki *et al*., 1978; Druffel and Benavides, 1986; Böhm *et al*., 1996). Measurements of $\delta^{13}C$ from marine surface waters made by the analysis of carbon isotopes in corals, sponges, clams and foraminifera corroborate the atmospheric decrease in $\delta^{13}C$ (Nozaki *et al*., 1978; Druffel and Benavides, 1986; Aharon, 1991; Beveridge and Shackleton, 1994; Böhm *et al*., 1996).

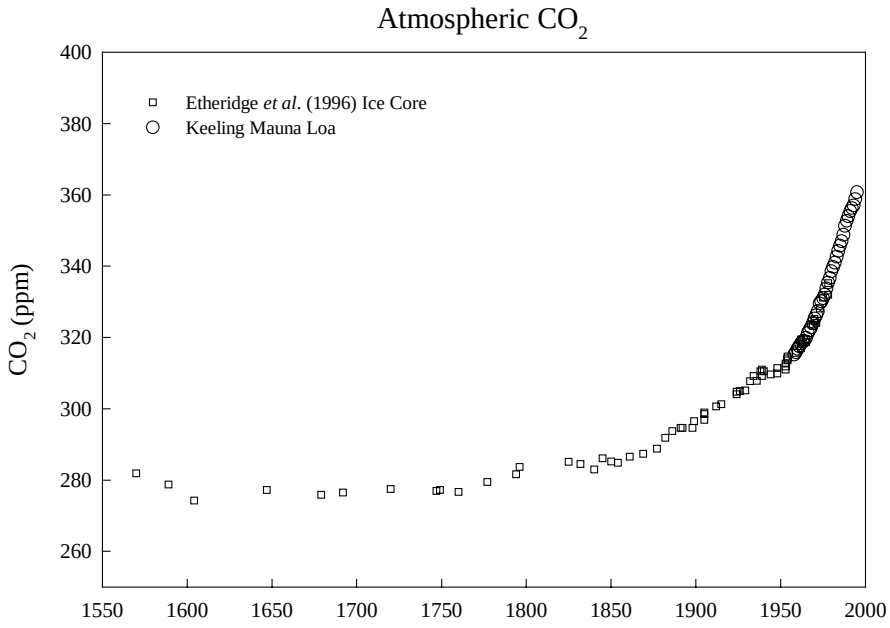

Figure 8.1 Atmospheric CO_2 from ice core and Mauna Loa.

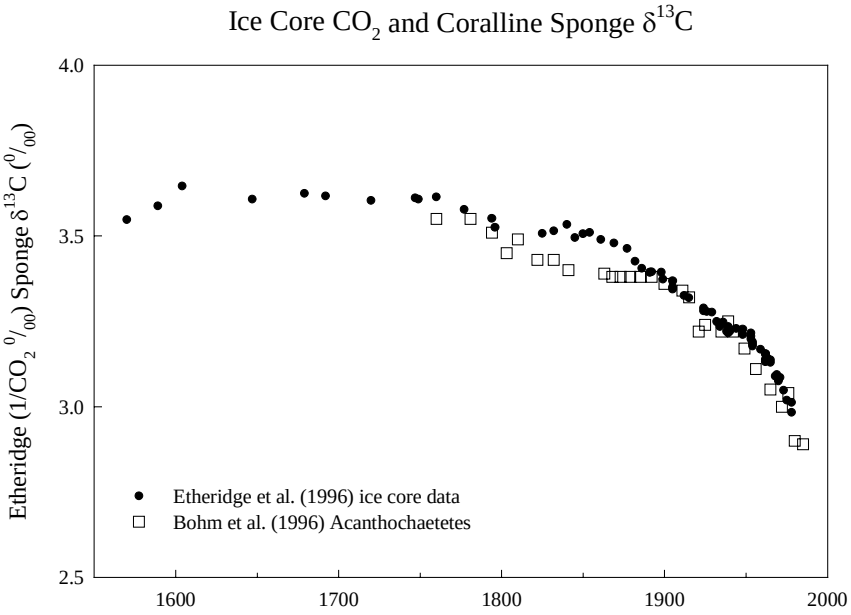

Figure 8.2 Ice core CO_2 and Calcite Coralline Sponge $\delta^{13}C$.

However metabolic and kinetic effects in corals, clams and foraminifera, appear to cause fractionation in the incorporation of carbon isotopes thereby complicating the reconstruction of marine water $\delta^{13}C$ and atmospheric CO_2 (McConnaughey, 1989; Aharon, 1991). Coralline sponges do not appear to be affected by carbon isotope

fractionation and can thus be used to reconstruct marine water $\delta^{13}C$ (Druffel and Benavides, 1986; Böhm *et al*., 1996) (Figure 8.2).

8.2 Background

Of the large number of species of sponges described throughout the globe only 15 species of recent sponges construct calcareous skeletons (Willenz and Pomponi, 1996). They are the living representatives of groups of sponges from the late Paleozoic and Mesozoic known as 'Stromatoporoidea', 'Chaetetida' and 'Sphinctozoa'. These groups of coralline sponges were the 'original' and main reef-building organisms before they were overtaken by hermatypic scleractinian corals (Reitner, 1989). Coralline sponges now inhabit areas with low light, caves, cryptic habitats and deep water where they are not in competition with hermatypic corals.

8.2.1 Astrosclera willeyana

General Information

The coralline demosponge *Astrosclera willeyana* has been observed to depths of 185m (Hartman, 1980). In shallower areas (~10m) they occupy reef caves and overhangs (Wörheide, 1998). Their shape is pyriform-half spherical (mushroom) and they are mostly bright orange in color (Figure 8.3). They are found widely distributed throughout the Indo-Pacific and are the most abundant coralline sponge in this area (Reitner *et al*., 1996). They have a in/exhalent water system that extends to the basal skeleton throughout the tissue layer. The living tissue can be several mm's thick encompassing 3 major zones: ectosome, choanosome and zone of epitaxial backfill (ZEB) (Wörheide, 1998).

Figure 8.3 Picture of Astrosclera willeyana collected from Myrmidon Reef.

Biomineralization in Astrosclera willeyana

In the ectosome (100-300 μm thick) aragonite crystal formation begins, ultimately leading to the formation of aragonite spherulites (Wörheide, 1998). In the top section of the choanosome the spherulites fuse together to begin forming the basal skeleton but space is still available for tissue and bacteria (Wörheide, 1998). As the soft tissue slowly moves upward in the ZEB, the remaining vacant space is filled by epitaxially growing skeleton. This secondary infilling may make up 50% or more of the basal skeleton (Wörheide, 1998). It is crucial to understand the calcification process of coralline sponges, which imply that at any given position below the top of the basal skeleton the material constitutes a time average equivalent to the time/distance from the outer tissue surface to the beginning of the basal skeleton (Druffel and Benavides, 1986; Böhm *et al*., 1996; Wörheide, 1998). The average growth rate of several *Astrosclera* measured by Wörheide (1998) was 0.2 mm yr^{-1} significantly less than the tissue thickness (1 to several mm's) making the recovery of seasonal records impossible.

8.2.2 Coralline Sponges as Environmental Recorders

Stable Isotopes

Coralline sponges appear to provide a means for reconstructing marine $\delta^{13}C$ of the dissolved inorganic carbon pool (DIC) as they have been shown to incorporate both oxygen and carbon in isotopic equilibrium with the DIC of seawater (Druffel and Benavides, 1986; Böhm *et al*., 1996; Wörheide, 1998). Records of $\delta^{13}C$ in coralline sponges show depleted ^{13}C values and correlate with atmospheric $\delta^{13}C$ and $1/CO_2$ (Figure 8.2) and appear to be useful for reconstructing past marine and atmospheric CO_2 levels (Druffel and Benavides, 1986; Böhm *et al*., 1996; Wörheide, 1998).

The oxygen isotopes ($\delta^{18}O$) in coralline sponges have not been extensively studied for the reconstruction water temperature. In the publication by (Böhm *et al*., 1996), the mean $\delta^{18}O$ values from both *Ceratoporella nicholsoni* and *Acanthochaetetes wellsi* provided accurate mean water temperatures for Jamaica and New Caledonia respectively. In the Great Barrier Reef the sponge *Astrosclera willeyana* also seems to reconstruct long-term water temperature variations (Figure 8.4) (Wörheide, 1998). They attribute the negative trend in the $\delta^{18}O$ from the early 1900's to reflect recent global warming of ~ 1 °C.

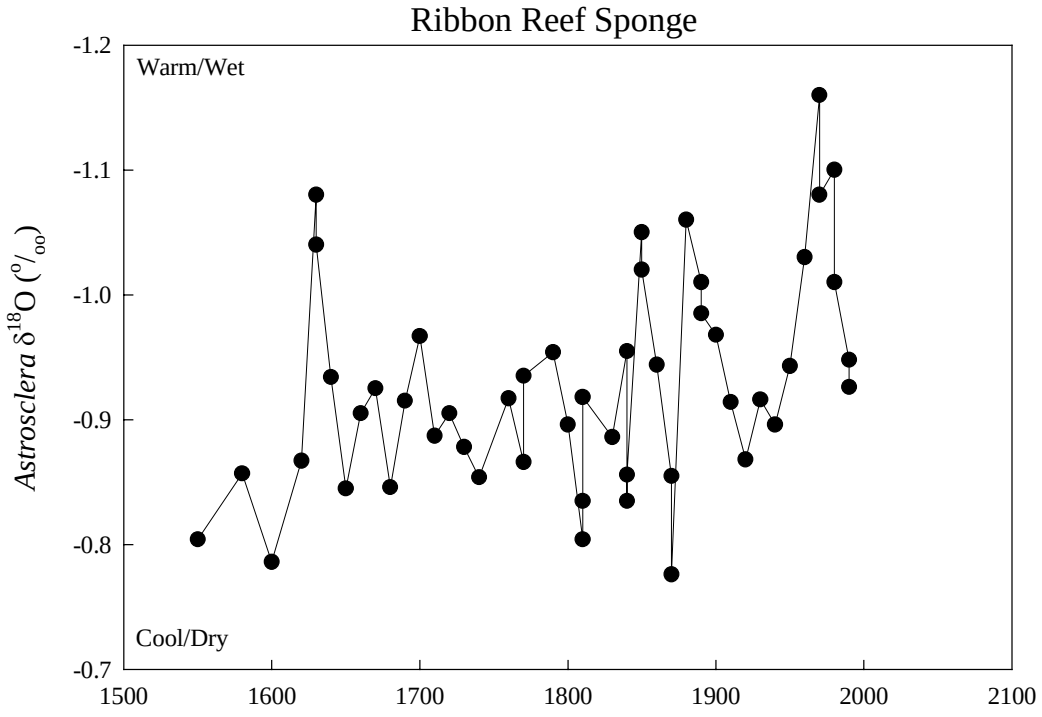

Figure 8.4 *Astroslcera willeyana* $\delta^{18}O$ from Ribbon Reef #10. Data from Wörheide (1998).

8.2.3 Dating and Growth Rates

Growth rates of coralline sponges have been measured by direct staining, (Alizarin Red-S (Dunstan and Sacco, 1982) and calcien (Willenz and Hartman, 1985) and by ^{14}C and ^{210}Pb (Benavides and Druffel, 1986; Wörheide, 1998). Growth rates estimated from staining are in the range of 0.1 - 0.2 mm yr^{-1} (Dunstan and Sacco, 1982; Willenz and Hartman, 1985). Dating using ^{14}C and ^{210}Pb give slightly higher growth rates 0.2 - 0.3 mm yr^{-1} (Benavides and Druffel, 1986; Wörheide, 1998). Due to the slow growth rates and limitations of radiometric dating, no direct comparisons have been made between these methods. Recently, thermal ionization mass spectrometry measurements of U-series isotopes for dating sponges has shown promise. Coralline sponges contain relatively high uranium (7-10 ppm) and low initial thorium making them ideal for dating, and the possibility of dating relatively young samples (~100 yrs.) to high precision is also feasible (J. Rubenstone, pers. comm.). In addition to the radiometric dates, plateaus in the CO_2 curve in the 1940's and ~1850's (shown by $\delta^{13}C$ plateaus) may be useful time markers (Figure 8.1, 8.2).

8.3 Locations

Coralline sponges have been analyzed from five locations from the Southwest Pacific. These sites are: Otta Island, Caroline Islands, Federated States of Micronesia, Robert's Reef, Fiji and three sites on the GBR (Figure 8.5). The collection sites from the GBR are Ribbon Reef #10, Ruby Reef, and Myrmidon Reef (Figure 8.6). Site information is listed in Table 8.1.

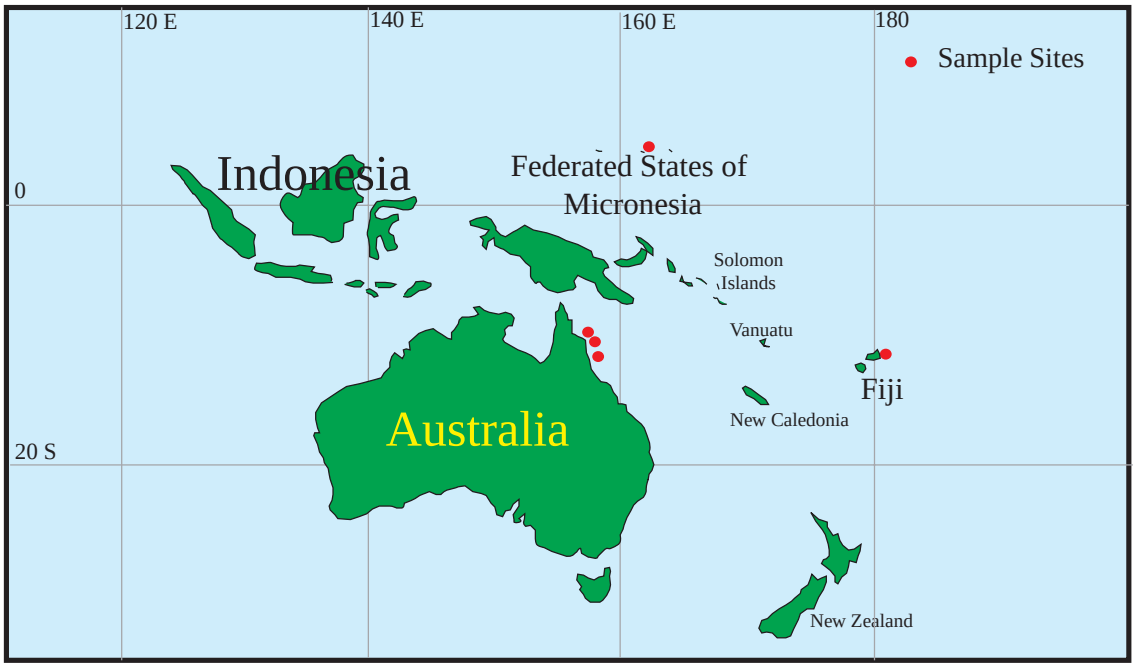

Figure 8.5 Map showing the five sample locations of the coralline sponges analyzed for this project. Samples from Otta Island, Fiji and Ruby Reef were collected by J. Hooper

Table 8.1 Summary of *Astrosclera willeyana* coralline sponge collection.

Location	Latitude/Longitude	Collection Depth (m)	Collection Date	Approx. record length (yrs.)	SST Range (°C)
Ruby Reef, GBR	15.42.7 S 145.48.2 E	26	22/2/95	50	23-29
Ribbon Reef, GBR	14.40.56 S 145.40.56 E	21	8/8/98	120	25-30
Myrmidon Reef, GBR	18.6 S 147.5 E	17	1/18/99	160	26-30
Otta Island, Caroline Islands	7.12.0 N 151.51.0 E	25	8/8/94	80	26-30
Robert's Reef, Fiji	16.42.9 S 179.48.2 W	42	29/10/96	110	25-29

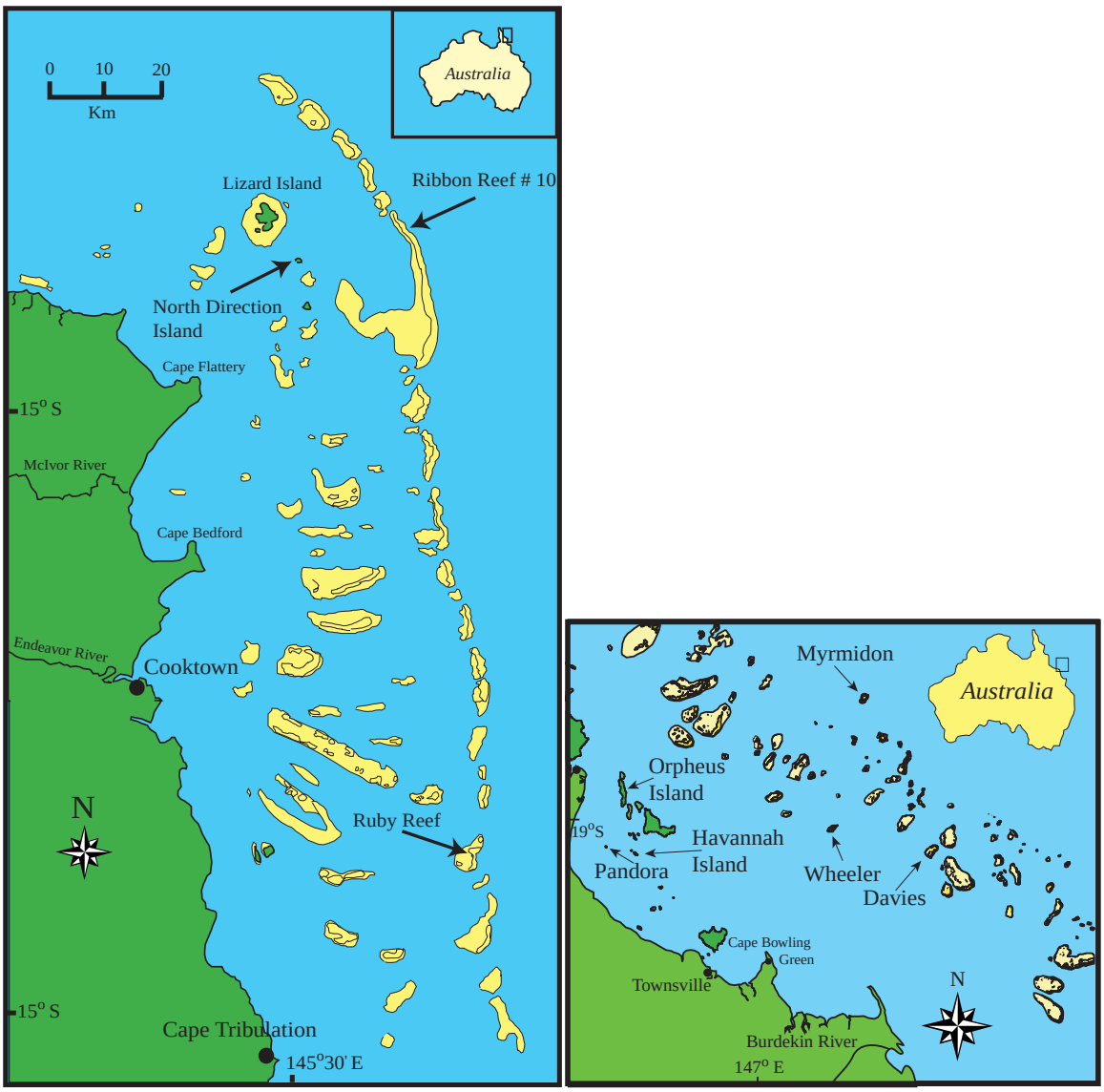

Figure 8.6 Close-up maps showing collection sites of coralline sponge on the GBR.

8.4 Analytical Methods

All coralline sponges were identified to be *Astrosclera willeyana* (Lister, 1900). The trace element data was collected using the methods described in Chapters 2 & 3 except that the laser sampling slit size was reduced to image a 20x100 μm rectangle on the sample. This was chosen to provide ~ 10 pulses per year assuming a growth rate of 0.2 mm yr^{-1}. A laser track on the Myrmidon Reef sponge is shown in Figure 2.7. The Ribbon Reef #10 sample was also analyzed for $\delta^{18}O$ and $\delta^{13}C$. Samples were milled in 0.25 mm increments using RSES's automated mill (Gagan *et al.*, 1994; McCulloch *et al.*, 1994) but only every other sample was analyzed. A subsample approximately 150-200 μg was analyzed on a Finnigan MAT 251 with a Kiel carbonate device using 105%

H_3PO_4 at 90ºC (Gagan *et al*., 1994). The working gas had the following isotopic composition, $\delta^{18}O_{V\text{-}PDB}$ = -1.63‰; $\delta^{13}C_{V\text{-}PDB}$ = +2.13‰. Data was corrected for ^{17}O interference using the method of Santrock *et al*. (1985) and normalized such that a sample of solid NBS 19 analyzed by this method would yield $\delta^{18}O_{V\text{-}PDB}$ = -2.20‰; $\delta^{13}C_{V\text{-}PDB}$ = +1.95‰. Average analytical precision is ± 0.05‰ for $\delta^{18}O$ and ±0.03‰ for $\delta^{13}C$ on a typical sample (Gagan *et al*., 1994).

8.4.1 Density Measurements

The density of the coralline sponges was measured on the gamma densitometer at AIMS. The methods are described by Chalker *et al*. (1985) and Chalker and Barnes (1990). For the sponge analyses, the beam diameter was masked with a 1mm diameter (round) lead castle. This was the smallest size currently available.

8.5 Results

8.5.1 Sponge Density and Skeleton Thickening

Samples from Fiji, Ribbon Reef #10 and Otta Island were analyzed using the AIMS densitometer. Multiple tracks were analyzed on each sample. It was apparent by visual examination that away from the living edge the density variations were very small (if any) and did not correspond to any environmental or annual patterns. Combined visual examination and the density scans on the sponge slabs showed an increase in density away from the outer "living" edge until approximately 5mm from that edge when the density approached that of pure aragonite (2.93 g cm^{-3}). The density tracks from the Ribbon Reef sponge are shown alongside a SEM image of the sponge (Figure 8.7). The outer ~ 2 mm has a similar density of ~1 g cm^{-3}. At approximately 3 mm from the edge the density increases until it reaches ~ 2.9 g cm^{-3} at 5-6 cm from the outer edge (Figure 8.7). All sponges analyzed in this study exhibited this pattern.

These density profiles suggest that thickening of aragonite occurs throughout the "living" tissue layer. This observation was confirmed by staining experiments in which the ZEB near the base of the "living" layer was shown to be a site of high calcification

(Wörheide *et al.*, 1997; Wörheide, 1998). The calcification appears to occur in two main stages, the outer 2 mm grows and extends while building the framework. This is accompanied by thickening of the ZEB until near solid aragonite is formed at the base of the "living" tissue layer (Figure 8.7).

Therefore the trace elements are being incorporated into the $CaCO_3$ skeleton over an extended period in essentially side-by-side locations. This results in a smoothing of environmental signals over the entire "living" tissue layer, 5-6 mm in this case. Potentially if the smoothing was equal over the entire 5-6 mm then a smoothing function of ~ 20 years would be occurring. More probable, it may be that ~ 1/3 of the skeletal material is deposited initially (t = 0) with the remaining 2/3 deposited over the bottom 2-3 mm "tissue" layer (Figure 8.7). Thus *Astrosclera* smoothes any incorporated signal preserved in its skeleton. If this smoothing function is consistent (ear-by-year) then the recovered record would be reliable, albeit smoothed. If the smoothing is not consistent then small-scale amplitude variations would not be robust throughout the lifetime of the sponge resulting in a misinterpretation of the included signals. A similar type of smoothing has been postulated for *Porites* corals (Taylor *et al*., 1993; Barnes *et al*., 1995; Taylor *et al*., 1995). Density and growth variation models of Taylor *et al*. (1993) imply that thickening of skeletal components should smooth the included signal. In contrast to *Porites*, the coralline sponge *Astrosclera willeyana* clearly exhibit prolonged density thickening resulting in smoothing of the incorporated signals.

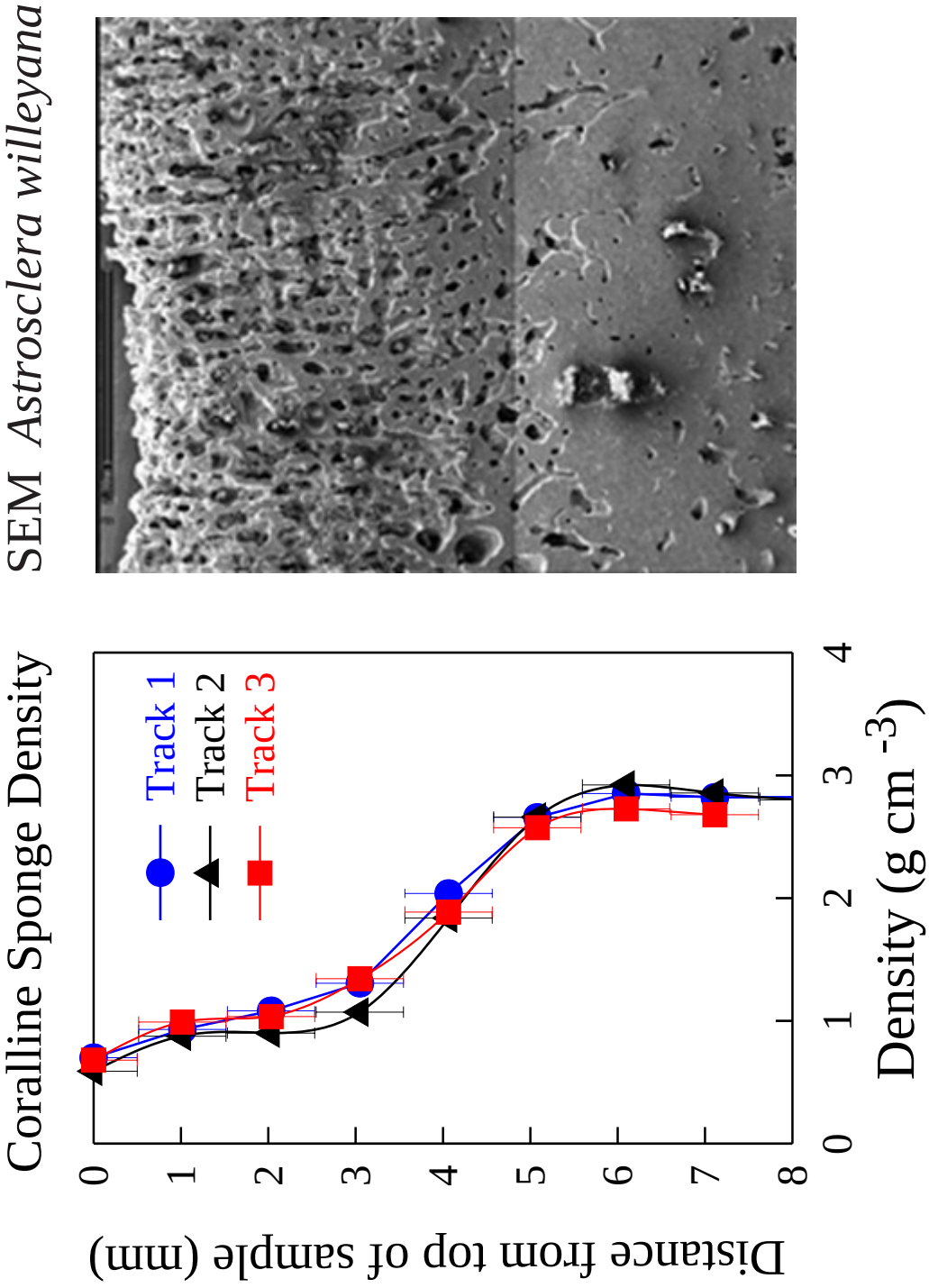

Figure 8.7 Gamma densitometry and scanning electon microscopy (SEM) image of the Ribbon Reef #10 coralline sponge. The scale is approximately equal for both images.

8.5.2 Trace elements in Astrosclera willeyana (General)

The boron, magnesium and barium in *Astrosclera willeyana* are 2-5 times lower than average *Porites* coral with concentrations of 20, 200 and 4 ppm respectively. The strontium and uranium concentration are 1-2.5 times higher than *Porites* corals with concentrations of ~9000 and ~10 ppm respectively. The high-resolution (20 μm) trace element analyses are shown for the Ruby Reef sponge in Figure 8.7. There is little similarity or correlation between most of the five elemental ratios at high resolution ($r < 0.36$) except for Sr/Ca vs. B/Ca that has a correlation coefficient of 0.49. However when data is averaged at a more coarse resolution (0.1 mm) then higher correlations appear. For example, the correlation coefficient between Sr/Ca and B/Ca increases to 0.71 (Table 8.2).

Table 8.2 Correlation Coefficients at 0.1 mm and 20μm resolution Ruby Reef, GBR $p < 0.001$. The 20μm resolution correlations are shown in parentheses.

	B/Ca	Mg/Ca	Sr/Ca	Ba/Ca
B/Ca				
Mg/Ca	0.31 (0.22)			
Sr/Ca	0.71 (0.49)	0.25 (0.17)		
Ba/Ca	0.51 0.32()	0.45 (0.24)	0.61 (0.36)	
U/Ca	0.25 (0.17)	N.A.	0.32 (0.22)	N.A.

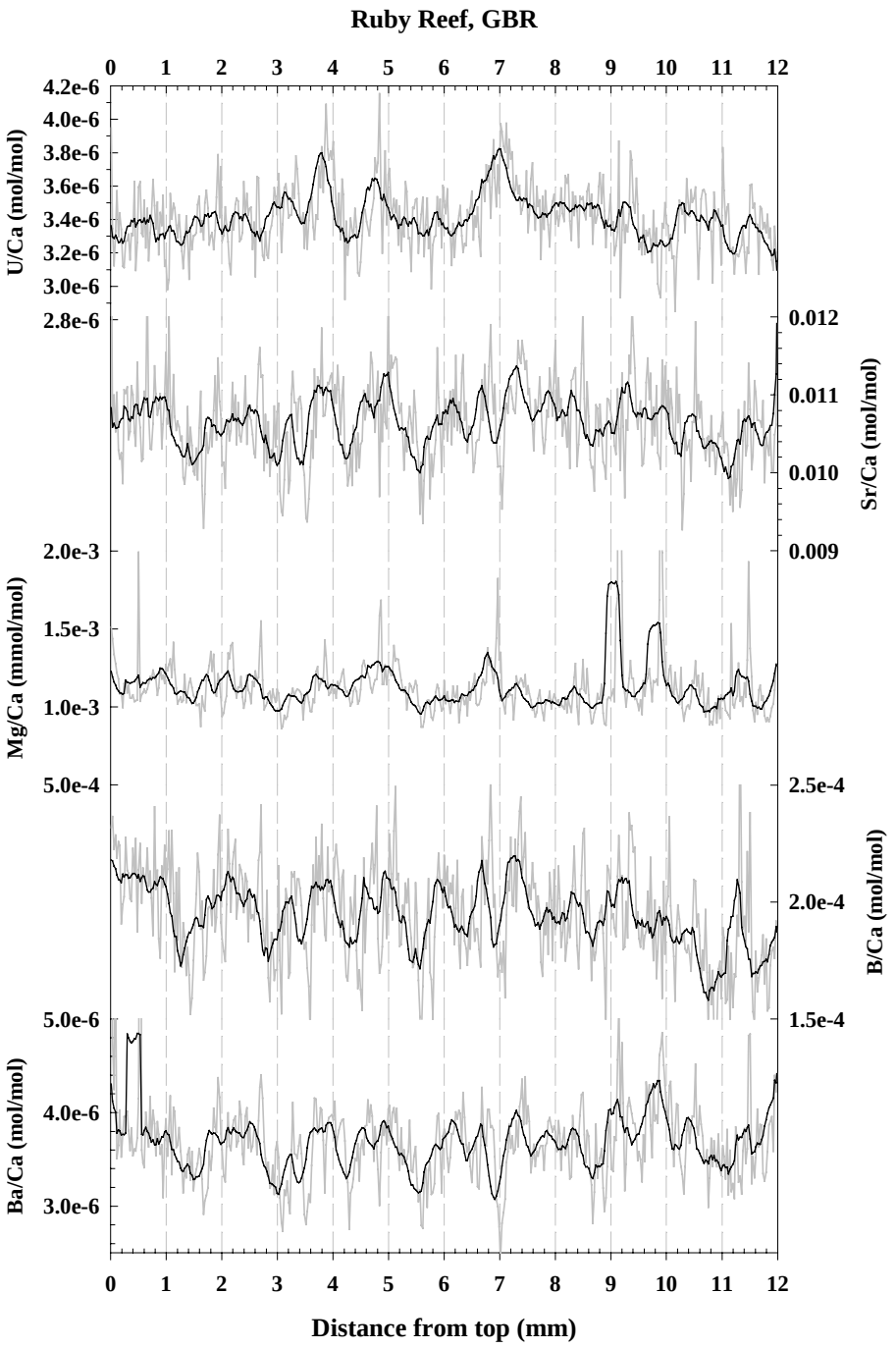

Figure 8.7 High resolution trace elements from the Ruby Reef sponge (gray line). A running average equivalent to 0.1 mm is also shown (black line).

The other samples show similar relationships although not all elements are always correlated. One significant difference between trace elements in corals and *Astrosclera willeyana* is that Mg/Ca is positively correlated to the other elements whereas in corals it is negatively correlated (Table 8.2). For comparison the trace element profiles and elemental correlations from the Otta Island and Fiji sponges are shown in Figures 8.9, 8.10 and Tables 8.3, 8.4 respectively.

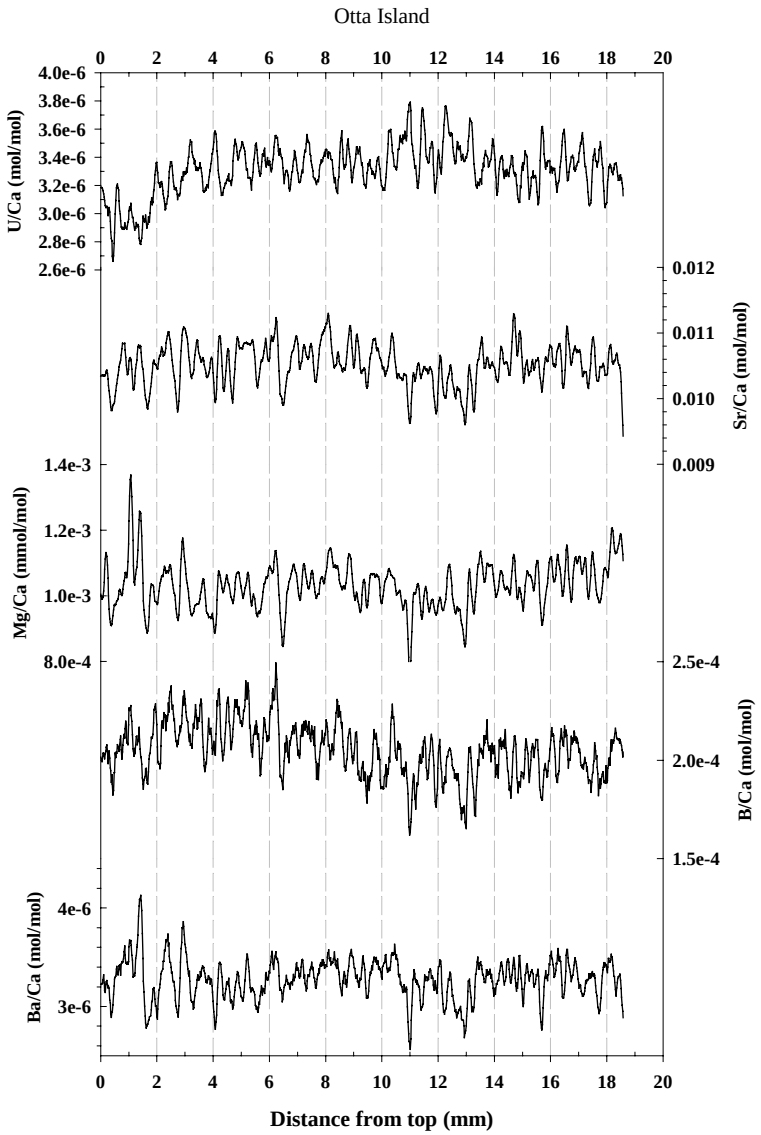

Figure 8.8 Trace element profiles from the Otta Island *Astrosclera willeyana* sample. Resolution is 0.1 mm running average.

Table 8.3 Correlation Coefficients (0.1 mm resolution) Otta Island $p < 0.001$.

	B/Ca	Mg/Ca	Sr/Ca	Ba/Ca
B/Ca				
Mg/Ca	0.44			
Sr/Ca	0.56	0.62		
Ba/Ca	0.40	0.71	0.69	
U/Ca	N.A.	0.21	N.A.	0.31

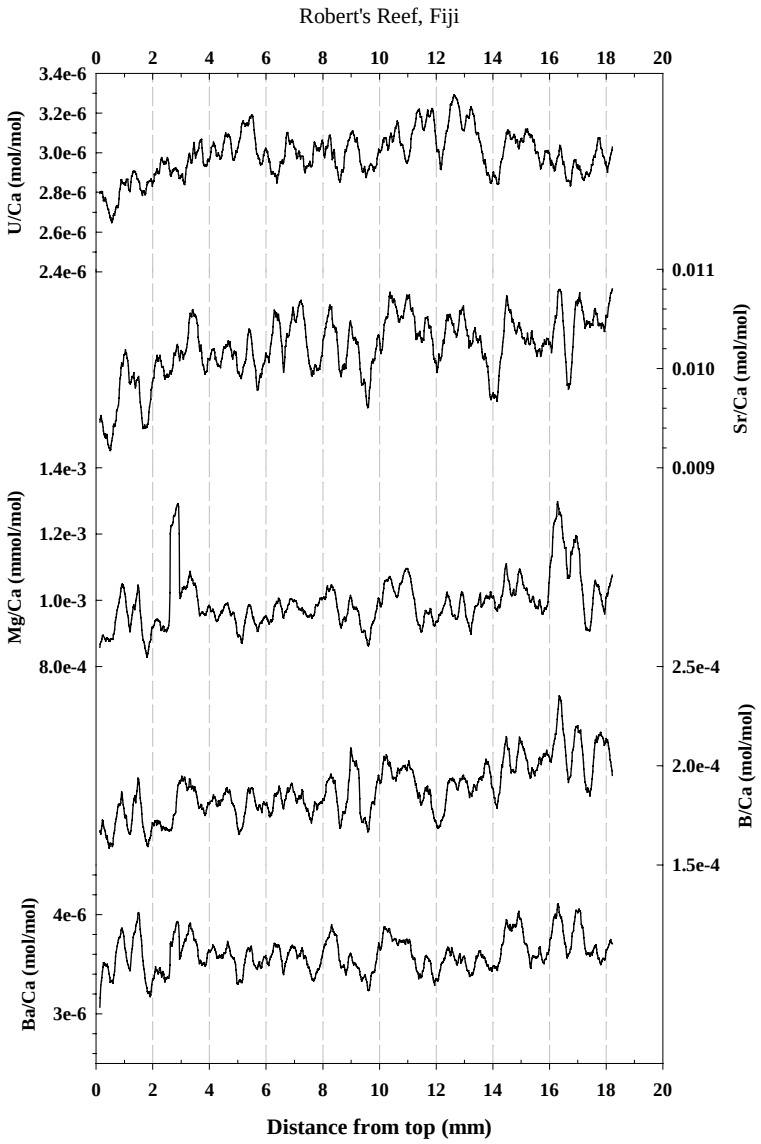

Figure 8.9 Trace element profiles from the Robert's Reef *Astrosclera willeyana* sample. Resolution is 0.1 mm running average.

Table 8.4 Correlation Coefficients (0.1 mm) Robert's Reef, Fiji $p < 0.001$.

	B/Ca	Mg/Ca	Sr/Ca	Ba/Ca
B/Ca				
Mg/Ca	0.68			
Sr/Ca	0.69	0.52		
Ba/Ca	0.67	0.81	0.58	
U/Ca	0.31	N.A.	0.59	N.A.

8.5.3 Sponge Dating and Sr/Ca Proxy Records

One of the difficulties with using coralline sponges is translating distance to time. In corals, annual growth bands and trace element cycles permit the generation of time series data relatively easily. Coralline sponges do not exhibit annual growth bands nor do they have very clear annual cycles. One way to overcome this problem is by isotopic dating. Various dating methods ^{14}C, ^{210}Pb or U-series make it possible to obtain an age for the oldest parts and subsets of the sponge. This enables the determination of an average growth rate. Using these methods and direct staining of skeleton provides average growth rates that range from 0.1 –0.3 mm yr^{-1} (Dunstan and Sacco, 1982; Benavides and Druffel, 1986; Willenz and Pomponi, 1996; Wörheide, 1998). Direct staining and ^{14}C from another sponge collected at Ribbon Reef #10 suggested a growth rate of 0.23 mm yr^{-1} (Wörheide, 1998). U-series was attempted on the Myrmidon and Ribbon Reef sponges. Small sample sizes and low ^{230}Th yields prevented an age calculation from these sponges. Further attempts using a recently purchased mass spectrometer with ion counting facilities will occur in the future.

The relatively uniform growth rates reported for coralline sponges (Druffel and Benavides, 1986; Wörheide, 1998) provide a starting point for the dating of these sponges. As a first approximation “annual” cycles were counted from the Myrmidon and Ribbon Reef sponges. The “annual” cycles are not always clear but provide a starting point for age determinations (Figure 8.10). Average growth rates of 0.25 and 0.23 mm yr^{-1} for Myrmidon and Ribbon Reef were used to construct a time series for the datasets. The average growth rates for Ruby Reef, Otta Island and Robert’s Reef were 0.2, 0.21 and 0.18 mm yr^{-1} respectively. Since the sponges are most likely smoothing the included signal, a filter equivalent to a 5 yr. running mean was applied to the data.

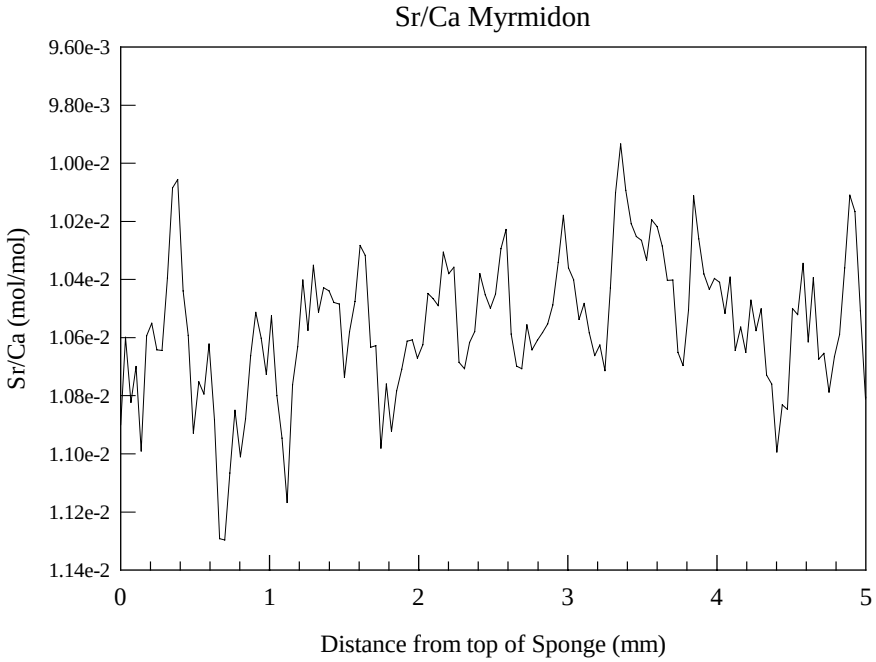

Figure 8.10 Subsection of Sr/Ca from Myrmidon reef sponge used to obtain starting point growth rate.

In corals Sr/Ca ratios are the most robust recorder of ocean temperature fluctuations. Other elements (B, Mg, Ba, U) in these sponges do not show good similarities to instrumental SST and are not shown. The instrumental SST record used was the optimally smoothed MOHSST5 from Kaplan *et al*. (1998). This dataset is at a 5º x 5º grid and covers most of the world. The data is available as an anomaly relative to the 1951-1980 average SST. The Kaplan SSTA (as it will be referred to) was smoothed with a five year running mean to facilitate comparisons with the sponge Sr/Ca. Sr/Ca anomalies relative to 1951-1980 (Sr/CaA) were also applied to the sponge data to enable direct comparisons with the Kaplan SSTA dataset.

The comparison between the Myrmidon sponge Sr/CaA and the Kaplan SSTA are shown in Figure 8.11. The Sr/CaA dataset was modified slightly on the assumption that the growth rate may not always be constant. The Sr/CaA dataset was tuned with a few "marker" points to enhance the correlation with the instrumental temperature. This method was applied to all the five samples with the tuning "marker points" and the adjusted Sr/CaA and Kaplan SSTA (5 yr. smoothed) being shown in Figures 8.12 - 8.16.

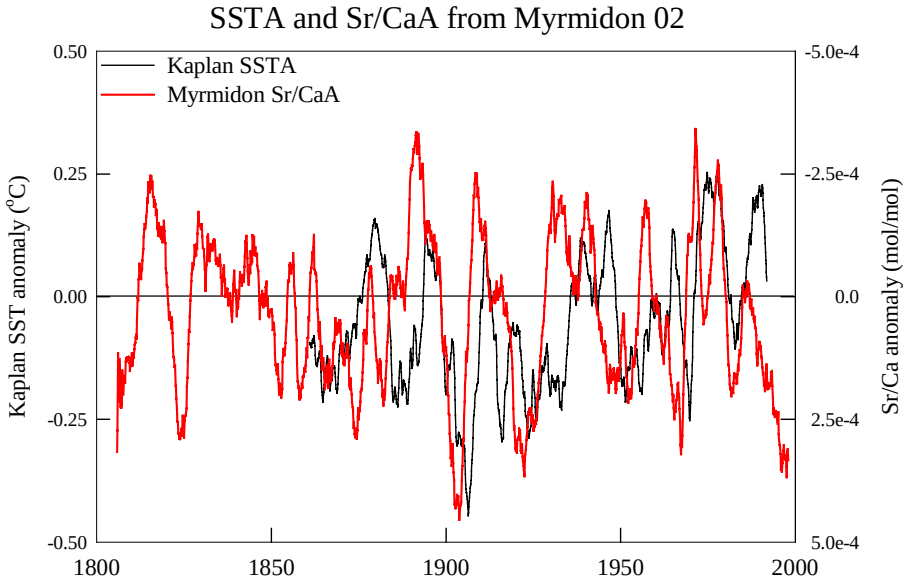

Figure 8.11 Sr/Ca anomaly (red) and Kaplan SSTA (black) vs. time for the Myrmidon *Astrosclera willeyana* sponge. The Myrmidon average value is 0.0104 mol/mol.

8.5.4 Sr/Ca Anomaly (Sr/CaA) and Kaplan SST Anomaly (SSTA)

Using this method, comparisons between SSTA and *Astrosclera willeyana* Sr/CaA can be assessed. During the overlapping time period 1860-1990 there is good agreement between SSTA and Sr/CaA for the Myrmidon sponge (Figure 8.12). The Ribbon Reef #10 Sr/CaA shows time periods with patterns similar to the SSTA but the amplitude is not always the same (Figure 8.13) resulting in a lower correlation coefficient. The Ruby Reef sponge Sr/CaA also displays a good coherence with SSTA except for the top portion (1982-1990) where the Sr/CaA does not show the increasing temperature trend (Figure 8.14). The Otta Island sponge Sr/CaA follows the SSTA trend quite well from ~ 1940 to 1990 (Figure 8.15). From 1910 to 1940 the SSTA suggests the average temperature was cooler whereas the sponge Sr/CaA suggest the average temperature was the same. However the "decadal" type cycles are reproduced by both dataset indicating that Sr/CaA captures the temperature variation if not the correct offset (Figure 8.15). The Robert's Reef, Fiji sponge again shows some coherence between sponge Sr/CaA and SSTA but there are amplitude differences and missing "decadal" cycles when compared to the Kaplan SSTA (Figure 8.16).

Overall, the Sr/CaA datasets show a remarkable coherence to the Kaplan SSTA. However there are still problems with Sr/CaA amplitude and "decadal" cyclicity. Potential problems and limitations with the Kaplan SSTA dataset include SST errors that are shown on every graph. In some cases early data 1860-1900 and ~1940 the error estimate is as large as the SSTA value. But at a resolution of 5 years (smoothed) this error estimate is most likely too large. The sponge Sr/CaA has a few potential problems that include the smoothing due to aragonite infilling and thickening. If this smoothing function does not remain constant through time the recovered Sr/CaA signal will vary in amplitude. This could lead to erroneous Sr/CaA shifts that are larger or smaller than the actual water temperature variation. A variable growth rate may also play a role in the Sr/CaA/SSTA misfits but the "marker point" tuning should reduce this (see dating section).

Another factor to consider is the collection location and depth of the sponges. All the samples were collected from 17-25 m water depth except for the Fiji sample that was collected from a depth of 42m (Table 8.1). The water temperature at depth may be slightly different than a surface derived SST dataset like Kaplan SSTA. Also changes in upwelling or thermocline depth could affect the water temperature surrounding the sponge and not a surface SST measurement. A final factor is that this comparison is between a regional signal (5^{o} x 5^{o} grid) and a point source (1 sponge). Therefore the fit/misfit between the datasets would represent a worse case scenario it terms of temperature reconstruction. However when using sponges (or corals) for paleo-reconstructions an important consideration is how well they capture regional variation and not just local small-scale processes. In this case, coralline sponges are doing a reasonable job of recording regional SST variation from the seclusion of their cavern homes.

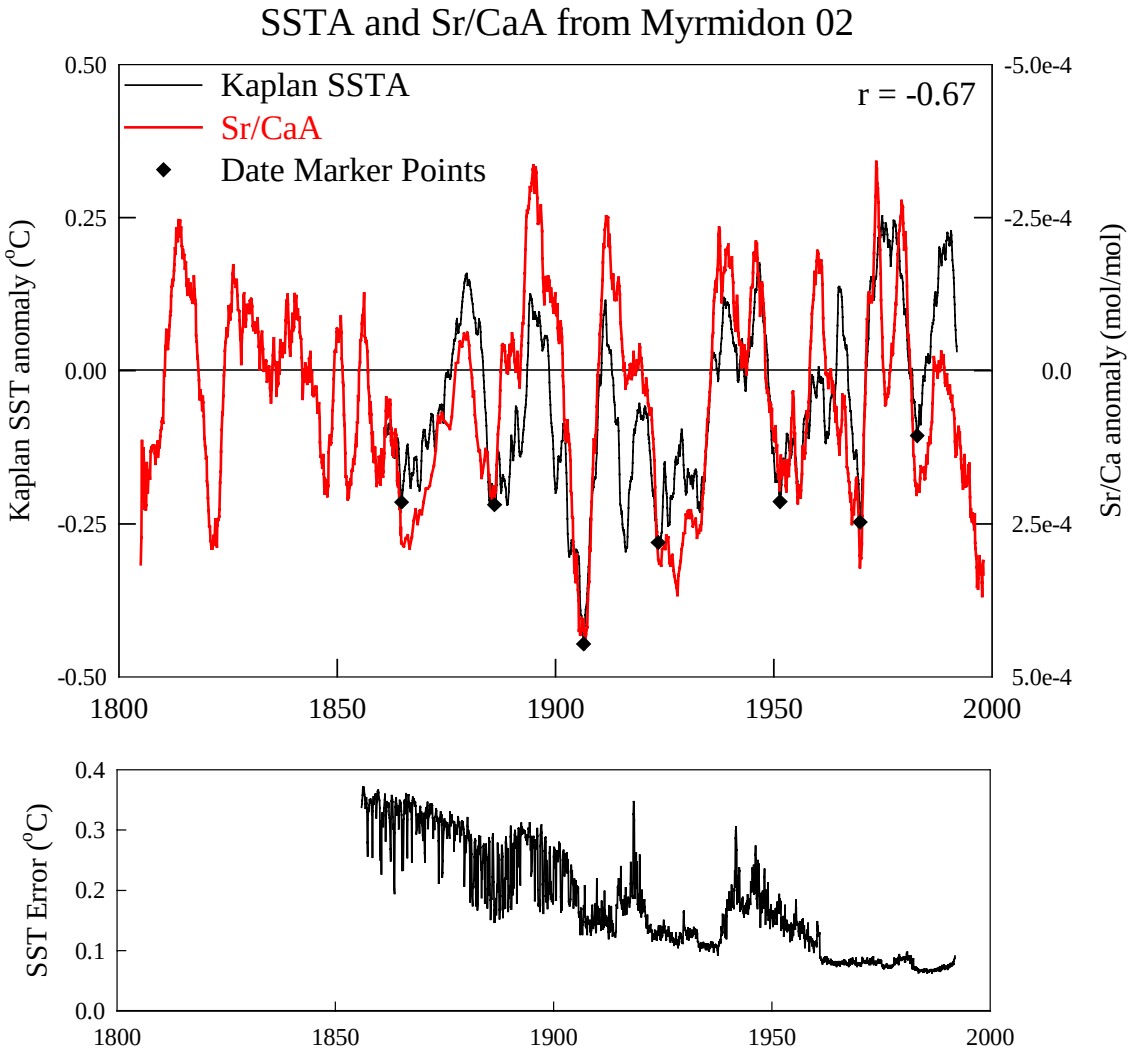

Figure 8.12 (top) Myrmidon Sr/CaA "marker point" adjusted (red) and Kaplan SSTA (147.5E, 17.5S) (black) vs. time. The "marker points" used to tune the Sr/CaA are shown as diamonds on the graph. Correlation coefficient based on overlapping sample periods. (bottom) Kaplan SSTA error estimate.

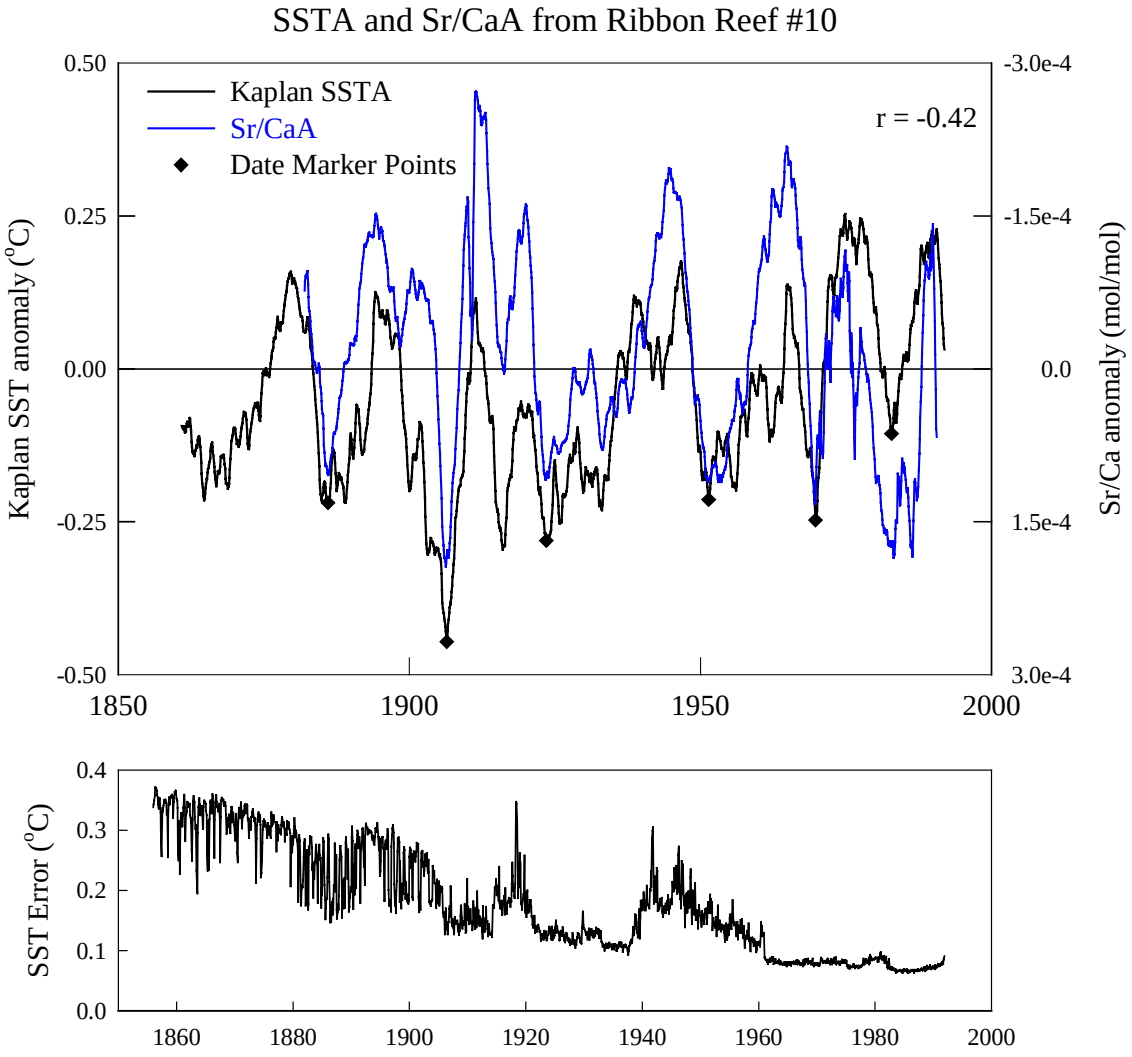

Figure 8.13 (top) Ribbon Reef Sr/CaA "marker point" adjusted (red) and Kaplan SSTA (147.5E, 17.5S) (black) vs. time. The "marker points" used to tune the Sr/CaA are shown as diamonds on the graph. Correlation coefficient based on overlapping sample periods. (bottom) Kaplan SSTA error estimate.

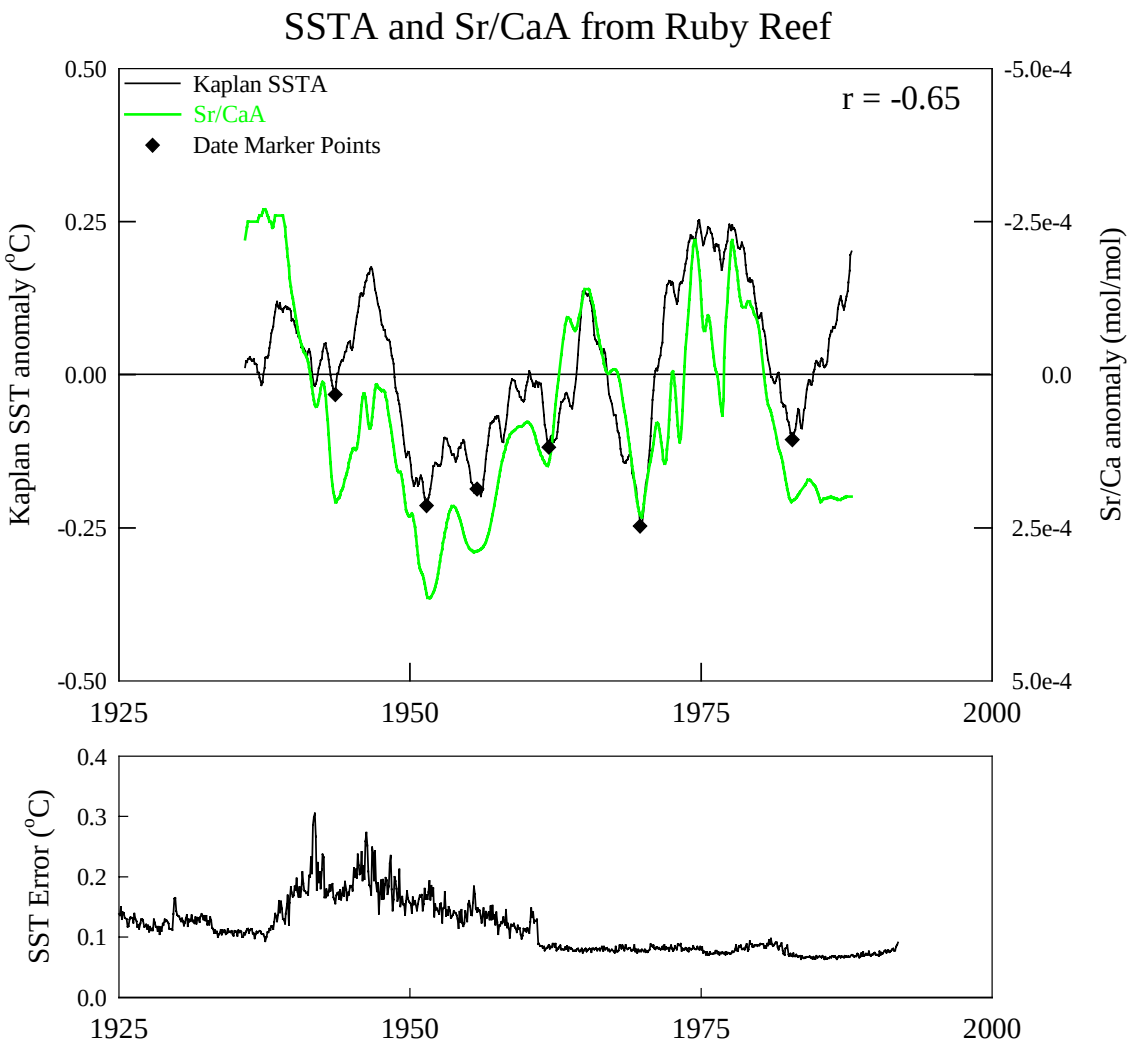

Figure 8.14 (top) Ruby Reef Sr/CaA "marker point" adjusted (red) and Kaplan SSTA (147.5E, 17.5S) (black) vs. time. The "marker points" used to tune the Sr/CaA are shown as diamonds on the graph. Correlation coefficient based on overlapping sample periods. (bottom) Kaplan SSTA error estimate.

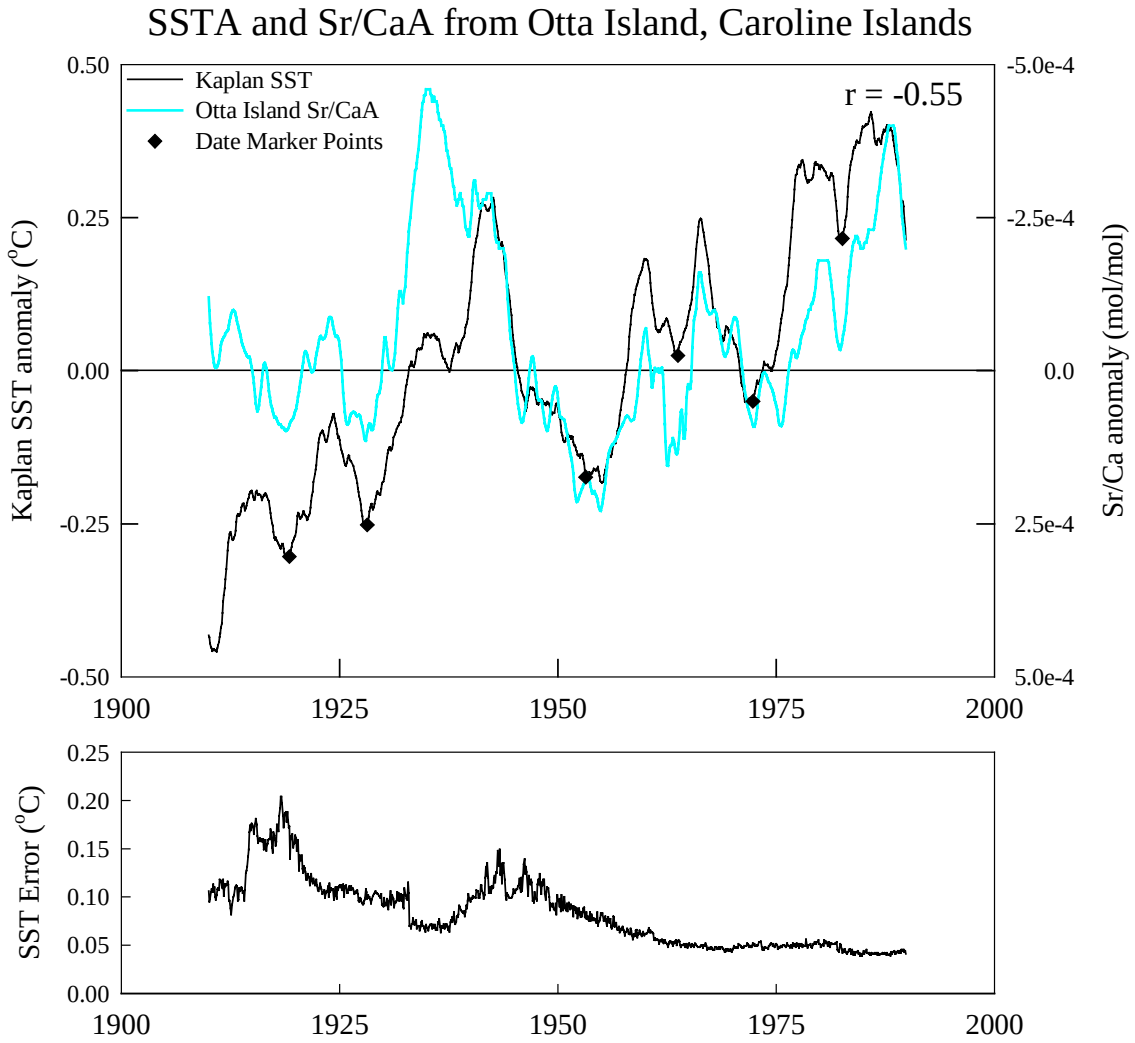

Figure 8.15 (top) Otta Island Sr/CaA "marker point" adjusted (red) and Kaplan SSTA (147.5E, 17.5S) (black) vs. time. The "marker points" used to tune the Sr/CaA are shown as diamonds on the graph. Correlation coefficient based on overlapping sample periods. (bottom) Kaplan SSTA error estimate.

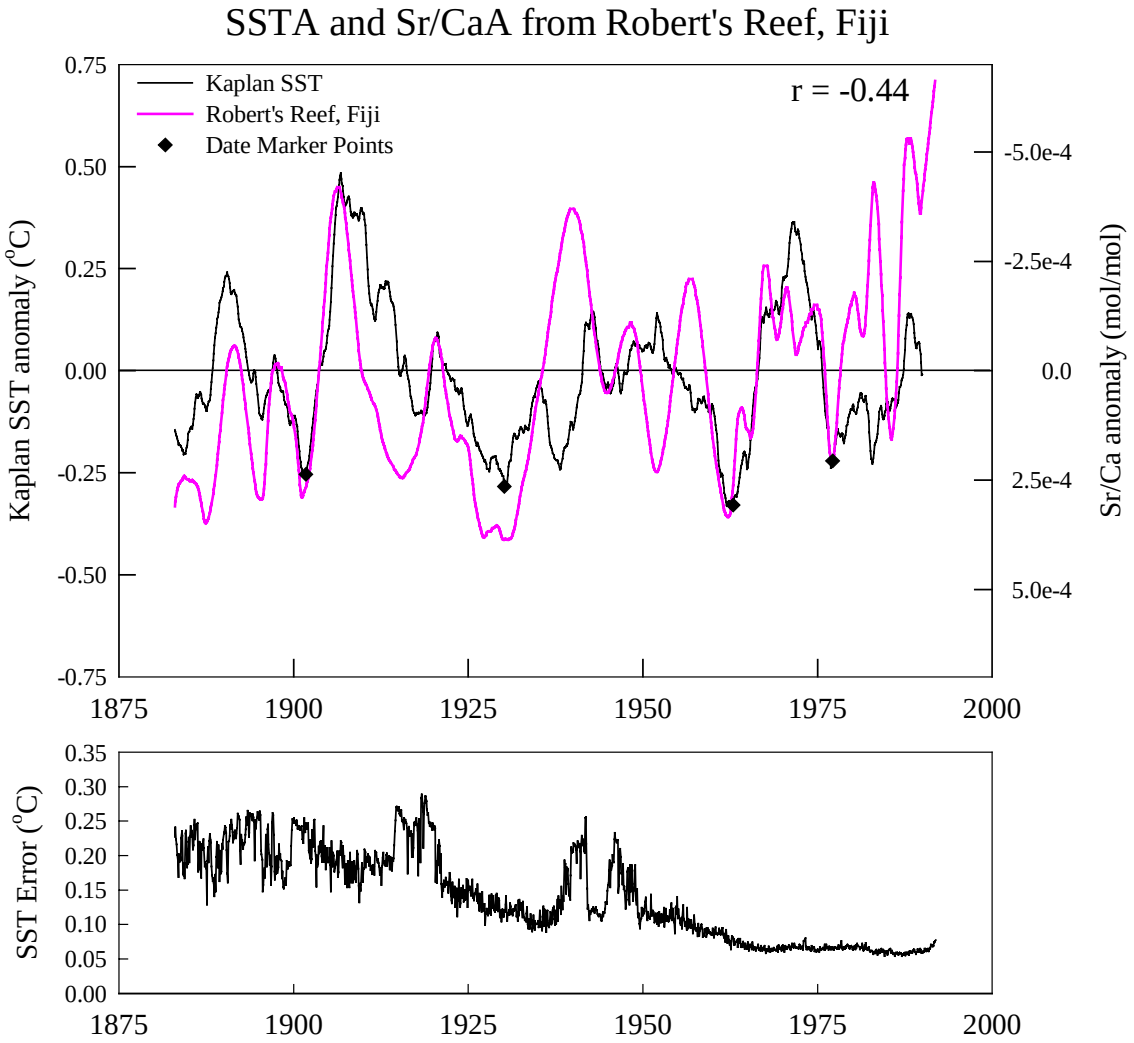

Figure 8.16 (top) Robert's Reef, Fiji Sr/CaA "marker point" adjusted (red) and Kaplan SSTA (147.5E, 17.5S) (black) vs. time. The "marker points" used to tune the Sr/CaA are shown as diamonds on the graph. Correlation coefficient based on overlapping sample periods. (bottom) Kaplan SSTA error estimate.

8.5.5 GBR Sponge Sr/CaA Comparison

The Sr/CaA from three GBR sponges is shown in Figure 8.17. The Myrmidon and Ruby Reef sponges have a reasonable correlation (r = 0.59) and a similar temperature dependence as shown by the amplitude variation of Sr/CaA. The Ribbon Reef #10 sponge has a smaller amplitude variation but is also reasonably correlated to the Myrmidon sponge (r = 0.53). The Ruby Reef and Ribbon Reef#10 sample are only weakly correlated (r = 0.41). All three sponges suggest similar decadal trends in water temperature but they are not always the same. This may be related to local effects on the sponge Sr/Ca. Interestingly, all three sponges show a rapid cool snap just after 1975 that is not observed by the Kaplan SSTA (Figures 8.14, 8.18).

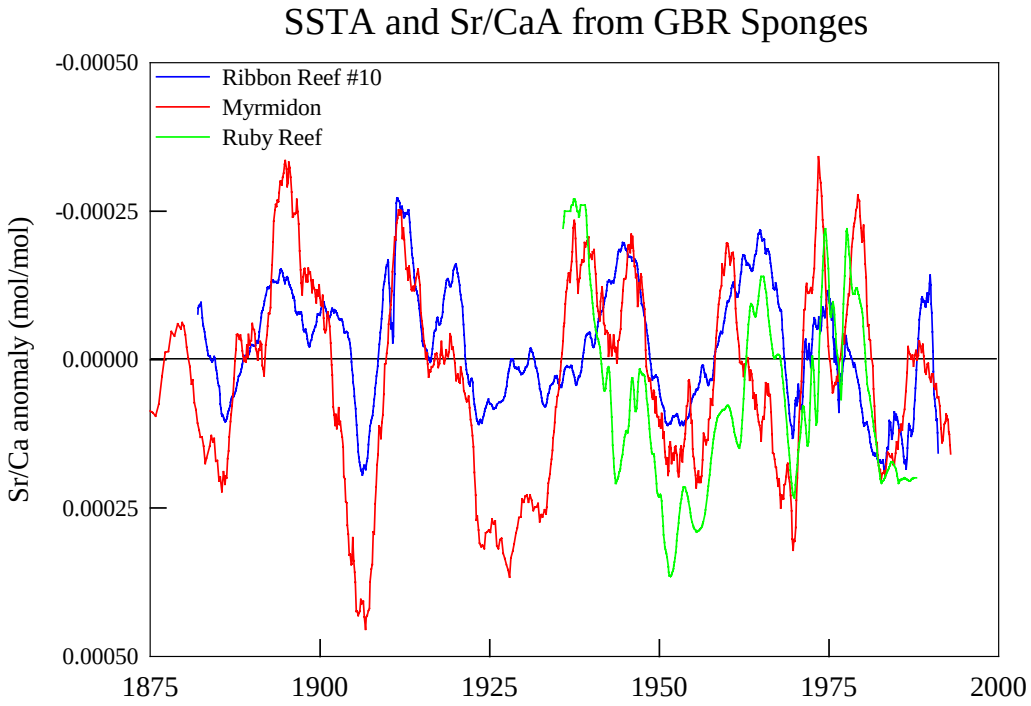

Figure 8.17 Ribbon Reef #10 (blue), Myrmidon (red) and Ruby Reef (green) Sr/CaA vs. time.

8.5.6 Sr/CaA Temperature Dependence

The magnitude of change of sponge Sr/Ca per ºC is significantly larger than for corals. A SST variation of 1ºC is equivalent to a change in coral Sr/Ca of ~ 0.07 mmol/mol (see Chapter 6). Sponge Sr/Ca varies by ~ 0.2-0.9 mmol/mol per ºC (Figure 8.18, Table 8.5). The Sr/Ca – SST sensitivity inferred from the sponges with high correlations to SST (Myrmidon, Ruby and Otta Island) range from 0.76 to 0.9 mmol/mol (Table 8.5). The lower correlated datasets range from 0.28 to 0.56 mmol/mol per ºC (Table 8.5). These are the Ribbon Reef and Fiji samples respectively. The causes of variability in temperature sensitivity are not understood but may be related to calibration misfits, SST errors, smoothing functions as described previously, or real variations intrinsic to the individual sponges.

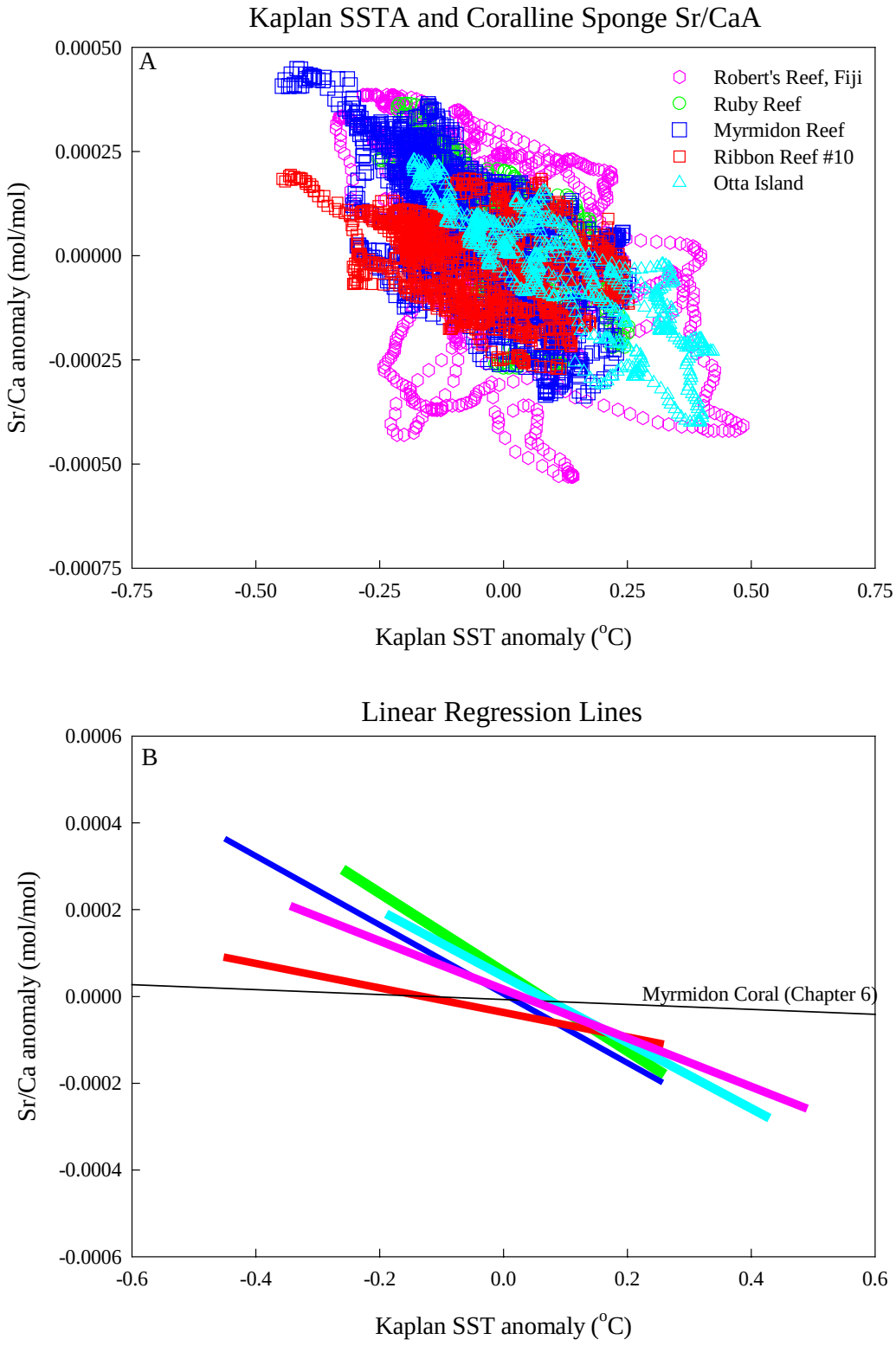

Figure 8.18 A) Scatter plot of Sr/CaA vs. SSTA from all samples. B) Linear Regression lines from all samples. Data prior to 1940 was removed from the Otta Island linear regression to increase the correlation because the slope of the equation was very sensitive to the offsets between SSTA and Sr/CaA prior to 1935. Also shown for comparison is the coral from Myrmidon Reef (Chapter 6).

Table 8.5 Linear Regression equations for Sr/CaA/SSTA and Sr/Ca/SST

	a[1]	b[1]	r
Sr/CaA (mol/mol)			
Myrmidon Reef	5.78e-6	7.94e-4	-0.67
Ribbon Reef	-3.14e-5	2.51e-4	-0.42
Ruby Reef	5.66e-5	9.09e-4	-0.70
Otta Island	4.63e-5	7.61e-4	-0.86
Robert's Reef	1.61e-5	5.61e-4	-0.44
Myrmidon Reef Coral	-7.16e-6	5.65e-5	-0.79
Sr/Ca (mol/mol)			
Myrmidon Reef	0.031	7.94e-4	-0.67
Ribbon Reef	0.018	2.51e-4	-0.42
Ruby Reef	0.034	9.09e-4	-0.70
Otta Island	0.033	7.61e-4	-0.86
Robert's Reef	0.026	5.61e-4	-0.44
Myrmidon Reef Coral	0.01042	5.65e-5	-0.79

[1] Calibration equation is X/Ca = a – b * SST.

It is also useful to examine the relationships between the absolute Sr/Ca (not the anomaly) and the Kaplan SST. Using the mean values (1951-1980) from A. Kaplan (pers. comm.), the 5º x 5º grid dataset was reconstructed and compared to the sponge Sr/Ca (same 5 yr. resolution). The comparisons and correlations are the same but the difference in the average Sr/Ca concentration between the locations is apparent (Figure 8.19). The GBR sponge Sr/Ca/SST linear regressions are fairly close together, close enough to be explained by the differences in local SST (~ 0.5 ºC) between the 3 locations. The offset between the Fiji Sr/Ca/SST data may be due to the difference between surface water temperature and the temperature at 42m. This temperature difference has not been quantified and is only speculation. However, the Sr/Ca data from Otta Island cannot be easily explained. This phenomenon could be related to the differences observed for coral Sr/Ca/SST variations. One interesting observation is that if the calibrations for the GBR sponges were extended to 29ºC the Otta Island sponge values would be ~ 0.008 mol/mol (Figure 8.19) slightly below the seawater value. This suggests an additional influence on sponge Sr/Ca aside from temperature causing mean sponge Sr/Ca values to be relatively similar regardless of the absolute temperature (Figure 8.19). This indicates that Sr/Ca ratios in coralline sponges appear to respond to temperature anomalies rather than differences in absolute temperature.

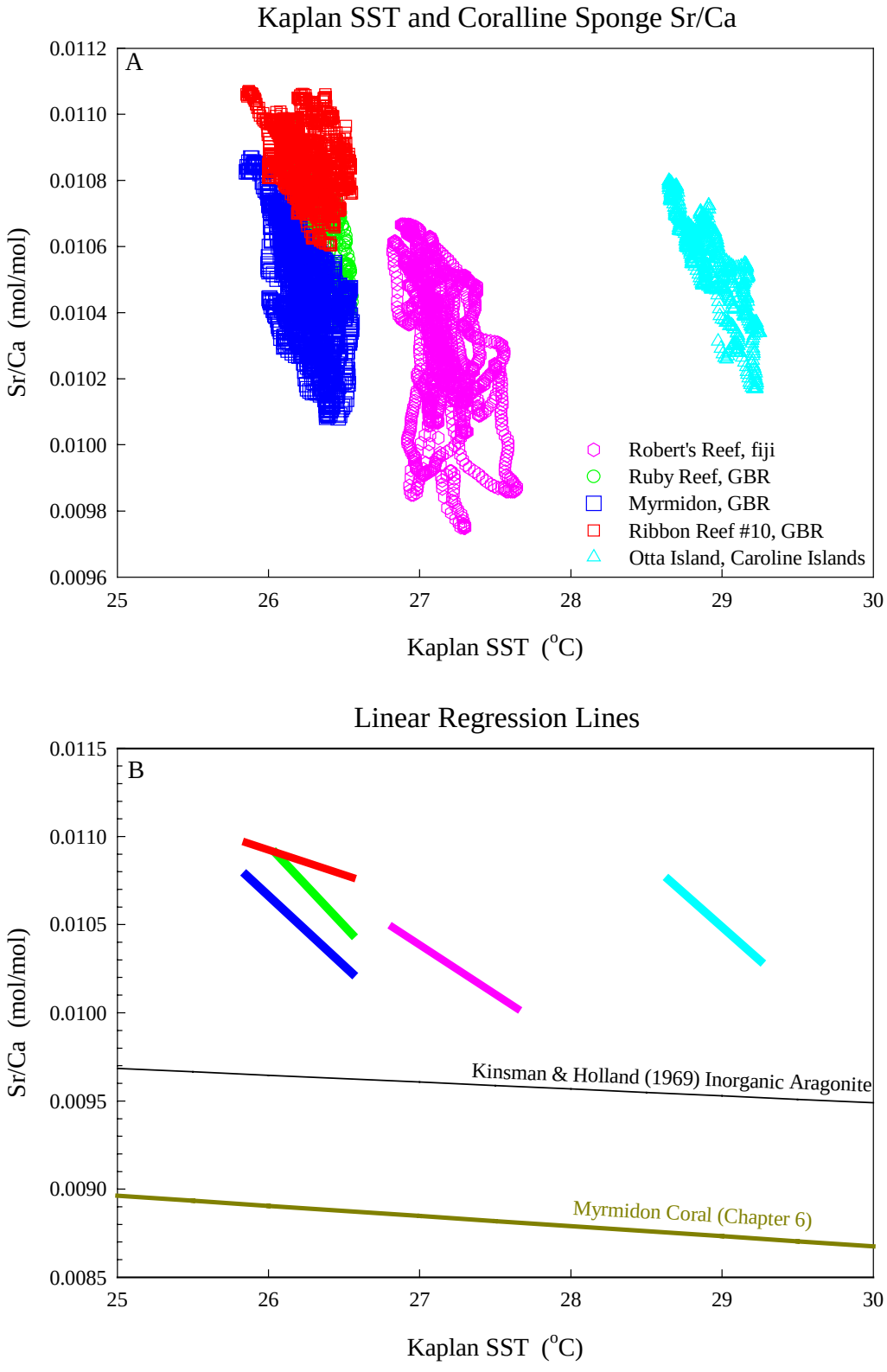

Figure 8.19 A) Sponge Sr/Ca vs. Kaplan SST. B) Linear regression lines for sponge Sr/Ca and SST. The inorganic aragonite line from Kinsman and Holland (1969) and the Myrmidon coral (Chapter 6) are shown for comparison.

Figure 8.19B also shows the slopes and location of the Kinsman and Holland (1969) theoretical inorganic aragonite Sr/Ca/SST regression line. Sponges are considerably

above this line. The Sr/Ca values from the GBR sponges indicate a distribution coefficient between seawater Sr/Ca and sponge Sr/Ca of ~1.26, the average GBR coral distribution coefficient is ~1.05. For comparison, the inorganic distribution coefficient is 1.15 at 30ºC (see Figure 4.4, Kinsman and Holland, 1969). The sponge distribution coefficient is similar to the value obtained by Delaney *et al*. (1996) for *Halimeda* aragonite (1.3).

Regardless of the causes for the relatively constant average Sr/Ca ratios over large ranges in mean SST, the large ΔSr/Ca per ºC enables less precise and more rapid method analyses (e.g. LA-ICP-MS) of Sr/Ca to be accurate to ~0.2º (see LA-ICP-MS errors Chapter 3). This tracer still needs to be verified by reproducing multiple samples from each location in the same manner as corals are being analyzed now.

8.5.7 Stable Isotopes

The stable isotope measurements undertaken on the Ribbon Reef sponge are shown in Figure 8.20, 8.22. The $\delta^{18}O$ values range from –0.82‰ to –1.2‰ (PDB) while the $\delta^{13}C$ values max at 4.62‰ (PDB) and rapidly decrease toward the youngest part of the sponge with a final value of 3.95‰. Using the dating methods from the Sr/CaA, time series of $\delta^{18}O$ and $\delta^{13}C$ were constructed. The $\delta^{13}C$ data show the increase in atmospheric and ocean ^{12}C due to the preferential release of ^{12}C during fossil fuel burning (Figure 8.20). The sponge shows the major onset occurring ~ 1900 that is similar to the $\delta^{13}C$ atmospheric composite shown by Böhm *et al*. (1996). This signal is clear and appears in all published sponge samples (Druffel and Benavides, 1986; Böhm *et al*., 1996; Wörheide, 1998). The ability of sponges to record this $\delta^{13}C$ seawater change so faithfully most likely results from sponges being in close equilibrium with respect to $\delta^{13}C$ and $\delta^{18}O$ and seawater (Druffel and Benavides, 1986; Böhm *et al*., 1996; Wörheide, 1998). The decrease in $\delta^{13}C$ can be seen in some coral records but it is not as clear as in sponges (e.g. Nozaki *et al*., 1978).

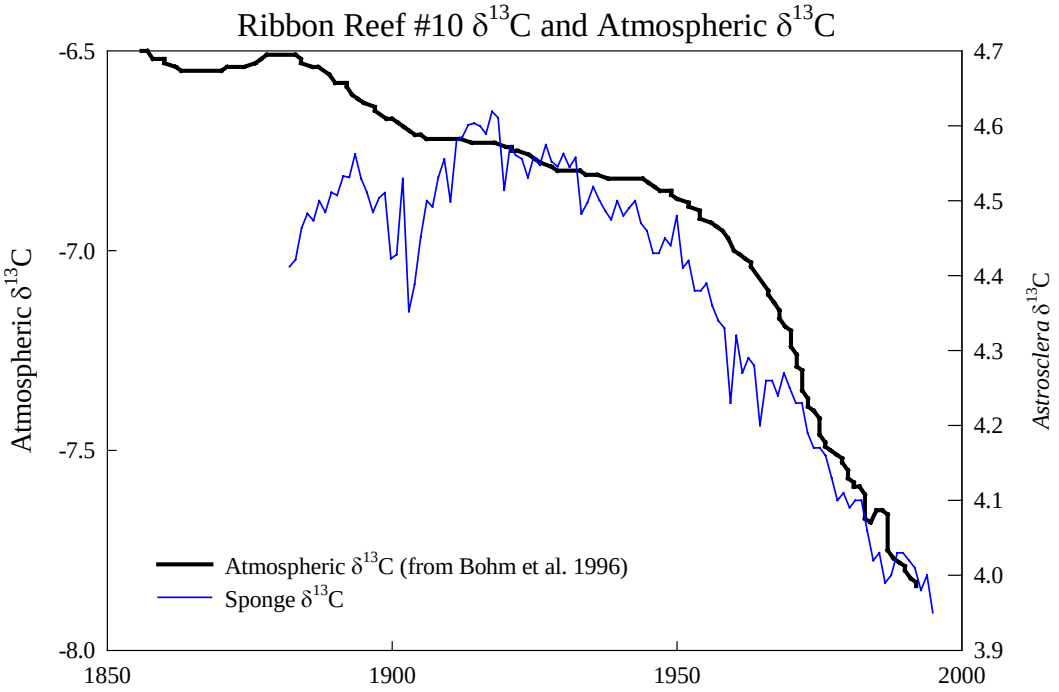

Figure 8.20 Atmospheric $\delta^{13}C$ and Ribbon Reef #10 $\delta^{13}C$ vs. time. $\delta^{13}C$ data was fit to time using the Sr/CaA dating method. Atmospheric $\delta^{13}C$ curve comes from the curve generated in Böhm *et al*. (1996).

The $\delta^{18}O$ measurement was converted to SST using the Equation 8.1:

Equation 8.1 $T(^oC) = (20.0 \pm 0.2) - (4.42 \pm 0.1) * (\delta_{aragonite} - \delta_{water})$

from Böhm *et al*. (2000)

$\delta^{18}O$water = 0.36 SMOW from Wörheide (1998)

The data was plotted and compared to the Kaplan SST (mean added back in) and is shown Figure 8.21. Using this equation the average SST at Ribbon Reef is reproduced by the sponge $\delta^{18}O$. However the "decadal" cyclisity recorded by the SST is not reproduced as well by $\delta^{18}O$ as by Sr/Ca. This may be attributed to the sampling density (much lower resolution) or the fact the $\delta^{18}O$ can also influenced by fresh water flux. The $\delta^{18}O$ suggests that temperature was much cooler ~1900-1920 than either the Kaplan SST or the Sr/Ca. Summer rainfall around 1900 from this section of Queensland (and GBR) was lower than normal (Lough, 1991) that may help account for some of this cooling. On a positive note, their equation (Böhm *et al*., 2000), based on a combination of sponge, mollusc, foram, gastrapod and synthetic aragonite, produces very reasonable SST values indicating that the $\delta^{18}O$ may be more robust across genera and locations

than Sr/Ca. Although like suggested for Sr/Ca more testing on multiple samples is required.

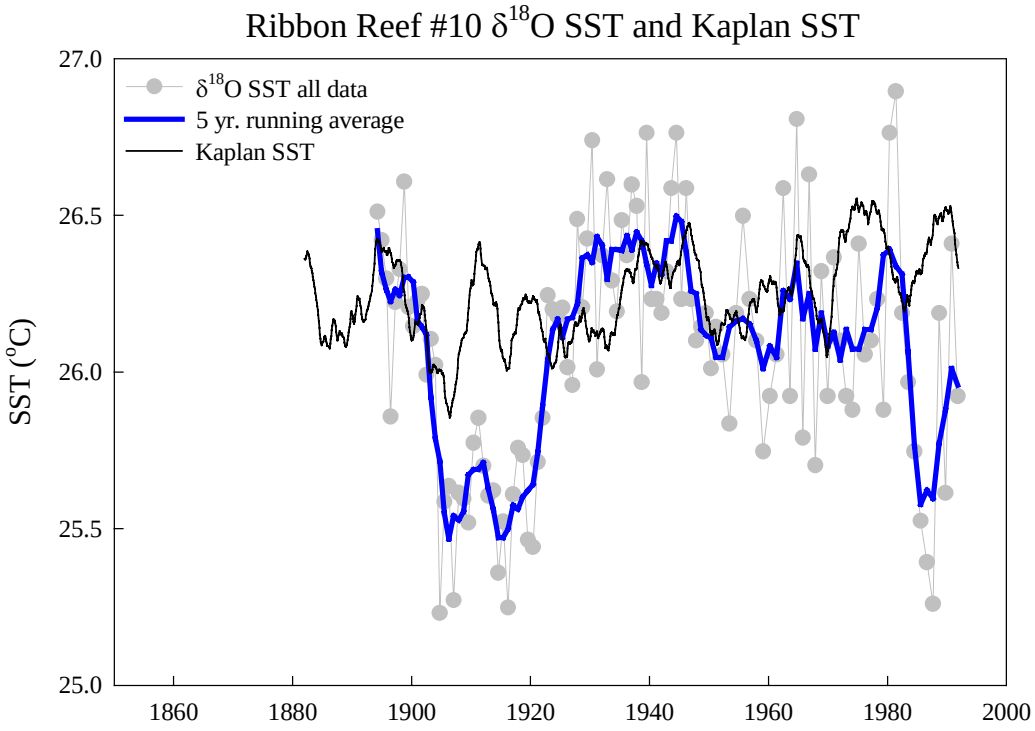

Figure 8.21 SST from Ribbon Reef #10 $\delta^{18}O$ using Equation 8.1. Gray line and circles are the raw data, distance b/w samples is 0.5. Blue line is 5 yr. running average. The data was fit to time using the Sr/CaA "marker" method. The Kaplan SST dataset is in black.

8.6 Conclusions

Multiple elements B, Mg, Sr, Ba, U were measured in the coralline sponge *Astrosclera willeyana* from five locations around the Southwest Pacific. Using dating methods based on counting "annual" cycles and "expected" average growth rates of ~0.2 mm yr^{-1} time series were constructed for these five samples. Out of the five elements only Sr/Ca showed variations consistent with regional SST variations.

Density measurements near the outer surface of the sponges indicate that thickening and addition of $CaCO_3$ occurs over distance of 2-3mm. The initial $CaCO_3$ deposition appears to not be thickened until approximately 2-3 mm from the outside "living" edge. This suggests that the sponges are smoothing the included trace element signal, maybe as much as 5-20 years. Based on the comparison between smoothed SST and smoothed

Sr/Ca the smoothing may be ~ 5 years. Care is still needed in interpreting Sr/Ca data as sponges from different regions correlate best with temperature anomalies rather than absolute temperature.

When Sr/Ca data was smoothed to a five year running average correlations appeared with the SST dataset of Kaplan *et al*. (1998). These comparisons suggest that Sr/Ca varies by ~0.7-0.9 mmol/mol per ºC. This is 7-12 times larger than coral Sr/Ca, which is around 0.07 mmol/mol per ºC. If this relationship holds up then less precise methods (e.g. LA-ICP-MS) and not necessarily TIMS would be needed to reconstruct SST from sponges on the order of 0.2 ºC or less.

The $\delta^{13}C$ data from the Ribbon Reef sponge records the atmospheric and oceanic increase in ^{12}C due to fossil fuel burning since the 1900's. All published sponge $\delta^{13}C$ show this result clearly. Using a temperature equation for sponge $\delta^{18}O$ from Böhm *et al*. (2000) the $\delta^{18}O$ from the ribbon reef sponge suggest the water temperature averages ~26.1 ºC. This is in good agreement with the Kaplan SST that suggests the average water temperature was 26.3 ºC. The $\delta^{18}O$ also suggests that the 1890-1920's were cooler and drier than present.

Overall, coralline sponges appear to show that they will be useful for providing water temperature. However problems such as dating, constant growth rates and signal smoothing (is it constant?) need to be addressed before full-scale use of these proxies can occur. Assessing the variability between sponges from one location is high on the list of priorities for establishing them as a new proxy.

Chapter 9: Summary and Conclusions

9.1 Method

A preliminary part of this project focused on providing fully quantitative measurements of the element boron, magnesium, strontium, calcium, barium and uranium from coral and sponge $CaCO_3$ by LA-ICP-MS. The construction of a well-characterized pressed powder (crushed coral) pellet standard provided this capability. Using this standard, accuracies of 1-4% for Mg/Ca, Sr/Ca, Ba/Ca and U/Ca were achieved. The daily reproducibility of this technique has been shown to be between 0.5 – 2.5% while the long-term (monthly) reproducibility is on the order of 1 – 3.5%. These results indicate that LA-ICP-MS is a viable tool for extracting elemental ratios of B/Ca, Mg/Ca, Sr/Ca, Ba/Ca and U/Ca from corals and coralline sponges.

The concentration of minor elements Mn, Zn, Pb, Y, La, Ce and the other REE's have also been analyzed by LA-ICP-MS using a calcium silicate glass standard (NIST 614) produced by the United States National Institute of Standards. A full comparison between alternative methods, solution ICP-MS and TIMS vs. LA-ICP-MS for these elements has not been carried out. However, when using this standard (NIST 614) an estimate of the barium concentration is accurate within 10% and uranium is within 3.5%. The other elements can only be assessed by their reproducibility, which is good even when concentrations are near detection limits. The next step for this standard is to compare LA-ICP-MS results with solution ICP-MS or TIMS analyses to obtain a clearer picture of this standards accuracy at calibrating minor elemental concentrations in corals.

9.2 Japan Coral

A *Porites* coral collected from one of the most northern reefs in Japan displayed a slow growth rate (~ 5 mm yr^{-1}). This coral lived in an area where SST ranged from ~ 15 – 29

ºC. The "arched" shape of the elemental ratios of Sr/Ca and U/Ca suggested increased extension in summer relative to winter. The sharp narrow winters suggested a marked decrease and/or cessation of extension/calcification during the cold winters when daily SST could reach ~12 ºC. The B/Ca and Mg/Ca signals also suggested that other factors aside from temperature could affect these proxies. This was seen, as monthly variations equal to ~1/2 the annual cycle and they could not be attributed to SST fluctuations. Ba/Ca was shown to vary in response to wind shifts causing winter upwelling and secondary summer upwelling events coincident with El Niño summers. Suggesting the usefulness of Ba/Ca as a potential El Niño proxy in the Japan area.

9.3 GBR Coral Transect

Six corals collected from the transect across the central GBR displayed variations consistent with their location across the shelf. Inshore reef corals are characterized by luminescent bands that indicate periods of rainfall-induced runoff from the Burdekin River. The elemental tracer Ba/Ca also shows increases that correspond to the increased sedimentation associated with these flood plumes. The mid-shelf and outer reef corals do not show the influence of runoff because of their distance from the river outfall. However some "anomalous" Ba/Ca spikes were also found in the mid-shelf Davies and inshore Orpheus coral that did not correspond to runoff. Its cause has not been elucidated. Horizontal variability was also examined via a 12 x 12 mm surface scan on the Orpheus coral. This scan suggested that Ba/Ca flood and "anomalous" signals are at least consistent for 12 mm across the same time horizon.

Manganese was measured and only the inshore corals show good annual cycles. The timing of the Mn cycles suggests increased solar radiation and the weakening of the winter southeasterly may be involved in the coral Mn variability. The increase of solar radiation may act to increase photoreduction of Mn oxides and decrease Mn particle formation. The low solar radiation and higher winds during winter may cause particle resuspension and formation. Thus providing a source for the higher summer seawater Mn concentration.

The SST proxies (B/Ca, Mg/Ca, Sr/Ca, U/Ca) from this transect suggest Sr/Ca and B/Ca are the most robust across the inshore to outer GBR. Sr/Ca and to some extent B/Ca

appear to be unaffected by coastline proximity and runoff. Mg/Ca and U/Ca appear to be influenced by parameters other than SST. This is in agreement with recent studies suggesting that Mg/Ca and U/Ca variation is not purely temperature dependent (Schrag, 1999). The U/Ca concentration in the inshore corals is slightly elevated relative to the mid-shelf and outer reef corals suggesting that dilution of U/Ca by runoff does not occur on the GBR (Shen and Dunbar, 1995; Wei *et al*., 2000).

9.4 Misima Island Corals

The corals from Misima Island clearly document increased sedimentation by way of minor elemental incorporation into the coral skeletons. Mn, Y, La and Ce all show elemental increases that coincide with the commencement of open-pit mining. The open-pit mining caused an increase in nearshore sediment by way of nearby creeks. The most likely source for the increase in coral Mn, Y, La and Ce was the weathered topsoil (feldspar and greenstone) that can contain high quantities of Mn oxides. A clear trend between the distance from the mine and the corals metal concentration existed for Mn, Y, La and Ce.

The elements lead and zinc did not increase until "fresh" rock was exposed by mining ~ 1 year after mine construction commenced. Zinc and lead are present as sulfides in the ore body, sphalerite (ZnS) and galena (PbS). Mine soils contain zinc and lead at concentrations of 200-800 ppm and 70-600 ppm respectively. Sulfate concentration was measure in the Cooktown creek and indicated that values were 10-30ppm (pre-mining) and increased to ~ 200 ppm in 1994 and subsequent measurements suggest the levels have stabilized at 450 ppm. The increase in creek sulfate is most likely related to the oxidation of sulfides (ZnS and PbS) releasing Zn and Pb to the environment.

Coral REE patterns suggest a similarity with the Fly and Sepik estuary waters off mainland PNG. When the coral data is normalized to Coral Sea seawater the LREE's and MREE's show enrichment while the HREE's show significant depletion. This nearshore REE pattern was termed an "island weathering signature" by Sholkovitz *et al*. (1999). This pattern was shown to affect the seawater REE pattern of sites distal to PNG (Sholkovitz *et al*., 1999). Particulates from the Fly and Sepik rivers do not have exactly the same REE pattern as the estuary waster. When the particles were leached in

seawater they released REE's with the same enriched MREE pattern as the Fly and Sepik estuary water. The fact that the corals REE pattern is similar to the dissolved estuary pattern hints at the incorporation of metals (REE's at least) into corals as a dissolved state and not as particulates. The consistent metal patterns within and between sites suggest that a consistent mode of metal incorporation is being measured and not detritus particles trapped in skeletal cavities. This method could be either by seawater dissolved metals or possibly coral polyp feeding. Either mechanism could cause the increase in metals recorded in the coral from Misima Island.

9.5 Coralline Sponges

Coralline sponges can provide records of the environment surrounding them as they grow. The recovered record from *Astrosclera willeyana* will be smoothed due to the extensive infilling of secondary aragonite at the base of the "living" tissue layer. Gamma densitometry profiles suggest that this thickening could take place over a distance of 2-3 mm. Assuming a growth rate of ~0.2 mm yr^{-1} and by counting "annual" cycles of Sr/Ca an approximate age model was constructed for five sponges from the Southwest Pacific. When an anomaly is computed for the Sr/Ca data and smoothed by a five year running mean correlations appeared with the SST anomaly dataset of Kaplan *et al*. (1998). Using a few "marker points" these correlations were improved and temperature dependence was computed. There is variability between the different location Sr/Ca-SST dependence but the three samples with good correlations to SST suggest that this temperature dependence is 7 – 12 times higher than corals (sponge ~0.7 – 0.9 mmol/mol ΔSr/Ca pre ºC vs. ~0.07 mmol/mol ΔSr/Ca per ºC for corals).

Stable isotope records from one sponge show good agreement between sponge $\delta^{13}C$ and atmospheric $\delta^{13}C$. The decrease in $\delta^{13}C$ (atmospheric and seawater) reflects the increase in atmospheric ^{12}C due to the burning of fossil fuels. Using a temperature equation from Böhm *et al*. (2000) the $\delta^{18}O$ data suggest the Ribbon Reef site had an average SST of 26.2 ºC, which is in good agreement with the Kaplan SST value of 26.3 ºC (A. Kaplan pers. comm.). Suggesting that $\delta^{18}O$ is useful to provide SST variation especially in areas little influenced by $\delta^{18}O$ seawater changes (fresh water flux).

9.6 What's Next

Overall this project has shown the usefulness of the LA-ICP-MS as a tool to provide rapid and accurate trace element profiles from corals and coralline sponges. However there is still further work to be done. More comparisons between analytical techniques especially for the minor elements need to be performed. The construction of a doped $CaCO_3$ standard that is homogenous would be a great achievement.

As far as analyses go, I believe the next step is to use these rapid analytical techniques to create multiple, long time-series records from corals. Using barium and manganese to distinguish runoff events and particle interactions from time periods before European settlement in Queensland would provide valuable information about the changing land use practices. Obtaining simultaneous measurements of B/Ca, Mg/Ca, Sr/Ca and U/Ca can elucidate temperature variations throughout the last centuries to examine if temperature dependence on these elements changes through time. The collection of records from sponges is still in the beginning stages. Reproducibility of sponge records from the same location needs to be assessed. Comparisons between corals and sponges from the same location could potentially provide information from surface waters and waters at depth. This could help aid in our understanding of water circulation and potentially thermocline variation.

References

Aharon, P., (1991), Recorders of reef environment histories: stable isotopes in corals, giant clams, and calcareous algae: *Coral Reefs*, v. 10, p. 71-90.

Alibert, C., and McCulloch, M.T., (1997), Strontium/calcium ratios in modern *Porites* corals from the Great Barrier Reef as a proxy for sea surface temperature: Calibration of the thermometer and monitoring of ENSO: *Paleoceanography*, v. 12, p. 345-363.

Allison, N., (1996a), Comparative determinations of trace and minor elements in coral aragonite by ion microprobe analysis, with preliminary results from Phuket, southern Thailand: *Geochimica et Cosmochimica Acta*, v. 60, p. 3457-3470.

Allison, N., (1996b), Geochemical anomalies in coral skeletons and their possible implications for palaeoenvironmental analyses: *Marine Chemistry*, v. 55, p. 367-379.

Allison, N., and Tudhope, A.W. (1992) Nature and significance of geochemical variations in coral skeletons as determined by ion microprobe analysis. *Seventh International Coral Reef Symposium*, 173-178.

Amiel, A.J., Friedman, G.M., and Miller, D.S., (1973a), Distribution and nature of incorporation of trace elements in modern aragonitic corals: *Sedimentology*, v. 20, p. 47-64.

Amiel, A.J., Miller, D.S., and Friedman, G.M., (1973b), Incorporation of uranium in modern corals: *Sedimentology*, v. 20, p. 523-528.

Bacon, M.P., and Edmond, J.M., (1972), Barium at GEOSECS III in the Southwest Pacific: *Earth and Planetary Science Letters*, v. 16, p. 66-74.

Barnard, L.A., Macintyre, I.G., and Pierce, J.W., (1974), Possible environmental index in tropical reef corals: *Nature*, v. 252, p. 219-220.

Barnes, D.J., and Lough, J.M., (1992), Systematic variations in the depth of skeleton occupied by coral tissue in massive colonies of *Porites* from the Great Barrier Reef: *Journal of Experimental Marine Biology Ecology*, v. 159, p. 113-128.

Barnes, D.J., and Lough, J.M., (1999), *Porites* growth characteristics in a changed environment: Misima Island, Papua New Guinea: *Coral Reefs*, v. 18, p. 213-218.

Barnes, D.J., Taylor, R.B., and Lough, J.M., (1995), On the inclusion of trace materials into massive coral skeletons. Part II: distortions in skeletal records of annual climate cycles due to growth processes: *Journal of Experimental Marine Biology Ecology*, v. 194, p. 251-275.

Bastidas, C., and Garcia, E., (1999), Metal content on the reef coral *Porites astreoides*: an evaluation of river influence and 35 years of chronology: *Marine Pollution Bulletin*, v. 38, p. 899-907.

Beck, J.W., Edwards., R.L., Ito, E., Taylor, F.W., Recy, J., Rougerie, F., Joannot, P., and Henin, C., (1992), Sea-Surface Temperature from Coral Skeletal Strontium/Calcium Ratios: *Science*, v. 257, p. 644-647.

Benavides, L.M., and Druffel, E.R.M., (1986), Sclerosponge growth rate as determined by ^{210}Pb and $\Delta^{14}C$ chronologies: *Coral Reefs*, v. 4, p. 221-224.

Bender, M.L., Klinkhammer, G.P., and Spencer, D.W., (1977), Manganese in seawater and the marine manganese balance: *Deep Sea Research*, v. 24, p. 799-812.

Bernat, M., Church, T., and Allegre, C.J., (1972), Barium and strontium concentrations in Pacific and Mediterranean sea water profiles by direct isotope dilution mass spectrometry: *Earth and Planetary Science Letters*, v. 16, p. 75-80.

Berner, R.A., (1975), The role of magnesium in the crystal growth of calcite and aragonite from sea water: *Geochimica et Cosmochimica Acta*, v. 39, p. 489-504.

Beveridge, N.A.S., and Shackleton, N.J., (1994), Carbon isotopes in recent planktonic foraminifera: A record of anthropogenic CO_2 invasion of the surface water: *Earth and Planetary Science Letters*, v. 126, p. 259-273.

Bloch, S., (1980), Some factors controlling the concentration of uranium in the world ocean: *Geochimica et Cosmochimica Acta*, v. 44, p. 373-377.

Böhm, F., Joachimski, M.M., Dullo, W.-C., Eisenhauer, A., Lehnert, H., Reitner, J., and Wörheide, G., (2000), Oxygen isotope fractionation in marine aragonite of coralline sponges: *Geochimica et Cosmochimica Acta*, v. 64, p. 1695-1703.

Böhm, F., Joachimski, M.M., Lehnert, H., Morgenroth, G., Kretschmer, W., Vacelet, J., and Dullo, W.-C., (1996), Carbon isotope records from extant Caribbean and South Pacific sponges: Evolution of $\delta^{13}C$ in surface water DIC: *Earth and Planetary Science Letters*, v. 139, p. 291-303.

Boto, K., and Isdale, P., (1985), Fluorescent bands in massive corals result from terrestrial fulvic acid inputs to nearshore zone: *Nature*, v. 315, p. 396-397.

Boyle, E.A., Sclater, F., and Edmond, J.M., (1976), On the marine geochemistry of cadmium: *Nature*, v. 263, p. 42-44.

Brass, G.W., and Turekian, K.K., (1974), Strontium distribution in GEOSECS Oceanic Profiles: *Earth and Planetary Science Letters*, v. 23, p. 141-148.

Broecker, W.S., and Peng, T.H., (1982), *Tracers in the Sea*: New York, Lamont-Doherty Geological Observatory.

Brown, B.E., (1987), Heavy metals pollution on coral reefs, *in Human Impacts on Coral Reefs: Facts and Recommendations*: French Polynesia, (ed. Salvat, B.), Antenne Museum E. P. H. E.

Brown, B.E., and Holley, M.C., (1982), Metal levels associated with tin dredging and smelting and their effect upon intertidal reef flats at Ko Phuket, Thailand: *Coral Reefs*, v. 1, p. 131-137.

Brown, B.E., Tudhope, A.W., LeTissier, M.D.A., and Scoffin, T.P., (1991), A novel mechanism for iron incorporation into coral skeletons: *Coral Reefs*, v. 10, p. 211-215.

Buddemeier, R.W., and Kinzie, R.A., (1975), The chronometric reliability of contemporary corals, *in Growth Rhythms and the History of the Earth's Rotation*: New York, (ed. Rosenberg, G.D., and Runcorn, S.K.), Wiley & Sons, p. 135-147.

Buddemeier, R.W., Schneider, R.C., and Smith, S.V. (1981) The alkaline earth chemistry of corals. *Fourth International Coral Reef Symposium*, 81-85.

Butler, I.B., and Nesbitt, R.W., (1999), Trace element distribution in the chalcopyrite wall of a black smoker chimney: insights from laser ablation inductively coupled plasma mass spectrometry (LA-ICP-MS): *Earth and Planetary Science Letters*, v. 167, p. 335-345.

Carroll, J., Falkner, K.K., Brown, E.T., and Moore, W.S., (1993), The role of the Ganges-Brahmaputra mixing zone in supplying barium and ^{226}Ra to the Bay of Bengal: *Geochimica et Cosmochimica Acta*, v. 57, p. 2981-2990.

Chalker, B., Barnes, D., and Isdale, P., (1985), Calibration of X-ray densitometry for the measurement of coral skeletal density: *Coral Reefs*, v. 4, p. 95-100.

Chalker, B.E., and Barnes, D.J., (1990), Gamma densitometry for the measurement of skeletal density: *Coral Reefs*, v. 9, p. 11-23.

Chave, K.E., (1954), Aspects of the biogeochemistry of magnesium 1. Calcareous marine organisms, v. 62, p. 266-283.

Chen, A., Doherty, W., and Gregoire, C., (1997), Application of laser sampling microprobe inductively coupled plasma mass spectrometry to the *in situ* trace

element analysis of geological materials: *Journal of Analytical Atomic Spectrometry*, v. 12, p. 653-659.

Chester, R., (1990), *Marine Geochemistry*: London, Unwin Hyman Ltd., 698 p.

Christ., C.L., Clark, J.R., and Jr., H.T.E., (1955), Crystal structure of Rutherfordine, UO_2CO_3: *Science*, v. 121, p. 472-473.

Cross, T.S., and Cross, B.W., (1983), U, Sr, Mg in Holocene and Pleistocene corals *A. palmata* and *M. annularis*: *Journal of Sedimentary Petrology*, v. 53, p. 587-594.

Crossland, C.J. (1981) Seasonal growth of *Acropora* cf. *formosa* and *Pocillopora damicornis* on a high latitude reef (Houtman Abrolhos, Western Australia). *Fourth International Coral Reef Symposium*, 663-667.

Dehairs, F., Chesselet, R., and Jedwab, J., (1980), Discrete suspended particles of barite and the barium cycle in the open ocean: *Earth and Planetary Science Letters*, v. 49, p. 528-550.

Delaney, M.L., Linn, L.J., and Davies, P.J., (1996), Trace and minor element ratios in *Halimeda* aragonite from the Great Barrier Reef: *Coral Reefs*, v. 15, p. 181-189.

Delaney, M.L., Linn, L.J., and Druffel, E.R.M., (1993), Seasonal cycles of manganese and cadmium in coral from the Galapagos Islands: *Geochimica et Cosmochimica Acta*, v. 57, p. 347-354.

Denton, G.R.W., and Burdon-Jones, C., (1986), Trace metals in corals from the Great Barrier Reef: *Marine Pollution Bulletin*, v. 17, p. 209-213.

de Villiers, S., Shen, G.T., and Nelson, B.K., (1994), The Sr/Ca-temperature relationship in coralline aragonite: Influence of variability in (Sr/Ca) seawater and skeletal growth parameters: *Geochimica et Cosmochimica Acta*, v. 58, p. 197-208.

Djogic, R., Sipos, L., and Branica, M., (1986), Characterization of uranium (VI) in seawater: *Limnology Oceanography*, v. 31, p. 1122-1131.

Dodd, J.R., (1967), Magnesium and strontium in calcareous skeletons: a review: *Journal of Paleontology*, v. 41, p. 1313-1329.

Dodge, R.E., and Gilbert, T.R., (1984), Chronology of lead pollution contained in banded coral skeletons: *Marine Biology*, v. 82, p. 9-13.

Dodge, R.E., Jickells, T.D., Knap, A.H., Boyd, S., and Bak, R.P.M., (1984), Reef-building coral skeletons as chemical pollution (Phosphorus) indicators: *Marine Pollution Bulletin*, v. 15, p. 178-187.

Dodge, R.E., and Vaisnys, J.R., (1975), Hermatypic coral growth banding as an environmental recorder: *Nature*, v. 258, p. 706-708.

Done, T.J., and Turak, E., (1994), Independent review of fringing coral reef effects. Report prepared for Misima Mines Pty Ltd, Environmental Monitoring Program: Townsville, Australian Institute of Marine Science, p. 48.

Druffel, E.R.M., and Benavides, L.M., (1986), Input of excess CO_2 to the surface ocean based on $^{13}C/^{12}C$ ratios in a banded Jamaican sclerosponge: *Nature*, v. 321, p. 58-61.

Dunstan, P., and Sacco, W.K., (1982), The sclerosponges of Chalet Caribe Reef: *Discovery*, v. 16, p. 13-17.

Edmond, J.M., Spivack, A., Grant, B.C., M-Hui, H., Zexiam, C., Sung, C., and Xiuxhau, Z., (1985), Chemical dynamics of the Changjiang estuary: *Continental Shelf Research*, v. 4, p. 17-36.

Eggins, S.M., Kinsley, L.P.J., and Shelly, J.M.G., (1998), Deposition and element fractionation processes during atmospheric pressure laser sampling for analysis by ICP-MS: *Applied Surface Science*, v. 127-129, p. 278-286.

Fallon, S.J., (1996), Uranium/Calcium Variations in Fijian and Hawaiian *Porites* spp. Corals [Masters thesis]: San Diego, University of San Diego.

Fallon, S.J., McCulloch, M.T., and Sinclair, D.J. (1997) Coral Growth: Trace elements reveal intra-annual variations in growth rate from a *Porites* Coral, Shirigai Bay, Japan. *Australian Coral Reef Society Conference*, 91-98.

Fallon, S.J., McCulloch, M.T., Marshall, J., and Alibert, C. (1999a) High resolution environmental records from the Great Barrier Reef (GBR): a trace element study of *Porites* corals and coralline sponges. *American Geophysical Union Fall Meeting, Abstracts with Programs*.

Fallon, S.J., McCulloch, M.T., van Woesik, R., and Sinclair, D.J., (1999b), Corals at their latitudinal limits: Laser ablation trace element systematics in *Porites* from Shirigai Bay, Japan: *Earth and Planetary Science Letters*, v. 172, p. 221-238.

Flor, T.H., and Moore, W.S., (1977), Radium/Calcium and Uranium/Calcium determinations for Western Atlantic reef corals: *3rd International Coral Reef Symposium, Miami*, v. 2, p. 555-561.

Folk, R.L., (1974), The natural history of crystalline calcium carbonate: effect of magnesium content and salinity: *Journal of Sedimentary Petrology*, v. 44, p. 40-53.

Freidli, H., Lotscher, H., Oeschger, H., Siegenthaler, U., and Stauffer, B., (1986), Ice core record of the $^{13}C/^{12}C$ ratio of atmospheric CO_2 in the past two centuries: *Nature*, v. 324, p. 237-238.

Furst, M., Lowenstam, H.A., and Burnett, D.S., (1976), Radiographic study of the distribution of boron in recent mollusc shells: *Geochimica et Cosmochimica Acta*, v. 40, p. 1381-1386.

Gagan, M.K., Ayliffe, L.K., Beck, J.W., Cole, J.E., Druffel, E.R.M., Dunbar, R.B., and Schrag, D.P., (2000), New views of tropical paleoclimates from coral: *Quaternary Science Reviews*, v. 19, p. 45-65.

Gagan, M.K., Ayliffe, L.K., Hopley, D., Cali, J.A., Mortimer, G.E., Chappell, J., McCulloch, M.T., and Head, M.J., (1998), Temperature and surface-ocean water balance of the mid-Holocene tropical Western Pacific: *Science*, v. 279, p. 1014-1017.

Gagan, M.K., Chivas, A.R., and Isdale, P.J., (1994), High-resolution isotopic records from corals using ocean temperature and mass-spawning chronometers: *Earth and Planetary Science Letters*, v. 121, p. 549-558.

Gaillardet, J., and Allegre, C.J., (1995), Boron isotopic compositions of corals: Seawater or diagenesis record?: *Earth and Planetary Science Letters*, v. 136, p. 665-676.

Given, R.K., and Wilkinson, B.H., (1985), Kinetic control of morphology, composition and mineralogy of abiotic sedimentary carbonates: *Journal of Sedimentary Petrology*, v. 55, p. 109-119.

Goreau, T.J., (1977), Coral skeletal chemistry: physiological and environmental regulation of stable isotopes and trace metals in *Montastrea annularis*: *Procedures Royal Society London, Series B*, v. Vol. 196, p. 291-315.

Greegor, R.B., Pingitore, N.E., and Lytle, F.W., (1997), Strontianite in coral skeletal aragonite: *Science*, v. 275, p. 1452-1454.

Gunther, D., Frischknecht, R., Heinrich, C.A., and Kahlert, H.-J., (1997), Capabilities of an argon fluoride 193 nm excimer laser for laser ablation inductively coupled plasma mass spectrometry microanalysis of geological materials: *Journal of Analytical Atomic Spectrometry*, v. 12, p. 939-944.

Guzman, H.M., and Jarvis, K.E., (1996), Vanadium century record from Caribbean reef corals: a tracer of oil pollution in Panama: *Ambio*, v. 25, p. 523-526.

Guzman, H.M., and Jimenez, C.E., (1992), Contamination of coral reefs by heavy metals along the Caribbean coast of Central America: *Marine Pollution Bulletin*, v. 24, p. 554-561.

Gvirtzman, G., Friedman, G.M., and Miller, D.S., (1973), Control and distribution of uranium in coral reefs during diagenesis: *Journal of Sedimentary Petrology*, v. 42, p. 985-997.

Hanna, R.G., and Muir, G.L., (1990), Red Sea corals as biomonitors of trace metal pollution: *Environmental Monitoring and Assessment*, v. 14, p. 211-222.

Hanor, J.S., (1969), Barite in seawater: *Geochimica et Cosmochimica Acta*, v. 33, p. 894-898.

Hanor, J.S., and Chan, L., (1977), Non-conservative behavior of barium during mixing on Mississippi river and Gulf of Mexico waters: *Earth and Planetary Science Letters*, v. 37, p. 242-250.

Harland, A.D., and Brown, B.E., (1989), Metal tolerance in the scleractinian coral *Porites lutea*: *Marine Pollution Bulletin*, v. 20, p. 353-357.

Harriss, R.C., and Almy, C.C., (1964), A preliminary investigation into the incorporation and distribution of minor elements in the skeletal material of scleractinian corals: *Bulletin of Marine Science Gulf of Caribbean*, v. 19, p. 418-423.

Hart, S.R., and Cohen, A.L., (1996), An ion probe study of annual cycles of Sr/Ca and other trace elements in corals: *Geochimica et Cosmochimica Acta*, v. 60, p. 3075-3084.

Hart, S.R., Cohen, A.L., and Ramsay, P. (1997) Microscale analysis of Sr/Ca and Ba/Ca in *Porites*. *8th International Coral Reef Symposium*, 1707-1712.

Hartman, W.D., (1980), Ecology of recent sclerosponges, *in Living and Fossil Sponges - Notes for a short course (Sedimenta VIII)*, (ed. Hartman, W.D., Wendt, J.B., and Wiedenmayer, F.), , p. 253-255.

Hemming, N.G., Guilderson, T.P., and Fairbanks, R.G., (1998), Seasonal variations in the boron isotopic composition of coral: a productivity signal?: *Global Biogeochemical Cycles*, v. 12, p. 581-586.

Hemming, N.G., and Hanson, G.N., (1992), Boron isotopic composition and concentration in modern marine carbonates: *Geochimica et Cosmochimica Acta*, v. 56, p. 537-543.

Hemming, N.G., Reeder, R.J., and Hanson, G.N., (1995), Mineral-fluid partitioning and isotopic fractionation of boron in synthetic calcium carbonate: *Geochimica et Cosmochimica Acta*, v. 59, p. 371-379.

Hershey, J.P., Fernandez, M., Milne, P.J., and Millero, F.J., (1986), The ionization of boric acid in NaCl, Na-Ca-Cl and Na-Mg-Cl solutions at 25^{o}C: *Geochimica et Cosmochimica Acta*, v. 50, p. 143-148.

Highsmith, R.C., (1979), Coral growth rates and environmental control of density banding: *Journal of Experimental Marine Biology and Ecology*, v. 37, p. 105-125.

Holland, H.D., (1978), *The Chemistry of the Atmosphere and Oceans*: New York, John Wiley & Sons, 351 p.

Horn, I., Hinton, R.W., Jackson, S.E., and Longerich, H.P., (1997), Ultra-trace element analysis of NIST SRM 616 and 614 using laser ablation microprobe-inductively coupled plasma-mass spectrometry (LAM-ICP-MS): a comparison with secondary ion mass spectrometry (SIMS): *Geostandards Newsletter*, v. 21, p. 191-203.

Houck, J.E., Buddemeier, R.W., Smith, S.V., and Jokiel, P.L., (1977), The response of coral growth rate and skeletal strontium content to light intensity and water temperature: *3rd International Coral Reef Symposium*, v. 2, p. 425-431.

Howard, L.S., and Brown, B.E., (1984), Heavy metals and reef corals: *Oceanography and Marine Biology: Annual Review*, v. 22, p. 195-210.

Howard, L.S., and Brown, B.E., (1986), Metals in tissues and skeleton of *Fungia fungites* from Phuket Thailand: *Bulletin of Marine Science*, v. 17, p. 569-570.

Howard, L.S., and Brown, B.E., (1987), Metals in *Pocillopora damicornis* exposed to tin smelter effluent: *Marine Pollution Bulletin*, v. 18, p. 451-454.

Ichikuni, M., and Kikuchi, K., (1972), Retention of boron by travertines: *Chemical Geology*, v. 9, p. 13-21.

Isdale, P., (1984), Fluorescent bands in massive corals record centuries of coastal rainfall: *Nature*, v. 310, p. 578-579.

Isdale, P.J., and Daniel, E., (1989), The design and deployment of a new lightweight submarine fixed drilling system for the acquisition and preparation of coral cores: *Marine Technology Society Journal*, v. 23, p. 3-8.

Isdale, P.J., Stewart, B.J., Tickle, K.S., and Lough, J.M., (1998), Palaeohydrological variation in a tropical river catchment: a reconstruction using fluorescent bands in coral of the Great Barrier Reef, Australia: *The Holocene*, v. 8, p. 1-8.

Jacques, T.G., Pilson, M.E.Q., Cummings, C., and Marshall, N. (1977) Laboratory observations on respiration, photosynthesis, and factors affecting calcification in the temperate coral *Astrangia danae*. *Third International Coral Reef Symposium*, 455-461.

Jarvis, K.E., and Williams, J.G., (1993), Laser ablation inductively coupled plasma mass spectrometry (LA-ICP-MS): a rapid technique for the direct, quantitative determination of major, trace and rare-earth elements in geological samples: *Chemical Geology*, v. 106, p. 251-262.

Kakihana, H., Kotaka, M., Satoh, S., Nomura, M., and Okamoto, M., (1977), Fundamental studies on the ion exchange separation of boron isotopes: *Bulletin of Chemistry Society Japan*, v. 50, p. 158-163.

Kaplan, A., Cane, M., Kushnir, Y., Clement, A.C., Blumenthal, M.B., and Rajagopalan, B., (1998), Analyses of global sea surface temperature 1856-1991: *Journal of Geophysical Research*, v. 103, p. 18567-18589.

Katz, A., (1973), The interaction of magnesium with calcite during crystal growth at 25-90^{o}C and one atmosphere: *Geochimica et Cosmochimica Acta*, v. 37, p. 1563-1586.

Kinsman, D.J.J., (1969), Interpretation of Sr^{+2} concentrations in carbonate minerals and rocks: *Journal of Sedimentary Petrology*, v. 39, p. 486-508.

Kinsman, D.J.J., (1970), Trace cations in aragonite: *Geological Society of America Abstracts*, v. 2, p. 596-597.

Kinsman, D.J.J., and Holland, H.D., (1969), The co-precipitation of cations with $CaCO_3$-IV. The co-precipitation of Sr^{2+} with aragonite between 16 and 96 ^{o}C: *Geochimica et Cosmochimica Acta*, v. 33, p. 1-17.

Kitano, Y., Okumura, M., and Idogaki, M., (1978), Coprecipitation of borate-boron with calcium carbonate: *Geochemical Journal*, v. 12, p. 183-189.

Kitano, Y., and Oomori, T., (1971), The coprecipitation of uranium with calcium carbonate: *Journal of the Oceanographic Society of Japan*, v. 27, p. 34-42.

Klinkhammer, G.P., and Bender, M.L., (1980), The distribution of manganese in the Pacific Ocean: *Earth and Planetary Science Letters*, v. 46, p. 361-384.

Knox, S., Turner, D.R., Dickson, A.G., Liddicoat, M.I., Whitfield, M., and Butler, E.I., (1981), Statistical analysis of estuarine profiles: application to manganese and ammonium in the Tamar estuary: *Estuarine and Coastal Shelf Science*, v. 13, p. 357-71.

Knutson, D.W., Buddemeier, R.W., and Smith, S.V., (1972), Coral chronometers: seasonal growth bands in reef corals: *Science*, v. 177, p. 270-272.

Kolesar, P.T., (1978), Magnesium in calcite from a coralline alga: *Journal of Sedimentary Petrology*, v. 48, p. 815-820.

Ku, T., Knauss, K.G., and Mathieu, G.G., (1977), Uranium in open ocean: concentration and isotopic composition: *Deep-Sea Research*, v. 24, p. 1005-1017.

Kuhl, M., Cohen, Y., Dalsgaard, T., Jorgensen, B.B., and Reusbech, N.P., (1995), Microenvironments and photosynthesis of zooxanthellae in scleractinian corals studied with microsensors of O_2, pH and light: *Marine Ecology Progress Series*, v. 117, p. 159-172.

Lahann, R.W., (1978), A chemical model for calcite crystal growth and morphology control: *Journal of Sedimentary Petrology*, v. 48, p. 337-344.

Langmuir, D., (1978), Uranium solution-mineral equilibria at low temperatures with applications to sedimentary ore deposits: *Geochimica et Cosmochimica Acta*, v. 42, p. 547-569.

Lea, D.W., and Martin, P.A., (1996), A rapid mass spectrometric method for the simultaneous analysis of barium, cadmium, and strontium in foraminifera shells: *Geochimica et Cosmochimica Acta*, v. 60, p. 3143-3149.

Lea, D.W., Shen, G.T., and Boyle, E.A., (1989), Coralline barium records temporal variability in equatorial Pacific upwelling: *Nature*, v. Vol. 340, p. 373-376.

LeCornec, F., and Correge, T., (1997), Determination of uranium to calcium and strontium to calcium ratios in corals by inductively coupled plasma mass spectrometry: *Journal of Analytical Atomic Spectrometry*, v. 12, p. 969-973.

Lewis, R.W., and Wilson, G.I., (1990), Misima gold deposit, *in Geology of the Mineral Deposits of Australia and Papua New Guinea*, Volume 2: Melbourne, (ed. Hughes, F.E.), The Australasian Institute of Mining and Metallurgy, p. 1741-1745.

Linn, L.J., Delaney, M.L., and Druffel, E.R.M., (1990), Trace metals in contemporary and seventeenth-century Galapagos coral: records of seasonal and annual variation: *Geochimica et Cosmochimica Acta*, v. 54, p. 387-394.

Lister, J.J., (1900), *Astrosclera willeyana*, the type of a new family of sponges: *Zoological Results*, v. 4, p. 461-482.

Livingston, H.G., and Thompson, G., (1971), Trace element concentrations in some modern corals: *Limnology Oceanography*, v. 16, p. 786-796.

Lorens, R.B., and Bender, M.L., (1980), The impact of solution chemistry on *Mytilus edulis* calcite and aragonite: *Geochimica et Cosmochimica Acta*, v. 44, p. 1265-1278.

Lough, J.M., (1991), Rainfall variations in Queensland, Australia: 1891-1986: *International Journal of Climatology*, v. 11, p. 745-768.

Lough, J.M., Barnes, D.J., Devereux, M.J., Tobin, B.J., and Tobin, S., (1999), Variability in growth characteristics of massive Porites on the Great Barrier Reef: Townsville, CRC Reef Research Centre, p. 95.

Lukas, R., and Lindstrom, E., (1991), The mixed layer of the Western Equatorial Pacific Ocean: *Journal of Geophysical Research*, v. 96, p. 3343-3357.

Macintyre, I.G., and Smith, S.V. (1974) X-Radiographic studies of skeletal development in coral colonies. *Second International Coral Reef Symp.*, 277-287.

Magini, A., Sonntag, C., Bertsch, G., and Muller, E., (1979), Evidence for a higher natural uranium content in world rivers: *Nature*, v. 278, p. 337-339.

Marshall, J.F., (in prep), [PhD thesis]: Canberra, The Australian National University.

Martin, J.H., (1970), *Limnology Oceanography*, v. 15, p. 756-761.

McAllister, F., King, B., and Done, T., (1999), Burdekin River Plume Modeling: Townsville, Qld., CRC Reef Report.

McConchie, D., and Harriott, V.J. (1992) The partitioning of metals between tissue and skeletal parts of corals: application in pollution monitoring. *Seventh International Coral Reef Symposium*, 97-103.

McConnaughey, T., (1989), ^{13}C and ^{18}O isotopic disequilibrium in biological carbonates: I. Patterns: *Geochimica et Cosmochimica Acta*, v. 53, p. 151-162.

McCulloch, M.T., Gagan, M.K., Mortimer, G.E., Chivas, A.R., and Isdale, P.J., (1994), A high-resolution Sr/Ca and $\delta^{18}O$ coral record from the Great Barrier Reef, Australia, and the 1982-1983 El Niño: *Geochimica et Cosmochimica Acta*, v. 58 No. 12, p. 2747-2754.

Meece, D.E., and Benninger, L.K., (1993), The coprecipitation of Pu and other radionuclides with $CaCO_3$: *Geochimica et Cosmochimica Acta*, v. 57, p. 1447-1458.

Min, G.R., Edwards, R.L., Taylor, F.W., Recy, J., Gallup, C.D., and Beck, J.W., (1995), Annual cycles of U/Ca in coral skeletons and U/Ca thermometry: *Geochimica et Cosmochimica Acta*, v. 59, p. 2025-2043.

Mitsuguchi, T., Matsumoto, E., Abe, O., Uchida, T., and Isdale, P.J., (1996), Mg/Ca thermometry in coral skeletons: *Science*, v. 274, p. 961-963.

Mitterer, R.A., (1978), Amino acid composition and metal binding capability of the skeletal protein of corals: *Bulletin of Marine Science*, v. 28, p. 173-180.

Monnin, C., Jeandel, C., Cattaldo, T., and Dehairs, F., (1999), The marine barite saturation state of the world's oceans: *Marine Chemistry*, v. 65, p. 253-261.

Morrison, C.A., Lambert, D.D., Morrison, R.J.S., Ahlers, W.W., and Nicholls, I.A., (1995), Laser ablation-inductively coupled plasma-mass spectrometry: an investigation of elemental responses and matrix effects in the analysis of geostandard materials: *Chemical Geology*, v. 119, p. 13-29.

Mucci, A., Canuel, R., and Zhong, S., (1989), The solubility of calcite and aragonite in sulfate-free seawater and the seeded growth kinetics and composition of the precipitates at 25^{o}C: *Chemical Geology*, v. 74, p. 309-320.

Naqvi, S.A.S., Nath, B.N., and Balaram, V., (1996), Signatures of rare-earth elements in banded corals of Kalpeni atoll - Lakshadweep archipelago in response to monsoonal variations: *Indian Journal of Marine Science*, v. 25, p. 1-4.

Nesbitt, R.W., Hirata, T., Butler, I.B., and Milton, J.A., (1997), UV laser ablation ICP-MS: some applications in the earth sciences: *Geostandards Newsletter*, v. 20, p. 231-243.

Nozaki, Y., Rye, D.M., Turekian, K.K., and Dodge, R.E., (1978), A 200 year record of carbon-13 and carbon-14 variations in a Bermuda coral: *Geophysical Research Letters*, v. 5, p. 825-828.

NSR, (1987), Misima project environmental plan, Placer (PNG) Pty Ltd., p. 159.

Oomori, T., Kaneshima, H., and Maezato, Y., (1987), Distribution coefficient of Mg^{2+} ions between calcite and solution at 10-50^{o}C: *Marine Chemistry*, v. 20, p. 327-336.

Oomori, T., Kaneshima, K., Nakamura, Y., and Kitano, Y., (1982), Seasonal variations of minor elements in coral skeletons: *Galaxea*, v. 1, p. 77-86.

Paillard, D., Labeyrie, L., and Yiou, P., (1996), Macintosh program performs time-series analysis, *Eos Trans. AGU*, Volume 77, p. 379.

Palmer, M.R., and Edmond, J.M., (1993), Uranium in river water: *Geochimica et Cosmochimica Acta*, v. 57, p. 4947-4955.

Pearce, N.J.G., Perkins, W.T., and Fuge, R., (1992), Developments in the quantitative and semiquantitative determination of trace elements in carbonates by laser ablation inductively coupled plasma mass spectrometry: *Journal of Analytical Atomic Spectrometry*, v. 7, p. 595-598.

Perkins, W.T., Fuge, R., and Pearce, N.J.G., (1991), Quantitative analysis of trace elements in carbonates using laser ablation inductively coupled plasma mass spectrometry: *Journal of Analytical Atomic Spectrometry*, v. 6, p. 445-449.

Perkins, W.T., Pearce, N.J.G., and Westgate, J.A., (1997), The development of laser ablation ICP-MS and calibration strategies: Examples from the analysis of trace elements in volcanic glass shards and sulfide minerals: *Geostandards Newsletter*, v. 21, p. 175-190.

Pingitore, N.E., Rangel, Y., and Kwarteng, A., (1989), Barium variation in *Acropora palmata* and *Monastrea annularis*: *Coral Reefs*, v. 8, p. 31-36.

Rasmussen, C.E. (1988) The use of strontium as an indicator of anthropogenically altered environmental parameters. *6th International Coral Reef Symposium*, 325-330.

Reitner, J. (1989) Lower and Mid-Cretaceous coralline sponge communities of the Boreal and Tethyan realms in comparison with the modern ones. *3rd International Cretaceous Symposium*, 851-878.

Reitner, J., Wörheide, G., Theil, V., and Gautret, P., (1996), Reef caves and cryptic habitats of Indo-Pacific reefs - Distribution patterns of coralline sponges and microbialites, *in Global and Regional Controls on Biogenic Sedimentation. I. Reef Evolution. Research Reports*, Volume Sb2, (ed. Reitner, J., Neuweiler, F., and Gunkel, F.), Gottinger Arb. Geol. Palaont., p. 91-100.

Riley, J.P., and Chester, R., (1971), *Introduction to Marine Chemistry*: London, Academic Press, 465 p.

Sanal, A., Nugent, M., Reeder, R.J., and Bijma, J., (2000), Seawater pH control on the boron isotopic composition of calcite: Evidence from inorganic calcite precipitation experiments: *Geochimica et Cosmochimica Acta*, v. 64, p. 1551-1555.

Santrock, J., Studley, S.A., and Hayes, J.M., (1985), Isotopic Analyses Based on the Mass Spectrum of Carbon Dioxide: *Analytical Chemistry*, v. 57, p. 1444-1448.

Scherer, M., and Seitz, H., (1980), Rare-earth element distribution in Holocene and Pleistocene corals and their distribution during diagenesis: *Chemical Geology*, v. 28, p. 279-289.

Schifano, G., (1982), Temperature-magnesium relationships in the shell carbonate of some modern marine gastropods: Chemical Geology, v. 35, p. 321-332.

Schneider, R.C., and Smith, S.V., (1982), Skeletal Sr Content and Density in *Porites* spp. in Relation to Environmental Factors: *Marine Biology*, v. 66, p. 121-131.

Schofield, A., and Haskin, L., (1964), Rare-earth distribution patterns in eight terrestrial materials: *Geochimica et Cosmochimica Acta*, v. 28, p. 437-446.

Schrag, D.P., (1999), Rapid analysis of high-precision Sr/Ca ratios in corals and other marine carbonates: *Paleoceanography*, v. 14, p. 97-102.

Schroeder, J.H., Miller, D.S., and Friedman, G.M., (1970), Uranium distributions in recent skeletal carbonates: *Journal of Sedimentary Petrology*, v. 40, p. 672-681.

Schwarcz, H.P., Agyei, E.K., and McCullen, C.C., (1969), Boron isotopic fractionation during clay adsorption from seawater: *Earth and Planetary Science Letters*, v. 6, p. 1-5.

Scott, P.J.B., (1990), Chronic pollution recorded in coral skeletons in Hong Kong: *Journal of Experimental Biology and Ecology*, v. 139, p. 51-64.

Sen, S., Stebbins, J.F., Hemming, N.G., and Ghosh, B., (1994), Coordination environments of B impurities in calcite and aragonite polymorphs: A ^{11}B MAS NMR study: *American Mineralogist*, v. 79, p. 819-825.

Shen, C.-C., Lee, T., Chen, C.-Y., Wang, C.-H., Dai, C.-F., and Li, L.-A., (1996), The calibration of D[Sr/Ca] versus sea surface temperature relationship for *Porites* corals: *Geochimica et Cosmochimica Acta*, v. 60, p. 3849-3858.

Shen, G.T., and Boyle, E.A., (1987), Lead in corals: reconstruction of historical industrial fluxes to the surface ocean: *Earth and Planetary Science Letters*, v. 82, p. 289-304.

Shen, G.T., and Boyle, E.A., (1988), Determination of lead, cadmium, and other trace metals in annually-banded corals: *Chemical Geology*, v. 67, p. 47-62.

Shen, G.T., Boyle, E.A., and Lea, D.W., (1987), Cadmium in corals as a tracer of historical upwelling and industrial fallout: *Nature*, v. 328, p. 794-796.

Shen, G.T., Campbell, T.M., Dunbar, R.B., Wellington, G.M., Colgan, M.W., and Glynn, P.W., (1991), Paleochemistry of manganese in corals from the Galapagos Islands: *Coral Reefs*, v. 10, p. 91-100.

Shen, G.T., Cole, J.E., Lea, D.W., Linn, L.J., McConnaughey, T.A., and Fairbanks, R.G., (1992a), Surface ocean variability at Galapagos from 1936-1982: calibration of geochemical tracers in corals: *Paleoceanography*, v. 7, p. 563-588.

Shen, G.T., Linn, L.J., Cambell, T.M., Cole, J.E., and Fairbanks, R.G., (1992b), A chemical indicator of trade wind reversal in corals from the Western Tropical Pacific: *Journal of Geophysical Research*, v. 97, p. 12,689-12,697.

Shen, G.T., and Dunbar, R.B., (1995), Environmental controls on Uranium in reef corals: *Geochimica et Cosmochimica Acta*, v. 59, p. 2009-2024.

Shen, G.T., and Sanford, C.L., (1990), Trace element indicators of climate change in annually-banded corals, *in Global Consequences of the 1982-83 El Nino-Southern Oscillation*, (ed. Glynn, P.W.), Elsevier.

Sholkovitz, E., and Shen, G.T., (1995), The incorporation of rare earth elements in modern corals: *Geochimica et Cosmochimica Acta*, v. 59, p. 2749-2756.

Sholkovitz, E.R., (1993), The geochemistry of rare earth elements in the Amazon River estuary: *Geochimica et Cosmochimica Acta*, v. 57, p. 2181-2190.

Sholkovitz, E.R., (1995), The aquatic chemistry of rare earth elements in rivers and estuaries: *Aquatic Geochemistry*, v. 1, p. 1-34.

Sholkovitz, E.R., Elderfield, H., Szymczak, R., and Casey, K., (1999), Island weathering: river sources of rare earth elements to the Western Pacific Ocean: *Marine Chemistry*, v. 68, p. 39-57.

Sinclair, D., Kinsley, L., and McCulloch, M., (1998), High resolution analysis of trace elements in corals by laser ablation ICP-MS: *Geochimica et Cosmochimica Acta*, v. 62, p. 1889-1901.

Sinclair, D.J., (1999), High-Spatial Resolution Analysis of Trace Elements in Corals Using Laser Ablation ICP-MS [PhD thesis]: Canberra, The Australian National University.

Slutz, R.J., Lubker, S.J., Hiscox, J.D., Woodruff, S.D., Jenne, R.L., Joseph, D.H., Steuer, P.M., and Elms, J.D., (1985), Comprehensive Ocean-Atmosphere Data Set: Boulder, NOAA Environmental Research Laboratory.

Smith, S.V., Buddemeier, R.W., Redalje, R.C., and Houck, J.E., (1979), Strontium-Calcium thermometry in coral skeletons: *Science*, v. 204, p. 404-406.

Spalding, R.F., and Sackett, W.M., (1972), Uranium in runoff from the Gulf of Mexico distributive province: anomalous concentrations: *Science*, v. 175, p. 629-631.

Speer, J.A., (1983), Crystal chemistry and phase relations of orthorhombic carbonates, *in Carbonates: Mineralogy and Chemistry*, (ed. Reeder, R.J.), Mineralogical Society of America, p. 145-190.

Spivack, A.J., Palmer, M.R., and Edmond, J.M., (1987), The sedimentary cycle of the boron isotopes: *Geochimica et Cosmochimica Acta*, v. 51, p. 1939-1949.

Spivack, A.J., You, C.F., and Smith, H.J., (1993), Foraminiferal boron isotope ratios as a proxy for surface ocean pH over the past 21 Myr: *Nature*, v. 363, p. 149-151.

Spivak, A.J., and Edmond, J.M., (1987), Boron isotope exchange between seawater and the oceanic crust: *Geochimica et Cosmochimica Acta*, v. 51, p. 1033-1043.

St.John, B.E. (1974) Heavy metals in the skeletal carbonate of scleractinian corals. *Second International Coral Reef Symposium*, 461-469.

Sunda, W.G., and Huntsman, S.A., (1988), Effect of sunlight on redox cycles of manganese in the southwestern Sargasso Sea: *Deep-Sea Research*, v. 35, p. 1297-1317.

Swart, P.K., (1981), The strontium, magnesium and sodium composition of recent scleractinian coral skeletons as standards for palaeoenvironmental analysis: *Palaeogeography, Palaeoclimatology, Palaeoecology*, v. 34, p. 115-136.

Swart, P.K., and Hubbard, J.A.E.B., (1982), Uranium in scleractinian coral skeletons: *Coral Reefs*, v. 1, p. 13-19.

Sylvester, P.J., and Ghaderi, M., (1997), Trace element analysis of scheelite by excimer laser ablation-inductively coupled plasma-mass spectrometry (ELA-ICP-MS) using a synthetic silicate glass standard: *Chemical Geology*, v. 141, p. 49-65.

Taylor, R.B., Barnes, D.J., and Lough, J.M., (1993), Simple models of density band formation in massive corals: *Journal of Experimental Marine Biology and Ecology*, v. 167, p. 109-125.

Taylor, R.B., Barnes, D.J., and Lough, J.M., (1995), On the inclusion of trace materials into massive coral skeletons. 1. Materials occurring in the environment in short pulses: *Journal of Experimental Marine Biology and Ecology*, v. 185, p. 255-278.

Taylor, S.R., and Mclennan, S.M., (1985), *The continental crust: its composition and evolution*, Blackwell Scientific Publications.

Thompson, G., and Livingston, H.D., (1970), Strontium and Uranium concentrations in aragonite precipitated by some modern corals: *Earth and Planetary Science Letters*, v. 8, p. 439-442.

Tudhope, A.W., Lea, D.W., Shimmield, G.B., Chilcott, C.P., and Head, S., (1996), Monsoon climate and Arabian Sea coastal upwelling recorded in massive corals from Southern Oman: *Palaios*, v. 11, p. 347-361.

Tudhope, A.W., Lea, D.W., Shimmield, G.B., Chilcott, C.P., Scoffin, T.P., Fallick, A.E., and Jebb, M. (1997) Climatic records from massive *Porites* corals in Papua New Guinea: A comparison of skeletal Ba/Ca, skeletal $\delta^{18}O$ and coastal rainfall. *8th International Coral Reef Symposium*, 1719-1724.

Van Woesik, R., (1995), Coral communities at high latitude are not pseudopopulations: evidence of spawning at 32ºN, Japan: *Coral Reefs*, v. 14, p. 119-120.

Veeh, H.H., and Turekian, K.K., (1968), Cobalt, Silver, and Uranium concentrations of reef-building corals in the Pacific Ocean: *Limnology Oceanography*, v. 13, p. 304-308.

Veizler, J., (1983), Trace elements and isotopes in sedimentary carbonates, *in Carbonates: Mineralogy and Chemistry*, (ed. Reeder, R.J.), p. 265-299.

Vengosh, A., Kolodny, Y., Starinsky, A., Chivas, A.R., and McCulloch, M.T., (1991), Coprecipitation and isotopic fractionation of boron in modern carbonates: *Geochimica et Cosmochimica Acta*, v. 55, p. 2901-2910.

Veron, J.E.N., (1992), *Hermatyptic Corals of Japan*: Townsville, Queensland, Australian Institute of Marine Science.

Walls, R.A., Ragland, P.C., and Crisp, E.L., (1977), Experimental and natural early diagenetic mobility of Sr and Mg in biogenic carbonates: *Geochimica et Cosmochimica Acta*, v. 41, p. 1731-1737.

Weber, J.N., (1973a), Incorporation of strontium into reef coral skeletal carbonate: *Geochemica et Cosmochimica Acta*, v. 37, p. 2173-2190.

Weber, J.N., (1973b), Temperature dependence of magnesium in echinoid and asteroid skeletal calcite: a reinterpretation of its significance: *Journal of Geology*, v. 81, p. 543-556.

Weber, J.N., (1974), Skeletal chemistry of scleractinian reef corals: uptake of magnesium from seawater: *American Journal of Science*, v. 274, p. 84-93.

Weber, J.N., and Woodhead, P.M., (1972), Temperature dependence of oxygen 18 concentration in reef coral carbonates: *Journal of Geophysical Research*, v. 77, p. 463-473.

Wei, G., Sun, M., Li, X., and Nie, B., (2000), Mg/Ca, Sr/Ca and U/ca ratios of a *Porites* coral from Sanya Bay, Hainan Island, South China Sea and their relationships to sea surface temperature: *Palaeogeography, Palaeoclimatology, Palaeoecology*, v. 162, p. 59-74.

Wellington, G.M., and Glynn, P.W., (1983), Environmental influences on skeletal banding in eastern Pacific (Panama) corals.: *Coral Reefs*, v. 1, p. 215-222.

Willenz, P., and Hartman, W.D. (1985) Calcification rate of *Ceratoporella nicholsoni* (Porifera : Sclerospongiae) : An *in situ* study with calcein. *Fifth International Coral Reef Congress*, 113-118.

Willenz, P., and Pomponi, S.A., (1996), A new deep sea coralline sponge from Turks and Caicos Islands : *Willardia caicosensis* gen *et* sp. nov. (Demospongiae : Hadromerida): *Biologie*, v. 66 suppl., p. 205-218.

Wörheide, G., (1998), The reef cave dwelling ultraconservative coralline demosponge *Astrosclera willeyana* Lister 19010 from the Indo-Pacific: *Facies*, v. 38, p. 1-88.

Wörheide, G., Gautret, P., Reitner, J., Böhm, F., Joachimski, M.M., Thiel, V., Michaelis, W., and Massault, M., (1997), Basal skeletal formation, role and preservation of intracrystalline organic matrices, and isotope record in the coralline sponge *Astrosclera willeyana* Lister, 1900: *Bol. R. Soc. Esp. Hist. Nat.*, v. 91, p. 355-374.

Zhang, J., and Nozaki, Y., (1996), Rare earth elements and yttrium in seawater: ICP-MS determinations in the East Caroline, Coral Sea, and South Fiji basins of the western South Pacific: *Geochimica et Cosmochimica Acta*, v. 60, p. 4631-4644.

Appendix 1: LA-ICP-MS Data Tables

Table A.1 Daily/Montly Reproducibility of Astrosclera willeyana Pressed Pellet

Sample	Date	B/Ca	1 σ B/Ca	Mg/Ca	1 σ Mg/Ca	Sr/Ca	1 σ Sr/Ca	Ba/Ca	1 σ Ba/Ca	U/Ca	1 σ U/Ca
Astrosclera	26-May-99	2.22E-04	6.66E-06	1.23E-03	4.66E-05	1.060E-02	1.696E-04	4.12E-06	1.40E-07	2.64E-06	8.18E-08
	26-May-99	2.19E-04	6.56E-06	1.18E-03	4.50E-05	1.058E-02	1.692E-04	3.80E-06	1.29E-07	2.66E-06	8.25E-08
	26-May-99	2.24E-04	6.72E-06	1.18E-03	4.48E-05	1.057E-02	1.691E-04	3.76E-06	1.28E-07	2.77E-06	8.59E-08
	26-May-99	2.15E-04	6.45E-06	1.27E-03	4.82E-05	1.065E-02	1.704E-04	4.18E-06	1.42E-07	2.65E-06	8.22E-08
	26-May-99	2.23E-04	6.68E-06	1.21E-03	4.60E-05	1.053E-02	1.685E-04	3.91E-06	1.33E-07	2.70E-06	8.37E-08
Astrosclera	28-May-99	2.17E-04	8.90E-06	1.25E-03	7.55E-05	1.060E-02	2.551E-04	3.64E-06	2.77E-07	2.63E-06	6.67E-08
	28-May-99	2.13E-04	7.78E-06	1.27E-03	8.30E-05	1.067E-02	2.584E-04	3.73E-06	3.08E-07	2.65E-06	1.20E-07
	28-May-99	2.15E-04	8.85E-06	1.27E-03	1.26E-04	1.060E-02	2.821E-04	3.61E-06	2.67E-07	2.63E-06	7.88E-08
	28-May-99	2.14E-04	8.30E-06	1.26E-03	5.68E-05	1.068E-02	2.227E-04	3.78E-06	3.26E-07	2.64E-06	7.28E-08
	28-May-99	2.10E-04	7.93E-06	1.32E-03	1.38E-04	1.060E-02	2.773E-04	3.66E-06	2.57E-07	2.64E-06	8.95E-08
	28-May-99	2.13E-04	6.37E-06	1.30E-03	1.37E-04	1.068E-02	2.263E-04	3.71E-06	1.83E-07	2.66E-06	1.01E-07
	28-May-99	2.15E-04	8.22E-06	1.24E-03	4.72E-05	1.071E-02	2.856E-04	3.81E-06	3.12E-07	2.65E-06	8.64E-08
	28-May-99	2.21E-04	1.51E-05	1.26E-03	8.56E-05	1.069E-02	2.364E-04	3.67E-06	3.10E-07	2.67E-06	8.40E-08
Astrosclera	28-May-99	2.21E-04	6.49E-06	1.24E-03	2.32E-04	1.055E-02	2.090E-04	3.78E-06	1.55E-07	2.76E-06	8.30E-08
	28-May-99	2.21E-04	7.87E-06	1.19E-03	9.77E-05	1.054E-02	2.016E-04	3.86E-06	2.26E-07	2.76E-06	9.87E-08
	28-May-99	2.20E-04	8.68E-06	1.19E-03	9.82E-05	1.054E-02	2.042E-04	3.89E-06	1.77E-07	2.76E-06	1.14E-07
	28-May-99	2.24E-04	8.41E-06	1.16E-03	6.23E-05	1.063E-02	2.127E-04	3.85E-06	1.60E-07	2.79E-06	1.01E-07
	28-May-99	2.29E-04	6.41E-06	1.23E-03	1.58E-04	1.065E-02	2.162E-04	3.90E-06	2.20E-07	2.79E-06	1.00E-07
	28-May-99	2.27E-04	7.74E-06	1.15E-03	1.01E-04	1.053E-02	2.418E-04	3.88E-06	1.53E-07	2.76E-06	7.77E-08
	28-May-99	2.24E-04	6.35E-06	1.11E-03	3.19E-05	1.059E-02	1.904E-04	3.81E-06	1.41E-07	2.78E-06	9.66E-08
Astrosclera	29-May-99	2.28E-04	9.73E-06	1.26E-03	1.02E-04	1.058E-02	2.431E-04	3.94E-06	3.05E-07	2.64E-06	1.01E-07
	29-May-99	2.24E-04	8.47E-06	1.28E-03	7.77E-05	1.059E-02	2.493E-04	3.81E-06	2.82E-07	2.59E-06	9.31E-08
	29-May-99	2.26E-04	6.59E-06	1.29E-03	5.59E-05	1.062E-02	2.372E-04	3.81E-06	3.17E-07	2.61E-06	7.59E-08
	29-May-99	2.23E-04	7.35E-06	1.27E-03	7.93E-05	1.065E-02	2.158E-04	3.89E-06	3.55E-07	2.61E-06	1.18E-07
	29-May-99	2.27E-04	8.01E-06	1.26E-03	6.65E-05	1.059E-02	2.344E-04	3.84E-06	3.06E-07	2.64E-06	9.50E-08

Sample	Date	B/Ca	1 σ B/Ca	Mg/Ca	1 σ Mg/Ca	Sr/Ca	1 σ Sr/Ca	Ba/Ca	1 σ Ba/Ca	U/Ca	1σ U/Ca
	29-May-99	2.28E-04	2.49E-05	1.25E-03	8.03E-05	1.069E-02	2.069E-04	3.78E-06	3.18E-07	2.63E-06	6.32E-08
	29-May-99	2.26E-04	8.99E-06	1.24E-03	5.14E-05	1.066E-02	2.248E-04	3.77E-06	3.03E-07	2.62E-06	1.07E-07
Astrosclera	29-May-99	2.21E-04	7.88E-06	1.19E-03	5.77E-05	1.053E-02	2.141E-04	3.82E-06	2.46E-07	2.66E-06	8.45E-08
	29-May-99	2.20E-04	8.73E-06	1.19E-03	7.66E-05	1.054E-02	2.308E-04	3.73E-06	2.39E-07	2.67E-06	9.01E-08
	29-May-99	2.21E-04	8.55E-06	1.21E-03	7.61E-05	1.051E-02	2.346E-04	3.71E-06	2.16E-07	2.70E-06	8.71E-08
	29-May-99	2.22E-04	9.36E-06	1.18E-03	7.32E-05	1.052E-02	2.813E-04	3.78E-06	2.77E-07	2.70E-06	9.58E-08
	29-May-99	2.24E-04	6.21E-06	1.21E-03	7.48E-05	1.056E-02	2.254E-04	3.69E-06	1.16E-07	2.73E-06	8.70E-08
	29-May-99	2.24E-04	7.14E-06	1.19E-03	5.90E-05	1.047E-02	2.386E-04	3.75E-06	2.12E-07	2.71E-06	8.02E-08
Astrosclera	25-Jun-99	2.26E-04	9.44E-06	1.20E-03	1.40E-04	1.053E-02	1.606E-04	3.97E-06	3.95E-07	2.71E-06	9.18E-08
	25-Jun-99	2.19E-04	8.26E-06	1.28E-03	1.53E-04	1.066E-02	1.635E-04	3.54E-06	2.46E-07	2.62E-06	9.31E-08
	25-Jun-99	2.17E-04	9.95E-06	1.27E-03	9.79E-05	1.072E-02	1.993E-04	3.65E-06	2.38E-07	2.61E-06	9.59E-08
	25-Jun-99	2.22E-04	1.03E-05	1.25E-03	1.42E-04	1.074E-02	2.038E-04	3.57E-06	2.03E-07	2.70E-06	1.06E-07
	25-Jun-99	2.19E-04	1.16E-05	1.23E-03	4.18E-05	1.068E-02	2.095E-04	3.72E-06	2.65E-07	2.67E-06	9.22E-08
	25-Jun-99	2.27E-04	1.34E-05	1.25E-03	1.56E-04	1.072E-02	1.587E-04	3.79E-06	2.00E-07	2.87E-06	1.13E-07
	25-Jun-99	2.33E-04	1.68E-05	1.24E-03	1.71E-04	1.070E-02	2.131E-04	3.89E-06	1.96E-07	2.90E-06	1.05E-07
Astrosclera	26-Jun-99	2.32E-04	6.50E-06	1.19E-03	4.06E-05	1.078E-02	1.725E-04	3.90E-06	1.25E-07	2.82E-06	8.16E-08
	26-Jun-99	2.26E-04	6.34E-06	1.21E-03	4.10E-05	1.068E-02	1.709E-04	3.78E-06	1.21E-07	2.75E-06	7.98E-08
	26-Jun-99	2.39E-04	6.69E-06	1.28E-03	4.36E-05	1.059E-02	1.695E-04	3.82E-06	1.22E-07	2.80E-06	8.11E-08
	26-Jun-99	2.30E-04	6.43E-06	1.22E-03	4.15E-05	1.064E-02	1.703E-04	3.90E-06	1.25E-07	2.75E-06	7.97E-08
	26-Jun-99	2.39E-04	6.69E-06	1.28E-03	4.36E-05	1.059E-02	1.695E-04	3.82E-06	1.22E-07	2.80E-06	8.11E-08
	26-Jun-99	2.30E-04	6.43E-06	1.22E-03	4.15E-05	1.064E-02	1.703E-04	3.90E-06	1.25E-07	2.75E-06	7.97E-08
Astrosclera	28-Jul-99	2.23E-04	6.24E-06	1.26E-03	4.29E-05	1.082E-02	1.732E-04	3.78E-06	1.21E-07	2.87E-06	8.32E-08
	28-Jul-99	2.19E-04	6.12E-06	1.28E-03	4.36E-05	1.073E-02	1.717E-04	3.80E-06	1.22E-07	2.86E-06	8.28E-08
	28-Jul-99	2.33E-04	6.53E-06	1.21E-03	4.11E-05	1.080E-02	1.728E-04	3.81E-06	1.22E-07	2.78E-06	8.05E-08

Table 10.1 Shirigai Bay *Porites* data

Distance from top (mm)	B/Ca (mol/mol)	Mg/Ca (mol/mol)	Sr/Ca (mol/mol)	Ba/Ca (mol/mol)	U/Ca (mol/mol)
0.000	6.49E-04	4.60E-03	9.04E-03	5.57E-06	1.15E-06
0.166	6.01E-04	3.71E-03	9.37E-03	5.12E-06	1.36E-06
0.333	5.98E-04	3.64E-03	9.44E-03	4.93E-06	1.37E-06
0.499	6.09E-04	3.37E-03	9.38E-03	5.06E-06	1.41E-06
0.666	6.51E-04	3.74E-03	9.51E-03	4.82E-06	1.35E-06
0.832	6.47E-04	3.89E-03	9.54E-03	5.09E-06	1.44E-06
0.999	6.20E-04	3.17E-03	9.69E-03	4.54E-06	1.53E-06
1.165	6.40E-04	3.16E-03	9.61E-03	4.79E-06	1.55E-06
1.332	5.54E-04	3.06E-03	9.61E-03	4.55E-06	1.60E-06
1.498	5.68E-04	2.87E-03	9.76E-03	4.41E-06	1.46E-06
1.665	5.99E-04	3.19E-03	9.78E-03	4.85E-06	1.50E-06
1.831	5.75E-04	2.91E-03	9.70E-03	4.67E-06	1.52E-06
1.998	5.65E-04	3.33E-03	9.65E-03	4.24E-06	1.49E-06
2.164	5.94E-04	3.26E-03	9.47E-03	4.64E-06	1.39E-06
2.331	5.73E-04	3.28E-03	9.60E-03	4.44E-06	1.38E-06
2.497	5.73E-04	3.09E-03	9.45E-03	4.21E-06	1.44E-06
2.664	5.12E-04	2.57E-03	9.63E-03	4.35E-06	1.55E-06
2.830	5.77E-04	3.35E-03	9.47E-03	4.46E-06	1.36E-06
2.997	5.84E-04	3.59E-03	9.37E-03	4.39E-06	1.27E-06
3.163	6.04E-04	3.49E-03	9.58E-03	4.16E-06	1.38E-06
3.330	6.15E-04	3.61E-03	9.65E-03	4.11E-06	1.39E-06
3.496	5.94E-04	3.83E-03	9.54E-03	4.25E-06	1.46E-06
3.663	5.53E-04	4.14E-03	9.52E-03	4.13E-06	1.29E-06
3.829	5.46E-04	4.52E-03	9.39E-03	3.99E-06	1.24E-06
3.996	5.63E-04	4.22E-03	9.36E-03	4.00E-06	1.28E-06
4.162	5.63E-04	4.29E-03	9.05E-03	4.38E-06	1.23E-06
4.328	5.19E-04	3.41E-03	9.08E-03	4.73E-06	1.21E-06
4.495	5.50E-04	3.41E-03	9.30E-03	4.70E-06	1.27E-06
4.661	5.65E-04	3.50E-03	9.24E-03	4.39E-06	1.33E-06
4.828	5.77E-04	3.47E-03	9.33E-03	4.06E-06	1.33E-06
4.994	6.08E-04	3.63E-03	9.20E-03	4.35E-06	1.29E-06
5.161	5.96E-04	3.14E-03	9.41E-03	4.13E-06	1.32E-06
5.327	5.85E-04	3.16E-03	9.62E-03	4.62E-06	1.43E-06
5.494	5.76E-04	3.19E-03	9.57E-03	4.23E-06	1.49E-06
5.660	6.32E-04	3.79E-03	9.60E-03	4.66E-06	1.46E-06
5.827	6.30E-04	4.21E-03	9.61E-03	4.51E-06	1.45E-06
5.993	6.20E-04	3.33E-03	9.81E-03	4.54E-06	1.38E-06
6.160	6.36E-04	4.00E-03	9.62E-03	4.74E-06	1.47E-06
6.326	6.33E-04	3.82E-03	9.70E-03	4.76E-06	1.52E-06
6.493	5.98E-04	3.41E-03	9.83E-03	5.10E-06	1.55E-06
6.659	5.91E-04	3.03E-03	9.66E-03	4.36E-06	1.54E-06
6.826	6.40E-04	3.29E-03	9.54E-03	4.36E-06	1.52E-06
6.992	6.15E-04	3.13E-03	9.56E-03	4.20E-06	1.45E-06
7.159	5.83E-04	3.11E-03	9.51E-03	4.13E-06	1.40E-06
7.325	5.65E-04	3.54E-03	9.14E-03	4.20E-06	1.19E-06
7.492	5.46E-04	3.96E-03	8.82E-03	4.46E-06	1.10E-06
7.658	4.90E-04	3.59E-03	9.25E-03	4.62E-06	1.29E-06
7.825	5.15E-04	4.38E-03	8.95E-03	4.66E-06	1.03E-06
7.991	5.10E-04	4.14E-03	8.99E-03	4.92E-06	1.11E-06
8.158	5.05E-04	3.88E-03	8.97E-03	4.90E-06	1.11E-06
8.324	5.10E-04	3.81E-03	8.93E-03	4.48E-06	1.18E-06
8.490	5.31E-04	3.76E-03	9.27E-03	4.47E-06	1.44E-06

LA-ICP-MS data

Distance from top (mm)	B/Ca (mol/mol)	Mg/Ca (mol/mol)	Sr/Ca (mol/mol)	Ba/Ca (mol/mol)	U/Ca (mol/mol)
8.823	5.62E-04	3.72E-03	9.32E-03	5.03E-06	1.31E-06
8.990	5.56E-04	3.96E-03	9.17E-03	4.61E-06	1.15E-06
9.156	5.76E-04	3.72E-03	9.27E-03	4.73E-06	1.23E-06
9.323	6.03E-04	3.54E-03	9.48E-03	4.85E-06	1.34E-06
9.489	6.17E-04	3.35E-03	9.36E-03	4.50E-06	1.29E-06
9.656	6.24E-04	3.39E-03	9.59E-03	4.92E-06	1.39E-06
9.822	5.81E-04	3.06E-03	9.52E-03	4.30E-06	1.44E-06
9.989	5.94E-04	3.11E-03	9.56E-03	4.36E-06	1.48E-06
10.155	6.18E-04	2.88E-03	9.88E-03	4.85E-06	1.64E-06
10.322	6.40E-04	2.98E-03	9.72E-03	5.38E-06	1.61E-06
10.488	6.28E-04	3.37E-03	9.68E-03	5.04E-06	1.43E-06
10.655	6.51E-04	3.17E-03	9.56E-03	4.92E-06	1.45E-06
10.821	6.44E-04	3.10E-03	9.72E-03	4.78E-06	1.49E-06
10.988	6.48E-04	2.92E-03	9.55E-03	5.38E-06	1.47E-06
11.154	6.77E-04	3.01E-03	9.95E-03	4.82E-06	1.52E-06
11.321	6.67E-04	3.29E-03	9.85E-03	4.91E-06	1.41E-06
11.487	6.59E-04	3.42E-03	9.48E-03	4.79E-06	1.31E-06
11.654	6.35E-04	3.48E-03	9.10E-03	4.58E-06	1.25E-06
11.820	6.02E-04	3.60E-03	9.36E-03	4.65E-06	1.15E-06
11.987	5.80E-04	4.13E-03	9.08E-03	4.58E-06	9.96E-07
12.153	5.72E-04	4.18E-03	8.87E-03	4.59E-06	1.03E-06
12.320	5.96E-04	4.17E-03	8.93E-03	4.42E-06	9.92E-07
12.486	5.54E-04	4.11E-03	9.04E-03	4.35E-06	9.89E-07
12.652	5.50E-04	3.93E-03	8.99E-03	4.79E-06	1.04E-06
12.819	5.65E-04	3.90E-03	9.04E-03	4.59E-06	1.07E-06
12.985	5.64E-04	3.72E-03	8.99E-03	4.49E-06	1.16E-06
13.152	5.48E-04	3.76E-03	9.01E-03	4.48E-06	1.09E-06
13.318	5.64E-04	3.40E-03	8.89E-03	4.31E-06	1.17E-06
13.485	5.89E-04	3.48E-03	9.18E-03	4.61E-06	1.12E-06
13.651	6.11E-04	3.80E-03	8.88E-03	4.43E-06	1.06E-06
13.818	5.78E-04	3.49E-03	9.03E-03	4.07E-06	1.11E-06
13.984	5.94E-04	3.26E-03	9.29E-03	4.55E-06	1.23E-06
14.151	5.87E-04	2.91E-03	9.25E-03	4.35E-06	1.33E-06
14.317	5.81E-04	2.66E-03	9.49E-03	4.76E-06	1.52E-06
14.484	6.26E-04	2.96E-03	9.59E-03	5.22E-06	1.53E-06
14.650	6.51E-04	3.11E-03	9.73E-03	5.05E-06	1.43E-06
14.817	6.57E-04	3.00E-03	9.73E-03	5.07E-06	1.46E-06
14.983	6.20E-04	2.62E-03	9.84E-03	4.92E-06	1.58E-06
15.150	6.15E-04	2.63E-03	9.92E-03	4.33E-06	1.59E-06
15.316	5.87E-04	2.81E-03	9.50E-03	4.50E-06	1.55E-06
15.483	6.84E-04	3.53E-03	9.34E-03	4.66E-06	1.27E-06
15.649	6.32E-04	3.84E-03	9.15E-03	4.75E-06	1.19E-06
15.816	5.86E-04	3.51E-03	8.99E-03	4.70E-06	1.16E-06
15.982	5.79E-04	3.47E-03	9.16E-03	4.52E-06	1.23E-06
16.149	5.96E-04	3.20E-03	9.16E-03	4.28E-06	1.34E-06
16.315	5.94E-04	3.87E-03	9.12E-03	4.49E-06	1.06E-06
16.482	6.13E-04	3.79E-03	9.36E-03	4.89E-06	1.11E-06
16.648	6.34E-04	3.33E-03	9.35E-03	4.45E-06	1.21E-06
16.814	6.11E-04	3.34E-03	9.15E-03	4.12E-06	1.19E-06
16.981	6.57E-04	3.46E-03	8.91E-03	4.30E-06	1.14E-06
17.147	6.22E-04	3.45E-03	9.24E-03	4.15E-06	1.13E-06
17.314	6.21E-04	3.55E-03	9.14E-03	4.39E-06	1.07E-06
17.480	5.51E-04	3.46E-03	9.03E-03	4.33E-06	1.05E-06
17.647	5.37E-04	3.56E-03	8.87E-03	4.44E-06	1.04E-06
17.813	5.29E-04	3.75E-03	8.89E-03	4.04E-06	1.04E-06
17.980	5.57E-04	4.02E-03	8.91E-03	4.70E-06	1.03E-06
18.146	5.55E-04	3.83E-03	8.93E-03	4.57E-06	1.01E-06

Distance from top (mm)	B/Ca (mol/mol)	Mg/Ca (mol/mol)	Sr/Ca (mol/mol)	Ba/Ca (mol/mol)	U/Ca (mol/mol)
18.479	5.50E-04	3.56E-03	8.96E-03	4.54E-06	1.05E-06
18.646	5.81E-04	3.48E-03	9.18E-03	4.99E-06	1.11E-06
18.812	5.79E-04	3.29E-03	9.40E-03	4.61E-06	1.23E-06
18.979	5.92E-04	2.92E-03	9.67E-03	4.62E-06	1.42E-06
19.145	5.95E-04	2.72E-03	9.70E-03	4.65E-06	1.56E-06
19.312	6.08E-04	2.64E-03	9.54E-03	4.70E-06	1.58E-06
19.478	5.86E-04	2.69E-03	9.79E-03	4.79E-06	1.55E-06
19.645	5.94E-04	2.65E-03	9.92E-03	4.95E-06	1.59E-06
19.811	6.10E-04	2.84E-03	9.81E-03	5.09E-06	1.57E-06
19.978	6.10E-04	2.90E-03	9.69E-03	4.88E-06	1.59E-06
20.144	5.92E-04	2.60E-03	9.71E-03	4.63E-06	1.63E-06
20.311	5.60E-04	2.61E-03	9.72E-03	4.70E-06	1.60E-06
20.477	6.18E-04	2.69E-03	9.95E-03	5.32E-06	1.54E-06
20.644	6.48E-04	2.72E-03	9.71E-03	4.61E-06	1.45E-06
20.810	6.75E-04	3.00E-03	9.54E-03	5.38E-06	1.37E-06
20.976	6.36E-04	3.19E-03	9.45E-03	4.71E-06	1.29E-06
21.143	6.30E-04	3.29E-03	9.39E-03	4.42E-06	1.24E-06
21.309	6.02E-04	3.19E-03	9.35E-03	4.24E-06	1.21E-06
21.476	5.64E-04	3.19E-03	9.04E-03	4.34E-06	1.16E-06
21.642	5.17E-04	3.62E-03	8.95E-03	4.27E-06	1.07E-06
21.809	5.44E-04	4.32E-03	8.67E-03	3.75E-06	8.88E-07
21.975	5.12E-04	4.08E-03	8.89E-03	4.03E-06	9.68E-07
22.142	5.27E-04	4.09E-03	8.91E-03	4.31E-06	9.21E-07
22.308	5.51E-04	4.08E-03	9.04E-03	4.38E-06	9.56E-07
22.475	5.39E-04	4.16E-03	8.89E-03	4.37E-06	9.30E-07
22.641	5.62E-04	3.91E-03	9.13E-03	4.38E-06	1.01E-06
22.808	5.34E-04	4.07E-03	8.90E-03	4.48E-06	1.04E-06
22.974	5.10E-04	3.87E-03	8.89E-03	4.27E-06	1.06E-06
23.141	4.97E-04	3.42E-03	9.01E-03	4.41E-06	1.06E-06
23.307	5.18E-04	3.21E-03	9.19E-03	4.56E-06	1.23E-06
23.474	5.31E-04	3.15E-03	9.37E-03	4.69E-06	1.33E-06
23.640	5.58E-04	2.61E-03	9.55E-03	4.34E-06	1.52E-06
23.807	5.66E-04	2.61E-03	9.65E-03	4.36E-06	1.56E-06
23.973	5.60E-04	2.43E-03	9.70E-03	4.54E-06	1.62E-06
24.140	5.94E-04	2.68E-03	9.66E-03	4.67E-06	1.70E-06
24.306	6.09E-04	2.77E-03	9.79E-03	4.75E-06	1.64E-06
24.473	5.99E-04	2.75E-03	9.69E-03	4.76E-06	1.58E-06
24.639	5.98E-04	2.79E-03	9.69E-03	4.93E-06	1.55E-06
24.806	5.92E-04	2.95E-03	9.84E-03	5.08E-06	1.61E-06
24.972	5.87E-04	3.35E-03	9.52E-03	4.83E-06	1.52E-06
25.138	5.63E-04	3.28E-03	9.29E-03	4.37E-06	1.42E-06
25.305	5.86E-04	3.34E-03	9.02E-03	4.40E-06	1.27E-06
25.471	5.91E-04	3.75E-03	9.15E-03	4.32E-06	1.14E-06
25.638	6.15E-04	3.23E-03	9.40E-03	4.15E-06	1.23E-06
25.804	5.86E-04	2.95E-03	9.31E-03	4.26E-06	1.26E-06
25.971	5.67E-04	2.99E-03	9.03E-03	4.11E-06	1.26E-06
26.137	5.47E-04	2.90E-03	9.22E-03	4.25E-06	1.23E-06
26.304	5.19E-04	2.96E-03	9.16E-03	4.44E-06	1.23E-06
26.470	5.19E-04	3.15E-03	9.12E-03	4.17E-06	1.13E-06
26.637	5.56E-04	3.46E-03	9.11E-03	4.19E-06	1.08E-06
26.803	5.41E-04	3.25E-03	8.96E-03	4.22E-06	1.09E-06
26.970	5.55E-04	3.47E-03	9.04E-03	4.00E-06	1.07E-06
27.136	5.83E-04	3.90E-03	9.35E-03	4.63E-06	1.23E-06
27.303	6.06E-04	3.72E-03	9.39E-03	4.64E-06	1.35E-06
27.469	6.27E-04	3.55E-03	8.98E-03	3.97E-06	1.15E-06
27.636	6.01E-04	3.47E-03	9.00E-03	4.15E-06	1.14E-06
27.802	6.09E-04	3.43E-03	9.23E-03	3.96E-06	1.17E-06

LA-ICP-MS data

Distance from top (mm)	B/Ca (mol/mol)	Mg/Ca (mol/mol)	Sr/Ca (mol/mol)	Ba/Ca (mol/mol)	U/Ca (mol/mol)
28.135	6.10E-04	3.09E-03	9.57E-03	4.27E-06	1.29E-06
28.302	6.34E-04	3.09E-03	9.41E-03	4.43E-06	1.37E-06
28.468	6.33E-04	2.87E-03	9.59E-03	4.96E-06	1.62E-06
28.635	6.16E-04	2.86E-03	9.91E-03	4.54E-06	1.64E-06
28.801	5.62E-04	2.66E-03	9.95E-03	4.49E-06	1.72E-06
28.968	6.12E-04	2.92E-03	9.65E-03	4.53E-06	1.62E-06
29.134	5.98E-04	2.97E-03	9.42E-03	4.61E-06	1.39E-06
29.300	5.66E-04	2.56E-03	9.66E-03	4.73E-06	1.49E-06
29.467	6.13E-04	2.74E-03	9.43E-03	4.55E-06	1.40E-06
29.633	6.05E-04	2.34E-03	9.86E-03	4.43E-06	1.51E-06
29.800	5.66E-04	2.30E-03	9.92E-03	4.75E-06	1.51E-06
29.966	5.66E-04	2.76E-03	9.71E-03	4.98E-06	1.41E-06
30.133	5.50E-04	2.99E-03	9.46E-03	4.61E-06	1.43E-06
30.299	5.28E-04	3.02E-03	9.10E-03	4.37E-06	1.20E-06
30.466	5.39E-04	2.94E-03	9.07E-03	4.35E-06	1.26E-06
30.632	5.33E-04	2.82E-03	9.34E-03	3.99E-06	1.25E-06
30.799	5.27E-04	3.45E-03	9.09E-03	4.06E-06	1.16E-06
30.965	5.15E-04	3.80E-03	9.18E-03	4.19E-06	1.14E-06
31.132	5.27E-04	3.78E-03	9.24E-03	4.05E-06	1.21E-06
31.298	5.05E-04	3.68E-03	8.99E-03	4.17E-06	1.10E-06
31.465	4.92E-04	4.02E-03	8.95E-03	4.06E-06	1.00E-06
31.631	4.87E-04	4.02E-03	8.85E-03	3.76E-06	9.34E-07
31.798	4.99E-04	4.01E-03	8.77E-03	3.62E-06	9.33E-07
31.964	4.99E-04	3.90E-03	8.73E-03	3.67E-06	9.40E-07
32.131	4.79E-04	3.09E-03	8.85E-03	3.73E-06	1.10E-06
32.297	4.68E-04	3.01E-03	8.78E-03	3.57E-06	1.07E-06
32.464	5.03E-04	3.44E-03	8.93E-03	3.90E-06	1.05E-06
32.630	5.10E-04	3.52E-03	9.14E-03	4.23E-06	1.08E-06
32.797	5.08E-04	3.71E-03	9.14E-03	4.11E-06	1.14E-06
32.963	5.13E-04	3.52E-03	8.96E-03	4.10E-06	1.12E-06
33.130	5.41E-04	3.30E-03	9.33E-03	4.15E-06	1.16E-06
33.296	5.34E-04	3.00E-03	9.35E-03	4.25E-06	1.21E-06
33.462	5.39E-04	2.99E-03	9.22E-03	4.34E-06	1.22E-06
33.629	5.77E-04	2.92E-03	9.21E-03	4.28E-06	1.28E-06
33.795	5.70E-04	3.21E-03	9.56E-03	4.59E-06	1.46E-06
33.962	5.32E-04	3.39E-03	9.60E-03	5.00E-06	1.65E-06
34.128	5.16E-04	2.62E-03	9.78E-03	4.84E-06	1.73E-06
34.295	5.51E-04	3.46E-03	9.83E-03	5.08E-06	1.57E-06
34.461	5.86E-04	3.08E-03	9.77E-03	5.22E-06	1.59E-06
34.628	5.73E-04	3.52E-03	9.50E-03	5.06E-06	1.53E-06
34.794	4.93E-04	3.68E-03	9.70E-03	4.79E-06	1.57E-06
34.961	5.58E-04	3.22E-03	9.75E-03	4.60E-06	1.40E-06
35.127	5.78E-04	3.37E-03	9.38E-03	4.32E-06	1.35E-06
35.294	5.36E-04	3.46E-03	9.27E-03	4.36E-06	1.24E-06
35.460	5.29E-04	3.60E-03	9.07E-03	4.12E-06	1.07E-06
35.627	5.48E-04	3.83E-03	8.95E-03	3.93E-06	9.95E-07
35.793	5.24E-04	3.96E-03	9.08E-03	4.05E-06	1.04E-06
35.960	5.29E-04	4.15E-03	9.02E-03	4.17E-06	9.22E-07
36.126	5.01E-04	4.07E-03	8.92E-03	3.95E-06	9.87E-07
36.293	5.12E-04	4.42E-03	9.01E-03	4.25E-06	1.03E-06
36.459	5.16E-04	3.37E-03	8.92E-03	4.33E-06	1.22E-06
36.626	5.16E-04	3.79E-03	9.01E-03	4.10E-06	1.12E-06
36.792	5.18E-04	4.08E-03	9.12E-03	4.03E-06	1.12E-06
36.959	5.40E-04	3.87E-03	9.02E-03	4.35E-06	1.10E-06
37.125	5.38E-04	3.92E-03	8.99E-03	4.30E-06	1.08E-06
37.292	5.36E-04	3.62E-03	8.91E-03	3.65E-06	1.12E-06
37.458	5.22E-04	3.53E-03	8.88E-03	3.80E-06	1.03E-06

Distance from top (mm)	B/Ca (mol/mol)	Mg/Ca (mol/mol)	Sr/Ca (mol/mol)	Ba/Ca (mol/mol)	U/Ca (mol/mol)
37.791	5.24E-04	3.42E-03	9.02E-03	3.98E-06	1.04E-06
37.957	4.98E-04	3.28E-03	8.84E-03	4.04E-06	1.05E-06
38.124	5.03E-04	3.28E-03	8.87E-03	4.04E-06	1.05E-06
38.290	5.01E-04	3.30E-03	9.02E-03	3.79E-06	1.03E-06
38.457	5.51E-04	3.56E-03	9.27E-03	3.94E-06	1.14E-06
38.623	5.80E-04	3.39E-03	9.10E-03	4.05E-06	1.20E-06
38.790	5.84E-04	3.14E-03	9.27E-03	4.20E-06	1.26E-06
38.956	5.84E-04	3.17E-03	9.42E-03	4.53E-06	1.40E-06
39.123	5.70E-04	3.08E-03	9.51E-03	4.53E-06	1.40E-06
39.289	5.83E-04	2.82E-03	9.82E-03	4.54E-06	1.60E-06
39.456	5.41E-04	2.57E-03	1.02E-02	5.07E-06	1.71E-06
39.622	5.17E-04	2.57E-03	9.89E-03	4.76E-06	1.51E-06
39.789	5.44E-04	3.23E-03	9.63E-03	4.85E-06	1.38E-06
39.955	5.66E-04	3.52E-03	9.50E-03	4.78E-06	1.40E-06
40.122	5.60E-04	2.92E-03	9.66E-03	4.55E-06	1.44E-06
40.288	5.77E-04	3.02E-03	9.60E-03	4.22E-06	1.31E-06
40.455	5.38E-04	3.07E-03	9.47E-03	4.08E-06	1.21E-06
40.621	5.13E-04	3.18E-03	9.32E-03	4.10E-06	1.23E-06
40.788	5.09E-04	3.50E-03	9.29E-03	4.20E-06	1.18E-06
40.954	5.20E-04	3.67E-03	9.29E-03	4.40E-06	1.20E-06
41.121	5.32E-04	3.73E-03	9.34E-03	4.11E-06	1.18E-06
41.287	5.30E-04	3.20E-03	9.09E-03	3.95E-06	1.20E-06
41.454	4.86E-04	3.16E-03	9.52E-03	4.35E-06	1.24E-06
41.620	4.94E-04	3.87E-03	9.20E-03	4.18E-06	1.16E-06
41.786	5.07E-04	3.58E-03	8.94E-03	4.09E-06	1.06E-06
41.953	5.00E-04	3.44E-03	9.01E-03	3.99E-06	1.13E-06
42.119	5.15E-04	3.99E-03	9.11E-03	4.20E-06	1.06E-06
42.286	5.22E-04	3.79E-03	9.17E-03	4.25E-06	1.17E-06
42.452	5.11E-04	3.89E-03	8.99E-03	4.44E-06	1.12E-06
42.619	4.64E-04	3.94E-03	8.87E-03	4.02E-06	9.80E-07
42.785	4.64E-04	4.06E-03	9.18E-03	4.54E-06	1.03E-06
42.952	5.07E-04	4.07E-03	9.01E-03	3.80E-06	1.05E-06
43.118	5.25E-04	3.77E-03	8.99E-03	4.14E-06	1.07E-06
43.285	5.01E-04	3.88E-03	8.95E-03	4.36E-06	1.06E-06
43.451	5.17E-04	3.95E-03	8.97E-03	4.35E-06	9.96E-07
43.618	5.53E-04	3.93E-03	9.07E-03	4.07E-06	9.77E-07
43.784	5.78E-04	3.71E-03	9.06E-03	4.00E-06	1.04E-06
43.951	5.28E-04	3.82E-03	9.00E-03	4.38E-06	1.00E-06
44.117	5.41E-04	4.11E-03	9.05E-03	4.68E-06	1.02E-06
44.284	5.44E-04	3.88E-03	9.14E-03	4.23E-06	9.94E-07
44.450	5.37E-04	3.53E-03	9.13E-03	4.00E-06	1.07E-06
44.617	5.42E-04	3.55E-03	8.99E-03	3.95E-06	9.87E-07
44.783	5.34E-04	3.56E-03	9.03E-03	3.80E-06	9.42E-07
44.950	5.38E-04	3.72E-03	9.27E-03	4.23E-06	1.02E-06
45.116	5.20E-04	3.23E-03	8.93E-03	4.05E-06	1.14E-06
45.283	5.50E-04	3.49E-03	9.06E-03	4.17E-06	1.13E-06
45.449	5.93E-04	3.73E-03	9.42E-03	4.43E-06	1.14E-06
45.616	5.37E-04	3.26E-03	9.45E-03	4.51E-06	1.27E-06
45.782	5.13E-04	2.68E-03	9.57E-03	4.64E-06	1.49E-06
45.948	5.76E-04	2.79E-03	9.60E-03	5.07E-06	1.44E-06
46.115	5.41E-04	3.06E-03	9.59E-03	4.79E-06	1.32E-06
46.281	5.32E-04	3.39E-03	9.60E-03	4.41E-06	1.29E-06
46.448	5.79E-04	3.58E-03	9.41E-03	4.46E-06	1.20E-06
46.614	5.96E-04	3.78E-03	9.18E-03	4.32E-06	1.13E-06
46.781	5.69E-04	3.35E-03	9.07E-03	4.44E-06	1.21E-06
46.947	5.57E-04	3.09E-03	9.23E-03	4.67E-06	1.13E-06
47.114	5.86E-04	3.23E-03	9.03E-03	4.60E-06	1.07E-06

LA-ICP-MS data

Distance from top (mm)	B/Ca (mol/mol)	Mg/Ca (mol/mol)	Sr/Ca (mol/mol)	Ba/Ca (mol/mol)	U/Ca (mol/mol)
47.451	5.79E-04	3.49E-03	9.35E-03	4.20E-06	1.11E-06
47.621	5.74E-04	3.51E-03	9.01E-03	3.96E-06	1.10E-06
47.792	5.57E-04	3.48E-03	8.89E-03	4.14E-06	1.12E-06
47.962	5.03E-04	3.36E-03	8.58E-03	4.07E-06	1.11E-06
48.132	5.15E-04	3.27E-03	8.82E-03	3.83E-06	1.15E-06
48.303	5.06E-04	3.27E-03	8.81E-03	4.00E-06	1.11E-06
48.473	5.18E-04	3.12E-03	8.71E-03	4.23E-06	1.14E-06
48.644	5.32E-04	3.48E-03	8.60E-03	4.33E-06	1.06E-06
48.814	4.73E-04	3.55E-03	8.75E-03	3.80E-06	1.02E-06
48.984	5.54E-04	3.39E-03	8.88E-03	4.01E-06	1.13E-06
49.155	5.55E-04	3.43E-03	8.87E-03	4.08E-06	1.15E-06
49.325	5.84E-04	3.47E-03	9.07E-03	4.20E-06	1.18E-06
49.496	5.94E-04	3.36E-03	9.17E-03	4.24E-06	1.27E-06
49.666	5.86E-04	3.22E-03	8.88E-03	4.40E-06	1.24E-06
49.836	6.10E-04	3.50E-03	8.79E-03	4.48E-06	1.12E-06
50.007	6.07E-04	3.69E-03	9.10E-03	4.42E-06	1.13E-06
50.177	6.22E-04	3.58E-03	9.05E-03	4.23E-06	1.13E-06
50.348	5.68E-04	3.14E-03	9.19E-03	4.21E-06	1.30E-06
50.518	6.40E-04	3.17E-03	9.17E-03	4.82E-06	1.38E-06
50.688	6.48E-04	3.23E-03	9.22E-03	4.85E-06	1.39E-06
50.859	6.25E-04	2.75E-03	9.44E-03	4.66E-06	1.60E-06
51.029	6.47E-04	2.59E-03	9.95E-03	5.11E-06	1.74E-06
51.200	6.42E-04	2.67E-03	9.67E-03	5.05E-06	1.74E-06
51.370	6.49E-04	2.48E-03	9.78E-03	4.92E-06	1.80E-06
51.540	6.41E-04	2.54E-03	9.75E-03	4.89E-06	1.75E-06
51.711	6.43E-04	2.67E-03	9.53E-03	4.54E-06	1.63E-06
51.881	6.38E-04	2.55E-03	9.74E-03	4.89E-06	1.60E-06
52.052	6.30E-04	2.58E-03	9.67E-03	4.16E-06	1.57E-06
52.222	6.35E-04	2.59E-03	9.44E-03	4.72E-06	1.52E-06
52.392	6.06E-04	3.11E-03	9.34E-03	4.74E-06	1.45E-06
52.563	5.82E-04	2.90E-03	9.36E-03	4.31E-06	1.36E-06
52.733	6.31E-04	3.04E-03	9.19E-03	4.20E-06	1.20E-06
52.904	6.27E-04	3.10E-03	9.16E-03	3.92E-06	1.19E-06
53.074	6.06E-04	3.28E-03	9.03E-03	3.98E-06	1.14E-06
53.244	5.58E-04	3.21E-03	8.86E-03	3.93E-06	1.17E-06
53.415	5.77E-04	3.42E-03	9.00E-03	4.26E-06	1.13E-06
53.585	5.54E-04	3.52E-03	9.07E-03	4.46E-06	1.13E-06
53.756	5.37E-04	3.44E-03	9.01E-03	4.18E-06	1.11E-06
53.926	5.34E-04	3.23E-03	8.95E-03	4.35E-06	1.11E-06
54.096	5.01E-04	3.08E-03	8.74E-03	4.03E-06	1.12E-06
54.267	5.55E-04	3.30E-03	8.90E-03	4.01E-06	1.12E-06
54.437	4.96E-04	3.04E-03	8.97E-03	4.56E-06	1.14E-06
54.608	4.99E-04	2.88E-03	8.97E-03	4.48E-06	1.20E-06
54.778	5.45E-04	2.91E-03	9.08E-03	4.82E-06	1.18E-06
54.948	5.13E-04	3.03E-03	8.90E-03	4.36E-06	1.16E-06
55.119	5.32E-04	3.13E-03	8.84E-03	4.29E-06	1.12E-06
55.289	5.71E-04	3.32E-03	9.00E-03	4.30E-06	1.15E-06
55.460	5.58E-04	3.47E-03	9.06E-03	4.75E-06	1.21E-06
55.630	5.46E-04	3.43E-03	9.21E-03	4.88E-06	1.20E-06
55.800	5.56E-04	3.08E-03	9.14E-03	4.33E-06	1.30E-06
55.971	5.34E-04	3.07E-03	9.17E-03	4.18E-06	1.24E-06
56.141	5.63E-04	3.29E-03	9.05E-03	4.13E-06	1.25E-06
56.312	5.86E-04	3.52E-03	9.13E-03	4.16E-06	1.23E-06
56.482	5.79E-04	3.64E-03	9.13E-03	4.27E-06	1.18E-06
56.652	5.90E-04	3.46E-03	9.12E-03	3.78E-06	1.18E-06
56.823	5.78E-04	2.95E-03	9.45E-03	3.92E-06	1.27E-06
56.993	5.71E-04	2.87E-03	9.30E-03	4.01E-06	1.23E-06

Distance from top (mm)	B/Ca (mol/mol)	Mg/Ca (mol/mol)	Sr/Ca (mol/mol)	Ba/Ca (mol/mol)	U/Ca (mol/mol)
57.334	5.94E-04	3.19E-03	9.22E-03	4.07E-06	1.28E-06
57.504	6.46E-04	2.86E-03	9.59E-03	4.58E-06	1.33E-06
57.675	6.81E-04	3.90E-03	9.48E-03	4.43E-06	1.29E-06
57.845	6.61E-04	4.11E-03	9.37E-03	4.55E-06	1.26E-06
58.016	6.37E-04	3.01E-03	9.36E-03	4.54E-06	1.40E-06
58.186	6.54E-04	3.18E-03	9.67E-03	5.13E-06	1.53E-06
58.356	6.63E-04	2.90E-03	9.72E-03	4.85E-06	1.62E-06
58.527	6.37E-04	3.30E-03	9.92E-03	4.88E-06	1.60E-06
58.697	6.30E-04	3.19E-03	9.62E-03	4.88E-06	1.50E-06
58.868	6.16E-04	2.70E-03	9.49E-03	4.71E-06	1.53E-06
59.038	6.36E-04	3.10E-03	9.48E-03	4.82E-06	1.45E-06
59.208	6.37E-04	3.00E-03	9.52E-03	4.36E-06	1.32E-06
59.379	6.26E-04	3.19E-03	9.23E-03	4.03E-06	1.28E-06
59.549	6.17E-04	3.91E-03	8.94E-03	4.22E-06	1.19E-06
59.720	5.82E-04	3.66E-03	8.97E-03	4.13E-06	1.10E-06
59.890	5.67E-04	3.92E-03	9.01E-03	4.37E-06	1.04E-06
60.060	6.16E-04	3.88E-03	9.15E-03	4.53E-06	1.14E-06
60.231	6.01E-04	3.81E-03	9.12E-03	4.37E-06	1.18E-06
60.401	5.71E-04	3.51E-03	9.03E-03	3.96E-06	1.21E-06
60.572	5.70E-04	3.47E-03	8.91E-03	4.32E-06	1.14E-06
60.742	5.82E-04	3.52E-03	8.80E-03	4.30E-06	1.03E-06
60.912	6.05E-04	3.62E-03	9.03E-03	3.98E-06	1.10E-06
61.083	5.74E-04	3.31E-03	8.95E-03	3.83E-06	1.10E-06
61.253	5.37E-04	3.50E-03	9.19E-03	4.29E-06	1.14E-06
61.424	5.30E-04	3.71E-03	8.93E-03	4.09E-06	1.14E-06
61.594	5.42E-04	3.61E-03	8.91E-03	3.82E-06	1.03E-06
61.764	5.73E-04	3.99E-03	8.89E-03	4.12E-06	1.05E-06
61.935	5.79E-04	3.66E-03	9.10E-03	4.62E-06	1.10E-06
62.105	6.02E-04	3.48E-03	9.16E-03	4.49E-06	1.17E-06
62.276	5.93E-04	3.77E-03	9.36E-03	4.08E-06	1.23E-06
62.446	6.03E-04	3.47E-03	8.98E-03	4.07E-06	1.11E-06
62.616	5.91E-04	4.03E-03	9.19E-03	4.36E-06	1.19E-06
62.787	6.04E-04	4.19E-03	9.38E-03	4.07E-06	1.20E-06
62.957	6.28E-04	4.00E-03	9.20E-03	3.86E-06	1.14E-06
63.128	6.16E-04	4.61E-03	9.30E-03	4.17E-06	1.16E-06
63.298	5.72E-04	3.78E-03	9.11E-03	4.11E-06	1.24E-06
63.468	5.95E-04	4.14E-03	9.22E-03	4.37E-06	1.24E-06
63.639	6.21E-04	4.17E-03	9.45E-03	4.13E-06	1.23E-06
63.809	6.47E-04	3.67E-03	9.35E-03	3.99E-06	1.25E-06
63.980	6.57E-04	3.39E-03	9.28E-03	4.73E-06	1.32E-06
64.150	7.10E-04	4.00E-03	9.44E-03	4.72E-06	1.35E-06
64.320	6.56E-04	4.06E-03	9.60E-03	4.74E-06	1.60E-06
64.491	6.13E-04	3.10E-03	9.80E-03	5.23E-06	1.75E-06
64.661	6.50E-04	3.36E-03	1.00E-02	5.18E-06	1.77E-06
64.832	6.29E-04	3.08E-03	9.71E-03	4.82E-06	1.75E-06
65.002	6.28E-04	2.95E-03	9.67E-03	4.84E-06	1.70E-06
65.172	6.32E-04	3.02E-03	9.75E-03	4.82E-06	1.66E-06
65.343	6.34E-04	2.86E-03	9.84E-03	4.91E-06	1.66E-06
65.513	6.00E-04	2.76E-03	9.85E-03	4.61E-06	1.64E-06
65.684	6.06E-04	2.87E-03	9.54E-03	4.68E-06	1.52E-06
65.854	6.27E-04	2.96E-03	9.37E-03	4.56E-06	1.35E-06
66.024	6.24E-04	2.50E-03	9.35E-03	4.09E-06	1.34E-06
66.195	6.14E-04	2.61E-03	9.22E-03	4.22E-06	1.31E-06
66.365	6.32E-04	2.53E-03	9.56E-03	4.81E-06	1.34E-06
66.536	6.58E-04	2.77E-03	9.38E-03	4.80E-06	1.27E-06
66.706	6.11E-04	2.95E-03	9.39E-03	4.05E-06	1.30E-06
66.876	6.09E-04	2.65E-03	9.41E-03	3.99E-06	1.25E-06

LA-ICP-MS data

Distance from top (mm)	B/Ca (mol/mol)	Mg/Ca (mol/mol)	Sr/Ca (mol/mol)	Ba/Ca (mol/mol)	U/Ca (mol/mol)
67.217	5.65E-04	4.04E-03	9.01E-03	4.41E-06	9.79E-07
67.388	5.10E-04	3.02E-03	9.08E-03	4.13E-06	1.11E-06
67.558	5.04E-04	2.77E-03	9.27E-03	4.14E-06	1.17E-06
67.728	5.38E-04	3.41E-03	8.95E-03	4.17E-06	1.14E-06
67.899	5.28E-04	3.43E-03	9.16E-03	4.18E-06	1.18E-06
68.069	5.40E-04	3.14E-03	9.14E-03	3.83E-06	1.11E-06
68.240	5.65E-04	3.21E-03	9.01E-03	3.93E-06	1.07E-06
68.410	5.50E-04	3.38E-03	9.04E-03	4.27E-06	1.02E-06
68.580	5.43E-04	3.84E-03	9.00E-03	4.61E-06	1.04E-06
68.751	5.28E-04	4.00E-03	9.15E-03	4.60E-06	1.00E-06
68.921	5.45E-04	3.96E-03	8.98E-03	4.08E-06	1.00E-06
69.092	5.34E-04	3.86E-03	8.89E-03	4.01E-06	9.90E-07
69.262	5.25E-04	3.62E-03	8.74E-03	4.08E-06	1.00E-06
69.432	5.11E-04	3.63E-03	8.88E-03	4.21E-06	9.95E-07
69.603	5.04E-04	3.38E-03	8.81E-03	4.35E-06	9.59E-07
69.773	5.03E-04	3.48E-03	8.97E-03	4.66E-06	1.03E-06
69.944	5.28E-04	3.12E-03	9.23E-03	4.74E-06	1.12E-06
70.114	5.88E-04	3.63E-03	9.10E-03	4.81E-06	1.17E-06
70.284	6.14E-04	3.25E-03	9.11E-03	4.25E-06	1.16E-06
70.455	6.05E-04	3.15E-03	9.09E-03	4.53E-06	1.10E-06
70.625	6.13E-04	3.27E-03	9.23E-03	4.65E-06	1.20E-06
70.796	6.28E-04	3.29E-03	9.05E-03	4.27E-06	1.24E-06
70.966	6.39E-04	3.14E-03	9.23E-03	4.32E-06	1.24E-06
71.136	6.21E-04	3.23E-03	9.22E-03	4.67E-06	1.24E-06
71.307	6.05E-04	3.31E-03	9.35E-03	4.42E-06	1.31E-06
71.477	6.36E-04	2.66E-03	9.66E-03	4.68E-06	1.49E-06
71.648	6.27E-04	2.89E-03	9.62E-03	4.59E-06	1.52E-06
71.818	6.56E-04	3.11E-03	9.68E-03	4.92E-06	1.53E-06
71.988	6.53E-04	3.39E-03	1.02E-02	5.30E-06	1.67E-06
72.159	6.09E-04	3.18E-03	9.86E-03	4.64E-06	1.60E-06
72.329	5.57E-04	3.14E-03	9.74E-03	4.57E-06	1.57E-06
72.500	5.55E-04	3.11E-03	9.51E-03	4.77E-06	1.50E-06
72.670	6.44E-04	2.97E-03	9.45E-03	4.65E-06	1.42E-06
72.840	6.20E-04	2.94E-03	9.64E-03	4.82E-06	1.43E-06
73.011	6.38E-04	2.95E-03	9.72E-03	4.55E-06	1.51E-06
73.181	6.05E-04	2.67E-03	9.91E-03	4.67E-06	1.52E-06
73.352	6.70E-04	3.18E-03	9.70E-03	5.07E-06	1.40E-06
73.522	6.33E-04	3.39E-03	9.62E-03	4.72E-06	1.36E-06
73.692	6.43E-04	3.19E-03	9.56E-03	4.84E-06	1.29E-06
73.863	6.28E-04	2.81E-03	9.65E-03	4.68E-06	1.45E-06
74.033	6.44E-04	3.06E-03	9.58E-03	4.87E-06	1.28E-06
74.204	6.43E-04	3.56E-03	9.77E-03	4.94E-06	1.41E-06
74.374	6.64E-04	3.18E-03	9.34E-03	4.79E-06	1.32E-06
74.544	6.66E-04	3.23E-03	9.27E-03	4.68E-06	1.24E-06
74.715	6.31E-04	3.66E-03	9.40E-03	4.32E-06	1.17E-06
74.885	6.33E-04	3.55E-03	9.24E-03	4.26E-06	1.05E-06
75.056	5.98E-04	2.83E-03	9.35E-03	4.45E-06	1.23E-06
75.226	6.04E-04	3.06E-03	9.34E-03	4.42E-06	1.31E-06
75.396	6.01E-04	2.93E-03	9.43E-03	4.43E-06	1.40E-06
75.567	6.23E-04	3.29E-03	9.63E-03	4.75E-06	1.35E-06
75.737	6.03E-04	3.02E-03	9.46E-03	4.70E-06	1.23E-06
75.908	6.01E-04	3.37E-03	9.44E-03	4.95E-06	1.22E-06
76.078	5.73E-04	3.60E-03	9.08E-03	4.68E-06	1.09E-06
76.248	5.57E-04	3.72E-03	8.95E-03	4.36E-06	1.04E-06
76.419	5.79E-04	3.74E-03	8.97E-03	4.22E-06	1.07E-06
76.589	5.90E-04	3.51E-03	9.15E-03	4.39E-06	1.06E-06
76.760	5.57E-04	3.39E-03	8.97E-03	4.31E-06	9.33E-07

Distance from top (mm)	B/Ca (mol/mol)	Mg/Ca (mol/mol)	Sr/Ca (mol/mol)	Ba/Ca (mol/mol)	U/Ca (mol/mol)
77.100	5.53E-04	2.89E-03	9.18E-03	4.66E-06	1.24E-06
77.271	5.77E-04	3.12E-03	9.19E-03	4.31E-06	1.17E-06
77.441	5.61E-04	2.83E-03	9.52E-03	4.66E-06	1.18E-06
77.612	5.46E-04	2.83E-03	9.62E-03	4.65E-06	1.23E-06
77.782	5.42E-04	3.20E-03	9.12E-03	4.35E-06	1.15E-06
77.952	5.60E-04	3.44E-03	9.01E-03	4.08E-06	1.06E-06
78.123	5.02E-04	3.34E-03	9.07E-03	3.98E-06	1.13E-06
78.293	4.87E-04	3.48E-03	9.23E-03	4.13E-06	1.17E-06
78.464	4.87E-04	3.27E-03	9.21E-03	4.18E-06	1.24E-06
78.634	5.46E-04	3.18E-03	9.21E-03	4.23E-06	1.15E-06
78.804	5.55E-04	3.48E-03	8.97E-03	3.74E-06	1.06E-06
78.975	5.81E-04	3.95E-03	8.66E-03	3.95E-06	9.61E-07
79.145	6.07E-04	5.08E-03	8.99E-03	4.00E-06	1.06E-06
79.316	5.62E-04	5.03E-03	9.16E-03	3.82E-06	1.13E-06
79.486	5.49E-04	4.05E-03	9.19E-03	4.03E-06	1.10E-06
79.656	5.35E-04	3.44E-03	8.82E-03	3.74E-06	1.00E-06
79.827	5.29E-04	3.56E-03	8.99E-03	4.03E-06	1.05E-06
79.997	5.44E-04	3.52E-03	9.08E-03	3.75E-06	1.07E-06
80.168	5.41E-04	3.57E-03	9.04E-03	4.02E-06	1.05E-06
80.338	5.69E-04	3.46E-03	9.05E-03	4.35E-06	1.09E-06
80.508	5.21E-04	3.57E-03	9.14E-03	3.90E-06	1.18E-06
80.679	5.64E-04	3.87E-03	9.09E-03	4.09E-06	1.06E-06
80.849	5.57E-04	5.21E-03	9.51E-03	4.10E-06	1.25E-06
81.020	5.73E-04	5.33E-03	9.70E-03	4.33E-06	1.35E-06
81.190	5.66E-04	4.16E-03	9.62E-03	4.53E-06	1.31E-06
81.360	5.80E-04	3.47E-03	9.55E-03	3.91E-06	1.35E-06
81.531	6.77E-04	3.54E-03	9.46E-03	4.40E-06	1.32E-06
81.701	6.01E-04	3.23E-03	9.58E-03	4.36E-06	1.41E-06
81.872	5.68E-04	3.40E-03	9.66E-03	4.54E-06	1.43E-06
82.042	5.91E-04	5.10E-03	9.52E-03	4.44E-06	1.44E-06
82.212	6.51E-04	4.29E-03	9.54E-03	4.66E-06	1.45E-06
82.383	6.26E-04	3.67E-03	9.73E-03	4.71E-06	1.49E-06
82.553	6.16E-04	2.91E-03	9.61E-03	4.94E-06	1.64E-06
82.724	6.11E-04	3.65E-03	1.00E-02	4.70E-06	1.62E-06
82.894	6.02E-04	3.62E-03	9.99E-03	4.69E-06	1.60E-06
83.064	5.72E-04	3.90E-03	9.89E-03	4.52E-06	1.47E-06
83.235	5.76E-04	4.06E-03	9.76E-03	4.40E-06	1.39E-06
83.405	5.83E-04	3.80E-03	9.55E-03	4.42E-06	1.39E-06
83.576	5.73E-04	3.24E-03	9.50E-03	4.68E-06	1.33E-06
83.746	6.08E-04	2.80E-03	9.62E-03	4.31E-06	1.50E-06
83.916	5.85E-04	3.00E-03	9.74E-03	4.28E-06	1.47E-06
84.087	5.74E-04	3.17E-03	9.42E-03	4.14E-06	1.27E-06
84.257	5.88E-04	3.43E-03	9.12E-03	4.34E-06	1.09E-06
84.428	5.67E-04	3.49E-03	9.27E-03	4.30E-06	1.16E-06
84.598	5.97E-04	3.45E-03	9.26E-03	4.17E-06	1.05E-06
84.768	5.57E-04	3.28E-03	9.35E-03	4.32E-06	1.10E-06
84.939	5.34E-04	3.60E-03	9.32E-03	4.09E-06	1.18E-06
85.109	5.22E-04	3.80E-03	9.09E-03	4.57E-06	1.04E-06
85.280	5.67E-04	3.75E-03	9.00E-03	4.10E-06	9.76E-07
85.450	5.53E-04	3.67E-03	9.08E-03	4.36E-06	1.05E-06
85.620	5.82E-04	3.59E-03	8.95E-03	4.13E-06	1.04E-06
85.791	5.53E-04	3.82E-03	9.16E-03	4.24E-06	1.07E-06
85.961	4.94E-04	3.83E-03	8.89E-03	4.03E-06	9.99E-07
86.132	5.13E-04	3.76E-03	8.66E-03	3.97E-06	9.64E-07
86.302	5.88E-04	3.59E-03	8.73E-03	3.70E-06	9.23E-07
86.472	5.97E-04	3.80E-03	8.92E-03	3.82E-06	9.37E-07
86.640	5.54E-04	3.63E-03	9.01E-03	3.78E-06	9.95E-07

Table 10.2 Orpheus Island, GBR *Porites* data

Time	Distance from top (mm)	B/Ca (mol/mol)	Mg/Ca (mol/mol)	Sr/Ca (mol/mol)	Ba/Ca (mol/mol)	U/Ca (mol/mol)	Mn ($\mu g\ g^{-1}$)
1992.43	0.00	3.750E-04	3.756E-03	9.061E-03	5.763E-06	1.252E-06	0.346
1992.38	0.30	3.946E-04	4.563E-03	8.846E-03	5.199E-06	1.007E-06	0.347
1992.35	0.59	3.984E-04	4.475E-03	8.739E-03	5.052E-06	1.058E-06	0.312
1992.33	0.89	4.049E-04	4.020E-03	8.935E-03	4.740E-06	1.120E-06	0.326
1992.31	1.18	4.062E-04	3.867E-03	8.867E-03	4.307E-06	1.119E-06	0.279
1992.29	1.48	3.990E-04	4.211E-03	8.938E-03	5.162E-06	1.080E-06	0.303
1992.27	1.77	3.989E-04	4.150E-03	8.898E-03	6.197E-06	1.060E-06	0.313
1992.24	2.07	3.919E-04	4.395E-03	8.907E-03	7.892E-06	1.035E-06	0.324
1992.22	2.36	3.973E-04	4.207E-03	8.846E-03	5.814E-06	1.090E-06	0.326
1992.20	2.66	3.889E-04	4.299E-03	8.802E-03	4.833E-06	1.058E-06	0.368
1992.18	2.95	3.778E-04	3.902E-03	8.819E-03	5.072E-06	1.108E-06	0.400
1992.15	3.25	3.951E-04	4.123E-03	8.872E-03	5.486E-06	1.066E-06	0.373
1992.13	3.54	4.104E-04	4.361E-03	8.734E-03	4.108E-06	9.223E-07	0.318
1992.10	3.84	4.457E-04	4.270E-03	8.784E-03	5.452E-06	9.956E-07	0.378
1992.08	4.13	4.302E-04	4.022E-03	8.719E-03	6.222E-06	9.903E-07	0.374
1992.05	4.43	4.582E-04	4.160E-03	8.869E-03	6.913E-06	9.893E-07	0.300
1992.02	4.72	4.679E-04	4.527E-03	8.750E-03	8.166E-06	9.457E-07	0.286
1991.99	5.02	4.512E-04	4.529E-03	8.779E-03	7.055E-06	9.583E-07	0.285
1991.96	5.32	4.536E-04	4.485E-03	8.817E-03	6.674E-06	1.010E-06	0.273
1991.94	5.61	4.281E-04	4.230E-03	8.746E-03	6.139E-06	1.035E-06	0.269
1991.91	5.91	4.100E-04	4.033E-03	8.867E-03	6.353E-06	1.055E-06	0.245
1991.88	6.20	4.100E-04	3.996E-03	8.678E-03	5.128E-06	1.072E-06	0.216
1991.85	6.50	4.119E-04	3.937E-03	8.757E-03	4.944E-06	1.093E-06	0.219
1991.82	6.79	4.152E-04	3.873E-03	8.811E-03	5.152E-06	1.106E-06	0.232
1991.80	7.09	4.331E-04	3.609E-03	8.848E-03	4.895E-06	1.170E-06	0.310
1991.77	7.38	4.438E-04	3.629E-03	8.895E-03	4.632E-06	1.177E-06	0.353
1991.74	7.68	4.551E-04	3.668E-03	8.988E-03	4.172E-06	1.160E-06	0.218
1991.71	7.97	4.665E-04	3.676E-03	8.962E-03	3.785E-06	1.202E-06	0.210
1991.68	8.27	4.563E-04	3.771E-03	8.925E-03	3.163E-06	1.136E-06	0.216
1991.65	8.56	4.668E-04	3.849E-03	8.881E-03	2.877E-06	1.115E-06	0.220
1991.62	8.86	4.701E-04	3.687E-03	8.992E-03	2.897E-06	1.190E-06	0.197
1991.59	9.15	4.813E-04	3.748E-03	8.965E-03	3.191E-06	1.194E-06	0.190
1991.56	9.45	4.825E-04	3.766E-03	8.932E-03	3.227E-06	1.162E-06	0.174
1991.52	9.75	4.661E-04	3.803E-03	8.908E-03	3.497E-06	1.115E-06	0.176
1991.49	10.04	4.562E-04	3.756E-03	8.982E-03	3.999E-06	1.178E-06	0.183
1991.46	10.34	4.632E-04	3.681E-03	8.979E-03	4.106E-06	1.202E-06	0.200
1991.44	10.63	4.603E-04	3.601E-03	8.946E-03	4.045E-06	1.164E-06	0.223
1991.42	10.93	4.640E-04	3.615E-03	9.005E-03	3.208E-06	1.176E-06	0.221
1991.40	11.22	4.684E-04	3.699E-03	8.921E-03	3.244E-06	1.160E-06	0.208
1991.38	11.52	4.678E-04	3.728E-03	8.984E-03	3.627E-06	1.147E-06	0.209
1991.36	11.81	4.581E-04	3.673E-03	8.963E-03	3.636E-06	1.144E-06	0.208
1991.34	12.11	4.649E-04	3.776E-03	9.028E-03	3.733E-06	1.126E-06	0.184
1991.32	12.40	4.717E-04	3.951E-03	8.885E-03	4.031E-06	1.086E-06	0.197
1991.30	12.70	4.589E-04	4.031E-03	8.908E-03	4.400E-06	1.101E-06	0.209
1991.28	12.99	4.658E-04	3.995E-03	8.897E-03	4.507E-06	1.074E-06	0.200
1991.26	13.29	4.420E-04	3.977E-03	8.882E-03	4.643E-06	1.068E-06	0.199
1991.24	13.58	4.403E-04	4.245E-03	8.840E-03	5.889E-06	1.021E-06	0.202
1991.22	13.88	4.337E-04	4.230E-03	8.839E-03	7.173E-06	1.000E-06	0.238
1991.20	14.17	4.356E-04	4.263E-03	8.849E-03	5.964E-06	1.000E-06	0.279
1991.18	14.47	4.183E-04	4.497E-03	8.691E-03	5.310E-06	9.647E-07	0.301
1991.16	14.77	4.283E-04	4.352E-03	8.823E-03	5.519E-06	1.003E-06	0.287
1991.14	15.06	4.427E-04	4.220E-03	8.804E-03	6.507E-06	9.862E-07	0.249
1991.12	15.36	4.187E-04	4.267E-03	8.717E-03	8.235E-06	9.134E-07	0.307

Time	Distance from top (mm)	B/Ca (mol/mol)	Mg/Ca (mol/mol)	Sr/Ca (mol/mol)	Ba/Ca (mol/mol)	U/Ca (mol/mol)	Mn ($\mu g\ g^{-1}$)
1991.10	15.65	3.906E-04	4.178E-03	8.577E-03	8.657E-06	9.370E-07	0.364
1991.08	15.95	4.131E-04	4.249E-03	8.624E-03	6.616E-06	9.483E-07	0.426
1991.04	16.83	4.212E-04	3.883E-03	8.631E-03	9.275E-06	1.002E-06	0.504
1991.02	17.13	3.970E-04	4.174E-03	8.748E-03	6.249E-06	9.945E-07	0.381
1991.01	17.42	3.985E-04	4.462E-03	8.665E-03	7.654E-06	9.729E-07	0.339
1990.99	17.72	4.363E-04	4.481E-03	8.766E-03	9.095E-06	9.686E-07	0.319
1990.98	18.01	4.150E-04	4.611E-03	8.704E-03	1.091E-05	9.590E-07	0.315
1990.96	18.31	4.135E-04	4.791E-03	8.561E-03	1.025E-05	8.978E-07	0.312
1990.94	18.60	4.356E-04	4.973E-03	8.707E-03	1.027E-05	9.026E-07	0.315
1990.91	18.90	4.104E-04	4.810E-03	8.534E-03	1.039E-05	9.340E-07	0.305
1990.89	19.19	4.115E-04	4.360E-03	8.633E-03	1.107E-05	9.819E-07	0.320
1990.87	19.49	4.070E-04	4.176E-03	8.683E-03	1.145E-05	1.032E-06	0.316
1990.84	19.79	4.111E-04	4.030E-03	8.874E-03	9.078E-06	1.049E-06	0.281
1990.82	20.08	4.058E-04	4.083E-03	8.651E-03	5.865E-06	1.007E-06	0.282
1990.79	20.38	4.136E-04	4.178E-03	8.810E-03	4.944E-06	1.064E-06	0.279
1990.77	20.67	4.104E-04	4.038E-03	8.729E-03	4.513E-06	1.042E-06	0.282
1990.75	20.97	4.114E-04	3.918E-03	8.817E-03	4.792E-06	1.084E-06	0.269
1990.72	21.26	4.155E-04	3.744E-03	8.966E-03	4.716E-06	1.145E-06	0.233
1990.70	21.56	4.284E-04	3.705E-03	8.966E-03	4.397E-06	1.149E-06	0.243
1990.67	21.85	4.607E-04	3.800E-03	8.987E-03	3.481E-06	1.133E-06	0.272
1990.65	22.15	4.702E-04	3.827E-03	8.947E-03	3.210E-06	1.132E-06	0.262
1990.63	22.44	4.760E-04	3.831E-03	9.049E-03	3.341E-06	1.170E-06	0.269
1990.60	22.74	4.924E-04	3.798E-03	9.011E-03	3.369E-06	1.168E-06	0.255
1990.58	23.03	4.866E-04	3.740E-03	8.883E-03	3.450E-06	1.165E-06	0.260
1990.55	23.33	4.978E-04	3.377E-03	9.148E-03	3.136E-06	1.268E-06	0.227
1990.53	23.62	4.929E-04	3.503E-03	9.054E-03	2.801E-06	1.248E-06	0.185
1990.51	23.92	5.109E-04	3.431E-03	9.104E-03	2.839E-06	1.267E-06	0.192
1990.48	24.22	5.192E-04	3.323E-03	9.294E-03	3.178E-06	1.283E-06	0.318
1990.47	24.51	5.311E-04	3.487E-03	9.169E-03	3.783E-06	1.259E-06	0.283
1990.45	24.81	5.403E-04	3.524E-03	9.113E-03	3.879E-06	1.231E-06	0.195
1990.44	25.10	5.319E-04	3.493E-03	9.052E-03	4.266E-06	1.186E-06	0.177
1990.42	25.40	5.225E-04	3.538E-03	9.049E-03	4.558E-06	1.178E-06	0.170
1990.41	25.69	5.034E-04	3.557E-03	9.135E-03	4.198E-06	1.149E-06	0.195
1990.39	25.99	4.952E-04	3.792E-03	9.031E-03	3.930E-06	1.148E-06	0.212
1990.38	26.28	4.858E-04	4.154E-03	8.887E-03	4.033E-06	1.061E-06	0.205
1990.36	26.58	4.629E-04	4.151E-03	8.996E-03	4.346E-06	1.048E-06	0.185
1990.34	26.87	4.695E-04	4.087E-03	8.916E-03	4.559E-06	1.039E-06	0.191
1990.33	27.17	4.550E-04	4.119E-03	8.900E-03	4.400E-06	1.058E-06	0.234
1990.31	27.46	4.398E-04	4.186E-03	8.767E-03	3.850E-06	1.054E-06	0.272
1990.30	27.76	4.328E-04	4.023E-03	8.901E-03	4.366E-06	1.105E-06	0.242
1990.28	28.05	4.177E-04	3.935E-03	8.863E-03	4.689E-06	1.067E-06	0.232
1990.27	28.35	4.241E-04	4.075E-03	8.850E-03	4.341E-06	1.035E-06	0.294
1990.26	28.64	4.196E-04	4.119E-03	8.734E-03	4.229E-06	1.036E-06	0.310
1990.25	28.94	4.128E-04	4.146E-03	8.846E-03	4.312E-06	1.062E-06	0.343
1990.24	29.24	4.173E-04	3.828E-03	8.846E-03	4.219E-06	1.096E-06	0.321
1990.23	29.53	4.339E-04	3.738E-03	8.898E-03	5.223E-06	1.152E-06	0.298
1990.21	29.83	4.317E-04	3.727E-03	8.817E-03	6.938E-06	1.136E-06	0.270
1990.20	30.12	4.107E-04	3.950E-03	8.798E-03	7.442E-06	1.046E-06	0.283
1990.19	30.42	3.800E-04	4.365E-03	8.818E-03	6.293E-06	9.877E-07	0.330
1990.17	30.71	3.996E-04	4.277E-03	8.818E-03	4.972E-06	1.033E-06	0.364
1990.15	31.01	4.080E-04	4.295E-03	8.890E-03	4.408E-06	1.015E-06	0.374
1990.12	31.30	4.126E-04	4.254E-03	8.803E-03	4.765E-06	1.013E-06	0.368
1990.10	31.60	4.201E-04	4.264E-03	8.641E-03	5.283E-06	1.004E-06	0.354
1990.08	31.89	4.150E-04	4.202E-03	8.713E-03	7.444E-06	9.686E-07	0.370
1990.06	32.19	4.154E-04	4.271E-03	8.742E-03	7.077E-06	9.625E-07	0.336

LA-ICP-MS data

Time	Distance from top (mm)	B/Ca (mol/mol)	Mg/Ca (mol/mol)	Sr/Ca (mol/mol)	Ba/Ca (mol/mol)	U/Ca (mol/mol)	Mn ($\mu g\ g^{-1}$)
1990.04	32.48	4.131E-04	4.288E-03	8.796E-03	5.760E-06	9.820E-07	0.295
1990.01	32.78	4.200E-04	4.263E-03	8.751E-03	5.849E-06	9.708E-07	0.280
1989.99	33.07	4.073E-04	4.433E-03	8.674E-03	6.722E-06	9.392E-07	0.270
1989.97	33.37	4.086E-04	4.220E-03	8.745E-03	8.010E-06	9.950E-07	0.273
1989.95	33.66	4.111E-04	4.035E-03	8.668E-03	8.215E-06	9.829E-07	0.246
1989.92	33.96	4.175E-04	4.289E-03	8.649E-03	8.879E-06	9.096E-07	0.240
1989.90	34.26	4.436E-04	4.408E-03	8.599E-03	9.325E-06	9.431E-07	0.219
1989.88	34.55	4.633E-04	4.231E-03	8.842E-03	8.545E-06	9.995E-07	0.255
1989.87	34.85	4.645E-04	4.207E-03	8.778E-03	7.905E-06	9.752E-07	0.296
1989.85	35.14	4.479E-04	4.255E-03	8.774E-03	7.724E-06	9.735E-07	0.324
1989.83	35.44	4.299E-04	4.361E-03	8.680E-03	7.857E-06	9.843E-07	0.317
1989.81	35.73	4.310E-04	4.163E-03	8.810E-03	6.713E-06	1.010E-06	0.303
1989.79	36.03	3.996E-04	4.151E-03	8.784E-03	6.164E-06	1.030E-06	0.301
1989.77	36.32	4.035E-04	3.993E-03	8.804E-03	6.206E-06	1.051E-06	0.263
1989.75	36.62	4.153E-04	3.905E-03	8.819E-03	5.759E-06	1.078E-06	0.264
1989.73	36.91	4.108E-04	3.657E-03	8.896E-03	5.128E-06	1.140E-06	0.318
1989.71	37.21	4.316E-04	3.734E-03	8.931E-03	4.739E-06	1.160E-06	0.317
1989.69	37.50	4.396E-04	3.776E-03	8.904E-03	4.013E-06	1.185E-06	0.303
1989.67	37.80	4.611E-04	3.572E-03	8.988E-03	3.695E-06	1.223E-06	0.308
1989.65	38.09	4.769E-04	3.535E-03	9.085E-03	3.669E-06	1.206E-06	0.280
1989.64	38.39	4.905E-04	3.462E-03	9.077E-03	2.998E-06	1.267E-06	0.262
1989.61	38.69	4.934E-04	3.441E-03	9.163E-03	3.023E-06	1.273E-06	0.230
1989.59	38.98	5.070E-04	3.406E-03	9.089E-03	2.826E-06	1.252E-06	0.207
1989.57	39.28	5.155E-04	3.298E-03	9.174E-03	2.964E-06	1.269E-06	0.207
1989.55	39.57	5.192E-04	3.426E-03	9.155E-03	3.269E-06	1.282E-06	0.190
1989.53	39.87	5.185E-04	3.263E-03	9.184E-03	3.087E-06	1.250E-06	0.173
1989.51	40.16	5.088E-04	3.391E-03	9.071E-03	3.092E-06	1.228E-06	0.190
1989.49	40.46	5.116E-04	3.521E-03	9.180E-03	3.085E-06	1.244E-06	0.186
1989.47	40.75	5.015E-04	3.608E-03	9.060E-03	3.259E-06	1.191E-06	0.199
1989.45	41.05	5.025E-04	3.721E-03	9.025E-03	3.538E-06	1.175E-06	0.194
1989.43	41.34	4.798E-04	3.553E-03	8.959E-03	3.420E-06	1.206E-06	0.185
1989.41	41.64	4.644E-04	3.586E-03	9.020E-03	3.649E-06	1.199E-06	0.202
1989.39	41.93	4.560E-04	3.681E-03	9.016E-03	3.896E-06	1.138E-06	0.207
1989.37	42.23	4.538E-04	3.798E-03	8.917E-03	4.430E-06	1.126E-06	0.218
1989.35	42.52	4.362E-04	3.595E-03	8.899E-03	4.521E-06	1.190E-06	0.208
1989.33	42.82	4.263E-04	3.566E-03	9.055E-03	4.546E-06	1.179E-06	0.204
1989.31	43.11	4.171E-04	3.703E-03	8.915E-03	4.834E-06	1.130E-06	0.226
1989.29	43.41	4.107E-04	4.102E-03	8.883E-03	5.257E-06	1.085E-06	0.250
1989.27	43.71	4.030E-04	3.790E-03	8.866E-03	4.670E-06	1.123E-06	0.257
1989.24	44.00	3.989E-04	3.971E-03	8.844E-03	5.264E-06	1.066E-06	0.250
1989.22	44.30	4.177E-04	4.156E-03	8.837E-03	5.281E-06	1.031E-06	0.254
1989.20	44.59	3.803E-04	4.170E-03	8.835E-03	5.404E-06	1.071E-06	0.269
1989.18	44.89	3.782E-04	4.161E-03	8.748E-03	4.894E-06	1.035E-06	0.287
1989.16	45.18	3.887E-04	4.009E-03	8.794E-03	4.555E-06	1.065E-06	0.300
1989.14	45.48	3.847E-04	4.119E-03	8.915E-03	4.820E-06	1.066E-06	0.268
1989.12	45.77	3.833E-04	3.889E-03	8.865E-03	5.197E-06	1.109E-06	0.238
1989.10	46.07	3.909E-04	4.024E-03	8.795E-03	6.422E-06	1.057E-06	0.230
1989.08	46.36	3.968E-04	4.256E-03	8.700E-03	5.404E-06	1.005E-06	0.257
1989.06	46.66	3.853E-04	3.951E-03	8.789E-03	5.192E-06	1.035E-06	0.250
1989.04	46.95	3.739E-04	4.164E-03	8.717E-03	5.634E-06	1.013E-06	0.293
1989.02	47.25	3.745E-04	4.127E-03	8.755E-03	5.030E-06	9.788E-07	0.314
1988.99	47.54	3.900E-04	4.058E-03	8.822E-03	4.464E-06	9.994E-07	0.301
1988.96	47.84	3.954E-04	4.039E-03	8.777E-03	4.986E-06	1.024E-06	0.341
1988.92	48.14	3.957E-04	3.732E-03	8.809E-03	4.706E-06	1.097E-06	0.319

Table 10.3 Havannah Island, GBR *Porites* data

Time	Distance from top (mm)	B/Ca (mol/mol)	Mg/Ca (mol/mol)	Sr/Ca (mol/mol)	Ba/Ca (mol/mol)	U/Ca (mol/mol)	Mn ($\mu g\ g^{-1}$)
1998.71	0.42	4.556E-04	3.106E-03	8.533E-03	4.181E-06	1.118E-06	0.285
1998.65	0.73	4.326E-04	2.932E-03	8.579E-03	4.003E-06	1.173E-06	0.252
1998.60	1.03	4.362E-04	2.726E-03	8.590E-03	4.006E-06	1.248E-06	0.243
1998.54	1.33	4.218E-04	2.463E-03	9.027E-03	4.002E-06	1.444E-06	0.223
1998.48	1.63	4.163E-04	2.104E-03	9.232E-03	4.129E-06	1.564E-06	0.211
1998.42	1.93	4.152E-04	2.426E-03	9.062E-03	4.072E-06	1.445E-06	0.249
1998.36	2.24	4.516E-04	2.975E-03	9.058E-03	4.233E-06	1.404E-06	0.325
1998.30	2.54	4.431E-04	3.048E-03	8.942E-03	4.113E-06	1.328E-06	0.324
1998.25	2.84	4.406E-04	3.339E-03	8.993E-03	4.331E-06	1.302E-06	0.384
1998.19	3.14	4.372E-04	3.750E-03	8.898E-03	4.659E-06	1.264E-06	0.399
1998.13	3.45	4.292E-04	4.059E-03	8.705E-03	4.931E-06	1.151E-06	0.394
1998.12	3.75	4.173E-04	4.026E-03	8.793E-03	5.316E-06	1.140E-06	0.378
1998.10	4.05	4.162E-04	3.846E-03	8.762E-03	5.397E-06	1.212E-06	0.377
1998.09	4.35	4.168E-04	3.473E-03	8.863E-03	5.844E-06	1.324E-06	0.451
1998.07	4.65	3.542E-04	3.128E-03	8.783E-03	7.793E-06	1.287E-06	0.571
1998.06	4.96	3.256E-04	3.084E-03	8.539E-03	8.044E-06	1.141E-06	0.524
1998.04	5.26	3.438E-04	2.961E-03	8.772E-03	7.778E-06	1.262E-06	0.456
1998.03	5.56	3.560E-04	2.945E-03	8.676E-03	6.951E-06	1.175E-06	0.389
1998.01	5.86	4.017E-04	3.583E-03	8.656E-03	4.519E-06	1.096E-06	0.339
1998.00	6.17	4.133E-04	3.225E-03	8.877E-03	3.972E-06	1.248E-06	0.309
1997.98	6.47	4.113E-04	3.033E-03	8.915E-03	3.740E-06	1.271E-06	0.300
1997.97	6.77	3.904E-04	3.073E-03	8.877E-03	3.577E-06	1.295E-06	0.347
1997.95	7.07	3.936E-04	3.159E-03	9.096E-03	3.681E-06	1.381E-06	0.384
1997.94	7.37	3.887E-04	2.958E-03	8.880E-03	3.498E-06	1.400E-06	0.426
1997.92	7.68	4.046E-04	2.955E-03	8.959E-03	3.694E-06	1.452E-06	0.467
1997.91	7.98	4.166E-04	2.846E-03	9.121E-03	3.717E-06	1.492E-06	0.477
1997.89	8.28	3.933E-04	3.320E-03	8.876E-03	3.555E-06	1.281E-06	0.459
1997.88	8.58	4.059E-04	3.022E-03	9.005E-03	3.553E-06	1.437E-06	0.429
1997.86	8.89	3.911E-04	2.902E-03	9.318E-03	3.639E-06	1.590E-06	0.393
1997.85	9.19	3.859E-04	2.808E-03	9.388E-03	3.794E-06	1.587E-06	0.375
1997.83	9.49	3.787E-04	2.599E-03	9.371E-03	3.706E-06	1.498E-06	0.391
1997.82	9.79	3.785E-04	2.440E-03	9.364E-03	3.674E-06	1.549E-06	0.442
1997.80	10.09	3.576E-04	2.574E-03	9.291E-03	3.709E-06	1.578E-06	0.471
1997.79	10.40	3.454E-04	2.205E-03	9.505E-03	3.902E-06	1.778E-06	0.419
1997.77	10.70	3.801E-04	2.518E-03	9.241E-03	3.691E-06	1.536E-06	0.349
1997.76	11.00	3.882E-04	2.715E-03	9.257E-03	3.707E-06	1.464E-06	0.333
1997.74	11.30	3.971E-04	2.484E-03	9.109E-03	3.710E-06	1.451E-06	0.340
1997.73	11.61	4.037E-04	2.570E-03	9.045E-03	3.648E-06	1.450E-06	0.365
1997.71	11.91	4.083E-04	2.757E-03	9.008E-03	3.658E-06	1.479E-06	0.383
1997.70	12.21	4.069E-04	2.743E-03	9.006E-03	3.645E-06	1.439E-06	0.385
1997.68	12.51	4.026E-04	2.618E-03	9.034E-03	3.715E-06	1.511E-06	0.361
1997.67	12.81	4.110E-04	2.484E-03	9.078E-03	3.751E-06	1.581E-06	0.329
1997.65	13.12	4.049E-04	2.325E-03	9.218E-03	3.741E-06	1.593E-06	0.306
1997.64	13.42	4.185E-04	2.352E-03	9.095E-03	3.650E-06	1.560E-06	0.293
1997.62	13.72	3.974E-04	2.246E-03	9.329E-03	3.804E-06	1.608E-06	0.272
1997.61	14.02	4.120E-04	2.476E-03	9.204E-03	3.737E-06	1.528E-06	0.266
1997.59	14.33	3.979E-04	2.151E-03	9.366E-03	3.764E-06	1.688E-06	0.260
1997.58	14.63	4.188E-04	2.214E-03	9.322E-03	3.764E-06	1.654E-06	0.232
1997.56	14.93	4.056E-04	2.285E-03	9.424E-03	3.835E-06	1.684E-06	0.218
1997.55	15.23	4.240E-04	2.118E-03	9.475E-03	3.778E-06	1.738E-06	0.206
1997.53	15.53	4.256E-04	2.219E-03	9.544E-03	3.923E-06	1.810E-06	0.196
1997.52	15.84	4.480E-04	2.494E-03	9.242E-03	3.843E-06	1.613E-06	0.189

LA-ICP-MS data

Time	Distance from top (mm)	B/Ca (mol/mol)	Mg/Ca (mol/mol)	Sr/Ca (mol/mol)	Ba/Ca (mol/mol)	U/Ca (mol/mol)	Mn ($\mu g\ g^{-1}$)
1997.50	16.14	4.569E-04	2.503E-03	9.483E-03	3.992E-06	1.725E-06	0.175
1997.48	16.44	4.498E-04	2.968E-03	9.092E-03	3.910E-06	1.493E-06	0.202
1997.47	16.74	4.488E-04	2.797E-03	9.158E-03	3.980E-06	1.602E-06	0.195
1997.45	17.05	4.229E-04	2.670E-03	9.318E-03	4.058E-06	1.571E-06	0.219
1997.43	17.35	4.382E-04	3.073E-03	9.020E-03	4.010E-06	1.461E-06	0.215
1997.41	17.65	4.323E-04	2.970E-03	9.140E-03	4.047E-06	1.554E-06	0.213
1997.40	17.95	4.196E-04	2.786E-03	9.143E-03	3.935E-06	1.505E-06	0.221
1997.38	18.25	4.409E-04	3.269E-03	9.020E-03	3.811E-06	1.422E-06	0.217
1997.36	18.56	4.408E-04	3.184E-03	9.033E-03	3.709E-06	1.436E-06	0.194
1997.35	18.86	4.406E-04	2.703E-03	9.105E-03	3.643E-06	1.488E-06	0.182
1997.33	19.16	4.063E-04	2.815E-03	9.058E-03	4.001E-06	1.421E-06	0.200
1997.31	19.46	4.170E-04	2.820E-03	9.185E-03	4.683E-06	1.521E-06	0.233
1997.30	19.77	4.053E-04	2.665E-03	9.255E-03	5.384E-06	1.566E-06	0.264
1997.28	20.07	4.125E-04	2.787E-03	9.186E-03	5.596E-06	1.546E-06	0.290
1997.26	20.37	3.970E-04	2.727E-03	9.423E-03	5.565E-06	1.615E-06	0.296
1997.25	20.67	3.822E-04	2.762E-03	9.149E-03	5.883E-06	1.508E-06	0.278
1997.23	20.97	3.753E-04	2.457E-03	9.333E-03	5.983E-06	1.594E-06	0.253
1997.21	21.28	3.728E-04	2.699E-03	9.236E-03	5.984E-06	1.548E-06	0.237
1997.19	21.58	3.739E-04	2.443E-03	9.356E-03	6.005E-06	1.687E-06	0.217
1997.18	21.88	3.846E-04	2.481E-03	9.246E-03	5.946E-06	1.716E-06	0.228
1997.16	22.18	3.898E-04	2.981E-03	9.197E-03	6.113E-06	1.558E-06	0.297
1997.14	22.49	3.934E-04	2.851E-03	9.151E-03	5.776E-06	1.672E-06	0.306
1997.13	22.79	3.707E-04	2.787E-03	9.068E-03	4.994E-06	1.545E-06	0.307
1997.11	23.09	3.932E-04	3.090E-03	8.946E-03	4.381E-06	1.417E-06	0.328
1997.09	23.39	4.006E-04	3.388E-03	8.836E-03	3.862E-06	1.279E-06	0.331
1997.08	23.69	3.919E-04	3.328E-03	8.972E-03	3.746E-06	1.321E-06	0.309
1997.06	24.00	4.019E-04	3.395E-03	8.974E-03	3.683E-06	1.333E-06	0.305
1997.04	24.30	3.983E-04	3.190E-03	9.174E-03	3.799E-06	1.446E-06	0.304
1997.02	24.60	3.963E-04	3.082E-03	9.006E-03	3.556E-06	1.412E-06	0.261
1997.01	24.90	3.975E-04	3.491E-03	8.896E-03	3.551E-06	1.361E-06	0.244
1996.99	25.21	3.994E-04	3.254E-03	9.147E-03	3.559E-06	1.410E-06	0.234
1996.97	25.51	3.908E-04	3.033E-03	9.072E-03	3.591E-06	1.556E-06	0.254
1996.96	25.81	3.907E-04	3.265E-03	9.063E-03	3.656E-06	1.518E-06	0.286
1996.94	26.11	3.890E-04	3.579E-03	8.934E-03	3.481E-06	1.413E-06	0.299
1996.93	26.41	3.761E-04	3.298E-03	8.915E-03	3.366E-06	1.434E-06	0.290
1996.92	26.72	3.849E-04	3.062E-03	8.966E-03	3.511E-06	1.533E-06	0.296
1996.91	27.02	3.803E-04	3.080E-03	8.990E-03	3.599E-06	1.619E-06	0.337
1996.90	27.32	3.873E-04	2.952E-03	8.994E-03	3.604E-06	1.617E-06	0.341
1996.90	27.62	3.844E-04	3.131E-03	9.031E-03	3.592E-06	1.508E-06	0.340
1996.89	27.93	3.746E-04	2.926E-03	8.977E-03	4.061E-06	1.468E-06	0.325
1996.88	28.23	4.037E-04	3.176E-03	8.986E-03	3.437E-06	1.303E-06	0.308
1996.87	28.53	3.953E-04	2.939E-03	9.001E-03	3.466E-06	1.339E-06	0.296
1996.86	28.83	4.049E-04	2.869E-03	9.067E-03	3.494E-06	1.380E-06	0.285
1996.85	29.13	4.080E-04	3.041E-03	8.908E-03	3.416E-06	1.317E-06	0.273
1996.84	29.44	4.105E-04	2.922E-03	9.084E-03	3.488E-06	1.391E-06	0.293
1996.83	29.74	4.047E-04	2.650E-03	9.167E-03	3.644E-06	1.476E-06	0.279
1996.83	30.04	4.273E-04	2.792E-03	9.162E-03	3.579E-06	1.454E-06	0.258
1996.82	30.34	4.237E-04	2.650E-03	9.139E-03	3.585E-06	1.475E-06	0.228
1996.81	30.65	4.075E-04	2.561E-03	9.310E-03	3.792E-06	1.640E-06	0.218
1996.80	30.95	4.147E-04	2.874E-03	9.163E-03	3.584E-06	1.467E-06	0.230
1996.79	31.25	4.063E-04	2.993E-03	9.113E-03	3.570E-06	1.467E-06	0.237
1996.78	31.55	4.066E-04	2.723E-03	9.316E-03	3.617E-06	1.603E-06	0.238
1996.77	31.85	4.256E-04	2.980E-03	8.961E-03	3.460E-06	1.318E-06	0.223
1996.76	32.16	3.791E-04	2.847E-03	8.735E-03	3.264E-06	1.208E-06	0.238
1996.75	32.46	3.991E-04	2.670E-03	8.833E-03	3.284E-06	1.302E-06	0.238

Time	Distance from top (mm)	B/Ca (mol/mol)	Mg/Ca (mol/mol)	Sr/Ca (mol/mol)	Ba/Ca (mol/mol)	U/Ca (mol/mol)	Mn ($\mu g\ g^{-1}$)
1996.75	32.76	4.122E-04	2.624E-03	8.907E-03	3.489E-06	1.310E-06	0.229
1996.74	33.06	4.307E-04	2.632E-03	8.974E-03	3.544E-06	1.322E-06	0.219
1996.73	33.37	4.191E-04	2.647E-03	8.866E-03	3.469E-06	1.313E-06	0.214
1996.72	33.67	4.301E-04	2.714E-03	8.995E-03	3.625E-06	1.332E-06	0.209
1996.71	33.97	4.171E-04	2.712E-03	8.926E-03	3.591E-06	1.295E-06	0.173
1996.70	34.27	4.293E-04	2.885E-03	8.964E-03	3.574E-06	1.273E-06	0.179
1996.69	34.57	4.090E-04	2.777E-03	8.915E-03	3.519E-06	1.315E-06	0.184
1996.68	34.88	4.120E-04	3.122E-03	8.924E-03	3.631E-06	1.285E-06	0.202
1996.67	35.18	4.132E-04	2.877E-03	8.931E-03	3.488E-06	1.327E-06	0.205
1996.67	35.48	4.397E-04	3.079E-03	8.878E-03	3.319E-06	1.291E-06	0.201
1996.66	35.78	4.247E-04	2.829E-03	9.095E-03	3.233E-06	1.434E-06	0.194
1996.65	36.09	4.374E-04	2.766E-03	9.279E-03	2.966E-06	1.513E-06	0.171
1996.64	36.39	4.253E-04	2.697E-03	9.240E-03	2.768E-06	1.525E-06	0.188
1996.63	36.69	4.282E-04	2.618E-03	9.311E-03	3.012E-06	1.573E-06	0.195
1996.62	36.99	4.312E-04	2.604E-03	9.305E-03	3.329E-06	1.612E-06	0.163
1996.60	37.29	4.282E-04	2.605E-03	9.309E-03	3.447E-06	1.642E-06	0.145
1996.58	37.60	4.218E-04	2.682E-03	9.405E-03	3.684E-06	1.621E-06	0.150
1996.56	37.90	4.392E-04	3.025E-03	9.411E-03	3.928E-06	1.532E-06	0.155
1996.54	38.20	4.261E-04	2.735E-03	9.185E-03	3.656E-06	1.549E-06	0.156
1996.52	38.50	4.300E-04	2.676E-03	9.220E-03	3.810E-06	1.555E-06	0.211
1996.50	38.81	4.379E-04	3.037E-03	8.971E-03	3.748E-06	1.444E-06	0.288
1996.48	39.11	4.101E-04	3.293E-03	8.881E-03	3.867E-06	1.321E-06	0.250
1996.46	39.41	4.139E-04	3.213E-03	8.879E-03	3.960E-06	1.328E-06	0.259
1996.43	39.71	3.927E-04	2.943E-03	8.990E-03	3.869E-06	1.397E-06	0.256
1996.41	40.01	3.827E-04	3.122E-03	8.991E-03	3.864E-06	1.486E-06	0.267
1996.39	40.32	4.138E-04	2.899E-03	9.091E-03	4.182E-06	1.484E-06	0.265
1996.37	40.62	4.353E-04	3.044E-03	8.867E-03	4.029E-06	1.406E-06	0.259
1996.35	41.04	4.187E-04	2.994E-03	8.771E-03	3.768E-06	1.280E-06	0.228
1996.33	41.38	4.505E-04	3.461E-03	8.686E-03	3.697E-06	1.241E-06	0.225
1996.31	41.71	4.273E-04	3.512E-03	8.803E-03	3.735E-06	1.323E-06	0.241
1996.29	42.05	4.413E-04	3.685E-03	8.749E-03	3.963E-06	1.236E-06	0.244
1996.26	42.39	4.519E-04	3.323E-03	8.822E-03	3.954E-06	1.330E-06	0.222
1996.22	42.73	4.562E-04	3.402E-03	8.845E-03	3.994E-06	1.345E-06	0.206
1996.18	43.07	4.556E-04	3.363E-03	8.927E-03	4.064E-06	1.434E-06	0.243
1996.15	43.41	4.404E-04	3.222E-03	8.869E-03	4.266E-06	1.405E-06	0.273
1996.11	43.75	4.272E-04	3.503E-03	8.865E-03	4.609E-06	1.299E-06	0.265
1996.08	44.09	4.129E-04	3.924E-03	8.770E-03	5.032E-06	1.261E-06	0.268
1996.07	44.43	4.047E-04	3.651E-03	8.672E-03	4.747E-06	1.286E-06	0.332
1996.05	44.77	3.893E-04	3.382E-03	8.900E-03	4.565E-06	1.443E-06	0.285
1996.04	45.11	3.951E-04	3.483E-03	8.783E-03	4.864E-06	1.295E-06	0.312
1996.03	45.45	3.875E-04	3.418E-03	8.825E-03	4.716E-06	1.322E-06	0.378
1996.02	45.79	3.911E-04	3.656E-03	8.837E-03	4.567E-06	1.371E-06	0.420
1996.00	46.13	3.967E-04	3.663E-03	8.769E-03	4.737E-06	1.404E-06	0.418
1995.99	46.47	4.122E-04	3.461E-03	8.812E-03	4.824E-06	1.381E-06	0.371
1995.98	46.81	3.885E-04	3.432E-03	8.774E-03	4.475E-06	1.337E-06	0.321
1995.96	47.15	3.902E-04	3.336E-03	8.744E-03	4.215E-06	1.432E-06	0.286
1995.95	47.49	3.944E-04	3.250E-03	8.798E-03	3.999E-06	1.503E-06	0.277
1995.94	47.83	3.937E-04	3.579E-03	8.695E-03	3.836E-06	1.482E-06	0.307
1995.93	48.17	4.269E-04	3.606E-03	8.798E-03	3.762E-06	1.447E-06	0.354
1995.91	48.51	4.295E-04	3.359E-03	8.748E-03	3.750E-06	1.453E-06	0.356
1995.90	48.85	4.279E-04	3.403E-03	8.832E-03	3.800E-06	1.441E-06	0.329
1995.89	49.19	4.325E-04	3.407E-03	8.794E-03	3.820E-06	1.358E-06	0.336
1995.87	49.53	4.304E-04	3.267E-03	8.764E-03	3.961E-06	1.365E-06	0.320
1995.86	49.86	4.319E-04	3.148E-03	8.873E-03	4.440E-06	1.366E-06	0.321
1995.85	50.20	4.255E-04	2.831E-03	8.763E-03	4.322E-06	1.371E-06	0.298

LA-ICP-MS data

Time	Distance from top (mm)	B/Ca (mol/mol)	Mg/Ca (mol/mol)	Sr/Ca (mol/mol)	Ba/Ca (mol/mol)	U/Ca (mol/mol)	Mn ($\mu g\ g^{-1}$)
1995.84	50.54	4.215E-04	2.707E-03	9.035E-03	4.426E-06	1.440E-06	0.282
1995.82	50.88	4.310E-04	2.678E-03	9.031E-03	4.046E-06	1.462E-06	0.274
1995.81	51.22	4.244E-04	3.102E-03	8.781E-03	3.626E-06	1.376E-06	0.294
1995.80	51.56	4.088E-04	2.924E-03	8.899E-03	3.650E-06	1.385E-06	0.310
1995.78	51.90	3.933E-04	2.999E-03	8.670E-03	3.614E-06	1.327E-06	0.266
1995.77	52.24	4.382E-04	2.752E-03	8.869E-03	3.683E-06	1.451E-06	0.252
1995.76	52.58	4.364E-04	2.501E-03	9.057E-03	3.610E-06	1.523E-06	0.257
1995.75	52.92	4.357E-04	2.630E-03	8.974E-03	3.448E-06	1.451E-06	0.239
1995.73	53.26	4.470E-04	2.562E-03	9.019E-03	3.570E-06	1.442E-06	0.216
1995.72	53.60	4.408E-04	2.638E-03	8.956E-03	3.627E-06	1.450E-06	0.218
1995.71	53.94	4.345E-04	2.697E-03	8.767E-03	3.560E-06	1.362E-06	0.251
1995.69	54.28	4.278E-04	2.577E-03	8.854E-03	3.519E-06	1.413E-06	0.234
1995.68	54.62	4.352E-04	2.513E-03	8.824E-03	3.534E-06	1.452E-06	0.232
1995.67	54.96	4.646E-04	2.683E-03	8.936E-03	3.689E-06	1.418E-06	0.204
1995.66	55.30	4.649E-04	2.392E-03	9.040E-03	3.609E-06	1.544E-06	0.189
1995.64	55.64	4.783E-04	2.484E-03	9.108E-03	3.668E-06	1.543E-06	0.172
1995.63	55.98	4.815E-04	2.161E-03	9.232E-03	3.617E-06	1.641E-06	0.149
1995.60	56.32	4.927E-04	2.662E-03	9.107E-03	3.792E-06	1.538E-06	0.180
1995.58	56.66	4.979E-04	3.143E-03	9.149E-03	3.827E-06	1.541E-06	0.205
1995.55	57.00	4.753E-04	2.537E-03	9.164E-03	3.711E-06	1.595E-06	0.187
1995.52	57.34	4.777E-04	2.736E-03	9.070E-03	3.720E-06	1.476E-06	0.213
1995.49	57.68	4.675E-04	2.565E-03	9.062E-03	3.662E-06	1.545E-06	0.166
1995.47	58.01	4.707E-04	2.578E-03	9.120E-03	3.703E-06	1.571E-06	0.161
1995.44	58.35	4.859E-04	2.796E-03	9.082E-03	3.934E-06	1.509E-06	0.170
1995.41	58.69	4.668E-04	2.800E-03	9.036E-03	3.778E-06	1.445E-06	0.174
1995.39	59.03	4.600E-04	3.005E-03	9.113E-03	4.101E-06	1.428E-06	0.174
1995.36	59.37	4.689E-04	3.183E-03	8.950E-03	3.835E-06	1.356E-06	0.201
1995.33	59.71	4.570E-04	3.505E-03	8.888E-03	3.767E-06	1.269E-06	0.211
1995.30	60.05	4.167E-04	3.009E-03	9.056E-03	3.826E-06	1.486E-06	0.224
1995.28	60.39	4.372E-04	3.453E-03	8.970E-03	3.801E-06	1.333E-06	0.202
1995.25	60.73	4.497E-04	3.780E-03	8.909E-03	3.838E-06	1.316E-06	0.210
1995.24	61.07	4.458E-04	3.483E-03	8.990E-03	4.014E-06	1.397E-06	0.237
1995.23	61.41	4.606E-04	3.749E-03	8.934E-03	4.187E-06	1.333E-06	0.253
1995.22	61.75	4.295E-04	3.536E-03	8.918E-03	4.257E-06	1.401E-06	0.307
1995.21	62.09	4.341E-04	3.366E-03	8.932E-03	4.272E-06	1.388E-06	0.311
1995.19	62.43	4.296E-04	3.137E-03	9.011E-03	4.402E-06	1.473E-06	0.293
1995.18	62.77	4.309E-04	3.052E-03	9.081E-03	4.324E-06	1.591E-06	0.312
1995.17	63.11	4.882E-04	3.362E-03	9.011E-03	4.231E-06	1.491E-06	0.336
1995.16	63.45	4.596E-04	3.515E-03	8.867E-03	3.931E-06	1.356E-06	0.309
1995.15	63.79	4.405E-04	3.462E-03	8.946E-03	3.965E-06	1.428E-06	0.269
1995.14	64.13	4.480E-04	3.284E-03	9.046E-03	3.974E-06	1.467E-06	0.249
1995.13	64.47	4.329E-04	3.527E-03	8.964E-03	3.998E-06	1.340E-06	0.249
1995.12	64.81	4.234E-04	3.520E-03	8.974E-03	3.961E-06	1.394E-06	0.254
1995.11	65.15	4.180E-04	3.377E-03	8.983E-03	3.987E-06	1.408E-06	0.275
1995.09	65.49	4.091E-04	3.498E-03	8.881E-03	3.874E-06	1.303E-06	0.292
1995.08	65.82	3.996E-04	3.196E-03	8.799E-03	3.797E-06	1.318E-06	0.300
1995.07	66.16	4.232E-04	3.286E-03	8.829E-03	3.723E-06	1.257E-06	0.276
1995.06	66.50	4.338E-04	3.308E-03	8.888E-03	3.905E-06	1.367E-06	0.273
1995.05	66.84	3.870E-04	2.913E-03	8.916E-03	4.222E-06	1.403E-06	0.314
1995.04	67.18	3.825E-04	3.044E-03	8.813E-03	4.249E-06	1.325E-06	0.386
1995.03	67.52	3.913E-04	3.026E-03	8.756E-03	3.905E-06	1.282E-06	0.382
1995.02	67.86	3.954E-04	2.873E-03	8.904E-03	4.146E-06	1.445E-06	0.368
1995.01	68.20	3.994E-04	2.956E-03	8.905E-03	3.767E-06	1.361E-06	0.380
1994.99	68.54	4.156E-04	3.210E-03	8.790E-03	3.645E-06	1.278E-06	0.427
1994.98	68.88	4.445E-04	3.445E-03	8.758E-03	3.692E-06	1.282E-06	0.433

Time	Distance from top (mm)	B/Ca (mol/mol)	Mg/Ca (mol/mol)	Sr/Ca (mol/mol)	Ba/Ca (mol/mol)	U/Ca (mol/mol)	Mn ($\mu g\ g^{-1}$)
1994.97	69.22	4.250E-04	3.326E-03	8.711E-03	3.607E-06	1.235E-06	0.438
1994.96	69.56	4.164E-04	3.363E-03	8.800E-03	3.709E-06	1.250E-06	0.429
1994.95	69.90	4.195E-04	3.420E-03	8.831E-03	3.691E-06	1.274E-06	0.514
1994.94	70.24	3.980E-04	3.646E-03	8.845E-03	3.875E-06	1.239E-06	0.617
1994.93	70.58	4.023E-04	3.574E-03	8.832E-03	3.767E-06	1.291E-06	0.554
1994.92	70.92	3.921E-04	3.471E-03	8.706E-03	3.714E-06	1.273E-06	0.474
1994.91	71.26	3.865E-04	3.224E-03	8.626E-03	3.497E-06	1.210E-06	0.350
1994.89	71.60	3.887E-04	3.510E-03	8.688E-03	3.523E-06	1.151E-06	0.300
1994.88	71.94	3.896E-04	3.479E-03	8.690E-03	3.480E-06	1.162E-06	0.323
1994.87	72.28	4.154E-04	3.546E-03	8.849E-03	3.532E-06	1.238E-06	0.310
1994.86	72.62	4.184E-04	3.407E-03	8.730E-03	3.595E-06	1.294E-06	0.294
1994.85	72.96	4.263E-04	3.221E-03	8.942E-03	3.746E-06	1.448E-06	0.297
1994.84	73.30	4.111E-04	3.224E-03	8.985E-03	3.826E-06	1.476E-06	0.314
1994.83	73.64	4.068E-04	3.210E-03	8.958E-03	3.728E-06	1.423E-06	0.309
1994.82	73.97	4.103E-04	2.826E-03	9.014E-03	3.727E-06	1.540E-06	0.301
1994.81	74.31	4.278E-04	2.937E-03	8.986E-03	3.622E-06	1.478E-06	0.300
1994.79	74.65	4.392E-04	2.917E-03	9.014E-03	3.621E-06	1.381E-06	0.307
1994.78	74.99	4.259E-04	3.010E-03	8.955E-03	3.708E-06	1.372E-06	0.303
1994.77	75.33	4.466E-04	3.027E-03	8.974E-03	3.843E-06	1.409E-06	0.298
1994.76	75.67	4.204E-04	3.026E-03	8.938E-03	3.948E-06	1.404E-06	0.296
1994.75	76.01	4.223E-04	3.131E-03	8.868E-03	3.866E-06	1.381E-06	0.286
1994.74	76.35	4.237E-04	3.050E-03	8.954E-03	3.571E-06	1.392E-06	0.303
1994.73	76.69	4.084E-04	2.904E-03	8.823E-03	3.422E-06	1.404E-06	0.338
1994.72	77.03	3.979E-04	3.024E-03	8.811E-03	3.432E-06	1.319E-06	0.326
1994.71	77.37	4.169E-04	2.918E-03	8.874E-03	3.509E-06	1.433E-06	0.300
1994.69	77.71	4.258E-04	2.777E-03	9.007E-03	3.642E-06	1.514E-06	0.310
1994.68	78.05	4.316E-04	2.686E-03	9.038E-03	3.683E-06	1.431E-06	0.295
1994.67	78.39	4.368E-04	2.749E-03	8.957E-03	3.588E-06	1.399E-06	0.225
1994.66	78.73	4.328E-04	2.776E-03	8.907E-03	3.577E-06	1.397E-06	0.196
1994.65	79.07	4.515E-04	2.590E-03	9.266E-03	3.736E-06	1.518E-06	0.204
1994.64	79.41	4.762E-04	2.628E-03	9.032E-03	3.822E-06	1.514E-06	0.222
1994.63	79.75	4.762E-04	2.428E-03	9.348E-03	3.826E-06	1.614E-06	0.204
1994.61	80.09	4.575E-04	2.712E-03	9.161E-03	3.818E-06	1.552E-06	0.188
1994.60	80.43	4.857E-04	3.019E-03	9.096E-03	3.949E-06	1.454E-06	0.168
1994.58	80.77	4.587E-04	2.737E-03	9.115E-03	3.785E-06	1.489E-06	0.155
1994.57	81.11	4.528E-04	2.693E-03	9.124E-03	3.910E-06	1.511E-06	0.162
1994.55	81.45	4.415E-04	2.859E-03	8.967E-03	3.864E-06	1.453E-06	0.174
1994.54	81.79	4.592E-04	3.037E-03	9.151E-03	4.009E-06	1.533E-06	0.176
1994.52	82.12	4.578E-04	3.298E-03	9.004E-03	4.032E-06	1.425E-06	0.168
1994.51	82.46	4.149E-04	3.121E-03	8.841E-03	3.863E-06	1.369E-06	0.162
1994.49	82.82	4.343E-04	3.544E-03	8.930E-03	3.922E-06	1.372E-06	0.181
1994.48	83.12	4.364E-04	3.771E-03	8.973E-03	3.908E-06	1.358E-06	0.161
1994.46	83.43	4.283E-04	3.718E-03	9.050E-03	3.850E-06	1.402E-06	0.179
1994.45	83.73	4.243E-04	3.614E-03	9.040E-03	3.817E-06	1.393E-06	0.201
1994.43	84.04	4.164E-04	3.687E-03	9.025E-03	3.896E-06	1.346E-06	0.204
1994.42	84.34	4.169E-04	3.526E-03	9.001E-03	4.006E-06	1.365E-06	0.204
1994.40	84.64	4.331E-04	3.637E-03	8.935E-03	4.148E-06	1.368E-06	0.212
1994.38	84.95	4.053E-04	3.785E-03	8.941E-03	4.131E-06	1.227E-06	0.218
1994.37	85.25	4.062E-04	3.218E-03	8.961E-03	4.154E-06	1.395E-06	0.216
1994.35	85.55	4.110E-04	3.297E-03	8.976E-03	4.154E-06	1.378E-06	0.215
1994.34	85.86	4.076E-04	3.430E-03	8.844E-03	4.268E-06	1.284E-06	0.207
1994.32	86.16	4.057E-04	3.405E-03	8.863E-03	4.650E-06	1.298E-06	0.185
1994.31	86.46	4.245E-04	2.997E-03	9.135E-03	4.987E-06	1.521E-06	0.207
1994.29	86.77	4.375E-04	3.309E-03	8.887E-03	4.641E-06	1.369E-06	0.228
1994.28	87.07	4.114E-04	3.567E-03	8.792E-03	4.156E-06	1.259E-06	0.229
1994.26	87.37	4.212E-04	3.174E-03	8.947E-03	4.122E-06	1.337E-06	0.252

LA-ICP-MS data

Time	Distance from top (mm)	B/Ca (mol/mol)	Mg/Ca (mol/mol)	Sr/Ca (mol/mol)	Ba/Ca (mol/mol)	U/Ca (mol/mol)	Mn ($\mu g\ g^{-1}$)
1994.25	87.68	4.031E-04	3.133E-03	8.934E-03	4.030E-06	1.370E-06	0.269
1994.23	87.98	3.945E-04	3.243E-03	8.808E-03	4.014E-06	1.301E-06	0.271
1994.22	88.28	3.879E-04	3.116E-03	8.818E-03	3.922E-06	1.310E-06	0.262
1994.20	88.59	4.170E-04	3.474E-03	8.905E-03	3.854E-06	1.235E-06	0.235
1994.18	88.89	4.088E-04	3.510E-03	8.882E-03	3.833E-06	1.207E-06	0.227
1994.17	89.19	4.077E-04	3.711E-03	8.706E-03	3.869E-06	1.154E-06	0.245
1994.15	89.50	3.747E-04	3.644E-03	8.577E-03	3.771E-06	1.080E-06	0.310
1994.14	89.80	3.688E-04	3.864E-03	8.801E-03	4.160E-06	1.187E-06	0.413
1994.12	90.11	3.776E-04	3.935E-03	8.871E-03	4.233E-06	1.197E-06	0.419
1994.11	90.41	3.689E-04	3.636E-03	8.810E-03	3.961E-06	1.202E-06	0.372
1994.09	90.71	3.666E-04	3.833E-03	8.835E-03	3.782E-06	1.209E-06	0.455
1994.08	91.02	3.668E-04	3.878E-03	8.826E-03	3.808E-06	1.257E-06	0.543
1994.06	91.32	3.582E-04	3.734E-03	8.946E-03	3.932E-06	1.339E-06	0.527
1994.05	91.62	3.529E-04	3.966E-03	8.858E-03	4.036E-06	1.250E-06	0.458
1994.03	91.93	3.768E-04	4.086E-03	8.879E-03	3.963E-06	1.272E-06	0.381
1994.02	92.23	3.656E-04	3.438E-03	9.018E-03	3.981E-06	1.421E-06	0.373
1994.00	92.53	3.548E-04	3.247E-03	8.894E-03	3.809E-06	1.350E-06	0.381
1993.99	92.84	3.693E-04	3.605E-03	8.814E-03	3.838E-06	1.229E-06	0.414
1993.97	93.14	3.653E-04	3.746E-03	8.767E-03	3.839E-06	1.164E-06	0.431
1993.95	93.44	3.815E-04	3.759E-03	8.902E-03	3.891E-06	1.216E-06	0.423
1993.94	93.75	3.843E-04	3.887E-03	8.766E-03	3.704E-06	1.157E-06	0.394
1993.92	94.05	3.860E-04	3.617E-03	9.014E-03	3.749E-06	1.637E-06	0.330
1993.91	94.35	3.697E-04	3.428E-03	9.051E-03	3.642E-06	1.420E-06	0.286
1993.89	94.66	3.921E-04	3.333E-03	8.924E-03	3.759E-06	1.356E-06	0.259
1993.88	94.96	3.942E-04	3.398E-03	8.833E-03	3.558E-06	1.252E-06	0.263
1993.86	95.26	3.917E-04	3.481E-03	8.822E-03	3.492E-06	1.245E-06	0.275
1993.85	95.57	4.039E-04	3.375E-03	8.841E-03	3.661E-06	1.275E-06	0.283
1993.83	95.87	3.917E-04	3.452E-03	8.916E-03	3.784E-06	1.392E-06	0.301
1993.82	96.18	3.945E-04	3.341E-03	9.027E-03	3.792E-06	1.393E-06	0.280
1993.80	96.48	3.924E-04	3.447E-03	8.894E-03	3.713E-06	1.320E-06	0.252
1993.79	96.78	3.997E-04	3.270E-03	8.898E-03	3.740E-06	1.349E-06	0.245
1993.77	97.09	3.821E-04	2.973E-03	8.955E-03	3.648E-06	1.692E-06	0.236
1993.75	97.39	3.956E-04	3.217E-03	8.895E-03	3.685E-06	1.301E-06	0.238
1993.74	97.69	4.093E-04	3.265E-03	9.024E-03	3.850E-06	1.333E-06	0.260
1993.72	98.00	4.025E-04	3.108E-03	8.942E-03	3.764E-06	1.404E-06	0.266
1993.71	98.30	4.093E-04	3.196E-03	8.977E-03	3.789E-06	1.355E-06	0.258
1993.69	98.60	4.164E-04	3.160E-03	8.981E-03	3.917E-06	1.356E-06	0.241
1993.68	98.91	3.962E-04	3.284E-03	8.968E-03	3.869E-06	1.364E-06	0.240
1993.66	99.21	4.133E-04	3.184E-03	8.943E-03	3.758E-06	1.328E-06	0.248
1993.65	99.51	4.258E-04	3.027E-03	8.934E-03	3.741E-06	1.326E-06	0.194
1993.63	99.82	4.317E-04	2.904E-03	9.014E-03	3.849E-06	1.370E-06	0.163
1993.62	100.12	4.373E-04	2.840E-03	8.960E-03	3.894E-06	1.417E-06	0.205
1993.60	100.42	4.491E-04	2.958E-03	8.995E-03	3.860E-06	1.340E-06	0.225
1993.59	100.73	4.466E-04	2.967E-03	9.044E-03	3.923E-06	1.369E-06	0.216
1993.57	101.03	4.615E-04	2.863E-03	9.264E-03	4.079E-06	1.615E-06	0.197
1993.56	101.33	4.637E-04	2.980E-03	9.191E-03	4.182E-06	1.531E-06	0.190
1993.54	101.64	4.466E-04	2.816E-03	9.189E-03	4.102E-06	1.517E-06	0.228
1993.52	101.94	4.427E-04	2.791E-03	9.091E-03	4.131E-06	1.477E-06	0.251
1993.51	102.25	4.455E-04	2.974E-03	9.166E-03	4.097E-06	1.427E-06	0.222
1993.49	102.55	4.580E-04	3.153E-03	9.134E-03	4.084E-06	1.466E-06	0.194
1993.47	102.85	4.537E-04	3.126E-03	9.151E-03	4.031E-06	1.481E-06	0.186
1993.45	103.16	4.599E-04	3.069E-03	9.213E-03	4.073E-06	1.546E-06	0.159
1993.44	103.46	4.601E-04	3.051E-03	9.133E-03	4.001E-06	1.504E-06	0.143
1993.42	103.76	4.611E-04	3.411E-03	9.026E-03	4.135E-06	1.372E-06	0.155
1993.40	104.07	4.407E-04	3.288E-03	8.982E-03	4.012E-06	1.339E-06	0.154
1993.38	104.37	4.335E-04	3.309E-03	8.944E-03	3.978E-06	1.348E-06	0.157

Time	Distance from top (mm)	B/Ca (mol/mol)	Mg/Ca (mol/mol)	Sr/Ca (mol/mol)	Ba/Ca (mol/mol)	U/Ca (mol/mol)	Mn ($\mu g\ g^{-1}$)
1993.37	104.67	4.184E-04	3.191E-03	9.091E-03	3.893E-06	1.425E-06	0.158
1993.35	104.98	4.069E-04	3.072E-03	9.116E-03	3.966E-06	1.498E-06	0.173
1993.33	105.28	4.170E-04	3.174E-03	8.999E-03	3.867E-06	1.365E-06	0.163
1993.31	105.58	4.195E-04	3.346E-03	9.078E-03	4.001E-06	1.463E-06	0.159
1993.30	105.89	4.218E-04	3.424E-03	9.130E-03	4.028E-06	1.390E-06	0.162
1993.28	106.19	4.372E-04	3.295E-03	9.047E-03	3.944E-06	1.399E-06	0.173
1993.26	106.49	4.542E-04	3.199E-03	9.165E-03	3.935E-06	1.512E-06	0.156
1993.24	106.80	4.535E-04	2.961E-03	9.248E-03	3.948E-06	1.555E-06	0.146
1993.23	107.10	4.418E-04	3.126E-03	9.113E-03	3.946E-06	1.452E-06	0.137
1993.21	107.40	4.517E-04	3.286E-03	9.050E-03	3.880E-06	1.388E-06	0.138
1993.19	107.71	4.336E-04	3.395E-03	8.945E-03	3.862E-06	1.324E-06	0.147
1993.18	108.01	4.379E-04	3.268E-03	8.988E-03	3.934E-06	1.394E-06	0.157
1993.16	108.32	4.164E-04	3.455E-03	8.834E-03	3.946E-06	1.272E-06	0.162
1993.14	108.62	4.348E-04	3.629E-03	8.974E-03	4.227E-06	1.278E-06	0.180
1993.12	108.92	3.879E-04	4.098E-03	8.911E-03	4.157E-06	1.167E-06	0.232
1993.11	109.23	3.999E-04	4.137E-03	8.731E-03	4.130E-06	1.128E-06	0.278
1993.09	109.53	3.927E-04	3.790E-03	8.786E-03	4.081E-06	1.143E-06	0.289
1993.07	109.83	3.931E-04	3.744E-03	8.809E-03	4.041E-06	1.214E-06	0.272
1993.05	110.14	3.972E-04	3.924E-03	8.865E-03	4.242E-06	1.164E-06	0.274
1993.04	110.44	3.876E-04	3.421E-03	8.944E-03	4.256E-06	1.314E-06	0.286
1993.02	110.74	3.868E-04	3.444E-03	8.779E-03	4.072E-06	1.283E-06	0.269
1993.00	111.05	3.831E-04	3.697E-03	8.823E-03	4.067E-06	1.245E-06	0.245
1992.98	111.35	3.808E-04	3.696E-03	8.977E-03	4.208E-06	1.315E-06	0.282
1992.97	111.65	3.748E-04	3.774E-03	8.766E-03	4.052E-06	1.228E-06	0.326
1992.95	111.96	3.729E-04	3.498E-03	8.979E-03	4.200E-06	1.359E-06	0.361
1992.93	112.26	4.044E-04	2.998E-03	9.059E-03	4.173E-06	1.459E-06	0.347
1992.92	112.56	3.881E-04	3.160E-03	9.213E-03	4.152E-06	1.495E-06	0.296
1992.90	112.87	3.637E-04	3.083E-03	9.201E-03	3.890E-06	1.558E-06	0.278
1992.88	113.17	3.627E-04	3.283E-03	9.031E-03	3.833E-06	1.494E-06	0.261
1992.86	113.47	3.764E-04	2.814E-03	9.138E-03	3.991E-06	1.606E-06	0.268
1992.85	113.78	3.894E-04	2.615E-03	9.179E-03	3.718E-06	1.518E-06	0.254
1992.83	114.08	3.903E-04	3.027E-03	9.173E-03	3.722E-06	1.469E-06	0.200
1992.81	114.39	3.760E-04	2.837E-03	9.243E-03	3.752E-06	1.553E-06	0.227
1992.79	114.69	4.177E-04	3.527E-03	9.055E-03	3.823E-06	1.391E-06	0.256
1992.78	114.99	4.252E-04	3.372E-03	9.056E-03	3.669E-06	1.437E-06	0.259
1992.76	115.30	4.337E-04	2.864E-03	9.147E-03	3.657E-06	1.555E-06	0.299
1992.74	115.60	4.418E-04	2.973E-03	9.191E-03	3.768E-06	1.498E-06	0.292
1992.72	115.90	4.247E-04	3.345E-03	9.074E-03	3.729E-06	1.394E-06	0.240
1992.71	116.21	4.187E-04	3.498E-03	9.145E-03	3.771E-06	1.375E-06	0.235
1992.69	116.51	4.159E-04	3.247E-03	9.233E-03	3.770E-06	1.477E-06	0.255
1992.67	116.81	3.923E-04	2.992E-03	9.343E-03	3.737E-06	1.498E-06	0.258
1992.65	117.12	3.916E-04	3.148E-03	9.185E-03	3.786E-06	1.529E-06	0.255
1992.64	117.42	3.688E-04	2.788E-03	9.319E-03	3.682E-06	1.614E-06	0.246
1992.62	117.72	3.843E-04	2.265E-03	9.631E-03	3.825E-06	1.761E-06	0.247
1992.59	118.03	3.969E-04	2.362E-03	9.510E-03	3.679E-06	1.624E-06	0.220
1992.56	118.33	3.893E-04	2.305E-03	9.480E-03	3.779E-06	1.634E-06	0.201
1992.53	118.63	4.049E-04	2.697E-03	9.284E-03	3.862E-06	1.550E-06	0.217
1992.49	118.94	4.195E-04	2.938E-03	9.144E-03	3.917E-06	1.450E-06	0.209
1992.46	119.24	4.275E-04	2.907E-03	9.160E-03	3.953E-06	1.488E-06	0.204
1992.43	119.54	4.180E-04	2.701E-03	9.145E-03	3.944E-06	1.598E-06	0.218

Table 10.4 Pandora Reef, GBR *Porites* data 1-98a

Time	Distance from top (mm)	B/Ca (mol/mol)	Mg/Ca (mol/mol)	Sr/Ca (mol/mol)	Ba/Ca (mol/mol)	U/Ca (mol/mol)	Mn ($\mu g\ g^{-1}$)
1998.79	0.14	5.265E-04	3.414E-03	8.777E-03	4.907E-06	1.288E-06	0.194
1998.75	0.49	5.298E-04	3.082E-03	8.865E-03	4.930E-06	1.310E-06	0.188
1998.69	0.85	5.577E-04	2.940E-03	9.088E-03	4.748E-06	1.438E-06	0.185
1998.64	1.20	5.705E-04	2.879E-03	9.157E-03	4.499E-06	1.433E-06	0.222
1998.58	1.55	5.606E-04	2.686E-03	9.088E-03	4.324E-06	1.433E-06	0.259
1998.52	1.90	5.471E-04	2.615E-03	9.244E-03	4.323E-06	1.454E-06	0.271
1998.46	2.26	5.946E-04	2.898E-03	9.191E-03	4.253E-06	1.376E-06	0.282
1998.40	2.61	5.434E-04	2.830E-03	9.182E-03	4.515E-06	1.385E-06	0.278
1998.35	2.96	4.968E-04	3.229E-03	9.061E-03	4.504E-06	1.343E-06	0.262
1998.29	3.31	4.053E-04	3.511E-03	8.757E-03	4.435E-06	1.133E-06	0.261
1998.23	3.67	3.634E-04	3.446E-03	8.703E-03	4.447E-06	1.089E-06	0.249
1998.21	4.02	3.925E-04	3.857E-03	8.795E-03	4.538E-06	1.078E-06	0.240
1998.19	4.37	4.200E-04	4.033E-03	8.739E-03	4.694E-06	1.068E-06	0.252
1998.17	4.73	3.990E-04	4.086E-03	8.810E-03	5.048E-06	1.111E-06	0.249
1998.15	5.08	3.882E-04	4.564E-03	8.716E-03	5.918E-06	1.061E-06	0.241
1998.14	5.43	3.737E-04	4.787E-03	8.752E-03	6.502E-06	9.927E-07	0.259
1998.12	5.78	3.818E-04	4.475E-03	8.803E-03	6.989E-06	1.082E-06	0.275
1998.11	6.14	3.778E-04	4.297E-03	8.844E-03	6.745E-06	1.135E-06	0.311
1998.10	6.49	3.512E-04	3.958E-03	8.855E-03	6.967E-06	1.197E-06	0.323
1998.08	6.84	3.254E-04	4.162E-03	8.667E-03	9.129E-06	1.158E-06	0.318
1998.08	7.19	3.420E-04	4.037E-03	8.591E-03	9.268E-06	1.117E-06	0.267
1998.07	7.55	3.898E-04	3.588E-03	8.846E-03	8.364E-06	1.250E-06	0.290
1998.06	7.90	4.466E-04	3.498E-03	8.901E-03	6.096E-06	1.303E-06	0.339
1998.06	8.25	4.414E-04	3.073E-03	8.992E-03	4.675E-06	1.407E-06	0.326
1998.05	8.60	4.245E-04	3.030E-03	8.973E-03	3.786E-06	1.336E-06	0.347
1998.04	8.96	4.376E-04	3.324E-03	8.971E-03	3.843E-06	1.319E-06	0.359
1998.04	9.31	4.204E-04	3.700E-03	8.747E-03	3.658E-06	1.255E-06	0.345
1998.03	9.66	4.203E-04	3.542E-03	8.687E-03	3.781E-06	1.238E-06	0.282
1998.02	10.01	4.074E-04	3.514E-03	8.629E-03	3.654E-06	1.266E-06	0.237
1998.02	10.37	4.316E-04	3.713E-03	8.862E-03	3.719E-06	1.302E-06	0.237
1998.01	10.72	4.281E-04	3.751E-03	8.989E-03	3.927E-06	1.343E-06	0.342
1998.00	11.07	4.307E-04	3.671E-03	8.993E-03	3.963E-06	1.363E-06	0.439
1998.00	11.43	4.161E-04	4.021E-03	8.787E-03	3.978E-06	1.223E-06	0.418
1997.99	11.78	4.247E-04	3.824E-03	8.927E-03	3.914E-06	1.259E-06	0.289
1997.98	12.13	4.296E-04	3.578E-03	8.967E-03	3.848E-06	1.287E-06	0.265
1997.98	12.48	4.426E-04	3.548E-03	8.991E-03	3.953E-06	1.355E-06	0.261
1997.97	12.84	4.421E-04	3.799E-03	9.045E-03	3.853E-06	1.273E-06	0.264
1997.96	13.19	4.073E-04	4.135E-03	8.695E-03	3.804E-06	1.166E-06	0.268
1997.94	13.54	4.034E-04	3.623E-03	8.862E-03	3.780E-06	1.309E-06	0.227
1997.89	13.89	4.548E-04	3.389E-03	8.950E-03	3.854E-06	1.344E-06	0.187
1997.84	14.25	4.695E-04	3.362E-03	8.977E-03	3.900E-06	1.314E-06	0.172
1997.79	14.60	4.929E-04	3.019E-03	9.079E-03	3.998E-06	1.403E-06	0.154
1997.74	14.95	4.737E-04	2.940E-03	9.173E-03	3.974E-06	1.381E-06	0.162
1997.69	15.30	4.868E-04	3.114E-03	9.078E-03	4.012E-06	1.410E-06	0.167
1997.64	15.66	4.950E-04	3.262E-03	9.205E-03	3.899E-06	1.481E-06	0.157
1997.60	16.01	4.980E-04	3.063E-03	9.260E-03	4.049E-06	1.538E-06	0.152
1997.55	16.36	4.884E-04	2.904E-03	9.217E-03	4.114E-06	1.587E-06	0.167
1997.50	16.72	5.069E-04	3.004E-03	9.252E-03	4.197E-06	1.475E-06	0.182
1997.46	17.07	4.768E-04	2.719E-03	9.147E-03	4.031E-06	1.430E-06	0.180
1997.42	17.42	4.722E-04	3.082E-03	8.948E-03	4.068E-06	1.335E-06	0.194
1997.37	17.77	4.886E-04	3.282E-03	9.014E-03	4.207E-06	1.263E-06	0.212
1997.33	18.13	4.873E-04	3.553E-03	8.889E-03	4.155E-06	1.182E-06	0.200
1997.28	18.48	5.035E-04	3.606E-03	8.977E-03	4.077E-06	1.180E-06	0.193

Time	Distance from top (mm)	B/Ca (mol/mol)	Mg/Ca (mol/mol)	Sr/Ca (mol/mol)	Ba/Ca (mol/mol)	U/Ca (mol/mol)	Mn ($\mu g\ g^{-1}$)
1997.27	18.83	4.884E-04	3.482E-03	8.968E-03	3.994E-06	1.212E-06	0.213
1997.26	19.18	5.045E-04	3.380E-03	8.969E-03	4.093E-06	1.249E-06	0.226
1997.23	19.54	5.018E-04	3.476E-03	9.052E-03	4.755E-06	1.288E-06	0.251
1997.21	19.89	4.686E-04	3.653E-03	8.930E-03	5.820E-06	1.201E-06	0.225
1997.18	20.24	4.616E-04	3.547E-03	8.856E-03	6.711E-06	1.191E-06	0.229
1997.16	20.59	4.545E-04	3.724E-03	8.733E-03	7.127E-06	1.133E-06	0.243
1997.13	20.95	4.406E-04	3.467E-03	8.861E-03	6.930E-06	1.172E-06	0.269
1997.11	21.30	4.242E-04	3.357E-03	8.830E-03	7.045E-06	1.187E-06	0.258
1997.09	21.65	3.945E-04	3.421E-03	8.849E-03	7.372E-06	1.230E-06	0.254
1997.06	22.00	3.722E-04	3.739E-03	8.568E-03	6.083E-06	1.126E-06	0.245
1997.05	22.36	3.893E-04	4.026E-03	8.614E-03	4.889E-06	1.125E-06	0.276
1997.05	22.71	3.883E-04	4.184E-03	8.742E-03	4.508E-06	1.094E-06	0.272
1997.04	23.06	4.114E-04	4.310E-03	8.760E-03	3.974E-06	1.104E-06	0.298
1997.04	23.42	4.176E-04	4.115E-03	8.778E-03	3.749E-06	1.124E-06	0.295
1997.03	23.77	4.335E-04	4.181E-03	8.778E-03	3.617E-06	1.094E-06	0.270
1997.02	24.12	4.115E-04	3.957E-03	8.808E-03	3.600E-06	1.144E-06	0.282
1997.02	24.47	4.297E-04	4.620E-03	8.741E-03	3.707E-06	1.054E-06	0.308
1997.01	24.83	4.387E-04	4.439E-03	8.817E-03	3.684E-06	1.046E-06	0.301
1997.01	25.18	4.465E-04	4.042E-03	8.851E-03	3.570E-06	1.132E-06	0.313
1997.00	25.53	4.094E-04	4.343E-03	8.853E-03	3.493E-06	1.062E-06	0.309
1996.99	25.88	4.025E-04	4.445E-03	8.744E-03	3.507E-06	1.084E-06	0.394
1996.99	26.24	4.265E-04	4.147E-03	8.889E-03	3.555E-06	1.150E-06	0.423
1996.98	26.59	3.979E-04	4.014E-03	8.916E-03	3.495E-06	1.129E-06	0.491
1996.97	26.94	3.993E-04	3.917E-03	8.764E-03	3.432E-06	1.097E-06	0.471
1996.96	27.29	4.217E-04	4.194E-03	8.835E-03	3.527E-06	1.098E-06	0.563
1996.95	27.65	4.264E-04	4.463E-03	8.782E-03	3.481E-06	1.080E-06	0.662
1996.94	28.00	4.221E-04	4.305E-03	8.709E-03	3.464E-06	1.057E-06	0.586
1996.92	28.35	4.161E-04	3.896E-03	8.808E-03	3.484E-06	1.179E-06	0.500
1996.89	28.70	4.103E-04	3.500E-03	8.972E-03	3.634E-06	1.252E-06	0.343
1996.87	29.06	4.271E-04	3.408E-03	8.889E-03	3.605E-06	1.278E-06	0.323
1996.85	29.41	4.403E-04	3.382E-03	8.872E-03	3.633E-06	1.209E-06	0.312
1996.82	29.76	4.400E-04	3.217E-03	8.939E-03	3.543E-06	1.309E-06	0.317
1996.80	30.12	4.474E-04	2.887E-03	8.976E-03	3.672E-06	1.414E-06	0.334
1996.77	30.47	4.389E-04	3.086E-03	8.887E-03	3.465E-06	1.295E-06	0.296
1996.75	30.82	4.524E-04	2.917E-03	9.106E-03	3.543E-06	1.362E-06	0.246
1996.73	31.17	4.585E-04	3.023E-03	9.068E-03	3.585E-06	1.310E-06	0.213
1996.70	31.53	4.674E-04	3.215E-03	9.082E-03	3.760E-06	1.336E-06	0.215
1996.68	31.88	4.912E-04	3.194E-03	9.091E-03	3.788E-06	1.308E-06	0.233
1996.66	32.23	4.721E-04	3.017E-03	9.169E-03	3.726E-06	1.360E-06	0.272
1996.64	32.58	4.652E-04	2.966E-03	9.172E-03	3.559E-06	1.335E-06	0.254
1996.62	32.94	4.663E-04	2.982E-03	9.320E-03	3.505E-06	1.444E-06	0.202
1996.59	33.29	4.725E-04	2.927E-03	9.300E-03	3.289E-06	1.380E-06	0.178
1996.57	33.64	4.869E-04	2.977E-03	9.138E-03	2.927E-06	1.396E-06	0.198
1996.56	33.99	4.528E-04	3.179E-03	9.144E-03	3.002E-06	1.327E-06	0.220
1996.54	34.35	4.875E-04	3.187E-03	9.252E-03	3.245E-06	1.390E-06	0.224
1996.51	34.70	4.919E-04	3.177E-03	9.430E-03	3.611E-06	1.490E-06	0.219
1996.50	35.05	4.707E-04	3.591E-03	9.052E-03	3.774E-06	1.232E-06	0.184
1996.48	35.40	4.765E-04	3.450E-03	9.036E-03	3.860E-06	1.295E-06	0.170
1996.46	35.76	4.775E-04	3.607E-03	9.112E-03	4.045E-06	1.321E-06	0.187
1996.43	36.11	4.582E-04	3.793E-03	8.973E-03	4.038E-06	1.309E-06	0.196
1996.42	36.46	4.390E-04	3.904E-03	9.104E-03	4.064E-06	1.372E-06	0.188
1996.40	36.82	4.361E-04	3.574E-03	9.038E-03	4.071E-06	1.303E-06	0.253
1996.38	37.17	4.325E-04	3.675E-03	8.926E-03	4.076E-06	1.213E-06	0.318
1996.36	37.52	4.417E-04	3.517E-03	8.827E-03	3.954E-06	1.240E-06	0.342
1996.34	37.87	4.733E-04	3.763E-03	8.952E-03	4.027E-06	1.221E-06	0.369

LA-ICP-MS data

Time	Distance from top (mm)	B/Ca (mol/mol)	Mg/Ca (mol/mol)	Sr/Ca (mol/mol)	Ba/Ca (mol/mol)	U/Ca (mol/mol)	Mn ($\mu g\ g^{-1}$)
1996.32	38.23	4.628E-04	3.690E-03	9.011E-03	3.964E-06	1.261E-06	0.394
1996.30	38.58	4.211E-04	3.730E-03	8.976E-03	3.825E-06	1.219E-06	0.334
1996.28	38.93	4.173E-04	3.599E-03	8.971E-03	3.794E-06	1.316E-06	0.322
1996.26	39.28	4.295E-04	3.396E-03	8.839E-03	4.029E-06	1.237E-06	0.319
1996.24	39.64	4.399E-04	3.994E-03	8.981E-03	4.164E-06	1.149E-06	0.360
1996.22	39.99	4.219E-04	3.869E-03	8.997E-03	4.243E-06	1.227E-06	0.385
1996.20	40.34	3.855E-04	4.481E-03	8.806E-03	4.872E-06	1.118E-06	0.341
1996.18	40.69	4.072E-04	4.301E-03	8.722E-03	5.124E-06	1.117E-06	0.328
1996.16	41.05	3.753E-04	4.230E-03	8.690E-03	4.995E-06	1.051E-06	0.356
1996.14	41.40	3.853E-04	3.835E-03	8.614E-03	4.834E-06	1.121E-06	0.334
1996.12	41.75	3.998E-04	3.853E-03	8.816E-03	4.645E-06	1.188E-06	0.373
1996.10	42.11	3.846E-04	4.015E-03	8.695E-03	4.279E-06	1.170E-06	0.400
1996.07	42.46	3.767E-04	4.048E-03	8.644E-03	4.465E-06	1.189E-06	0.527
1996.06	42.81	4.130E-04	4.024E-03	8.789E-03	4.125E-06	1.267E-06	0.526
1996.04	43.16	4.276E-04	3.975E-03	8.727E-03	3.761E-06	1.214E-06	0.635
1996.02	43.52	4.310E-04	3.849E-03	8.765E-03	3.625E-06	1.141E-06	0.681
1996.00	43.87	4.171E-04	4.130E-03	8.663E-03	3.610E-06	1.122E-06	0.541
1995.98	44.22	4.261E-04	4.075E-03	8.784E-03	3.562E-06	1.103E-06	0.465
1995.96	44.57	4.279E-04	4.145E-03	8.601E-03	3.369E-06	1.055E-06	0.479
1995.94	44.93	4.421E-04	4.080E-03	8.653E-03	3.496E-06	1.059E-06	0.503
1995.92	45.28	4.398E-04	4.326E-03	8.658E-03	3.513E-06	1.038E-06	0.446
1995.90	45.63	4.458E-04	3.989E-03	8.643E-03	3.440E-06	1.081E-06	0.406
1995.88	45.98	4.383E-04	3.761E-03	8.739E-03	3.510E-06	1.128E-06	0.285
1995.86	46.34	4.508E-04	3.671E-03	8.690E-03	3.556E-06	1.158E-06	0.279
1995.84	46.69	4.582E-04	3.476E-03	8.727E-03	3.524E-06	1.163E-06	0.361
1995.82	47.04	4.450E-04	3.492E-03	8.744E-03	3.540E-06	1.159E-06	0.332
1995.80	47.34	4.490E-04	3.256E-03	8.878E-03	3.639E-06	1.207E-06	0.264
1995.78	47.74	4.732E-04	2.780E-03	8.945E-03	3.573E-06	1.389E-06	0.211
1995.76	48.08	4.858E-04	3.161E-03	8.850E-03	3.681E-06	1.271E-06	0.172
1995.74	48.42	4.767E-04	3.235E-03	8.760E-03	3.617E-06	1.245E-06	0.201
1995.72	48.76	4.767E-04	3.029E-03	8.917E-03	3.725E-06	1.308E-06	0.204
1995.70	49.11	4.949E-04	3.009E-03	8.996E-03	3.742E-06	1.373E-06	0.183
1995.68	49.45	5.645E-04	2.939E-03	9.133E-03	3.750E-06	1.409E-06	0.174
1995.66	49.79	5.308E-04	3.063E-03	9.153E-03	3.799E-06	1.406E-06	0.166
1995.64	50.13	5.496E-04	3.228E-03	9.178E-03	3.915E-06	1.445E-06	0.176
1995.60	50.47	5.454E-04	2.989E-03	9.245E-03	3.883E-06	1.421E-06	0.202
1995.57	50.82	5.428E-04	2.634E-03	9.184E-03	3.713E-06	1.419E-06	0.212
1995.53	51.16	5.464E-04	2.615E-03	9.107E-03	3.714E-06	1.368E-06	0.213
1995.50	51.50	5.343E-04	2.677E-03	9.137E-03	3.750E-06	1.349E-06	0.236
1995.46	51.84	5.237E-04	2.719E-03	9.211E-03	3.812E-06	1.331E-06	0.210
1995.43	52.19	5.083E-04	3.167E-03	9.046E-03	3.725E-06	1.180E-06	0.173
1995.39	52.53	4.899E-04	2.785E-03	9.087E-03	3.799E-06	1.347E-06	0.216
1995.36	52.87	5.013E-04	3.375E-03	8.935E-03	3.838E-06	1.223E-06	0.291
1995.32	53.21	5.127E-04	3.290E-03	8.957E-03	3.832E-06	1.163E-06	0.334
1995.29	53.55	4.824E-04	3.349E-03	8.891E-03	4.048E-06	1.151E-06	0.295
1995.25	53.90	4.423E-04	3.725E-03	8.584E-03	3.993E-06	1.045E-06	0.304
1995.23	54.24	4.334E-04	3.618E-03	8.710E-03	3.990E-06	1.104E-06	0.312
1995.22	54.58	4.071E-04	3.674E-03	8.833E-03	3.920E-06	1.128E-06	0.356
1995.20	54.92	3.906E-04	4.059E-03	8.580E-03	3.797E-06	1.050E-06	0.435
1995.18	55.27	3.663E-04	3.985E-03	8.584E-03	3.852E-06	1.003E-06	0.526
1995.17	55.61	3.666E-04	4.035E-03	8.683E-03	3.710E-06	1.018E-06	0.490
1995.15	55.95	3.631E-04	4.164E-03	8.583E-03	3.645E-06	9.804E-07	0.473
1995.13	56.29	3.489E-04	4.229E-03	8.743E-03	3.643E-06	1.080E-06	0.494
1995.12	56.63	3.404E-04	4.138E-03	8.538E-03	3.594E-06	9.691E-07	0.419
1995.11	56.98	3.447E-04	4.192E-03	8.607E-03	3.711E-06	1.044E-06	0.425

Time	Distance from top (mm)	B/Ca (mol/mol)	Mg/Ca (mol/mol)	Sr/Ca (mol/mol)	Ba/Ca (mol/mol)	U/Ca (mol/mol)	Mn ($\mu g\ g^{-1}$)
1995.10	57.32	4.155E-04	3.920E-03	8.794E-03	3.731E-06	1.156E-06	0.440
1995.09	57.66	4.564E-04	4.027E-03	8.877E-03	3.814E-06	1.173E-06	0.487
1995.08	58.00	4.396E-04	3.904E-03	8.755E-03	3.762E-06	1.177E-06	0.481
1995.07	58.35	4.366E-04	3.566E-03	8.897E-03	3.672E-06	1.233E-06	0.378
1995.06	58.69	4.435E-04	3.729E-03	8.782E-03	3.653E-06	1.209E-06	0.386
1995.05	59.03	4.464E-04	3.750E-03	8.893E-03	3.613E-06	1.194E-06	0.414
1995.04	59.37	4.721E-04	3.817E-03	8.781E-03	3.688E-06	1.153E-06	0.525
1995.03	59.71	4.452E-04	3.496E-03	8.768E-03	3.607E-06	1.135E-06	0.454
1995.02	60.06	4.598E-04	3.651E-03	8.750E-03	3.575E-06	1.120E-06	0.350
1995.01	60.40	4.468E-04	3.448E-03	8.785E-03	3.568E-06	1.145E-06	0.347
1995.00	60.74	4.528E-04	3.451E-03	8.746E-03	3.489E-06	1.102E-06	0.314
1994.97	61.08	4.535E-04	3.194E-03	8.837E-03	3.517E-06	1.180E-06	0.330
1994.94	61.43	4.470E-04	3.521E-03	8.721E-03	3.483E-06	1.135E-06	0.331
1994.92	61.77	4.311E-04	3.484E-03	8.584E-03	3.417E-06	1.150E-06	0.192
1994.89	62.11	4.606E-04	3.392E-03	8.766E-03	3.441E-06	1.207E-06	0.189
1994.86	62.45	4.614E-04	3.284E-03	8.765E-03	3.331E-06	1.192E-06	0.206
1994.83	62.79	4.573E-04	3.243E-03	8.899E-03	3.394E-06	1.239E-06	0.221
1994.80	63.14	4.781E-04	3.303E-03	8.793E-03	3.423E-06	1.217E-06	0.292
1994.78	63.48	4.874E-04	3.143E-03	8.812E-03	3.483E-06	1.204E-06	0.280
1994.75	63.82	4.974E-04	3.062E-03	8.829E-03	3.539E-06	1.212E-06	0.283
1994.72	64.16	5.124E-04	2.724E-03	9.033E-03	3.853E-06	1.307E-06	0.248
1994.69	64.50	5.252E-04	2.642E-03	9.056E-03	3.631E-06	1.279E-06	0.230
1994.66	64.85	5.459E-04	2.546E-03	9.212E-03	3.790E-06	1.436E-06	0.224
1994.64	65.19	5.106E-04	2.543E-03	9.225E-03	3.668E-06	1.482E-06	0.218
1994.59	65.53	5.173E-04	2.958E-03	9.155E-03	3.833E-06	1.400E-06	0.219
1994.54	65.87	5.430E-04	2.683E-03	9.262E-03	4.049E-06	1.452E-06	0.207
1994.49	66.22	5.457E-04	3.041E-03	9.143E-03	3.913E-06	1.352E-06	0.176
1994.44	66.56	5.397E-04	3.796E-03	9.062E-03	4.277E-06	1.196E-06	0.163
1994.43	66.90	5.544E-04	3.642E-03	9.045E-03	4.103E-06	1.262E-06	0.145
1994.40	67.24	5.337E-04	3.360E-03	9.112E-03	4.231E-06	1.276E-06	0.194
1994.37	67.58	5.239E-04	3.108E-03	9.141E-03	3.983E-06	1.320E-06	0.200
1994.34	67.93	5.066E-04	2.860E-03	9.129E-03	4.090E-06	1.341E-06	0.161
1994.31	68.27	5.024E-04	3.402E-03	8.956E-03	4.498E-06	1.225E-06	0.162
1994.28	68.61	4.772E-04	3.402E-03	8.801E-03	4.802E-06	1.158E-06	0.178
1994.25	68.95	4.667E-04	3.870E-03	8.706E-03	5.490E-06	1.097E-06	0.178
1994.23	69.30	4.374E-04	3.606E-03	8.724E-03	6.087E-06	1.204E-06	0.183
1994.20	69.64	4.358E-04	3.606E-03	8.820E-03	6.012E-06	1.164E-06	0.196
1994.18	69.98	4.220E-04	3.669E-03	8.740E-03	6.142E-06	1.108E-06	0.221
1994.16	70.32	4.032E-04	3.712E-03	8.727E-03	5.496E-06	1.045E-06	0.270
1994.14	70.66	4.032E-04	3.988E-03	8.650E-03	4.358E-06	1.029E-06	0.266
1994.11	71.01	3.688E-04	3.756E-03	8.627E-03	3.637E-06	1.009E-06	0.253
1994.09	71.35	3.960E-04	3.939E-03	8.622E-03	3.736E-06	1.032E-06	0.235
1994.07	71.69	3.898E-04	3.975E-03	8.689E-03	3.760E-06	1.055E-06	0.231
1994.05	72.03	3.779E-04	4.243E-03	8.555E-03	3.799E-06	9.568E-07	0.248
1994.02	72.38	3.713E-04	4.340E-03	8.750E-03	3.923E-06	9.603E-07	0.265
1994.02	72.72	3.796E-04	4.436E-03	8.712E-03	3.705E-06	9.899E-07	0.256
1994.01	73.06	3.825E-04	3.983E-03	8.822E-03	3.812E-06	1.097E-06	0.276
1994.01	73.40	3.983E-04	4.579E-03	8.647E-03	3.627E-06	9.667E-07	0.284
1994.00	73.74	3.975E-04	3.724E-03	8.533E-03	3.513E-06	1.040E-06	0.310
1994.00	74.09	4.137E-04	3.685E-03	8.634E-03	3.535E-06	1.086E-06	0.361
1994.00	74.43	4.554E-04	3.812E-03	8.779E-03	4.701E-06	1.134E-06	0.378
1993.99	74.77	4.625E-04	3.901E-03	8.729E-03	3.967E-06	1.049E-06	0.387
1993.99	75.11	4.650E-04	3.677E-03	8.731E-03	3.832E-06	1.103E-06	0.386
1993.98	75.46	4.417E-04	3.603E-03	8.758E-03	3.631E-06	1.142E-06	0.298
1993.98	75.80	4.559E-04	3.877E-03	8.853E-03	3.807E-06	1.157E-06	0.298

LA-ICP-MS data

Time	Distance from top (mm)	B/Ca (mol/mol)	Mg/Ca (mol/mol)	Sr/Ca (mol/mol)	Ba/Ca (mol/mol)	U/Ca (mol/mol)	Mn ($\mu g\ g^{-1}$)
1993.97	76.14	4.436E-04	4.025E-03	8.711E-03	3.718E-06	1.093E-06	0.296
1993.97	76.48	4.365E-04	3.503E-03	8.734E-03	3.482E-06	1.174E-06	0.252
1993.96	76.82	4.467E-04	3.119E-03	8.829E-03	3.557E-06	1.222E-06	0.266
1993.96	77.17	4.610E-04	3.084E-03	8.804E-03	3.552E-06	1.230E-06	0.258
1993.95	77.51	4.490E-04	3.405E-03	8.831E-03	3.626E-06	1.141E-06	0.287
1993.95	77.85	4.329E-04	3.236E-03	8.685E-03	3.451E-06	1.147E-06	0.273
1993.94	78.19	4.312E-04	3.226E-03	8.678E-03	3.474E-06	1.110E-06	0.324
1993.93	78.54	4.623E-04	3.483E-03	8.791E-03	3.805E-06	1.143E-06	0.368
1993.92	78.88	4.776E-04	3.457E-03	8.904E-03	3.948E-06	1.164E-06	0.398
1993.91	79.22	4.703E-04	3.471E-03	8.772E-03	3.909E-06	1.209E-06	0.428
1993.90	79.56	4.602E-04	3.684E-03	8.797E-03	3.859E-06	1.161E-06	0.383
1993.89	79.90	4.711E-04	3.696E-03	8.861E-03	3.836E-06	1.137E-06	0.310
1993.83	80.25	4.648E-04	3.352E-03	8.904E-03	3.785E-06	1.168E-06	0.238
1993.77	80.59	4.873E-04	3.075E-03	9.128E-03	3.892E-06	1.345E-06	0.285
1993.71	80.93	5.191E-04	2.986E-03	9.055E-03	3.940E-06	1.346E-06	0.321
1993.66	81.27	5.321E-04	3.154E-03	9.020E-03	3.986E-06	1.337E-06	0.299
1993.60	81.62	5.252E-04	2.957E-03	9.034E-03	3.901E-06	1.389E-06	0.247
1993.54	81.96	5.168E-04	2.791E-03	9.252E-03	3.930E-06	1.440E-06	0.203
1993.51	82.30	5.211E-04	2.753E-03	9.263E-03	3.914E-06	1.382E-06	0.153
1993.49	82.64	5.046E-04	3.005E-03	9.012E-03	3.837E-06	1.269E-06	0.187
1993.47	82.98	5.080E-04	3.351E-03	9.114E-03	4.020E-06	1.241E-06	0.255
1993.44	83.33	5.498E-04	3.820E-03	9.047E-03	4.120E-06	1.201E-06	0.266
1993.42	83.67	5.299E-04	3.615E-03	9.044E-03	4.003E-06	1.175E-06	0.281
1993.40	84.01	5.037E-04	3.203E-03	8.873E-03	3.783E-06	1.185E-06	0.262
1993.38	84.35	5.078E-04	2.721E-03	9.067E-03	3.792E-06	1.351E-06	0.212
1993.36	84.70	5.170E-04	2.896E-03	9.058E-03	3.785E-06	1.303E-06	0.165
1993.34	85.04	5.044E-04	3.168E-03	8.983E-03	3.879E-06	1.227E-06	0.154
1993.32	85.38	4.969E-04	3.296E-03	9.014E-03	3.980E-06	1.211E-06	0.148
1993.30	85.72	4.814E-04	3.688E-03	8.899E-03	4.153E-06	1.160E-06	0.160
1993.27	86.06	4.680E-04	3.487E-03	9.001E-03	4.080E-06	1.209E-06	0.174
1993.25	86.41	4.957E-04	3.466E-03	8.827E-03	4.107E-06	1.209E-06	0.172
1993.23	86.75	4.665E-04	3.776E-03	8.802E-03	4.132E-06	1.155E-06	0.246
1993.21	87.09	4.662E-04	3.806E-03	8.777E-03	4.318E-06	1.088E-06	0.293
1993.19	87.31	4.415E-04	3.948E-03	8.887E-03	4.181E-06	1.044E-06	0.306
1993.18	87.74	4.352E-04	3.491E-03	8.902E-03	4.288E-06	1.274E-06	0.348
1993.17	88.08	4.388E-04	3.385E-03	8.953E-03	4.161E-06	1.288E-06	0.379
1993.15	88.43	4.240E-04	3.350E-03	8.826E-03	3.980E-06	1.255E-06	0.421
1993.14	88.77	4.378E-04	3.252E-03	8.953E-03	3.956E-06	1.267E-06	0.478
1993.13	89.12	4.420E-04	3.392E-03	8.840E-03	3.854E-06	1.198E-06	0.512
1993.11	89.46	4.287E-04	3.288E-03	8.872E-03	4.032E-06	1.292E-06	0.458
1993.10	89.81	4.437E-04	3.768E-03	8.828E-03	4.253E-06	1.163E-06	0.396
1993.09	90.15	4.548E-04	3.735E-03	8.852E-03	3.992E-06	1.157E-06	0.422
1993.07	90.50	4.392E-04	3.738E-03	8.905E-03	4.084E-06	1.155E-06	0.424
1993.06	90.84	4.186E-04	3.654E-03	8.734E-03	4.000E-06	1.137E-06	0.404
1993.05	91.19	4.113E-04	3.734E-03	8.696E-03	3.850E-06	1.103E-06	0.372
1993.03	91.53	4.251E-04	3.884E-03	8.750E-03	3.943E-06	1.072E-06	0.408
1993.02	91.88	4.284E-04	3.874E-03	8.638E-03	3.831E-06	1.056E-06	0.509
1993.01	92.22	4.483E-04	3.601E-03	8.833E-03	3.820E-06	1.164E-06	0.549
1993.00	92.57	4.605E-04	3.769E-03	8.825E-03	3.746E-06	1.109E-06	0.455
1992.98	92.91	4.468E-04	3.910E-03	8.721E-03	3.598E-06	1.065E-06	0.450
1992.97	93.26	4.291E-04	3.509E-03	8.883E-03	3.650E-06	1.182E-06	0.441
1992.96	93.60	4.151E-04	3.468E-03	8.789E-03	3.635E-06	1.216E-06	0.362
1992.94	93.95	3.925E-04	4.052E-03	8.626E-03	3.524E-06	1.039E-06	0.307
1992.93	94.29	4.311E-04	4.150E-03	8.731E-03	3.671E-06	1.111E-06	0.343
1992.91	94.64	4.113E-04	3.742E-03	8.717E-03	3.602E-06	1.190E-06	0.511

Time	Distance from top (mm)	B/Ca (mol/mol)	Mg/Ca (mol/mol)	Sr/Ca (mol/mol)	Ba/Ca (mol/mol)	U/Ca (mol/mol)	Mn ($\mu g\ g^{-1}$)
1992.90	94.98	4.316E-04	3.309E-03	8.872E-03	3.779E-06	1.325E-06	0.653
1992.89	95.33	4.457E-04	3.216E-03	8.930E-03	4.001E-06	1.360E-06	0.559
1992.87	95.67	4.533E-04	3.065E-03	8.907E-03	4.278E-06	1.346E-06	0.405
1992.86	96.02	4.443E-04	3.081E-03	8.836E-03	4.174E-06	1.242E-06	0.349
1992.84	96.36	4.380E-04	3.027E-03	8.833E-03	4.226E-06	1.269E-06	0.396
1992.83	96.71	4.429E-04	2.879E-03	8.868E-03	4.467E-06	1.288E-06	0.380
1992.81	97.05	4.736E-04	3.002E-03	8.875E-03	3.798E-06	1.314E-06	0.334
1992.80	97.40	4.543E-04	3.273E-03	8.839E-03	3.357E-06	1.228E-06	0.297
1992.78	97.74	4.620E-04	3.350E-03	8.917E-03	3.528E-06	1.266E-06	0.359
1992.77	98.09	4.604E-04	3.186E-03	8.933E-03	3.829E-06	1.247E-06	0.325
1992.76	98.43	4.591E-04	3.410E-03	8.879E-03	3.919E-06	1.208E-06	0.260
1992.71	98.78	4.916E-04	3.032E-03	9.047E-03	3.922E-06	1.317E-06	0.222
1992.66	99.12	4.941E-04	3.022E-03	9.122E-03	3.932E-06	1.303E-06	0.207
1992.61	99.47	5.360E-04	2.739E-03	9.136E-03	4.061E-06	1.370E-06	0.184
1992.58	99.81	5.274E-04	2.959E-03	9.325E-03	4.304E-06	1.421E-06	0.187
1992.55	100.16	5.216E-04	3.060E-03	9.182E-03	4.405E-06	1.414E-06	0.177
1992.53	100.50	5.205E-04	3.159E-03	9.199E-03	4.400E-06	1.390E-06	0.223
1992.51	100.85	5.215E-04	2.962E-03	9.148E-03	4.181E-06	1.262E-06	0.246
1992.50	101.19	4.900E-04	3.171E-03	8.991E-03	4.092E-06	1.100E-06	0.285
1992.48	101.54	4.961E-04	3.414E-03	8.790E-03	3.959E-06	1.049E-06	0.308
1992.46	101.88	4.805E-04	3.544E-03	9.017E-03	4.074E-06	1.252E-06	0.213
1992.45	102.23	4.912E-04	3.149E-03	9.045E-03	3.984E-06	1.320E-06	0.236
1992.43	102.57	4.975E-04	3.333E-03	9.006E-03	4.083E-06	1.317E-06	0.231
1992.41	102.92	4.623E-04	3.196E-03	8.979E-03	4.011E-06	1.257E-06	0.217
1992.40	103.26	4.697E-04	3.518E-03	8.853E-03	4.113E-06	1.176E-06	0.227
1992.38	103.61	5.008E-04	3.534E-03	8.834E-03	4.393E-06	1.173E-06	0.236
1992.36	103.95	4.873E-04	3.474E-03	8.890E-03	4.515E-06	1.204E-06	0.243
1992.35	104.30	4.662E-04	3.782E-03	8.982E-03	4.582E-06	1.213E-06	0.268
1992.33	104.64	4.833E-04	3.325E-03	8.998E-03	4.656E-06	1.273E-06	0.336
1992.31	104.99	4.844E-04	3.701E-03	9.107E-03	4.520E-06	1.206E-06	0.302
1992.30	105.33	4.814E-04	3.722E-03	8.921E-03	4.593E-06	1.228E-06	0.255
1992.28	105.68	4.383E-04	3.507E-03	8.905E-03	4.593E-06	1.220E-06	0.205
1992.26	106.02	3.989E-04	4.051E-03	8.655E-03	4.321E-06	1.057E-06	0.222
1992.25	106.37	4.062E-04	4.547E-03	8.768E-03	4.143E-06	1.025E-06	0.255
1992.23	106.71	3.998E-04	4.291E-03	8.771E-03	3.981E-06	1.091E-06	0.301
1992.22	107.06	3.982E-04	4.715E-03	8.656E-03	3.880E-06	9.758E-07	0.363
1992.20	107.40	3.982E-04	4.362E-03	8.606E-03	3.781E-06	1.065E-06	0.393
1992.18	107.75	4.034E-04	3.859E-03	8.839E-03	3.721E-06	1.097E-06	0.412
1992.17	108.09	4.067E-04	3.760E-03	8.755E-03	3.656E-06	1.116E-06	0.424
1992.15	108.44	4.113E-04	3.827E-03	8.684E-03	3.411E-06	1.097E-06	0.455
1992.13	108.78	4.128E-04	4.220E-03	8.807E-03	3.340E-06	1.060E-06	0.444
1992.12	109.13	4.351E-04	4.306E-03	8.640E-03	3.448E-06	1.006E-06	0.506
1992.10	109.47	4.061E-04	4.009E-03	8.719E-03	3.985E-06	1.033E-06	0.477
1992.08	109.82	4.197E-04	3.848E-03	8.656E-03	4.058E-06	1.077E-06	0.474
1992.07	110.16	4.220E-04	4.078E-03	8.688E-03	3.671E-06	1.095E-06	0.357
1992.05	110.51	4.297E-04	3.906E-03	8.753E-03	3.469E-06	1.103E-06	0.471
1992.03	110.85	4.545E-04	3.990E-03	8.678E-03	3.341E-06	1.021E-06	0.711
1992.02	111.20	4.467E-04	4.144E-03	8.680E-03	3.563E-06	1.026E-06	0.649
1992.00	111.54	4.613E-04	3.951E-03	8.749E-03	3.491E-06	1.071E-06	0.469
1991.98	111.89	4.382E-04	3.744E-03	8.760E-03	3.500E-06	1.124E-06	0.468
1991.97	112.23	4.571E-04	3.643E-03	8.733E-03	3.615E-06	1.149E-06	0.446
1991.95	112.58	4.281E-04	3.538E-03	8.659E-03	3.740E-06	1.131E-06	0.466
1991.93	112.92	4.253E-04	3.832E-03	8.718E-03	3.885E-06	1.143E-06	0.434
1991.92	113.27	4.354E-04	3.807E-03	8.775E-03	3.937E-06	1.139E-06	0.394
1991.90	113.61	4.315E-04	4.197E-03	8.615E-03	4.055E-06	1.077E-06	0.309

LA-ICP-MS data

Time	Distance from top (mm)	B/Ca (mol/mol)	Mg/Ca (mol/mol)	Sr/Ca (mol/mol)	Ba/Ca (mol/mol)	U/Ca (mol/mol)	Mn ($\mu g\ g^{-1}$)
1991.88	113.96	4.116E-04	4.299E-03	8.608E-03	4.009E-06	1.046E-06	0.318
1991.87	114.30	4.460E-04	4.024E-03	8.813E-03	4.176E-06	1.157E-06	0.358
1991.85	114.65	4.468E-04	3.329E-03	8.796E-03	4.053E-06	1.174E-06	0.366
1991.83	114.99	4.572E-04	3.459E-03	8.706E-03	4.020E-06	1.079E-06	0.343
1991.82	115.34	4.678E-04	3.720E-03	8.711E-03	3.930E-06	1.102E-06	0.344
1991.80	115.68	4.737E-04	3.313E-03	8.821E-03	3.811E-06	1.235E-06	0.317
1991.78	116.03	4.679E-04	3.211E-03	8.804E-03	3.737E-06	1.195E-06	0.304
1991.77	116.37	4.586E-04	3.369E-03	8.817E-03	4.159E-06	1.239E-06	0.269
1991.71	116.72	4.804E-04	2.981E-03	8.876E-03	4.367E-06	1.324E-06	0.274
1991.65	117.06	4.999E-04	2.897E-03	9.052E-03	4.606E-06	1.424E-06	0.241
1991.59	117.41	5.060E-04	2.709E-03	9.131E-03	4.809E-06	1.481E-06	0.234
1991.53	117.75	5.180E-04	2.874E-03	9.027E-03	5.143E-06	1.395E-06	0.217
1991.47	118.10	5.302E-04	2.848E-03	9.150E-03	5.261E-06	1.371E-06	0.198
1991.46	118.44	5.041E-04	2.657E-03	9.127E-03	5.078E-06	1.451E-06	0.199
1991.44	118.79	4.891E-04	2.925E-03	9.019E-03	4.860E-06	1.400E-06	0.195
1991.42	119.13	4.965E-04	3.193E-03	9.133E-03	5.044E-06	1.300E-06	0.232
1991.41	119.48	4.777E-04	2.900E-03	9.095E-03	5.107E-06	1.366E-06	0.204
1991.39	119.82	4.837E-04	2.969E-03	9.031E-03	5.000E-06	1.264E-06	0.204
1991.37	120.17	4.954E-04	3.189E-03	8.833E-03	5.071E-06	1.209E-06	0.217
1991.35	120.51	4.776E-04	2.835E-03	9.026E-03	5.196E-06	1.275E-06	0.203
1991.34	120.86	4.916E-04	2.965E-03	9.070E-03	5.485E-06	1.286E-06	0.213
1991.32	121.20	4.800E-04	3.270E-03	9.052E-03	5.521E-06	1.298E-06	0.187
1991.30	121.55	4.478E-04	2.791E-03	9.087E-03	5.490E-06	1.443E-06	0.190
1991.29	121.89	4.406E-04	3.291E-03	9.067E-03	5.629E-06	1.317E-06	0.168
1991.27	122.24	4.285E-04	3.144E-03	8.984E-03	5.714E-06	1.312E-06	0.189
1991.25	122.58	4.116E-04	3.078E-03	9.057E-03	5.292E-06	1.403E-06	0.189
1991.24	122.93	4.230E-04	3.376E-03	8.975E-03	5.164E-06	1.430E-06	0.283
1991.22	123.27	4.473E-04	3.191E-03	9.108E-03	5.696E-06	1.438E-06	0.290
1991.20	123.62	4.205E-04	3.195E-03	9.043E-03	5.928E-06	1.416E-06	0.245
1991.19	123.96	4.144E-04	3.136E-03	9.113E-03	6.022E-06	1.507E-06	0.301
1991.17	124.31	4.008E-04	2.704E-03	9.318E-03	6.339E-06	1.708E-06	0.244
1991.15	124.65	3.843E-04	2.359E-03	9.619E-03	5.986E-06	1.879E-06	0.197
1991.14	125.00	3.620E-04	2.228E-03	9.399E-03	6.103E-06	1.842E-06	0.179
1991.12	125.34	3.666E-04	2.636E-03	9.217E-03	7.602E-06	1.596E-06	0.198
1991.10	125.69	3.907E-04	3.006E-03	9.060E-03	9.684E-06	1.414E-06	0.419
1991.08	126.03	4.154E-04	3.019E-03	8.997E-03	1.038E-05	1.341E-06	0.552
1991.06	126.38	3.902E-04	2.984E-03	8.927E-03	9.297E-06	1.415E-06	0.481
1991.04	126.72	4.202E-04	3.395E-03	8.985E-03	6.010E-06	1.396E-06	0.357
1991.02	127.07	4.245E-04	3.937E-03	8.769E-03	5.048E-06	1.094E-06	0.280
1991.00	127.41	4.342E-04	3.731E-03	8.868E-03	4.519E-06	1.225E-06	0.296
1990.98	127.76	4.049E-04	3.372E-03	8.876E-03	4.072E-06	1.353E-06	0.306
1990.96	128.10	4.244E-04	3.870E-03	8.711E-03	3.937E-06	1.262E-06	0.349
1990.94	128.45	4.305E-04	3.858E-03	8.786E-03	4.095E-06	1.220E-06	0.339
1990.92	128.67	4.206E-04	3.403E-03	8.818E-03	4.143E-06	1.229E-06	0.330

Table 10.5 Pandora Reef 1-98b Reef 2 *Porites* data

Time	Distance from top (mm)	B/Ca (mol/mol)	Mg/Ca (mol/mol)	Sr/Ca (mol/mol)	Ba/Ca (mol/mol)	U/Ca (mol/mol)
1998.35	0.00	4.494E-04	2.699E-03	8.991E-03	4.626E-06	1.677E-06
1998.33	0.26	4.081E-04	3.136E-03	8.755E-03	4.526E-06	1.464E-06
1998.29	0.53	4.108E-04	3.378E-03	8.657E-03	4.439E-06	1.363E-06
1998.26	0.79	4.066E-04	3.414E-03	8.749E-03	4.746E-06	1.322E-06
1998.23	1.06	4.122E-04	3.290E-03	8.726E-03	4.748E-06	1.268E-06
1998.20	1.32	4.232E-04	3.503E-03	8.764E-03	5.193E-06	1.217E-06
1998.17	1.59	4.121E-04	3.821E-03	8.893E-03	5.700E-06	1.257E-06
1998.13	1.85	3.888E-04	3.620E-03	8.689E-03	6.009E-06	1.161E-06
1998.10	2.12	3.763E-04	3.510E-03	8.948E-03	6.326E-06	1.307E-06
1998.07	2.38	3.615E-04	3.666E-03	8.971E-03	7.498E-06	1.274E-06
1998.07	2.65	3.444E-04	3.074E-03	8.946E-03	8.231E-06	1.411E-06
1998.06	2.91	3.467E-04	3.303E-03	8.830E-03	8.299E-06	1.283E-06
1998.06	3.18	3.741E-04	3.522E-03	8.605E-03	8.280E-06	1.228E-06
1998.06	3.44	4.155E-04	2.939E-03	8.874E-03	6.340E-06	1.412E-06
1998.05	3.71	4.310E-04	3.115E-03	8.961E-03	4.811E-06	1.454E-06
1998.05	3.97	4.417E-04	3.203E-03	8.934E-03	4.231E-06	1.439E-06
1998.05	4.24	4.354E-04	3.252E-03	8.824E-03	3.864E-06	1.436E-06
1998.04	4.50	4.448E-04	4.120E-03	8.742E-03	3.797E-06	1.291E-06
1998.04	4.77	4.272E-04	4.414E-03	8.814E-03	3.754E-06	1.247E-06
1998.03	5.03	4.162E-04	3.805E-03	8.863E-03	3.823E-06	1.338E-06
1998.03	5.30	4.223E-04	3.485E-03	9.126E-03	3.708E-06	1.363E-06
1998.03	5.56	4.197E-04	3.694E-03	8.920E-03	3.779E-06	1.306E-06
1998.02	5.83	4.300E-04	3.534E-03	8.908E-03	3.682E-06	1.253E-06
1998.02	6.09	4.244E-04	3.184E-03	9.004E-03	3.757E-06	1.398E-06
1998.01	6.36	4.436E-04	3.566E-03	8.956E-03	3.857E-06	1.305E-06
1998.01	6.62	4.348E-04	3.706E-03	8.764E-03	3.863E-06	1.233E-06
1998.01	6.89	4.129E-04	3.618E-03	8.744E-03	3.939E-06	1.165E-06
1998.00	7.15	4.327E-04	3.691E-03	8.904E-03	3.935E-06	1.208E-06
1998.00	7.42	4.066E-04	3.204E-03	9.051E-03	4.034E-06	1.367E-06
1997.99	7.68	3.969E-04	3.074E-03	8.955E-03	3.882E-06	1.376E-06
1997.99	7.95	4.131E-04	3.251E-03	8.897E-03	3.846E-06	1.264E-06
1997.99	8.21	4.518E-04	3.193E-03	8.956E-03	3.865E-06	1.367E-06
1997.98	8.48	4.651E-04	3.189E-03	8.967E-03	3.926E-06	1.306E-06
1997.98	8.74	4.536E-04	3.349E-03	8.943E-03	3.922E-06	1.247E-06
1997.97	9.01	4.618E-04	3.026E-03	9.021E-03	3.849E-06	1.246E-06
1997.97	9.27	4.644E-04	2.949E-03	9.105E-03	3.859E-06	1.265E-06
1997.97	9.54	4.808E-04	3.013E-03	9.048E-03	3.863E-06	1.268E-06
1997.96	9.80	4.765E-04	2.834E-03	9.169E-03	3.956E-06	1.302E-06
1997.92	10.07	4.783E-04	2.724E-03	9.108E-03	3.760E-06	1.321E-06
1997.88	10.33	4.682E-04	2.555E-03	9.300E-03	4.025E-06	1.388E-06
1997.84	10.60	4.679E-04	2.480E-03	9.293E-03	3.902E-06	1.392E-06
1997.80	10.86	4.854E-04	2.541E-03	9.262E-03	3.847E-06	1.429E-06
1997.76	11.12	5.153E-04	2.633E-03	9.258E-03	3.950E-06	1.462E-06
1997.72	11.39	4.959E-04	2.511E-03	9.440E-03	3.943E-06	1.500E-06
1997.68	11.65	5.054E-04	2.486E-03	9.314E-03	3.762E-06	1.484E-06
1997.64	11.92	4.645E-04	2.141E-03	9.665E-03	3.984E-06	1.692E-06
1997.60	12.18	4.802E-04	2.282E-03	9.673E-03	4.100E-06	1.704E-06
1997.56	12.45	4.627E-04	2.360E-03	9.378E-03	4.028E-06	1.580E-06
1997.52	12.71	4.766E-04	2.599E-03	9.373E-03	4.186E-06	1.582E-06
1997.48	12.98	4.881E-04	2.506E-03	9.422E-03	4.243E-06	1.571E-06
1997.44	13.24	4.755E-04	2.469E-03	9.413E-03	4.162E-06	1.616E-06

LA-ICP-MS data

Time	Distance from top (mm)	B/Ca (mol/mol)	Mg/Ca (mol/mol)	Sr/Ca (mol/mol)	Ba/Ca (mol/mol)	U/Ca (mol/mol)
1997.40	13.51	4.780E-04	2.465E-03	9.471E-03	4.292E-06	1.586E-06
1997.36	13.77	4.649E-04	2.452E-03	9.268E-03	4.070E-06	1.591E-06
1997.32	14.04	4.653E-04	2.584E-03	9.219E-03	4.193E-06	1.533E-06
1997.28	14.30	4.516E-04	2.968E-03	9.076E-03	4.105E-06	1.348E-06
1997.27	14.57	4.475E-04	2.930E-03	9.265E-03	4.601E-06	1.441E-06
1997.25	14.83	4.586E-04	3.161E-03	9.108E-03	5.189E-06	1.420E-06
1997.23	15.10	4.509E-04	3.406E-03	8.929E-03	6.221E-06	1.288E-06
1997.22	15.36	4.245E-04	2.953E-03	9.012E-03	7.557E-06	1.348E-06
1997.20	15.63	4.318E-04	3.105E-03	9.007E-03	7.694E-06	1.369E-06
1997.18	15.89	4.207E-04	2.821E-03	9.052E-03	7.166E-06	1.462E-06
1997.17	16.16	4.009E-04	2.784E-03	9.185E-03	7.395E-06	1.432E-06
1997.15	16.42	4.054E-04	3.536E-03	8.880E-03	7.470E-06	1.231E-06
1997.13	16.69	4.121E-04	3.424E-03	8.921E-03	7.583E-06	1.210E-06
1997.12	16.95	3.998E-04	3.493E-03	8.809E-03	7.197E-06	1.205E-06
1997.10	17.22	3.700E-04	3.526E-03	8.889E-03	6.489E-06	1.175E-06
1997.08	17.48	3.580E-04	3.416E-03	9.009E-03	5.051E-06	1.252E-06
1997.07	17.75	3.785E-04	3.601E-03	8.795E-03	4.820E-06	1.174E-06
1997.05	18.01	3.888E-04	3.759E-03	8.762E-03	4.423E-06	1.156E-06
1997.03	18.28	4.012E-04	3.461E-03	9.001E-03	4.424E-06	1.248E-06
1997.02	18.54	4.046E-04	3.478E-03	8.873E-03	4.180E-06	1.220E-06
1997.00	18.81	4.154E-04	3.494E-03	8.949E-03	3.804E-06	1.223E-06
1996.99	19.07	4.057E-04	3.695E-03	8.815E-03	3.750E-06	1.176E-06
1996.98	19.34	4.057E-04	3.632E-03	9.055E-03	3.778E-06	1.247E-06
1996.97	19.60	4.166E-04	3.967E-03	8.811E-03	3.702E-06	1.129E-06
1996.96	19.87	4.141E-04	4.043E-03	8.865E-03	3.720E-06	1.075E-06
1996.95	20.13	4.136E-04	3.973E-03	8.874E-03	3.731E-06	1.235E-06
1996.94	20.40	4.046E-04	3.975E-03	8.878E-03	3.647E-06	1.196E-06
1996.92	20.66	4.105E-04	3.965E-03	8.890E-03	3.676E-06	1.252E-06
1996.91	20.93	3.976E-04	3.803E-03	8.904E-03	3.581E-06	1.258E-06
1996.90	21.19	4.017E-04	3.413E-03	9.020E-03	3.742E-06	1.343E-06
1996.89	21.46	4.020E-04	3.762E-03	9.016E-03	3.679E-06	1.254E-06
1996.88	21.72	4.045E-04	3.736E-03	8.914E-03	3.718E-06	1.212E-06
1996.87	21.98	4.138E-04	3.440E-03	9.032E-03	3.666E-06	1.286E-06
1996.86	22.25	4.394E-04	3.761E-03	8.918E-03	3.708E-06	1.231E-06
1996.85	22.51	4.278E-04	3.658E-03	8.881E-03	3.548E-06	1.213E-06
1996.84	22.78	4.503E-04	3.488E-03	9.072E-03	3.717E-06	1.323E-06
1996.83	23.04	4.353E-04	3.332E-03	9.120E-03	3.607E-06	1.370E-06
1996.82	23.31	4.125E-04	3.341E-03	8.957E-03	3.698E-06	1.243E-06
1996.81	23.57	4.128E-04	3.619E-03	8.720E-03	3.547E-06	1.248E-06
1996.80	23.84	4.287E-04	3.210E-03	8.961E-03	3.769E-06	1.376E-06
1996.78	24.10	4.265E-04	3.201E-03	9.029E-03	3.727E-06	1.411E-06
1996.77	24.37	4.194E-04	3.378E-03	9.200E-03	3.847E-06	1.418E-06
1996.76	24.63	4.446E-04	3.100E-03	9.135E-03	3.829E-06	1.479E-06
1996.75	24.90	4.242E-04	2.922E-03	9.120E-03	3.757E-06	1.399E-06
1996.74	25.16	4.248E-04	3.118E-03	9.119E-03	3.688E-06	1.372E-06
1996.73	25.43	4.208E-04	2.800E-03	9.098E-03	3.689E-06	1.408E-06
1996.72	25.69	4.268E-04	2.918E-03	9.086E-03	3.686E-06	1.353E-06
1996.71	25.96	4.407E-04	3.577E-03	9.020E-03	3.640E-06	1.254E-06
1996.70	26.22	4.275E-04	3.151E-03	8.870E-03	3.656E-06	1.309E-06
1996.69	26.49	4.399E-04	3.290E-03	8.933E-03	3.670E-06	1.237E-06
1996.68	26.75	4.613E-04	2.940E-03	8.992E-03	3.629E-06	1.276E-06
1996.67	27.02	4.660E-04	2.862E-03	8.976E-03	3.714E-06	1.299E-06
1996.66	27.28	4.503E-04	2.693E-03	9.079E-03	3.697E-06	1.289E-06
1996.64	27.55	4.558E-04	2.662E-03	9.199E-03	3.726E-06	1.358E-06

Time	Distance from top (mm)	B/Ca (mol/mol)	Mg/Ca (mol/mol)	Sr/Ca (mol/mol)	Ba/Ca (mol/mol)	U/Ca (mol/mol)
1996.63	27.81	4.726E-04	2.547E-03	9.216E-03	3.774E-06	1.430E-06
1996.62	28.08	4.503E-04	2.364E-03	9.262E-03	3.813E-06	1.494E-06
1996.61	28.34	4.790E-04	2.463E-03	9.260E-03	3.707E-06	1.485E-06
1996.60	28.61	4.627E-04	2.388E-03	9.267E-03	3.519E-06	1.481E-06
1996.59	28.87	4.776E-04	2.495E-03	9.166E-03	3.312E-06	1.444E-06
1996.58	29.14	4.710E-04	2.335E-03	9.224E-03	3.128E-06	1.498E-06
1996.57	29.40	4.482E-04	2.431E-03	9.139E-03	2.862E-06	1.412E-06
1996.56	29.67	4.507E-04	2.595E-03	9.104E-03	2.759E-06	1.389E-06
1996.54	29.93	4.501E-04	2.466E-03	9.207E-03	2.830E-06	1.449E-06
1996.53	30.20	4.558E-04	2.580E-03	9.156E-03	3.469E-06	1.382E-06
1996.51	30.46	4.529E-04	2.680E-03	9.056E-03	3.573E-06	1.329E-06
1996.50	30.73	4.540E-04	2.896E-03	9.058E-03	3.668E-06	1.382E-06
1996.48	30.99	4.785E-04	3.055E-03	9.144E-03	3.869E-06	1.385E-06
1996.47	31.26	4.548E-04	2.942E-03	8.995E-03	3.795E-06	1.409E-06
1996.46	31.52	4.405E-04	3.003E-03	9.066E-03	3.940E-06	1.454E-06
1996.44	31.79	4.566E-04	2.966E-03	9.079E-03	3.973E-06	1.473E-06
1996.43	32.05	4.384E-04	2.969E-03	9.256E-03	4.215E-06	1.488E-06
1996.41	32.32	4.365E-04	3.314E-03	8.901E-03	4.175E-06	1.370E-06
1996.40	32.58	4.258E-04	3.040E-03	9.140E-03	4.130E-06	1.472E-06
1996.38	32.84	4.503E-04	3.520E-03	8.971E-03	4.196E-06	1.326E-06
1996.37	33.11	4.202E-04	3.536E-03	8.778E-03	4.018E-06	1.184E-06
1996.35	33.37	4.160E-04	3.548E-03	8.815E-03	3.997E-06	1.194E-06
1996.34	33.64	4.298E-04	3.565E-03	8.913E-03	4.104E-06	1.250E-06
1996.32	33.90	4.324E-04	3.381E-03	8.842E-03	4.110E-06	1.292E-06
1996.31	34.17	4.311E-04	3.318E-03	8.981E-03	4.066E-06	1.425E-06
1996.29	34.43	4.425E-04	3.517E-03	8.833E-03	4.271E-06	1.357E-06
1996.28	34.70	4.516E-04	3.682E-03	8.892E-03	4.498E-06	1.395E-06
1996.27	34.96	4.469E-04	3.355E-03	8.788E-03	4.349E-06	1.365E-06
1996.25	35.23	4.423E-04	3.377E-03	8.977E-03	4.468E-06	1.401E-06
1996.24	35.49	4.397E-04	3.771E-03	8.816E-03	4.837E-06	1.294E-06
1996.22	35.76	4.358E-04	3.884E-03	8.676E-03	4.925E-06	1.279E-06
1996.21	36.02	4.186E-04	3.980E-03	8.565E-03	4.961E-06	1.226E-06
1996.19	36.29	3.881E-04	3.789E-03	8.695E-03	5.206E-06	1.141E-06
1996.19	36.55	3.874E-04	3.764E-03	8.681E-03	5.205E-06	1.140E-06
1996.18	36.82	3.878E-04	3.761E-03	8.738E-03	5.184E-06	1.148E-06
1996.17	37.08	3.881E-04	3.775E-03	8.739E-03	5.169E-06	1.155E-06
1996.17	37.35	3.917E-04	3.776E-03	8.806E-03	5.180E-06	1.168E-06
1996.16	37.61	3.935E-04	3.803E-03	8.802E-03	5.145E-06	1.168E-06
1996.15	37.88	3.873E-04	3.803E-03	8.839E-03	5.110E-06	1.172E-06
1996.15	38.14	3.857E-04	3.796E-03	8.767E-03	5.035E-06	1.152E-06
1996.14	38.41	3.874E-04	3.787E-03	8.771E-03	4.993E-06	1.150E-06
1996.14	38.67	3.893E-04	3.782E-03	8.793E-03	4.999E-06	1.163E-06
1996.13	38.94	3.866E-04	3.742E-03	8.784E-03	5.006E-06	1.168E-06
1996.12	39.20	3.874E-04	3.691E-03	8.756E-03	5.014E-06	1.184E-06
1996.12	39.47	3.882E-04	3.607E-03	8.725E-03	5.040E-06	1.192E-06
1996.11	39.73	3.842E-04	3.532E-03	8.700E-03	5.034E-06	1.207E-06
1996.10	40.00	3.835E-04	3.439E-03	8.719E-03	5.018E-06	1.231E-06
1996.10	40.26	3.872E-04	3.370E-03	8.699E-03	5.013E-06	1.238E-06
1996.09	40.53	3.856E-04	3.328E-03	8.716E-03	4.995E-06	1.268E-06
1996.09	40.79	3.818E-04	3.316E-03	8.753E-03	4.987E-06	1.278E-06
1996.08	41.06	3.774E-04	3.319E-03	8.784E-03	4.966E-06	1.282E-06
1996.07	41.32	3.765E-04	3.344E-03	8.830E-03	4.902E-06	1.294E-06
1996.07	41.59	3.784E-04	3.381E-03	8.812E-03	4.842E-06	1.294E-06
1996.06	41.85	3.776E-04	3.422E-03	8.830E-03	4.728E-06	1.285E-06

LA-ICP-MS data

Time	Distance from top (mm)	B/Ca (mol/mol)	Mg/Ca (mol/mol)	Sr/Ca (mol/mol)	Ba/Ca (mol/mol)	U/Ca (mol/mol)
1996.06	42.12	3.816E-04	3.457E-03	8.807E-03	4.669E-06	1.277E-06
1996.05	42.38	3.810E-04	3.485E-03	8.801E-03	4.658E-06	1.262E-06
1996.04	42.65	3.798E-04	3.527E-03	8.773E-03	4.605E-06	1.261E-06
1996.04	42.91	3.805E-04	3.560E-03	8.770E-03	4.557E-06	1.259E-06
1996.03	43.18	3.833E-04	3.548E-03	8.751E-03	4.510E-06	1.259E-06
1996.02	43.44	3.853E-04	3.523E-03	8.730E-03	4.495E-06	1.255E-06
1996.02	43.70	3.912E-04	3.490E-03	8.709E-03	4.495E-06	1.254E-06
1996.01	43.97	3.955E-04	3.619E-03	8.767E-03	4.445E-06	1.218E-06
1996.01	44.23	3.831E-04	3.550E-03	8.750E-03	4.509E-06	1.169E-06
1996.00	44.50	3.904E-04	3.583E-03	8.766E-03	4.422E-06	1.157E-06
1995.99	44.76	3.943E-04	3.480E-03	8.828E-03	4.307E-06	1.265E-06
1995.99	45.03	4.177E-04	3.397E-03	8.809E-03	4.027E-06	1.331E-06
1995.98	45.29	4.401E-04	3.933E-03	8.840E-03	3.821E-06	1.199E-06
1995.97	45.56	4.358E-04	3.792E-03	8.817E-03	3.806E-06	1.205E-06
1995.97	45.82	4.419E-04	4.053E-03	8.687E-03	3.856E-06	1.195E-06
1995.96	46.09	4.331E-04	4.151E-03	8.723E-03	3.687E-06	1.163E-06

Table 10.6 Myrmidon Reef 2 *Porites* data

Time	Distance from top (mm)	B/Ca (mol/mol)	Mg/Ca (mol/mol)	Sr/Ca (mol/mol)	Ba/Ca (mol/mol)	U/Ca (mol/mol)	Mn ($\mu g\ g^{-1}$)
1996.33	0.00	4.126E-04	4.569E-03	8.700E-03	8.747E-06	9.787E-07	0.168
1996.29	0.26	3.952E-04	4.664E-03	8.688E-03	8.717E-06	9.871E-07	0.136
1996.25	0.51	4.112E-04	4.500E-03	8.711E-03	7.555E-06	1.049E-06	0.149
1996.21	0.77	4.319E-04	4.357E-03	8.611E-03	6.625E-06	1.021E-06	0.186
1996.17	1.03	4.359E-04	4.403E-03	8.829E-03	4.605E-06	1.005E-06	0.157
1996.13	1.29	4.310E-04	4.368E-03	8.815E-03	3.862E-06	9.964E-07	0.160
1996.08	1.54	4.115E-04	4.122E-03	8.623E-03	4.161E-06	9.931E-07	0.163
1996.04	1.80	4.441E-04	4.040E-03	8.747E-03	3.995E-06	1.051E-06	0.116
1996.00	2.06	4.335E-04	3.930E-03	8.844E-03	3.601E-06	1.093E-06	0.120
1995.96	2.31	4.106E-04	3.655E-03	8.739E-03	3.222E-06	1.082E-06	0.126
1995.92	2.57	4.222E-04	3.637E-03	8.834E-03	2.969E-06	1.103E-06	0.097
1995.88	2.83	4.311E-04	3.781E-03	8.894E-03	2.738E-06	1.053E-06	0.103
1995.83	3.09	4.424E-04	3.864E-03	8.840E-03	3.262E-06	1.055E-06	0.117
1995.79	3.34	4.521E-04	3.880E-03	8.780E-03	3.235E-06	1.135E-06	0.129
1995.75	3.60	4.483E-04	3.774E-03	8.824E-03	2.819E-06	1.103E-06	0.117
1995.70	3.86	4.513E-04	3.782E-03	8.967E-03	3.403E-06	1.048E-06	0.102
1995.66	4.11	4.801E-04	3.957E-03	8.984E-03	3.837E-06	1.114E-06	0.118
1995.62	4.37	5.124E-04	3.770E-03	9.065E-03	3.279E-06	1.173E-06	0.128
1995.58	4.63	5.113E-04	4.022E-03	9.033E-03	3.497E-06	1.114E-06	0.151
1995.55	4.88	4.990E-04	4.353E-03	9.067E-03	4.072E-06	1.014E-06	0.154
1995.52	5.14	4.882E-04	4.431E-03	9.041E-03	4.820E-06	9.734E-07	0.169
1995.48	5.40	4.826E-04	4.284E-03	9.003E-03	4.926E-06	1.058E-06	0.166
1995.45	5.66	4.719E-04	4.131E-03	8.906E-03	4.081E-06	1.042E-06	0.153
1995.42	5.91	4.599E-04	4.190E-03	8.814E-03	3.263E-06	1.012E-06	0.151
1995.38	6.17	4.538E-04	4.218E-03	8.892E-03	3.769E-06	1.016E-06	0.143
1995.35	6.43	4.548E-04	4.299E-03	8.912E-03	3.259E-06	1.001E-06	0.167
1995.32	6.68	4.473E-04	4.078E-03	8.941E-03	3.194E-06	1.046E-06	0.176
1995.28	6.94	4.419E-04	4.296E-03	8.777E-03	3.338E-06	1.009E-06	0.167
1995.25	7.20	4.224E-04	4.493E-03	8.702E-03	2.785E-06	9.686E-07	0.178
1995.21	7.46	4.339E-04	4.393E-03	8.788E-03	2.644E-06	9.974E-07	0.171
1995.18	7.71	4.248E-04	4.240E-03	8.722E-03	2.959E-06	9.584E-07	0.150
1995.15	7.97	4.105E-04	3.941E-03	8.684E-03	2.916E-06	1.005E-06	0.173
1995.12	8.23	4.067E-04	3.791E-03	8.860E-03	3.131E-06	1.065E-06	0.143
1995.05	8.48	4.242E-04	3.633E-03	8.791E-03	2.626E-06	1.080E-06	0.139
1995.00	8.74	4.448E-04	3.670E-03	8.797E-03	2.599E-06	1.105E-06	0.160
1994.93	9.00	4.640E-04	3.558E-03	9.055E-03	2.871E-06	1.253E-06	0.140
1994.88	9.26	4.738E-04	3.546E-03	9.077E-03	3.056E-06	1.239E-06	0.128
1994.81	9.51	4.908E-04	3.594E-03	9.107E-03	2.822E-06	1.253E-06	0.122
1994.76	9.77	5.047E-04	3.719E-03	9.106E-03	2.639E-06	1.189E-06	0.129
1994.69	10.03	5.139E-04	3.722E-03	9.068E-03	2.528E-06	1.131E-06	0.130
1994.64	10.28	5.209E-04	3.835E-03	9.204E-03	2.968E-06	1.150E-06	0.126
1994.59	10.54	4.930E-04	4.152E-03	9.098E-03	3.300E-06	1.075E-06	0.133
1994.54	10.80	4.838E-04	4.221E-03	9.157E-03	3.126E-06	1.068E-06	0.142
1994.50	11.06	4.861E-04	4.135E-03	9.022E-03	3.285E-06	1.048E-06	0.141
1994.45	11.31	4.835E-04	3.896E-03	9.068E-03	3.365E-06	1.196E-06	0.149
1994.41	11.57	4.824E-04	4.001E-03	9.027E-03	2.856E-06	1.136E-06	0.115
1994.36	11.83	4.634E-04	4.140E-03	8.934E-03	2.749E-06	1.006E-06	0.151
1994.31	12.08	4.705E-04	4.203E-03	8.963E-03	2.737E-06	1.029E-06	0.138
1994.27	12.34	4.822E-04	4.156E-03	8.899E-03	2.633E-06	1.022E-06	0.132
1994.22	12.60	4.558E-04	4.082E-03	8.938E-03	2.625E-06	1.077E-06	0.142
1994.18	12.85	4.305E-04	4.087E-03	8.807E-03	2.410E-06	9.807E-07	0.156
1994.13	13.11	4.453E-04	4.122E-03	8.772E-03	2.348E-06	1.007E-06	0.161

LA-ICP-MS data

Time	Distance from top (mm)	B/Ca (mol/mol)	Mg/Ca (mol/mol)	Sr/Ca (mol/mol)	Ba/Ca (mol/mol)	U/Ca (mol/mol)	Mn ($\mu g\ g^{-1}$)
1994.08	13.37	4.345E-04	3.999E-03	8.716E-03	2.235E-06	1.007E-06	0.182
1994.04	13.63	4.177E-04	4.009E-03	8.908E-03	2.217E-06	1.024E-06	0.187
1993.98	13.88	4.336E-04	3.913E-03	8.799E-03	2.430E-06	1.082E-06	0.180
1993.93	14.14	4.288E-04	3.999E-03	8.695E-03	2.290E-06	1.020E-06	0.196
1993.88	14.40	4.353E-04	4.083E-03	8.708E-03	2.949E-06	9.797E-07	0.187
1993.82	14.65	4.731E-04	4.376E-03	8.967E-03	3.286E-06	1.007E-06	0.148
1993.77	14.91	4.619E-04	4.092E-03	8.872E-03	2.895E-06	1.032E-06	0.137
1993.72	15.17	4.876E-04	4.219E-03	8.966E-03	2.883E-06	1.063E-06	0.124
1993.66	15.43	4.911E-04	3.984E-03	8.998E-03	2.983E-06	1.110E-06	0.134
1993.61	15.68	4.790E-04	3.724E-03	8.980E-03	2.835E-06	1.170E-06	0.140
1993.55	15.94	4.894E-04	3.652E-03	9.103E-03	3.031E-06	1.152E-06	0.132
1993.50	16.20	5.310E-04	4.117E-03	9.170E-03	3.067E-06	1.101E-06	0.132
1993.47	16.45	5.139E-04	4.077E-03	9.159E-03	3.430E-06	1.104E-06	0.132
1993.44	16.71	4.972E-04	4.125E-03	9.081E-03	3.202E-06	1.078E-06	0.144
1993.42	16.97	5.124E-04	4.074E-03	9.154E-03	2.949E-06	1.105E-06	0.122
1993.39	17.23	5.085E-04	4.292E-03	9.074E-03	2.990E-06	1.032E-06	0.129
1993.36	17.48	4.889E-04	4.239E-03	8.982E-03	3.078E-06	1.047E-06	0.129
1993.33	17.74	4.964E-04	4.212E-03	9.103E-03	3.065E-06	1.001E-06	0.123
1993.30	18.00	4.672E-04	4.059E-03	8.970E-03	2.738E-06	1.000E-06	0.144
1993.28	18.25	4.713E-04	3.953E-03	8.928E-03	2.983E-06	1.011E-06	0.159
1993.25	18.51	4.447E-04	4.033E-03	8.877E-03	2.755E-06	1.011E-06	0.215
1993.22	18.77	4.233E-04	3.966E-03	8.892E-03	2.603E-06	1.032E-06	0.212
1993.19	19.03	4.145E-04	3.971E-03	8.899E-03	2.662E-06	9.964E-07	0.207
1993.16	19.28	3.980E-04	4.148E-03	8.793E-03	3.311E-06	9.795E-07	0.188
1993.14	19.54	4.070E-04	4.564E-03	8.753E-03	3.202E-06	9.766E-07	0.179
1993.11	19.80	4.210E-04	4.102E-03	8.837E-03	2.976E-06	1.061E-06	0.186
1993.08	20.05	4.238E-04	4.200E-03	8.742E-03	2.719E-06	9.750E-07	0.145
1993.05	20.31	4.215E-04	4.107E-03	8.863E-03	3.101E-06	9.775E-07	0.154
1993.02	20.57	4.266E-04	3.926E-03	8.821E-03	2.631E-06	1.014E-06	0.211
1993.00	20.82	4.409E-04	3.962E-03	8.842E-03	2.567E-06	1.015E-06	0.148
1992.97	21.08	4.143E-04	3.796E-03	8.745E-03	2.764E-06	1.044E-06	0.145
1992.94	21.34	4.019E-04	3.632E-03	8.758E-03	2.410E-06	1.050E-06	0.129
1992.91	21.60	3.902E-04	3.547E-03	8.784E-03	2.878E-06	1.081E-06	0.121
1992.88	21.85	4.206E-04	3.993E-03	8.897E-03	3.675E-06	1.090E-06	0.128
1992.86	22.11	4.366E-04	4.221E-03	8.804E-03	3.898E-06	1.047E-06	0.127
1992.83	22.37	4.407E-04	4.076E-03	8.881E-03	3.908E-06	1.097E-06	0.126
1992.80	22.62	4.456E-04	4.368E-03	8.865E-03	3.462E-06	1.000E-06	0.126
1992.77	22.88	4.577E-04	4.167E-03	8.878E-03	3.493E-06	1.040E-06	0.141
1992.74	23.14	4.644E-04	4.261E-03	8.832E-03	3.167E-06	1.011E-06	0.180
1992.72	23.40	4.595E-04	4.050E-03	8.857E-03	3.041E-06	1.002E-06	0.165
1992.69	23.65	4.824E-04	3.761E-03	9.034E-03	2.922E-06	1.079E-06	0.180
1992.66	23.91	4.831E-04	3.796E-03	8.886E-03	2.783E-06	1.056E-06	0.137
1992.63	24.17	4.872E-04	3.816E-03	8.942E-03	2.750E-06	1.037E-06	0.164
1992.60	24.42	4.988E-04	3.700E-03	8.988E-03	2.844E-06	1.061E-06	0.145
1992.58	24.68	5.177E-04	3.761E-03	8.944E-03	2.847E-06	1.083E-06	0.210
1992.52	24.94	4.984E-04	3.626E-03	8.994E-03	2.835E-06	1.107E-06	0.319
1992.47	25.20	4.759E-04	3.590E-03	9.006E-03	2.843E-06	1.112E-06	0.164
1992.41	25.45	4.773E-04	3.954E-03	8.973E-03	2.930E-06	1.050E-06	0.145
1992.36	25.71	4.498E-04	4.119E-03	8.913E-03	2.636E-06	1.001E-06	0.152
1992.30	25.97	4.602E-04	4.005E-03	8.902E-03	2.585E-06	1.065E-06	0.128
1992.25	26.22	4.582E-04	3.906E-03	8.902E-03	2.722E-06	1.076E-06	0.125
1992.20	26.48	4.388E-04	3.492E-03	8.840E-03	2.577E-06	1.166E-06	0.150
1992.14	26.74	4.312E-04	3.360E-03	8.721E-03	2.528E-06	1.165E-06	0.132
1992.09	26.99	4.199E-04	3.374E-03	8.800E-03	2.870E-06	1.148E-06	0.171
1992.03	27.25	4.157E-04	3.632E-03	8.857E-03	3.984E-06	1.127E-06	0.342

Time	Distance from top (mm)	B/Ca (mol/mol)	Mg/Ca (mol/mol)	Sr/Ca (mol/mol)	Ba/Ca (mol/mol)	U/Ca (mol/mol)	Mn ($\mu g\ g^{-1}$)
1991.98	27.51	4.329E-04	3.676E-03	8.927E-03	6.612E-06	1.171E-06	0.148
1991.92	27.77	4.425E-04	3.482E-03	8.909E-03	4.859E-06	1.174E-06	0.172
1991.87	28.02	4.849E-04	3.744E-03	9.017E-03	3.213E-06	1.157E-06	0.176
1991.81	28.28	4.680E-04	3.642E-03	8.999E-03	2.737E-06	1.162E-06	0.168
1991.76	28.54	4.828E-04	3.709E-03	8.999E-03	2.836E-06	1.155E-06	0.135
1991.71	28.79	4.988E-04	3.682E-03	9.114E-03	3.245E-06	1.204E-06	0.112
1991.65	29.05	4.831E-04	3.540E-03	9.149E-03	3.024E-06	1.180E-06	0.130
1991.60	29.31	5.119E-04	3.825E-03	8.986E-03	2.714E-06	1.147E-06	0.129
1991.55	29.57	5.099E-04	3.794E-03	8.978E-03	2.514E-06	1.086E-06	0.191
1991.51	29.82	4.944E-04	3.589E-03	9.077E-03	2.483E-06	1.184E-06	0.160
1991.46	30.08	4.945E-04	3.782E-03	9.035E-03	2.684E-06	1.171E-06	0.163
1991.42	30.34	4.676E-04	3.887E-03	8.956E-03	2.673E-06	1.087E-06	0.158
1991.38	30.59	4.646E-04	4.405E-03	8.913E-03	2.970E-06	1.019E-06	0.174
1991.33	30.85	4.395E-04	4.352E-03	8.953E-03	2.702E-06	1.030E-06	0.176
1991.29	31.11	4.360E-04	4.218E-03	8.837E-03	2.487E-06	1.034E-06	0.165
1991.26	31.37	4.533E-04	4.219E-03	8.988E-03	2.548E-06	1.058E-06	0.176
1991.23	31.62	4.491E-04	4.221E-03	8.870E-03	2.327E-06	9.540E-07	0.194
1991.21	31.88	4.403E-04	4.067E-03	8.793E-03	2.180E-06	9.831E-07	0.168
1991.18	32.14	4.327E-04	3.845E-03	8.833E-03	2.000E-06	9.976E-07	0.160
1991.16	32.39	4.392E-04	3.729E-03	8.751E-03	2.141E-06	1.018E-06	0.179
1991.13	32.65	4.193E-04	3.415E-03	8.829E-03	2.255E-06	1.039E-06	0.178
1991.10	32.91	4.216E-04	3.986E-03	8.759E-03	2.354E-06	9.937E-07	0.160
1991.08	33.17	4.390E-04	4.117E-03	8.793E-03	2.464E-06	9.930E-07	0.150
1991.05	33.42	4.270E-04	3.911E-03	8.843E-03	3.416E-06	1.035E-06	0.168
1991.02	33.68	4.183E-04	3.789E-03	8.882E-03	3.869E-06	1.068E-06	0.272
1991.00	33.94	4.009E-04	3.956E-03	8.712E-03	3.499E-06	9.868E-07	0.139
1990.97	34.19	4.116E-04	3.603E-03	8.830E-03	3.629E-06	1.066E-06	0.178
1990.94	34.45	4.031E-04	3.488E-03	8.764E-03	3.197E-06	1.044E-06	0.166
1990.87	34.71	4.495E-04	3.655E-03	8.970E-03	3.218E-06	1.106E-06	0.190
1990.80	34.96	4.721E-04	3.582E-03	8.991E-03	3.673E-06	1.177E-06	0.162
1990.73	35.22	4.526E-04	3.604E-03	8.995E-03	2.932E-06	1.131E-06	0.121
1990.65	35.48	4.808E-04	3.557E-03	8.989E-03	2.853E-06	1.108E-06	0.147
1990.58	35.74	4.849E-04	3.531E-03	8.901E-03	2.680E-06	1.135E-06	0.153
1990.51	35.99	4.905E-04	3.639E-03	9.026E-03	2.872E-06	1.157E-06	0.213
1990.48	36.25	4.859E-04	3.985E-03	8.987E-03	2.521E-06	1.030E-06	0.156
1990.45	36.51	4.781E-04	3.791E-03	9.009E-03	2.635E-06	1.103E-06	0.181
1990.42	36.76	4.659E-04	3.828E-03	9.069E-03	2.717E-06	1.093E-06	0.182
1990.39	37.02	4.597E-04	3.797E-03	9.037E-03	2.788E-06	1.081E-06	0.163
1990.36	37.28	4.665E-04	3.826E-03	9.024E-03	2.909E-06	1.123E-06	0.159
1990.33	37.54	4.424E-04	3.868E-03	8.928E-03	2.724E-06	1.020E-06	0.170
1990.30	37.79	4.351E-04	3.856E-03	8.726E-03	2.541E-06	9.346E-07	0.146
1990.27	38.05	4.535E-04	4.089E-03	8.916E-03	2.574E-06	9.440E-07	0.156
1990.24	38.31	4.320E-04	4.010E-03	8.735E-03	2.611E-06	9.433E-07	0.155
1990.21	38.56	4.083E-04	4.071E-03	8.720E-03	2.574E-06	9.398E-07	0.157
1990.19	38.82	4.098E-04	4.162E-03	8.664E-03	2.345E-06	9.236E-07	0.132
1990.16	39.08	4.322E-04	3.854E-03	8.658E-03	2.473E-06	9.782E-07	0.123
1990.13	39.34	3.952E-04	3.895E-03	8.747E-03	2.530E-06	9.938E-07	0.132
1990.10	39.59	3.851E-04	3.857E-03	8.775E-03	2.612E-06	1.025E-06	0.135
1990.07	39.85	3.916E-04	4.166E-03	8.690E-03	2.731E-06	9.740E-07	0.141
1990.04	40.11	3.749E-04	3.599E-03	8.851E-03	2.512E-06	1.058E-06	0.149
1990.00	40.36	4.012E-04	3.789E-03	8.685E-03	2.783E-06	1.037E-06	0.149
1989.97	40.62	4.085E-04	3.458E-03	8.754E-03	2.070E-06	1.095E-06	0.135
1989.93	40.88	4.344E-04	3.482E-03	8.936E-03	2.324E-06	1.162E-06	0.142
1989.90	41.14	4.446E-04	3.639E-03	8.906E-03	2.724E-06	1.120E-06	0.159
1989.86	41.39	4.353E-04	3.298E-03	8.846E-03	2.688E-06	1.174E-06	0.150

LA-ICP-MS data

Time	Distance from top (mm)	B/Ca (mol/mol)	Mg/Ca (mol/mol)	Sr/Ca (mol/mol)	Ba/Ca (mol/mol)	U/Ca (mol/mol)	Mn ($\mu g\ g^{-1}$)
1989.83	41.65	4.397E-04	3.539E-03	8.822E-03	3.355E-06	1.089E-06	0.150
1989.79	41.91	4.609E-04	3.739E-03	9.033E-03	4.122E-06	1.104E-06	0.144
1989.76	42.16	4.600E-04	3.984E-03	8.936E-03	3.156E-06	1.097E-06	0.160
1989.72	42.42	4.696E-04	3.746E-03	8.970E-03	2.433E-06	1.120E-06	0.162
1989.69	42.68	5.062E-04	3.732E-03	9.067E-03	2.348E-06	1.200E-06	0.177
1989.65	42.93	4.927E-04	3.733E-03	9.020E-03	2.412E-06	1.179E-06	0.179
1989.62	43.19	5.184E-04	3.958E-03	9.073E-03	2.108E-06	1.041E-06	0.181
1989.49	43.45	4.874E-04	3.973E-03	8.982E-03	2.052E-06	1.043E-06	0.179
1989.37	43.71	4.697E-04	3.891E-03	9.050E-03	2.470E-06	1.073E-06	0.193
1989.24	43.96	4.789E-04	3.929E-03	9.043E-03	2.467E-06	1.116E-06	0.155
1989.12	44.22	4.755E-04	4.062E-03	9.046E-03	2.527E-06	1.032E-06	0.165
1988.99	44.48	4.718E-04	3.988E-03	8.873E-03	2.658E-06	1.036E-06	0.143
1988.87	44.73	4.471E-04	4.194E-03	8.884E-03	2.876E-06	1.004E-06	0.117
1988.74	44.99	4.480E-04	4.075E-03	8.898E-03	3.345E-06	1.074E-06	0.146
1988.62	45.25	4.454E-04	3.844E-03	8.945E-03	3.677E-06	1.095E-06	0.153
1988.49	45.51	4.495E-04	4.420E-03	8.786E-03	3.044E-06	9.329E-07	0.145
1988.37	45.76	4.482E-04	4.304E-03	8.806E-03	2.958E-06	9.845E-07	0.136

Table 10.7 Davies Reef 2 *Porites* data

Time	Distance from top (mm)	B/Ca (mol/mol)	Mg/Ca (mol/mol)	Sr/Ca (mol/mol)	Ba/Ca (mol/mol)	U/Ca (mol/mol)	Mn ($\mu g\ g^{-1}$)
1993.77	0.14	4.173E-04	3.666E-03	8.823E-03	1.895E-04	1.080E-06	0.110
1993.75	0.45	4.225E-04	3.630E-03	8.874E-03	7.012E-05	1.063E-06	0.152
1993.73	0.75	4.339E-04	3.526E-03	8.833E-03	7.165E-05	1.046E-06	0.133
1993.71	1.06	4.347E-04	3.269E-03	8.914E-03	7.604E-05	1.131E-06	0.130
1993.69	1.37	4.523E-04	3.353E-03	8.892E-03	8.586E-05	1.179E-06	0.139
1993.66	1.68	4.622E-04	3.276E-03	8.849E-03	8.560E-05	1.171E-06	0.118
1993.64	1.99	4.926E-04	3.162E-03	9.030E-03	8.428E-05	1.207E-06	0.120
1993.62	2.30	5.143E-04	3.211E-03	8.999E-03	8.106E-05	1.193E-06	0.161
1993.60	2.61	5.184E-04	3.302E-03	9.030E-03	8.264E-05	1.185E-06	0.142
1993.58	2.92	5.139E-04	3.272E-03	9.064E-03	6.442E-05	1.160E-06	0.146
1993.56	3.23	5.062E-04	3.221E-03	8.921E-03	5.844E-05	1.155E-06	0.133
1993.54	3.53	5.164E-04	3.286E-03	9.134E-03	5.909E-05	1.234E-06	0.127
1993.42	3.84	4.993E-04	3.594E-03	9.016E-03	6.329E-05	1.110E-06	0.140
1993.39	4.15	4.840E-04	4.234E-03	8.926E-03	8.903E-05	1.025E-06	0.155
1993.36	4.46	4.706E-04	3.763E-03	8.872E-03	7.323E-05	1.120E-06	0.178
1993.33	4.77	4.624E-04	3.998E-03	8.818E-03	7.639E-05	1.034E-06	0.119
1993.31	5.08	4.636E-04	4.021E-03	8.835E-03	6.955E-05	1.028E-06	0.112
1993.30	5.39	4.819E-04	3.744E-03	8.975E-03	6.548E-05	1.116E-06	0.124
1993.29	5.70	4.623E-04	3.716E-03	8.911E-03	5.665E-05	1.093E-06	0.144
1993.28	6.00	4.396E-04	3.747E-03	8.915E-03	4.366E-05	1.078E-06	0.139
1993.27	6.31	4.379E-04	3.964E-03	8.830E-03	4.369E-05	1.055E-06	0.147
1993.25	6.62	4.152E-04	3.770E-03	8.867E-03	3.662E-05	1.068E-06	0.141
1993.24	6.93	3.935E-04	3.562E-03	8.838E-03	2.985E-05	1.138E-06	0.164
1993.23	7.24	3.940E-04	3.648E-03	8.778E-03	1.946E-05	1.123E-06	0.149
1993.22	7.55	3.948E-04	3.537E-03	8.827E-03	2.137E-05	1.217E-06	0.157
1993.20	7.86	4.018E-04	3.747E-03	8.880E-03	2.135E-05	1.114E-06	0.177
1993.19	8.17	4.047E-04	3.933E-03	8.672E-03	1.236E-05	9.489E-07	0.166
1993.16	8.47	3.995E-04	3.959E-03	8.790E-03	1.142E-05	1.053E-06	0.133
1993.12	8.78	4.075E-04	4.290E-03	8.760E-03	1.055E-05	9.373E-07	0.108
1993.09	9.09	4.084E-04	3.904E-03	8.799E-03	6.254E-06	1.039E-06	0.139
1993.05	9.40	4.422E-04	3.730E-03	8.751E-03	5.878E-06	1.026E-06	0.098
1993.01	9.71	4.348E-04	3.599E-03	8.856E-03	7.440E-06	1.051E-06	0.125
1992.98	10.02	4.211E-04	3.427E-03	8.830E-03	6.382E-06	1.032E-06	0.174
1992.94	10.33	4.300E-04	3.762E-03	8.724E-03	6.412E-06	9.844E-07	0.125
1992.92	10.64	4.253E-04	3.755E-03	8.784E-03	6.869E-06	1.016E-06	0.117
1992.89	10.94	4.580E-04	3.956E-03	8.940E-03	6.215E-06	1.010E-06	0.142
1992.86	11.25	4.350E-04	4.068E-03	8.805E-03	5.898E-06	9.869E-07	0.128
1992.84	11.56	4.331E-04	3.911E-03	8.898E-03	6.778E-06	1.001E-06	0.136
1992.81	11.87	4.338E-04	3.888E-03	8.805E-03	5.669E-06	1.002E-06	0.148
1992.78	12.18	4.411E-04	3.733E-03	8.933E-03	5.388E-06	1.027E-06	0.167
1992.76	12.49	4.550E-04	3.669E-03	9.046E-03	6.053E-06	1.122E-06	0.370
1992.73	12.80	4.395E-04	3.224E-03	9.181E-03	4.968E-06	1.216E-06	0.140
1992.71	13.11	4.887E-04	3.298E-03	9.016E-03	4.502E-06	1.188E-06	0.119
1992.68	13.42	4.982E-04	3.430E-03	9.166E-03	6.084E-06	1.183E-06	0.108
1992.65	13.72	4.700E-04	3.255E-03	9.091E-03	6.531E-06	1.172E-06	0.129
1992.63	14.03	5.096E-04	3.571E-03	9.081E-03	5.400E-06	1.071E-06	0.123
1992.60	14.34	5.237E-04	3.636E-03	9.042E-03	4.602E-06	1.046E-06	0.133
1992.57	14.65	5.262E-04	3.259E-03	9.120E-03	3.855E-06	1.179E-06	0.148
1992.55	14.96	5.760E-04	3.435E-03	9.302E-03	4.861E-06	1.147E-06	0.147
1992.50	15.27	5.195E-04	3.292E-03	9.090E-03	3.876E-06	1.181E-06	0.138
1992.45	15.58	4.815E-04	3.442E-03	9.034E-03	3.454E-06	1.166E-06	0.114
1992.40	15.89	4.737E-04	3.527E-03	9.003E-03	3.025E-06	1.083E-06	0.119

LA-ICP-MS data

Time	Distance from top (mm)	B/Ca (mol/mol)	Mg/Ca (mol/mol)	Sr/Ca (mol/mol)	Ba/Ca (mol/mol)	U/Ca (mol/mol)	Mn ($\mu g\ g^{-1}$)
1992.35	16.19	4.580E-04	3.889E-03	8.993E-03	3.073E-06	9.991E-07	0.104
1992.30	16.50	4.427E-04	4.029E-03	8.927E-03	3.660E-06	9.854E-07	0.103
1992.26	16.81	4.516E-04	4.205E-03	8.824E-03	3.832E-06	9.243E-07	0.089
1992.21	17.12	4.584E-04	3.826E-03	8.755E-03	3.305E-06	1.016E-06	0.103
1992.19	17.43	4.608E-04	3.589E-03	8.915E-03	2.926E-06	1.103E-06	0.108
1992.17	17.74	4.717E-04	3.701E-03	8.914E-03	3.267E-06	1.032E-06	0.134
1992.15	18.05	4.561E-04	3.692E-03	8.928E-03	3.333E-06	1.019E-06	0.117
1992.13	18.36	4.655E-04	3.888E-03	8.823E-03	3.372E-06	9.719E-07	0.106
1992.11	18.66	4.405E-04	3.817E-03	8.851E-03	3.746E-06	1.023E-06	0.128
1992.09	18.97	4.217E-04	3.952E-03	8.835E-03	2.843E-06	9.864E-07	0.137
1992.07	19.28	4.025E-04	3.643E-03	8.784E-03	2.585E-06	1.052E-06	0.114
1992.05	19.59	3.999E-04	3.648E-03	8.906E-03	3.122E-06	1.066E-06	0.115
1992.03	19.90	4.051E-04	3.885E-03	8.874E-03	3.491E-06	1.035E-06	0.118
1992.01	20.21	4.159E-04	4.033E-03	8.854E-03	3.887E-06	1.033E-06	0.109
1991.99	20.52	4.233E-04	4.307E-03	8.889E-03	3.511E-06	9.408E-07	0.118
1991.97	20.83	4.138E-04	4.302E-03	8.745E-03	4.322E-06	9.005E-07	0.127
1991.95	21.13	4.255E-04	4.146E-03	8.792E-03	3.057E-06	9.544E-07	0.127
1991.93	21.44	4.539E-04	3.993E-03	8.890E-03	2.684E-06	1.026E-06	0.150
1991.91	21.75	4.173E-04	3.891E-03	8.748E-03	2.988E-06	1.015E-06	0.133
1991.89	22.06	4.281E-04	3.987E-03	8.856E-03	3.001E-06	1.015E-06	0.122
1991.87	22.37	4.320E-04	3.911E-03	8.826E-03	2.519E-06	1.041E-06	0.115
1991.83	22.68	4.544E-04	3.934E-03	8.830E-03	2.579E-06	1.040E-06	0.128
1991.80	22.99	4.539E-04	3.823E-03	9.010E-03	2.685E-06	1.060E-06	0.119
1991.77	23.30	4.742E-04	3.717E-03	8.948E-03	3.354E-06	1.061E-06	0.113
1991.74	23.61	4.737E-04	3.644E-03	9.133E-03	3.829E-06	1.033E-06	0.126
1991.71	23.91	4.768E-04	3.745E-03	8.991E-03	4.682E-06	1.039E-06	0.121
1991.68	24.22	4.816E-04	3.854E-03	8.988E-03	4.135E-06	1.041E-06	0.120
1991.65	24.53	5.123E-04	3.903E-03	9.007E-03	3.144E-06	1.063E-06	0.139
1991.62	24.84	4.972E-04	3.720E-03	9.106E-03	3.071E-06	1.031E-06	0.143
1991.59	25.15	5.055E-04	3.821E-03	8.975E-03	2.885E-06	1.015E-06	0.147
1991.56	25.46	5.233E-04	4.050E-03	8.998E-03	3.972E-06	1.006E-06	0.124
1991.52	25.77	5.000E-04	3.605E-03	8.913E-03	3.261E-06	1.056E-06	0.114
1991.49	26.08	5.207E-04	3.427E-03	9.054E-03	3.111E-06	1.106E-06	0.115
1991.46	26.38	5.108E-04	3.333E-03	9.131E-03	2.585E-06	1.058E-06	0.102
1991.44	26.69	5.154E-04	3.590E-03	9.090E-03	2.710E-06	1.110E-06	0.097
1991.43	27.00	5.104E-04	3.627E-03	9.104E-03	2.603E-06	1.116E-06	0.076
1991.41	27.31	5.004E-04	3.475E-03	8.963E-03	2.556E-06	1.091E-06	0.093
1991.39	27.62	5.030E-04	3.308E-03	8.990E-03	2.254E-06	1.097E-06	0.082
1991.38	27.93	5.215E-04	3.434E-03	9.020E-03	2.403E-06	1.120E-06	0.065
1991.36	28.24	4.683E-04	3.676E-03	8.990E-03	2.601E-06	1.061E-06	0.078
1991.34	28.55	4.790E-04	3.960E-03	8.970E-03	2.428E-06	1.017E-06	0.085
1991.32	28.85	4.821E-04	4.319E-03	8.886E-03	2.654E-06	9.621E-07	0.088
1991.31	29.16	4.557E-04	4.184E-03	8.930E-03	2.504E-06	1.015E-06	0.109
1991.29	29.47	4.570E-04	4.013E-03	8.942E-03	2.557E-06	1.022E-06	0.108
1991.27	29.78	4.709E-04	4.000E-03	9.001E-03	2.288E-06	9.846E-07	0.109
1991.25	30.09	4.725E-04	4.071E-03	8.956E-03	2.522E-06	9.686E-07	0.102
1991.24	30.40	4.765E-04	4.140E-03	8.905E-03	2.503E-06	9.684E-07	0.118
1991.22	30.71	4.630E-04	4.081E-03	8.895E-03	2.343E-06	9.690E-07	0.123
1991.20	31.02	4.507E-04	4.397E-03	8.906E-03	2.492E-06	8.973E-07	0.139
1991.18	31.32	4.568E-04	4.336E-03	8.821E-03	3.025E-06	9.147E-07	0.139
1991.17	31.63	4.618E-04	4.339E-03	8.811E-03	2.853E-06	9.238E-07	0.124
1991.15	31.94	4.615E-04	4.275E-03	8.863E-03	2.899E-06	9.442E-07	0.135
1991.13	32.25	4.522E-04	4.285E-03	8.780E-03	2.807E-06	8.787E-07	0.130
1991.12	32.56	4.341E-04	4.421E-03	8.674E-03	3.904E-06	8.790E-07	0.149
1991.09	32.87	4.082E-04	4.146E-03	8.691E-03	3.090E-06	9.292E-07	0.211

Time	Distance from top (mm)	B/Ca (mol/mol)	Mg/Ca (mol/mol)	Sr/Ca (mol/mol)	Ba/Ca (mol/mol)	U/Ca (mol/mol)	Mn ($\mu g\ g^{-1}$)
1991.06	33.18	4.174E-04	4.250E-03	8.744E-03	2.728E-06	9.049E-07	0.177
1991.04	33.49	4.068E-04	4.593E-03	8.743E-03	2.768E-06	8.725E-07	0.151
1991.01	33.80	4.137E-04	4.610E-03	8.758E-03	2.313E-06	9.212E-07	0.137
1990.99	34.10	4.309E-04	4.321E-03	8.853E-03	1.899E-06	9.243E-07	0.107
1990.96	34.41	4.529E-04	4.310E-03	8.730E-03	2.315E-06	9.193E-07	0.106
1990.94	34.72	4.433E-04	4.007E-03	8.816E-03	3.907E-06	9.622E-07	0.105
1990.91	35.03	4.313E-04	4.247E-03	8.738E-03	4.185E-06	9.007E-07	0.100
1990.89	35.34	4.241E-04	4.273E-03	8.812E-03	3.318E-06	8.908E-07	0.111
1990.86	35.65	4.396E-04	4.542E-03	8.953E-03	3.409E-06	9.103E-07	0.122
1990.84	35.96	4.539E-04	4.145E-03	8.838E-03	2.837E-06	9.155E-07	0.145
1990.81	36.27	4.753E-04	4.284E-03	8.930E-03	2.500E-06	9.237E-07	0.137
1990.79	36.57	4.841E-04	4.122E-03	8.921E-03	2.435E-06	9.734E-07	0.111
1990.76	36.88	5.265E-04	4.123E-03	8.929E-03	2.381E-06	9.671E-07	0.113
1990.74	37.19	5.102E-04	3.956E-03	8.940E-03	2.307E-06	9.724E-07	0.127
1990.71	37.50	4.924E-04	3.537E-03	9.072E-03	2.286E-06	1.056E-06	0.107
1990.65	37.81	4.783E-04	3.208E-03	8.976E-03	2.172E-06	1.106E-06	0.113
1990.60	38.12	5.116E-04	3.437E-03	9.020E-03	2.433E-06	1.114E-06	0.124
1990.54	38.43	5.053E-04	3.291E-03	9.087E-03	2.370E-06	1.145E-06	0.104
1990.48	38.74	5.195E-04	3.510E-03	9.151E-03	2.395E-06	1.134E-06	0.086
1990.45	39.04	5.343E-04	3.491E-03	9.048E-03	2.208E-06	1.101E-06	0.108
1990.42	39.35	5.359E-04	3.873E-03	8.967E-03	1.973E-06	1.031E-06	0.097
1990.40	39.66	5.238E-04	4.138E-03	8.991E-03	2.489E-06	1.043E-06	0.106
1990.37	39.97	4.998E-04	4.216E-03	8.885E-03	2.392E-06	9.877E-07	0.118
1990.34	40.28	4.780E-04	4.098E-03	8.929E-03	1.941E-06	9.173E-07	0.100
1990.31	40.59	5.000E-04	4.214E-03	8.826E-03	2.095E-06	9.558E-07	0.105
1990.28	40.90	4.941E-04	4.204E-03	8.726E-03	1.938E-06	8.997E-07	0.098
1990.25	41.21	4.716E-04	4.236E-03	8.740E-03	2.101E-06	9.213E-07	0.093
1990.23	41.51	4.656E-04	4.470E-03	8.789E-03	2.648E-06	8.858E-07	0.112
1990.21	41.82	4.692E-04	4.481E-03	8.743E-03	2.755E-06	9.012E-07	0.121
1990.19	42.13	4.530E-04	4.138E-03	8.793E-03	2.446E-06	9.275E-07	0.098
1990.17	42.44	4.534E-04	4.262E-03	8.686E-03	2.563E-06	9.080E-07	0.103
1990.14	42.75	4.396E-04	4.287E-03	8.698E-03	2.506E-06	8.887E-07	0.114
1990.12	43.06	4.300E-04	4.057E-03	8.609E-03	2.585E-06	8.971E-07	0.107
1990.10	43.37	4.204E-04	3.880E-03	8.727E-03	2.639E-06	9.264E-07	0.103
1990.08	43.68	3.962E-04	3.136E-03	8.782E-03	3.289E-06	1.142E-06	0.134
1990.06	43.99	3.879E-04	3.024E-03	8.949E-03	4.320E-06	1.175E-06	0.132
1990.04	44.29	3.834E-04	3.361E-03	8.843E-03	3.634E-06	1.111E-06	0.127
1990.03	44.60	3.941E-04	3.591E-03	8.832E-03	3.932E-06	1.064E-06	0.131
1990.01	44.91	3.751E-04	3.122E-03	8.914E-03	3.313E-06	1.170E-06	0.157
1989.99	45.22	3.956E-04	3.496E-03	8.841E-03	3.683E-06	1.105E-06	0.147
1989.97	45.53	3.943E-04	3.506E-03	8.815E-03	3.351E-06	1.108E-06	0.149
1989.95	45.84	4.107E-04	3.426E-03	8.849E-03	3.483E-06	1.109E-06	0.174
1989.94	46.15	4.246E-04	3.236E-03	8.966E-03	3.854E-06	1.139E-06	0.149
1989.92	46.46	4.084E-04	2.925E-03	8.907E-03	3.819E-06	1.134E-06	0.162
1989.90	46.76	4.100E-04	3.035E-03	8.858E-03	3.882E-06	1.112E-06	0.151
1989.88	47.07	4.256E-04	3.445E-03	8.880E-03	3.881E-06	1.042E-06	0.150
1989.87	47.38	4.218E-04	3.386E-03	8.820E-03	4.174E-06	1.056E-06	0.158
1989.84	47.69	4.165E-04	3.360E-03	8.864E-03	3.813E-06	1.101E-06	0.188
1989.81	48.00	4.466E-04	3.270E-03	8.949E-03	4.615E-06	1.162E-06	0.140
1989.78	48.31	4.138E-04	3.078E-03	8.999E-03	6.051E-06	1.220E-06	0.204
1989.75	48.62	4.176E-04	3.222E-03	9.116E-03	6.840E-06	1.245E-06	0.277
1989.73	48.87	3.988E-04	3.058E-03	8.954E-03	6.094E-06	1.269E-06	0.173
1989.70	49.04	4.139E-04	2.695E-03	9.190E-03	2.998E-06	1.334E-06	0.112
1989.67	49.38	4.196E-04	2.945E-03	9.251E-03	2.740E-06	1.280E-06	0.132
1989.64	49.72	4.264E-04	3.172E-03	9.150E-03	2.540E-06	1.198E-06	0.113

LA-ICP-MS data

Time	Distance from top (mm)	B/Ca (mol/mol)	Mg/Ca (mol/mol)	Sr/Ca (mol/mol)	Ba/Ca (mol/mol)	U/Ca (mol/mol)	Mn ($\mu g\ g^{-1}$)
1989.61	50.06	4.544E-04	2.889E-03	9.157E-03	2.358E-06	1.248E-06	0.112
1989.59	50.40	4.693E-04	2.910E-03	9.116E-03	2.217E-06	1.295E-06	0.117
1989.56	50.74	5.149E-04	2.995E-03	9.318E-03	2.163E-06	1.257E-06	0.110
1989.51	51.08	5.217E-04	3.368E-03	9.146E-03	2.337E-06	1.214E-06	0.111
1989.46	51.42	5.088E-04	3.557E-03	9.156E-03	2.092E-06	1.098E-06	0.098
1989.41	51.76	5.057E-04	3.521E-03	8.947E-03	1.840E-06	1.122E-06	0.144
1989.37	52.10	4.915E-04	3.460E-03	9.119E-03	1.863E-06	1.159E-06	0.180
1989.32	52.44	4.816E-04	3.689E-03	8.908E-03	1.774E-06	1.133E-06	0.156
1989.27	52.79	4.690E-04	4.049E-03	8.845E-03	2.021E-06	1.060E-06	0.145
1989.25	53.13	4.548E-04	3.782E-03	8.902E-03	1.847E-06	1.032E-06	0.137
1989.23	53.47	4.554E-04	4.076E-03	8.944E-03	2.039E-06	9.352E-07	0.131
1989.21	53.81	4.458E-04	3.578E-03	8.997E-03	1.985E-06	1.069E-06	0.122
1989.19	54.15	4.478E-04	3.695E-03	8.989E-03	2.080E-06	1.021E-06	0.114
1989.17	54.49	4.325E-04	3.474E-03	8.781E-03	1.973E-06	1.038E-06	0.101
1989.14	54.83	4.637E-04	3.596E-03	8.903E-03	2.128E-06	1.026E-06	0.121
1989.12	55.17	4.223E-04	3.846E-03	8.961E-03	2.288E-06	1.085E-06	0.099
1989.10	55.51	3.851E-04	4.108E-03	8.865E-03	2.272E-06	9.621E-07	0.122
1989.08	55.85	3.961E-04	4.388E-03	8.687E-03	2.485E-06	9.351E-07	0.141
1989.06	56.19	3.936E-04	3.699E-03	8.800E-03	1.977E-06	1.020E-06	0.142
1989.04	56.53	3.985E-04	3.465E-03	8.849E-03	2.130E-06	1.035E-06	0.130
1989.02	56.88	4.167E-04	3.848E-03	8.803E-03	2.097E-06	9.196E-07	0.196
1989.00	57.22	4.047E-04	3.555E-03	8.898E-03	2.082E-06	1.015E-06	0.225
1988.98	57.56	4.079E-04	3.789E-03	8.783E-03	1.893E-06	9.866E-07	0.334
1988.96	57.90	4.097E-04	3.606E-03	8.774E-03	2.381E-06	1.023E-06	0.149
1988.94	58.24	3.831E-04	3.572E-03	8.734E-03	2.230E-06	1.046E-06	0.140
1988.92	58.58	4.046E-04	3.636E-03	8.955E-03	2.408E-06	1.079E-06	0.175
1988.90	58.92	3.979E-04	3.518E-03	8.795E-03	2.049E-06	1.056E-06	0.175
1988.88	59.26	4.053E-04	3.938E-03	8.704E-03	3.766E-06	1.028E-06	0.242
1988.86	59.60	4.053E-04	4.103E-03	8.799E-03	4.537E-06	9.882E-07	0.272
1988.83	59.94	3.974E-04	3.909E-03	8.852E-03	4.189E-06	9.772E-07	0.219
1988.81	60.28	4.119E-04	3.824E-03	8.663E-03	3.591E-06	9.687E-07	0.239
1988.79	60.63	4.291E-04	3.377E-03	8.804E-03	3.255E-06	1.040E-06	0.168
1988.77	60.97	4.540E-04	3.338E-03	8.869E-03	2.959E-06	1.126E-06	0.124
1988.75	61.31	4.503E-04	3.254E-03	9.014E-03	2.394E-06	1.076E-06	0.111
1988.73	61.65	4.686E-04	3.341E-03	8.900E-03	2.029E-06	1.079E-06	0.118
1988.65	61.99	4.909E-04	3.170E-03	8.996E-03	2.082E-06	1.194E-06	0.094
1988.58	62.33	5.056E-04	2.806E-03	9.196E-03	1.872E-06	1.198E-06	0.103
1988.56	62.67	5.214E-04	3.097E-03	9.188E-03	1.758E-06	1.150E-06	0.104
1988.53	63.01	5.092E-04	3.244E-03	9.144E-03	1.858E-06	1.228E-06	0.104
1988.51	63.35	5.072E-04	3.474E-03	9.086E-03	1.952E-06	1.054E-06	0.142
1988.49	63.69	4.949E-04	3.689E-03	9.113E-03	1.934E-06	1.101E-06	0.115
1988.47	64.03	4.867E-04	3.546E-03	8.973E-03	1.981E-06	1.128E-06	0.111
1988.45	64.37	4.939E-04	3.604E-03	8.991E-03	2.075E-06	1.098E-06	0.114
1988.42	64.72	4.798E-04	3.180E-03	9.042E-03	1.720E-06	1.142E-06	0.108
1988.40	65.06	4.608E-04	3.548E-03	8.960E-03	2.090E-06	1.091E-06	0.112
1988.38	65.40	4.717E-04	3.723E-03	8.974E-03	2.033E-06	1.069E-06	0.099
1988.36	65.74	4.414E-04	3.548E-03	8.941E-03	2.052E-06	1.076E-06	0.084
1988.34	66.08	4.365E-04	3.397E-03	8.913E-03	2.085E-06	1.136E-06	0.092
1988.32	66.42	4.322E-04	3.426E-03	8.941E-03	2.085E-06	1.079E-06	0.114
1988.29	66.76	4.469E-04	3.787E-03	8.909E-03	2.152E-06	1.030E-06	0.108
1988.27	67.10	4.580E-04	3.377E-03	8.895E-03	1.917E-06	1.139E-06	0.135
1988.25	67.44	4.326E-04	3.544E-03	8.741E-03	1.787E-06	1.034E-06	0.107
1988.22	67.78	4.228E-04	3.684E-03	8.747E-03	1.854E-06	9.911E-07	0.141
1988.20	68.12	4.294E-04	3.682E-03	8.885E-03	2.002E-06	1.050E-06	0.118
1988.17	68.46	4.316E-04	3.711E-03	8.769E-03	2.276E-06	1.071E-06	0.139

Time	Distance from top (mm)	B/Ca (mol/mol)	Mg/Ca (mol/mol)	Sr/Ca (mol/mol)	Ba/Ca (mol/mol)	U/Ca (mol/mol)	Mn ($\mu g\ g^{-1}$)
1988.14	68.81	4.074E-04	4.051E-03	8.731E-03	2.251E-06	1.008E-06	0.089
1988.12	69.15	4.048E-04	3.833E-03	8.940E-03	2.285E-06	1.108E-06	0.093
1988.09	69.49	4.236E-04	3.712E-03	8.893E-03	2.311E-06	1.033E-06	0.095
1988.06	69.83	4.227E-04	3.463E-03	8.764E-03	2.347E-06	1.052E-06	0.103
1988.04	70.17	4.485E-04	3.548E-03	8.980E-03	2.251E-06	1.062E-06	0.123
1988.01	70.51	4.523E-04	3.424E-03	8.816E-03	2.047E-06	1.086E-06	0.117
1987.98	70.85	4.419E-04	3.202E-03	8.837E-03	2.462E-06	1.167E-06	0.134
1987.96	71.19	4.373E-04	3.229E-03	8.863E-03	5.206E-06	1.128E-06	0.156
1987.93	71.53	4.149E-04	3.538E-03	8.968E-03	4.469E-06	1.090E-06	0.123
1987.90	71.87	4.113E-04	3.489E-03	8.865E-03	2.857E-06	1.124E-06	0.117
1987.88	72.21	4.320E-04	3.582E-03	8.864E-03	2.598E-06	1.093E-06	0.120
1987.85	72.55	4.840E-04	3.763E-03	8.953E-03	2.224E-06	1.116E-06	0.171
1987.82	72.90	4.973E-04	3.520E-03	9.014E-03	1.970E-06	1.162E-06	0.309
1987.80	73.24	5.083E-04	3.669E-03	8.986E-03	1.896E-06	1.120E-06	0.096
1987.77	73.58	5.043E-04	3.706E-03	8.860E-03	1.762E-06	1.056E-06	0.118
1987.71	73.92	5.119E-04	3.636E-03	9.006E-03	1.889E-06	1.076E-06	0.175
1987.65	74.26	5.370E-04	3.373E-03	9.030E-03	1.615E-06	1.126E-06	0.104
1987.60	74.60	5.421E-04	3.345E-03	9.044E-03	1.793E-06	1.190E-06	0.085
1987.54	74.94	5.292E-04	3.236E-03	9.139E-03	1.679E-06	1.148E-06	0.124
1987.51	75.28	5.178E-04	3.718E-03	9.025E-03	1.925E-06	1.058E-06	0.119
1987.48	75.62	5.142E-04	3.707E-03	8.910E-03	1.742E-06	1.040E-06	0.106
1987.45	75.96	4.802E-04	3.537E-03	9.062E-03	1.817E-06	1.092E-06	0.071
1987.43	76.30	5.016E-04	3.207E-03	9.116E-03	1.731E-06	1.137E-06	0.075
1987.40	76.64	5.169E-04	3.490E-03	9.010E-03	1.686E-06	1.051E-06	0.114
1987.37	76.99	4.852E-04	3.524E-03	8.864E-03	1.672E-06	1.025E-06	0.115
1987.34	77.33	4.732E-04	3.582E-03	8.901E-03	1.570E-06	1.082E-06	0.072
1987.31	77.67	4.630E-04	3.770E-03	8.878E-03	1.627E-06	9.958E-07	0.068
1987.29	78.01	4.394E-04	3.699E-03	8.820E-03	1.711E-06	1.041E-06	0.075
1987.26	78.35	4.250E-04	3.999E-03	8.795E-03	1.866E-06	9.882E-07	0.071
1987.23	78.69	4.063E-04	3.815E-03	8.617E-03	1.741E-06	9.673E-07	0.078
1987.20	79.03	4.346E-04	3.573E-03	8.922E-03	1.830E-06	9.860E-07	0.082
1987.17	79.37	4.042E-04	3.503E-03	8.789E-03	1.948E-06	1.026E-06	0.096
1987.15	79.71	4.115E-04	3.584E-03	8.724E-03	2.247E-06	9.534E-07	0.094
1987.12	80.05	4.005E-04	3.320E-03	8.685E-03	2.164E-06	1.022E-06	0.084
1987.09	80.39	3.984E-04	3.566E-03	8.711E-03	1.962E-06	1.001E-06	0.089
1987.06	80.73	3.915E-04	3.916E-03	8.765E-03	2.104E-06	9.760E-07	0.095
1987.03	81.08	3.864E-04	3.902E-03	8.780E-03	2.012E-06	1.011E-06	0.542
1987.01	81.42	4.096E-04	3.980E-03	8.776E-03	2.339E-06	9.848E-07	0.091
1986.98	81.76	4.027E-04	3.717E-03	8.572E-03	2.124E-06	9.818E-07	0.111
1986.95	82.10	4.050E-04	3.445E-03	8.754E-03	2.173E-06	9.858E-07	0.106
1986.92	82.44	4.418E-04	3.591E-03	8.802E-03	2.089E-06	9.752E-07	0.098
1986.89	82.78	4.330E-04	3.559E-03	8.947E-03	2.017E-06	9.798E-07	0.112
1986.87	83.12	4.532E-04	3.549E-03	8.815E-03	2.589E-06	1.040E-06	0.108
1986.84	83.46	4.331E-04	3.374E-03	8.845E-03	3.693E-06	1.058E-06	0.109
1986.81	83.80	5.038E-04	3.499E-03	8.928E-03	2.893E-06	1.066E-06	0.101
1986.78	84.14	4.299E-04	3.645E-03	8.873E-03	2.293E-06	1.033E-06	0.094
1986.76	84.48	4.380E-04	3.504E-03	8.884E-03	2.045E-06	1.054E-06	0.097
1986.73	84.83	4.366E-04	3.275E-03	8.851E-03	1.915E-06	1.072E-06	0.140
1986.70	85.17	4.639E-04	3.249E-03	8.901E-03	1.942E-06	1.124E-06	0.100
1986.67	85.51	4.879E-04	3.488E-03	9.043E-03	2.009E-06	1.045E-06	0.092
1986.64	85.85	4.918E-04	3.556E-03	9.079E-03	1.881E-06	1.047E-06	0.091
1986.62	86.19	4.929E-04	3.390E-03	8.922E-03	1.908E-06	1.132E-06	0.074
1986.59	86.53	4.845E-04	3.127E-03	8.997E-03	1.759E-06	1.172E-06	0.081
1986.56	86.87	4.753E-04	3.459E-03	9.023E-03	2.024E-06	1.104E-06	0.095
1986.53	87.21	4.940E-04	3.351E-03	9.159E-03	1.938E-06	1.110E-06	0.093

LA-ICP-MS data

Time	Distance from top (mm)	B/Ca (mol/mol)	Mg/Ca (mol/mol)	Sr/Ca (mol/mol)	Ba/Ca (mol/mol)	U/Ca (mol/mol)	Mn ($\mu g\ g^{-1}$)
1986.50	87.55	4.996E-04	3.364E-03	8.919E-03	1.847E-06	1.101E-06	0.094
1986.48	87.89	5.014E-04	3.236E-03	9.012E-03	1.902E-06	1.165E-06	0.115
1986.45	88.23	5.023E-04	3.230E-03	8.995E-03	1.874E-06	1.144E-06	0.160
1986.42	88.57	4.685E-04	3.487E-03	8.989E-03	2.245E-06	1.090E-06	0.094
1986.39	88.92	4.601E-04	3.352E-03	8.916E-03	2.119E-06	1.142E-06	0.132
1986.36	89.26	4.547E-04	3.633E-03	8.925E-03	2.296E-06	1.125E-06	0.084
1986.34	89.60	3.935E-04	3.085E-03	9.085E-03	2.117E-06	1.282E-06	0.150
1986.31	89.94	4.325E-04	3.422E-03	9.127E-03	6.073E-06	1.194E-06	0.133
1986.28	90.28	4.488E-04	3.465E-03	8.965E-03	3.902E-06	1.066E-06	0.116
1986.25	90.62	4.434E-04	3.328E-03	8.971E-03	2.206E-06	1.105E-06	0.095
1986.22	90.96	4.269E-04	3.508E-03	8.896E-03	1.923E-06	1.031E-06	0.101
1986.20	91.30	4.598E-04	3.643E-03	8.922E-03	2.163E-06	1.023E-06	0.120
1986.17	91.64	4.300E-04	3.653E-03	8.789E-03	2.154E-06	1.044E-06	0.118
1986.14	91.98	3.863E-04	3.654E-03	8.733E-03	2.094E-06	1.053E-06	0.139
1986.11	92.32	3.927E-04	3.872E-03	8.737E-03	2.266E-06	1.037E-06	0.130
1986.08	92.66	4.198E-04	4.068E-03	8.761E-03	2.100E-06	9.421E-07	0.133
1986.06	93.01	4.251E-04	4.145E-03	8.712E-03	2.291E-06	9.942E-07	0.152
1986.03	93.35	4.367E-04	4.056E-03	8.733E-03	2.275E-06	1.005E-06	0.110
1986.00	93.69	3.964E-04	3.495E-03	8.675E-03	2.096E-06	1.032E-06	0.109
1985.97	94.03	4.047E-04	3.397E-03	8.798E-03	2.190E-06	1.008E-06	0.127
1985.94	94.37	4.179E-04	3.592E-03	8.832E-03	2.127E-06	1.077E-06	0.158
1985.92	94.71	4.198E-04	3.796E-03	8.854E-03	2.316E-06	1.010E-06	0.137

Table 10.8 Davies Reef 8 *Porites* data

Time	Distance from top (mm)	B/Ca (mol/mol)	Mg/Ca (mol/mol)	Sr/Ca (mol/mol)	Ba/Ca (mol/mol)	U/Ca (mol/mol)	Mn ($\mu g\ g^{-1}$)
1993.77	0.14	4.735E-04	4.406E-03	9.152E-03	3.918E-05	9.897E-07	0.302
1993.73	0.48	4.680E-04	4.207E-03	9.322E-03	4.685E-05	1.067E-06	0.224
1993.69	0.82	4.642E-04	3.947E-03	9.134E-03	2.620E-05	1.099E-06	0.136
1993.65	1.16	5.246E-04	4.475E-03	9.047E-03	1.854E-05	9.478E-07	0.103
1993.62	1.50	5.091E-04	4.383E-03	8.939E-03	2.513E-05	9.383E-07	0.092
1993.58	1.84	4.995E-04	3.805E-03	8.978E-03	1.758E-05	1.064E-06	0.078
1993.54	2.18	5.165E-04	3.963E-03	9.135E-03	2.239E-05	1.035E-06	0.087
1993.52	2.52	5.098E-04	3.821E-03	9.059E-03	1.841E-05	1.066E-06	0.089
1993.50	2.86	5.112E-04	3.842E-03	9.014E-03	2.129E-05	1.035E-06	0.075
1993.48	3.20	4.919E-04	3.649E-03	9.081E-03	1.807E-05	1.045E-06	0.065
1993.46	3.54	4.991E-04	3.776E-03	9.027E-03	1.246E-05	1.001E-06	0.073
1993.44	3.88	4.898E-04	4.082E-03	9.072E-03	2.514E-05	1.012E-06	0.102
1993.42	4.22	4.716E-04	4.186E-03	8.933E-03	1.658E-05	9.416E-07	0.103
1993.40	4.56	4.590E-04	4.123E-03	9.039E-03	1.699E-05	1.015E-06	0.112
1993.38	4.90	4.380E-04	4.087E-03	8.952E-03	1.157E-05	9.850E-07	0.109
1993.37	5.24	4.218E-04	4.220E-03	8.916E-03	1.054E-05	9.886E-07	0.106
1993.35	5.58	4.244E-04	4.492E-03	9.009E-03	1.766E-05	9.539E-07	0.156
1993.33	5.92	4.200E-04	4.557E-03	8.932E-03	1.144E-05	9.377E-07	0.122
1993.31	6.26	4.012E-04	4.444E-03	8.855E-03	1.182E-05	9.491E-07	0.137
1993.29	6.60	4.165E-04	4.286E-03	8.907E-03	1.140E-05	9.780E-07	0.166
1993.27	6.94	4.034E-04	4.513E-03	8.823E-03	9.453E-06	9.473E-07	0.149
1993.25	7.28	3.784E-04	4.454E-03	8.838E-03	7.224E-06	9.349E-07	0.125
1993.23	7.62	3.894E-04	4.652E-03	8.839E-03	7.360E-06	9.094E-07	0.145
1993.21	7.96	3.872E-04	4.911E-03	8.736E-03	5.641E-06	8.814E-07	0.112
1993.19	8.30	3.678E-04	4.754E-03	8.724E-03	4.502E-06	8.638E-07	0.099
1993.17	8.64	3.745E-04	4.602E-03	8.793E-03	4.990E-06	9.388E-07	0.108
1993.16	8.98	3.701E-04	4.413E-03	8.758E-03	5.548E-06	9.200E-07	0.102
1993.14	9.32	3.857E-04	4.647E-03	8.838E-03	3.628E-06	9.178E-07	0.094
1993.12	9.66	3.837E-04	4.776E-03	8.764E-03	3.367E-06	8.782E-07	0.108
1993.10	10.01	3.711E-04	4.939E-03	8.754E-03	4.413E-06	8.498E-07	0.122
1993.09	10.35	3.774E-04	4.591E-03	8.761E-03	3.137E-06	8.939E-07	0.104
1993.07	10.69	3.722E-04	4.365E-03	8.697E-03	2.687E-06	9.211E-07	0.089
1993.05	11.03	3.807E-04	4.327E-03	8.855E-03	3.832E-06	9.333E-07	0.111
1993.03	11.37	3.911E-04	4.669E-03	8.820E-03	3.913E-06	9.154E-07	0.109
1993.01	11.71	3.712E-04	4.346E-03	8.784E-03	2.868E-06	9.269E-07	0.090
1993.00	12.05	3.605E-04	4.127E-03	8.769E-03	3.083E-06	9.483E-07	0.087
1992.98	12.39	3.613E-04	4.437E-03	8.824E-03	2.915E-06	9.310E-07	0.102
1992.96	12.73	3.884E-04	4.803E-03	8.856E-03	3.872E-06	8.732E-07	0.123
1992.94	13.07	3.727E-04	4.455E-03	8.696E-03	2.922E-06	8.882E-07	0.095
1992.92	13.41	3.824E-04	4.598E-03	8.799E-03	3.251E-06	8.844E-07	0.087
1992.90	13.75	4.140E-04	4.392E-03	8.904E-03	2.947E-06	9.779E-07	0.089
1992.87	14.09	4.180E-04	4.436E-03	8.856E-03	3.926E-06	9.066E-07	0.100
1992.85	14.43	4.248E-04	4.314E-03	8.868E-03	3.905E-06	9.394E-07	0.093
1992.83	14.77	4.272E-04	4.294E-03	8.882E-03	3.517E-06	9.816E-07	0.101
1992.81	15.11	4.198E-04	4.056E-03	8.893E-03	3.485E-06	9.672E-07	0.095
1992.78	15.45	4.315E-04	4.001E-03	8.946E-03	4.138E-06	1.028E-06	0.102
1992.76	15.79	4.336E-04	3.793E-03	8.935E-03	3.013E-06	1.076E-06	0.092
1992.74	16.13	4.360E-04	3.780E-03	8.932E-03	3.445E-06	1.085E-06	0.091
1992.71	16.47	4.420E-04	3.783E-03	9.034E-03	3.372E-06	1.020E-06	0.088
1992.69	16.81	4.775E-04	3.904E-03	9.029E-03	3.063E-06	1.054E-06	0.080
1992.67	17.15	4.892E-04	3.860E-03	9.079E-03	3.308E-06	1.053E-06	0.079
1992.65	17.49	4.923E-04	4.121E-03	9.044E-03	3.547E-06	9.875E-07	0.079
1992.62	17.83	4.780E-04	4.072E-03	9.126E-03	4.254E-06	1.018E-06	0.081

LA-ICP-MS data

Time	Distance from top (mm)	B/Ca (mol/mol)	Mg/Ca (mol/mol)	Sr/Ca (mol/mol)	Ba/Ca (mol/mol)	U/Ca (mol/mol)	Mn ($\mu g\ g^{-1}$)
1992.58	18.17	4.668E-04	3.932E-03	8.993E-03	3.453E-06	1.027E-06	0.086
1992.54	18.51	4.770E-04	3.930E-03	9.031E-03	3.038E-06	1.023E-06	0.074
1992.50	18.85	5.082E-04	3.990E-03	9.039E-03	3.341E-06	1.034E-06	0.076
1992.46	19.19	4.774E-04	3.994E-03	8.949E-03	3.740E-06	1.024E-06	0.088
1992.42	19.53	4.521E-04	3.815E-03	9.019E-03	3.854E-06	1.057E-06	0.092
1992.40	19.87	4.386E-04	3.977E-03	8.923E-03	3.441E-06	1.002E-06	0.083
1992.38	20.21	4.249E-04	4.552E-03	8.851E-03	3.692E-06	9.131E-07	0.105
1992.36	20.55	4.111E-04	4.468E-03	8.887E-03	3.443E-06	9.176E-07	0.093
1992.34	20.90	3.965E-04	4.569E-03	8.787E-03	3.252E-06	9.199E-07	0.103
1992.32	21.24	4.071E-04	4.540E-03	8.844E-03	3.119E-06	9.226E-07	0.098
1992.30	21.58	3.962E-04	4.342E-03	8.818E-03	3.513E-06	9.481E-07	0.108
1992.28	21.92	3.839E-04	4.357E-03	8.871E-03	3.596E-06	9.545E-07	0.115
1992.26	22.26	3.881E-04	4.420E-03	8.736E-03	3.126E-06	9.328E-07	0.097
1992.25	22.60	3.739E-04	4.340E-03	8.864E-03	3.434E-06	9.425E-07	0.090
1992.23	22.94	3.563E-04	4.214E-03	8.650E-03	3.566E-06	9.186E-07	0.082
1992.21	23.28	3.509E-04	4.161E-03	8.799E-03	3.470E-06	9.361E-07	0.087
1992.19	23.62	3.449E-04	4.195E-03	8.727E-03	2.843E-06	9.177E-07	0.088
1992.17	23.96	3.492E-04	4.120E-03	8.726E-03	2.611E-06	9.090E-07	0.096
1992.15	24.30	3.608E-04	3.972E-03	8.781E-03	2.803E-06	9.291E-07	0.100
1992.13	24.64	3.701E-04	4.136E-03	8.695E-03	3.318E-06	8.878E-07	0.099
1992.11	24.98	3.625E-04	4.080E-03	8.799E-03	2.968E-06	8.862E-07	0.111
1992.09	25.32	3.813E-04	4.189E-03	8.759E-03	2.828E-06	9.237E-07	0.124
1992.08	25.66	3.839E-04	4.299E-03	8.862E-03	2.653E-06	9.009E-07	0.122
1992.06	26.00	3.784E-04	4.096E-03	8.710E-03	2.788E-06	9.124E-07	0.118
1992.04	26.34	3.910E-04	4.432E-03	8.713E-03	3.327E-06	9.109E-07	0.123
1992.02	26.68	3.880E-04	4.896E-03	8.769E-03	3.156E-06	8.422E-07	0.131
1992.00	27.02	3.846E-04	4.884E-03	8.739E-03	2.965E-06	8.239E-07	0.112
1991.98	27.36	3.893E-04	4.652E-03	8.760E-03	3.412E-06	8.633E-07	0.141
1991.96	27.70	3.931E-04	4.537E-03	8.702E-03	2.645E-06	8.927E-07	0.109
1991.93	28.04	3.653E-04	4.347E-03	8.806E-03	3.287E-06	8.869E-07	0.104
1991.89	28.38	3.659E-04	4.362E-03	8.760E-03	2.245E-06	8.857E-07	0.093
1991.85	28.72	3.882E-04	4.194E-03	8.844E-03	2.294E-06	9.289E-07	0.088
1991.82	29.06	4.042E-04	4.101E-03	8.912E-03	2.518E-06	9.924E-07	0.085
1991.78	29.40	4.226E-04	4.115E-03	8.888E-03	2.114E-06	9.985E-07	0.084
1991.74	29.74	4.135E-04	4.019E-03	8.988E-03	2.581E-06	9.948E-07	0.085
1991.71	30.08	4.216E-04	3.561E-03	9.046E-03	2.240E-06	1.094E-06	0.075
1991.67	30.42	4.493E-04	3.714E-03	9.104E-03	2.955E-06	1.163E-06	0.095
1991.64	30.76	4.624E-04	3.627E-03	9.126E-03	2.753E-06	1.205E-06	0.082
1991.58	31.10	4.862E-04	3.803E-03	9.074E-03	2.338E-06	1.118E-06	0.080
1991.52	31.44	4.930E-04	3.661E-03	9.172E-03	5.279E-06	1.144E-06	0.093
1991.46	31.78	4.937E-04	3.524E-03	9.160E-03	6.549E-06	1.087E-06	0.066
1991.42	32.13	5.021E-04	3.694E-03	8.966E-03	2.929E-06	1.017E-06	0.076
1991.37	32.47	4.976E-04	3.817E-03	8.975E-03	3.216E-06	1.024E-06	0.082
1991.33	32.81	4.751E-04	3.921E-03	8.917E-03	2.394E-06	9.565E-07	0.068
1991.31	33.15	4.820E-04	3.794E-03	9.074E-03	2.321E-06	1.008E-06	0.074
1991.29	33.49	4.408E-04	3.783E-03	8.915E-03	2.710E-06	1.037E-06	0.091
1991.27	33.83	4.167E-04	3.910E-03	8.898E-03	2.844E-06	1.001E-06	0.089
1991.25	34.17	4.009E-04	3.894E-03	8.894E-03	2.839E-06	9.888E-07	0.087
1991.23	34.51	3.876E-04	3.706E-03	8.789E-03	2.948E-06	1.046E-06	0.090
1991.22	34.85	4.045E-04	4.125E-03	8.850E-03	2.754E-06	9.446E-07	0.103
1991.20	35.19	3.906E-04	3.908E-03	8.956E-03	3.165E-06	9.929E-07	0.103
1991.19	35.53	3.964E-04	4.080E-03	8.804E-03	3.001E-06	1.005E-06	0.110
1991.17	35.87	4.047E-04	4.065E-03	8.955E-03	2.964E-06	1.006E-06	0.138
1991.15	36.21	3.798E-04	4.174E-03	8.681E-03	3.102E-06	9.201E-07	0.158
1991.14	36.55	3.610E-04	3.920E-03	8.799E-03	5.321E-06	9.868E-07	0.160

Time	Distance from top (mm)	B/Ca (mol/mol)	Mg/Ca (mol/mol)	Sr/Ca (mol/mol)	Ba/Ca (mol/mol)	U/Ca (mol/mol)	Mn ($\mu g\ g^{-1}$)
1991.12	36.89	3.683E-04	3.939E-03	8.878E-03	3.164E-06	9.978E-07	0.143
1991.11	37.23	3.949E-04	3.856E-03	8.806E-03	2.526E-06	1.005E-06	0.132
1991.09	37.57	4.028E-04	3.772E-03	8.836E-03	2.462E-06	1.022E-06	0.145
1991.08	37.91	3.952E-04	4.293E-03	8.692E-03	2.679E-06	8.999E-07	0.151
1991.06	38.25	4.138E-04	4.421E-03	8.745E-03	2.652E-06	8.865E-07	0.136
1991.05	38.59	4.133E-04	4.021E-03	8.865E-03	2.469E-06	9.451E-07	0.109
1991.03	38.93	4.051E-04	4.488E-03	8.770E-03	2.769E-06	8.674E-07	0.118
1991.02	39.27	3.968E-04	4.358E-03	8.843E-03	2.685E-06	9.397E-07	0.103
1991.00	39.61	3.914E-04	3.734E-03	8.896E-03	2.653E-06	1.042E-06	0.097
1990.99	39.95	4.102E-04	3.827E-03	8.949E-03	3.134E-06	9.876E-07	0.111
1990.97	40.29	4.174E-04	4.167E-03	8.858E-03	3.073E-06	9.444E-07	0.117
1990.96	40.63	4.335E-04	4.123E-03	8.829E-03	3.077E-06	9.640E-07	0.107
1990.94	40.97	4.243E-04	4.084E-03	8.789E-03	2.408E-06	9.606E-07	0.089
1990.91	41.31	4.056E-04	4.284E-03	8.910E-03	3.296E-06	1.013E-06	0.098
1990.87	41.65	4.108E-04	3.792E-03	8.919E-03	2.990E-06	1.048E-06	0.103
1990.84	41.99	4.323E-04	3.628E-03	8.925E-03	2.948E-06	1.056E-06	0.099
1990.80	42.33	4.441E-04	3.646E-03	9.005E-03	2.830E-06	1.066E-06	0.098
1990.76	42.67	4.472E-04	3.587E-03	8.959E-03	3.008E-06	1.061E-06	0.114
1990.73	43.02	4.529E-04	3.714E-03	9.000E-03	2.608E-06	1.066E-06	0.074
1990.69	43.36	4.946E-04	3.880E-03	9.054E-03	2.945E-06	1.092E-06	0.074
1990.66	43.70	5.052E-04	3.741E-03	9.222E-03	2.959E-06	1.162E-06	0.069
1990.62	44.04	4.949E-04	3.567E-03	9.085E-03	3.701E-06	1.147E-06	0.086
1990.59	44.38	5.416E-04	3.679E-03	9.099E-03	3.280E-06	1.187E-06	0.087
1990.55	44.72	5.014E-04	3.424E-03	9.196E-03	3.539E-06	1.228E-06	0.078
1990.52	45.06	4.868E-04	3.585E-03	9.048E-03	3.117E-06	1.157E-06	0.096
1990.48	45.40	4.493E-04	3.751E-03	9.132E-03	2.950E-06	1.129E-06	0.101
1990.45	45.74	4.476E-04	3.989E-03	8.967E-03	3.134E-06	1.026E-06	0.129
1990.41	46.06	4.197E-04	3.549E-03	8.835E-03	3.730E-06	9.851E-07	0.156

Table 10.9 Wheeler Reef *Porites* data

Time	Distance from top (mm)	B/Ca (mol/mol)	Mg/Ca (mol/mol)	Sr/Ca (mol/mol)	Ba/Ca (mol/mol)	U/Ca (mol/mol)
1985.64	0.00	5.510E-04	3.692E-03	8.775E-03	3.440E-05	1.130E-06
1985.62	0.37	5.250E-04	3.651E-03	8.787E-03	3.730E-05	1.160E-06
1985.60	0.74	5.110E-04	3.482E-03	8.893E-03	3.490E-05	1.200E-06
1985.58	1.11	4.990E-04	3.384E-03	8.862E-03	3.920E-05	1.200E-06
1985.56	1.47	5.050E-04	3.302E-03	8.824E-03	4.350E-05	1.190E-06
1985.54	1.84	5.180E-04	3.209E-03	8.892E-03	4.090E-05	1.220E-06
1985.52	2.21	5.200E-04	3.163E-03	8.980E-03	3.540E-05	1.260E-06
1985.50	2.58	5.430E-04	3.143E-03	9.081E-03	2.810E-05	1.320E-06
1985.48	2.95	5.140E-04	3.553E-03	9.020E-03	3.900E-05	1.130E-06
1985.46	3.32	4.960E-04	4.046E-03	9.009E-03	4.790E-05	1.120E-06
1985.44	3.69	4.790E-04	4.032E-03	8.885E-03	5.000E-05	1.130E-06
1985.42	4.05	4.610E-04	4.097E-03	8.949E-03	8.400E-05	1.050E-06
1985.40	4.42	4.620E-04	3.943E-03	8.962E-03	5.100E-05	1.130E-06
1985.39	4.79	4.610E-04	3.668E-03	8.880E-03	5.990E-05	1.180E-06
1985.37	5.16	4.450E-04	3.880E-03	8.974E-03	3.860E-05	1.110E-06
1985.35	5.53	4.400E-04	3.976E-03	8.916E-03	1.900E-05	9.780E-07
1985.33	5.90	4.500E-04	4.248E-03	8.741E-03	1.070E-05	9.620E-07
1985.31	6.27	4.490E-04	3.972E-03	8.632E-03	1.010E-05	1.040E-06
1985.29	6.63	4.380E-04	4.047E-03	8.656E-03	1.030E-05	1.010E-06
1985.27	7.00	4.310E-04	4.152E-03	8.810E-03	7.570E-06	9.720E-07
1985.25	7.37	4.290E-04	4.354E-03	8.580E-03	7.180E-06	9.110E-07
1985.23	7.74	4.200E-04	4.113E-03	8.557E-03	9.310E-06	9.160E-07
1985.21	8.11	4.200E-04	4.016E-03	8.709E-03	1.040E-05	9.640E-07
1985.19	8.48	4.160E-04	4.016E-03	8.477E-03	7.380E-06	9.360E-07
1985.17	8.85	4.020E-04	4.226E-03	8.646E-03	5.840E-06	9.650E-07
1985.15	9.21	3.900E-04	4.251E-03	8.538E-03	4.890E-06	9.220E-07
1985.14	9.58	4.310E-04	3.751E-03	8.776E-03	6.990E-06	1.060E-06
1985.12	9.95	4.130E-04	3.889E-03	8.531E-03	4.290E-06	1.050E-06
1985.10	10.32	4.190E-04	4.086E-03	8.584E-03	3.940E-06	9.750E-07
1985.08	10.69	4.280E-04	3.884E-03	8.704E-03	4.730E-06	1.050E-06
1985.06	11.06	4.130E-04	3.945E-03	8.577E-03	3.660E-06	9.310E-07
1985.04	11.43	4.250E-04	4.210E-03	8.624E-03	3.810E-06	9.430E-07
1985.02	11.79	4.180E-04	3.959E-03	8.616E-03	4.000E-06	9.880E-07
1985.00	12.16	4.260E-04	3.609E-03	8.743E-03	4.450E-06	1.080E-06
1984.98	12.53	4.240E-04	3.474E-03	8.702E-03	5.510E-06	1.090E-06
1984.96	12.90	4.320E-04	3.793E-03	8.662E-03	6.290E-06	1.060E-06
1984.94	13.27	4.350E-04	3.836E-03	8.752E-03	6.360E-06	1.090E-06
1984.92	13.64	4.410E-04	3.932E-03	8.751E-03	6.490E-06	1.050E-06
1984.90	14.01	4.460E-04	3.910E-03	8.755E-03	6.340E-06	1.050E-06
1984.89	14.37	4.550E-04	3.848E-03	8.773E-03	5.830E-06	1.060E-06
1984.87	14.74	4.670E-04	3.955E-03	8.771E-03	4.620E-06	1.040E-06
1984.85	15.11	4.700E-04	4.067E-03	8.839E-03	3.860E-06	1.070E-06
1984.83	15.48	4.660E-04	4.159E-03	8.779E-03	3.810E-06	1.020E-06
1984.81	15.85	4.680E-04	4.089E-03	8.737E-03	3.680E-06	1.040E-06
1984.79	16.22	4.760E-04	3.807E-03	8.848E-03	3.580E-06	1.090E-06
1984.77	16.59	4.780E-04	3.638E-03	8.836E-03	3.480E-06	1.130E-06
1984.75	16.96	4.810E-04	3.588E-03	8.824E-03	3.040E-06	1.080E-06
1984.73	17.32	4.840E-04	3.587E-03	8.816E-03	2.900E-06	1.110E-06
1984.71	17.69	4.830E-04	3.679E-03	8.826E-03	3.130E-06	1.130E-06
1984.69	18.06	4.730E-04	3.630E-03	8.930E-03	3.200E-06	1.160E-06
1984.67	18.43	4.840E-04	3.492E-03	8.810E-03	3.090E-06	1.170E-06
1984.65	18.80	4.820E-04	3.546E-03	8.887E-03	3.370E-06	1.140E-06
1984.64	19.17	4.740E-04	3.582E-03	8.811E-03	3.150E-06	1.120E-06

Time	Distance from top (mm)	B/Ca (mol/mol)	Mg/Ca (mol/mol)	Sr/Ca (mol/mol)	Ba/Ca (mol/mol)	U/Ca (mol/mol)
1984.62	19.54	4.670E-04	3.537E-03	8.792E-03	2.790E-06	1.090E-06
1984.60	19.90	4.750E-04	3.513E-03	8.935E-03	2.990E-06	1.130E-06
1984.58	20.27	4.740E-04	3.339E-03	9.094E-03	3.140E-06	1.190E-06
1984.56	20.64	4.730E-04	3.180E-03	9.160E-03	3.560E-06	1.280E-06
1984.54	21.01	5.020E-04	3.203E-03	9.127E-03	3.570E-06	1.300E-06
1984.52	21.38	5.100E-04	3.016E-03	9.142E-03	3.430E-06	1.330E-06
1984.50	21.75	5.140E-04	3.042E-03	9.102E-03	3.660E-06	1.360E-06
1984.48	22.12	5.280E-04	2.986E-03	9.202E-03	3.430E-06	1.300E-06
1984.46	22.48	5.210E-04	3.256E-03	9.147E-03	3.560E-06	1.270E-06
1984.44	22.85	5.180E-04	3.214E-03	8.983E-03	3.620E-06	1.250E-06
1984.42	23.22	5.100E-04	3.651E-03	9.052E-03	4.040E-06	1.150E-06
1984.40	23.59	5.120E-04	3.724E-03	8.856E-03	4.130E-06	1.090E-06
1984.39	23.96	4.990E-04	3.401E-03	8.958E-03	4.860E-06	1.210E-06
1984.37	24.33	4.890E-04	3.415E-03	8.817E-03	5.650E-06	1.120E-06
1984.35	24.70	4.450E-04	3.680E-03	8.798E-03	3.800E-06	1.090E-06
1984.33	25.06	4.440E-04	3.899E-03	8.819E-03	3.280E-06	1.060E-06
1984.31	25.43	4.490E-04	3.640E-03	8.910E-03	3.960E-06	1.140E-06
1984.29	25.80	4.550E-04	3.836E-03	8.826E-03	4.660E-06	1.110E-06
1984.27	26.17	4.740E-04	3.864E-03	8.722E-03	5.590E-06	1.030E-06
1984.25	26.54	4.560E-04	4.174E-03	8.710E-03	3.920E-06	9.840E-07
1984.23	26.91	4.380E-04	4.111E-03	8.715E-03	3.960E-06	9.810E-07
1984.21	27.28	4.560E-04	4.093E-03	8.672E-03	3.910E-06	9.690E-07
1984.19	27.64	4.460E-04	3.639E-03	8.818E-03	4.650E-06	1.090E-06
1984.17	28.01	4.360E-04	3.689E-03	8.800E-03	4.420E-06	1.070E-06
1984.15	28.38	4.090E-04	3.991E-03	8.680E-03	3.810E-06	1.020E-06
1984.14	28.75	4.190E-04	4.111E-03	8.760E-03	4.390E-06	9.920E-07
1984.12	29.12	4.200E-04	4.125E-03	8.602E-03	4.380E-06	9.850E-07
1984.10	29.49	4.310E-04	3.975E-03	8.798E-03	4.940E-06	1.000E-06
1984.08	29.86	4.400E-04	4.123E-03	8.699E-03	3.620E-06	9.780E-07
1984.06	30.22	4.610E-04	4.507E-03	8.751E-03	4.020E-06	9.630E-07
1984.04	30.59	4.530E-04	4.706E-03	8.713E-03	4.590E-06	9.250E-07
1984.02	30.96	4.390E-04	4.118E-03	8.823E-03	3.740E-06	9.740E-07
1984.00	31.33	4.390E-04	3.746E-03	8.744E-03	4.040E-06	1.070E-06
1983.98	31.70	4.270E-04	3.700E-03	8.702E-03	3.000E-06	1.010E-06
1983.96	32.07	4.240E-04	3.612E-03	8.788E-03	2.960E-06	1.120E-06
1983.94	32.44	4.290E-04	3.558E-03	8.843E-03	4.120E-06	1.190E-06
1983.92	32.80	4.090E-04	3.828E-03	8.761E-03	2.250E-06	1.050E-06
1983.90	33.17	4.070E-04	3.903E-03	8.637E-03	3.200E-06	1.010E-06
1983.89	33.54	4.340E-04	3.611E-03	8.638E-03	3.370E-06	1.060E-06
1983.87	33.91	4.240E-04	3.373E-03	8.781E-03	3.310E-06	1.110E-06
1983.85	34.28	4.230E-04	3.616E-03	8.923E-03	3.460E-06	1.120E-06
1983.83	34.65	4.450E-04	3.550E-03	8.827E-03	3.930E-06	1.200E-06
1983.81	35.02	4.150E-04	3.505E-03	8.837E-03	3.670E-06	1.140E-06
1983.79	35.38	4.270E-04	3.359E-03	8.979E-03	2.710E-06	1.170E-06
1983.77	35.75	4.180E-04	3.639E-03	8.833E-03	2.470E-06	1.170E-06
1983.75	36.12	4.230E-04	3.495E-03	8.904E-03	2.690E-06	1.170E-06
1983.73	36.49	4.340E-04	3.552E-03	8.986E-03	2.450E-06	1.190E-06
1983.71	36.86	4.530E-04	3.496E-03	9.029E-03	2.420E-06	1.250E-06
1983.69	37.23	4.700E-04	3.623E-03	8.918E-03	3.930E-06	1.140E-06
1983.67	37.60	4.880E-04	3.621E-03	8.949E-03	4.550E-06	1.160E-06
1983.65	37.96	4.860E-04	3.692E-03	8.890E-03	3.580E-06	1.170E-06
1983.64	38.33	4.980E-04	3.587E-03	8.958E-03	3.310E-06	1.160E-06
1983.62	38.70	4.830E-04	3.331E-03	8.886E-03	2.970E-06	1.120E-06
1983.60	39.07	5.280E-04	2.992E-03	9.130E-03	3.390E-06	1.360E-06
1983.58	39.44	5.130E-04	3.076E-03	9.049E-03	3.800E-06	1.280E-06

LA-ICP-MS data

Time	Distance from top (mm)	B/Ca (mol/mol)	Mg/Ca (mol/mol)	Sr/Ca (mol/mol)	Ba/Ca (mol/mol)	U/Ca (mol/mol)
1983.56	39.81	5.050E-04	3.035E-03	9.029E-03	3.960E-06	1.280E-06
1983.54	40.18	4.610E-04	3.087E-03	9.022E-03	3.810E-06	1.260E-06
1983.52	40.54	4.700E-04	3.272E-03	9.014E-03	3.430E-06	1.200E-06
1983.50	40.91	4.670E-04	3.350E-03	9.038E-03	3.120E-06	1.160E-06
1983.48	41.28	4.730E-04	3.438E-03	8.965E-03	3.230E-06	1.140E-06
1983.46	41.65	4.540E-04	3.488E-03	8.908E-03	3.300E-06	1.120E-06
1983.44	42.02	4.660E-04	3.492E-03	8.889E-03	3.450E-06	1.110E-06
1983.42	42.39	4.760E-04	3.466E-03	8.900E-03	3.660E-06	1.110E-06
1983.40	42.76	4.780E-04	3.457E-03	8.858E-03	3.320E-06	1.070E-06
1983.39	43.12	4.770E-04	3.540E-03	8.925E-03	2.990E-06	1.070E-06
1983.37	43.49	4.700E-04	3.544E-03	8.908E-03	2.770E-06	1.080E-06
1983.35	43.86	4.630E-04	3.568E-03	8.844E-03	2.870E-06	1.090E-06
1983.33	44.23	4.600E-04	3.723E-03	8.816E-03	3.370E-06	1.080E-06
1983.31	44.60	4.690E-04	3.654E-03	8.804E-03	3.830E-06	1.050E-06
1983.29	44.97	4.690E-04	3.872E-03	8.809E-03	3.820E-06	1.060E-06
1983.27	45.34	4.360E-04	4.067E-03	8.762E-03	3.870E-06	1.030E-06
1983.25	45.70	4.510E-04	4.175E-03	8.713E-03	3.810E-06	9.910E-07
1983.23	46.07	4.400E-04	4.200E-03	8.771E-03	3.130E-06	9.870E-07
1983.21	46.44	4.350E-04	4.065E-03	8.797E-03	2.930E-06	1.020E-06
1983.19	46.81	4.270E-04	4.137E-03	8.791E-03	2.810E-06	1.010E-06
1983.17	47.18	4.350E-04	4.205E-03	8.755E-03	2.900E-06	9.980E-07
1983.15	47.55	4.400E-04	4.195E-03	8.694E-03	3.170E-06	1.000E-06

Table 10.10 Ruby Reef, GBR *Astrosclera willeyana* Sr/Ca

Distance from top (mm)	Sr/Ca (mol/mol)	Distance con't (mm)	Sr/Ca (mol/mol)	Distance con't (mm)	Sr/Ca (mol/mol)
0.006	1.200E-02	1.038	1.113E-02	2.070	1.024E-02
0.026	1.170E-02	1.058	1.113E-02	2.089	1.032E-02
0.045	1.146E-02	1.077	1.102E-02	2.109	1.034E-02
0.065	1.128E-02	1.096	1.102E-02	2.128	1.054E-02
0.084	1.100E-02	1.116	1.099E-02	2.148	1.064E-02
0.104	1.061E-02	1.135	1.077E-02	2.167	1.072E-02
0.123	1.045E-02	1.155	1.073E-02	2.186	1.071E-02
0.143	1.046E-02	1.174	1.076E-02	2.206	1.070E-02
0.162	1.037E-02	1.194	1.068E-02	2.225	1.082E-02
0.182	1.039E-02	1.213	1.058E-02	2.245	1.082E-02
0.201	1.045E-02	1.233	1.056E-02	2.264	1.070E-02
0.221	1.050E-02	1.252	1.042E-02	2.284	1.068E-02
0.240	1.065E-02	1.272	1.029E-02	2.303	1.060E-02
0.260	1.070E-02	1.291	1.015E-02	2.323	1.056E-02
0.279	1.067E-02	1.311	1.023E-02	2.342	1.066E-02
0.298	1.084E-02	1.330	1.023E-02	2.362	1.063E-02
0.318	1.088E-02	1.350	1.017E-02	2.381	1.065E-02
0.337	1.078E-02	1.369	1.012E-02	2.401	1.067E-02
0.357	1.078E-02	1.388	1.033E-02	2.420	1.072E-02
0.376	1.072E-02	1.408	1.039E-02	2.440	1.079E-02
0.396	1.068E-02	1.427	1.046E-02	2.459	1.078E-02
0.415	1.085E-02	1.447	1.029E-02	2.478	1.078E-02
0.435	1.087E-02	1.466	1.022E-02	2.498	1.066E-02
0.454	1.081E-02	1.486	1.026E-02	2.517	1.063E-02
0.474	1.077E-02	1.505	1.021E-02	2.537	1.052E-02
0.493	1.067E-02	1.525	1.012E-02	2.556	1.049E-02
0.513	1.060E-02	1.544	1.023E-02	2.576	1.048E-02
0.532	1.064E-02	1.564	1.033E-02	2.595	1.061E-02
0.551	1.059E-02	1.583	1.036E-02	2.615	1.064E-02
0.571	1.059E-02	1.603	1.024E-02	2.634	1.091E-02
0.590	1.090E-02	1.622	1.012E-02	2.654	1.099E-02
0.610	1.094E-02	1.641	1.009E-02	2.673	1.124E-02
0.629	1.107E-02	1.661	1.006E-02	2.693	1.119E-02
0.649	1.106E-02	1.680	1.006E-02	2.712	1.111E-02
0.668	1.106E-02	1.700	9.915E-03	2.731	1.098E-02
0.688	1.098E-02	1.719	9.958E-03	2.751	1.087E-02
0.707	1.089E-02	1.739	1.017E-02	2.770	1.067E-02
0.727	1.066E-02	1.758	1.033E-02	2.790	1.052E-02
0.746	1.066E-02	1.778	1.042E-02	2.809	1.031E-02
0.766	1.074E-02	1.797	1.052E-02	2.829	1.025E-02
0.785	1.080E-02	1.817	1.053E-02	2.848	1.028E-02
0.805	1.085E-02	1.836	1.067E-02	2.868	1.020E-02
0.824	1.090E-02	1.856	1.070E-02	2.887	1.036E-02
0.843	1.095E-02	1.875	1.084E-02	2.907	1.031E-02
0.863	1.083E-02	1.895	1.089E-02	2.926	1.045E-02
0.882	1.077E-02	1.914	1.096E-02	2.946	1.056E-02
0.902	1.070E-02	1.933	1.092E-02	2.965	1.063E-02
0.921	1.075E-02	1.953	1.078E-02	2.985	1.055E-02
0.941	1.090E-02	1.972	1.072E-02	3.004	1.041E-02
0.960	1.088E-02	1.992	1.059E-02	3.023	1.021E-02
0.980	1.089E-02	2.011	1.037E-02	3.043	1.008E-02
0.999	1.113E-02	2.031	1.028E-02	3.062	9.941E-03
1.019	1.120E-02	2.050	1.031E-02	3.082	9.791E-03

LA-ICP-MS data

Distance con't (mm)	Sr/Ca (mol/mol)	Distance con't (mm)	Sr/Ca (mol/mol)	Distance con't (mm)	Sr/Ca (mol/mol)
3.101	9.867E-03	4.133	1.105E-02	5.165	1.117E-02
3.121	9.960E-03	4.152	1.083E-02	5.184	1.096E-02
3.140	1.007E-02	4.172	1.067E-02	5.203	1.084E-02
3.160	1.005E-02	4.191	1.058E-02	5.223	1.068E-02
3.179	1.016E-02	4.211	1.052E-02	5.242	1.062E-02
3.199	1.030E-02	4.230	1.040E-02	5.262	1.049E-02
3.218	1.051E-02	4.250	1.014E-02	5.281	1.042E-02
3.238	1.055E-02	4.269	1.010E-02	5.301	1.039E-02
3.257	1.059E-02	4.289	1.006E-02	5.320	1.047E-02
3.276	1.074E-02	4.308	1.016E-02	5.340	1.051E-02
3.296	1.082E-02	4.328	1.012E-02	5.359	1.054E-02
3.315	1.091E-02	4.347	1.024E-02	5.379	1.054E-02
3.335	1.091E-02	4.366	1.022E-02	5.398	1.061E-02
3.354	1.089E-02	4.386	1.033E-02	5.418	1.075E-02
3.374	1.086E-02	4.405	1.025E-02	5.437	1.071E-02
3.393	1.074E-02	4.425	1.033E-02	5.456	1.067E-02
3.413	1.063E-02	4.444	1.030E-02	5.476	1.066E-02
3.432	1.059E-02	4.464	1.033E-02	5.495	1.049E-02
3.452	1.035E-02	4.483	1.038E-02	5.515	1.039E-02
3.471	1.015E-02	4.503	1.056E-02	5.534	1.028E-02
3.491	9.961E-03	4.522	1.050E-02	5.554	1.004E-02
3.510	9.709E-03	4.542	1.059E-02	5.573	9.898E-03
3.530	9.718E-03	4.561	1.073E-02	5.593	9.808E-03
3.549	9.763E-03	4.581	1.084E-02	5.612	9.793E-03
3.568	9.789E-03	4.600	1.085E-02	5.632	9.958E-03
3.588	9.972E-03	4.620	1.093E-02	5.651	1.003E-02
3.607	1.023E-02	4.639	1.099E-02	5.671	1.010E-02
3.627	1.039E-02	4.658	1.111E-02	5.690	1.012E-02
3.646	1.053E-02	4.678	1.116E-02	5.710	1.023E-02
3.666	1.073E-02	4.697	1.107E-02	5.729	1.023E-02
3.685	1.087E-02	4.717	1.102E-02	5.748	1.017E-02
3.705	1.098E-02	4.736	1.108E-02	5.768	1.015E-02
3.724	1.114E-02	4.756	1.106E-02	5.787	1.013E-02
3.744	1.114E-02	4.775	1.076E-02	5.807	1.025E-02
3.763	1.115E-02	4.795	1.072E-02	5.826	1.050E-02
3.783	1.121E-02	4.814	1.068E-02	5.846	1.059E-02
3.802	1.112E-02	4.834	1.065E-02	5.865	1.075E-02
3.821	1.102E-02	4.853	1.071E-02	5.885	1.072E-02
3.841	1.100E-02	4.873	1.064E-02	5.904	1.070E-02
3.860	1.099E-02	4.892	1.050E-02	5.924	1.077E-02
3.880	1.094E-02	4.911	1.072E-02	5.943	1.069E-02
3.899	1.100E-02	4.931	1.085E-02	5.963	1.059E-02
3.919	1.107E-02	4.950	1.098E-02	5.982	1.051E-02
3.938	1.110E-02	4.970	1.114E-02	6.001	1.047E-02
3.958	1.114E-02	4.989	1.115E-02	6.021	1.068E-02
3.977	1.117E-02	5.009	1.123E-02	6.040	1.071E-02
3.997	1.105E-02	5.028	1.140E-02	6.060	1.071E-02
4.016	1.112E-02	5.048	1.151E-02	6.079	1.064E-02
4.036	1.108E-02	5.067	1.144E-02	6.099	1.071E-02
4.055	1.107E-02	5.087	1.139E-02	6.118	1.075E-02
4.075	1.096E-02	5.106	1.133E-02	6.138	1.077E-02
4.094	1.094E-02	5.126	1.131E-02	6.157	1.080E-02
4.113	1.104E-02	5.145	1.124E-02	6.177	1.083E-02
6.196	1.093E-02	7.228	1.100E-02	8.259	1.077E-02
6.216	1.091E-02	7.247	1.096E-02	8.279	1.086E-02
6.235	1.082E-02	7.267	1.103E-02	8.298	1.096E-02

Distance con't (mm)	Sr/Ca (mol/mol)	Distance con't (mm)	Sr/Ca (mol/mol)	Distance con't (mm)	Sr/Ca (mol/mol)
6.255	1.088E-02	7.286	1.111E-02	8.318	1.099E-02
6.274	1.100E-02	7.306	1.114E-02	8.337	1.099E-02
6.293	1.097E-02	7.325	1.130E-02	8.357	1.080E-02
6.313	1.096E-02	7.345	1.137E-02	8.376	1.078E-02
6.332	1.089E-02	7.364	1.147E-02	8.396	1.077E-02
6.352	1.092E-02	7.383	1.150E-02	8.415	1.076E-02
6.371	1.092E-02	7.403	1.151E-02	8.435	1.097E-02
6.391	1.082E-02	7.422	1.153E-02	8.454	1.093E-02
6.410	1.071E-02	7.442	1.147E-02	8.473	1.108E-02
6.430	1.055E-02	7.461	1.143E-02	8.493	1.114E-02
6.449	1.054E-02	7.481	1.129E-02	8.512	1.123E-02
6.469	1.041E-02	7.500	1.115E-02	8.532	1.118E-02
6.488	1.036E-02	7.520	1.113E-02	8.551	1.105E-02
6.508	1.035E-02	7.539	1.094E-02	8.571	1.072E-02
6.527	1.031E-02	7.559	1.075E-02	8.590	1.061E-02
6.546	1.027E-02	7.578	1.080E-02	8.610	1.048E-02
6.566	1.031E-02	7.598	1.061E-02	8.629	1.039E-02
6.585	1.035E-02	7.617	1.062E-02	8.649	1.019E-02
6.605	1.046E-02	7.636	1.069E-02	8.668	1.014E-02
6.624	1.061E-02	7.656	1.076E-02	8.688	1.025E-02
6.644	1.066E-02	7.675	1.087E-02	8.707	1.034E-02
6.663	1.080E-02	7.695	1.092E-02	8.726	1.035E-02
6.683	1.089E-02	7.714	1.078E-02	8.746	1.045E-02
6.702	1.091E-02	7.734	1.079E-02	8.765	1.060E-02
6.722	1.092E-02	7.753	1.074E-02	8.785	1.067E-02
6.741	1.101E-02	7.773	1.066E-02	8.804	1.062E-02
6.761	1.104E-02	7.792	1.059E-02	8.824	1.043E-02
6.780	1.121E-02	7.812	1.053E-02	8.843	1.033E-02
6.800	1.120E-02	7.831	1.053E-02	8.863	1.033E-02
6.819	1.117E-02	7.851	1.073E-02	8.882	1.036E-02
6.838	1.119E-02	7.870	1.086E-02	8.902	1.037E-02
6.858	1.125E-02	7.890	1.091E-02	8.921	1.044E-02
6.877	1.110E-02	7.909	1.100E-02	8.941	1.056E-02
6.897	1.098E-02	7.928	1.104E-02	8.960	1.064E-02
6.916	1.061E-02	7.948	1.119E-02	8.980	1.077E-02
6.936	1.053E-02	7.967	1.125E-02	8.999	1.073E-02
6.955	1.038E-02	7.987	1.110E-02	9.018	1.067E-02
6.975	1.027E-02	8.006	1.109E-02	9.038	1.058E-02
6.994	1.006E-02	8.026	1.112E-02	9.057	1.052E-02
7.014	9.997E-03	8.045	1.109E-02	9.077	1.057E-02
7.033	1.002E-02	8.065	1.106E-02	9.096	1.059E-02
7.053	1.028E-02	8.084	1.081E-02	9.116	1.043E-02
7.072	1.033E-02	8.104	1.078E-02	9.135	1.060E-02
7.091	1.043E-02	8.123	1.071E-02	9.155	1.065E-02
7.111	1.056E-02	8.143	1.073E-02	9.174	1.069E-02
7.130	1.076E-02	8.162	1.060E-02	9.194	1.055E-02
7.150	1.090E-02	8.181	1.057E-02	9.213	1.040E-02
7.169	1.099E-02	8.201	1.047E-02	9.233	1.045E-02
7.189	1.088E-02	8.220	1.062E-02	9.252	1.063E-02
7.208	1.092E-02	8.240	1.062E-02	9.271	1.065E-02
9.291	1.068E-02	10.323	1.011E-02	11.354	1.026E-02
9.310	1.088E-02	10.342	1.007E-02	11.374	1.019E-02
9.330	1.130E-02	10.361	1.023E-02	11.393	1.030E-02
9.349	1.148E-02	10.381	1.022E-02	11.413	1.045E-02
9.369	1.155E-02	10.400	1.029E-02	11.432	1.061E-02
9.388	1.154E-02	10.420	1.036E-02	11.451	1.074E-02

LA-ICP-MS data

Distance con't (mm)	Sr/Ca (mol/mol)	Distance con't (mm)	Sr/Ca (mol/mol)	Distance con't (mm)	Sr/Ca (mol/mol)
9.408	1.144E-02	10.439	1.039E-02	11.471	1.070E-02
9.427	1.133E-02	10.459	1.064E-02	11.490	1.062E-02
9.447	1.119E-02	10.478	1.070E-02	11.510	1.056E-02
9.466	1.099E-02	10.498	1.080E-02	11.529	1.070E-02
9.486	1.080E-02	10.517	1.094E-02	11.549	1.074E-02
9.505	1.062E-02	10.537	1.100E-02	11.568	1.072E-02
9.525	1.052E-02	10.556	1.097E-02	11.588	1.062E-02
9.544	1.049E-02	10.576	1.099E-02	11.607	1.072E-02
9.563	1.046E-02	10.595	1.072E-02	11.627	1.071E-02
9.583	1.053E-02	10.615	1.073E-02	11.646	1.083E-02
9.602	1.062E-02	10.634	1.062E-02	11.666	1.069E-02
9.622	1.073E-02	10.653	1.050E-02	11.685	1.072E-02
9.641	1.086E-02	10.673	1.051E-02	11.705	1.059E-02
9.661	1.100E-02	10.692	1.042E-02	11.724	1.042E-02
9.680	1.100E-02	10.712	1.034E-02	11.743	1.046E-02
9.700	1.105E-02	10.731	1.033E-02	11.763	1.049E-02
9.719	1.094E-02	10.751	1.036E-02	11.782	1.041E-02
9.739	1.079E-02	10.770	1.033E-02	11.802	1.041E-02
9.758	1.084E-02	10.790	1.040E-02	11.821	1.027E-02
9.778	1.073E-02	10.809	1.039E-02	11.841	1.029E-02
9.797	1.057E-02	10.829	1.031E-02	11.860	1.040E-02
9.816	1.055E-02	10.848	1.034E-02	11.880	1.022E-02
9.836	1.044E-02	10.868	1.031E-02	11.899	1.034E-02
9.855	1.046E-02	10.887	1.028E-02	11.919	1.033E-02
9.875	1.062E-02	10.906	1.034E-02	11.938	1.054E-02
9.894	1.055E-02	10.926	1.034E-02	11.958	1.077E-02
9.914	1.065E-02	10.945	1.042E-02	11.977	1.103E-02
9.933	1.081E-02	10.965	1.056E-02	11.990	1.130E-02
9.953	1.086E-02	10.984	1.050E-02		
9.972	1.109E-02	11.004	1.049E-02		
9.992	1.102E-02	11.023	1.046E-02		
10.011	1.087E-02	11.043	1.043E-02		
10.031	1.098E-02	11.062	1.043E-02		
10.050	1.092E-02	11.082	1.021E-02		
10.070	1.081E-02	11.101	1.003E-02		
10.089	1.077E-02	11.121	1.010E-02		
10.108	1.064E-02	11.140	9.970E-03		
10.128	1.081E-02	11.160	9.893E-03		
10.147	1.079E-02	11.179	9.893E-03		
10.167	1.075E-02	11.198	9.768E-03		
10.186	1.071E-02	11.218	9.855E-03		
10.206	1.070E-02	11.237	1.006E-02		
10.225	1.054E-02	11.257	9.964E-03		
10.245	1.045E-02	11.276	1.001E-02		
10.264	1.020E-02	11.296	1.002E-02		
10.284	1.021E-02	11.315	1.004E-02		
10.303	1.006E-02	11.335	1.014E-02		

Table 10.11 Robert's Reef, Fiji *Astrosclera willeyana* Sr/Ca

Distance from top (mm)	Sr/Ca (mol/mol)	Distance con't (mm)	Sr/Ca (mol/mol)	Distance con't (mm)	Sr/Ca (mol/mol)
0.129	9.838E-03	1.152	1.034E-02	2.176	1.024E-02
0.148	9.866E-03	1.172	1.023E-02	2.195	1.022E-02
0.167	9.906E-03	1.191	1.023E-02	2.214	1.025E-02
0.187	9.877E-03	1.210	1.020E-02	2.234	1.025E-02
0.206	9.851E-03	1.229	1.022E-02	2.253	1.027E-02
0.225	9.834E-03	1.249	1.025E-02	2.272	1.021E-02
0.245	9.787E-03	1.268	1.027E-02	2.292	1.021E-02
0.264	9.745E-03	1.287	1.026E-02	2.311	1.014E-02
0.283	9.713E-03	1.307	1.025E-02	2.330	1.014E-02
0.303	9.685E-03	1.326	1.030E-02	2.350	1.012E-02
0.322	9.710E-03	1.345	1.024E-02	2.369	1.013E-02
0.341	9.671E-03	1.365	1.017E-02	2.388	1.008E-02
0.360	9.674E-03	1.384	1.013E-02	2.407	1.003E-02
0.380	9.707E-03	1.403	1.014E-02	2.427	9.987E-03
0.399	9.680E-03	1.423	1.019E-02	2.446	1.001E-02
0.418	9.605E-03	1.442	1.020E-02	2.465	1.001E-02
0.438	9.594E-03	1.461	1.019E-02	2.485	9.996E-03
0.457	9.569E-03	1.481	1.021E-02	2.504	1.002E-02
0.476	9.568E-03	1.500	1.022E-02	2.523	9.999E-03
0.496	9.539E-03	1.519	1.016E-02	2.543	9.981E-03
0.515	9.550E-03	1.538	1.004E-02	2.562	9.984E-03
0.534	9.594E-03	1.558	9.938E-03	2.581	1.000E-02
0.554	9.643E-03	1.577	9.885E-03	2.601	1.002E-02
0.573	9.670E-03	1.596	9.823E-03	2.620	1.003E-02
0.592	9.715E-03	1.616	9.761E-03	2.639	1.001E-02
0.612	9.795E-03	1.635	9.704E-03	2.659	9.988E-03
0.631	9.817E-03	1.654	9.648E-03	2.678	1.002E-02
0.650	9.792E-03	1.674	9.657E-03	2.697	1.004E-02
0.669	9.802E-03	1.693	9.644E-03	2.716	1.007E-02
0.689	9.847E-03	1.712	9.667E-03	2.736	1.013E-02
0.708	9.855E-03	1.732	9.641E-03	2.755	1.018E-02
0.727	9.947E-03	1.751	9.631E-03	2.774	1.015E-02
0.747	9.967E-03	1.770	9.638E-03	2.794	1.015E-02
0.766	9.989E-03	1.790	9.630E-03	2.813	1.018E-02
0.785	1.001E-02	1.809	9.652E-03	2.832	1.019E-02
0.805	1.009E-02	1.828	9.653E-03	2.852	1.023E-02
0.824	1.018E-02	1.847	9.700E-03	2.871	1.024E-02
0.843	1.030E-02	1.867	9.768E-03	2.890	1.022E-02
0.863	1.033E-02	1.886	9.819E-03	2.910	1.015E-02
0.882	1.041E-02	1.905	9.856E-03	2.929	1.012E-02
0.901	1.046E-02	1.925	9.889E-03	2.948	1.008E-02
0.921	1.044E-02	1.944	9.985E-03	2.968	1.012E-02
0.940	1.042E-02	1.963	9.999E-03	2.987	1.016E-02
0.959	1.045E-02	1.983	1.005E-02	3.006	1.018E-02
0.978	1.054E-02	2.002	1.006E-02	3.025	1.016E-02
0.998	1.054E-02	2.021	1.009E-02	3.045	1.017E-02
1.017	1.055E-02	2.041	1.008E-02	3.064	1.011E-02
1.036	1.059E-02	2.060	1.015E-02	3.083	1.009E-02
1.056	1.057E-02	2.079	1.020E-02	3.103	1.013E-02
1.075	1.056E-02	2.099	1.023E-02	3.122	1.015E-02
1.094	1.050E-02	2.118	1.025E-02	3.141	1.015E-02
1.114	1.047E-02	2.137	1.025E-02	3.161	1.017E-02
1.133	1.041E-02	2.156	1.029E-02	3.180	1.019E-02

LA-ICP-MS data

Distance con't (mm)	Sr/Ca (mol/mol)	Distance con't (mm)	Sr/Ca (mol/mol)	Distance con't (mm)	Sr/Ca (mol/mol)
3.199	1.021E-02	4.223	1.011E-02	5.246	1.007E-02
3.219	1.024E-02	4.242	1.008E-02	5.266	1.006E-02
3.238	1.031E-02	4.261	1.007E-02	5.285	1.009E-02
3.257	1.036E-02	4.281	1.004E-02	5.304	1.015E-02
3.277	1.046E-02	4.300	1.002E-02	5.324	1.019E-02
3.296	1.050E-02	4.319	1.004E-02	5.343	1.029E-02
3.315	1.055E-02	4.339	1.003E-02	5.362	1.034E-02
3.334	1.055E-02	4.358	1.002E-02	5.381	1.037E-02
3.354	1.053E-02	4.377	1.002E-02	5.401	1.040E-02
3.373	1.052E-02	4.397	1.001E-02	5.420	1.037E-02
3.392	1.059E-02	4.416	1.007E-02	5.439	1.039E-02
3.412	1.059E-02	4.435	1.010E-02	5.459	1.035E-02
3.431	1.057E-02	4.455	1.010E-02	5.478	1.031E-02
3.450	1.054E-02	4.474	1.016E-02	5.497	1.025E-02
3.470	1.053E-02	4.493	1.019E-02	5.517	1.018E-02
3.489	1.055E-02	4.512	1.021E-02	5.536	1.014E-02
3.508	1.053E-02	4.532	1.022E-02	5.555	1.010E-02
3.528	1.052E-02	4.551	1.021E-02	5.575	1.008E-02
3.547	1.050E-02	4.570	1.021E-02	5.594	1.004E-02
3.566	1.046E-02	4.590	1.024E-02	5.613	1.002E-02
3.585	1.044E-02	4.609	1.023E-02	5.633	9.980E-03
3.605	1.032E-02	4.628	1.023E-02	5.652	9.910E-03
3.624	1.027E-02	4.648	1.025E-02	5.671	9.822E-03
3.643	1.022E-02	4.667	1.028E-02	5.690	9.785E-03
3.663	1.017E-02	4.686	1.025E-02	5.710	9.788E-03
3.682	1.023E-02	4.706	1.023E-02	5.729	9.794E-03
3.701	1.023E-02	4.725	1.027E-02	5.748	9.861E-03
3.721	1.016E-02	4.744	1.021E-02	5.768	9.904E-03
3.740	1.010E-02	4.763	1.019E-02	5.787	9.924E-03
3.759	1.004E-02	4.783	1.019E-02	5.806	9.948E-03
3.779	1.004E-02	4.802	1.012E-02	5.826	9.917E-03
3.798	1.002E-02	4.821	1.010E-02	5.845	9.949E-03
3.817	9.989E-03	4.841	1.014E-02	5.864	9.993E-03
3.837	9.943E-03	4.860	1.015E-02	5.884	1.002E-02
3.856	9.948E-03	4.879	1.017E-02	5.903	1.005E-02
3.875	9.967E-03	4.899	1.017E-02	5.922	1.004E-02
3.894	9.967E-03	4.918	1.013E-02	5.941	1.006E-02
3.914	9.975E-03	4.937	1.016E-02	5.961	1.008E-02
3.933	1.003E-02	4.957	1.011E-02	5.980	1.015E-02
3.952	1.010E-02	4.976	1.003E-02	5.999	1.016E-02
3.972	1.010E-02	4.995	9.974E-03	6.019	1.013E-02
3.991	1.010E-02	5.015	9.953E-03	6.038	1.011E-02
4.010	1.009E-02	5.034	9.966E-03	6.057	1.012E-02
4.030	1.010E-02	5.053	9.940E-03	6.077	1.012E-02
4.049	1.015E-02	5.072	9.924E-03	6.096	1.006E-02
4.068	1.015E-02	5.092	9.925E-03	6.115	1.012E-02
4.088	1.019E-02	5.111	9.899E-03	6.135	1.015E-02
4.107	1.019E-02	5.130	9.906E-03	6.154	1.022E-02
4.126	1.019E-02	5.150	9.942E-03	6.173	1.025E-02
4.146	1.019E-02	5.169	9.966E-03	6.193	1.028E-02
4.165	1.020E-02	5.188	1.001E-02	6.212	1.034E-02
4.184	1.016E-02	5.208	1.002E-02	6.231	1.036E-02
4.203	1.010E-02	5.227	1.004E-02	6.250	1.042E-02
6.270	1.052E-02	7.293	1.063E-02	8.317	1.062E-02
6.289	1.059E-02	7.313	1.055E-02	8.336	1.050E-02
6.308	1.057E-02	7.332	1.051E-02	8.355	1.044E-02

Distance con't (mm)	Sr/Ca (mol/mol)	Distance con't (mm)	Sr/Ca (mol/mol)	Distance con't (mm)	Sr/Ca (mol/mol)
6.328	1.056E-02	7.351	1.049E-02	8.375	1.042E-02
6.347	1.052E-02	7.371	1.044E-02	8.394	1.042E-02
6.366	1.056E-02	7.390	1.040E-02	8.413	1.042E-02
6.386	1.055E-02	7.409	1.031E-02	8.433	1.040E-02
6.405	1.049E-02	7.428	1.025E-02	8.452	1.037E-02
6.424	1.054E-02	7.448	1.022E-02	8.471	1.041E-02
6.444	1.054E-02	7.467	1.019E-02	8.491	1.036E-02
6.463	1.048E-02	7.486	1.013E-02	8.510	1.029E-02
6.482	1.046E-02	7.506	1.008E-02	8.529	1.023E-02
6.502	1.041E-02	7.525	1.005E-02	8.549	1.015E-02
6.521	1.033E-02	7.544	1.003E-02	8.568	1.007E-02
6.540	1.028E-02	7.564	9.992E-03	8.587	9.989E-03
6.559	1.023E-02	7.583	1.000E-02	8.606	9.975E-03
6.579	1.017E-02	7.602	9.939E-03	8.626	9.945E-03
6.598	1.005E-02	7.622	9.925E-03	8.645	9.921E-03
6.617	9.962E-03	7.641	9.965E-03	8.664	9.953E-03
6.637	1.002E-02	7.660	9.978E-03	8.684	9.982E-03
6.656	1.011E-02	7.680	9.944E-03	8.703	1.002E-02
6.675	1.022E-02	7.699	1.000E-02	8.722	1.003E-02
6.695	1.023E-02	7.718	1.002E-02	8.742	9.992E-03
6.714	1.028E-02	7.737	1.004E-02	8.761	1.005E-02
6.733	1.035E-02	7.757	1.003E-02	8.780	1.004E-02
6.753	1.033E-02	7.776	1.001E-02	8.800	1.000E-02
6.772	1.032E-02	7.795	9.980E-03	8.819	1.000E-02
6.791	1.033E-02	7.815	9.989E-03	8.838	1.010E-02
6.811	1.033E-02	7.834	9.984E-03	8.858	1.013E-02
6.830	1.038E-02	7.853	9.986E-03	8.877	1.021E-02
6.849	1.043E-02	7.873	1.000E-02	8.896	1.028E-02
6.868	1.045E-02	7.892	9.993E-03	8.915	1.033E-02
6.888	1.047E-02	7.911	1.003E-02	8.935	1.039E-02
6.907	1.049E-02	7.931	1.008E-02	8.954	1.046E-02
6.926	1.054E-02	7.950	1.012E-02	8.973	1.048E-02
6.946	1.062E-02	7.969	1.012E-02	8.993	1.046E-02
6.965	1.057E-02	7.988	1.016E-02	9.012	1.043E-02
6.984	1.054E-02	8.008	1.029E-02	9.031	1.041E-02
7.004	1.049E-02	8.027	1.030E-02	9.051	1.035E-02
7.023	1.048E-02	8.046	1.032E-02	9.070	1.031E-02
7.042	1.048E-02	8.066	1.034E-02	9.089	1.029E-02
7.062	1.047E-02	8.085	1.040E-02	9.109	1.030E-02
7.081	1.052E-02	8.104	1.041E-02	9.128	1.031E-02
7.100	1.052E-02	8.124	1.045E-02	9.147	1.031E-02
7.119	1.058E-02	8.143	1.047E-02	9.166	1.026E-02
7.139	1.062E-02	8.162	1.051E-02	9.186	1.029E-02
7.158	1.063E-02	8.182	1.053E-02	9.205	1.025E-02
7.177	1.067E-02	8.201	1.054E-02	9.224	1.027E-02
7.197	1.067E-02	8.220	1.059E-02	9.244	1.026E-02
7.216	1.067E-02	8.240	1.062E-02	9.263	1.022E-02
7.235	1.069E-02	8.259	1.064E-02	9.282	1.016E-02
7.255	1.065E-02	8.278	1.060E-02	9.302	1.006E-02
7.274	1.065E-02	8.297	1.061E-02	9.321	9.995E-03
9.340	9.959E-03	10.364	1.073E-02	11.387	1.034E-02
9.360	9.864E-03	10.383	1.077E-02	11.407	1.035E-02
9.379	9.835E-03	10.402	1.071E-02	11.426	1.037E-02
9.398	9.846E-03	10.422	1.072E-02	11.445	1.032E-02
9.418	9.838E-03	10.441	1.073E-02	11.465	1.031E-02
9.437	9.860E-03	10.460	1.068E-02	11.484	1.027E-02

LA-ICP-MS data

Distance con't (mm)	Sr/Ca (mol/mol)	Distance con't (mm)	Sr/Ca (mol/mol)	Distance con't (mm)	Sr/Ca (mol/mol)
9.456	9.890E-03	10.480	1.066E-02	11.503	1.027E-02
9.475	9.865E-03	10.499	1.068E-02	11.522	1.030E-02
9.495	9.851E-03	10.518	1.070E-02	11.542	1.030E-02
9.514	9.770E-03	10.538	1.068E-02	11.561	1.029E-02
9.533	9.720E-03	10.557	1.064E-02	11.580	1.038E-02
9.553	9.638E-03	10.576	1.062E-02	11.600	1.046E-02
9.572	9.621E-03	10.596	1.062E-02	11.619	1.051E-02
9.591	9.607E-03	10.615	1.058E-02	11.638	1.050E-02
9.611	9.613E-03	10.634	1.056E-02	11.658	1.051E-02
9.630	9.701E-03	10.653	1.053E-02	11.677	1.051E-02
9.649	9.777E-03	10.673	1.047E-02	11.696	1.052E-02
9.669	9.810E-03	10.692	1.049E-02	11.716	1.049E-02
9.688	9.886E-03	10.711	1.047E-02	11.735	1.044E-02
9.707	1.000E-02	10.731	1.050E-02	11.754	1.041E-02
9.727	1.006E-02	10.750	1.052E-02	11.774	1.043E-02
9.746	1.007E-02	10.769	1.052E-02	11.793	1.043E-02
9.765	1.009E-02	10.789	1.052E-02	11.812	1.042E-02
9.784	1.006E-02	10.808	1.052E-02	11.831	1.036E-02
9.804	1.008E-02	10.827	1.051E-02	11.851	1.030E-02
9.823	1.008E-02	10.847	1.051E-02	11.870	1.030E-02
9.842	1.010E-02	10.866	1.058E-02	11.889	1.024E-02
9.862	1.017E-02	10.885	1.060E-02	11.909	1.014E-02
9.881	1.020E-02	10.905	1.064E-02	11.928	1.009E-02
9.900	1.023E-02	10.924	1.066E-02	11.947	1.010E-02
9.920	1.030E-02	10.943	1.070E-02	11.967	1.006E-02
9.939	1.032E-02	10.962	1.074E-02	11.986	1.008E-02
9.958	1.034E-02	10.982	1.070E-02	12.005	1.005E-02
9.978	1.034E-02	11.001	1.073E-02	12.025	9.962E-03
9.997	1.031E-02	11.020	1.071E-02	12.044	9.972E-03
10.016	1.025E-02	11.040	1.073E-02	12.063	1.001E-02
10.036	1.019E-02	11.059	1.074E-02	12.083	1.007E-02
10.055	1.015E-02	11.078	1.067E-02	12.102	1.014E-02
10.074	1.018E-02	11.098	1.061E-02	12.121	1.011E-02
10.093	1.019E-02	11.117	1.060E-02	12.140	1.011E-02
10.113	1.022E-02	11.136	1.058E-02	12.160	1.008E-02
10.132	1.030E-02	11.156	1.060E-02	12.179	1.010E-02
10.151	1.038E-02	11.175	1.061E-02	12.198	1.013E-02
10.171	1.044E-02	11.194	1.055E-02	12.218	1.019E-02
10.190	1.046E-02	11.214	1.053E-02	12.237	1.024E-02
10.209	1.049E-02	11.233	1.052E-02	12.256	1.028E-02
10.229	1.050E-02	11.252	1.046E-02	12.276	1.026E-02
10.248	1.052E-02	11.271	1.038E-02	12.295	1.029E-02
10.267	1.051E-02	11.291	1.029E-02	12.314	1.035E-02
10.287	1.052E-02	11.310	1.035E-02	12.334	1.040E-02
10.306	1.055E-02	11.329	1.030E-02	12.353	1.048E-02
10.325	1.063E-02	11.349	1.033E-02	12.372	1.049E-02
10.344	1.073E-02	11.368	1.035E-02	12.392	1.054E-02
12.411	1.052E-02	13.434	1.029E-02	14.458	1.063E-02
12.430	1.048E-02	13.454	1.030E-02	14.477	1.069E-02
12.449	1.054E-02	13.473	1.026E-02	14.496	1.073E-02
12.469	1.052E-02	13.492	1.029E-02	14.516	1.072E-02
12.488	1.055E-02	13.512	1.029E-02	14.535	1.064E-02
12.507	1.053E-02	13.531	1.029E-02	14.554	1.064E-02
12.527	1.050E-02	13.550	1.033E-02	14.574	1.059E-02
12.546	1.048E-02	13.570	1.032E-02	14.593	1.058E-02
12.565	1.046E-02	13.589	1.026E-02	14.612	1.056E-02

Distance con't (mm)	Sr/Ca (mol/mol)	Distance con't (mm)	Sr/Ca (mol/mol)	Distance con't (mm)	Sr/Ca (mol/mol)
12.585	1.044E-02	13.608	1.019E-02	14.632	1.059E-02
12.604	1.043E-02	13.627	1.016E-02	14.651	1.056E-02
12.623	1.045E-02	13.647	1.011E-02	14.670	1.050E-02
12.643	1.037E-02	13.666	1.010E-02	14.690	1.047E-02
12.662	1.037E-02	13.685	1.009E-02	14.709	1.050E-02
12.681	1.035E-02	13.705	1.012E-02	14.728	1.047E-02
12.700	1.035E-02	13.724	1.015E-02	14.748	1.046E-02
12.720	1.032E-02	13.743	1.012E-02	14.767	1.042E-02
12.739	1.034E-02	13.763	1.011E-02	14.786	1.038E-02
12.758	1.036E-02	13.782	1.006E-02	14.805	1.038E-02
12.778	1.039E-02	13.801	1.002E-02	14.825	1.035E-02
12.797	1.044E-02	13.821	1.002E-02	14.844	1.036E-02
12.816	1.049E-02	13.840	9.965E-03	14.863	1.039E-02
12.836	1.057E-02	13.859	9.883E-03	14.883	1.041E-02
12.855	1.058E-02	13.878	9.798E-03	14.902	1.043E-02
12.874	1.055E-02	13.898	9.739E-03	14.921	1.046E-02
12.894	1.059E-02	13.917	9.709E-03	14.941	1.046E-02
12.913	1.059E-02	13.936	9.686E-03	14.960	1.041E-02
12.932	1.061E-02	13.956	9.693E-03	14.979	1.041E-02
12.952	1.060E-02	13.975	9.719E-03	14.999	1.039E-02
12.971	1.063E-02	13.994	9.743E-03	15.018	1.035E-02
12.990	1.055E-02	14.014	9.755E-03	15.037	1.032E-02
13.009	1.050E-02	14.033	9.732E-03	15.056	1.030E-02
13.029	1.048E-02	14.052	9.702E-03	15.076	1.031E-02
13.048	1.042E-02	14.072	9.733E-03	15.095	1.030E-02
13.067	1.040E-02	14.091	9.716E-03	15.114	1.030E-02
13.087	1.039E-02	14.110	9.721E-03	15.134	1.026E-02
13.106	1.033E-02	14.130	9.713E-03	15.153	1.024E-02
13.125	1.033E-02	14.149	9.671E-03	15.172	1.027E-02
13.145	1.033E-02	14.168	9.707E-03	15.192	1.029E-02
13.164	1.021E-02	14.187	9.765E-03	15.211	1.030E-02
13.183	1.024E-02	14.207	9.884E-03	15.230	1.035E-02
13.203	1.028E-02	14.226	9.926E-03	15.250	1.029E-02
13.222	1.023E-02	14.245	1.001E-02	15.269	1.025E-02
13.241	1.024E-02	14.265	1.007E-02	15.288	1.025E-02
13.261	1.025E-02	14.284	1.011E-02	15.308	1.024E-02
13.280	1.026E-02	14.303	1.012E-02	15.327	1.025E-02
13.299	1.027E-02	14.323	1.015E-02	15.346	1.030E-02
13.318	1.035E-02	14.342	1.022E-02	15.365	1.036E-02
13.338	1.038E-02	14.361	1.026E-02	15.385	1.038E-02
13.357	1.038E-02	14.381	1.031E-02	15.404	1.030E-02
13.376	1.041E-02	14.400	1.038E-02	15.423	1.030E-02
13.396	1.036E-02	14.419	1.050E-02	15.443	1.025E-02
13.415	1.032E-02	14.439	1.056E-02	15.462	1.026E-02
15.481	1.025E-02	16.505	1.041E-02	17.528	1.043E-02
15.501	1.020E-02	16.524	1.033E-02	17.548	1.049E-02
15.520	1.018E-02	16.543	1.024E-02	17.567	1.052E-02
15.539	1.016E-02	16.563	1.014E-02	17.586	1.059E-02
15.559	1.012E-02	16.582	1.007E-02	17.606	1.060E-02
15.578	1.015E-02	16.601	9.959E-03	17.625	1.060E-02
15.597	1.018E-02	16.621	9.836E-03	17.644	1.054E-02
15.617	1.019E-02	16.640	9.833E-03	17.664	1.055E-02
15.636	1.018E-02	16.659	9.845E-03	17.683	1.055E-02
15.655	1.019E-02	16.679	9.792E-03	17.702	1.050E-02
15.674	1.017E-02	16.698	9.809E-03	17.721	1.044E-02
15.694	1.012E-02	16.717	9.841E-03	17.741	1.043E-02

LA-ICP-MS data

Distance con't (mm)	Sr/Ca (mol/mol)	Distance con't (mm)	Sr/Ca (mol/mol)	Distance con't (mm)	Sr/Ca (mol/mol)
15.713	1.013E-02	16.737	9.849E-03	17.760	1.045E-02
15.732	1.018E-02	16.756	9.908E-03	17.779	1.044E-02
15.752	1.023E-02	16.775	9.995E-03	17.799	1.044E-02
15.771	1.025E-02	16.795	1.006E-02	17.818	1.045E-02
15.790	1.023E-02	16.814	1.014E-02	17.837	1.041E-02
15.810	1.025E-02	16.833	1.022E-02	17.857	1.045E-02
15.829	1.029E-02	16.852	1.035E-02	17.876	1.045E-02
15.848	1.027E-02	16.872	1.042E-02	17.895	1.044E-02
15.868	1.026E-02	16.891	1.051E-02	17.915	1.042E-02
15.887	1.025E-02	16.910	1.060E-02	17.934	1.038E-02
15.906	1.030E-02	16.930	1.067E-02	17.953	1.037E-02
15.926	1.030E-02	16.949	1.068E-02	17.973	1.043E-02
15.945	1.029E-02	16.968	1.067E-02	17.992	1.052E-02
15.964	1.030E-02	16.988	1.064E-02	18.011	1.054E-02
15.983	1.024E-02	17.007	1.069E-02	18.030	1.052E-02
16.003	1.025E-02	17.026	1.066E-02	18.050	1.052E-02
16.022	1.027E-02	17.046	1.071E-02	18.069	1.059E-02
16.041	1.024E-02	17.065	1.076E-02	18.088	1.062E-02
16.061	1.022E-02	17.084	1.068E-02	18.108	1.066E-02
16.080	1.016E-02	17.103	1.068E-02	18.127	1.068E-02
16.099	1.021E-02	17.123	1.066E-02	18.146	1.071E-02
16.119	1.032E-02	17.142	1.062E-02	18.166	1.076E-02
16.138	1.037E-02	17.161	1.059E-02	18.185	1.076E-02
16.157	1.040E-02	17.181	1.057E-02	18.204	1.079E-02
16.177	1.045E-02	17.200	1.054E-02	18.224	1.080E-02
16.196	1.047E-02	17.219	1.050E-02		
16.215	1.053E-02	17.239	1.047E-02		
16.234	1.051E-02	17.258	1.041E-02		
16.254	1.054E-02	17.277	1.043E-02		
16.273	1.061E-02	17.297	1.044E-02		
16.292	1.072E-02	17.316	1.048E-02		
16.312	1.078E-02	17.335	1.045E-02		
16.331	1.079E-02	17.355	1.046E-02		
16.350	1.079E-02	17.374	1.047E-02		
16.370	1.080E-02	17.393	1.046E-02		
16.389	1.078E-02	17.412	1.047E-02		
16.408	1.077E-02	17.432	1.042E-02		
16.428	1.075E-02	17.451	1.043E-02		
16.447	1.064E-02	17.470	1.045E-02		
16.466	1.056E-02	17.490	1.045E-02		
16.486	1.048E-02	17.509	1.044E-02		

Table 10.12 Otta Island, Caroline Islands *Astrosclera willeyana* Sr/Ca

Distance from top (mm)	Sr/Ca (mol/mol)	Distance con't (mm)	Sr/Ca (mol/mol)	Distance con't (mm)	Sr/Ca (mol/mol)
0.007	1.035E-02	1.050	1.055E-02	2.093	1.066E-02
0.026	1.033E-02	1.069	1.065E-02	2.113	1.065E-02
0.046	1.038E-02	1.089	1.059E-02	2.132	1.063E-02
0.066	1.035E-02	1.109	1.049E-02	2.152	1.072E-02
0.085	1.034E-02	1.128	1.027E-02	2.172	1.080E-02
0.105	1.035E-02	1.148	1.015E-02	2.191	1.083E-02
0.125	1.038E-02	1.168	1.005E-02	2.211	1.063E-02
0.144	1.031E-02	1.188	1.019E-02	2.231	1.068E-02
0.164	1.039E-02	1.207	1.019E-02	2.250	1.063E-02
0.184	1.035E-02	1.227	1.033E-02	2.270	1.068E-02
0.203	1.044E-02	1.247	1.052E-02	2.290	1.069E-02
0.223	1.048E-02	1.266	1.054E-02	2.309	1.074E-02
0.243	1.038E-02	1.286	1.051E-02	2.329	1.087E-02
0.262	1.029E-02	1.306	1.070E-02	2.349	1.093E-02
0.282	1.023E-02	1.325	1.081E-02	2.368	1.092E-02
0.302	1.008E-02	1.345	1.086E-02	2.388	1.101E-02
0.321	1.006E-02	1.365	1.077E-02	2.408	1.105E-02
0.341	9.951E-03	1.384	1.074E-02	2.428	1.099E-02
0.361	9.834E-03	1.404	1.082E-02	2.447	1.100E-02
0.381	9.853E-03	1.424	1.087E-02	2.467	1.089E-02
0.400	9.766E-03	1.443	1.071E-02	2.487	1.082E-02
0.420	9.840E-03	1.463	1.054E-02	2.506	1.079E-02
0.440	9.921E-03	1.483	1.046E-02	2.526	1.066E-02
0.459	9.941E-03	1.502	1.046E-02	2.546	1.058E-02
0.479	9.887E-03	1.522	1.044E-02	2.565	1.052E-02
0.499	9.949E-03	1.542	1.027E-02	2.585	1.039E-02
0.518	1.002E-02	1.561	1.012E-02	2.605	1.034E-02
0.538	1.015E-02	1.581	1.001E-02	2.624	1.033E-02
0.558	1.020E-02	1.601	1.002E-02	2.644	1.027E-02
0.577	1.025E-02	1.621	9.972E-03	2.664	1.021E-02
0.597	1.024E-02	1.640	9.948E-03	2.683	1.003E-02
0.617	1.040E-02	1.660	9.771E-03	2.703	9.996E-03
0.636	1.042E-02	1.680	9.860E-03	2.723	9.823E-03
0.656	1.049E-02	1.699	9.901E-03	2.742	9.750E-03
0.676	1.054E-02	1.719	1.002E-02	2.762	9.825E-03
0.695	1.056E-02	1.739	9.968E-03	2.782	9.941E-03
0.715	1.058E-02	1.758	1.010E-02	2.801	1.012E-02
0.735	1.062E-02	1.778	1.016E-02	2.821	1.039E-02
0.754	1.079E-02	1.798	1.028E-02	2.841	1.054E-02
0.774	1.087E-02	1.817	1.026E-02	2.861	1.077E-02
0.794	1.087E-02	1.837	1.043E-02	2.880	1.089E-02
0.814	1.076E-02	1.857	1.049E-02	2.900	1.099E-02
0.833	1.089E-02	1.876	1.069E-02	2.920	1.101E-02
0.853	1.087E-02	1.896	1.056E-02	2.939	1.113E-02
0.873	1.078E-02	1.916	1.051E-02	2.959	1.107E-02
0.892	1.058E-02	1.935	1.052E-02	2.979	1.108E-02
0.912	1.053E-02	1.955	1.055E-02	2.998	1.109E-02
0.932	1.041E-02	1.975	1.049E-02	3.018	1.105E-02
0.951	1.041E-02	1.994	1.050E-02	3.038	1.097E-02
0.971	1.027E-02	2.014	1.041E-02	3.057	1.098E-02
0.991	1.044E-02	2.034	1.045E-02	3.077	1.094E-02
1.010	1.062E-02	2.054	1.050E-02	3.097	1.086E-02
1.030	1.067E-02	2.073	1.067E-02	3.116	1.069E-02

LA-ICP-MS data

Distance con't (mm)	Sr/Ca (mol/mol)	Distance con't (mm)	Sr/Ca (mol/mol)	Distance con't (mm)	Sr/Ca (mol/mol)
3.136	1.060E-02	4.179	1.070E-02	5.222	1.082E-02
3.156	1.060E-02	4.199	1.091E-02	5.242	1.083E-02
3.175	1.053E-02	4.219	1.099E-02	5.262	1.084E-02
3.195	1.042E-02	4.238	1.094E-02	5.281	1.085E-02
3.215	1.027E-02	4.258	1.095E-02	5.301	1.081E-02
3.234	1.032E-02	4.278	1.089E-02	5.321	1.084E-02
3.254	1.034E-02	4.297	1.066E-02	5.341	1.080E-02
3.274	1.043E-02	4.317	1.056E-02	5.360	1.087E-02
3.294	1.034E-02	4.337	1.028E-02	5.380	1.090E-02
3.313	1.041E-02	4.356	1.013E-02	5.400	1.089E-02
3.333	1.057E-02	4.376	1.009E-02	5.419	1.090E-02
3.353	1.070E-02	4.396	1.012E-02	5.439	1.081E-02
3.372	1.073E-02	4.415	1.014E-02	5.459	1.074E-02
3.392	1.078E-02	4.435	1.030E-02	5.478	1.068E-02
3.412	1.082E-02	4.455	1.043E-02	5.498	1.050E-02
3.431	1.096E-02	4.474	1.054E-02	5.518	1.042E-02
3.451	1.090E-02	4.494	1.068E-02	5.537	1.028E-02
3.471	1.080E-02	4.514	1.073E-02	5.557	1.017E-02
3.490	1.067E-02	4.534	1.078E-02	5.577	1.013E-02
3.510	1.063E-02	4.553	1.078E-02	5.596	1.019E-02
3.530	1.071E-02	4.573	1.062E-02	5.616	1.029E-02
3.549	1.058E-02	4.593	1.038E-02	5.636	1.038E-02
3.569	1.055E-02	4.612	1.025E-02	5.655	1.033E-02
3.589	1.055E-02	4.632	1.019E-02	5.675	1.046E-02
3.608	1.058E-02	4.652	1.014E-02	5.695	1.058E-02
3.628	1.064E-02	4.671	1.000E-02	5.714	1.062E-02
3.648	1.065E-02	4.691	9.877E-03	5.734	1.058E-02
3.668	1.057E-02	4.711	9.929E-03	5.754	1.053E-02
3.687	1.052E-02	4.730	1.016E-02	5.774	1.061E-02
3.707	1.047E-02	4.750	1.037E-02	5.793	1.074E-02
3.727	1.045E-02	4.770	1.043E-02	5.813	1.071E-02
3.746	1.039E-02	4.789	1.055E-02	5.833	1.072E-02
3.766	1.032E-02	4.809	1.068E-02	5.852	1.091E-02
3.786	1.030E-02	4.829	1.085E-02	5.872	1.091E-02
3.805	1.035E-02	4.848	1.095E-02	5.892	1.093E-02
3.825	1.035E-02	4.868	1.094E-02	5.911	1.070E-02
3.845	1.038E-02	4.888	1.094E-02	5.931	1.059E-02
3.864	1.040E-02	4.908	1.085E-02	5.951	1.062E-02
3.884	1.045E-02	4.927	1.080E-02	5.970	1.059E-02
3.904	1.057E-02	4.947	1.077E-02	5.990	1.050E-02
3.923	1.063E-02	4.967	1.072E-02	6.010	1.064E-02
3.943	1.060E-02	4.986	1.083E-02	6.029	1.071E-02
3.963	1.066E-02	5.006	1.075E-02	6.049	1.092E-02
3.982	1.053E-02	5.026	1.073E-02	6.069	1.099E-02
4.002	1.041E-02	5.045	1.081E-02	6.088	1.096E-02
4.022	1.024E-02	5.065	1.075E-02	6.108	1.085E-02
4.041	1.008E-02	5.085	1.085E-02	6.128	1.086E-02
4.061	9.937E-03	5.104	1.088E-02	6.148	1.091E-02
4.081	9.891E-03	5.124	1.081E-02	6.167	1.096E-02
4.101	1.000E-02	5.144	1.086E-02	6.187	1.097E-02
4.120	1.009E-02	5.163	1.088E-02	6.207	1.105E-02
4.140	1.034E-02	5.183	1.080E-02	6.226	1.119E-02
4.160	1.057E-02	5.203	1.090E-02	6.246	1.131E-02
6.266	1.121E-02	7.309	1.063E-02	8.352	1.055E-02
6.285	1.099E-02	7.328	1.065E-02	8.372	1.048E-02
6.305	1.077E-02	7.348	1.062E-02	8.391	1.049E-02

Distance con't (mm)	Sr/Ca (mol/mol)	Distance con't (mm)	Sr/Ca (mol/mol)	Distance con't (mm)	Sr/Ca (mol/mol)
6.325	1.068E-02	7.368	1.065E-02	8.411	1.063E-02
6.344	1.046E-02	7.388	1.053E-02	8.431	1.073E-02
6.364	1.012E-02	7.407	1.064E-02	8.450	1.075E-02
6.384	1.005E-02	7.427	1.071E-02	8.470	1.064E-02
6.403	1.003E-02	7.447	1.078E-02	8.490	1.054E-02
6.423	1.003E-02	7.466	1.088E-02	8.509	1.052E-02
6.443	1.004E-02	7.486	1.084E-02	8.529	1.051E-02
6.462	9.916E-03	7.506	1.080E-02	8.549	1.051E-02
6.482	9.842E-03	7.525	1.075E-02	8.568	1.048E-02
6.502	9.947E-03	7.545	1.063E-02	8.588	1.036E-02
6.521	9.927E-03	7.565	1.059E-02	8.608	1.044E-02
6.541	9.947E-03	7.584	1.044E-02	8.628	1.044E-02
6.561	1.013E-02	7.604	1.026E-02	8.647	1.048E-02
6.581	1.021E-02	7.624	1.030E-02	8.667	1.048E-02
6.600	1.024E-02	7.643	1.023E-02	8.687	1.040E-02
6.620	1.032E-02	7.663	1.024E-02	8.706	1.041E-02
6.640	1.037E-02	7.683	1.028E-02	8.726	1.055E-02
6.659	1.042E-02	7.702	1.034E-02	8.746	1.061E-02
6.679	1.042E-02	7.722	1.048E-02	8.765	1.072E-02
6.699	1.042E-02	7.742	1.059E-02	8.785	1.081E-02
6.718	1.037E-02	7.761	1.068E-02	8.805	1.090E-02
6.738	1.050E-02	7.781	1.075E-02	8.824	1.097E-02
6.758	1.055E-02	7.801	1.087E-02	8.844	1.106E-02
6.777	1.065E-02	7.821	1.083E-02	8.864	1.117E-02
6.797	1.072E-02	7.840	1.095E-02	8.883	1.110E-02
6.817	1.073E-02	7.860	1.093E-02	8.903	1.107E-02
6.836	1.070E-02	7.880	1.105E-02	8.923	1.093E-02
6.856	1.078E-02	7.899	1.093E-02	8.942	1.075E-02
6.876	1.075E-02	7.919	1.105E-02	8.962	1.065E-02
6.895	1.086E-02	7.939	1.099E-02	8.982	1.054E-02
6.915	1.085E-02	7.958	1.110E-02	9.001	1.036E-02
6.935	1.092E-02	7.978	1.101E-02	9.021	1.050E-02
6.954	1.103E-02	7.998	1.115E-02	9.041	1.057E-02
6.974	1.092E-02	8.017	1.109E-02	9.061	1.070E-02
6.994	1.090E-02	8.037	1.120E-02	9.080	1.095E-02
7.014	1.089E-02	8.057	1.114E-02	9.100	1.098E-02
7.033	1.072E-02	8.076	1.128E-02	9.120	1.098E-02
7.053	1.058E-02	8.096	1.134E-02	9.139	1.098E-02
7.073	1.039E-02	8.116	1.127E-02	9.159	1.084E-02
7.092	1.038E-02	8.135	1.118E-02	9.179	1.079E-02
7.112	1.057E-02	8.155	1.108E-02	9.198	1.073E-02
7.132	1.053E-02	8.175	1.101E-02	9.218	1.054E-02
7.151	1.052E-02	8.194	1.097E-02	9.238	1.048E-02
7.171	1.064E-02	8.214	1.073E-02	9.257	1.036E-02
7.191	1.070E-02	8.234	1.067E-02	9.277	1.035E-02
7.210	1.083E-02	8.254	1.068E-02	9.297	1.045E-02
7.230	1.080E-02	8.273	1.052E-02	9.316	1.044E-02
7.250	1.082E-02	8.293	1.046E-02	9.336	1.042E-02
7.269	1.077E-02	8.313	1.045E-02	9.356	1.042E-02
7.289	1.072E-02	8.332	1.049E-02	9.375	1.046E-02
9.395	1.053E-02	10.438	1.074E-02	11.481	1.047E-02
9.415	1.036E-02	10.458	1.064E-02	11.501	1.052E-02
9.434	1.025E-02	10.478	1.052E-02	11.521	1.048E-02
9.454	1.013E-02	10.497	1.051E-02	11.541	1.046E-02
9.474	1.018E-02	10.517	1.040E-02	11.560	1.041E-02
9.494	1.017E-02	10.537	1.025E-02	11.580	1.044E-02

LA-ICP-MS data

Distance con't (mm)	Sr/Ca (mol/mol)	Distance con't (mm)	Sr/Ca (mol/mol)	Distance con't (mm)	Sr/Ca (mol/mol)
9.513	1.022E-02	10.556	1.033E-02	11.600	1.050E-02
9.533	1.036E-02	10.576	1.035E-02	11.619	1.040E-02
9.553	1.054E-02	10.596	1.043E-02	11.639	1.035E-02
9.572	1.054E-02	10.615	1.035E-02	11.659	1.039E-02
9.592	1.073E-02	10.635	1.033E-02	11.678	1.042E-02
9.612	1.062E-02	10.655	1.028E-02	11.698	1.049E-02
9.631	1.072E-02	10.674	1.035E-02	11.718	1.049E-02
9.651	1.074E-02	10.694	1.032E-02	11.737	1.046E-02
9.671	1.087E-02	10.714	1.029E-02	11.757	1.041E-02
9.690	1.091E-02	10.734	1.025E-02	11.777	1.045E-02
9.710	1.092E-02	10.753	1.029E-02	11.796	1.038E-02
9.730	1.084E-02	10.773	1.034E-02	11.816	1.029E-02
9.749	1.098E-02	10.793	1.042E-02	11.836	1.015E-02
9.769	1.093E-02	10.812	1.038E-02	11.855	1.003E-02
9.789	1.086E-02	10.832	1.030E-02	11.875	9.918E-03
9.808	1.070E-02	10.852	1.041E-02	11.895	9.922E-03
9.828	1.076E-02	10.871	1.038E-02	11.914	9.751E-03
9.848	1.074E-02	10.891	1.024E-02	11.934	9.794E-03
9.868	1.081E-02	10.911	1.005E-02	11.954	9.764E-03
9.887	1.074E-02	10.930	9.858E-03	11.974	9.889E-03
9.907	1.061E-02	10.950	9.747E-03	11.993	1.006E-02
9.927	1.067E-02	10.970	9.708E-03	12.013	1.028E-02
9.946	1.057E-02	10.989	9.637E-03	12.033	1.044E-02
9.966	1.062E-02	11.009	9.527E-03	12.052	1.067E-02
9.986	1.058E-02	11.029	9.723E-03	12.072	1.058E-02
10.005	1.047E-02	11.048	9.926E-03	12.092	1.073E-02
10.025	1.045E-02	11.068	1.013E-02	12.111	1.060E-02
10.045	1.047E-02	11.088	1.024E-02	12.131	1.044E-02
10.064	1.045E-02	11.108	1.038E-02	12.151	1.033E-02
10.084	1.052E-02	11.127	1.042E-02	12.170	1.015E-02
10.104	1.030E-02	11.147	1.039E-02	12.190	1.004E-02
10.123	1.033E-02	11.167	1.028E-02	12.210	1.011E-02
10.143	1.040E-02	11.186	1.024E-02	12.229	9.997E-03
10.163	1.040E-02	11.206	1.028E-02	12.249	1.003E-02
10.182	1.047E-02	11.226	1.042E-02	12.269	1.001E-02
10.202	1.040E-02	11.245	1.041E-02	12.288	9.991E-03
10.222	1.052E-02	11.265	1.050E-02	12.308	1.014E-02
10.241	1.055E-02	11.285	1.056E-02	12.328	1.025E-02
10.261	1.064E-02	11.304	1.052E-02	12.348	1.033E-02
10.281	1.071E-02	11.324	1.055E-02	12.367	1.034E-02
10.301	1.073E-02	11.344	1.047E-02	12.387	1.033E-02
10.320	1.084E-02	11.363	1.034E-02	12.407	1.045E-02
10.340	1.108E-02	11.383	1.031E-02	12.426	1.051E-02
10.360	1.093E-02	11.403	1.028E-02	12.446	1.053E-02
10.379	1.098E-02	11.422	1.038E-02	12.466	1.051E-02
10.399	1.098E-02	11.442	1.044E-02	12.485	1.036E-02
10.419	1.084E-02	11.462	1.036E-02	12.505	1.028E-02
12.525	1.021E-02	13.568	1.105E-02	14.611	1.072E-02
12.544	1.019E-02	13.588	1.081E-02	14.631	1.081E-02
12.564	1.013E-02	13.607	1.066E-02	14.650	1.107E-02
12.584	1.011E-02	13.627	1.053E-02	14.670	1.123E-02
12.603	1.001E-02	13.647	1.043E-02	14.690	1.129E-02
12.623	9.987E-03	13.666	1.044E-02	14.709	1.136E-02
12.643	1.001E-02	13.686	1.052E-02	14.729	1.119E-02
12.662	1.018E-02	13.706	1.048E-02	14.749	1.113E-02
12.682	1.022E-02	13.725	1.062E-02	14.768	1.096E-02

Distance con't (mm)	Sr/Ca (mol/mol)	Distance con't (mm)	Sr/Ca (mol/mol)	Distance con't (mm)	Sr/Ca (mol/mol)
12.702	1.014E-02	13.745	1.069E-02	14.788	1.075E-02
12.721	1.010E-02	13.765	1.058E-02	14.808	1.069E-02
12.741	1.014E-02	13.784	1.059E-02	14.828	1.055E-02
12.761	1.014E-02	13.804	1.054E-02	14.847	1.072E-02
12.781	1.015E-02	13.824	1.042E-02	14.867	1.091E-02
12.800	1.001E-02	13.843	1.047E-02	14.887	1.099E-02
12.820	9.895E-03	13.863	1.050E-02	14.906	1.105E-02
12.840	9.947E-03	13.883	1.043E-02	14.926	1.104E-02
12.859	9.864E-03	13.902	1.060E-02	14.946	1.090E-02
12.879	9.825E-03	13.922	1.057E-02	14.965	1.081E-02
12.899	9.862E-03	13.942	1.050E-02	14.985	1.059E-02
12.918	9.753E-03	13.961	1.055E-02	15.005	1.049E-02
12.938	9.644E-03	13.981	1.045E-02	15.024	1.030E-02
12.958	9.586E-03	14.001	1.046E-02	15.044	1.018E-02
12.977	9.578E-03	14.021	1.051E-02	15.064	1.023E-02
12.997	9.760E-03	14.040	1.032E-02	15.083	1.039E-02
13.017	9.924E-03	14.060	1.034E-02	15.103	1.050E-02
13.036	9.937E-03	14.080	1.034E-02	15.123	1.049E-02
13.056	1.015E-02	14.099	1.020E-02	15.142	1.057E-02
13.076	1.036E-02	14.119	1.030E-02	15.162	1.061E-02
13.095	1.051E-02	14.139	1.025E-02	15.182	1.058E-02
13.115	1.054E-02	14.158	1.029E-02	15.201	1.040E-02
13.135	1.049E-02	14.178	1.045E-02	15.221	1.033E-02
13.154	1.028E-02	14.198	1.061E-02	15.241	1.032E-02
13.174	1.036E-02	14.217	1.077E-02	15.261	1.044E-02
13.194	1.020E-02	14.237	1.083E-02	15.280	1.045E-02
13.214	1.005E-02	14.257	1.079E-02	15.300	1.035E-02
13.233	9.960E-03	14.276	1.074E-02	15.320	1.045E-02
13.253	9.843E-03	14.296	1.071E-02	15.339	1.062E-02
13.273	9.689E-03	14.316	1.062E-02	15.359	1.060E-02
13.292	9.869E-03	14.335	1.050E-02	15.379	1.056E-02
13.312	9.972E-03	14.355	1.051E-02	15.398	1.044E-02
13.332	1.006E-02	14.375	1.056E-02	15.418	1.037E-02
13.351	1.026E-02	14.394	1.054E-02	15.438	1.049E-02
13.371	1.036E-02	14.414	1.055E-02	15.457	1.056E-02
13.391	1.053E-02	14.434	1.058E-02	15.477	1.059E-02
13.410	1.067E-02	14.454	1.053E-02	15.497	1.060E-02
13.430	1.055E-02	14.473	1.053E-02	15.516	1.054E-02
13.450	1.055E-02	14.493	1.048E-02	15.536	1.060E-02
13.469	1.070E-02	14.513	1.037E-02	15.556	1.066E-02
13.489	1.078E-02	14.532	1.030E-02	15.575	1.061E-02
13.509	1.081E-02	14.552	1.041E-02	15.595	1.047E-02
13.528	1.085E-02	14.572	1.037E-02	15.615	1.036E-02
13.548	1.090E-02	14.591	1.055E-02	15.634	1.028E-02
15.654	1.029E-02	16.697	1.064E-02	17.741	1.043E-02
15.674	1.015E-02	16.717	1.048E-02	17.760	1.054E-02
15.694	1.003E-02	16.737	1.052E-02	17.780	1.049E-02
15.713	1.012E-02	16.756	1.055E-02	17.800	1.042E-02
15.733	1.033E-02	16.776	1.060E-02	17.819	1.052E-02
15.753	1.034E-02	16.796	1.071E-02	17.839	1.048E-02
15.772	1.046E-02	16.815	1.073E-02	17.859	1.050E-02
15.792	1.056E-02	16.835	1.068E-02	17.878	1.056E-02
15.812	1.062E-02	16.855	1.081E-02	17.898	1.055E-02
15.831	1.066E-02	16.874	1.081E-02	17.918	1.038E-02
15.851	1.062E-02	16.894	1.078E-02	17.937	1.037E-02
15.871	1.057E-02	16.914	1.069E-02	17.957	1.033E-02

LA-ICP-MS data

Distance con't (mm)	Sr/Ca (mol/mol)	Distance con't (mm)	Sr/Ca (mol/mol)	Distance con't (mm)	Sr/Ca (mol/mol)
15.890	1.054E-02	16.934	1.069E-02	17.977	1.039E-02
15.910	1.058E-02	16.953	1.073E-02	17.996	1.038E-02
15.930	1.061E-02	16.973	1.080E-02	18.016	1.031E-02
15.949	1.080E-02	16.993	1.063E-02	18.036	1.045E-02
15.969	1.082E-02	17.012	1.075E-02	18.055	1.065E-02
15.989	1.083E-02	17.032	1.074E-02	18.075	1.070E-02
16.008	1.070E-02	17.052	1.075E-02	18.095	1.075E-02
16.028	1.087E-02	17.071	1.063E-02	18.114	1.084E-02
16.048	1.081E-02	17.091	1.063E-02	18.134	1.082E-02
16.068	1.062E-02	17.111	1.041E-02	18.154	1.080E-02
16.087	1.049E-02	17.130	1.034E-02	18.174	1.067E-02
16.107	1.047E-02	17.150	1.028E-02	18.193	1.054E-02
16.127	1.051E-02	17.170	1.040E-02	18.213	1.047E-02
16.146	1.060E-02	17.189	1.040E-02	18.233	1.059E-02
16.166	1.043E-02	17.209	1.045E-02	18.252	1.054E-02
16.186	1.042E-02	17.229	1.034E-02	18.272	1.058E-02
16.205	1.070E-02	17.248	1.042E-02	18.292	1.058E-02
16.225	1.068E-02	17.268	1.046E-02	18.311	1.058E-02
16.245	1.077E-02	17.288	1.035E-02	18.331	1.064E-02
16.264	1.079E-02	17.308	1.023E-02	18.351	1.077E-02
16.284	1.075E-02	17.327	1.014E-02	18.370	1.066E-02
16.304	1.086E-02	17.347	1.014E-02	18.390	1.055E-02
16.323	1.089E-02	17.367	1.019E-02	18.410	1.054E-02
16.343	1.077E-02	17.386	1.037E-02	18.429	1.053E-02
16.363	1.076E-02	17.406	1.039E-02	18.449	1.047E-02
16.382	1.066E-02	17.426	1.054E-02	18.469	1.054E-02
16.402	1.038E-02	17.445	1.068E-02	18.488	1.040E-02
16.422	1.021E-02	17.465	1.081E-02	18.508	1.028E-02
16.441	1.010E-02	17.485	1.091E-02	18.528	1.010E-02
16.461	1.019E-02	17.504	1.099E-02	18.548	9.862E-03
16.481	1.021E-02	17.524	1.090E-02	18.567	9.554E-03
16.501	1.030E-02	17.544	1.092E-02	18.587	9.369E-03
16.520	1.039E-02	17.563	1.076E-02		
16.540	1.061E-02	17.583	1.067E-02		
16.560	1.101E-02	17.603	1.052E-02		
16.579	1.123E-02	17.622	1.027E-02		
16.599	1.108E-02	17.642	1.029E-02		
16.619	1.097E-02	17.662	1.028E-02		
16.638	1.091E-02	17.681	1.025E-02		
16.658	1.081E-02	17.701	1.029E-02		
16.678	1.077E-02	17.721	1.026E-02		

Table 10.13 Myrmidon Reef *Astrosclera willeyana* Sr/Ca.

Distance from top (mm)	Sr/Ca (mol/mol)	Distance con't (mm)	Sr/Ca (mol/mol)	Distance con't (mm)	Sr/Ca (mol/mol)
0.000	1.077E-02	1.852	1.103E-02	3.705	1.029E-02
0.035	1.117E-02	1.887	1.096E-02	3.740	1.047E-02
0.070	9.865E-03	1.922	1.014E-02	3.775	1.119E-02
0.105	1.143E-02	1.957	1.074E-02	3.810	1.043E-02
0.140	1.080E-02	1.992	1.095E-02	3.845	9.894E-03
0.175	1.074E-02	2.027	1.033E-02	3.879	1.002E-02
0.210	1.024E-02	2.062	1.060E-02	3.914	1.087E-02
0.245	1.067E-02	2.097	1.042E-02	3.949	1.026E-02
0.280	1.101E-02	2.132	1.038E-02	3.984	1.017E-02
0.315	1.025E-02	2.167	1.067E-02	4.019	1.076E-02
0.350	9.917E-03	2.202	9.863E-03	4.054	1.030E-02
0.384	1.008E-02	2.237	1.060E-02	4.089	1.049E-02
0.419	1.017E-02	2.272	1.061E-02	4.124	1.039E-02
0.454	1.106E-02	2.307	1.084E-02	4.159	1.105E-02
0.489	1.054E-02	2.342	1.067E-02	4.194	1.025E-02
0.524	1.118E-02	2.377	1.033E-02	4.229	1.065E-02
0.559	1.054E-02	2.412	1.073E-02	4.264	1.052E-02
0.594	1.067E-02	2.447	1.007E-02	4.299	1.057E-02
0.629	1.066E-02	2.481	1.055E-02	4.334	1.042E-02
0.664	1.132E-02	2.516	1.087E-02	4.369	1.120E-02
0.699	1.189E-02	2.551	9.929E-03	4.404	1.066E-02
0.734	1.068E-02	2.586	1.008E-02	4.439	1.112E-02
0.769	1.063E-02	2.621	1.067E-02	4.474	1.071E-02
0.804	1.125E-02	2.656	1.101E-02	4.509	1.070E-02
0.839	1.115E-02	2.691	1.041E-02	4.544	1.008E-02
0.874	1.024E-02	2.726	1.070E-02	4.578	1.078E-02
0.909	1.059E-02	2.761	1.056E-02	4.613	1.018E-02
0.944	1.071E-02	2.796	1.067E-02	4.648	1.089E-02
0.979	1.051E-02	2.831	1.060E-02	4.683	1.011E-02
1.014	1.097E-02	2.866	1.048E-02	4.718	1.102E-02
1.049	1.010E-02	2.901	1.058E-02	4.753	1.084E-02
1.083	1.133E-02	2.936	1.041E-02	4.788	1.051E-02
1.118	1.141E-02	2.971	1.004E-02	4.823	1.065E-02
1.153	1.077E-02	3.006	1.009E-02	4.858	1.061E-02
1.188	1.011E-02	3.041	1.095E-02	4.893	9.823E-03
1.223	1.101E-02	3.076	1.016E-02	4.928	9.897E-03
1.258	1.008E-02	3.111	1.051E-02	4.963	1.078E-02
1.293	1.063E-02	3.146	1.078E-02	4.998	1.085E-02
1.328	1.034E-02	3.180	1.046E-02	5.033	1.081E-02
1.363	1.057E-02	3.215	1.074E-02	5.068	1.050E-02
1.398	1.037E-02	3.250	1.068E-02	5.103	1.038E-02
1.433	1.038E-02	3.285	1.073E-02	5.138	1.052E-02
1.468	1.069E-02	3.320	9.883E-03	5.173	1.073E-02
1.503	1.039E-02	3.355	9.699E-03	5.208	1.052E-02
1.538	1.113E-02	3.390	1.022E-02	5.243	1.035E-02
1.573	1.022E-02	3.425	1.036E-02	5.277	1.036E-02
1.608	1.008E-02	3.460	1.004E-02	5.312	9.973E-03
1.643	1.055E-02	3.495	1.035E-02	5.347	9.956E-03
1.678	1.032E-02	3.530	1.040E-02	5.382	1.036E-02
1.713	1.103E-02	3.565	1.025E-02	5.417	1.016E-02
1.748	1.054E-02	3.600	9.938E-03	5.452	9.912E-03
1.782	1.137E-02	3.635	1.047E-02	5.487	1.024E-02
1.817	1.037E-02	3.670	1.045E-02	5.522	9.562E-03

LA-ICP-MS data

Distance con't (mm)	Sr/Ca (mol/mol)	Distance con't (mm)	Sr/Ca (mol/mol)	Distance con't (mm)	Sr/Ca (mol/mol)
5.557	1.037E-02	7.409	9.644E-03	9.262	1.072E-02
5.592	1.004E-02	7.444	9.395E-03	9.297	9.950E-03
5.627	9.878E-03	7.479	1.016E-02	9.332	1.086E-02
5.662	1.011E-02	7.514	9.811E-03	9.367	9.799E-03
5.697	1.017E-02	7.549	9.584E-03	9.402	1.077E-02
5.732	1.016E-02	7.584	9.380E-03	9.437	1.088E-02
5.767	1.001E-02	7.619	9.761E-03	9.471	1.051E-02
5.802	9.398E-03	7.654	9.681E-03	9.506	1.019E-02
5.837	9.811E-03	7.689	9.657E-03	9.541	1.086E-02
5.872	9.474E-03	7.724	9.952E-03	9.576	1.034E-02
5.907	9.837E-03	7.759	1.020E-02	9.611	1.010E-02
5.942	1.030E-02	7.794	9.879E-03	9.646	1.046E-02
5.976	1.027E-02	7.829	1.134E-02	9.681	9.832E-03
6.011	1.006E-02	7.864	1.118E-02	9.716	1.007E-02
6.046	1.028E-02	7.899	1.115E-02	9.751	9.953E-03
6.081	1.004E-02	7.934	1.094E-02	9.786	1.108E-02
6.116	1.039E-02	7.969	1.078E-02	9.821	1.004E-02
6.151	1.017E-02	8.004	1.098E-02	9.856	1.064E-02
6.186	1.114E-02	8.039	1.123E-02	9.891	1.016E-02
6.221	1.089E-02	8.073	1.018E-02	9.926	1.045E-02
6.256	1.091E-02	8.108	1.019E-02	9.961	1.098E-02
6.291	1.060E-02	8.143	1.035E-02	9.996	1.098E-02
6.326	1.052E-02	8.178	1.027E-02	10.031	1.014E-02
6.361	1.058E-02	8.213	1.072E-02	10.066	1.079E-02
6.396	1.035E-02	8.248	1.013E-02	10.101	1.126E-02
6.431	1.104E-02	8.283	1.022E-02	10.136	1.079E-02
6.466	1.111E-02	8.318	1.047E-02	10.170	1.051E-02
6.501	1.075E-02	8.353	1.157E-02	10.205	1.039E-02
6.536	1.018E-02	8.388	1.051E-02	10.240	1.004E-02
6.571	1.010E-02	8.423	1.093E-02	10.275	1.045E-02
6.606	1.086E-02	8.458	1.072E-02	10.310	1.024E-02
6.641	1.035E-02	8.493	1.088E-02	10.345	1.064E-02
6.675	1.020E-02	8.528	1.073E-02	10.380	1.007E-02
6.710	1.091E-02	8.563	1.038E-02	10.415	1.006E-02
6.745	1.023E-02	8.598	1.050E-02	10.450	9.869E-03
6.780	9.642E-03	8.633	1.078E-02	10.485	1.055E-02
6.815	1.054E-02	8.668	1.117E-02	10.520	1.033E-02
6.850	9.917E-03	8.703	1.085E-02	10.555	1.068E-02
6.885	1.004E-02	8.738	1.102E-02	10.590	1.021E-02
6.920	9.608E-03	8.772	1.063E-02	10.625	9.887E-03
6.955	1.053E-02	8.807	1.011E-02	10.660	1.019E-02
6.990	1.058E-02	8.842	1.044E-02	10.695	1.064E-02
7.025	1.005E-02	8.877	1.077E-02	10.730	9.950E-03
7.060	1.044E-02	8.912	9.753E-03	10.765	9.984E-03
7.095	1.019E-02	8.947	1.039E-02	10.800	1.056E-02
7.130	1.020E-02	8.982	1.025E-02	10.835	1.050E-02
7.165	1.069E-02	9.017	1.052E-02	10.869	9.902E-03
7.200	1.022E-02	9.052	1.031E-02	10.904	1.072E-02
7.235	1.060E-02	9.087	1.132E-02	10.939	1.009E-02
7.270	1.031E-02	9.122	1.075E-02	10.974	9.659E-03
7.305	1.043E-02	9.157	1.057E-02	11.009	1.059E-02
7.340	1.048E-02	9.192	1.038E-02	11.044	1.052E-02
7.374	9.889E-03	9.227	1.097E-02	11.079	9.803E-03
11.114	1.007E-02	12.966	1.047E-02	14.819	1.029E-02
11.149	9.611E-03	13.001	1.045E-02	14.854	1.026E-02
11.184	9.906E-03	13.036	1.026E-02	14.889	9.792E-03

Distance con't (mm)	Sr/Ca (mol/mol)	Distance con't (mm)	Sr/Ca (mol/mol)	Distance con't (mm)	Sr/Ca (mol/mol)
11.219	1.020E-02	13.071	1.048E-02	14.924	1.015E-02
11.254	1.042E-02	13.106	1.139E-02	14.959	1.044E-02
11.289	1.042E-02	13.141	1.066E-02	14.994	9.945E-03
11.324	1.064E-02	13.176	1.076E-02	15.029	9.966E-03
11.359	9.868E-03	13.211	1.083E-02	15.063	9.921E-03
11.394	1.008E-02	13.246	1.137E-02	15.098	9.885E-03
11.429	9.978E-03	13.281	1.018E-02	15.133	9.403E-03
11.464	1.003E-02	13.316	1.077E-02	15.168	1.039E-02
11.499	1.037E-02	13.351	1.045E-02	15.203	1.009E-02
11.534	1.111E-02	13.386	1.078E-02	15.238	1.069E-02
11.568	1.087E-02	13.421	1.042E-02	15.273	9.798E-03
11.603	1.048E-02	13.456	1.051E-02	15.308	1.038E-02
11.638	9.837E-03	13.491	1.103E-02	15.343	1.109E-02
11.673	1.101E-02	13.526	1.059E-02	15.378	1.022E-02
11.708	1.043E-02	13.561	1.060E-02	15.413	1.073E-02
11.743	1.101E-02	13.596	1.090E-02	15.448	1.044E-02
11.778	1.028E-02	13.631	1.027E-02	15.483	9.903E-03
11.813	1.063E-02	13.665	1.045E-02	15.518	1.017E-02
11.848	1.124E-02	13.700	1.050E-02	15.553	1.022E-02
11.883	1.085E-02	13.735	9.816E-03	15.588	1.059E-02
11.918	1.088E-02	13.770	1.042E-02	15.623	9.818E-03
11.953	1.185E-02	13.805	1.069E-02	15.658	9.781E-03
11.988	1.061E-02	13.840	1.021E-02	15.693	1.052E-02
12.023	1.043E-02	13.875	1.024E-02	15.728	1.039E-02
12.058	1.038E-02	13.910	1.030E-02	15.762	1.035E-02
12.093	1.039E-02	13.945	1.019E-02	15.797	1.001E-02
12.128	1.076E-02	13.980	1.023E-02	15.832	1.046E-02
12.163	1.017E-02	14.015	1.014E-02	15.867	1.012E-02
12.198	1.064E-02	14.050	1.071E-02	15.902	1.123E-02
12.233	9.913E-03	14.085	1.148E-02	15.937	1.040E-02
12.267	1.041E-02	14.120	1.070E-02	15.972	1.027E-02
12.302	1.023E-02	14.155	1.051E-02	16.007	1.043E-02
12.337	1.023E-02	14.190	1.095E-02	16.042	9.962E-03
12.372	1.047E-02	14.225	1.043E-02	16.077	1.054E-02
12.407	1.122E-02	14.260	1.054E-02	16.112	1.056E-02
12.442	1.089E-02	14.295	1.037E-02	16.147	1.028E-02
12.477	1.030E-02	14.330	1.049E-02	16.182	1.033E-02
12.512	9.751E-03	14.364	9.806E-03	16.217	1.058E-02
12.547	1.066E-02	14.399	1.019E-02	16.252	1.044E-02
12.582	1.053E-02	14.434	1.149E-02	16.287	1.076E-02
12.617	1.126E-02	14.469	1.003E-02	16.322	1.062E-02
12.652	1.060E-02	14.504	1.080E-02	16.357	1.066E-02
12.687	1.016E-02	14.539	1.057E-02	16.392	1.032E-02
12.722	1.037E-02	14.574	1.060E-02	16.427	1.040E-02
12.757	1.006E-02	14.609	1.052E-02	16.461	1.030E-02
12.792	1.054E-02	14.644	9.955E-03	16.496	1.006E-02
12.827	1.017E-02	14.679	1.107E-02	16.531	1.054E-02
12.862	1.024E-02	14.714	9.427E-03	16.566	1.056E-02
12.897	9.805E-03	14.749	1.040E-02	16.601	9.796E-03
12.932	1.097E-02	14.784	1.025E-02	16.636	9.959E-03
16.671	1.044E-02	18.524	1.055E-02	20.376	1.084E-02
16.706	1.025E-02	18.558	1.046E-02	20.411	1.034E-02
16.741	9.356E-03	18.593	1.087E-02	20.446	1.051E-02
16.776	1.028E-02	18.628	1.047E-02	20.481	1.091E-02
16.811	1.032E-02	18.663	1.085E-02	20.516	1.055E-02
16.846	1.019E-02	18.698	1.061E-02	20.551	1.048E-02

LA-ICP-MS data

Distance con't (mm)	Sr/Ca (mol/mol)	Distance con't (mm)	Sr/Ca (mol/mol)	Distance con't (mm)	Sr/Ca (mol/mol)
16.881	1.003E-02	18.733	1.071E-02	20.586	1.018E-02
16.916	1.000E-02	18.768	1.101E-02	20.621	1.056E-02
16.951	9.951E-03	18.803	1.051E-02	20.655	1.058E-02
16.986	9.839E-03	18.838	1.079E-02	20.690	1.061E-02
17.021	1.061E-02	18.873	1.071E-02	20.725	1.051E-02
17.056	1.083E-02	18.908	1.056E-02	20.760	1.096E-02
17.091	1.093E-02	18.943	1.050E-02	20.795	1.083E-02
17.126	1.030E-02	18.978	1.058E-02	20.830	1.097E-02
17.160	1.031E-02	19.013	1.066E-02	20.865	1.055E-02
17.195	1.003E-02	19.048	1.093E-02	20.900	1.095E-02
17.230	9.671E-03	19.083	1.082E-02	20.935	1.027E-02
17.265	9.606E-03	19.118	1.027E-02	20.970	1.010E-02
17.300	1.008E-02	19.153	1.056E-02	21.005	1.015E-02
17.335	9.917E-03	19.188	1.021E-02	21.040	1.057E-02
17.370	1.074E-02	19.223	9.801E-03	21.075	1.021E-02
17.405	1.065E-02	19.257	1.064E-02	21.110	9.549E-03
17.440	1.068E-02	19.292	1.060E-02	21.145	1.017E-02
17.475	1.016E-02	19.327	1.114E-02	21.180	1.049E-02
17.510	1.028E-02	19.362	1.062E-02	21.215	1.036E-02
17.545	1.025E-02	19.397	1.126E-02	21.250	1.057E-02
17.580	9.498E-03	19.432	1.084E-02	21.285	9.975E-03
17.615	1.069E-02	19.467	1.009E-02	21.320	1.017E-02
17.650	9.859E-03	19.502	1.062E-02	21.354	1.052E-02
17.685	1.009E-02	19.537	1.143E-02	21.389	1.038E-02
17.720	1.058E-02	19.572	1.043E-02	21.424	1.068E-02
17.755	1.005E-02	19.607	1.081E-02	21.459	1.006E-02
17.790	1.033E-02	19.642	9.935E-03	21.494	1.040E-02
17.825	1.030E-02	19.677	1.065E-02	21.529	1.029E-02
17.859	1.021E-02	19.712	1.085E-02	21.564	1.030E-02
17.894	1.044E-02	19.747	1.078E-02	21.599	1.015E-02
17.929	1.005E-02	19.782	1.018E-02	21.634	1.098E-02
17.964	1.066E-02	19.817	1.075E-02	21.669	1.049E-02
17.999	1.014E-02	19.852	1.086E-02	21.704	1.020E-02
18.034	1.039E-02	19.887	1.044E-02	21.739	1.080E-02
18.069	9.926E-03	19.922	1.078E-02	21.774	1.065E-02
18.104	9.930E-03	19.956	1.084E-02	21.809	1.006E-02
18.139	9.755E-03	19.991	1.037E-02	21.844	1.044E-02
18.174	9.581E-03	20.026	1.147E-02	21.879	1.057E-02
18.209	1.013E-02	20.061	1.069E-02	21.914	1.066E-02
18.244	1.039E-02	20.096	1.148E-02	21.949	1.032E-02
18.279	1.090E-02	20.131	1.106E-02	21.984	1.014E-02
18.314	1.011E-02	20.166	1.085E-02	22.019	1.101E-02
18.349	1.053E-02	20.201	1.088E-02	22.053	1.037E-02
18.384	1.052E-02	20.236	1.058E-02	22.088	1.051E-02
18.419	1.024E-02	20.271	1.074E-02	22.123	9.935E-03
18.454	1.068E-02	20.306	1.029E-02	22.158	1.003E-02
18.489	1.105E-02	20.341	1.034E-02	22.193	1.037E-02
22.228	1.022E-02	24.081	1.076E-02	25.933	1.073E-02
22.263	1.022E-02	24.116	1.029E-02	25.968	1.028E-02
22.298	9.871E-03	24.150	1.051E-02	26.003	1.038E-02
22.333	1.065E-02	24.185	1.052E-02	26.038	1.086E-02
22.368	1.062E-02	24.220	1.111E-02	26.073	1.002E-02
22.403	1.072E-02	24.255	1.079E-02	26.108	1.088E-02
22.438	9.954E-03	24.290	1.122E-02	26.143	1.043E-02
22.473	1.039E-02	24.325	1.055E-02	26.178	1.005E-02
22.508	1.009E-02	24.360	1.151E-02	26.213	1.093E-02

Distance con't (mm)	Sr/Ca (mol/mol)	Distance con't (mm)	Sr/Ca (mol/mol)	Distance con't (mm)	Sr/Ca (mol/mol)
22.543	1.075E-02	24.395	1.115E-02	26.248	9.785E-03
22.578	1.049E-02	24.430	1.096E-02	26.282	1.072E-02
22.613	1.043E-02	24.465	1.075E-02	26.317	9.608E-03
22.648	1.013E-02	24.500	9.678E-03	26.352	1.039E-02
22.683	1.122E-02	24.535	1.056E-02	26.387	9.892E-03
22.718	1.042E-02	24.570	1.122E-02	26.422	9.714E-03
22.752	1.055E-02	24.605	1.068E-02	26.457	9.663E-03
22.787	1.014E-02	24.640	1.108E-02	26.492	1.030E-02
22.822	1.009E-02	24.675	1.061E-02	26.527	1.056E-02
22.857	1.039E-02	24.710	1.136E-02	26.562	1.031E-02
22.892	9.760E-03	24.745	1.056E-02	26.597	1.114E-02
22.927	1.035E-02	24.780	1.150E-02	26.632	1.041E-02
22.962	1.003E-02	24.815	1.060E-02	26.667	1.016E-02
22.997	9.922E-03	24.850	1.143E-02	26.702	9.538E-03
23.032	9.742E-03	24.884	1.123E-02	26.737	1.058E-02
23.067	9.614E-03	24.919	1.059E-02	26.772	1.010E-02
23.102	9.976E-03	24.954	1.087E-02	26.807	9.867E-03
23.137	1.009E-02	24.989	1.071E-02	26.842	9.835E-03
23.172	1.018E-02	25.024	1.084E-02	26.877	1.093E-02
23.207	1.025E-02	25.059	1.028E-02	26.912	1.020E-02
23.242	1.071E-02	25.094	9.986E-03	26.947	1.057E-02
23.277	1.051E-02	25.129	1.076E-02	26.981	1.045E-02
23.312	9.996E-03	25.164	1.039E-02	27.016	9.870E-03
23.347	1.011E-02	25.199	1.031E-02	27.051	1.029E-02
23.382	1.058E-02	25.234	1.112E-02	27.086	1.049E-02
23.417	9.946E-03	25.269	1.122E-02	27.121	1.064E-02
23.451	1.022E-02	25.304	1.090E-02	27.156	1.029E-02
23.486	1.064E-02	25.339	1.100E-02	27.191	1.001E-02
23.521	9.788E-03	25.374	1.054E-02	27.226	1.010E-02
23.556	1.016E-02	25.409	1.005E-02	27.261	1.067E-02
23.591	9.973E-03	25.444	1.064E-02	27.296	1.046E-02
23.626	9.751E-03	25.479	1.040E-02	27.331	1.041E-02
23.661	9.835E-03	25.514	9.568E-03	27.366	9.951E-03
23.696	1.067E-02	25.549	1.102E-02	27.401	9.718E-03
23.731	9.839E-03	25.583	1.057E-02	27.436	9.933E-03
23.766	1.038E-02	25.618	1.073E-02	27.471	1.010E-02
23.801	1.078E-02	25.653	1.069E-02	27.506	1.056E-02
23.836	9.882E-03	25.688	1.004E-02	27.541	9.689E-03
23.871	1.049E-02	25.723	1.016E-02	27.576	9.916E-03
23.906	1.064E-02	25.758	1.023E-02	27.611	9.342E-03
23.941	1.059E-02	25.793	1.049E-02	27.646	9.807E-03
23.976	1.024E-02	25.828	1.038E-02	27.680	9.763E-03
24.011	1.091E-02	25.863	1.049E-02	27.715	9.529E-03
24.046	1.077E-02	25.898	9.923E-03	27.750	1.025E-02
27.785	1.063E-02	29.638	1.112E-02	31.490	1.087E-02
27.820	1.006E-02	29.673	9.857E-03	31.525	1.062E-02
27.855	1.002E-02	29.708	1.125E-02	31.560	1.039E-02
27.890	9.880E-03	29.743	1.075E-02	31.595	1.103E-02
27.925	9.662E-03	29.777	1.083E-02	31.630	1.063E-02
27.960	9.461E-03	29.812	1.052E-02	31.665	1.087E-02
27.995	1.006E-02	29.847	1.031E-02	31.700	1.019E-02
28.030	1.020E-02	29.882	1.010E-02	31.735	1.131E-02
28.065	1.089E-02	29.917	1.043E-02	31.770	1.127E-02
28.100	1.050E-02	29.952	1.068E-02	31.805	1.072E-02
28.135	9.583E-03	29.987	1.022E-02	31.840	1.073E-02
28.170	1.022E-02	30.022	1.021E-02	31.874	1.042E-02

LA-ICP-MS data

Distance con't (mm)	Sr/Ca (mol/mol)	Distance con't (mm)	Sr/Ca (mol/mol)	Distance con't (mm)	Sr/Ca (mol/mol)
28.205	1.046E-02	30.057	1.040E-02	31.909	1.092E-02
28.240	1.046E-02	30.092	1.044E-02	31.944	1.025E-02
28.275	1.029E-02	30.127	1.061E-02	31.979	1.088E-02
28.310	1.107E-02	30.162	1.073E-02	32.014	1.040E-02
28.345	1.029E-02	30.197	1.115E-02	32.049	1.143E-02
28.379	1.040E-02	30.232	1.059E-02	32.084	1.052E-02
28.414	1.053E-02	30.267	1.062E-02	32.119	1.072E-02
28.449	1.017E-02	30.302	1.136E-02	32.154	1.055E-02
28.484	9.868E-03	30.337	1.085E-02	32.189	1.019E-02
28.519	1.040E-02	30.372	1.085E-02	32.224	9.995E-03
28.554	1.047E-02	30.407	1.069E-02	32.259	1.099E-02
28.589	9.974E-03	30.442	1.101E-02	32.294	1.060E-02
28.624	1.047E-02	30.476	1.030E-02	32.329	1.067E-02
28.659	1.039E-02	30.511	1.066E-02	32.364	1.034E-02
28.694	1.098E-02	30.546	1.041E-02	32.399	1.027E-02
28.729	1.062E-02	30.581	1.086E-02	32.434	1.083E-02
28.764	1.082E-02	30.616	9.874E-03	32.469	1.103E-02
28.799	1.055E-02	30.651	1.012E-02	32.504	1.076E-02
28.834	1.062E-02	30.686	1.011E-02	32.539	1.025E-02
28.869	1.070E-02	30.721	9.869E-03	32.573	1.077E-02
28.904	1.047E-02	30.756	1.011E-02	32.608	1.079E-02
28.939	1.038E-02	30.791	1.090E-02	32.643	1.088E-02
28.974	1.031E-02	30.826	1.053E-02	32.678	1.056E-02
29.009	1.037E-02	30.861	1.107E-02	32.713	1.017E-02
29.044	9.704E-03	30.896	1.062E-02	32.748	1.051E-02
29.078	1.004E-02	30.931	1.039E-02	32.783	1.019E-02
29.113	9.819E-03	30.966	1.071E-02	32.818	1.113E-02
29.148	1.036E-02	31.001	9.791E-03	32.853	1.042E-02
29.183	1.002E-02	31.036	9.748E-03	32.888	1.022E-02
29.218	1.017E-02	31.071	1.025E-02	32.923	1.008E-02
29.253	1.102E-02	31.106	1.003E-02	32.958	1.030E-02
29.288	1.004E-02	31.141	1.007E-02	32.993	1.089E-02
29.323	1.016E-02	31.175	9.941E-03	33.028	1.078E-02
29.358	1.030E-02	31.210	1.038E-02	33.063	1.025E-02
29.393	1.007E-02	31.245	9.999E-03	33.098	9.666E-03
29.428	1.037E-02	31.280	1.081E-02	33.133	1.055E-02
29.463	1.024E-02	31.315	9.713E-03	33.168	1.020E-02
29.498	1.103E-02	31.350	1.095E-02	33.203	1.028E-02
29.533	9.888E-03	31.385	1.030E-02	33.238	1.066E-02
29.568	1.061E-02	31.420	1.022E-02	33.272	1.038E-02
29.603	9.936E-03	31.455	1.022E-02	33.307	1.072E-02
33.342	1.073E-02	35.195	9.528E-03	37.047	1.015E-02
33.377	1.081E-02	35.230	1.043E-02	37.082	1.056E-02
33.412	1.079E-02	35.265	1.080E-02	37.117	1.036E-02
33.447	9.998E-03	35.300	1.106E-02	37.152	9.697E-03
33.482	1.102E-02	35.335	1.002E-02	37.187	1.120E-02
33.517	9.991E-03	35.369	1.016E-02	37.222	1.048E-02
33.552	1.053E-02	35.404	1.044E-02	37.257	1.041E-02
33.587	1.103E-02	35.439	9.977E-03	37.292	1.052E-02
33.622	1.061E-02	35.474	1.038E-02	37.327	1.068E-02
33.657	1.043E-02	35.509	9.883E-03	37.362	1.032E-02
33.692	9.420E-03	35.544	1.028E-02	37.397	1.082E-02
33.727	1.037E-02	35.579	1.011E-02	37.432	1.071E-02
33.762	1.040E-02	35.614	1.023E-02	37.466	1.111E-02
33.797	1.028E-02	35.649	9.816E-03	37.501	1.041E-02
33.832	1.092E-02	35.684	1.093E-02	37.536	1.068E-02

Distance con't (mm)	Sr/Ca (mol/mol)	Distance con't (mm)	Sr/Ca (mol/mol)	Distance con't (mm)	Sr/Ca (mol/mol)
33.867	1.088E-02	35.719	1.063E-02	37.571	1.106E-02
33.902	1.012E-02	35.754	1.021E-02	37.606	1.060E-02
33.937	1.046E-02	35.789	1.051E-02	37.641	1.142E-02
33.971	1.049E-02	35.824	1.119E-02	37.676	1.108E-02
34.006	1.036E-02	35.859	1.097E-02	37.711	1.073E-02
34.041	1.072E-02	35.894	1.046E-02	37.746	1.065E-02
34.076	9.950E-03	35.929	1.123E-02	37.781	1.046E-02
34.111	1.090E-02	35.964	1.081E-02	37.816	1.084E-02
34.146	1.045E-02	35.999	1.091E-02	37.851	9.377E-03
34.181	1.099E-02	36.034	1.098E-02	37.886	1.080E-02
34.216	9.833E-03	36.068	1.165E-02	37.921	1.058E-02
34.251	1.151E-02	36.103	1.046E-02	37.956	1.125E-02
34.286	1.086E-02	36.138	1.049E-02	37.991	1.021E-02
34.321	1.062E-02	36.173	1.029E-02	38.026	1.004E-02
34.356	1.117E-02	36.208	1.056E-02	38.061	1.043E-02
34.391	1.098E-02	36.243	1.005E-02	38.096	1.006E-02
34.426	1.079E-02	36.278	1.080E-02	38.131	1.010E-02
34.461	9.995E-03	36.313	1.076E-02	38.165	1.027E-02
34.496	1.023E-02	36.348	1.089E-02	38.200	1.040E-02
34.531	1.028E-02	36.383	1.056E-02	38.235	1.027E-02
34.566	1.033E-02	36.418	1.012E-02	38.270	9.551E-03
34.601	1.192E-02	36.453	1.049E-02	38.305	1.055E-02
34.636	1.017E-02	36.488	1.062E-02	38.340	1.100E-02
34.670	1.022E-02	36.523	1.014E-02	38.375	1.044E-02
34.705	1.033E-02	36.558	1.019E-02	38.410	1.000E-02
34.740	1.010E-02	36.593	1.035E-02	38.445	1.082E-02
34.775	1.064E-02	36.628	1.062E-02	38.480	1.002E-02
34.810	1.071E-02	36.663	9.822E-03	38.515	9.928E-03
34.845	1.044E-02	36.698	1.033E-02	38.550	9.698E-03
34.880	1.018E-02	36.733	1.009E-02	38.585	1.103E-02
34.915	1.038E-02	36.767	1.077E-02	38.620	1.100E-02
34.950	9.469E-03	36.802	9.793E-03	38.655	1.075E-02
34.985	1.117E-02	36.837	1.052E-02	38.690	1.054E-02
35.020	1.038E-02	36.872	1.006E-02	38.725	1.071E-02
35.055	1.044E-02	36.907	9.590E-03	38.760	1.072E-02
35.090	9.318E-03	36.942	9.942E-03	38.795	1.065E-02
35.125	1.083E-02	36.977	9.797E-03	38.830	1.061E-02
35.160	1.004E-02	37.012	1.066E-02	38.864	1.079E-02
38.899	9.731E-03	40.752	1.077E-02	42.604	1.038E-02
38.934	1.051E-02	40.787	1.022E-02	42.639	1.074E-02
38.969	1.081E-02	40.822	1.027E-02	42.674	1.028E-02
39.004	1.015E-02	40.857	1.039E-02	42.709	1.003E-02
39.039	1.038E-02	40.892	1.094E-02	42.744	1.029E-02
39.074	1.032E-02	40.927	1.007E-02	42.779	1.043E-02
39.109	8.976E-03	40.961	1.048E-02	42.814	1.007E-02
39.144	1.036E-02	40.996	1.027E-02	42.849	9.893E-03
39.179	1.013E-02	41.031	1.003E-02	42.884	1.033E-02
39.214	1.140E-02	41.066	1.028E-02	42.919	1.041E-02
39.249	9.755E-03	41.101	1.135E-02	42.954	1.049E-02
39.284	1.039E-02	41.136	9.948E-03	42.989	9.978E-03
39.319	1.020E-02	41.171	1.098E-02	43.024	1.063E-02
39.354	1.036E-02	41.206	1.070E-02	43.058	1.037E-02
39.389	1.038E-02	41.241	1.017E-02	43.093	1.016E-02
39.424	1.025E-02	41.276	1.096E-02	43.128	1.058E-02
39.459	1.084E-02	41.311	9.495E-03	43.163	1.042E-02
39.494	1.028E-02	41.346	1.059E-02	43.198	9.900E-03

LA-ICP-MS data

Distance con't (mm)	Sr/Ca (mol/mol)	Distance con't (mm)	Sr/Ca (mol/mol)	Distance con't (mm)	Sr/Ca (mol/mol)
39.529	1.044E-02	41.381	1.000E-02	43.233	1.065E-02
39.563	1.005E-02	41.416	1.058E-02	43.268	1.050E-02
39.598	1.058E-02	41.451	9.874E-03	43.303	1.084E-02
39.633	9.894E-03	41.486	1.025E-02	43.338	1.015E-02
39.668	1.013E-02	41.521	1.038E-02	43.373	1.010E-02
39.703	9.832E-03	41.556	1.068E-02	43.408	1.060E-02
39.738	1.045E-02	41.591	1.041E-02	43.443	1.089E-02
39.773	1.047E-02	41.626	1.062E-02	43.478	1.033E-02
39.808	1.000E-02	41.660	1.016E-02	43.513	1.014E-02
39.843	1.067E-02	41.695	1.008E-02	43.548	1.050E-02
39.878	1.070E-02	41.730	1.028E-02	43.583	9.509E-03
39.913	1.028E-02	41.765	1.027E-02	43.618	1.043E-02
39.948	1.015E-02	41.800	1.086E-02	43.653	9.587E-03
39.983	1.055E-02	41.835	1.061E-02	43.688	1.030E-02
40.018	9.708E-03	41.870	1.047E-02	43.723	1.024E-02
40.053	1.030E-02	41.905	1.044E-02	43.757	1.000E-02
40.088	1.049E-02	41.940	9.948E-03	43.792	9.578E-03
40.123	9.952E-03	41.975	1.005E-02	43.827	9.690E-03
40.158	1.060E-02	42.010	1.077E-02	43.862	1.032E-02
40.193	1.041E-02	42.045	1.011E-02	43.897	9.953E-03
40.228	1.024E-02	42.080	1.037E-02	43.932	1.017E-02
40.262	1.059E-02	42.115	1.030E-02	43.967	1.026E-02
40.297	1.109E-02	42.150	1.027E-02	44.002	1.058E-02
40.332	9.896E-03	42.185	9.936E-03	44.037	9.898E-03
40.367	1.073E-02	42.220	1.018E-02	44.072	9.894E-03
40.402	1.102E-02	42.255	1.088E-02	44.107	1.082E-02
40.437	9.930E-03	42.290	1.095E-02	44.142	1.103E-02
40.472	9.873E-03	42.325	1.087E-02	44.177	1.151E-02
40.507	1.005E-02	42.359	1.046E-02	44.212	1.014E-02
40.542	9.392E-03	42.394	9.410E-03	44.247	1.059E-02
40.577	9.971E-03	42.429	1.007E-02	44.282	1.063E-02
40.612	1.051E-02	42.464	9.848E-03	44.317	1.026E-02
40.647	1.043E-02	42.499	9.227E-03	44.352	1.047E-02
40.682	1.084E-02	42.534	1.070E-02	44.387	1.091E-02
40.717	1.076E-02	42.569	1.056E-02	44.422	1.052E-02
44.456	1.086E-02	46.309	1.057E-02	48.161	1.042E-02
44.491	1.054E-02	46.344	1.030E-02	48.196	1.060E-02
44.526	1.073E-02	46.379	1.012E-02	48.231	1.051E-02
44.561	1.041E-02	46.414	9.944E-03	48.266	1.035E-02
44.596	1.092E-02	46.449	1.039E-02	48.301	1.064E-02
44.631	1.033E-02	46.484	9.242E-03	48.336	1.039E-02
44.666	1.082E-02	46.519	1.043E-02	48.371	9.742E-03
44.701	1.058E-02	46.553	1.001E-02	48.406	1.079E-02
44.736	1.122E-02	46.588	9.886E-03	48.441	1.042E-02
44.771	1.012E-02	46.623	1.089E-02	48.476	1.050E-02
44.806	1.086E-02	46.658	1.058E-02	48.511	1.022E-02
44.841	1.062E-02	46.693	1.042E-02	48.546	1.099E-02
44.876	1.070E-02	46.728	9.344E-03	48.581	1.077E-02
44.911	1.084E-02	46.763	1.034E-02	48.616	9.780E-03
44.946	1.129E-02	46.798	9.663E-03	48.650	1.055E-02
44.981	1.049E-02	46.833	1.062E-02	48.685	1.085E-02
45.016	1.040E-02	46.868	9.884E-03	48.720	1.040E-02
45.051	1.063E-02	46.903	1.019E-02	48.755	1.113E-02
45.086	1.015E-02	46.938	1.066E-02	48.790	1.069E-02
45.121	1.090E-02	46.973	9.812E-03	48.825	1.034E-02
45.155	1.047E-02	47.008	1.053E-02	48.860	1.035E-02

Distance con't (mm)	Sr/Ca (mol/mol)	Distance con't (mm)	Sr/Ca (mol/mol)	Distance con't (mm)	Sr/Ca (mol/mol)
45.190	1.048E-02	47.043	1.009E-02	48.895	1.090E-02
45.225	1.109E-02	47.078	1.032E-02	48.930	1.019E-02
45.260	1.107E-02	47.113	9.910E-03	48.965	1.062E-02
45.295	1.087E-02	47.148	1.008E-02	49.000	1.071E-02
45.330	1.023E-02	47.183	1.040E-02		
45.365	1.067E-02	47.218	9.862E-03		
45.400	1.068E-02	47.252	1.065E-02		
45.435	1.078E-02	47.287	1.048E-02		
45.470	1.063E-02	47.322	1.056E-02		
45.505	1.055E-02	47.357	9.994E-03		
45.540	1.051E-02	47.392	1.028E-02		
45.575	1.003E-02	47.427	9.210E-03		
45.610	1.038E-02	47.462	1.038E-02		
45.645	1.016E-02	47.497	9.626E-03		
45.680	9.681E-03	47.532	9.636E-03		
45.715	1.021E-02	47.567	1.000E-02		
45.750	1.040E-02	47.602	1.040E-02		
45.785	1.001E-02	47.637	1.052E-02		
45.820	1.019E-02	47.672	1.030E-02		
45.854	1.040E-02	47.707	1.082E-02		
45.889	1.049E-02	47.742	1.017E-02		
45.924	1.030E-02	47.777	1.059E-02		
45.959	9.780E-03	47.812	1.007E-02		
45.994	1.062E-02	47.847	1.045E-02		
46.029	1.023E-02	47.882	1.093E-02		
46.064	1.104E-02	47.917	1.032E-02		
46.099	1.006E-02	47.951	1.046E-02		
46.134	1.012E-02	47.986	1.040E-02		
46.169	1.053E-02	48.021	1.015E-02		
46.204	1.058E-02	48.056	1.099E-02		
46.239	1.080E-02	48.091	1.083E-02		
46.274	1.017E-02	48.126	1.052E-02		

Table 10.14 Ribbon Reef #10 *Astrosclera willeyana* Sr/Ca

Distance from top (mm)	Sr/Ca (mol/mol)	Distance con't (mm)	Sr/Ca (mol/mol)	Distance con't (mm)	Sr/Ca (mol/mol)
0.000	1.132E-02	0.883	1.087E-02	1.766	1.063E-02
0.017	1.100E-02	0.899	1.098E-02	1.782	1.092E-02
0.033	1.140E-02	0.916	1.095E-02	1.799	1.085E-02
0.050	1.134E-02	0.933	1.078E-02	1.816	1.085E-02
0.067	1.140E-02	0.949	1.066E-02	1.832	1.077E-02
0.083	1.115E-02	0.966	1.072E-02	1.849	1.064E-02
0.100	1.125E-02	0.983	1.101E-02	1.866	1.070E-02
0.117	1.107E-02	0.999	1.087E-02	1.882	1.079E-02
0.133	1.143E-02	1.016	1.103E-02	1.899	1.045E-02
0.150	1.089E-02	1.033	1.066E-02	1.916	1.100E-02
0.167	1.123E-02	1.049	1.056E-02	1.932	1.111E-02
0.183	1.142E-02	1.066	1.079E-02	1.949	1.068E-02
0.200	1.122E-02	1.083	1.073E-02	1.966	1.110E-02
0.217	1.141E-02	1.099	1.067E-02	1.982	1.098E-02
0.233	1.109E-02	1.116	1.089E-02	1.999	1.116E-02
0.250	1.080E-02	1.133	1.060E-02	2.016	1.102E-02
0.267	1.068E-02	1.149	1.039E-02	2.032	1.127E-02
0.283	1.102E-02	1.166	1.090E-02	2.049	1.098E-02
0.300	1.107E-02	1.183	1.038E-02	2.065	1.084E-02
0.316	1.085E-02	1.199	1.071E-02	2.082	1.100E-02
0.333	1.101E-02	1.216	1.059E-02	2.099	1.124E-02
0.350	1.118E-02	1.233	1.048E-02	2.115	1.123E-02
0.366	1.122E-02	1.249	1.053E-02	2.132	1.100E-02
0.383	1.134E-02	1.266	1.064E-02	2.149	1.120E-02
0.400	1.098E-02	1.283	1.084E-02	2.165	1.117E-02
0.416	1.100E-02	1.299	1.058E-02	2.182	1.129E-02
0.433	1.040E-02	1.316	1.074E-02	2.199	1.120E-02
0.450	1.037E-02	1.333	1.045E-02	2.215	1.097E-02
0.466	1.062E-02	1.349	1.044E-02	2.232	1.090E-02
0.483	1.026E-02	1.366	1.056E-02	2.249	1.110E-02
0.500	1.071E-02	1.383	1.097E-02	2.265	1.134E-02
0.516	1.081E-02	1.399	1.039E-02	2.282	1.101E-02
0.533	1.061E-02	1.416	1.048E-02	2.299	1.110E-02
0.550	1.079E-02	1.433	1.067E-02	2.315	1.113E-02
0.566	1.131E-02	1.449	1.077E-02	2.332	1.128E-02
0.583	1.131E-02	1.466	1.083E-02	2.349	1.107E-02
0.600	1.130E-02	1.482	1.103E-02	2.365	1.109E-02
0.616	1.090E-02	1.499	1.121E-02	2.382	1.107E-02
0.633	1.057E-02	1.516	1.083E-02	2.399	1.115E-02
0.650	1.062E-02	1.532	1.102E-02	2.415	1.083E-02
0.666	1.054E-02	1.549	1.098E-02	2.432	1.120E-02
0.683	1.086E-02	1.566	1.140E-02	2.449	1.122E-02
0.700	1.059E-02	1.582	1.098E-02	2.465	1.111E-02
0.716	1.067E-02	1.599	1.094E-02	2.482	1.099E-02
0.733	1.084E-02	1.616	1.065E-02	2.499	1.110E-02
0.750	1.105E-02	1.632	1.109E-02	2.515	1.108E-02
0.766	1.112E-02	1.649	1.089E-02	2.532	1.132E-02
0.783	1.096E-02	1.666	1.080E-02	2.549	1.115E-02
0.800	1.076E-02	1.682	1.110E-02	2.565	1.095E-02
0.816	1.068E-02	1.699	1.094E-02	2.582	1.084E-02
0.833	1.054E-02	1.716	1.072E-02	2.599	1.086E-02
0.850	1.107E-02	1.732	1.081E-02	2.615	1.068E-02
0.866	1.062E-02	1.749	1.076E-02	2.632	1.093E-02

Distance con't (mm)	Sr/Ca (mol/mol)	Distance con't (mm)	Sr/Ca (mol/mol)	Distance con't (mm)	Sr/Ca (mol/mol)
2.648	1.071E-02	3.531	1.084E-02	4.414	1.092E-02
2.665	1.087E-02	3.548	1.083E-02	4.431	1.092E-02
2.682	1.090E-02	3.565	1.113E-02	4.447	1.071E-02
2.698	1.070E-02	3.581	1.079E-02	4.464	1.076E-02
2.715	1.092E-02	3.598	1.125E-02	4.481	1.100E-02
2.732	1.102E-02	3.615	1.121E-02	4.497	1.115E-02
2.748	1.138E-02	3.631	1.112E-02	4.514	1.132E-02
2.765	1.128E-02	3.648	1.138E-02	4.531	1.093E-02
2.782	1.143E-02	3.665	1.121E-02	4.547	1.115E-02
2.798	1.134E-02	3.681	1.112E-02	4.564	1.074E-02
2.815	1.126E-02	3.698	1.104E-02	4.581	1.075E-02
2.832	1.147E-02	3.715	1.117E-02	4.597	1.072E-02
2.848	1.161E-02	3.731	1.100E-02	4.614	1.094E-02
2.865	1.089E-02	3.748	1.068E-02	4.631	1.080E-02
2.882	1.048E-02	3.764	1.097E-02	4.647	1.100E-02
2.898	1.049E-02	3.781	1.074E-02	4.664	1.065E-02
2.915	1.045E-02	3.798	1.090E-02	4.681	1.073E-02
2.932	1.060E-02	3.814	1.122E-02	4.697	1.099E-02
2.948	1.113E-02	3.831	1.142E-02	4.714	1.072E-02
2.965	1.103E-02	3.848	1.137E-02	4.731	1.066E-02
2.982	1.093E-02	3.864	1.119E-02	4.747	1.125E-02
2.998	1.103E-02	3.881	1.125E-02	4.764	1.068E-02
3.015	1.091E-02	3.898	1.116E-02	4.781	1.090E-02
3.032	1.068E-02	3.914	1.141E-02	4.797	1.103E-02
3.048	1.065E-02	3.931	1.119E-02	4.814	1.098E-02
3.065	1.072E-02	3.948	1.118E-02	4.831	1.083E-02
3.082	1.084E-02	3.964	1.090E-02	4.847	1.091E-02
3.098	1.059E-02	3.981	1.087E-02	4.864	1.075E-02
3.115	1.097E-02	3.998	1.106E-02	4.881	1.077E-02
3.132	1.109E-02	4.014	1.102E-02	4.897	1.101E-02
3.148	1.082E-02	4.031	1.123E-02	4.914	1.052E-02
3.165	1.084E-02	4.048	1.088E-02	4.930	1.045E-02
3.181	1.097E-02	4.064	1.135E-02	4.947	1.094E-02
3.198	1.088E-02	4.081	1.085E-02	4.964	1.079E-02
3.215	1.125E-02	4.098	1.111E-02	4.980	1.068E-02
3.231	1.120E-02	4.114	1.107E-02	4.997	1.060E-02
3.248	1.085E-02	4.131	1.123E-02	5.014	1.071E-02
3.265	1.122E-02	4.148	1.092E-02	5.030	1.068E-02
3.281	1.083E-02	4.164	1.088E-02	5.047	1.073E-02
3.298	1.116E-02	4.181	1.081E-02	5.064	1.072E-02
3.315	1.109E-02	4.198	1.089E-02	5.080	1.111E-02
3.331	1.073E-02	4.214	1.073E-02	5.097	1.130E-02
3.348	1.111E-02	4.231	1.072E-02	5.114	1.074E-02
3.365	1.093E-02	4.248	1.095E-02	5.130	1.089E-02
3.381	1.085E-02	4.264	1.124E-02	5.147	1.085E-02
3.398	1.088E-02	4.281	1.120E-02	5.164	1.091E-02
3.415	1.103E-02	4.298	1.099E-02	5.180	1.058E-02
3.431	1.124E-02	4.314	1.098E-02	5.197	1.066E-02
3.448	1.116E-02	4.331	1.098E-02	5.214	1.055E-02
3.465	1.067E-02	4.347	1.086E-02	5.230	1.075E-02
3.481	1.111E-02	4.364	1.074E-02	5.247	1.061E-02
3.498	1.148E-02	4.381	1.114E-02	5.264	1.089E-02
3.515	1.116E-02	4.397	1.090E-02	5.280	1.079E-02
5.297	1.061E-02	6.180	1.117E-02	7.063	1.093E-02
5.314	1.064E-02	6.196	1.102E-02	7.079	1.089E-02
5.330	1.106E-02	6.213	1.082E-02	7.096	1.065E-02

LA-ICP-MS data

Distance con't (mm)	Sr/Ca (mol/mol)	Distance con't (mm)	Sr/Ca (mol/mol)	Distance con't (mm)	Sr/Ca (mol/mol)
5.347	1.101E-02	6.230	1.086E-02	7.113	1.082E-02
5.364	1.154E-02	6.246	1.097E-02	7.129	1.052E-02
5.380	1.116E-02	6.263	1.145E-02	7.146	1.057E-02
5.397	1.146E-02	6.280	1.085E-02	7.163	1.086E-02
5.414	1.133E-02	6.296	1.106E-02	7.179	1.067E-02
5.430	1.122E-02	6.313	1.118E-02	7.196	1.092E-02
5.447	1.114E-02	6.330	1.131E-02	7.213	1.068E-02
5.464	1.084E-02	6.346	1.113E-02	7.229	1.078E-02
5.480	1.084E-02	6.363	1.103E-02	7.246	1.087E-02
5.497	1.099E-02	6.380	1.079E-02	7.262	1.041E-02
5.513	1.090E-02	6.396	1.119E-02	7.279	1.054E-02
5.530	1.104E-02	6.413	1.117E-02	7.296	1.091E-02
5.547	1.102E-02	6.430	1.101E-02	7.312	1.052E-02
5.563	1.096E-02	6.446	1.087E-02	7.329	1.052E-02
5.580	1.097E-02	6.463	1.056E-02	7.346	1.066E-02
5.597	1.116E-02	6.480	1.053E-02	7.362	1.081E-02
5.613	1.070E-02	6.496	1.049E-02	7.379	1.120E-02
5.630	1.089E-02	6.513	1.082E-02	7.396	1.086E-02
5.647	1.100E-02	6.530	1.072E-02	7.412	1.084E-02
5.663	1.097E-02	6.546	1.075E-02	7.429	1.112E-02
5.680	1.089E-02	6.563	1.041E-02	7.446	1.099E-02
5.697	1.068E-02	6.580	1.115E-02	7.462	1.076E-02
5.713	1.110E-02	6.596	1.093E-02	7.479	1.093E-02
5.730	1.078E-02	6.613	1.068E-02	7.496	1.109E-02
5.747	1.113E-02	6.630	1.079E-02	7.512	1.135E-02
5.763	1.096E-02	6.646	1.046E-02	7.529	1.083E-02
5.780	1.089E-02	6.663	1.028E-02	7.546	1.099E-02
5.797	1.117E-02	6.679	1.061E-02	7.562	1.051E-02
5.813	1.108E-02	6.696	1.093E-02	7.579	1.063E-02
5.830	1.092E-02	6.713	1.079E-02	7.596	1.075E-02
5.847	1.114E-02	6.729	1.111E-02	7.612	1.065E-02
5.863	1.114E-02	6.746	1.107E-02	7.629	1.039E-02
5.880	1.104E-02	6.763	1.147E-02	7.646	1.019E-02
5.897	1.059E-02	6.779	1.109E-02	7.662	1.075E-02
5.913	1.082E-02	6.796	1.090E-02	7.679	1.030E-02
5.930	1.095E-02	6.813	1.112E-02	7.696	1.066E-02
5.947	1.081E-02	6.829	1.077E-02	7.712	1.083E-02
5.963	1.067E-02	6.846	1.075E-02	7.729	1.061E-02
5.980	1.054E-02	6.863	1.075E-02	7.746	1.082E-02
5.997	1.077E-02	6.879	1.085E-02	7.762	1.100E-02
6.013	1.040E-02	6.896	1.035E-02	7.779	1.095E-02
6.030	1.062E-02	6.913	1.091E-02	7.796	1.111E-02
6.047	1.037E-02	6.929	1.061E-02	7.812	1.082E-02
6.063	1.067E-02	6.946	1.046E-02	7.829	1.097E-02
6.080	1.075E-02	6.963	1.046E-02	7.845	1.109E-02
6.096	1.092E-02	6.979	1.068E-02	7.862	1.077E-02
6.113	1.117E-02	6.996	1.103E-02	7.879	1.061E-02
6.130	1.122E-02	7.013	1.084E-02	7.895	1.078E-02
6.146	1.081E-02	7.029	1.078E-02	7.912	1.040E-02
6.163	1.094E-02	7.046	1.137E-02	7.929	1.073E-02
7.945	1.085E-02	8.828	1.062E-02	9.711	1.078E-02
7.962	1.053E-02	8.845	1.091E-02	9.728	1.139E-02
7.979	1.067E-02	8.862	1.085E-02	9.744	1.093E-02
7.995	1.064E-02	8.878	1.089E-02	9.761	1.083E-02
8.012	1.095E-02	8.895	1.089E-02	9.778	1.072E-02
8.029	1.064E-02	8.912	1.100E-02	9.794	1.061E-02

Distance con't (mm)	Sr/Ca (mol/mol)	Distance con't (mm)	Sr/Ca (mol/mol)	Distance con't (mm)	Sr/Ca (mol/mol)
8.045	1.093E-02	8.928	1.106E-02	9.811	1.092E-02
8.062	1.042E-02	8.945	1.079E-02	9.828	1.064E-02
8.079	1.083E-02	8.961	1.067E-02	9.844	1.048E-02
8.095	1.076E-02	8.978	1.078E-02	9.861	1.056E-02
8.112	1.080E-02	8.995	1.064E-02	9.878	1.046E-02
8.129	1.084E-02	9.011	1.055E-02	9.894	1.059E-02
8.145	1.066E-02	9.028	1.096E-02	9.911	1.052E-02
8.162	1.081E-02	9.045	1.051E-02	9.928	1.079E-02
8.179	1.079E-02	9.061	1.080E-02	9.944	1.074E-02
8.195	1.092E-02	9.078	1.054E-02	9.961	1.073E-02
8.212	1.108E-02	9.095	1.072E-02	9.978	1.082E-02
8.229	1.105E-02	9.111	1.072E-02	9.994	1.092E-02
8.245	1.100E-02	9.128	1.041E-02	10.011	1.099E-02
8.262	1.097E-02	9.145	1.055E-02	10.028	1.121E-02
8.279	1.089E-02	9.161	1.078E-02	10.044	1.101E-02
8.295	1.107E-02	9.178	1.062E-02	10.061	1.135E-02
8.312	1.065E-02	9.195	1.090E-02	10.078	1.126E-02
8.329	1.095E-02	9.211	1.085E-02	10.094	1.099E-02
8.345	1.054E-02	9.228	1.077E-02	10.111	1.103E-02
8.362	1.080E-02	9.245	1.119E-02	10.127	1.144E-02
8.379	1.083E-02	9.261	1.116E-02	10.144	1.108E-02
8.395	1.089E-02	9.278	1.097E-02	10.161	1.120E-02
8.412	1.096E-02	9.295	1.141E-02	10.177	1.118E-02
8.428	1.071E-02	9.311	1.105E-02	10.194	1.088E-02
8.445	1.093E-02	9.328	1.098E-02	10.211	1.137E-02
8.462	1.073E-02	9.345	1.078E-02	10.227	1.128E-02
8.478	1.081E-02	9.361	1.151E-02	10.244	1.133E-02
8.495	1.073E-02	9.378	1.111E-02	10.261	1.099E-02
8.512	1.091E-02	9.395	1.107E-02	10.277	1.127E-02
8.528	1.129E-02	9.411	1.099E-02	10.294	1.086E-02
8.545	1.089E-02	9.428	1.122E-02	10.311	1.074E-02
8.562	1.092E-02	9.445	1.094E-02	10.327	1.118E-02
8.578	1.093E-02	9.461	1.113E-02	10.344	1.086E-02
8.595	1.132E-02	9.478	1.116E-02	10.361	1.125E-02
8.612	1.098E-02	9.495	1.121E-02	10.377	1.112E-02
8.628	1.108E-02	9.511	1.152E-02	10.394	1.107E-02
8.645	1.068E-02	9.528	1.125E-02	10.411	1.155E-02
8.662	1.055E-02	9.544	1.064E-02	10.427	1.085E-02
8.678	1.060E-02	9.561	1.099E-02	10.444	1.089E-02
8.695	1.064E-02	9.578	1.062E-02	10.461	1.031E-02
8.712	1.042E-02	9.594	1.092E-02	10.477	1.076E-02
8.728	1.094E-02	9.611	1.095E-02	10.494	1.105E-02
8.745	1.093E-02	9.628	1.063E-02	10.511	1.089E-02
8.762	1.093E-02	9.644	1.022E-02	10.527	1.100E-02
8.778	1.057E-02	9.661	1.069E-02	10.544	1.091E-02
8.795	1.045E-02	9.678	1.065E-02	10.561	1.087E-02
8.812	1.068E-02	9.694	1.090E-02	10.577	1.094E-02
10.594	1.125E-02	11.477	1.063E-02	12.360	1.079E-02
10.611	1.112E-02	11.493	1.068E-02	12.376	1.112E-02
10.627	1.107E-02	11.510	1.085E-02	12.393	1.095E-02
10.644	1.117E-02	11.527	1.079E-02	12.410	1.067E-02
10.661	1.099E-02	11.543	1.081E-02	12.426	1.065E-02
10.677	1.053E-02	11.560	1.069E-02	12.443	1.071E-02
10.694	1.076E-02	11.577	1.072E-02	12.459	1.094E-02
10.710	1.068E-02	11.593	1.068E-02	12.476	1.083E-02
10.727	1.068E-02	11.610	1.048E-02	12.493	1.103E-02

LA-ICP-MS data

Distance con't (mm)	Sr/Ca (mol/mol)	Distance con't (mm)	Sr/Ca (mol/mol)	Distance con't (mm)	Sr/Ca (mol/mol)
10.744	1.092E-02	11.627	1.080E-02	12.509	1.085E-02
10.760	1.093E-02	11.643	1.077E-02	12.526	1.084E-02
10.777	1.097E-02	11.660	1.076E-02	12.543	1.063E-02
10.794	1.081E-02	11.677	1.116E-02	12.559	1.071E-02
10.810	1.073E-02	11.693	1.099E-02	12.576	1.058E-02
10.827	1.105E-02	11.710	1.092E-02	12.593	1.042E-02
10.844	1.086E-02	11.727	1.059E-02	12.609	1.060E-02
10.860	1.096E-02	11.743	1.069E-02	12.626	1.060E-02
10.877	1.111E-02	11.760	1.083E-02	12.643	1.050E-02
10.894	1.090E-02	11.777	1.064E-02	12.659	1.107E-02
10.910	1.099E-02	11.793	1.051E-02	12.676	1.087E-02
10.927	1.120E-02	11.810	1.023E-02	12.693	1.068E-02
10.944	1.110E-02	11.827	1.043E-02	12.709	1.076E-02
10.960	1.094E-02	11.843	1.044E-02	12.726	1.058E-02
10.977	1.095E-02	11.860	1.076E-02	12.743	1.057E-02
10.994	1.097E-02	11.876	1.056E-02	12.759	1.062E-02
11.010	1.073E-02	11.893	1.073E-02	12.776	1.083E-02
11.027	1.053E-02	11.910	1.059E-02	12.793	1.103E-02
11.044	1.059E-02	11.926	1.080E-02	12.809	1.112E-02
11.060	1.100E-02	11.943	1.103E-02	12.826	1.103E-02
11.077	1.096E-02	11.960	1.099E-02	12.843	1.065E-02
11.094	1.123E-02	11.976	1.087E-02	12.859	1.122E-02
11.110	1.082E-02	11.993	1.083E-02	12.876	1.115E-02
11.127	1.061E-02	12.010	1.114E-02	12.893	1.128E-02
11.144	1.060E-02	12.026	1.082E-02	12.909	1.084E-02
11.160	1.060E-02	12.043	1.084E-02	12.926	1.098E-02
11.177	1.056E-02	12.060	1.062E-02	12.943	1.078E-02
11.194	1.075E-02	12.076	1.091E-02	12.959	1.079E-02
11.210	1.074E-02	12.093	1.045E-02	12.976	1.079E-02
11.227	1.074E-02	12.110	1.040E-02	12.993	1.073E-02
11.244	1.071E-02	12.126	1.056E-02	13.009	1.058E-02
11.260	1.087E-02	12.143	1.079E-02	13.026	1.079E-02
11.277	1.082E-02	12.160	1.060E-02	13.042	1.057E-02
11.293	1.035E-02	12.176	1.053E-02	13.059	1.068E-02
11.310	1.061E-02	12.193	1.095E-02	13.076	1.106E-02
11.327	1.050E-02	12.210	1.046E-02	13.092	1.079E-02
11.343	1.031E-02	12.226	1.051E-02	13.109	1.113E-02
11.360	1.042E-02	12.243	1.052E-02	13.126	1.074E-02
11.377	1.034E-02	12.260	1.045E-02	13.142	1.084E-02
11.393	1.040E-02	12.276	1.060E-02	13.159	1.093E-02
11.410	1.062E-02	12.293	1.081E-02	13.176	1.074E-02
11.427	1.059E-02	12.310	1.071E-02	13.192	1.079E-02
11.443	1.019E-02	12.326	1.064E-02	13.209	1.079E-02
11.460	1.059E-02	12.343	1.056E-02	13.226	1.055E-02
13.242	1.087E-02	14.125	1.108E-02	15.008	1.050E-02
13.259	1.084E-02	14.142	1.116E-02	15.025	1.081E-02
13.276	1.086E-02	14.159	1.095E-02	15.041	1.059E-02
13.292	1.108E-02	14.175	1.081E-02	15.058	1.075E-02
13.309	1.118E-02	14.192	1.092E-02	15.075	1.079E-02
13.326	1.090E-02	14.208	1.093E-02	15.091	1.054E-02
13.342	1.113E-02	14.225	1.088E-02	15.108	1.044E-02
13.359	1.106E-02	14.242	1.098E-02	15.125	1.052E-02
13.376	1.089E-02	14.258	1.092E-02	15.141	1.053E-02
13.392	1.099E-02	14.275	1.106E-02	15.158	1.049E-02
13.409	1.090E-02	14.292	1.141E-02	15.175	1.075E-02
13.426	1.088E-02	14.308	1.155E-02	15.191	1.083E-02

Distance con't (mm)	Sr/Ca (mol/mol)	Distance con't (mm)	Sr/Ca (mol/mol)	Distance con't (mm)	Sr/Ca (mol/mol)
13.442	1.096E-02	14.325	1.138E-02	15.208	1.069E-02
13.459	1.082E-02	14.342	1.111E-02	15.225	1.107E-02
13.476	1.138E-02	14.358	1.107E-02	15.241	1.106E-02
13.492	1.114E-02	14.375	1.114E-02	15.258	1.087E-02
13.509	1.111E-02	14.392	1.103E-02	15.275	1.103E-02
13.526	1.103E-02	14.408	1.098E-02	15.291	1.127E-02
13.542	1.083E-02	14.425	1.117E-02	15.308	1.076E-02
13.559	1.084E-02	14.442	1.076E-02	15.324	1.069E-02
13.576	1.109E-02	14.458	1.124E-02	15.341	1.089E-02
13.592	1.115E-02	14.475	1.100E-02	15.358	1.036E-02
13.609	1.128E-02	14.492	1.116E-02	15.374	1.041E-02
13.625	1.125E-02	14.508	1.102E-02	15.391	1.048E-02
13.642	1.105E-02	14.525	1.099E-02	15.408	1.066E-02
13.659	1.078E-02	14.542	1.120E-02	15.424	1.026E-02
13.675	1.095E-02	14.558	1.103E-02	15.441	1.052E-02
13.692	1.078E-02	14.575	1.091E-02	15.458	1.055E-02
13.709	1.078E-02	14.592	1.075E-02	15.474	1.082E-02
13.725	1.075E-02	14.608	1.097E-02	15.491	1.071E-02
13.742	1.100E-02	14.625	1.107E-02	15.508	1.070E-02
13.759	1.078E-02	14.642	1.095E-02	15.524	1.048E-02
13.775	1.052E-02	14.658	1.082E-02	15.541	1.107E-02
13.792	1.060E-02	14.675	1.088E-02	15.558	1.037E-02
13.809	1.080E-02	14.692	1.112E-02	15.574	1.041E-02
13.825	1.069E-02	14.708	1.076E-02	15.591	1.038E-02
13.842	1.082E-02	14.725	1.073E-02	15.608	1.035E-02
13.859	1.098E-02	14.741	1.098E-02	15.624	1.037E-02
13.875	1.080E-02	14.758	1.085E-02	15.641	1.027E-02
13.892	1.078E-02	14.775	1.078E-02	15.658	1.049E-02
13.909	1.083E-02	14.791	1.067E-02	15.674	1.061E-02
13.925	1.098E-02	14.808	1.088E-02	15.691	1.071E-02
13.942	1.085E-02	14.825	1.092E-02	15.708	1.094E-02
13.959	1.100E-02	14.841	1.096E-02	15.724	1.094E-02
13.975	1.136E-02	14.858	1.063E-02	15.741	1.078E-02
13.992	1.134E-02	14.875	1.109E-02	15.758	1.098E-02
14.009	1.111E-02	14.891	1.084E-02	15.774	1.085E-02
14.025	1.073E-02	14.908	1.082E-02	15.791	1.033E-02
14.042	1.095E-02	14.925	1.096E-02	15.808	1.075E-02
14.059	1.095E-02	14.941	1.093E-02	15.824	1.076E-02
14.075	1.088E-02	14.958	1.057E-02	15.841	1.097E-02
14.092	1.082E-02	14.975	1.107E-02	15.858	1.090E-02
14.109	1.097E-02	14.991	1.085E-02	15.874	1.069E-02
15.891	1.058E-02	16.774	1.050E-02	17.656	1.089E-02
15.907	1.054E-02	16.790	1.066E-02	17.673	1.101E-02
15.924	1.088E-02	16.807	1.055E-02	17.690	1.101E-02
15.941	1.081E-02	16.824	1.071E-02	17.706	1.083E-02
15.957	1.036E-02	16.840	1.079E-02	17.723	1.075E-02
15.974	1.080E-02	16.857	1.113E-02	17.740	1.088E-02
15.991	1.091E-02	16.874	1.086E-02	17.756	1.088E-02
16.007	1.077E-02	16.890	1.104E-02	17.773	1.081E-02
16.024	1.115E-02	16.907	1.121E-02	17.790	1.078E-02
16.041	1.095E-02	16.924	1.113E-02	17.806	1.115E-02
16.057	1.072E-02	16.940	1.123E-02	17.823	1.093E-02
16.074	1.069E-02	16.957	1.136E-02	17.840	1.089E-02
16.091	1.065E-02	16.974	1.111E-02	17.856	1.079E-02
16.107	1.094E-02	16.990	1.128E-02	17.873	1.096E-02
16.124	1.093E-02	17.007	1.109E-02	17.890	1.070E-02

LA-ICP-MS data

Distance con't (mm)	Sr/Ca (mol/mol)	Distance con't (mm)	Sr/Ca (mol/mol)	Distance con't (mm)	Sr/Ca (mol/mol)
16.141	1.110E-02	17.024	1.130E-02	17.906	1.073E-02
16.157	1.105E-02	17.040	1.091E-02	17.923	1.046E-02
16.174	1.090E-02	17.057	1.119E-02	17.940	1.088E-02
16.191	1.120E-02	17.073	1.091E-02	17.956	1.047E-02
16.207	1.123E-02	17.090	1.112E-02	17.973	1.072E-02
16.224	1.092E-02	17.107	1.080E-02	17.990	1.068E-02
16.241	1.086E-02	17.123	1.080E-02	18.006	1.080E-02
16.257	1.107E-02	17.140	1.048E-02	18.023	1.110E-02
16.274	1.108E-02	17.157	1.072E-02	18.040	1.054E-02
16.291	1.090E-02	17.173	1.071E-02	18.056	1.055E-02
16.307	1.118E-02	17.190	1.075E-02	18.073	1.077E-02
16.324	1.068E-02	17.207	1.084E-02	18.090	1.078E-02
16.341	1.084E-02	17.223	1.095E-02	18.106	1.072E-02
16.357	1.090E-02	17.240	1.100E-02	18.123	1.087E-02
16.374	1.085E-02	17.257	1.105E-02	18.140	1.133E-02
16.391	1.114E-02	17.273	1.101E-02	18.156	1.129E-02
16.407	1.071E-02	17.290	1.106E-02	18.173	1.105E-02
16.424	1.083E-02	17.307	1.097E-02	18.190	1.094E-02
16.441	1.080E-02	17.323	1.097E-02	18.206	1.074E-02
16.457	1.081E-02	17.340	1.081E-02	18.223	1.116E-02
16.474	1.102E-02	17.357	1.088E-02	18.239	1.106E-02
16.490	1.088E-02	17.373	1.106E-02	18.256	1.125E-02
16.507	1.082E-02	17.390	1.105E-02	18.273	1.105E-02
16.524	1.070E-02	17.407	1.147E-02	18.289	1.109E-02
16.540	1.112E-02	17.423	1.139E-02	18.306	1.080E-02
16.557	1.103E-02	17.440	1.117E-02	18.323	1.081E-02
16.574	1.052E-02	17.457	1.116E-02	18.339	1.061E-02
16.590	1.083E-02	17.473	1.086E-02	18.356	1.102E-02
16.607	1.103E-02	17.490	1.076E-02	18.373	1.084E-02
16.624	1.054E-02	17.507	1.090E-02	18.389	1.091E-02
16.640	1.079E-02	17.523	1.071E-02	18.406	1.115E-02
16.657	1.084E-02	17.540	1.057E-02	18.423	1.104E-02
16.674	1.097E-02	17.557	1.071E-02	18.439	1.088E-02
16.690	1.077E-02	17.573	1.062E-02	18.456	1.123E-02
16.707	1.066E-02	17.590	1.079E-02	18.473	1.109E-02
16.724	1.074E-02	17.607	1.084E-02	18.489	1.129E-02
16.740	1.035E-02	17.623	1.086E-02	18.506	1.142E-02
16.757	1.069E-02	17.640	1.108E-02	18.523	1.121E-02
18.539	1.135E-02	19.422	1.079E-02	20.305	1.086E-02
18.556	1.135E-02	19.439	1.095E-02	20.322	1.097E-02
18.573	1.122E-02	19.455	1.076E-02	20.338	1.095E-02
18.589	1.116E-02	19.472	1.062E-02	20.355	1.056E-02
18.606	1.093E-02	19.489	1.055E-02	20.372	1.083E-02
18.623	1.113E-02	19.505	1.034E-02	20.388	1.092E-02
18.639	1.091E-02	19.522	1.042E-02	20.405	1.124E-02
18.656	1.110E-02	19.539	1.017E-02	20.422	1.103E-02
18.673	1.099E-02	19.555	1.035E-02	20.438	1.101E-02
18.689	1.098E-02	19.572	1.048E-02	20.455	1.081E-02
18.706	1.108E-02	19.589	1.037E-02	20.472	1.105E-02
18.723	1.095E-02	19.605	1.084E-02	20.488	1.076E-02
18.739	1.086E-02	19.622	1.060E-02	20.505	1.113E-02
18.756	1.120E-02	19.639	1.067E-02	20.521	1.111E-02
18.773	1.089E-02	19.655	1.063E-02	20.538	1.075E-02
18.789	1.092E-02	19.672	1.048E-02	20.555	1.079E-02
18.806	1.072E-02	19.689	1.054E-02	20.571	1.063E-02
18.822	1.077E-02	19.705	1.068E-02	20.588	1.074E-02

Distance con't (mm)	Sr/Ca (mol/mol)	Distance con't (mm)	Sr/Ca (mol/mol)	Distance con't (mm)	Sr/Ca (mol/mol)
18.839	1.089E-02	19.722	1.059E-02	20.605	1.046E-02
18.856	1.079E-02	19.739	1.076E-02	20.621	1.055E-02
18.872	1.079E-02	19.755	1.083E-02	20.638	1.060E-02
18.889	1.051E-02	19.772	1.060E-02	20.655	1.045E-02
18.906	1.101E-02	19.789	1.060E-02	20.671	1.056E-02
18.922	1.094E-02	19.805	1.096E-02	20.688	1.012E-02
18.939	1.084E-02	19.822	1.090E-02	20.705	1.021E-02
18.956	1.101E-02	19.839	1.089E-02	20.721	1.065E-02
18.972	1.102E-02	19.855	1.110E-02	20.738	1.055E-02
18.989	1.110E-02	19.872	1.089E-02	20.755	1.052E-02
19.006	1.121E-02	19.889	1.114E-02	20.771	1.070E-02
19.022	1.073E-02	19.905	1.132E-02	20.788	1.053E-02
19.039	1.067E-02	19.922	1.113E-02	20.805	1.076E-02
19.056	1.097E-02	19.939	1.101E-02	20.821	1.078E-02
19.072	1.072E-02	19.955	1.121E-02	20.838	1.059E-02
19.089	1.074E-02	19.972	1.084E-02	20.855	1.027E-02
19.106	1.052E-02	19.988	1.119E-02	20.871	1.025E-02
19.122	1.063E-02	20.005	1.079E-02	20.888	1.039E-02
19.139	1.086E-02	20.022	1.081E-02	20.905	1.052E-02
19.156	1.084E-02	20.038	1.059E-02	20.921	1.062E-02
19.172	1.078E-02	20.055	1.067E-02	20.938	1.069E-02
19.189	1.084E-02	20.072	1.102E-02	20.955	1.073E-02
19.206	1.052E-02	20.088	1.088E-02	20.971	1.047E-02
19.222	1.068E-02	20.105	1.104E-02	20.988	1.071E-02
19.239	1.042E-02	20.122	1.091E-02	21.005	1.092E-02
19.256	1.021E-02	20.138	1.097E-02	21.021	1.070E-02
19.272	1.047E-02	20.155	1.129E-02	21.038	1.047E-02
19.289	1.080E-02	20.172	1.111E-02	21.055	1.033E-02
19.306	1.110E-02	20.188	1.135E-02	21.071	1.025E-02
19.322	1.085E-02	20.205	1.150E-02	21.088	1.018E-02
19.339	1.112E-02	20.222	1.126E-02	21.104	1.030E-02
19.356	1.102E-02	20.238	1.075E-02	21.121	1.025E-02
19.372	1.079E-02	20.255	1.054E-02	21.138	1.063E-02
19.389	1.089E-02	20.272	1.062E-02	21.154	1.054E-02
19.405	1.031E-02	20.288	1.064E-02	21.171	1.034E-02
21.188	1.055E-02	22.071	1.088E-02	22.953	1.068E-02
21.204	1.033E-02	22.087	1.108E-02	22.970	1.058E-02
21.221	1.049E-02	22.104	1.084E-02	22.987	1.074E-02
21.238	1.062E-02	22.121	1.118E-02	23.003	1.098E-02
21.254	1.046E-02	22.137	1.101E-02	23.020	1.063E-02
21.271	1.072E-02	22.154	1.096E-02	23.037	1.092E-02
21.288	1.079E-02	22.171	1.081E-02	23.053	1.087E-02
21.304	1.088E-02	22.187	1.106E-02	23.070	1.105E-02
21.321	1.073E-02	22.204	1.070E-02	23.087	1.076E-02
21.338	1.081E-02	22.221	1.065E-02	23.103	1.086E-02
21.354	1.105E-02	22.237	1.071E-02	23.120	1.098E-02
21.371	1.101E-02	22.254	1.072E-02	23.137	1.074E-02
21.388	1.081E-02	22.270	1.065E-02	23.153	1.058E-02
21.404	1.086E-02	22.287	1.033E-02	23.170	1.044E-02
21.421	1.063E-02	22.304	1.058E-02	23.187	1.052E-02
21.438	1.082E-02	22.320	1.072E-02	23.203	1.035E-02
21.454	1.073E-02	22.337	1.045E-02	23.220	1.044E-02
21.471	1.122E-02	22.354	1.063E-02	23.237	1.053E-02
21.488	1.085E-02	22.370	1.076E-02	23.253	1.047E-02
21.504	1.068E-02	22.387	1.041E-02	23.270	1.082E-02
21.521	1.068E-02	22.404	1.075E-02	23.287	1.082E-02

LA-ICP-MS data

Distance con't (mm)	Sr/Ca (mol/mol)	Distance con't (mm)	Sr/Ca (mol/mol)	Distance con't (mm)	Sr/Ca (mol/mol)
21.538	1.088E-02	22.420	1.077E-02	23.303	1.073E-02
21.554	1.082E-02	22.437	1.065E-02	23.320	1.057E-02
21.571	1.048E-02	22.454	1.068E-02	23.337	1.066E-02
21.588	1.062E-02	22.470	1.065E-02	23.353	1.072E-02
21.604	1.077E-02	22.487	1.083E-02	23.370	1.068E-02
21.621	1.098E-02	22.504	1.091E-02	23.387	1.092E-02
21.638	1.091E-02	22.520	1.098E-02	23.403	1.078E-02
21.654	1.098E-02	22.537	1.105E-02	23.420	1.064E-02
21.671	1.084E-02	22.554	1.104E-02	23.436	1.065E-02
21.687	1.082E-02	22.570	1.089E-02	23.453	1.068E-02
21.704	1.101E-02	22.587	1.073E-02	23.470	1.091E-02
21.721	1.133E-02	22.604	1.060E-02	23.486	1.126E-02
21.737	1.114E-02	22.620	1.063E-02	23.503	1.110E-02
21.754	1.131E-02	22.637	1.076E-02	23.520	1.098E-02
21.771	1.089E-02	22.654	1.087E-02	23.536	1.144E-02
21.787	1.090E-02	22.670	1.042E-02	23.553	1.124E-02
21.804	1.077E-02	22.687	1.073E-02	23.570	1.123E-02
21.821	1.060E-02	22.704	1.083E-02	23.586	1.133E-02
21.837	1.061E-02	22.720	1.058E-02	23.603	1.131E-02
21.854	1.079E-02	22.737	1.073E-02	23.620	1.135E-02
21.871	1.052E-02	22.754	1.081E-02	23.636	1.156E-02
21.887	1.079E-02	22.770	1.097E-02	23.653	1.127E-02
21.904	1.061E-02	22.787	1.077E-02	23.670	1.135E-02
21.921	1.101E-02	22.804	1.077E-02	23.686	1.112E-02
21.937	1.077E-02	22.820	1.082E-02	23.703	1.112E-02
21.954	1.095E-02	22.837	1.047E-02	23.720	1.102E-02
21.971	1.078E-02	22.853	1.058E-02	23.736	1.113E-02
21.987	1.108E-02	22.870	1.077E-02	23.753	1.120E-02
22.004	1.119E-02	22.887	1.035E-02	23.770	1.115E-02
22.021	1.069E-02	22.903	1.061E-02	23.786	1.168E-02
22.037	1.091E-02	22.920	1.047E-02	23.803	1.135E-02
22.054	1.095E-02	22.937	1.065E-02	23.820	1.121E-02
23.836	1.121E-02	24.719	1.020E-02	25.602	1.110E-02
23.853	1.089E-02	24.736	1.045E-02	25.619	1.089E-02
23.870	1.087E-02	24.752	1.025E-02	25.635	1.096E-02
23.886	1.107E-02	24.769	1.066E-02	25.652	1.064E-02
23.903	1.093E-02	24.786	1.037E-02	25.669	1.043E-02
23.920	1.080E-02	24.802	1.078E-02	25.685	1.041E-02
23.936	1.111E-02	24.819	1.067E-02	25.702	1.053E-02
23.953	1.096E-02	24.836	1.071E-02	25.719	1.064E-02
23.970	1.099E-02	24.852	1.066E-02	25.735	1.078E-02
23.986	1.114E-02	24.869	1.097E-02	25.752	1.092E-02
24.003	1.119E-02	24.886	1.059E-02	25.768	1.053E-02
24.019	1.133E-02	24.902	1.064E-02	25.785	1.057E-02
24.036	1.101E-02	24.919	1.084E-02	25.802	1.087E-02
24.053	1.112E-02	24.936	1.077E-02	25.818	1.077E-02
24.069	1.106E-02	24.952	1.119E-02	25.835	1.097E-02
24.086	1.110E-02	24.969	1.095E-02	25.852	1.081E-02
24.103	1.105E-02	24.986	1.106E-02	25.868	1.115E-02
24.119	1.101E-02	25.002	1.106E-02	25.885	1.103E-02
24.136	1.115E-02	25.019	1.081E-02	25.902	1.095E-02
24.153	1.107E-02	25.036	1.083E-02	25.918	1.097E-02
24.169	1.093E-02	25.052	1.071E-02	25.935	1.077E-02
24.186	1.086E-02	25.069	1.094E-02	25.952	1.057E-02
24.203	1.089E-02	25.086	1.110E-02	25.968	1.075E-02
24.219	1.100E-02	25.102	1.110E-02	25.985	1.056E-02

Distance con't (mm)	Sr/Ca (mol/mol)	Distance con't (mm)	Sr/Ca (mol/mol)	Distance con't (mm)	Sr/Ca (mol/mol)
24.236	1.090E-02	25.119	1.112E-02	26.002	1.073E-02
24.253	1.110E-02	25.136	1.095E-02	26.018	1.064E-02
24.269	1.085E-02	25.152	1.110E-02	26.035	1.092E-02
24.286	1.107E-02	25.169	1.094E-02	26.052	1.097E-02
24.303	1.096E-02	25.185	1.078E-02	26.068	1.074E-02
24.319	1.106E-02	25.202	1.061E-02	26.085	1.043E-02
24.336	1.096E-02	25.219	1.079E-02	26.102	1.047E-02
24.353	1.059E-02	25.235	1.083E-02	26.118	1.056E-02
24.369	1.065E-02	25.252	1.093E-02	26.135	1.072E-02
24.386	1.068E-02	25.269	1.089E-02	26.152	1.115E-02
24.403	1.063E-02	25.285	1.121E-02	26.168	1.118E-02
24.419	1.085E-02	25.302	1.097E-02	26.185	1.076E-02
24.436	1.091E-02	25.319	1.085E-02	26.202	1.069E-02
24.453	1.088E-02	25.335	1.083E-02	26.218	1.083E-02
24.469	1.111E-02	25.352	1.096E-02	26.235	1.088E-02
24.486	1.088E-02	25.369	1.108E-02	26.252	1.067E-02
24.503	1.094E-02	25.385	1.091E-02	26.268	1.086E-02
24.519	1.099E-02	25.402	1.086E-02	26.285	1.070E-02
24.536	1.089E-02	25.419	1.083E-02	26.301	1.034E-02
24.553	1.095E-02	25.435	1.075E-02	26.318	1.041E-02
24.569	1.093E-02	25.452	1.079E-02	26.335	1.095E-02
24.586	1.071E-02	25.469	1.067E-02	26.351	1.061E-02
24.602	1.066E-02	25.485	1.086E-02	26.368	1.062E-02
24.619	1.048E-02	25.502	1.047E-02	26.385	1.069E-02
24.636	1.030E-02	25.519	1.086E-02	26.401	1.087E-02
24.652	1.045E-02	25.535	1.055E-02	26.418	1.065E-02
24.669	1.044E-02	25.552	1.072E-02	26.435	1.072E-02
24.686	1.061E-02	25.569	1.095E-02	26.451	1.047E-02
24.702	1.059E-02	25.585	1.081E-02	26.468	1.043E-02
26.485	1.060E-02	27.368	1.072E-02	28.250	1.071E-02
26.501	1.069E-02	27.384	1.073E-02	28.267	1.070E-02
26.518	1.086E-02	27.401	1.073E-02	28.284	1.092E-02
26.535	1.076E-02	27.418	1.078E-02	28.300	1.080E-02
26.551	1.105E-02	27.434	1.071E-02	28.317	1.089E-02
26.568	1.034E-02	27.451	1.077E-02	28.334	1.090E-02
26.585	1.060E-02	27.467	1.086E-02	28.350	1.099E-02
26.601	1.061E-02	27.484	1.087E-02	28.367	1.070E-02
26.618	1.074E-02	27.501	1.091E-02	28.384	1.068E-02
26.635	1.073E-02	27.517	1.111E-02	28.400	1.068E-02
26.651	1.090E-02	27.534	1.115E-02	28.417	1.060E-02
26.668	1.068E-02	27.551	1.088E-02	28.434	1.049E-02
26.685	1.089E-02	27.567	1.110E-02	28.450	1.076E-02
26.701	1.093E-02	27.584	1.094E-02	28.467	1.079E-02
26.718	1.085E-02	27.601	1.081E-02	28.484	1.084E-02
26.735	1.074E-02	27.617	1.110E-02	28.500	1.081E-02
26.751	1.068E-02	27.634	1.110E-02	28.517	1.078E-02
26.768	1.085E-02	27.651	1.093E-02	28.534	1.080E-02
26.785	1.054E-02	27.667	1.106E-02	28.550	1.082E-02
26.801	1.063E-02	27.684	1.085E-02	28.567	1.071E-02
26.818	1.068E-02	27.701	1.078E-02	28.584	1.073E-02
26.835	1.071E-02	27.717	1.101E-02	28.600	1.065E-02
26.851	1.125E-02	27.734	1.126E-02	28.617	1.068E-02
26.868	1.105E-02	27.751	1.120E-02	28.633	1.078E-02
26.884	1.120E-02	27.767	1.113E-02	28.650	1.069E-02
26.901	1.128E-02	27.784	1.090E-02	28.667	1.080E-02
26.918	1.100E-02	27.801	1.090E-02	28.683	1.068E-02

LA-ICP-MS data

Distance con't (mm)	Sr/Ca (mol/mol)	Distance con't (mm)	Sr/Ca (mol/mol)	Distance con't (mm)	Sr/Ca (mol/mol)
26.934	1.086E-02	27.817	1.105E-02	28.700	1.078E-02
26.951	1.083E-02	27.834	1.088E-02	28.717	1.062E-02
26.968	1.129E-02	27.851	1.083E-02	28.733	1.055E-02
26.984	1.082E-02	27.867	1.119E-02	28.750	1.070E-02
27.001	1.094E-02	27.884	1.078E-02	28.767	1.059E-02
27.018	1.117E-02	27.901	1.105E-02	28.783	1.056E-02
27.034	1.115E-02	27.917	1.106E-02	28.800	1.108E-02
27.051	1.112E-02	27.934	1.105E-02	28.817	1.083E-02
27.068	1.118E-02	27.951	1.095E-02	28.833	1.126E-02
27.084	1.139E-02	27.967	1.083E-02	28.850	1.094E-02
27.101	1.108E-02	27.984	1.072E-02	28.867	1.082E-02
27.118	1.116E-02	28.001	1.052E-02	28.883	1.110E-02
27.134	1.120E-02	28.017	1.063E-02	28.900	1.121E-02
27.151	1.126E-02	28.034	1.053E-02		
27.168	1.105E-02	28.050	1.023E-02		
27.184	1.093E-02	28.067	1.077E-02		
27.201	1.130E-02	28.084	1.119E-02		
27.218	1.080E-02	28.100	1.112E-02		
27.234	1.078E-02	28.117	1.094E-02		
27.251	1.086E-02	28.134	1.070E-02		
27.268	1.063E-02	28.150	1.089E-02		
27.284	1.080E-02	28.167	1.085E-02		
27.301	1.074E-02	28.184	1.098E-02		
27.318	1.078E-02	28.200	1.066E-02		
27.334	1.096E-02	28.217	1.049E-02		
27.351	1.087E-02	28.234	1.072E-02		

Table 10.15 Ribbon Reef #10 *Astrosclera willeyana* stable isotope data

Distance from top (mm)	$\delta^{13}C$ ‰ PDB	$\delta^{18}O$ ‰ PDB	Distance con't (mm)	$\delta^{13}C$ ‰ PDB	$\delta^{18}O$ ‰ PDB	Distance con't (mm)	$\delta^{13}C$ ‰ PDB	$\delta^{18}O$ ‰ PDB
0.20	3.96	-0.90	21.20	4.47	-1.12	42.40	4.42	-1.09
0.40	3.95	-0.94	21.60	4.49	-1.13	42.80	4.41	-1.11
0.80	3.94	-0.97	22.00	4.50	-1.08			
1.20	4.00	-1.08	22.40	4.52	-1.11			
1.60	3.97	-0.90	22.80	4.50	-1.04			
2.00	4.01	-1.03	23.20	4.48	-1.06			
2.40	4.00	-0.94	23.60	4.56	-1.14			
2.80	3.99	-0.99	24.00	4.54	-1.08			
3.20	4.03	-1.04	24.40	4.56	-1.00			
3.60	4.02	-1.20	24.80	4.55	-1.16			
4.00	4.06	-1.17	25.20	4.55	-1.09			
4.40	4.10	-0.97	25.60	4.57	-1.04			
4.80	4.10	-1.05	26.00	4.55	-1.11			
5.20	4.09	-1.02	26.40	4.56	-0.99			
5.60	4.11	-1.01	26.80	4.53	-1.00			
6.00	4.10	-1.09	27.20	4.56	-1.04			
6.40	4.13	-0.97	27.60	4.56	-1.04			
6.80	4.16	-0.98	28.00	4.57	-1.04			
7.20	4.17	-1.02	28.40	4.51	-1.05			
7.60	4.17	-1.08	28.80	4.61	-0.96			
8.00	4.19	-0.98	29.20	4.62	-0.93			
8.40	4.23	-1.07	29.60	4.59	-0.87			
8.80	4.23	-0.93	30.00	4.60	-0.88			
9.20	4.05	-1.14	30.40	4.60	-0.94			
9.60	4.27	-0.95	30.80	4.60	-0.94			
10.00	4.24	-1.18	31.20	4.59	-0.91			
10.40	4.26	-0.98	31.60	4.58	-0.83			
10.80	4.26	-1.13	32.00	4.50	-0.89			
11.20	4.20	-1.01	32.40	4.56	-0.85			
11.60	4.28	-0.98	32.80	4.53	-0.91			
12.00	4.29	-0.94	33.20	4.49	-0.91			
12.40	4.27	-1.02	33.60	4.50	-0.93			
12.80	4.32	-1.05	34.00	4.45	-0.96			
13.20	4.23	-1.11	34.40	4.39	-0.95			
13.60	4.33	-1.04	34.80	4.35	-0.89			
14.00	4.34	-0.96	35.20	4.53	-0.91			
14.40	4.36	-1.01	35.60	4.43	-0.91			
14.80	4.39	-1.03	36.00	4.42	-0.83			
15.20	4.38	-1.00	36.40	4.51	-0.92			
15.60	4.38	-1.04	36.80	4.50	-0.90			
16.00	4.42	-1.03	37.20	4.48	-0.82			
16.40	4.41	-1.02	37.60	4.51	-1.00			
16.80	4.48	-1.05	38.00	4.53	-1.02			
17.20	4.44	-1.13	38.40	4.56	-1.00			
17.60	4.45	-1.05	38.80	4.53	-1.05			
18.00	4.43	-1.17	39.20	4.53	-1.05			
18.40	4.43	-1.13	39.60	4.51	-1.03			
18.80	4.46	-1.07	40.00	4.51	-1.04			
19.20	4.47	-1.04	40.40	4.48	-1.13			
19.60	4.50	-1.05	40.80	4.50	-1.07			
20.00	4.49	-1.05	41.20	4.47	-1.05			
20.40	4.48	-1.17	41.60	4.48	-0.97			
20.80	4.50	-0.99	42.00	4.46	-1.06			

Appendix 2: Publications

Coral Growth: Trace Elements Reveal Intra-annual Variations in Growth Rate from a *Porites* Coral, Shirigai Bay, Japan

Stewart J. Fallon, Malcolm T. McCulloch and Daniel J. Sinclair

Research School of Earth Sciences, Australian National University, Canberra ACT 2600

ABSTRACT

A *Porites* coral from Shirigai Bay, Japan was analysed for the trace elements strontium and uranium by Excimer Laser Ablation Inductively Coupled Plasma - Mass Spectrometry (ELA ICP-MS). This technique provides spatial resolution as small as 20-100 mm, equivalent to near-weekly resolution, even in corals with relatively slow growth rates (5 mm yr^{-1}). The Japanese *Porites* coral came from an environment with an exceptionally large annual range of SST of 13.5°C to 29°C. Elemental ratios of Sr/Ca, and U/Ca show seasonal cycles consistent with an instrumental SST record from nearby Komame (1980-1995). Trace element data indicate a large disparity between summer and winter extension rates with a large increase in the summer extension rate. Comparisons of the trace element profiles with computer simulations of trace element profiles during variable coral extension (Barnes *et al*., 1995) suggest a decrease and/or cessation of extension during winter in this coral.

INTRODUCTION

Coral reefs are generally located in tropical areas where it is rare for winter sea surface temperatures (SST's) to fall below 20°C. A few reefs exist at higher latitudes (SST ~20°C), in Bermuda, Houtman Abrolhos Islands (Western Australia), Red Sea and North Japan, because of the influx of warm tropical water (the Gulf Stream, Leeuwin Current and the Kuroshio Current). These corals can provide important information on the environmental factors controlling coral reef development during times of low SST or stress. By determining the intra-annual growth rates of these high latitude corals, we may be able to determine some of the optimal and sub-optimal environmental factors controlling coral growth.

Coral growth rates are traditionally determined by several methods: (1) Alizarin red S staining (Barnes, 1970; Buddemeier & Kinzie, 1975); (2) measuring annual density variations from X-radiographs (Knutson *et al*., 1972 & others); and (3) gamma densitometry (measuring the density directly from a thin slice of coral) (Chalker *et al*., 1985). Obtaining growth information from X-rays or gamma densitometry usually only provides the length of the high density and low density bands, thus giving an annual growth rate. Previously, the only way the intra-annual growth history of corals could be obtained was by staining (in the laboratory or field). Apart from being time consuming, there are problems associated with the stain diffusing through the skeleton, making it hard to measure the growth between stains. Here, we show how trace element analysis of corals can be used to show variations in intra-annual growth rates by using the seasonal cycles of the uranium/calcium (U/Ca) ratio measured in a *Porites* coral from Shirigai Bay, Japan.

In: Greenwood, J.G. & Hall, N.J., eds (1998)
Proceedings of the Australian Coral Reef Society 75th Anniversary Conference, Heron Island October 1997.
School of Marine Science, The University of Queensland, Brisbane. pp. 1-??.

BACKGROUND

Aragonitic coral skeletons contain growth bands such that one high density plus an adjacent less dense band represent skeletal formation over approximately one calendar year (Knutson *et al*., 1972 & others). Growth bands provide a record of annual extension rates. Since their initial description, these bands have been used as important tools for analysing coral growth rates and for providing a chronology for studies of environmental conditions in tropical marine regions (Barnes & Lough, 1993).

Corals also record environmental variations through the incorporation of trace elements into their skeletons. Incorporation of certain trace elements is dependent on the temperature of the surrounding sea water providing geochemical proxies which allow the reconstruction of temperature. Two elemental ratios, Sr/Ca (Smith *et al*., 1979; Beck *et al*., 1992; McCulloch *et al*. 1994) and U/Ca (Min *et al*., 1995; Shen & Dunbar, 1995) have been shown to exhibit a high correlation with sea water temperature.

Location

A 15cm long core was taken from a 2m diameter *Porites* coral in September 1993 from Shirigai Bay, near the southern tip of Shikoku Island, Japan (latitude 32°46´N, longitude 132° 42´E) (Figure 1). Shirigai Bay is one of the most northern coral communities in the world. The corals do not form typical coral reefs, they grow directly on non-carbonate rock substrate and occur as small outcrops (Veron, 1992). The northward flowing Kuroshio Current supplies the warm water necessary for hermatypic coral growth in this high latitude location, and *Porites* in this location have a wide temperature tolerance. Instrumental SST values at Komame, Shikoki Island, range from 13.5°C to 30°C.

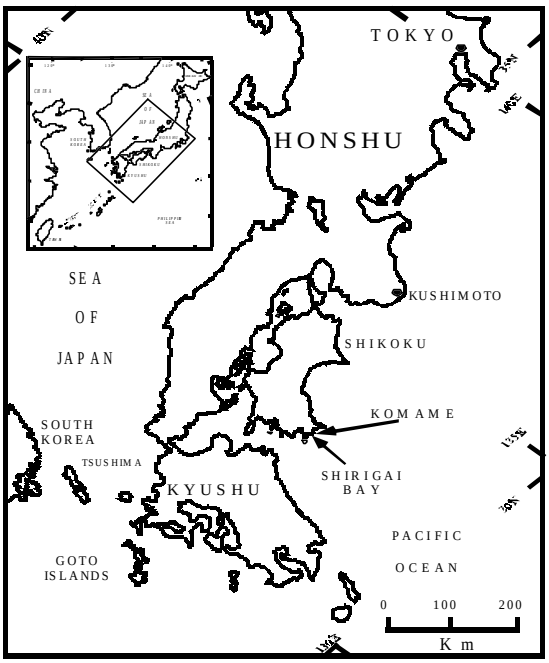

Figure 1. Map of sample locations in Japan. The coral was collected from Shirigai Bay, Shikoku Island (32°46´N, 132°42´E), the instrumental SST record used was from Komame.

LABORATORY METHODS

The 5 cm diameter core was slabbed (7mm thick) and X-rayed to reveal the density variations. The sample was cleaned with an ultrasonic probe in Milli-Q water and dried at 40°C. A sampling transect along the slice was chosen to follow the main axis of growth (Alibert & McCulloch, 1997). The coral was analysed by Excimer Laser Ablation Inductively Coupled Plasma - Mass Spectrometry (ELA ICP-MS) following techniques described elsewhere (Sinclair *et al*., 1998). Briefly, the corals were analysed in 20 x 45mm pieces, the size required for mounting on to the sample stage. The coral was then ablated with an ArF eximer laser (193nm). A rectangular slit was used to mask the beam to obtain a coverage of 50 x 500 mm on the coral surface. Ablated material was entrained in argon gas for analysis by ICP-MS (VG Elemental PQ2) (Figure 2). Counts were obtained for the isotopes ^{43}Ca, ^{84}Sr and ^{238}U with ^{43}Ca being used as the index isotope.

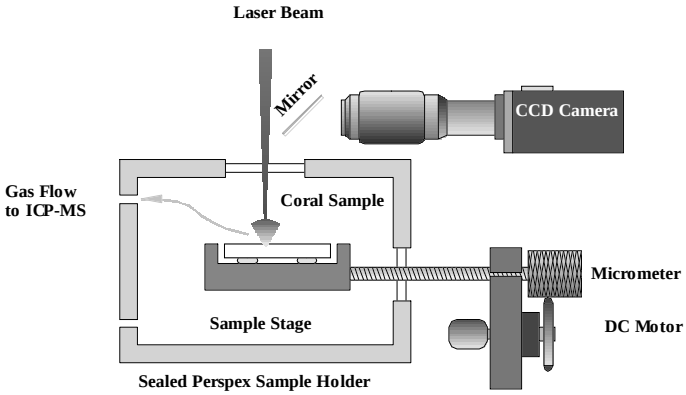

Figure 2. Schematic of laser ablation sample cell.

Standardisation was obtained by analysing a pressed powder disc made from cleaned and finely crushed Great Barrier Reef *Porites* coral. Using finely crushed coral powder provides elemental concentrations essentially identical to the unknown. The powder was mixed with a 2.5% polyvinyl alcohol binder and pressed at 20 tons (Perkins *et al*., 1991; Pearce *et al*., 1992). Calibration of the standard was performed by solution ICP-MS and thermal ionisation mass spectrometry (TIMS). Laser ablation estimates of Sr/Ca and U/Ca on two separate corals indicate the values are within error of solution ICP-MS and TIMS measurements (unpublished data). The precision of this technique, based on the standard deviation of a 60 second scan on the standard is 1.8% for Sr/Ca and 3.5% for U/Ca. The reproducibility, based on four replicates (during five months) over the same 86 mm length of sample was 2% for Sr/Ca and 5% for U/Ca. This translates into a temperature uncertainty of ± 2.5°C and ± 1°C respectively.

RESULTS AND DISCUSSION

The average annual extension (growth) measured from both the X-ray and from the distance between minimum U/Ca values was 5.3±1.2mm yr^{-1}. The measured U/Ca and Sr/Ca values ranged from (0.97-2.01 µmol/mol) and (8.58-0.2 µmol/mol) respectively. Variations in both elements show annual cycles very similar to the instrumental SST (Figure 3). This is consistent with a linear relationship between SST and U/Ca which will result in a trace element profile very similar to the shape of the SST curve.

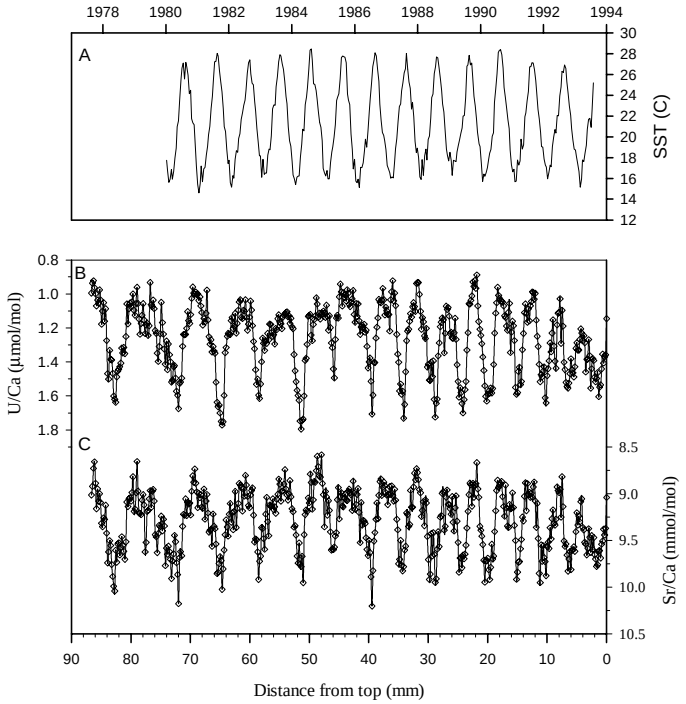

Figure 3. **A**. SST vs time from Komame, Japan. **B.** U/Ca (µmol/mol) vs distance from top of coral (mm). **C.** Sr/Ca (mmol/mol) vs distance from top of coral (mm). Note the "arched" shape of the trace element data compared to the SST data. This shape suggests a greater extension rate during summer when compare to winter.

The trace element (U/Ca and Sr/Ca) transects have a greater abundance of sample points during the summer months compared to winter (Figure 3). This suggests that there is a variation of the intra-annual extension of this coral. The arched shape of the trace element profiles are very similar to computer simulations of coral growth with variable intra-annual extension rates (Barnes *et al.*, 1995). Their simulations showed that trace element profiles took on an arched shape when summer extension increased relative to winter extension. Our data reproduces the sharp/narrow winter peaks observed by the computer simulated trace element profiles when winter extension is stopped (Barnes *et al.*, 1995). Using the simulations as a guide, we tested the correlation between U/Ca and SST by assuming variations in winter extension.

Assigning time to a coral proxy series generally involves correlating the "element"/Ca to SST maximum and minimum, and assuming linear growth between these "marker" points. Some researchers also match similar fine-scale features between the SST and "element"/Ca (Alibert & McCulloch, 1997). This approach is not adequate for our coral because of the extreme summer to winter growth bias we observe. The measured SST has approximately a sinusoidal pattern with the winter having a slightly higher abundance of points than summer (Figure 3A) whereas for the coral ~ 2 times more points (U/Ca) were sampled in summer vs winter (Figure 3B; C).

Based on the assumption that little to no extension was occurring during the winter, a time gap was inserted during the winter minimum. Using the minimum measured SST's as a guide, the effects of assuming non-uniform growth for different periods was examined (1week to 4 months).

The optimum fit for the U/Ca (and Sr/Ca) ratios was obtained for a ~2 month cessation of growth between early January and late March. Linear growth was then assumed to occur between the remaining interval, spring (April) and late fall (December). However, it should be noted that an absence of winter growth in the two month model is a simplifying assumption that cannot be readily resolved from very slow winter growth rates.

A comparison of the best fits for U/Ca and measured SST vs time is shown for the two cases, i.e. uniform annual growth (Figure 4A) versus an absence of winter growth (Figure 4B). The uniform annual growth model uses the simplistic approach of matching U/Ca to SST minimum and maximum. For uniform annual growth, a regression of U/Ca versus SST has an $r^2 = 0.51$

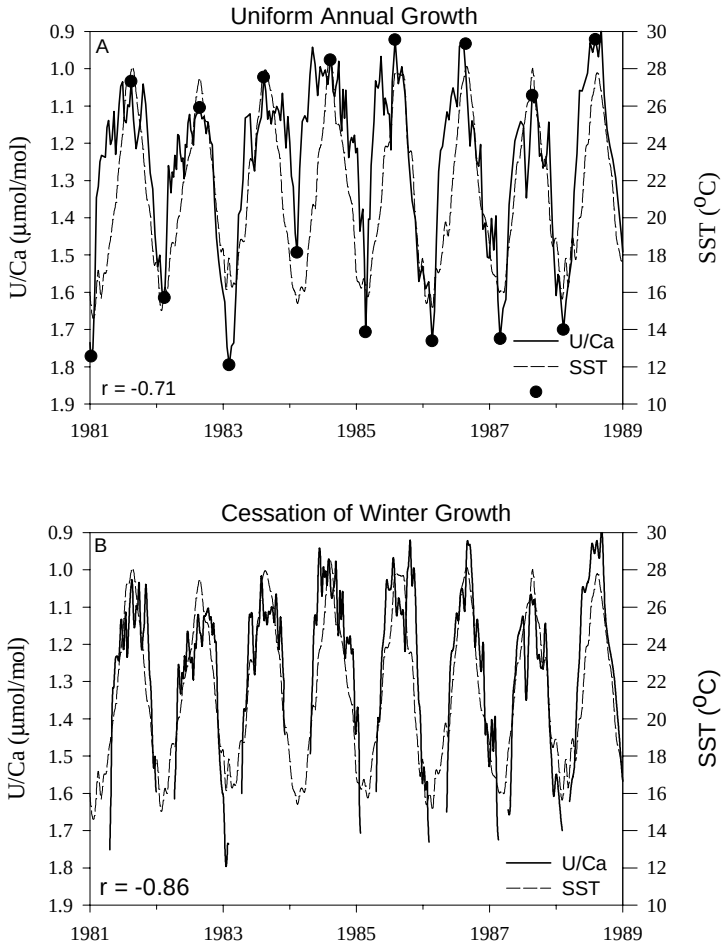

Figure 4. **(A)** U/Ca and Komame SST vs time assuming uniform growth between winter minimum and summer maximum SST. Note the U/Ca curve is much broader from early spring to late autumn. Correlation coefficient for this least squares regression is r = -0.71.
(B) U/Ca and SST vs time using 2 month cessation of growth model. By assuming little/no growth during the winter we assigned marker points then assumed linear growth between these points. The result is a better visual and statistical fit (r = -0.86).

($p<0.0001$) compared to $r^2 = 0.74$ ($p<0.0001$) for the ~2-month absence of winter growth. For the cessation model, SST values between the time markers (no extension) were removed from the linear regression (Figure 5). Although the best fit was obtained by assuming an absence or slowdown of winter growth there are still misfits between the two profiles, suggesting it may be difficult to reconstruct intra-annual SST from corals with varying intra-annual extension rates.

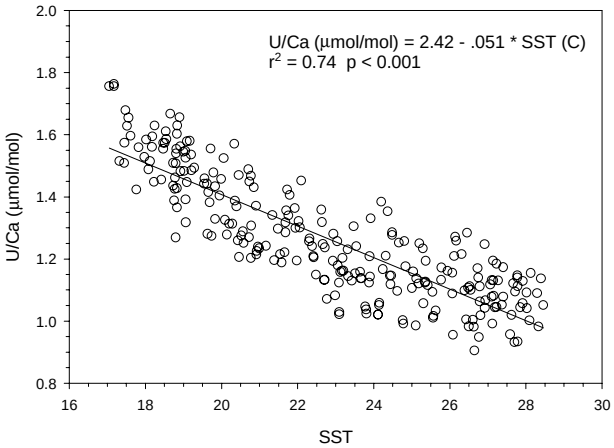

Figure 5. Linear regression of U/Ca (µmol/mol) vs SST. U/Ca (µmol/mol) = 2.42 - 0.051 * SST ($r^2 = 0.74$, $p < 0.0001$). SST values between the growth markers are not use in the linear regression.

The idea of a decreasing winter extension is not a new discovery in coral studies. Several publications have noted decreasing growth and calcification during cold winter temperatures (Buddemeier & Kinzie, 1975; Houck *et al*., 1977; Crossland, 1981; Wellington & Glynn, 1983). Their studies encompassed a wide range of locations and several different coral genera. For example, the growth of *Pavona* corals is 2x less on reefs of the western side of Galapagos when compared to other locations around the islands (Wellington & Glynn, 1983). This has been attributed to sustained periods of winter upwelling (SST 17-18°C). In studies of *Porites lobata*, Houck *et al*. (1977) noted a growth rate decrease of up to 2x the summer rate when SST approached 22°C. The evidence shown in these studies only suggests a decrease of winter growth and not a full cessation of growth.

Jacques *et al*. (1977), who used ^{45}Ca to determine calcification rates, suggested that calcification approaches zero as the temperature reaches 16°C. Our coral is surrounded by temperatures below 18°C for two to three months every year (Figure 3A). These observations, taken in conjunction with the trace element profiles of sharp winter peaks, lead us to the conclusion that cessation of winter growth is occurring. However, at this point we do not know the actual temperature at which cessation occurs.

CONCLUSIONS

Trace element analysis in corals provides a means of not only determining environmental conditions such as SST, but also for documenting the variations of intra-annual growth. Results reconfirm that the ELA-ICP-MS analyses of U/Ca and Sr/Ca in corals can provide proxy data for sea surface temperature with near-weekly resolution in corals with relatively slow growth

rates. The arched shape of our trace element profiles is indicative of increased summer extension compared to winter extension. This is corroborated by computer simulations of trace element profiles with little to no winter extension (Barnes *et al*., 1995). Our data suggest a decrease and/or a cessation of extension during winter.

ACKNOWLEDGEMENTS

We would like to thank R. van Woesik for supplying the coral sample, L. Kinsley for providing technical support for the ICP-MS and laser-ablation system, and two anonymous reviewers for helpful comments. Mr S. Fallon is supported by a Ph.D. scholarship from the Research School of Earth Sciences at the Australian National University.

REFERENCES

Alibert, C. & McCulloch, M.T. (1997) Strontium/calcium ratios in modern *Porites* corals from the Great Barrier Reef as a proxy for sea surface temperature: Calibration of the thermometer and monitoring of ENSO. *Paleoceanography* **12**(3): 345-363.

Barnes, D.J. (1970) Coral skeletons: An explanation of their growth and structure. *Science* **170**: 1305-1308.

Barnes, D.J. & Lough, J.M. (1993) On the nature and causes of density banding in massive coral skeletons. *Journal of Experimental Marine Biology Ecology* **167**: 91-108.

Barnes, D.J., Taylor, R.B. & Lough, J.M. (1995) On the inclusion of trace materials into massive coral skeletons. Part II: distortions in skeletal records of annual climate cycles due to growth processes. *Journal of Experimental Marine Biology Ecology* **194:** 251-275.

Beck, J.W., Edwards, R.L., Ito, E., Taylor, F.W., Recy, J., Rougerie, F., Joannot, P. & Henin, C. (1992) Sea-surface temperature from coral skeletal strontium/calcium ratios. *Science* **257**: 644-647.

Buddemeier, R.W. & Kinzie, R.A. (1975) The chronometric reliability of contemporary corals. In *Growth Rhythms and the History of the Earths's Rotation* (eds. Rosenberg, G.D. & Runcorn, S.K.) pp. 135-147. Wiley & Sons.

Chalker, B., Barnes, D.J. & Isdale, P. (1985) Calibration of X-ray densitometry for the measurement of coral skeletal density. *Coral Reefs* **4**: 95-100.

Crossland, C.J. (1981) Seasonal growth of *Acropora cf. formosa* and *Pocillopora damicornis* on a high latitude reef (Houtman Abrolhos, Western Australia). *Fourth International Coral Reef Symposium:* 663-667.

Houck, J.E., Buddemeier, R.W., Smith, S.V. & Jokiel, P.L. (1977) The response of coral growth rate and skeletal strontium content to light intensity and water temperature. *Third International Coral Reef Symposium* **2**: 425-431.

Jacques, T.G., Pilson, M.E.Q., Cummings, C. & Marshall, N. (1977) Laboratory observations on respiration, photosynthesis, and factors affecting calcification in the temperate coral *Astrangia danae*. *Third International Coral Reef Symposium* **2**: 455-461.

Knutson, D.W., Buddemeier, R.W. & Smith, S.V. (1972) Coral chronometers: seasonal growth bands in reef corals. *Science* **177**: 270-272.

McCulloch, M.T., Gagan, M.K., Mortimer, G.E., Chivas, A.R. & Isdale, P. J. (1994) A high-resolution Sr/Ca and $d^{18}O$ coral record from the Great Barrier Reef, Australia, and the 1982-1983 El Niño. *Geochimica et Cosmochimica Acta* **58**: 2747-2754.

Min, G.R., Edwards, R.L., Taylor, F.W., Recy, J., Gallup, C.D. & Beck, J.W. (1995) Annual cycles of U/Ca in coral skeletons and U/Ca thermometry. *Geochimica et Cosmochimica Acta* **59**: 2025-2043.

Pearce, N.J.G., Perkins, W.T. & Fuge, R. (1992) Developments in the quantitative and semiquantitative determination of trace elements in carbonates by laser ablation inductively coupled plasma mass spectrometry. *Journal of Analytical Atomic Spectrometry* **7**: 595-598.

Perkins, W.T., Fuge, R. & Pearce, N.J.G. (1991) Quantitative analysis of trace elements in carbonates using laser ablation inductively coupled plasma mass spectrometry. *Journal of Analytical Atomic Spectrometry* **6**: 445-449.

Shen, G.T. & Dunbar, R.B. (1995) Environmental controls on uranium in reef corals. *Geochimica et Cosmochimica Acta* **59**: 2009-2024.

Sinclair, D., Kinsley, L. & McCulloch, M.T. (1998) High resolution analysis of trace elements in corals by laser ablation ICP-MS. *Geochimica et Cosmochimica Acta* **212**(62/11): 1889-1901.

Smith, S.V., Buddemeier, R.W., Redalje, R.C. & Houck, J.E. (1979) Strontium-Calcium thermometry in coral skeletons. *Science* **204**: 404-406.

Veron, J.E.N. (1992) Hermatyptic Corals of Japan. *Australian Institute of Marine Scence Monographs* Vol. **9**: 234 pp .

Wellington, G.M. & Glynn, P.W. (1983) Environmental influences on skeletal banding in eastern Pacific (Panama) corals. Coral Reefs **1**: 215-222.

ELSEVIER

Earth and Planetary Science Letters 172 (1999) 221–238

EPSL

www.elsevier.com/locate/epsl

Corals at their latitudinal limits: laser ablation trace element systematics in *Porites* from Shirigai Bay, Japan

Stewart J. Fallon [a,*], Malcolm T. McCulloch [a], Robert van Woesik [b], Daniel J. Sinclair [a]

[a] *Research School of Earth Sciences, The Australian National University, Canberra, ACT 0200, Australia*
[b] *Department of Marine Sciences, University of the Ryukyus, Okinawa, Japan*

Received 8 March 1999; revised version received 29 July 1999; accepted 19 August 1999

Abstract

The rapid analytical technique of laser ablation–inductively coupled plasma–mass spectrometry (LA–ICP–MS) was used to measure the trace elements B, Mg, Sr, Ba and U in a high-latitude coral colony (*Porites lobata*) taken from Shirigai Bay, Japan (32ºN). A wide range of sea surface temperatures (SSTs 14.5–28ºC) and upwelling events influenced this coral. Cold winter SSTs caused a decrease and/or cessation of skeletal extension. Measurements of U/Ca and Sr/Ca indicate an approximately linear response to SSTs above 18ºC and a non-linear response below 18ºC. Mg/Ca and B/Ca measurements both showed annual cycles broadly consistent with SST variations, but also exhibited intra-annual fluctuations not associated with temperature, suggesting that the incorporation of Mg and B into the coral skeleton was not simply regulated by temperature. It is shown that Ba/Ca ratios provide a proxy for wind-induced seasonal upwelling. This is inferred from the strong correlations between the strength of zonal winds ~1 month prior to the SST minimum and the Ba/Ca maximum. Secondary upwelling events occurred during the summers of 1982, 1987, 1991 and 1992. These summers were cooler than average and were associated with El Niño Southern Oscillation events.

Keywords: Japan; Porites; chemical ratios; Sr/Ca; laser methods; inductively coupled plasma methods

1. Introduction

Corals growing at their latitudinal limits have been postulated as those most sensitive to global climatic changes [1,2]. Examining corals from locations where winter sea surface temperatures (SSTs) are extreme may further elucidate processes involving coral growth during glacial conditions when the majority of corals were living in colder waters [3]. A *Porites lobata* coral core was collected from one of the most northern coral reefs of Japan (Shirigai Bay, 32º46′N, 132º42′E) [4]. This location provides a 'unique' opportunity to study the response of trace element systematics and coral growth in an environment where the SSTs range from 14.5º to 28ºC. A new method, laser ablation–inductively coupled plasma–mass spectrometry (LA–ICP–MS) [5], is described here for the high-resolution measurement of the abundance of the elements B, Mg, Sr, Ba and U. It will be shown that the high-resolution capabilities of this technique provide a means to determine seasonal changes in coral growth, seasonal wind shifts and associated upwelling events,

* Corresponding author. Tel.: 61-2-6249-5472; Fax: 61-2-6249-0738; E-mail: stewart.fallon@anu.edu.au

0012-821X/99/$ – see front matter
PII: S0012-821X(99)00200-9

and traces of secondary upwelling associated with El Niño Southern Oscillation events.

Trace elements (B, Mg, Sr, Ba, U) provide geochemical proxies for reconstructing environmental conditions during coral growth. In various publications, the incorporation of the elements Sr [6–9], U [5,10,11], B [5,12] and Mg [5,12–14] have all been linked to seawater temperature. Barium has been associated with coastal river runoff but is predominantly used as an indicator of oceanic upwelling [15–17]. In this study we report the high-resolution measurements of U/Ca, Sr/Ca, Ba/Ca, B/Ca and Mg/Ca ratios and examine their response to a wide range of SSTs and upwelling events during approximately 16 years of coral growth. Moreover, time series records of environmental conditions are preserved in the aragonitic ($CaCO_3$) skeleton of corals in alternating high- and low-density band couplets that can be approximately correlated to annual growth [18–20].

1.1. Location

A 30 cm core was extracted from a 2 m diameter *Porites lobata* coral located 2 m below low-water datum in Shirigai Bay, Shikoku Island, Japan (32°46′N, 132°42′E) in 1993 (Fig. 1). Shirigai Bay supports a 2.5 ha reef coral community and is one of the most northern coral communities in the world. The warm Kuroshio Current, which originates in equatorial waters, extends north to Shirigai Bay and beyond. The bay has a wide diversity of corals, ∼63 scleractinian coral species, covering approximately 70% of the rocky substrate. No carbonate accumulation is evident. Outside the bay, tides flood to the west and ebb to the east. A deep channel (15 m) splits the bay entrance, which occasionally brings cold, nutrient-rich, jets of deep water into the bay. This form of 'local' upwelling is most likely related to shifting wind patterns, when the summer southwesterly is replaced by a northwesterly pattern. The SST in the bay ranges from ∼14.5°C in February to ∼28°C in August (Komame station data, see Fig. 1).

2. Analytical methods

The LA–ICP–MS system at the Research School of Earth Sciences consists of an ArF excimer laser (193 nm wavelength) connected to a modified VG Elemental PQ2+ [5,21,22]. The coral sample was cut parallel to the axis of growth in 7 mm slabs and X-rayed to reveal the density variations. A sampling transect along the slice was chosen to follow the main axis of growth [9]. The coral samples were then cut into 45 mm lengths and cleaned with an ultrasonic probe in Milli-Q water and dried overnight at 40°C. The samples were then mounted on the stage with a motor drive moving the sample underneath the laser at 30 μm/s. A rectangular slit was used to mask the beam to obtain a surface coverage on the coral of 50 μm wide parallel to the growth axis and 500 μm wide perpendicular to the growth axis. The size of this rectangular slit corresponds to sub-weekly resolution in corals (>100 samples/year). The laser was pulsed at 5 Hz using 50 MJ energy and a 50% partially reflecting mirror. The ablated material was entrained in argon and helium gas for analysis by ICP–MS where counts were obtained for the isotopes ^{10}B, ^{25}Mg, ^{43}Ca, ^{84}Sr, ^{138}Ba, and ^{238}U. The isotope ^{43}Ca (0.13% Ca) was used as an index isotope to account for variations in count rate due to coral surface porosity. Crosschecks were also undertaken using additional isotopes (^{11}B, ^{26}Mg, ^{46}Ca, ^{137}Ba) which gave identical results.

The analysis protocol follows techniques described in Sinclair et al. [5]. The coral was first cleaned using a laser energy of 100 MJ and a repetition rate of 50 Hz to expose a clean surface. The ICP–MS was then pre-conditioned to analyze the $CaCO_3$ by scanning the entire coral piece using sample collection parameters (5 Hz, 50 MJ). Backgrounds and standards were collected before and after the analysis of the coral to correct for any long-term machine drift. Under sample analysis conditions, this method removed approximately 0.1 μm of coral material with each laser pulse. When data was averaged to a resolution of 0.15 mm per sample (the resolution used in this study), we obtained an approximate volume of 0.0625 mm^3 vs. approximately 1.25 mm^3 for solution-based ICP–MS coral analyses.

2.1. Laser ablation standards

For LA–ICP–MS, an ideal standard should be chemically and physically matched to the unknown [22–26]. However, finding appropriate ma-

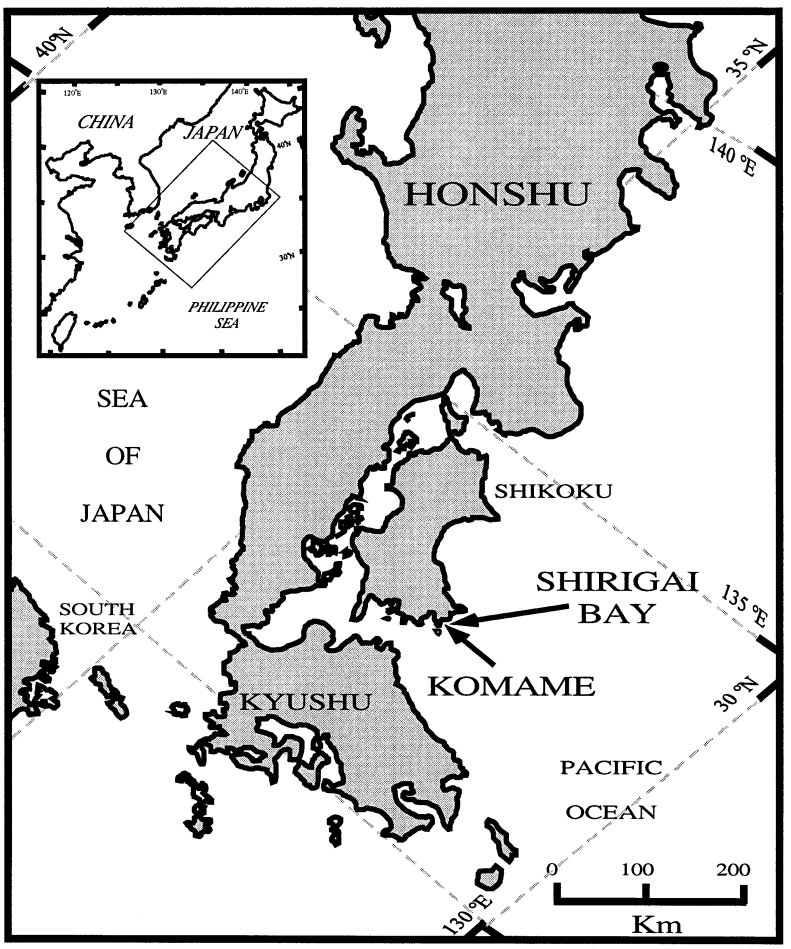

Fig. 1. Sampling location in Japan. The *Porites* coral core was collected from Shirigai Bay (32°46′N, 132°42′E), the instrumental SST record used was from Komame (an aquaculture station ~2–3 km south of Shirigai Bay).

trix-matched standards for the analysis of carbonates by LA–ICP–MS is difficult. Two in-house standards were used in this project. The first was a $CaSiO_3$ glass synthesized and described by Sinclair et al. [5]. However, this glass standard had problems with accuracy and long-term reproducibility. Sinclair et al. [5] concluded that matrix-related fractionation occurred when the coral silicate was used as a standard. Therefore the non-matrix-matched coral silicate standard does not provide the accuracy or long-term reproducibility necessary for fully quantitative analysis of corals and has been replaced. The current standard is a pressed powder disc similar to ones developed by Perkins et al. [26]. This disc was made from 5 g of a cleaned and finely crushed *Porites* coral from Davies Reef, Great Barrier Reef (GBR). This powder was then mixed with a 2.5% polyvinyl alcohol binder and pressed under high pressure into a 32 mm disc [25,26]. Using such finely crushed coral powder provides elemental concentrations essentially identical to the unknown. Calibration of the standard was performed by solution ICP–MS and thermal ionization mass spectrometry (TIMS).

In order to assess the accuracy of the pressed powder standard for Sr/Ca we compared a 35 mm laser track to the high-resolution TIMS Sr/Ca measurements on a coral from Davies Reef, GBR, called Davies 2 in Alibert and McCulloch [9]. The TIMS

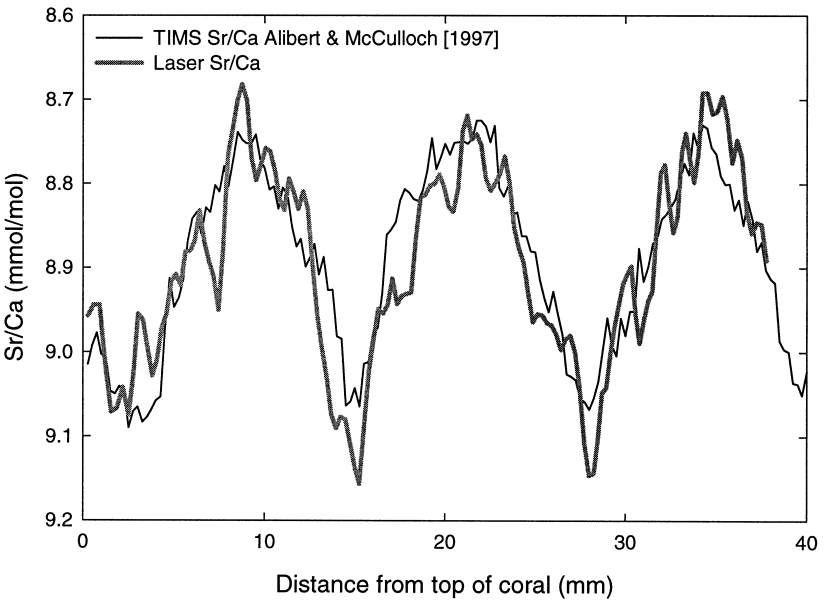

Fig. 2. Laser Sr/Ca and TIMS Sr/Ca vs. distance for the coral Davies 2 [9], showing the comparison between the two different analytical methods.

measurements cover almost 3 years of coral growth with both the mean values and some of the fine-scale variations in Sr/Ca being reproduced by the laser scan (Fig. 2).

The accuracy for the other elements (B, Mg, Ba and U) was tested on bulk milled samples of the Davies 2 coral. A summary of LA–ICP–MS data for the Davies 2 coral, using both the synthesized glass and pressed powder standards is shown in Table 1. Independent results by isotope dilution (solution ICP–MS and TIMS) are also given. Using our first pressed powder standard, all the elemental concentrations aside from boron and barium were within analytical error (Table 1). The boron concentration from the pressed powder standard laser analysis was slightly higher than expected, probably due to contamination during the pressing of the pellet because lithium metaborate was previously used in the press for XRF pellet manufacturing. The cause for the offset in barium has not been determined but may

Table 1
Comparison of Davies 2 coral by ID–ICP–MS and LA–ICP–MS using coral silicate glass and pressed powder disc

Method/standard	B/Ca (mmol/mol)	Mg/Ca (mmol/mol)	Sr/Ca (mmol/mol)	Ba/Ca (μmol/mol)	U/Ca (μmol/mol)
LA–ICP–MS					
Wollastonite glass [a]	0.489 ± 0.006 [b]	3.65 ± 0.05	8.06 ± 0.02	2.18 ± 0.04	0.785 ± 0.02
Pressed powder disc [a,c]	0.501 ± 0.015	4.11 ± 0.09	9.02 ± 0.11	3.04 ± 0.12	1.01 ± 0.03
Pressed powder disc [a,d]	0.472 ± 0.014	4.12 ± 0.09	8.97 ± 0.11	3.07 ± 0.12	1.01 ± 0.03
ID–ICP–MS	0.471 ± 0.005	4.14 ± 0.05	8.9087 ± 0.001 [e]	2.67 ± 0.03	1.03 ± 0.01

[a] All elemental concentrations in the coral silicate glass and pressed powder disc are based on ID–ICP–MS solution analysis except for boron in the wollastonite glass. Boron was lost during dissolution of glass.
[b] Boron concentration calibrated by 21 paired laser analyses of the wollastonite and NBS 612 glass.
[c] First pressed powder standard, based on 4 replicates.
[d] Second pressed powder standard, based on 4 replicates.
[e] Sr/Ca measured by ID–TIMS.

Table 2
Comparison of Huon Peninsula coral and coralline sponge by ID–ICP–MS and LA–ICP–MS using second pressed powder disc

Method/standard	B/Ca (mmol/mol)	Mg/Ca (mmol/mol)	Sr/Ca (mmol/mol)	Ba/Ca (μmol/mol)	U/Ca (μmol/mol)
Huon Peninsula, PNG coral					
ID–ICP–MS [a]	–	4.99 ± 0.11	8.90 ± 0.06	2.89 ± 0.03	1.09 ± 0.01
LA–ICP–MS [b]	0.528 ± 0.006	5.18 ± 0.23	8.96 ± 0.14	2.83 ± 0.12	1.06 ± 0.04
Coralline sponge, GBR					
ID–ICP–MS [c]	–	1.35 ± 0.09	10.68 ± 0.07	3.71 ± 0.04	2.75 ± 0.02
LA–ICP–MS [d]	0.171 ± 0.005	1.23 ± 0.15	10.59 ± 0.17	3.83 ± 0.16	2.71 ± 0.11

[a] Average of 5 measurements by ID–ICP–MS, B/Ca not measured.
[b] Average of 12 individual measurements made over a 1-month period using second coral pressed powder standard.
[c] Average of 5 measurements by ID–ICP–MS, B/Ca not measured.
[d] Average of 15 individual measurements made over a 1-month period using the second coral pressed powder standard.

be related to the distance between the milled sample and the laser tracks (>5 mm). A second pressed powder standard was constructed using a new clean press. The old pressed powder standard was cross-calibrated ($n = 13$) with the new pressed coral standard and the boron concentration in the new pressed powder standard was 8% lower than the original estimation, indicating some contamination. All the other elements were within error. Using the second pressed powder standard, the Davies 2 coral was re-analyzed and the boron concentration was within error of the solution estimate, but an offset still existed for the Ba/Ca (Table 1). The B/Ca values have been corrected using the new pressed powder standard.

Two other samples, a coral from Huon, Papua New Guinea, and a coralline sponge from the GBR were analyzed as a bulk pressed powder disc using the second pressed coral standard. These samples were prepared in the same manner as the coral pressed powder standard and were analyzed as pressed powder discs. Average values for 12 repeats of the Huon sample and 15 repeats for the coralline sponge are shown in Table 2. Independent analyses by isotope dilution solution ICP–MS are also given. All laser estimates of Mg, Sr, Ba and U, for these two samples are within error of the solution values (Table 2).

2.2. Precision and reproducibility

The three main components that contribute to the precision of this technique are counting statistics, calibration of the standard and heterogeneity of the standard. We can make estimates for each of these components, and they can be added in quadrature to give the final precision. The counting statistic errors are estimated by count rate and dwell time. The error associated with the calibration of the standard was our reproducibility and precision on the solution ICP–MS and TIMS measurements. The error for the heterogeneity of the standard was calculated as the standard deviation of a 60 s scan. Table 3 lists the estimates for the individual components and the overall precision for this technique as 3.8% for B/Ca, 4.2% for Mg/Ca, 1.6% for Sr/Ca, 4.3% for Ba/Ca and 3.9% for U/Ca (Table 3). This precision was between 1% and 4% greater than solution-based ID–ICP–MS analyses for these ratios.

Daily reproducibility was monitored by repeated measurements of the bulk Huon pressed powder disc and the bulk coralline sponge pressed powder disc. Repeated (×4) measurements of the coral from Shirigai Bay, over a 5-month period was used to estimate the long-term reproducibility. The four replicates for this coral are shown in Fig. 3. The daily and the long-term reproducibility for this technique is summarized in Table 3. Some of the variability of the long-term estimates may be due to inaccurate realigning of the laser tracks, which are not visible on the coral.

3. Results and discussion

A 9 cm length of the Shirigai Bay coral core was scanned for B, Mg, Sr, Ba and U. The Sr/Ca and U/Ca data are shown in Fig. 4. The average annual

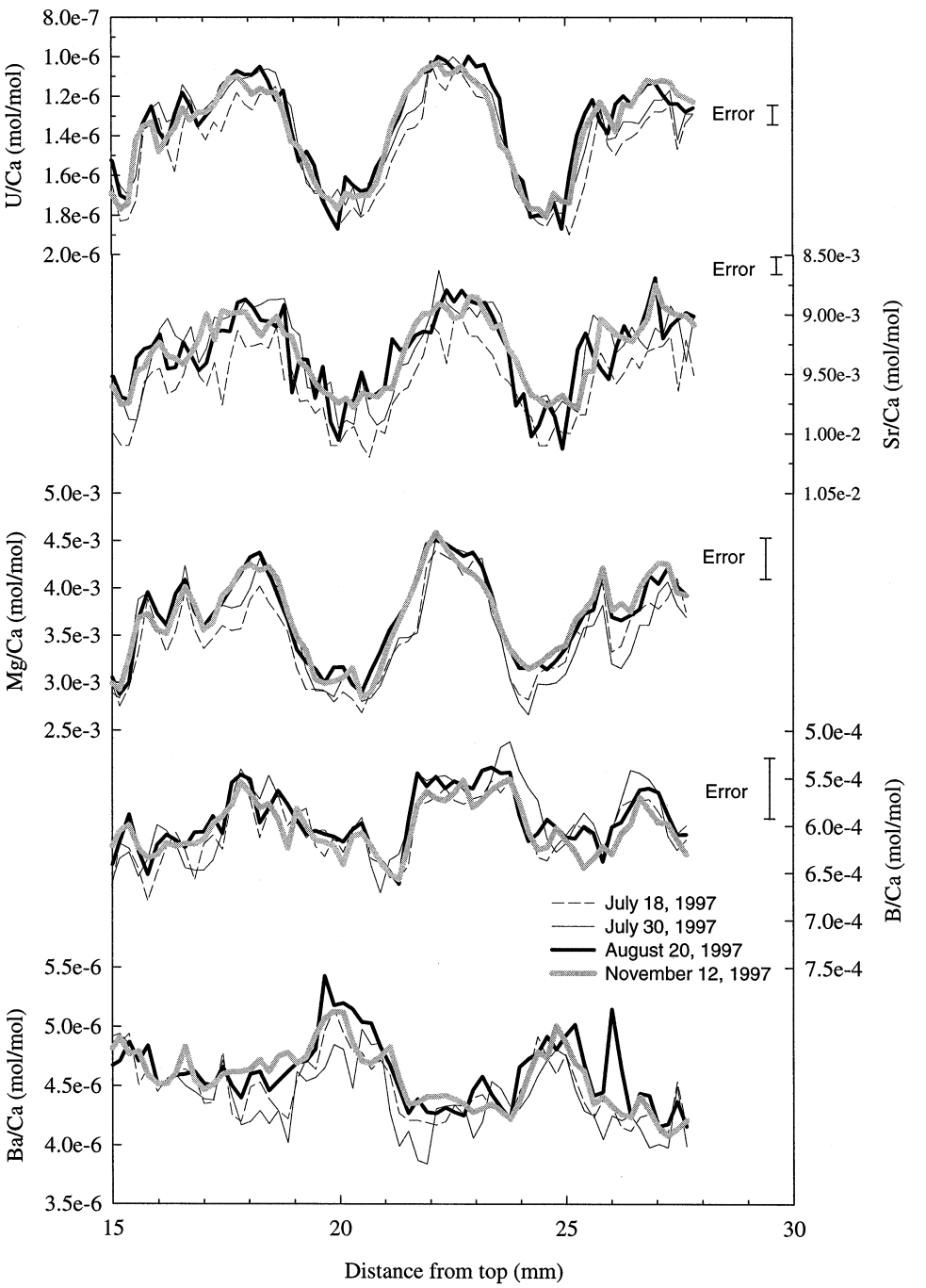

Fig. 3. Day to day reproducibility for the 5 elemental ratios (U/Ca, Sr/Ca, Mg/Ca, B/Ca and Ba/Ca) of the LA–ICP–MS method by measuring the Shirigai Bay *Porites* coral 4 times over a 5-month period.

Table 3
Analytical precision and reproducibility of the LA–ICP–MS system

Error	B/Ca	Mg/Ca	Sr/Ca	Ba/Ca	U/Ca
Counting uncertainty (%)	1.8	0.5	0.6	1.2	1.6
Calibration of standard (%)	1.1	1.7	0.02 [a]	1.0	0.9
Heterogeneity of standard (%) [b]	3.2	3.8	1.5	4.0	3.4
Overall precision (%)	3.8	4.2	1.6	4.3	3.9
Temperature equivalent (ºC) [c]	0.9	1.1	2.2	–	0.8
Daily reproducibility (%) [d]	1.3	1.4	0.5	1.6	1.4
Monthly reproducibility (%) [e]	2.5	4.9	1.1	3.3	3.3

[a] Calibrated using TIMS.
[b] 1σ standard deviation on a 60 s scan.
[c] Calculated from the temperature equations in this paper.
[d] Based on 1σ standard deviation of repeated ($n = 5$) daily measurements of the Huon pressed disc and coralline sponge pressed disc.
[e] Based on 1σ standard deviation of 4 replicates over a 86 mm length section of Shirigai Bay coral during a 5-month period (Fig. 3).

extension of this coral was 5.3 ± 1.2 mm/yr and the scan therefore covers approximately 16 years of coral growth. Each data point shown (Fig. 4) is a running average of 5 s of analytical time resulting in an effective resolution of 0.15 mm, which is similar to the coral calix depth. This sampling interval provides approximately fortnightly resolution.

3.1. Correlations between elements

Regression of Sr/Ca vs. U/Ca, B/Ca, Ba/Ca, and Mg/Ca are given in Fig. 5. A strong correlation ($r = 0.9$, $p < 0.0001$) exists between Sr/Ca and U/Ca which agrees with previous results [10]. However, the correlations between Sr/Ca and Mg/Ca and Sr/Ca and B/Ca ($r = -0.46$ and 0.53, respectively) are not as high as previously observed by Mitsuguchi et al. [14] and Sinclair et al. [5]. The low correlation between B/Ca, Mg/Ca and Sr/Ca indicates that these two elements (B and Mg) may be influenced by other factors aside from temperature.

3.2. Length to time translation

Translating from distance to time usually involves correlating the 'element'/Ca to SST maximum and minimum and assuming linear growth between these 'marker' points. This approach is not adequate for our *Porites* coral because of the extreme summer-to-winter growth bias. Evidence for a marked decrease, or cessation, of winter growth can be seen in Fig. 4, where the winters are under represented as sharp spikes compared to the broad peaks for summer. A quantitative representation of this effect is shown in the histogram of the number of data points sampled (equivalent to ~0.15 mm growth increments) (Fig. 6). The measured SST has approximately a sinusoidal pattern with the winter having a slightly higher abundance of points than the summer (Fig. 6A). However, for the *Porites* coral ~3 times more points (U/Ca and Sr/Ca) were sampled in summer versus winter (Fig. 6B,C). The 'arched' shape of the trace element profiles is very similar to model simulations of coral growth by Barnes et al. [27]. Simulations showed that trace element profiles took on an 'arched' shape when summer extension increased relative to winter extension. Our data reproduce the sharp/narrow winter peaks observed by the model-simulated trace element profiles when winter extension is stopped [27]. Using the simulations as a guide, we tested the correlation between U/Ca and SST by assuming variations in winter extension.

Based on the assumption that little to no growth was occurring during the winters, a time gap was inserted during each winter minimum. Using the minimum measured SSTs as a guide, the effects of assuming non-uniform growth for different periods was examined (from 1 week to 4 months). The optimum fit for the U/Ca (and Sr/Ca) ratios was obtained for a ~2 month cessation of growth between early January and late March when SSTs < 18ºC. Linear growth was then assumed to occur within the remaining interval, that is, from spring to late fall. It is noted that an absence of winter growth for the 2-month model

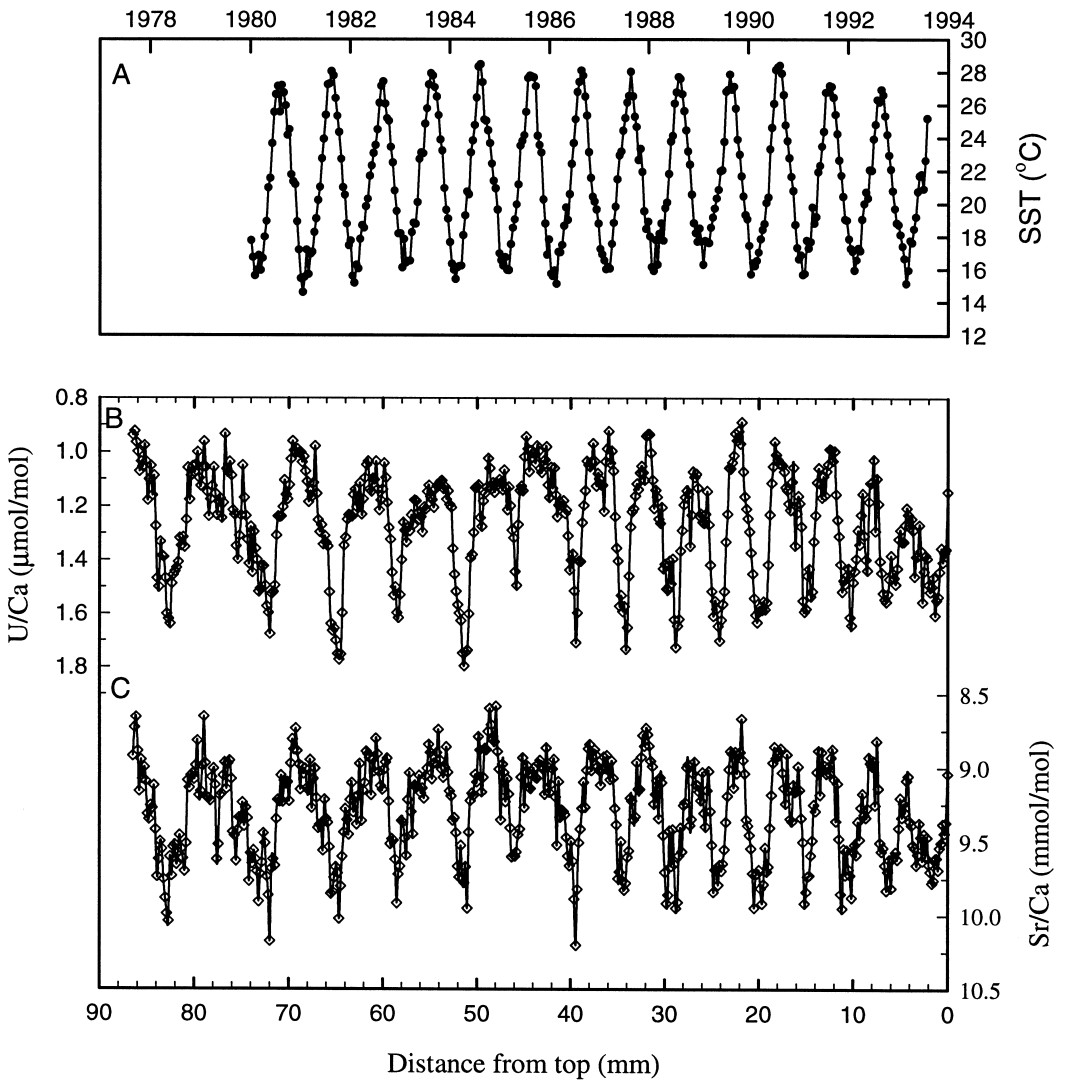

Fig. 4. (A) Fortnightly SSTs from Komame station. (B) U/Ca vs. distance from the top of the Shirigai Bay Porites coral. (C) Sr/Ca vs. distance from the top of the Shirigai Bay *Porites* coral. Diamonds represent individual measurements.

is a simplifying assumption that cannot be resolved from very slow (<1 mm/yr) winter growth rates.

Comparisons of the best fit for U/Ca and measured SST versus time is shown for uniform annual growth (Fig. 7A) and an absence of winter growth (Fig. 7B,C). For uniform annual growth, the relationship of U/Ca to SST had a correlation coefficient $r = -0.71$, compared to $r = -0.84$ for the 2-month cessation in winter growth. Inputting an absence of growth considerably improved the U/Ca and SST interpretation; however, there were still some outliers. This has been noted previously by McCulloch et al. [8] for coral growth during winter in the inshore region of the Great Barrier Reef where cool (<20°C) SSTs are sometimes recorded.

3.3. SST and elemental calibrations

The above chronology, including an absence of winter growth, was then used to compare the trace

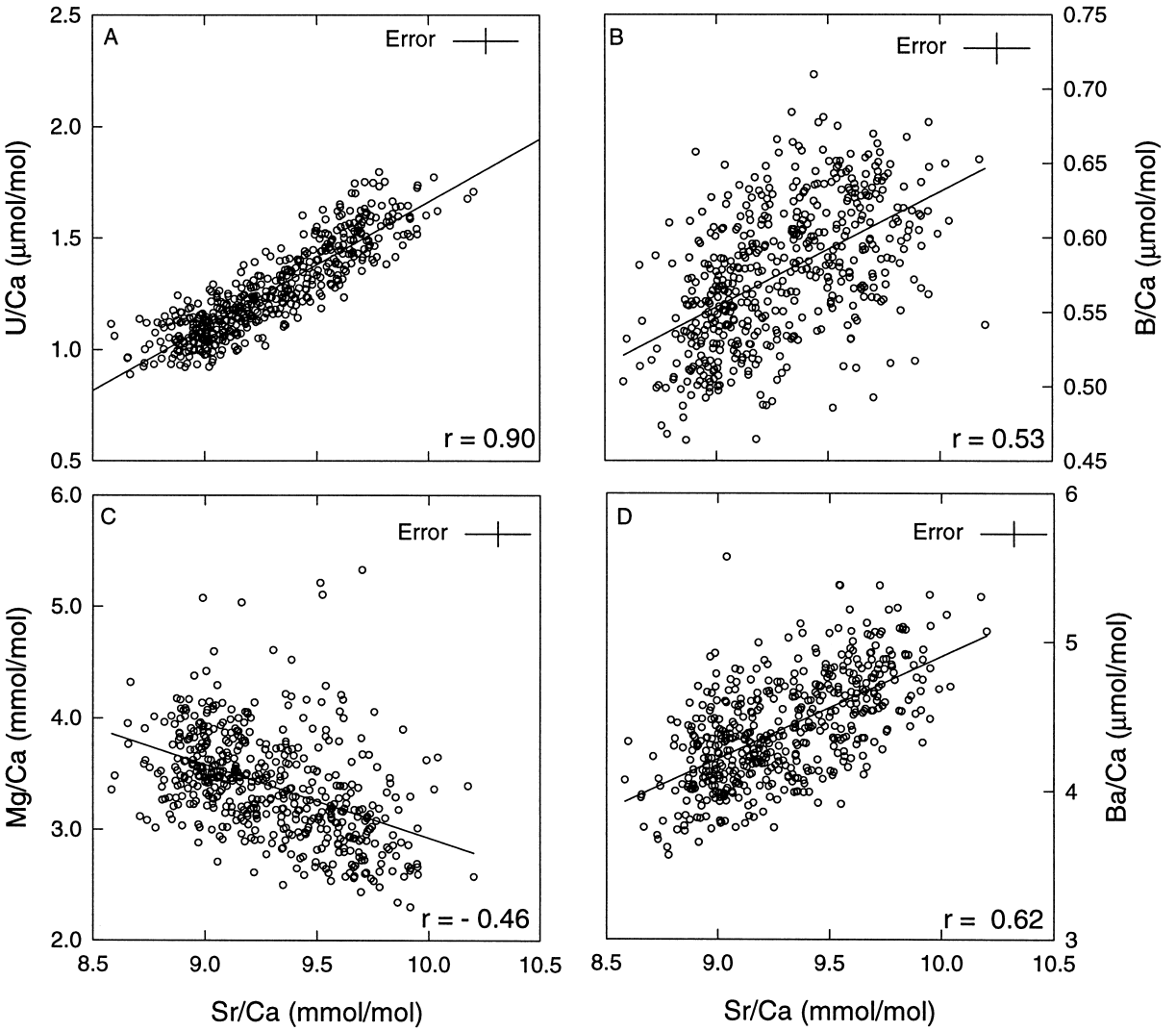

Fig. 5. (A) Linear regression of U/Ca vs. Sr/Ca. (B) Linear regression of B/Ca vs. Sr/Ca. (C) Linear regression of Mg/Ca vs. Sr/Ca. (D) Linear regression of Ba/Ca vs. Sr/Ca.

elements with fortnightly SSTs (Fig. 8). Using this time vs. distance fit, linear regressions between SSTs and the following, U/Ca, Sr/Ca, B/Ca and Mg/Ca, and are shown in Fig. 8. The least-squares regression equations for these elements are:

$$\mathrm{U/Ca} \times 10^6 = 2.26(\pm 0.05) - 0.044(\pm 0.022) \times \mathrm{SST(^oC)} \quad r = -0.84 \tag{1}$$

$$\mathrm{Sr/Ca} \times 10^3 = 10.76(\pm 0.08) - 0.063(\pm 0.003) \times \mathrm{SST(^oC)} \quad r = -0.77 \tag{2}$$

$$\mathrm{B/Ca} \times 10^3 = 0.767(\pm 0.015) - 0.009(\pm 0.001) \times \mathrm{SST(^oC)} \quad r = -0.74 \tag{3}$$

$$\mathrm{Mg/Ca} \times 10^3 = 1.38(\pm 0.161) + 0.088(\pm 0.007) \times \mathrm{SST(^oC)} \quad r = 0.66 \tag{4}$$

Under the assumption of cessation of growth, the regression equations do not encompass SSTs below 18ºC.

The calibrations presented here are similar to previously reported calibrations with some discrep-

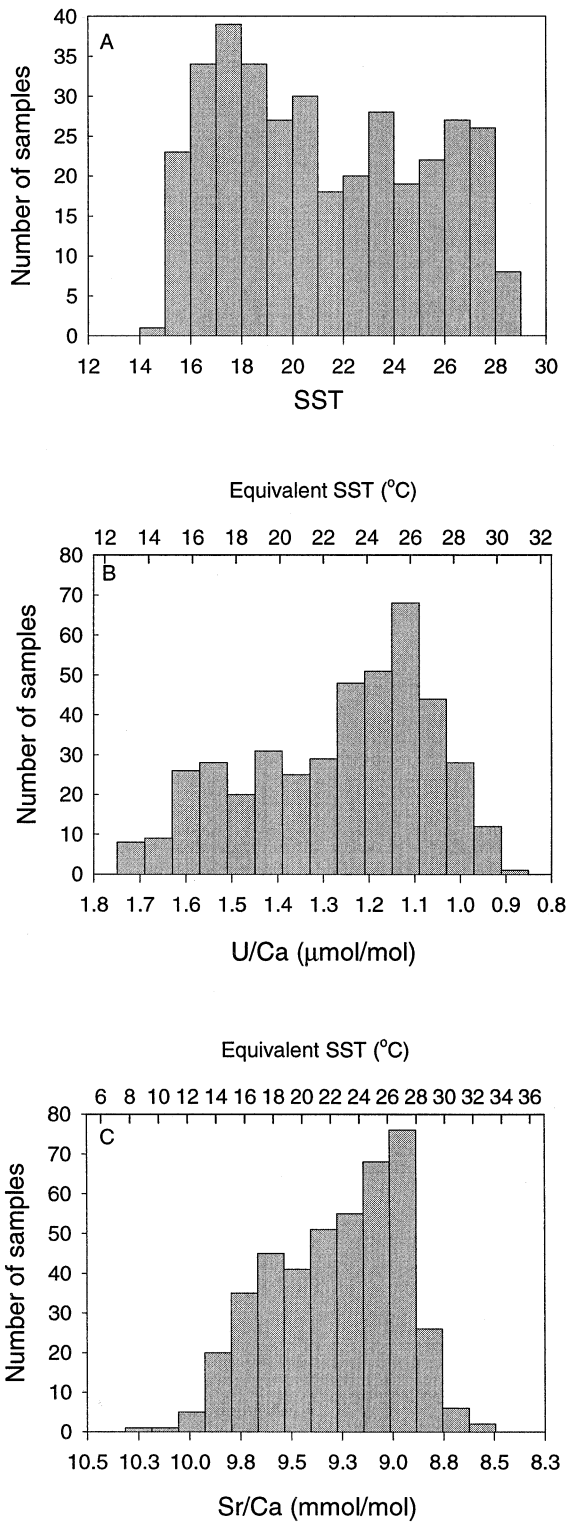

Fig. 6 (left). (A) Histogram of Komame sea surface temperatures (SSTs), number of observations vs. SSTs. Notice a slightly higher abundance of data points sampled between 16° and 19°C. (B) Histogram of U/Ca values. Notice a higher abundance of data points sampled between 1.25 and 1.1 μmol/mol, which is approximately equivalent to 23–26°C (top *x*-axis). (C) Histogram of Sr/Ca values. Notice a higher abundance of data points sampled between 9.2 and 8.9 mmol/mol, or at 24–28°C.

ancies (Fig. 8) [5,9,10,14,28,29]. The calibration of Sr/Ca to SST has been the most widely studied of the temperature proxies and several calibrations exist for the coral genera *Porites*. Calibrations from Alibert and McCulloch [9], de Villiers et al. [28] and Gagan et al. [29] are plotted for comparison with our dataset (Fig. 8A). There is a wide range of published calibrations. Even though there is some error associated with our laser ablation technique our calibration falls closely within the reported range (Fig. 8A), although no convincing explanation has been provided for the offsets reported between high-precision TIMS Sr/Ca calibrations. More importantly, the slope and temperature dependence provided by our calibration is very close to those previously reported [7,9,28–30].

Two previously reported calibrations for U/Ca and temperature from Min et al. [10] and Sinclair et al. [5] are plotted for comparison with our dataset (Fig. 8B). Our calibration is offset from Min et al. [10] and Sinclair et al. [5], and gives temperatures between 2° and 4°C higher, although the slope and temperature dependence are both very similar (Fig. 8B). It appears that discrepancies similar to those for Sr/Ca may exist for the U/Ca temperature calibrations.

Calibration lines for Mg/Ca, based on data from Mitsuguchi et al. [14], Sinclair et al. [5] and Wheeler

Fig. 7 (right). (A) U/Ca and Komame SSTs vs. time assuming uniform growth between winter minimum and summer maximum SSTs. Note that the U/Ca curve is much broader from early spring to late autumn. Correlation coefficient for this least-squares regression is $r = -0.71$. (B) U/Ca and SST vs. time using 2-month cessation of growth model. By assuming little/no growth during the winter (SST < 18°C) we assigned marker points then assumed linear growth between these points. The result is a better visual and statistical fit ($r = -0.84$). (C) Sr/Ca and SST vs. time using the 2-month cessation of growth model; this also provides a better fit between the data and SSTs.

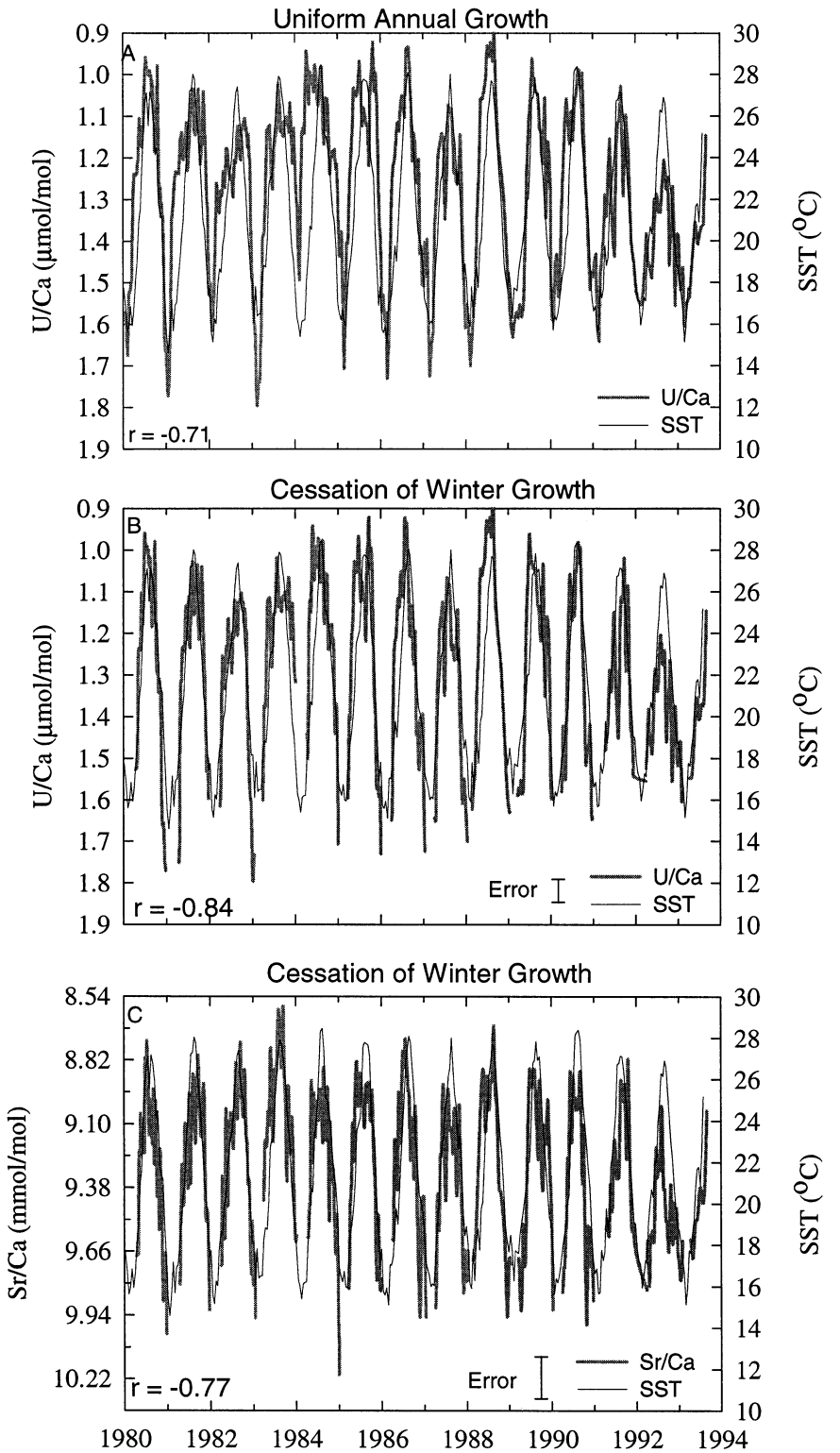
Uniform Annual Growth
A
U/Ca (µmol/mol)
SST (°C)
r = -0.71
U/Ca
SST
Cessation of Winter Growth
B
U/Ca (µmol/mol)
SST (°C)
Error
r = -0.84
U/Ca
SST
Cessation of Winter Growth
C
Sr/Ca (mmol/mol)
SST (°C)
r = -0.77
Error
Sr/Ca
SST
1980 1982 1984 1986 1988 1990 1992 1994

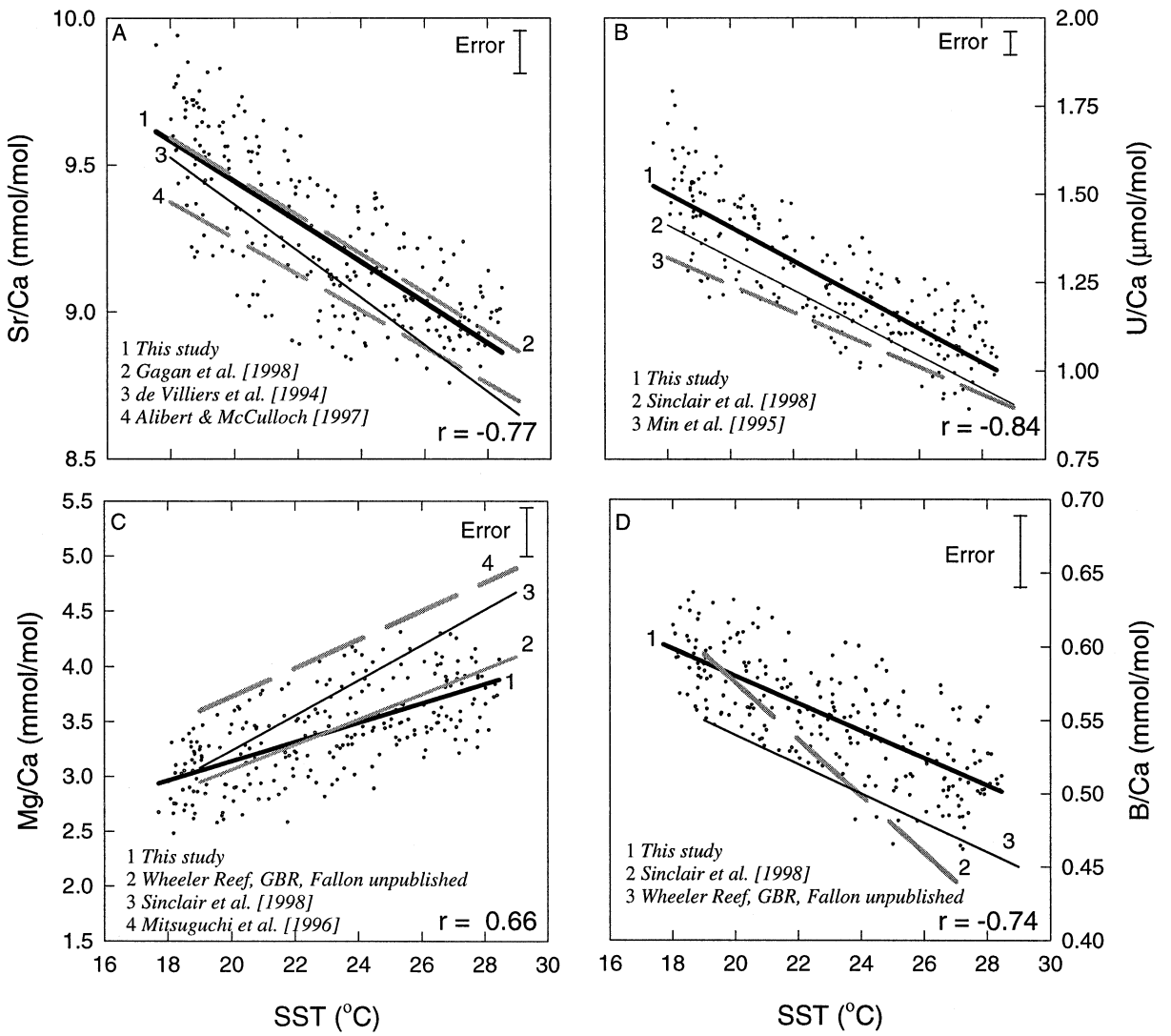

Fig. 8. (A) Linear regression of Sr/Ca vs. Komane SSTs. Also shown are calibration lines from de Villiers et al. [28], Alibert and McCulloch [9] and Gagan et al. [29]. (B) Linear regression of U/Ca vs. SST. Also shown are calibration lines from Sinclair et al. [5] and Min et al. [10]. (C) Linear regression of Mg/Ca vs. SSTs. Also shown are calibrations from Mitsuguchi et al. [14], Sinclair et al. [5] and a coral from Wheeler Reef (S.J. Fallon, unpubl.). (D) Linear regression of B/Ca vs. SST. Also shown are calibration lines from Sinclair et al. [5] and a coral from Wheeler Reef (S.J. Fallon, unpubl.).

Reef, GBR (S.J. Fallon, unpubl. data) are shown in Fig. 8C. The calibration from Wheeler Reef, GBR, is very similar to the Shirigai Bay *Porites* coral; however, a large offset (outside analytical error) exists for the data of Mitsuguchi et al. [14] (Fig. 8C). The calibration provided by Sinclair et al. [5] falls between this study and that of Mitsuguchi et al. [14], with a much steeper slope (Fig. 8C). We do not attribute these calibration offsets to inaccuracy of the laser method. More likely they are due to different environmental conditions in which the corals grew, or some species-specific effects, influencing the incorporation of magnesium.

The only previously published calibration for B/Ca is from Sinclair et al. [5]. There is a large discrepancy when their results are compared to our

data (Fig. 8D). The calibration for the coral from Wheeler Reef, GBR (S.J. Fallon, unpubl. data) is also shown for comparison. The slopes of the Shirigai Bay coral and the Wheeler Reef coral are very similar but the temperature offset is 4–6ºC (Fig. 8D). Clearly more work is needed in order to test boron as a temperature proxy.

3.4. Winter growth changes

Decreased extension and hence calcification during cold winter temperatures has been noted previously [31–34]. Such studies encompassed a wide range of locations and several different coral genera. For example, reduced growth rates of *Pavona* spp. corals on the western side of the Galapagos Islands, as opposed to other locations on the islands, have been attributed to reduced SSTs in winter that are onset by upwelling events (SSTs 17–18ºC) [34]. In studies on *Porites lobata*, Houck et al. [32] noted a two-fold decrease in growth when SSTs approached and extended below 22ºC. The evidence shown in other studies suggests a decrease in winter growth, and not a full cessation of growth as shown in the present study.

Jacques et al. [35] suggested that calcification rates approached zero as temperature reached 16ºC. Our *Porites* coral grew in temperatures below 16ºC for ~3–4 weeks every year and below 18ºC for 2–3 months (Fig. 4A). In conjunction with the trace element profiles showing sharp winter peaks and few samples, we conclude that *Porites* corals cease growing in winter at these high latitudes when the SSTs decline below 18ºC.

3.5. Mg/Ca

The annual cycles of Mg/Ca are clearly visible (Fig. 9A) and are weakly correlated with SST ($r = 0.66$) (Fig. 8C). This is generally consistent with previous measurements of the Mg/Ca ratio in corals [5,12–14]. However, a large variation across short distances (weeks to months) approaching 50–60% of the annual signal was observed in some of the records (Fig. 9A). This short-time scale variability cannot be associated with any SST variations. This micro-scale heterogeneity has also been observed in corals analyzed by Allison [36], Allison and Tudhope [37] and Sinclair et al. [5]. The high-resolution nature of laser and other micro-beam techniques may enhance the observation of this heterogeneity. In a study by Mitsuguchi et al. [14], a more coarse sampling approach was undertaken (each sample equivalent to ~3 weeks of growth) and this fine-scale heterogeneity was not observed. Indeed, it appears that bulk sampling may smooth some of the heterogeneity.

Amiel et al. [38] suggested that Mg^{2+} could occur both in adsorbed sites and in organic phases as well as in the crystal lattice, with the lattice component easily displaced by Ca^{2+} during leaching. Amiel et al. [38] also suggested that different amounts of organic phases, adjacent to each other, could possibly explain this fine-scale heterogeneity. The variability in the metal binding capacity of the coral tissue organic matrix, and its heterogeneity throughout the depth of the coral, may also play an important role [36,37,39]. Clearly more work is needed to understand the fine-scale variations of Mg in corals.

3.6. B/Ca

Hart and Cohen [12] and Sinclair et al. [5] suggested B/Ca ratio in corals as a palaeothermometer. However, the speciation of boron in seawater can be affected by many factors, including pH, temperature, borate to carbonate ratio in seawater, and biological and kinetic factors [40–42]. Sinclair et al. [5] noted a high correlation between B/Ca and SST ($r = -0.91$) for a mid-reef site in the GBR. In this study we observe a moderate correlation between B/Ca and SST ($r = -0.74$, $p < 0.0001$) (Fig. 8D, Fig. 9B). As mentioned previously for Mg/Ca, we also observed large elemental excursions across short distances approaching 60–70% of the annual signal (Fig. 7B). These large shifts, not attributable to SST, may limit the use of B/Ca as a palaeothermometer but when used in conjunction with U/Ca or Sr/Ca these fine-scale variations may be able to provide additional information on other environmental influences.

3.7. SST variations, upwelling and Ba/Ca

The summer SSTs during 1982, 1991 and 1992 were slightly cooler than the ‘average’ summer (Fig. 7A) which is consistent with the U/Ca values

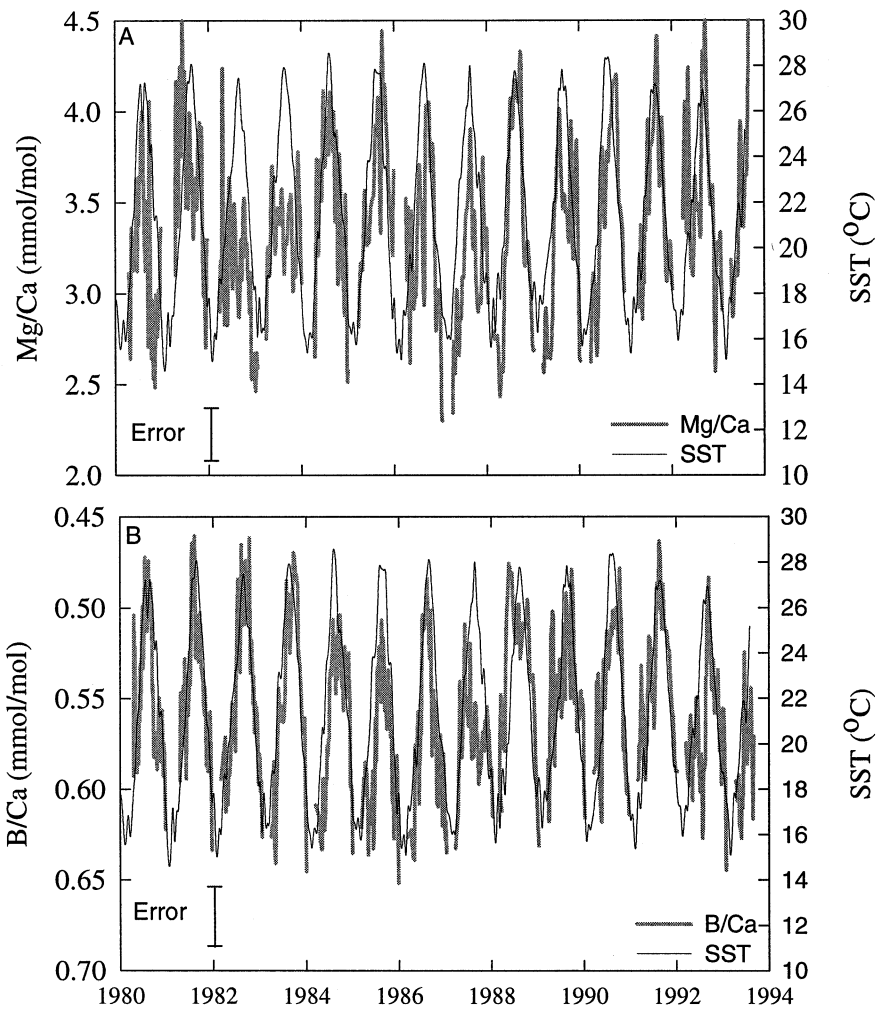

Fig. 9. (A) Mg/Ca and Komame SSTs vs. time using 2-month cessation of growth model. (B) B/Ca and Komame SSTs vs. time using 2-month cessation of growth model.

(for these same time periods) that also indicate cooler than normal summer water temperatures (Fig. 7B). These cooler summer temperatures coincide with years characterized as El Niño periods. One factor that may play a role in determining which years have cooler summer SSTs is seasonal upwelling. Along the coast of Shikoku (in Shirigai Bay specifically), seasonal upwelling occurs when the summer SW airflow is replaced by a winter NW wind pattern. Data from dives in the bay suggest that a deep-water channel (15 m) on the eastern side of the bay provides an access for cold, nutrient-rich, water to enter into the shallow coral zones.

Barium can substitute for calcium into the aragonitic crystal lattice of reef corals. The concentration of Ba in seawater increases from low values in warm surface water to high values in deep, cold, and nutrient-rich water. Therefore, cycles in the Ba/Ca ratio in corals, away from coastal river runoff, are most likely controlled by the strength of seasonal upwelling [15]. However, it has been suggested that the barium distribution coefficient has a slight temperature dependence but this has not been verified [15,17]. If this temperature dependence exists it will be small compared to the upwelling signature recorded by this coral.

The observed range of Ba/Ca in the *Porites* coral is approximately 3.9–5.1 μmol/mol. Using a distribution coefficient of 1.27 [15], the coralline Ba/Ca can be converted to an estimate of seawater barium content. The seawater barium concentration ranges from a low of 31 nmol/kg in the summer to a high of 41 nmol/kg in the winter. These values are consistent with inferred seawater barium concentrations from corals in an upwelling zone of the Galapagos, whose values ranged from 32 to 40 nmol/kg [15,17].

The Ba/Ca cycles in the *Porites* coral peak just after a positive peak in the zonal wind speed (Fig. 10A). The wind direction appears to be forcing upwelling, thereby bringing colder, Ba-enriched water to the surface. Wind data from COADS [43] indicate that the shift to the NW wind pattern usually precedes the winter SST minimum by ~1–2 months (Fig. 10A). The main inferred Ba/Ca upwelling peaks coincide with the U/Ca and Sr/Ca maximum and the SST minimum (Fig. 10B). Cross-correlation

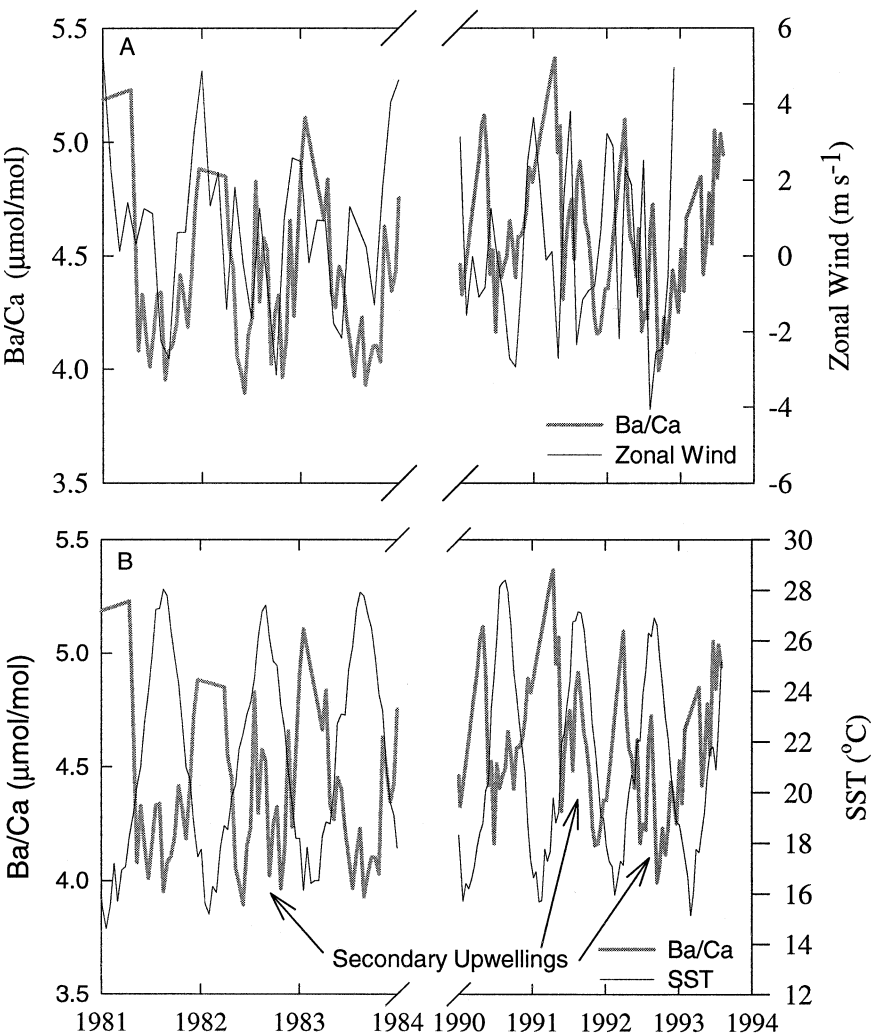

Fig. 10. (A) Ba/Ca and zonal wind velocity vs. time. Zonal wind dataset from COADS (2° × 2°) grid centred on 33°N, 133°E. Note positive zonal wind peaks lead Ba/Ca peaks by ~2 months. During the El Niño years (1982, 1987, 1991, 1992) multiple peaks in both the zonal wind and Ba/Ca occur. Cross-correlation indicates a 2-month lag by the Ba/Ca to the zonal winds $r = 0.51$. (B) Close-up of Ba/Ca and SST vs. time from 1981 to 1984 and from 1990 to 1994 showing secondary upwelling in the summers of 1982, 1991 and 1992.

indicates that the Ba/Ca lags the zonal wind by 2 months ($r = 0.51$ when lagged by 2 months, no lag $r = 0.25$). This winter upwelling contributes to the extremely cold winter SSTs measured in this area.

Secondary peaks in both the zonal winds and Ba/Ca (Fig. 10A) were recorded during the years 1982, 1987, 1991 and 1992, which exhibited cooler-than-average summer SSTs. It appears that changes in the 'normal' atmospheric wind patterns during these periods are associated with El Niño Southern Oscillation events. This wind pattern change can be observed in the *Porites* coral as a second increase in the Ba/Ca during the summer (Fig. 10B), suggesting that, in addition to the seasonal upwelling, a second upwelling event occurs during El Niño years. This secondary upwelling event is at least partly responsible for the cooler-than-average summer SSTs during 1982, 1987, 1991 and 1992 (Fig. 7B, Fig. 10B). If this double upwelling signature is consistent during all El Niño events it may be a useful proxy for the reconstruction of palaeo-El Niño in this area.

4. Conclusions

Excimer laser ablation–inductively coupled plasma–mass spectrometry (LA–ICP–MS) provides a rapid analytical technique to measure boron, magnesium, calcium, strontium and uranium concentrations in corals. The power of this technique lies in its ability to measure these elements simultaneously with appropriate spatial resolution regardless of coral extension rate.

The 'arched' shape of our trace element profiles is indicative of increased extension in summer relative to winter. Model simulations of trace element profiles corroborate this with little to no winter extension [27]. Our data suggest a marked decrease and/or cessation of extension during winter. A decrease or cessation of growth during cold winters has important implications for coral calcification and overall carbonate/reef accumulation.

U/Ca, Mg/Ca and B/Ca appear to exhibit similar calibration offsets as the Sr/Ca thermometer. It is expected, however, that as the database for these elements increases, factors influencing the temperature relationships and their (B, Mg, Sr, U) respective elemental budgets will be enhanced.

The Shirigai Bay *Porites* coral has an approximately linear response of U/Ca and Sr/Ca to SSTs above 18ºC. Below 18ºC there appears to be an increase in elemental incorporation during times of extreme cold and/or in times of little to no growth. The *Porites* coral reinforces the notion that factors aside from temperature (such as adsorbed sites or variability in metal binding capacity of the organic matrix) could be affecting the Mg/Ca ratio. It also appears that other factors are influencing the B/Ca ratio aside from temperature. The usefulness of Ba/Ca as an upwelling indicator is confirmed, and here we show how upwelling can influence SST. A secondary upwelling event occurs during El Niño summers, causing cooler summer SSTs, which may provide a proxy for detecting palaeo-events in similar locations.

Acknowledgements

We would like to thank Les Kinsley who provided technical support for the ICP–MS and laser-ablation system and the town of Otsuki, Japan, for inviting R. Van Woesik to study this reef. This paper benefited from comments by C. Stirling and two anonymous reviewers. Mr. S. Fallon is supported by an OPRS and a Ph.D. scholarship from the Research School of Earth Sciences at the Australian National University. ***[AH]***

References

[1] J.-P. Gattuso, M. Frankignoulle, I. Bourge, S. Romaine, R.W. Buddemeier, Effect of calcium carbonate saturation of seawater on coral calcification, Global Planet. Change 18 (1998) 37–46.

[2] J.A. Kleypas, R.W. Buddemeier, D. Archer, J.-P. Gattuso, C. Langdon, B.N. Opdyke, Geochemical consequences of increased atmospheric carbon dioxide on coral reefs, Science 284 (1999) 118–120.

[3] M.T. McCulloch, A.W. Tudhope, T.M. Esat, G.E. Mortimer, J. Chappell, B. Pillans, A.R. Chivas, A. Omura, Coral record of equatorial sea-surface temperatures during the penultimate deglaciation at Huon Peninsula, Science 283 (1999) 202–204.

[4] R. van Woesik, Coral communities at high latitude are not pseudopopulations: evidence of spawning at 32ºN, Japan, Coral Reefs 14 (1995) 119–120.

[5] D. Sinclair, L. Kinsley, M. McCulloch, High resolution

analysis of trace elements in corals by laser ablation ICP–MS, Geochim. Cosmochim. Acta 212 (62/11) (1998) 1889–1901.
[6] S.V. Smith, R.W. Buddemeier, R.C. Redalje, J.E. Houck, Strontium–calcium thermometry in coral skeletons, Science 204 (1979) 404–406.
[7] J.W. Beck, R.L. Edwards, E. Ito, F.W. Taylor, J. Recy, F. Rougerie, P. Joannot, C. Henin, Sea-surface temperature from coral skeletal strontium/calcium ratios, Science 257 (1992) 644–647.
[8] M.T. McCulloch, M.K. Gagan, G.E. Mortimer, A.R. Chivas, P.J. Isdale, A high-resolution Sr/Ca and $\delta^{18}O$ coral record from the Great Barrier Reef, Australia, and the 1982–1983 El Niño, Geochim. Cosmochim. Acta 58 (12) (1994) 2747–2754.
[9] C. Alibert, M.T. McCulloch, Strontium/calcium ratios in modern *Porites* corals from the Great Barrier Reef as a proxy for sea surface temperature: calibration of the thermometer and monitoring of ENSO, Paleoceanography 12 (3) (1997) 345–363.
[10] G.R. Min, R.L. Edwards, F.W. Taylor, J. Recy, C.D. Gallup, J.W. Beck, Annual cycles of U/Ca in coral skeletons and U/Ca thermometry, Geochim. Cosmochim. Acta 59 (1995) 2025–2043.
[11] G.T. Shen, R.B. Dunbar, Environmental controls on uranium in reef corals, Geochim. Cosmochim. Acta 59 (1995) 2009–2024.
[12] S.R. Hart, A.L. Cohen, An ion probe study of annual cycles of Sr/Ca and other trace elements in corals, Geochim. Cosmochim. Acta 60 (16) (1996) 3075–3084.
[13] T. Oomori, K. Kaneshima, Y. Nakamura, Y. Kitano, Seasonal variations of minor elements in coral skeletons, Galaxea 1 (1982) 77–86.
[14] T. Mitsuguchi, E. Matsumoto, O. Abe, T. Uchida, P.J. Isdale, Mg/Ca thermometry in coral skeletons, Science 274 (1996) 961–963.
[15] D.W. Lea, G.T. Shen, E.A. Boyle, Coralline barium records temporal variability in equatorial Pacific upwelling, Nature 340 (1989) 373–376.
[16] G.T. Shen, C.L. Sanford, Trace element indicators of climate change in annually-banded corals, in: P.W. Glynn (Ed.), Global Consequences of the 1982–83 El Nino Southern Oscillation, Elsevier, Amsterdam, 1990.
[17] G.T. Shen, J.E. Cole, D.W. Lea, L.J. Linn, T.A. McConnaughey, R.G. Fairbanks, Surface ocean variability at Galapagos from 1936–1982: calibration of geochemical tracers in corals, Paleoceanography 7 (5) (1992) 563–588.
[18] D.W. Knutson, R.W. Buddemeier, S.V. Smith, Coral chronometers: seasonal growth bands in reef corals, Science 177 (1972) 270–272.
[19] R.E. Dodge, J.R. Vaisnys, Hermatypic coral growth banding as an environmental recorder, Nature 258 (1975) 706–708.
[20] R.C. Highsmith, Coral growth rates and environmental control of density banding, J. Exp. Mar. Biol. Ecol. 37 (1979) 105–125.
[21] S.M. Eggins, L.P.J. Kinsley, J.M.G. Shelly, Deposition and element fractionation processes during atmospheric pressure laser sampling for analysis by ICP–MS, Appl. Surf. Sci. 127–129 (1998) 278–286.
[22] P.J. Sylvester, M. Ghaderi, Trace element analysis of scheelite by excimer laser ablation–inductively coupled plasma–mass spectrometry (ELA–ICP–MS) using a synthetic silicate glass standard, Chem. Geol. 141 (1997) 49–65.
[23] K.E. Jarvis, J.G. Williams, Laser ablation inductively coupled plasma mass spectrometry (LA–ICP–MS): a rapid technique for the direct, quantitative determination of major, trace and rare-earth elements in geological samples, Chem. Geol. 106 (1993) 251–262.
[24] C.A. Morrison, D.D. Lambert, R.J.S. Morrison, W.W. Ahlers, I.A. Nicholls, Laser ablation–inductively coupled plasma–mass spectrometry: an investigation of elemental responses and matrix effects in the analysis of geostandard materials, Chem. Geol. 119 (1995) 13–29.
[25] N.J.G. Pearce, W.T. Perkins, R. Fuge, Developments in the quantitative and semiquantitative determination of trace elements in carbonates by laser ablation inductively coupled plasma mass spectrometry, J. Anal. At. Spectr. 7 (1992) 595–598.
[26] W.T. Perkins, R. Fuge, N.J.G. Pearce, Quantitative analysis of trace elements in carbonates using laser ablation inductively coupled plasma mass spectrometry, J. Anal. At. Spectr. 6 (1991) 445–449.
[27] D.J. Barnes, R.B. Taylor, J.M. Lough, On the inclusion of trace materials into massive coral skeletons, Part II, Distortions in skeletal records of annual climate cycles due to growth processes, J. Exp. Mar. Biol. Ecol. 194 (1995) 251–275.
[28] S. de Villiers, G.T. Shen, B.K. Nelson, The Sr/Ca–temperature relationship in coralline aragonite: Influence of variability in (Sr/Ca)seawater and skeletal growth parameters, Geochim. Cosmochim. Acta 58 (1994) 197–208.
[29] M.K. Gagan, L.K. Ayliffe, D. Hopley, J.A. Cali, G.E. Mortimer, J. Chappell, M.T. McCulloch, M.J. Head, Temperature and surface-ocean water balance of the mid-Holocene tropical Western Pacific, Science 279 (1998) 1014–1017.
[30] C.-C. Shen, T. Lee, C.-Y. Chen, C.-H. Wang, C.-F. Dai, L.-A. Li, The calibration of D[Sr/Ca] versus sea surface temperature relationship for *Porites* corals, Geochim. Cosmochim. Acta 60 (20) (1996) 3849–3858.
[31] R.W. Buddemeier, R.A. Kinzie, The chronometric reliability of contemporary corals, in: G.D. Rosenberg, S.K. Runcorn (Eds.), Growth Rhythms and the History of the Earths's Rotation, Wiley, New York, 1975, pp. 135–147.
[32] J.E. Houck, R.W. Buddemeier, S.V. Smith, P.L. Jokiel, The response of coral growth rate and skeletal strontium content to light intensity and water temperature, 3rd Int. Coral Reef Symp. 2, 1977, pp. 425–431.
[33] C.J. Crossland, Seasonal growth of *Acropora* cf. *formosa* and *Pocillopora damicornis* on a high latitude reef (Houtman Abrolhos, Western Australia), 4th Int. Coral Reef Symp. 1, Manila, 1981, pp. 663–667.
[34] G.M. Wellington, P.W. Glynn, Environmental influences on

skeletal banding in eastern Pacific (Panama) corals, Coral Reefs 1 (1983) 215–222.
[35] T.G. Jacques, M.E.Q. Pilson, C. Cummings, N. Marshall, Laboratory observations on respiration, photosynthesis, and factors affecting calcification in the temperate coral *Astrangia danae*, in: D.L. Taylor (Ed.), Third International Coral Reef Symposium 2, University of Miami, Miami, FL, 1977, pp. 455–461.
[36] N. Allison, A.W. Tudhope, Nature and significance of geochemical variations in coral skeletons as determined by ion microprobe analysis, 7th Int. Coral Reef Symp. 1, Guam, 1992, pp. 173–178.
[37] N. Allison, Geochemical anomalies in coral skeletons and their possible implications for palaeoenvironmental analyses, Mar. Chem. 55 (1996) 367–379.
[38] A.J. Amiel, G.M. Friedman, D.S. Miller, Distribution and nature of incorporation of trace elements in modern aragonitic corals, Sedimentology 20 (1973) 47–64.
[39] R.A. Mitterer, Amino acid composition and metal binding capability of the skeletal protein of corals, Bull. Mar. Sci. 28 (1978) 173–180.
[40] A. Vengosh, Y. Kolodny, A. Starinsky, A.R. Chivas, M.T. McCulloch, Coprecipitation and isotopic fractionation of boron in modern carbonates, Geochim. Cosmochim. Acta 55 (1991) 2901–2910.
[41] N.G. Hemming, G.N. Hanson, Boron isotopic composition and concentration in modern marine carbonates, Geochim. Cosmochim. Acta 56 (1992) 537–543.
[42] J. Gaillardet, C.J. Allegre, Boron isotopic compositions of corals: seawater or diagenesis record?, Earth Planet. Sci. Lett. 136 (1995) 665–676.
[43] R.J. Slutz, S.J. Lubker, J.D. Hiscox, S.D. Woodruff, R.L. Jenne, D.H. Joseph, P.M. Steuer, J.D. Elms, Comprehensive Ocean–Atmosphere Data Set, NOAA Environmental Research Laboratory, Boulder, CO, 1985.